# Mathematical Omnibus: Thirty Lectures on Classic Mathematics

Dmitry Fuchs

Serge Tabachnikov

Department of Mathematics, University of California, Davis, CA 95616 .
Department of Mathematics, Penn State University, University Park, PA 16802 .

# Contents

# Preface

> For more than two thousand years some familiarity with mathematics has been regarded as an indispensable part of the intellectual equipment of every cultured person. Today the traditional place of mathematics in education is in grave danger.

These opening sentences to the preface of the classical book "What Is Mathematics?" were written by Richard Courant in 1941. It is somewhat soothing to learn that the problems that we tend to associate with the current situation were equally acute 65 years ago (and, most probably, way earlier as well). This is not to say that there are no clouds on the horizon, and by this book we hope to make a modest contribution to the continuation of the mathematical culture.

The first mathematical book that one of our mathematical heroes, Vladimir Arnold, read at the age of twelve, was "Von Zahlen und Figuren"[1] by Hans Rademacher and Otto Toeplitz. In his interview to the "Kvant" magazine, published in 1990, Arnold recalls that he worked on the book slowly, a few pages a day. We cannot help hoping that our book will play a similar role in the mathematical development of some prominent mathematician of the future.

We hope that this book will be of interest to anyone who likes mathematics, from high school students to accomplished researchers. We do not promise an easy ride: the majority of results are proved, and it will take a considerable effort from the reader to follow the details of the arguments. We hope that, in reward, the reader, at least sometimes, will be filled with awe by the harmony of the subject (this feeling is what drives most of mathematicians in their work!) To quote from "A Mathematician's Apology" by G. H. Hardy,

> The mathematician's patterns, like the painter's or the poet's, must be *beautiful*; the ideas, like the colors or the words, must fit together in a harmonious way. Beauty is the first test: there is no permanent place in the world for ugly mathematics.

For us too, beauty is the first test in the choice of topics for our own research, as well as the subject for popular articles and lectures, and consequently, in the choice of material for this book. We did not restrict ourselves to any particular area (say, number theory or geometry), our emphasis is on the diversity and the unity of mathematics. If, after reading our book, the reader becomes interested in a more systematic exposition of any particular subject, (s)he can easily find good sources in the literature.

About the subtitle: the dictionary definition of the word *classic*, used in the title, is "judged over a period of time to be of the highest quality and outstanding

[1] "The enjoyment of mathematics", in the English translation; the Russian title was a literal translation of the German original.

of its kind". We tried to select mathematics satisfying this rigorous criterion. The reader will find here theorems of Isaac Newton and Leonhard Euler, Augustin Louis Cauchy and Carl Gustav Jacob Jacobi, Michel Chasles and Pafnuty Chebyshev, Max Dehn and James Alexander, and many other great mathematicians of the past. Quite often we reach recent results of prominent contemporary mathematicians, such as Robert Connelly, John Conway and Vladimir Arnold.

There are about four hundred figures in this book. We fully agree with the dictum that a picture is worth a thousand words. The figures are mathematically precise – so a cubic curve is drawn by a computer as a locus of points satisfying an equation of degree three. In particular, the figures illustrate the importance of accurate drawing as an experimental tool in geometrical research. Two examples are given in Lecture 29: the Money-Coutts theorem, discovered by accurate drawing as late as in the 1970s, and a very recent theorem by Richard Schwartz on the Poncelet grid which he discovered by computer experimentation. Another example of using computer as an experimental tool is given in Lecture 3 (see the discussion of "privileged exponents").

We did not try to make different lectures similar in their length and level of difficulty: some are quite long and involved whereas others are considerably shorter and lighter. One lecture, "Cusps", stands out: it contains no proofs but only numerous examples, richly illustrated by figures; many of these examples are rigorously treated in other lectures. The lectures are independent of each other but the reader will notice some themes that reappear throughout the book. We do not assume much by way of preliminary knowledge: a standard calculus sequence will do in most cases, and quite often even calculus is not required (and this relatively low threshold does not leave out mathematically inclined high school students). We also believe that any reader, no matter how sophisticated, will find surprises in almost every lecture.

There are about 200 exercises in the book, many provided with solutions or answers. They further develop the topics discussed in the lectures; in many cases, they involve more advanced mathematics (then, instead of a solution, we give references to the literature).

This book stems from a good many articles we wrote for the Russian magazine "Kvant" over the years 1970–1990[2] and from numerous lectures that we gave over the years to various audiences in the Soviet Union and the United States (where we live since 1990). These include advanced high school students – the participants of the Canada/USA Binational Mathematical Camp in 2001 and 2002, undergraduate students attending the Mathematics Advanced Study Semesters (MASS) program at Penn State over the years 2000–2006, high school students – along with their teachers and parents – attending the Bay Area Mathematical Circle at Berkeley.

The book may be used for an undergraduate Honors Mathematics Seminar (there is more than enough material for a full academic year), various topics courses, Mathematical Clubs at high school or college, or simply as a "coffee table book" to browse through, at one's leisure.

To support the "coffee table book" claim, this volume is lavishly illustrated by an accomplished artist, Sergey Ivanov. Sergey was the artist-in-chief of the "Kvant" magazine in the 1980s, and then continued, in a similar position, in the 1990s, at its English-language cousin, "Quantum". Being a physicist by education, Ivanov's

[2]Available, in Russian, online at http://kvant.mccme.ru/

illustrations are not only aesthetically attractive but also reflect the mathematical content of the material.

We started this preface with a quotation; let us finish with another one. Max Dehn, whose theorems are mentioned here more than once, thus characterized mathematicians in his 1928 address [**22**]; we believe, his words apply to the subject of this book:

> At times the mathematician has the passion of a poet or a conqueror, the rigor of his arguments is that of a responsible statesman or, more simply, of a concerned father, and his tolerance and resignation are those of an old sage; he is revolutionary and conservative, skeptical and yet faithfully optimistic.

*Acknowledgments.* This book is dedicated to V. I. Arnold on the occasion of his 70th anniversary; his style of mathematical research and exposition has greatly influenced the authors over the years.

For two consecutive years, in 2005 and 2006, we participated in the "Research in Pairs" program at the Mathematics Institute at Oberwolfach. We are very grateful to this mathematicians' paradise where the administration, the cooks and nature conspire to boost one's creativity. Without our sojourns at MFO the completion of this project would still remain a distant future.

The second author is also grateful to Max-Planck-Institut for Mathematics in Bonn for its invariable hospitality.

Many thanks to John Duncan, Sergei Gelfand and Günter Ziegler who read the manuscript from beginning to end and whose detailed (and almost disjoint!) comments and criticism greatly improved the exposition.

The second author gratefully acknowledges partial NSF support.

Davis, CA and State College, PA
December 2006

# Algebra and Arithmetics

# *Chapter* 1

## ARITHMETIC AND COMBINATORICS

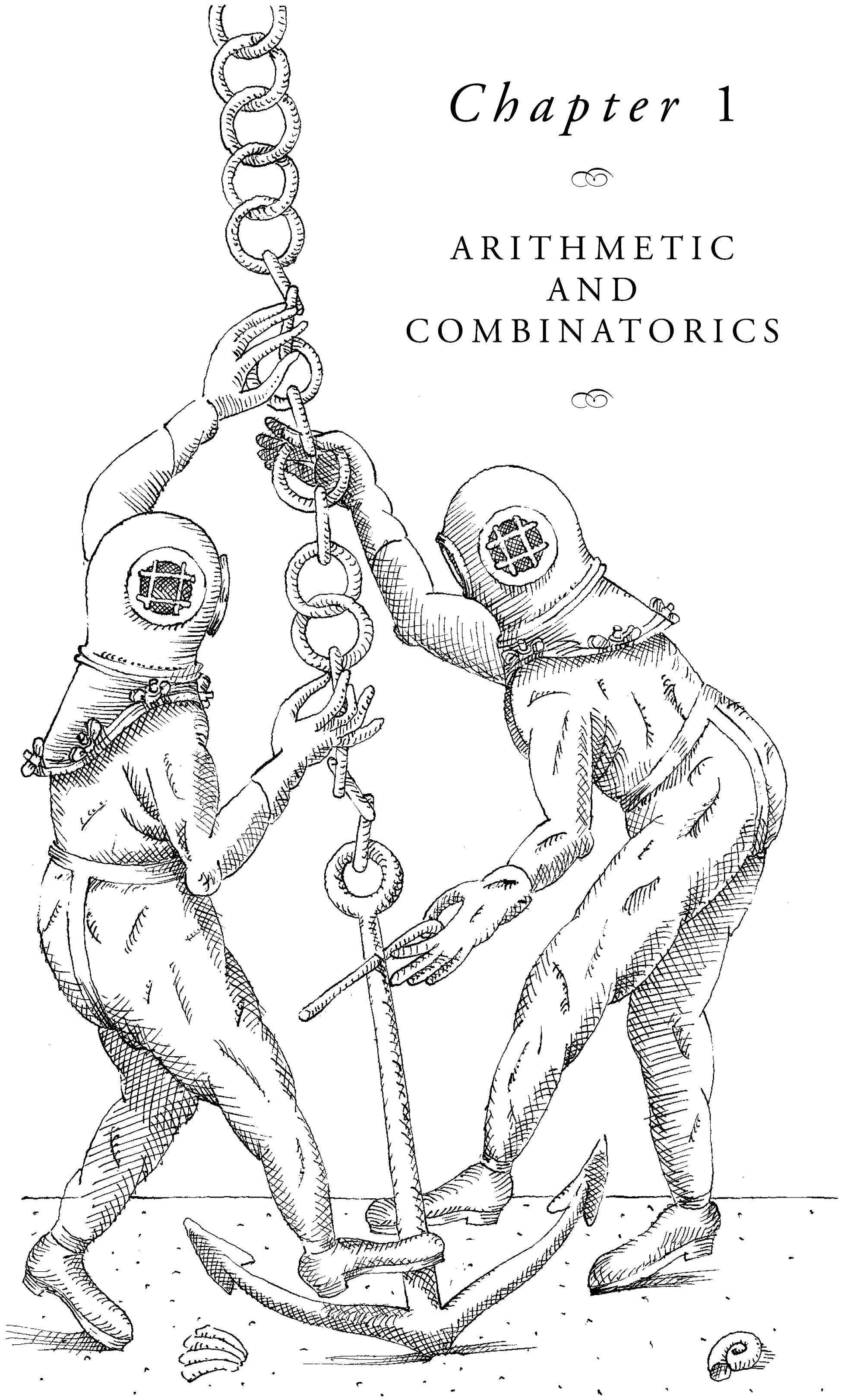

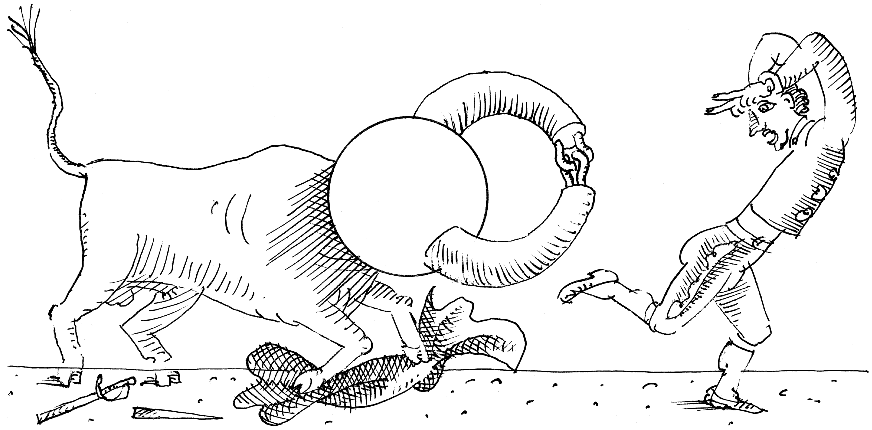

LECTURE 1

# Can a Number be Approximately Rational?

**1.1 Prologue.** *Alice*[1] (entering through a door on the left): I can prove that $\sqrt{2}$ is irrational.

*Bob* (entering through a door on the right): But it is so simple: take a calculator, press the button $\boxed{\sqrt{\ }}$ , then $\boxed{2}$ , and you will see the square root of 2 in the screen. It's obvious that it is irrational:

| | | | | | | | | | |
|---|---|---|---|---|---|---|---|---|---|
| 1. | 4 | 1 | 4 | 2 | 1 | 3 | 5 | 6 | 2 |

*Alice*: Some proof indeed! What if $\sqrt{2}$ is a periodic decimal fraction, but the period is longer than your screen? If you use your calculator to divide, say 25 by 17, you will also get a messy sequence of digits:

| | | | | | | | | | |
|---|---|---|---|---|---|---|---|---|---|
| 1. | 4 | 7 | 0 | 5 | 8 | 8 | 2 | 3 | 5 |

But this number is rational!

*Bob*: You may be right, but for numbers arising in real life problems my method usually gives the correct result. So, I can rely on my calculator in determining which numbers are rational, and which are irrational. The probability of mistake will be very low.

*Alice*: I do not agree with you (*leaves through a door on the left*).

*Bob*: And I do not agree with you (*leaves through a door on the right*).

[1]See D. Knuth, "Surreal Numbers".

**1.2 Who is right?** We asked many people, and everybody says: Alice. If you know nine (or ninety, or nine million) decimal digits of a number, you cannot say whether it is rational or irrational: there are infinitely many rational and irrational numbers with the same beginning of their decimal fraction.

But still the two numbers displayed in Section 1.1, however similar they might look, are different in one important way. The second one is very close to the rational number $\frac{25}{17}$: the difference between 1.470588235 and $\frac{25}{17}$ is approximately $3 \cdot 10^{-10}$. As for 1.414213562, there are no fractions with a two-digit denominator this close to it; actually, of such fractions, the closest to 1.414213562 is $\frac{99}{70}$, and the difference between the two numbers is approximately $7 \cdot 10^{-5}$. The shortest fraction approximating $\sqrt{2}$ with an error of $3 \cdot 10^{-10}$ is $\frac{47321}{33461}$, much longer than just $\frac{25}{17}$. What is more important, this difference between the two nine-digit decimal fractions (not transparent to the naked eye) can be easily detected by a primitive pocket calculator.

To give some support to Bob in his argument with Alice, you can show your friends a simple trick.

**1.3 A trick.** You will need a pocket calculator which can add, subtract, multiply and divide (a key $\boxed{x^{-1}}$ will be helpful). Have somebody give you two nine-digits decimals, say, between 0.5 and 1, for example,

$$0.635149023 \quad \text{and} \quad 0.728101457.$$

One of these numbers has to be obtained as a fraction with its denominator less than 1000 (known to the audience), another one should be random. You claim that you can find out in one minute which of the two numbers is a fraction and, in another minute, find the fraction itself. You are allowed to use your calculator (the audience will see what you do with it).

How to do it? We shall explain this in this lecture (see Section 1.13). Informally speaking, one of these numbers is "approximately rational", while the other is not – whatever this means.

**1.4 What is a good approximation?** Let $\alpha$ be an irrational number. How can we decide whether a fraction $\frac{p}{q}$ (which we can assume irreducible) is a good approximation for $\alpha$? The first thing which matters, is the error, $\left|\alpha - \frac{p}{q}\right|$; we want it to be small. But this is not all: a fraction should be convenient, that is, the numbers $p$ and $q$ should not be too big. It is reasonable to require that the denominator $q$ is not too big: the size of $p$ depends on $\alpha$ which is not related to the precision of the approximation. So, we want to minimize two numbers, the error $\left|\alpha - \frac{p}{q}\right|$ and the denominator $q$. But the two goals contradict each other: to make the error smaller we must take bigger denominators, and vice versa. To reconcile the two contradicting demands, we can combine them into one "indicator of quality" of an approximation. Let us call an approximation $\frac{p}{q}$ of $\alpha$ *good* if the product $\left|\alpha - \frac{p}{q}\right| \cdot q$ is small, say, less than $\frac{1}{100}$ or $\frac{1}{1000000}$. The idea seems reasonable, but the following theorem sounds discouraging.

THEOREM 1.1. *For any $\alpha$ and any $\varepsilon > 0$ there exist infinitely many fractions $\frac{p}{q}$ such that*

$$q\left|\alpha - \frac{p}{q}\right| < \varepsilon.$$

In other words, all numbers have arbitrarily good approximations, so we cannot distinguish numbers by the quality of their rational approximations.

Our proof of Theorem 1.1 is geometric, and the main geometric ingredient of this proof is a "lattice". Since lattices will be useful also in subsequent sections, we shall discuss their relevant properties in a separate section.

**1.5 Lattices.** Let $O$ be a point in the plane (the "origin"), and let $\mathbf{v} = \overrightarrow{OA}$ and $\mathbf{w} = \overrightarrow{OB}$ be two non-collinear vectors (which means that the points $O, A, B$ do not lie on one line). Consider the set of all points (endpoints of the vectors) $p\mathbf{v} + q\mathbf{w}$ (Figure 1.1). This is a lattice (generated by $\mathbf{v}$ and $\mathbf{w}$). We need the following two propositions (of which only the first is needed for the proof of Theorem 1.1).

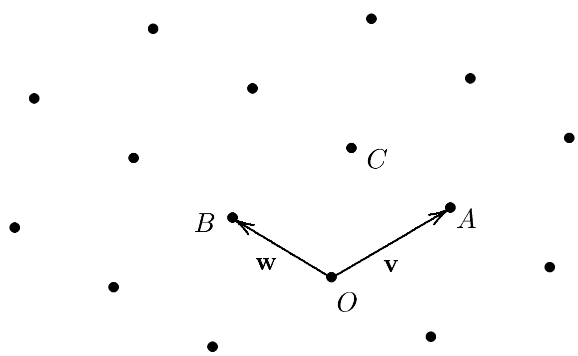


FIGURE 1.1. The lattice generated by $\mathbf{v}$ and $\mathbf{w}$

Let $\Lambda$ be a lattice in the plane generated by the vectors $\mathbf{v}$ and $\mathbf{w}$.

PROPOSITION 1.1. *Let $KLMN$ be a parallelogram such that the vertices $K, L$, and $M$ belong to $\Lambda$. Then $N$ also belongs to $\Lambda$.*

Proof. Let $\overrightarrow{OK} = a\mathbf{v} + b\mathbf{w}$, $\overrightarrow{OL} = c\mathbf{v} + d\mathbf{w}$, $\overrightarrow{OM} = e\mathbf{v} + f\mathbf{w}$. Then

$$\begin{aligned}\overrightarrow{ON} &= \overrightarrow{OK} + \overrightarrow{KN} = \overrightarrow{OK} + \overrightarrow{LM} = \overrightarrow{OK} + (\overrightarrow{OM} - \overrightarrow{OL}) \\ &= (a - c + e)\mathbf{v} + (b - d + f)\mathbf{w},\end{aligned}$$

hence $N \in \Lambda$. □

Denote the area of the "elementary" parallelogram $OACB$ (where $\overrightarrow{OC} = \overrightarrow{OA} + \overrightarrow{OB}$) by $s$.

PROPOSITION 1.2. *Let $KLMN$ be a parallelogram with vertices in $\Lambda$.*

*(a) The area of $KLMN$ is $ns$ where $n$ is a positive integer.*

*(b) If no point of $\Lambda$, other than $K, L, M, N$, lies inside the parallelogram $KLMN$ or on its boundary, then the area of $KLMN$ equals $s$.*

(For a more general statement, Pick's formula, see Exercise 1.1.)

Proof of (b). Let $\ell$ be the length of the longer of the two diagonals of $KLMN$.

Tile the plane by parallelograms parallel to $KLMN$. For a tile $\pi$, denote by $K_\pi$ the vertex of $\pi$ corresponding to $K$ under the parallel translation $KLMN \to \pi$. Then $\pi \leftrightarrow K_\pi$ is a one-to-one correspondence between the tiles and the points of the lattice $\Lambda$. (Indeed, no point of $\Lambda$ lies inside any tile or inside a side of any tile; hence, every point of $\Lambda$ is a $K_\pi$ for some $\pi$.) Let $D_R$ be the disk of radius $R$ centered at $O$, and let $N$ be the number of points of $\Lambda$ within $D_R$. Denote the points of $\Lambda$ within $D_R$ by $K_1, K_2, \dots, K_N$. Let $K_i = K_{\pi_i}$. The union of all tiles $\pi_i$ $(1 \le i \le N)$ contains $D_{R-\ell}$ and is contained in $D_{R+\ell}$. Thus, if the area of $KLMN$ is $S$, then

$$\pi(R-\ell)^2 \le NS \le \pi(R+\ell)^2.$$

The same is true (maybe, with a different $\ell$, but we can take the bigger of the two $\ell$'s) for the parallelogram $OACB$, which also does not contain any point of $\Lambda$ different from its vertices; thus,

$$\pi(R-\ell)^2 \le Ns \le \pi(R+\ell)^2.$$

Division of the inequalities shows that

$$\frac{(R-\ell)^2}{(R+\ell)^2} \le \frac{S}{s} \le \frac{(R+\ell)^2}{(R-\ell)^2},$$

and, since $\dfrac{(R-\ell)^2}{(R+\ell)^2}$ for big $R$ is arbitrarily close to 1, that $S = s$.

Proof of (a). First, notice that if a triangle $PQR$ with vertices in $\Lambda$ does not contain (either inside or on the boundary) points of $\Lambda$ different from $P, Q, R$, then its area is $\dfrac{s}{2}$: this triangle is a half of a parallelogram $PQRS$ which also contains no points of $\Lambda$ different from its vertices, and $S \in \Lambda$ by Proposition 1.1. Thus, the area of the parallelogram $PQRS$ is $s$ (by Part (b)) and the area of the triangle $PQR$ is $\dfrac{s}{2}$. Now, if our parallelogram $KLMN$ contains $q$ points of $\Lambda$ inside and $p$ points on the sides (other than $K, L, M, N$), then $p$ is even (opposite sides contain equal number of points of $\Lambda$) and the parallelogram $KLMN$ can be cut into $2q+p+2$ triangles with vertices in $\Lambda$ and with no other points inside or on the sides (see Figure 1.2), and its area is

$$(2q+p+2)\frac{s}{2} = (q+\frac{p}{2}+1)s = ns \text{ where } n = q+\frac{p}{2}+1 \in \mathbb{Z}.$$

(Why is the number of triangles $2q+p+2$? Compute the sum of the angles of all the triangles which equals, of course, $\pi$ times the number of triangles. Every point inside the parallelogram contributes $2\pi$ to this sum, every interior point of a side contributes $\pi$, and the four vertices contribute $2\pi$. Divide by $\pi$ to find the number of triangles.) $\square$

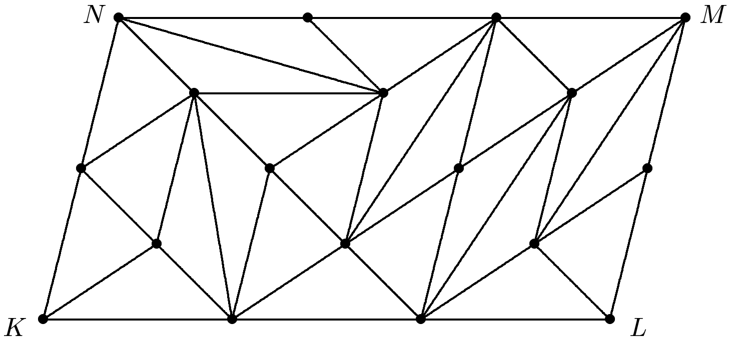


FIGURE 1.2. A dissection of a parallelogram into triangles

**1.6 Proof of Theorem 1.1.** Let $\alpha, p$, and $q$ be as in Theorem 1.1. Consider the lattice generated by the vectors $\mathbf{v} = (-1, 0)$ and $\mathbf{w} = (\alpha, 1)$. Then

$$p\mathbf{v} + q\mathbf{w} = (q\alpha - p, q) = \left(q\left(\alpha - \frac{p}{q}\right), q\right).$$

We want to prove that for infinitely many $(p, q)$ this point lies within the strip $-\varepsilon < x < \varepsilon$ shaded in Figure 1.3, left, or, in other words, that the shaded strip contains (for any $\varepsilon > 0$) infinitely many points of the lattice.

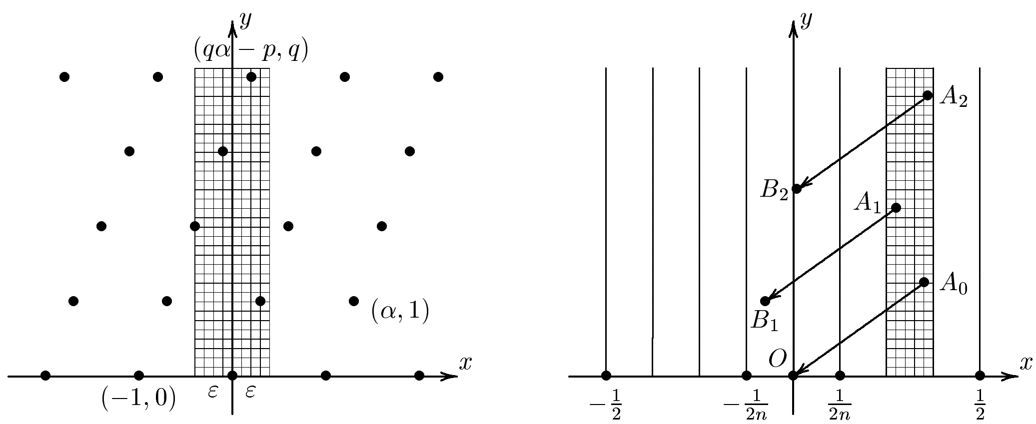


FIGURE 1.3. Proof of Theorem 1.1

This is obvious if $\varepsilon$ is not very small, say, if $\varepsilon = \dfrac{1}{2}$. Indeed, for every positive integer $q$, the horizontal line $y = q$ contains a sequence of points of the lattice with distance 1 between consecutive points; precisely one of these points will be inside the wide strip $|x| < \dfrac{1}{2}$. Hence the wide strip contains infinitely many points of the lattice with positive $y$-coordinates.

Choose a positive integer $n$ such that $\dfrac{1}{2n} < \varepsilon$ and cut the wide strip into $2n$ narrow strips of width $\dfrac{1}{2n}$. At least one of these narrow strips must contain infinitely many points with positive $y$-coordinates; let it be the strip shaded in Figure

1.3, right. Let $A_0, A_1, A_2, \ldots$ be the points in the shaded strip, numbered in the direction of increasing $y$-coordinate. For every $i > 0$, take the vector equal to $A_0O$ with the foot point $A_i$; let $B_i$ be the endpoint of this vector. Since $OA_0A_iB_i$ is a parallelogram and $O, A_0, A_i$ belong to the lattice, $B_i$ also belongs to the lattice. Furthermore, the $x$-coordinate of $B_i$ is equal to the difference between the $x$-coordinates of $A_i$ and $A_0$ (again, because $OA_0A_iB_i$ is a parallelogram). Thus, the absolute value of the $x$-coordinate of $B_i$ is less that $\dfrac{1}{2n} < \varepsilon$, that is, all the points $B_i$ lie in the shaded strip of Figure 1.3, left. □

**1.7 Quadratic approximations.** Theorem 1.1, no matter how beautiful its statement and proof are, sounds rather discouraging. If all numbers have arbitrarily good approximations, then we have no way to distinguish between numbers which possess or do not possess good approximations. To do better, we can try to work with a different indicator of quality which gives more weight to the denominator $q$. Let us now say that approximation $\dfrac{p}{q}$ of $\alpha$ is *good*, if the product $q^2\left|\alpha - \dfrac{p}{q}\right|$ is small.

The following theorem, proved a century ago, shows that this choice is reasonable.

THEOREM 1.2 (A. Hurwitz, E. Borel). *(a). For any $\alpha$, there exist infinitely many fractions $\dfrac{p}{q}$ such that*

$$q^2\left|\alpha - \frac{p}{q}\right| < \frac{1}{\sqrt{5}}.$$

*(b). There exists an irrational number $\alpha$ such that for any $\lambda > \sqrt{5}$ there are only finitely many fractions $\dfrac{p}{q}$ such that*

$$q^2\left|\alpha - \frac{p}{q}\right| < \frac{1}{\lambda}.$$

A proof of this result is contained in Section 1.12. It is based on the geometric construction of Section 1.6 and on properties of so-called continued fractions which will be discussed in Section 1.8. But before considering continued fractions, we want to satisfy a natural curiosity of the reader who may want to see the number which exists according to Part (b). What is this most irrational irrational number, the number, most averse to rational approximation? Surprisingly, this worst number is the number most loved by generations of artists, sculptors and architects: the golden ratio $\dfrac{1+\sqrt{5}}{2}$.[2]

**1.8 Continued fractions.**

[2]To be precise, the golden ratio is not unique: any other number, related to it in the sense of Exercise 1.8, is equally bad.

*1.8.1 Definitions and terminology.* A *finite continued fraction* is an expression of the form

$$a_0 + \cfrac{1}{a_1 + \cfrac{1}{a_2 + \cfrac{1}{\ddots + \cfrac{1}{a_{n-1} + \cfrac{1}{a_n}}}}}$$

where $a_0$ is an integer, $a_1, \dots, a_n$ are positive integers, and $n \geq 0$.

PROPOSITION 1.3. *Any rational number has a unique presentation as a finite continued fraction.*

Proof of existence. For an irreducible fraction $\frac{p}{q}$, we shall prove the existence of a continued fraction presentation using induction on $q$. For integers ($q = 1$), the existence is obvious. Assume that a continued fraction presentation exists for all fractions with denominators less than $q$. Let $r = \frac{p}{q}, a_0 = [r]$. Then $r = a_0 + \frac{p'}{q}$ with $0 < p' < q$, and $r = a_0 + \frac{1}{r'}$ where $r' = \frac{q}{p'}$. Since $p' < q$, there exists a continued fraction presentation

$$r' = a_1 + \cfrac{1}{a_2 + \cfrac{1}{\ddots + \cfrac{1}{a_{n-1} + \cfrac{1}{a_n}}}}$$

and, since $r' > 1$, $a_1 = [r'] \geq 1$. Thus,

$$r = a_0 + \frac{1}{r'} = a_0 + \cfrac{1}{a_1 + \cfrac{1}{a_2 + \cfrac{1}{\ddots + \cfrac{1}{a_{n-1} + \cfrac{1}{a_n}}}}}$$

Proof of uniqueness. If

$$r = a_0 + \cfrac{1}{a_1 + \cfrac{1}{a_2 + \cfrac{1}{\ddots + \cfrac{1}{a_{n-1} + \cfrac{1}{a_n}}}}}$$

then

$$a_0 = [r], \; a_1 = \left[\frac{1}{r - a_0}\right], \; a_2 = \left[\frac{1}{\frac{1}{r - a_0} - a_1}\right], \dots$$

which shows that $a_0, a_1, a_2, \ldots$ are uniquely determined by $r$. $\square$

The last line of formulas provides an algorithm for computing $a_0, a_1, a_2, \ldots$ for a given $r$. Moreover, this algorithm can be applied to an irrational number, $\alpha$, in place of $r$, in which case it provides an infinite sequence of integers, $a_0; a_1, a_2, \ldots,\ a_i > 0$ for $i > 0$. We write

$$\alpha = a_0 + \cfrac{1}{a_1 + \cfrac{1}{a_2 + \ddots}}$$

The numbers $a_0, a_1, a_2, \ldots$ are called *incomplete quotients* for $\alpha$. The number

$$r_n = a_0 + \cfrac{1}{a_1 + \cfrac{1}{\ddots + \cfrac{1}{a_{n-1} + \cfrac{1}{a_n}}}}$$

is called $n$-th *convergent* of $\alpha$. Obviously,

$$r_0 < r_2 < r_4 < \cdots < \alpha < \cdots < r_5 < r_3 < r_1.$$

The standard procedure for reducing multi-stage fractions yields values for the numerator and the denominator of $r_n$:

$$r_0 = \frac{a_0}{1},\ r_1 = \frac{a_0a_1 + 1}{a_1},\ r_2 = \frac{a_0a_1a_2 + a_0 + a_2}{a_1a_2 + 1},\ \ldots,$$

or $r_n = \dfrac{p_n}{q_n}$ where

$$\begin{array}{llll} p_0 = a_0, & p_1 = a_0a_1 + 1, & p_2 = a_0a_1a_2 + a_0 + a_2, & \ldots \\ q_0 = 1, & q_1 = a_1, & q_2 = a_1a_2 + 1, & \ldots \end{array}$$

From now on we shall use a short notation for continued fractions: an infinite continued fraction with the incomplete quotients $a_0, a_1, a_2, \ldots$ will be denoted by $[a_0; a_1, a_2, \ldots]$; a finite continued fraction with the incomplete quotients $a_0, a_1, \ldots, a_n$ will be denoted by $[a_0; a_1, \ldots, a_n]$.

*1.8.2 Several simple relations.*

PROPOSITION 1.4. *Let $a_0, a_1, \ldots, p_0, p_1, \ldots, q_0, q_1, \ldots$ be as above. Then*

*(a) $p_n = a_np_{n-1} + p_{n-2}$ $(n \geq 2)$;*
*(b) $q_n = a_nq_{n-1} + q_{n-2}$ $(n \geq 2)$;*
*(c) $p_{n-1}q_n - p_nq_{n-1} = (-1)^n$ $(n \geq 1)$.*

Proof of (a) and (b). We shall prove these results in a more general form, when $a_0, a_1, a_2, \ldots$ are arbitrary real numbers (not necessarily integers). For $n = 2$, we already have the necessary relations. Let $n > 2$ and assume that

$$\begin{aligned} p_{n-1} &= a_{n-1}p_{n-2} + p_{n-3}, \\ q_{n-1} &= a_{n-1}q_{n-2} + q_{n-3} \end{aligned}$$

for any $a_0, \ldots, a_{n-1}$. Apply these formulas to $a'_0 = a_0, \ldots, a'_{n-2} = a_{n-2}, a'_{n-1} = a_{n-1} + \dfrac{1}{a_n}$. Obviously, $p'_i = p_i, q'_i = q_i$ for $i \leq n-2$, and $p'_{n-1} = \dfrac{p_n}{a_n},\ q'_{n-1} = \dfrac{q_n}{a_n}$.

Thus,

$$\begin{aligned} p_n = a_n p'_{n-1} &= a_n(a'_{n-1}p_{n-2} + p_{n-3}) \\ &= a_n \left[ \left( a_{n-1} + \frac{1}{a_n} \right) p_{n-2} + p_{n-3} \right] \\ &= a_n(a_{n-1}p_{n-2} + p_{n-3}) + p_{n-2} \\ &= a_n p_{n-1} + p_{n-2}, \end{aligned}$$

and similarly $q_n = a_n q_{n-1} + q_{n-2}$.

Proof of (c). Induction on $n$. For $n = 1$:

$$p_0 q_1 - p_1 q_0 = a_0 a_1 - (a_0 a_1 + 1) \cdot 1 = -1.$$

If $n \geq 2$ and the equality holds for $n - 1$ in place of $n$, then

$$\begin{aligned} p_{n-1}q_n - p_n q_{n-1} &= p_{n-1}(a_n q_{n-1} + q_{n-2}) - (a_n p_{n-1} + p_{n-2})q_{n-1} \\ &= p_{n-1}q_{n-2} - p_{n-2}q_{n-1} \\ &= -(p_{n-2}q_{n-1} - p_{n-1}q_{n-2}) \\ &= -(-1)^{n-1} = (-1)^n. \end{aligned}$$

□

Corollary 1.3. $\lim_{n\to\infty} r_n = \alpha$.

Proof. Indeed, $r_n - r_{n-1} = \dfrac{p_n}{q_n} - \dfrac{p_{n-1}}{q_{n-1}} = \dfrac{p_n q_{n-1} - q_n p_{n-1}}{q_n q_{n-1}} = \dfrac{(-1)^{n-1}}{q_n q_{n-1}}$. Since $\alpha$ lies between $r_{n-1}$ and $r_n$, $|r_n - \alpha| < \dfrac{1}{q_n q_{n-1}}$, and the latter tends to 0 when $n$ tends to infinity. □

*1.8.3 Why continued fractions are better than decimal fractions.* Decimal fractions for rational numbers are either finite or periodic infinite. Decimal fractions for irrational numbers like $e, \pi$ or $\sqrt{2}$ are chaotic.

Continued fractions for rational numbers are always finite. Infinite periodic continued fractions correspond to "quadratic irrationalities", that is, to roots of quadratic equations with rational coefficients. We leave the proof of this statement as an exercise to the reader (see Exercises 1.4 and 1.5), but we give a couple of examples. Let

$$\alpha = [1; 1, 1, 1, \ldots], \ \beta = [2; 2, 2, 2, \ldots].$$

Then $\alpha = 1 + \dfrac{1}{\alpha}$, $\beta = 2 + \dfrac{1}{\beta}$, hence $\alpha^2 - \alpha - 1 = 0$, $\beta^2 - 2\beta - 1 = 0$, and therefore $\alpha = \dfrac{1+\sqrt{5}}{2}$, $\beta = 1 + \sqrt{2}$ (we take positive roots of the quadratic equations). Thus, $\alpha$ is the "golden ratio"; also $\sqrt{2} = \beta - 1 = [1; 2, 2, 2, \ldots]$.

*1.8.4 Why decimal fractions are better than continued fractions.* For decimal fractions, there are convenient algorithms for addition, subtraction, multiplication, and division (and even for extracting square roots). For continued fractions, there are almost no such algorithms. Say, if

$$[a_0; a_1, a_2, \ldots] + [b_0; b_1, b_2, \ldots] = [c_0; c_1, c_2, \ldots],$$

then there are no reasonable formulas expressing $c_i$'s via $a_i$'s and $b_i$'s. Besides the obvious relations

$$\begin{aligned} [a_0; a_1, a_2, \ldots] + n &= [a_0 + n, a_1, a_2, \ldots] \quad (\text{if } n \in \mathbb{Z}) \\ [a_0; a_1, a_2, \ldots]^{-1} &= [0; a_0, a_1, a_2, \ldots] \quad (\text{if } a_0 > 0), \end{aligned}$$

there are almost no formulas of this kind (see, however, Exercises 1.2 and 1.3).

**1.9 The Euclidean Algorithm.**

*1.9.1 Continued fractions and the Euclidean Algorithm.* The Euclidean algorithm is normally used for finding greatest common divisors. If $M$ and $N$ are two positive integers and $N > M$, then a repeated division with remainders yields a chain of equalities

$$\begin{aligned} N &= a_0M + b_0, \\ M &= a_1b_0 + b_1 \\ b_0 &= a_2b_1 + b_2 \\ &\cdots\cdots\cdots\cdots \\ b_{n-2} &= a_nb_{n-1} \end{aligned}$$

where all $a$'s and $b$'s are positive integers and

$$0 < b_{n-1} < b_{n-2} < \cdots < b_0 < M.$$

The number $b_{n-1}$ is the greatest common divisor of $M$ and $N$, and it can be calculated by means of the Euclidean Algorithm even if $M$ and $N$ are too big for explicit prime factorization. (It is worth mentioning that the Euclidean Algorithm may be applied not only to integers, but also to polynomials in one variable with complex, real, or rational coefficients.)

From our current point of view, however, the most important feature of the Euclidean Algorithm is its relation with continued fractions.

PROPOSITION 1.5. *(a) The numbers $a_0, a_1, \dots, a_n$ are the incomplete quotients of $\dfrac{N}{M}$,*

$$\frac{N}{M} = [a_0; a_1, \dots, a_n].$$

*(b) Let $\dfrac{p_i}{q_i}$ $(i = 0, 1, 2, \dots, n)$ be the convergents of $\dfrac{N}{M}$. Then $b_i = (-1)^i(Nq_i - Mp_i)$.*

Proof of (a).

$$\begin{aligned} \frac{N}{M} &= a_0 + \frac{b_0}{M} = a_0 + \frac{1}{M/b_0} \\ &= a_0 + \cfrac{1}{a_1 + \cfrac{b_1}{b_0}} = a_0 + \cfrac{1}{a_1 + \cfrac{1}{b_0/b_1}} \\ &= a_0 + \cfrac{1}{a_1 + \cfrac{1}{a_2 + \cfrac{b_2}{b_1}}} = a_0 + \cfrac{1}{a_1 + \cfrac{1}{a_2 + \cfrac{1}{b_1/b_2}}} \\ &= \cdots = [a_0; a_1, \dots, a_n]. \end{aligned}$$

Proof of (b). For $i = 0, 1$, the statement is obvious:

$$\begin{aligned} b_0 = N - Ma_0 &= Nq_0 - Mp_0; \\ b_1 = M - a_1b_0 &= M - Na_1 + Ma_0a_1 = M(a_0a_1 + 1) - Na_1 \\ &= -(Nq_1 - Mp_1). \end{aligned}$$

Then, by induction,

$$\begin{aligned} b_i = b_{i-2} - a_i b_{i-1} &= (-1)^i [Nq_{i-2} - Mp_{i-2} + a_i(Nq_{i-1} - Mp_{i-1})] \\ &= (-1)^i [N(a_i q_{i-1} + q_{i-2}) - M(a_i p_{i-1} + p_{i-2})] \\ &= (-1)^i (Nq_i - Mp_i). \end{aligned}$$

□

All of the above can be applied to the case when the integers $N, M$ are replaced by real numbers $\beta, \gamma > 0$. We get an infinite (if $\dfrac{\beta}{\gamma}$ is irrational) sequence of equalities,

$$\begin{aligned} \beta &= a_0\gamma + b_0, \\ \gamma &= a_1 b_0 + b_1, \\ b_0 &= a_2 b_1 + b_2, \\ &\dots\dots\dots\dots\dots\dots \end{aligned}$$

where $a_0$ is an integer, $a_1, a_2, \dots$ are positive integers, and the real numbers $b_i$ satisfy the inequalities

$$0 < \dots < b_2 < b_1 < b_0 < \gamma.$$

Proposition 1.5 can be generalized to this case:

PROPOSITION 1.6. *(a)* $\dfrac{\beta}{\gamma} = [a_0; a_1, a_2, \dots]$.

*(b) if* $\dfrac{p_i}{q_i}$ *is the i-th convergent of* $\dfrac{\beta}{\gamma}$*, then* $b_i = (-1)^i(\gamma q_i - \beta p_i)$.

(The proof is the same as above.)

*1.9.2 Geometric presentation of the Euclidean Algorithm.* It is shown in Figure 1.4.

Take a point $O$ in the plane and a line $\ell$ through it (vertical in Figure 1.4). Take points $A_{-2}$ and $A_{-1}$ at distance $\beta$ an $\gamma$ from $\ell$, both above the horizontal line through $O$: $A_{-2}$ to the right of $\ell$ and $A_{-1}$ to the left of $\ell$. Apply the vector $\overrightarrow{OA_{-1}}$ to the point $A_{-2}$ as many time as possible without crossing the line $\ell$. Let $A_0$ be the end of the last vector, thus the vector $\overrightarrow{A_0D}$ crosses $\ell$. Then apply the vector $\overrightarrow{OA_0}$ to the point $A_{-1}$ as many time as possible without crossing $\ell$; let $A_1$ be the end of the last vector. Then apply the vector $\overrightarrow{OA_1}$ to $A_0$ and get the point $A_2$, then $A_3, A_4$ (not shown in Figure 1.4), etc. We get two polygonal lines $A_{-2}A_0A_2A_4\dots$ and $A_{-1}A_1A_3\dots$ converging to $\ell$ from the two sides, and $\overrightarrow{A_{-2}A_0} = a_0\overrightarrow{OA_{-1}}, \overrightarrow{A_{-1}A_1} = a_1\overrightarrow{OA_0}, \overrightarrow{A_0A_2} = a_2\overrightarrow{OA_1}$, etc. This construction is related to the Euclidean algorithm via the column of formulas shown in Figure 1.4. In particular, $\dfrac{\beta}{\gamma} = [a_0; a_1, a_2, \dots]$.

Notice that if some point $A_n$ lies on the line $\ell$, then the ratio $\dfrac{\beta}{\gamma}$ is rational and equal to $[a_0; a_1, a_2, \dots, a_n]$.

The following observation is very important in the subsequent sections. All the points marked in Figure 1.4 (not only $A_{-2}, A_{-1}, A_0, A_1, A_2$, but also $B, C, D$) belong to the lattice $\Lambda$ generated by the vectors $\overrightarrow{OA_{-2}}$ and $\overrightarrow{OA_{-1}}$. Indeed, consider the sequence of parallelograms

$$A_{-1}A_{-2}B,\ A_{-1}OBC,\ A_{-1}OCA_0,\ A_{-1}OA_0D,\ DOA_0A_1,\ A_1OA_0A_2, \dots$$

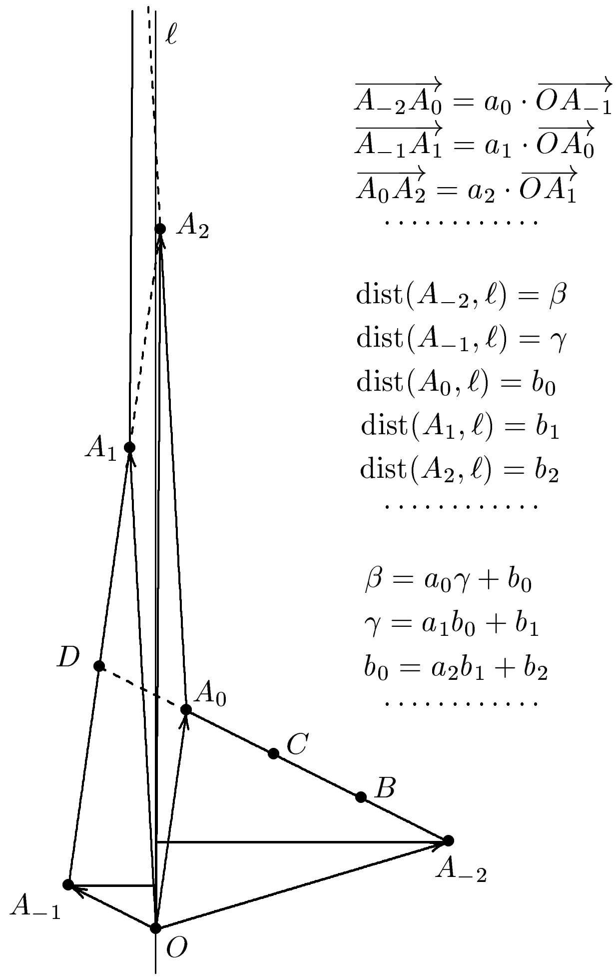


FIGURE 1.4. Geometric presentation of the Euclidean Algorithm

Since $A_{-1}, O, A_{-2}$ are points of the lattice, we successively deduce from Proposition 1.1 that $B, C, A_0, D, A_1, A_2, \ldots$ are points of the lattice.

Moreover, the following is true.

PROPOSITION 1.7. *No points of the lattice $\Lambda$ lie between the polygonal lines $A_{-2}A_0A_2A_4\ldots$ and $A_{-1}A_1A_3\ldots$ (and above $A_{-2}$ and $A_{-1}$).*

Proof. The domain between these polygonal lines is covered by the parallelograms $OA_{-2}BA_{-1}$, $OBCA_{-1}$, $OCA_0A_{-1}$, $OA_0DA_{-1}$, $OA_0A_1D$, $OA_0A_2A_1$, $OA_2EA_1$ (the point $E$ is well above Figure 1.4), etc. These parallelograms have equal areas (every two consecutive parallelograms have a common base and equal altitudes). Thus all of them have the same area as the parallelogram $OA_{-2}BA_{-1}$, and Proposition 1.2 (b) states that no one of them contains any point of $\Lambda$.$\square$

(By the way, the polygonal lines $A_{-2}A_0A_2A_4\ldots$ and $A_{-1}A_1A_3\ldots$ may be constructed as "Newton polygons". Suppose that there is a nail at every point of the lattice $\Lambda$ to the right of $\ell$ and above $A_{-2}$. Put a horizontal ruler on the plane so that it touches the nail at $A_{-2}$ and then rotate it clockwise so that it constantly touches at least one nail. The ruler will be rotating first around $A_{-2}$, then around $A_0$, then around $A_2$, etc, and it will sweep the exterior domain of the polygonal line $A_{-2}A_0A_2A_4\dots$.)

**1.10 Convergents as the best approximations.** Let $\alpha$ be a real number. In Section 1.6, we considered a lattice $\Lambda$ spanned by the vectors $(-1,0)$ and $(\alpha,1)$. For any $p$ and $q$, the point

$$p(-1,0)+q(\alpha,1)=(q\alpha-p,q)=\left(q\left(\alpha-\frac{p}{q}\right),q\right)$$

belongs to the lattice; our old indicator of quality of the approximation $\frac{p}{q}$ of $\alpha$ was equal to the distance of this point from the $y$ axis. The new indicator of quality, $q^2\left|\alpha-\frac{p}{q}\right|$, is the absolute value of the product of coordinates of this point. So, the question, for how many approximations $\frac{p}{q}$ of $\alpha$ this indicator of quality is less than $\varepsilon$, is equivalent to the question, how many points of the lattice $\Lambda$ above the $x$ axis $(q>0)$ lie within the "hyperbolic cross" $|xy|<\varepsilon$ (Figure 1.5).

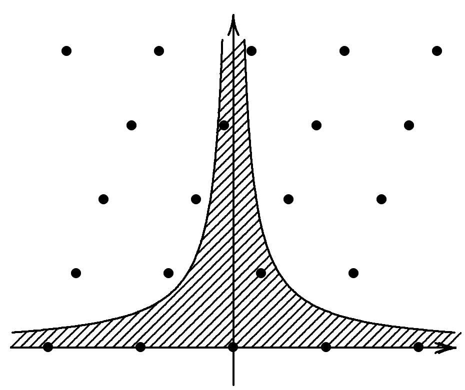

FIGURE 1.5. Lattice points in the "hyperbolic cross"

Let us apply the construction of Subsection 1.9.2 to the lattice $\Lambda$ with $A_{-2}=(\alpha,1)$ and $A_{-1}=(-1,0)$. What is the significance of the points $A_0,A_1,A_2,\dots$?

PROPOSITION 1.8. *For $n\geq 0$, $A_n=(q_n\alpha-p_n,q_n)$ where $p_n$ and $q_n$ are the numerator and denominator of the irreducible fraction equal to the $n$-th convergent of the number $\alpha$.*

Proof. Induction on $n$. For $n=0,1$ we check this directly: since $p_0=a_0,q_0=1,p_1=a_0a_1+1,q_1=a_0$ (see Section 1.8),

$$\begin{aligned}A_0=A_{-2}+a_0A_{-1}&=(\alpha,1)+a_0(-1,0)\\&=(\alpha-a_0,1)=(q_0\alpha-p_0,q_0),\\A_1=A_{-1}+a_1A_0&=(-1,0)+a_1(\alpha-a_0,1)\\&=(a_1\alpha-(a_0a_1+1),a_1)=(q_1\alpha-p_1,q_1).\end{aligned}$$

Furthermore, if $n \geq 2$ and the formulas for $A_{n-1}$ and $A_{n-2}$ are true, then

$$\begin{aligned} A_n &= A_{n-2} + a_n A_{n-1} = (q_{n-2}\alpha - p_{n-2}, q_{n-2}) + a_n(q_{n-1}\alpha - p_{n-1}, q_{n-1}) \\ &= ((a_n q_{n-1} + q_{n-2})\alpha - a_n p_{n-1} - p_{n-2}, a_n q_{n-1} + q_{n-2}) = (q_n\alpha - p_n, q_n). \end{aligned}$$

□

Proposition 1.8 shows that convergents are the best rational approximations of real numbers. In particular, the following holds.

PROPOSITION 1.9. *Let $\varepsilon > 0$. If for only finitely many convergents $\frac{p_n}{q_n}$, $q_n^2\left|\alpha - \frac{p_n}{q_n}\right| < \varepsilon$, then the whole set of fractions $\frac{p}{q}$ such that $q^2\left|\alpha - \frac{p}{q}\right| < \varepsilon$ is finite.*

Proof. The assumption implies that for some $n$, all the points $A_{n+1}, A_{n+2}, A_{n+3}, A_{n+4}$ lie outside the hyperbolic cross $|xy| < \varepsilon$. This means that the whole hyperbolic cross lies between the polygonal lines $A_{n+1}A_{n+3}A_{n+4}\dots$ and $A_{n+2}A_{n+4}A_{n+6}\dots$ (we use the convexity of a hyperbola: if the points $A_k$ and $A_{k+2}$ lie within a component of the domain $|xy| > \varepsilon$, then so does the whole segment $A_kA_{k+2}$). But according to Proposition 1.7, there are no points of the lattice between the two polygonal lines (and above $A_n$). Thus the hyperbolic cross $|xy| > \varepsilon$ contains no points of the lattice above $A_n$, whence the proposition. □

Notice that the expression $q^2\left|\alpha - \frac{p}{q}\right|$ is not very important for this proof. The same statement would hold for the indicator of quality calculated as $q^3\left|\alpha - \frac{p}{q}\right|$, or $q^{100}\left|\alpha - \frac{p}{q}\right|$, or, actually any expression $F\left(q, \left|\alpha - \frac{p}{q}\right|\right)$ where the function $F$ has the property that the domain $F(x, y) > \varepsilon$ within the first or the second quadrant is convex for any $\varepsilon$.

Thus, convergents provide the best approximations. For example, for the golden ratio $\frac{1+\sqrt{5}}{2} = [1; 1, 1, 1, \dots]$, the best approximations are

$$1,\ [1;1] = \frac{2}{1},\ [1;1,1] = \frac{3}{2},\ [1;1,1,1] = \frac{5}{3},\ [1;1,1,1,1] = \frac{8}{5}, \dots;$$

these are the ratios of consecutive Fibonacci numbers (which follows from Proposition 1.4(b)). For $\sqrt{2} = [1; 2, 2, 2, \dots]$ the best approximations are

$$\begin{aligned} 1,\quad &[1;2] = \frac{3}{2},\ [1;2,2] = \frac{7}{5},\ [1;2,2,2] = \frac{17}{12},\ [1;2,2,2,2] = \frac{41}{29}, \\ &[1;2,2,2,2,2] = \frac{99}{70}, \dots, [1;2,2,2,2,2,2,2,2,2,2,2,2] = \frac{47321}{33461}, \dots. \end{aligned}$$

We mentioned the last two approximations of $\sqrt{2}$ in Section 1.2; in particular, we stated that $\frac{99}{70}$ is the best approximation for $\sqrt{2}$ among the fractions with two-digit denominators.

What is most surprising, there exists a beautiful formula for the indicators of quality of convergents.

### 1.11 Indicator of quality for convergents.

THEOREM 1.4. *Let* $\frac{p_n}{q_n}$ *be the (irreducible) n-th convergent for the real number* $\alpha = [a_0; a_1, a_2, \ldots]$. *Then*

$$q_n^2 \left| \alpha - \frac{p_n}{q_n} \right| = \frac{1}{\lambda_n}$$

*where*

$$\lambda_n = a_{n+1} + \cfrac{1}{a_{n+2} + \cfrac{1}{a_{n+3} + \cfrac{1}{\ddots}}} + \cfrac{1}{a_n + \cfrac{1}{a_{n-1} + \cfrac{1}{\ddots + \cfrac{1}{a_1}}}}$$

The proof is based on the following lemma.

LEMMA 1.10. *Let points* $A, B$ *have coordinates* $(a_1, a_2), (-b_1, b_2)$ *in the standard rectangular coordinate system with the origin* $O$ *where* $a_1, a_2, b_1, b_2$ *are positive. Then the parallelogram* $OACB$ *(see Figure 1.6, left) has the area* $a_1b_2 + b_1a_2$.

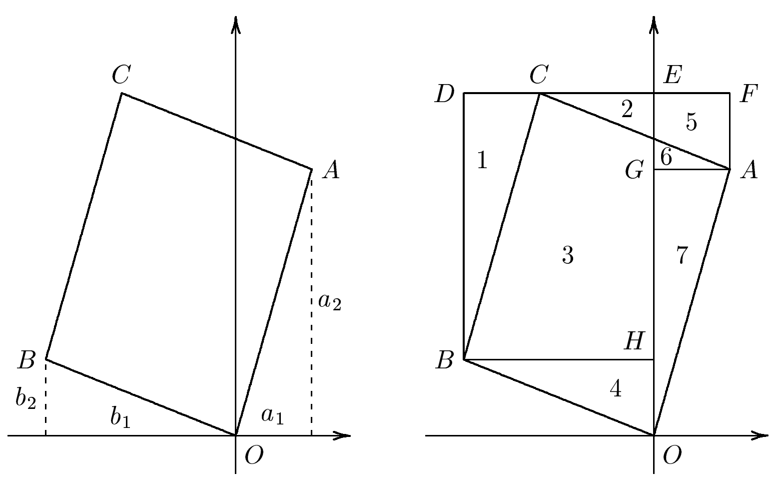


FIGURE 1.6. Computing the area of a parallelogram

Proof of Lemma. Add to the parallelogram (Figure 1.6, left) vertical lines through $A$ and $B$ and a horizontal line through $C$. We get a pentagon $OAFDB$ (see Figure 1.6, right). Divide it into 7 parts as shown in the figure and denote by $S_i$ the area of the part labeled $i$. Obviously, $EF = GA = a_1, DB = GD = a_2, AF = OH = b_2$. It is also obvious that $S_4 = S_2 + S_5$ and $S_1 = S_7$. Thus,

$$\begin{aligned} \text{area}(OACB) &= S_3 + S_4 + S_6 + S_7 = S_3 + (S_2 + S_5) + S_6 + S_1 \\ &= (S_1 + S_2 + S_3) + (S_5 + S_6) \\ &= \text{area}(HEDB) + \text{area}(AFEG) = b_1a_2 + a_1b_2. \end{aligned}$$

□

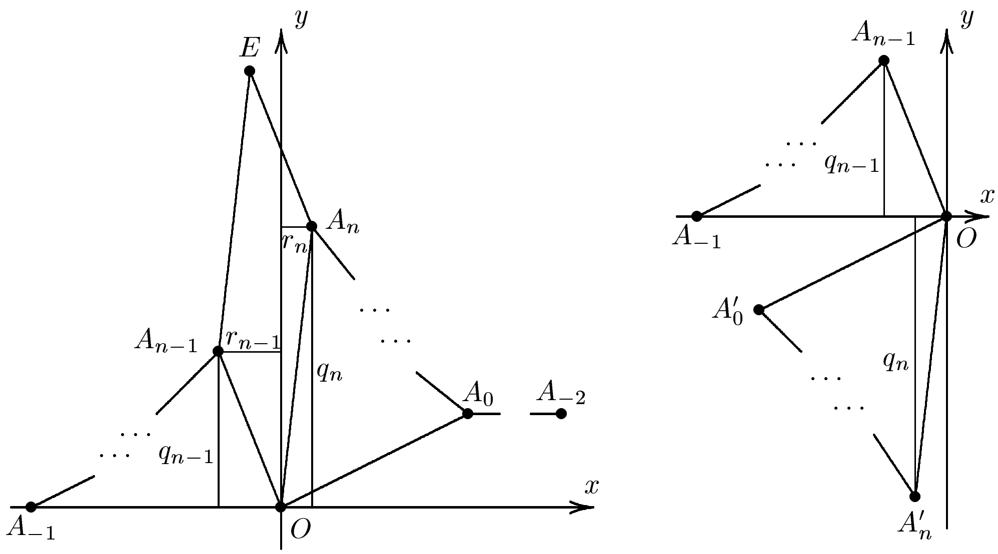


FIGURE 1.7. Proof of Theorem 1.4

Proof of Theorem. Consider Figure 1.7, left. It corresponds to the case when $n$ is even. We shall use the notation $r_k = |\alpha q_k - p_k|$. The coordinates of the points $A_{-2}, A_{-1}, A_{n-1}, A_n$ are $(\alpha, 1), (-1, 0), (-r_{n-1}, q_{n-1}), (r_n, q_n)$ (see Proposition 1.8). The area of the parallelogram $OA_nEA_{n-1}$ is 1 (see Proposition 1.7 and its proof). We have the following relations:

(1) $r_{n-1}q_n + r_nq_{n-1} = 1$;

(2) $\dfrac{r_{n-1}}{r_n} = [a_{n+1}; a_{n+2}, a_{n+3}, \dots]$;

(3) $\dfrac{q_n}{q_{n-1}} = [a_n; a_{n-1}, \dots, a_1]$.

Relation (1) is stated by Lemma 1.10. Relation (2) follows from Proposition 1.6 (a) (the Euclidean Algorithm for $\dfrac{r_{n-1}}{r_n}$ is part of the Euclidean Algorithm for $\dfrac{\alpha}{1}$ as presented in Figure 1.4). Relation (3) may seem less obvious, but it also follows from Proposition 1.6 (a). To see this, reflect the points $A_n, A_{n-2}, \dots, A_0$ in the origin as shown in Figure 1.7, right. We get a picture for the Euclidean Algorithm for $\dfrac{q_n}{q_{n-1}}$ (turned by 90° and reflected in the $x$ axis). The polygonal lines similar to $A_{-2}A_0A_2A_4\dots$ and $A_{-1}A_1A_3A_5\dots$ are $A'_nA'_{n-2}\dots A'_0$ and $A_{n-1}A_{n-3}\dots A_{-1}$. The second one ends at a point $A_{-1}$ on the $x$ axis which means (as was noticed in Subsection 1.9.2) that $\dfrac{q_n}{q_{n-1}}$ is a finite continued fraction $[a_n; a_{n-1}, a_{n-2}, \dots, a_1]$, as stated by Relation (3).

Now, we divide Relation (1) by $r_nq_n$ and compute $\lambda_n$:

$$\lambda_n = \frac{1}{r_nq_n} = \frac{r_{n-1}}{r_n} + \frac{q_{n-1}}{q_n} = [a_{n+1}; a_{n+2}, \dots] + \frac{1}{[a_n; a_{n-1}, \dots, a_1]}.$$

Also,

$$\lambda_{n-1} = \frac{1}{r_{n-1}q_{n-1}} = \frac{q_n}{q_{n-1}} + \frac{r_n}{r_{n-1}} = [a_n; a_{n-1}, \dots, a_1] + \frac{1}{[a_{n+1}; a_{n+2}, \dots]}.$$

This completes the proof of the theorem both for even and odd $n$.□

Theorem 1.4 shows that while convergents are the best rational approximations of real numbers, they are not all equally good. The approximation $\frac{p_n}{q_n}$ is really good if $\lambda_n$ is large, which means, since $a_{n+1} < \lambda_n < a_{n+1} + 2$, that the incomplete quotient $a_{n+1}$ is large. In this sense, neither the golden ratio, nor $\sqrt{2}$ have really good approximations. Let us consider the most frequently used irrational numbers, $\pi$ and $e$. It is not hard to convert decimal approximations provided by pocket calculators into fragments of continued fractions (we shall discuss this in detail in Section 1.13). In particular,

$$\pi = [3; 7, 15, 1, 293, 10, 3, 8, \dots], \quad e = [2; 1, 2, 1, 1, 4, 1, 1, 6, \dots].$$

We see that, unlike $e$, $\pi$ has some big incomplete quotients; the most notable are 15 and 293. The corresponding good approximations are

$$[3; 7] = \frac{22}{7}, \ [3; 1, 15, 1] = \frac{355}{113}.$$

The first was known to Archimedes; with its denominator 7, it gives the value of $\pi$ with the error $1.3 \cdot 10^{-3}$. The second one was discovered almost 4 centuries ago by Adriaen Metius. It has a remarkable (for a fraction with this denominator) precision of $2.7 \cdot 10^{-7}$ and gives 6 correct decimal digits of $\pi$. Nothing comparable exists for $e$: the best approximations (within the fragment of the continued fraction given above) are $\frac{19}{7}$ (the error is $\approx 4 \cdot 10^{-3}$) and $\frac{199}{71}$ (the error is $\approx 2.8 \cdot 10^{-5}$). For further information on the continued fraction for $\pi$ and $e$, see [**56**], Appendix II.

**1.12 Proof of the Hurwitz-Borel Theorem.** Let $\alpha = [a_0; a_1, a_2, \dots]$ be an irrational number. We need to prove that for infinitely many convergents $\frac{p_n}{q_n}$,

$$\lambda_n = \frac{1}{q_n(q_n\alpha - p_n)} > \sqrt{5},$$

and this is not always true if $\sqrt{5}$ is replaced by a bigger number.

*Case 1.* Let infinitely many $a_n$'s be at least 3. Then, for these $n$,

$$\lambda_{n-1} > a_n \geq 3 > \sqrt{5}.$$

*Case 2.* Let only finitely many $a_n$'s be greater than 2, but infinitely many of them equal to 2. Then, for infinitely many $n$, $a_{n+1} = 2, a_n \leq 2, a_{n+2} \leq 2$, and

$$\lambda_n = a_{n+1} + \cfrac{1}{a_{n+2} + \cfrac{1}{\ddots}} + \cfrac{1}{a_n + \cfrac{1}{\ddots}} \geq 2 + \frac{1}{3} + \frac{1}{3} = \frac{8}{3} > \sqrt{5}.$$

*Case 3.* For sufficiently big $m$, $a_m = 1$. Then, for $n > m$,

$$\lambda_n = [1; 1, 1, 1, \dots] + \frac{1}{[1; 1, 1, \dots, a_1]}.$$

The first summand is the golden ratio, $\frac{\sqrt{5}+1}{2}$, the second summand tends to $\left(\frac{\sqrt{5}+1}{2}\right)^{-1} = \frac{\sqrt{5}-1}{2}$ when $n \to \infty$ and is greater than $\frac{\sqrt{5}-1}{2}$ for every other $n$.

Thus, $\lambda_n > \dfrac{\sqrt{5}+1}{2} + \dfrac{\sqrt{5}-1}{2} = \sqrt{5}$ for infinitely many $n$, but, since $\lim\limits_{n\to\infty} \lambda_n = \sqrt{5}$, for any $\varepsilon > 0$, the inequality $\lambda_n > \sqrt{5}+\varepsilon$ holds only for finitely many $n$. □

Comments. It is clear from the proof that only in Case 3 can we not replace the constant $\sqrt{5}$ by a bigger constant. In this case the number $\alpha$ has the form $[a_0; a_1, \dots, a_n, 1, 1, 1, \dots]$. The most characteristic representative of this class is the golden ratio

$$\rho = \frac{\sqrt{5}+1}{2} = [1; 1, 1, 1, \dots].$$

One can prove that all numbers of this class are precisely those of the form $\dfrac{a\rho + b}{c\rho + d}$ with $a, b, c, d \in \mathbb{Z}$ and $ad - bc = \pm 1$. If $\alpha$ is not one of these numbers, then the constant $\sqrt{5}$ can be increased to $\sqrt{8}$. There are further results of this kind (see Exercises 1.11-1.14).

In conclusion, let us mention the following theorem, for which its author, Klaus Roth, was awarded a Fields medal in 1958.

Theorem 1.5 (Roth). *If $\alpha$ is a solution of an algebraic equation*

$$a_n x^n + a_{n-1} x^{n-1} + \dots + a_1 x + a_0 = 0$$

*with integral coefficients, then for any $\varepsilon > 0$, there exist only finitely many fractions $\dfrac{p}{q}$ such that*

$$\left| \alpha - \frac{p}{q} \right| < \frac{1}{q^{2+\varepsilon}}.$$

**1.13 Back to the trick.** In Section 1.3, we were given two 9-digit decimal fractions, of which one was obtained by a division of one 3-digit number by another, while the other one is a random sequence of digits. We need to determine which is which. If $\alpha$ is a 9-digit approximation of a fraction $\dfrac{p}{q}$ with a 3-digit denominator $q$, then

$$\left| \alpha - \frac{p}{q} \right| < \frac{1}{10^9} = \frac{1}{1000 \cdot (1000^2)} < \frac{1}{1000 q^2}.$$

By Theorem 1.4, this means that one of the incomplete quotients $a_{n+1}$ of $\alpha$ is greater than 1000, and the corresponding $q_n$ is less than 1000. How big can $n$ be? Since $q_n = a_n q_{n-1} + q_{n-2}$, the numbers $q_n$ grow at least as fast as the Fibonacci numbers $F_n$. Since $F_{15} = 987$, $n$ should be at most 15.

It is very easy to find the beginning fragment of the continued fraction for a given $\alpha$:

$$\begin{aligned}
& & [\alpha] &= a_0; \\
(\alpha - a_0)^{-1} &= \alpha_1, & [\alpha_1] &= a_1; \\
(\alpha_1 - a_1)^{-1} &= \alpha_2, & [\alpha_2] &= a_2; \\
(\alpha_2 - a_2)^{-1} &= \alpha_3, & [\alpha_3] &= a_3; \\
& \dots\dots\dots\dots & &
\end{aligned}$$

Using this algorithm, we can find a few incomplete fractions of the two numbers given in Section 1.3 relatively fast:

$$0.635149023 = [0; 1, 1, 1, 2, 1, 6, 13, 1204, 1, \dots]$$
$$0.728101457 = [0; 1, 2, 1, 2, 9, 1, 1, 1, 1, 3, 1, 15, 1, 59, 7, 1, 39, \dots]$$

Obviously, the first number, and not the second one, has a very good rational approximation, namely $[0; 1, 1, 1, 2, 1, 6, 13]$.

Next step: using the relations from Proposition 1.4 (a-b), we can find the corresponding convergents:

$$\begin{array}{lll} p_0 = a_0 = 0, & p_1 = a_0 a_1 + 1 = 1, & p_2 = 1 \cdot p_1 + p_0 = 1, \\ & p_3 = 1 \cdot p_2 + p_1 = 2, & p_4 = 2 \cdot p_3 + p_2 = 5, \\ & p_5 = 1 \cdot p_4 + p_3 = 7, & p_6 = 6 \cdot p_5 + p_4 = 47, \\ & p_7 = 13 \cdot p_6 + p_5 = 618. & \\ q_0 = 1, & q_1 = a_1 = 1, & q_2 = 1 \cdot q_1 + q_0 = 2, \\ & q_3 = 1 \cdot q_2 + q_1 = 3, & q_4 = 2 \cdot q_3 + q_2 = 8, \\ & q_5 = 1 \cdot q_4 + q_3 = 11, & q_6 = 6 \cdot q_5 + q_4 = 74, \\ & q_7 = 13 \cdot q_6 + q_5 = 973. & \end{array}$$

Final result: the first number is rational, it is $\dfrac{618}{973}$ (to be on the safe side, you can divide 618 by 973 using your calculator, and you will get precisely 0.635149023).

**1.14 Epilogue.** *Bob (enters through the door on the right)*: You were right, a calculator cannot give a proof that $\sqrt{2}$ is irrational.

*Alice (enters through the door on the left)*: No, you were right: using a calculator, you can certainly distinguish between numbers like $\sqrt{2}$ and $\dfrac{25}{17}$.

*Bob*: Yes, but still it is not a proof of irrationality. I read in a history book that when Pythagoras found a proof that $\sqrt{2}$ was irrational, he invited all his friends to a dinner to celebrate this discovery.

*Alice*: Well, we shall not invite all our friends, but let's have a nice dinner now. My pie is ready.

*Bob*: Oh, pi! There is a wonderful approximation for pi found by Metius!

*Alice*: But I don't mean this pi, I mean my apple pie.

*Bob*: Then let's go and try it. *(They leave together through a door in the middle).*

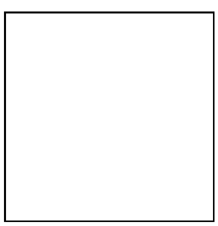

John Smith
January 23, 2010

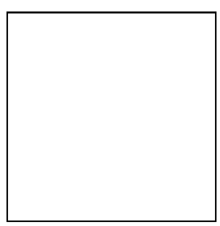

Martyn Green
August 2, 1936

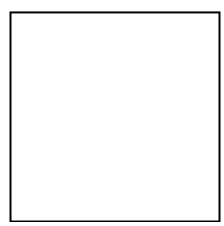

Henry Williams
June 6, 1944

**1.15 Exercises.**

1.1. (Pick's Formula.) Let $P$ be a non-self-intersecting polygon whose vertices are points of a lattice with the area of the elementary parallelogram $s$. Let $m$ be the number of points of the lattice inside $P$ and $n$ the number of points of the lattice on the boundary of $P$ (including the vertices). Prove that

$$\text{area}(P) = \left(n + \frac{m}{2} - 1\right) s \cdot$$

*Hint.* Cut $P$ into triangles with vertices in the points of the lattice and without other points of the lattice on the sides and inside and investigate how the right hand side of the equality behaves.

1.2. Prove that

$$-[a_0; a_1, a_2, \dots] = \begin{cases} [-1-a_0; 1, a_1-1, a_2, \dots], & \text{if } a_1 > 1, \\ [-1-a_0; a_2+1, a_3, \dots], & \text{if } a_1 = 1 \end{cases}$$

1.3. (a) Prove that if $a_0, a_2, a_4, a_6, \dots$ are divisible by $n$, then

$$\frac{[a_0; a_1, a_2, \dots]}{n} = \left[\frac{a_0}{n}; na_1, \frac{a_2}{n}, na_3, \dots\right].$$

(b) Prove that if $a_1, a_3, a_5, \dots$ are divisible by $n$, then

$$n[a_0; a_1, a_2, \dots] = [na_0, \frac{a_1}{n}, na_2, \frac{a_3}{n}, \dots].$$

1.4. Assume that

$$\alpha = [a_0; a_1, a_2 \dots]$$

is a periodic continuous fraction, that is, for some $r \geq 0$ and $d > 0$, $a_{m+d} = a_m$ for all $m \geq r$. Prove that $\alpha$ is a root of a quadratic equation with integer coefficients.

*Hint.* Begin with the case $r = 0$.

1.5. ** Prove the converse: if $\alpha$ is a root of a quadratic equation with integer coefficients, then $\alpha$ is represented by a periodic continued fraction.

1.6. Find the continued fractions representing $\sqrt{3}, \sqrt{5}, \sqrt{n^2+1}, \sqrt{n^2-1}$.

1.7. Using Exercises 1.6 and 1.3, find the continued fractions representing $4\sqrt{5}, \frac{\sqrt{5}}{2}$ and $\frac{1+\sqrt{3}}{2}$.

1.8. (Preparation to Exercise 1.9.) Let $\alpha, \beta$ be real numbers. We say that $\alpha$ is *related to* $\beta$, if $\alpha = \dfrac{a\beta+b}{c\beta+d}$ where $a, b, c, d$ are integers and $ad - bc = \pm 1$. Prove that if $\alpha$ is related to $\beta$, then $\beta$ is related to $\alpha$. Prove also that if $\alpha$ is related to $\beta$ and $\beta$ is related to $\gamma$, then $\alpha$ is related to $\gamma$.

1.9. * Let

$$\alpha = [a_0; a_1, a_2, \dots], \beta = [b_0; b_1, b_2, \dots]$$

be "almost identical" continued fractions, that is, there are non-negative integers $k, \ell$ such that $a_{k+m} = b_{\ell+m}$ for all $m \geq 0$. Prove that $\alpha$ and $\beta$ are related.

1.10. * Prove the converse: if $\alpha$ and $\beta$ are related, then their continued fractions are almost identical (see Exercise 1.9).

*Hint.* The following lemma might be useful. If $\alpha$ and $\beta$ are related, then there is a sequence of real numbers, $\alpha_0, \alpha_1, \dots, \alpha_N$ such that $\alpha_0 = \alpha$, $\alpha_N = \beta$, and for $1 \leq i \leq N$,

$$\alpha_i = -\alpha_{i-1}, \text{ or } \alpha_i = \alpha_{i-1} + 1, \text{ or } \alpha_i = \frac{1}{\alpha_{i-1}}.$$

1.11. Prove that if $\alpha$ is not related to the golden ratio (that is,

$$\alpha \neq [a_0; a_1, a_2, \dots, a_r, 1, 1, 1, \dots]),$$

then $\sqrt{5}$ in the Hurwitz-Borel Theorem can be replaced by $\sqrt{8}$.

1.12. Prove that if $\alpha$ is not related to the golden ratio or to $\sqrt{2}$, then $\sqrt{5}$ in the Hurwitz-Borel Theorem can be replaced by $\sqrt{\dfrac{221}{25}}$.

Remark to Exercises 1.11 and 1.12. The reader can extend the sequence $\sqrt{5}, \sqrt{8}, \sqrt{\dfrac{221}{25}}$ as long as he wishes (so, if $\alpha$ is not related to the golden ratio, $\sqrt{2}$ and one more specific number, then $\sqrt{5}$ in the Hurwitz-Borel Theorem can be replaced by a still bigger constant, and so on.) The resulting sequence will converge to 3.

1.13. Prove that there are uncountably many real numbers $\alpha$ with the following property: if $\lambda > 3$, then there are only finitely many fractions $\dfrac{p}{q}$ such that $\left|\alpha - \dfrac{p}{q}\right| < \dfrac{1}{\lambda q^2}$.

*Hint.* Try the numbers

$$[1; \underbrace{1, 1, \dots, 1}_{n_0}, 2, 2, \underbrace{1, 1, \dots, 1}_{n_1}, 2, 2, \underbrace{1, 1, \dots, 1}_{n_2}, 2, 2, 1, \dots]$$

where $n_0, n_1, n_2, \dots$ is an increasing sequence of integers.

1.14. ** The number 3 in Exercise 1.13 cannot be decreased.

1.15. Find the smallest number $\lambda_n$ with the following property. If $\alpha = [a_0; a_1, a_2, \dots]$ and $a_k \geq n$ for $k$ sufficiently large, then for any $\lambda > \lambda_n$ there are only finitely many fractions $\dfrac{p}{q}$ such that $\left|\alpha - \dfrac{p}{q}\right| < \dfrac{1}{\lambda q^2}$.

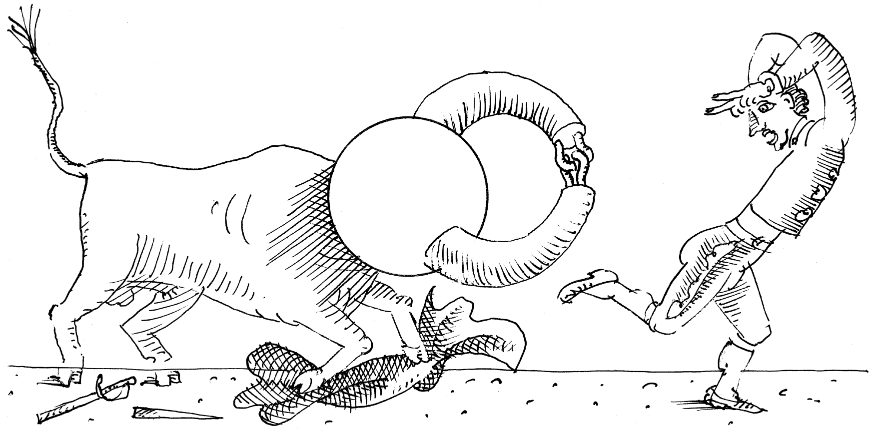

LECTURE 2

# Arithmetical Properties of Binomial Coefficients

**2.1 Binomial coefficients and Pascal's triangle.** We first encounter binomial coefficients in the chain of formulas

$$\begin{array}{ll} (a+b)^0 & = 1 \\ (a+b)^1 & = a+b \\ (a+b)^2 & = a^2+2ab+b^2 \\ (a+b)^3 & = a^3+3a^2b+3ab^2+b^3 \\ (a+b)^4 & = a^4+4a^3b+6a^2b^2+4ab^3+b^4 \\ & \dots\dots\dots\dots\dots\dots \end{array}$$

as the coefficients in the right hand sides. The coefficient of $a^m b^{n-m}$ (where $0 \leq m \leq n$) is denoted by $\binom{n}{m}$ (or, sometimes, by $C_n^m$) which is pronounced as "$n$ choose $m$" (we shall explain this below). There are two major ways to calculate the numbers $\binom{n}{m}$. One is given by the recursive Pascal Triangle Formula:

$$\binom{n}{m} = \binom{n-1}{m-1} + \binom{n-1}{m}$$

which has a simple proof:

$$\begin{aligned} \dots \quad &+\binom{n}{m} a^m b^{n-m} + \dots = (a+b)^n = (a+b)^{n-1}(a+b) \\ &= \left(\dots + \binom{n-1}{m-1} a^{m-1} b^{n-m} + \binom{n-1}{m} a^m b^{n-m-1} + \dots\right)(a+b) \\ &= \dots + \left(\binom{n-1}{m-1} + \binom{n-1}{m}\right) a^m b^{n-m} + \dots \end{aligned}$$

The second expression for the binomial coefficients is the formula

$$\binom{n}{m} = \frac{n(n-1)\dots(n-m+1)}{1\cdot 2\cdot\dots\cdot m} = \frac{n!}{m!(n-m)!}$$

which can be deduced from Pascal Triangle Formula by induction: it is obviously true for $n = 0$, and if it is true for $\binom{n-1}{k}$ (for all $k$ between 0 and $n-1$), then

$$\begin{aligned}\binom{n}{m} &= \binom{n-1}{m-1} + \binom{n-1}{m} = \frac{(n-1)!}{(m-1)!(n-m)!} + \frac{(n-1)!}{m!(n-m-1)!} \\ &= \frac{(n-1)!\cdot m + (n-1)!\cdot(n-m)}{m!(n-m)!} = \frac{(n-1)!\cdot n}{m!(n-m)!} = \frac{n!}{m!(n-m)!}\end{aligned}$$

The Pascal Triangle Formula gives rise to the Pascal Triangle, a beautiful triangular table which contains all the binomial coefficients and which can be extended downward infinitely.

| | | | | | | | | | | | | | | |
|---|---|---|---|---|---|---|---|---|---|---|---|---|---|---|
| 1 | | | | | | | | | | | | | | |
| 1 | 1 | | | | | | | | | | | | | |
| 1 | 2 | 1 | | | | | | | | | | | | |
| 1 | 3 | 3 | 1 | | | | | | | | | | | |
| 1 | 4 | 6 | 4 | 1 | | | | | | | | | | |
| 1 | 5 | 10 | 10 | 5 | 1 | | | | | | | | | |
| 1 | 6 | 15 | 20 | 15 | 6 | 1 | | | | | | | | |
| 1 | 7 | 21 | 35 | 35 | 21 | 7 | 1 | | | | | | | |
| 1 | 8 | 28 | 56 | 70 | 56 | 28 | 8 | 1 | | | | | | |
| 1 | 9 | 36 | 84 | 126 | 126 | 84 | 36 | 9 | 1 | | | | | |
| 1 | 10 | 45 | 120 | 210 | 252 | 210 | 120 | 45 | 10 | 1 | | | | |
| 1 | 11 | 55 | 165 | 330 | 462 | 462 | 330 | 165 | 55 | 11 | 1 | | | |
| 1 | 12 | 66 | 220 | 495 | 792 | 924 | 792 | 495 | 220 | 66 | 12 | 1 | | |
| 1 | 13 | 78 | 286 | 715 | 1287 | 1716 | 1716 | 1287 | 715 | 286 | 78 | 13 | 1 | |
| 1 | 14 | 91 | 364 | 1001 | 2002 | 3003 | 3432 | 3003 | 2002 | 1001 | 364 | 91 | 14 | 1 |

In this table, the $n$-th row (the top row with just one 1 has number 0) consists of the numbers

$$\binom{n}{0}, \binom{n}{1}, \dots, \binom{n}{n-1}, \binom{n}{n}.$$

The Pascal Triangle Formula means that every number in this table, with the exception of the upper 1, is equal to the sum of the two numbers above it (for example, 56 in the 8-th row is $21 + 35$). Here we regard the blank spots as zeros.

To legalize the last remark, we assume that $\binom{n}{m}$ is defined for all integers $n, m$, provided that $n \geq 0$: we set $\binom{n}{m} = 0$, if $m < 0$ or $m > n$. This does not contradict the Pascal Triangle Formula (provided $n \geq 1$), so we can use this formula for any $m$.

Let us deduce some immediate corollaries from the Binomial Formula

$$(a+b)^n = \binom{n}{0}a^n + \binom{n}{1}a^{n-1}b + \dots + \binom{n}{n-1}ab^{n-1} + \binom{n}{n}b^n.$$

Proposition 2.1. *(a)* $\binom{n}{0}+\binom{n}{1}+\cdots+\binom{n}{n-1}+\binom{n}{n}=2^n.$

*(b) If $n \geq 1$, then*

$$\binom{n}{0}-\binom{n}{1}+\cdots+(-1)^{n-1}\binom{n}{n-1}+(-1)^n\binom{n}{n}=0.$$

*(c) If $n \geq 1$, then*

$$\binom{n}{0}+\binom{n}{2}+\binom{n}{4}+\cdots=\binom{n}{1}+\binom{n}{3}+\binom{n}{5}+\cdots=2^{n-1}.$$

Proof. The Binomial Formula yields (a) if one takes $a=b=1$ and yields (b) if one takes $a=1, b=-1$. The formula (c) follows from (a) and (b). □

**2.2 Pascal Triangle, combinatorics and probability.**

Proposition 2.2. *There are $\binom{n}{m}$ ways to choose $m$ things out of a collection of $n$ (different) things.*

Remark 2.3. (1) This Proposition explains the term "$n$ choose $m$".
(2) If $m < 0$ or $m > n$, then there are no ways to choose $m$ things out of $n$. This fact matches the equality $\binom{n}{m}=0$ for $m<0$ or $m>n$.

Proof of Proposition. Again, induction. For $n=0$, the fact is obvious. Assume that the Proposition holds for the case of $n-1$ things. Let $n$ things be given ($n \geq 1$). Mark one of them. When we choose $m$ things out of our $n$ things, we either take, or do not take, the marked thing. If we take it, then we need to chose $m-1$ things out of the remaining $n-1$; this can be done in $\binom{n-1}{m-1}$ ways. If we do not take the marked thing, then we need to choose $m$ things out of $n-1$, which can be done in $\binom{n-1}{m}$ ways. Thus, the total number of choices is

$$\binom{n-1}{m-1}+\binom{n-1}{m}=\binom{n}{m},$$

and we are done. □

As an aside, this Proposition has immediate applications to probability. For example, if you randomly pull 4 cards out of a deck of 52 cards, the probability to get 4 aces is

$$\frac{1}{\binom{52}{4}}=\frac{4!\cdot 48!}{52!}=\frac{1}{270725}\approx 3.7\cdot 10^{-6}$$

(there are $\binom{52}{4}$ choices, and only one of them gives you 4 aces). The probability of getting 4 spades is higher: it is

$$\frac{\binom{13}{4}}{\binom{52}{4}}=\frac{13!\cdot 4!\cdot 48!}{4!\cdot 9!\cdot 52!}=\frac{11}{4165}\approx 2.64\cdot 10^{-3}$$

(the total number of choices of 4 cards is $\binom{52}{4}$, the number of choices of 4 spades is $\binom{13}{4}$).

**2.3 Pascal Triangle and trigonometry.** The reader is probably familiar with the formulas

$$\begin{aligned} \sin 2\theta &= 2\sin\theta\cos\theta, \\ \cos 2\theta &= \cos^2\theta - \sin^2\theta. \end{aligned}$$

And what about $\sin 3\theta$? $\cos 5\theta$? $\sin 12\theta$? All such formulas are contained in the Pascal Triangle:

| | | |
|---|---|---|
| $\cos 0\theta =$ | | $\mathbf{1}$ |
| $\cos 1\theta =$ | $\sin 1\theta =$ | $\mathbf{1}\cos\theta$ $\quad$ $\mathbf{1}\sin\theta$ |
| $\cos 2\theta =$ | $\sin 2\theta =$ | $\mathbf{1}\cos^2\theta$ $\quad$ $\mathbf{2}\cos\theta\sin\theta$ $\quad$ $-\mathbf{1}\sin^2\theta$ |
| $\cos 3\theta =$ | $\sin 3\theta =$ | $\mathbf{1}\cos^3\theta$ $\quad$ $\mathbf{3}\cos^2\theta\sin\theta$ $\quad$ $-\mathbf{3}\cos\theta\sin^2\theta$ $\quad$ $-\mathbf{1}\sin^3\theta$ |
| $\cos 4\theta =$ | $\sin 4\theta =$ | $\mathbf{1}\cos^4\theta$ $\quad$ $\mathbf{4}\cos^3\theta\sin\theta$ $\quad$ $-\mathbf{6}\cos^2\theta\sin^2\theta$ $\quad$ $-\mathbf{4}\cos\theta\sin^3\theta$ $\quad$ $+\mathbf{1}\sin^4\theta$ |

Can you see the Pascal Triangle here? It is slightly spoiled by the signs. Here is the result.

PROPOSITION 2.4.

$$\begin{aligned} \sin n\theta &= \binom{n}{1}\cos^{n-1}\theta\sin\theta - \binom{n}{3}\cos^{n-3}\theta\sin^3\theta + \binom{n}{5}\cos^{n-5}\theta\sin^5\theta - \dots \\ \cos n\theta &= \cos^n\theta - \binom{n}{2}\cos^{n-2}\theta\sin^2\theta + \binom{n}{4}\cos^{n-4}\theta\sin^4\theta - \dots \end{aligned}$$

Proof. Induction, as usual. For $n = 1$, the formulas are tautological. If the formulas for $\sin(n-1)\theta$ and $\cos(n-1)\theta$ $(n > 1)$ hold then

$$\begin{aligned} \sin\, n\theta = &\ \sin((n-1)\theta + \theta) = \sin(n-1)\theta\cos\theta + \sin\theta\cos(n-1)\theta \\ = &\ \left(\binom{n-1}{1}\cos^{n-2}\theta\sin\theta - \binom{n-1}{3}\cos^{n-4}\theta\sin^3\theta + \dots\right)\cos\theta + \\ &\ \sin\theta\left(\binom{n-1}{0}\cos^{n-1}\theta - \binom{n-1}{2}\cos^{n-3}\sin^2\theta + \dots\right) \\ = &\ \left(\binom{n-1}{0} + \binom{n-1}{1}\right)\cos^{n-1}\theta\sin\theta - \\ &\ \left(\binom{n-1}{2} + \binom{n-1}{3}\right)\cos^{n-3}\theta\sin^3\theta + \dots \\ = &\ \binom{n}{1}\cos^{n-1}\theta\sin\theta - \binom{n}{3}\cos^{n-3}\theta\sin^3\theta + \dots, \end{aligned}$$

and similarly for

$$\cos n\theta = \cos((n-1)\theta + \theta) = \cos(n-1)\theta\cos\theta - \sin(n-1)\theta\sin\theta,$$

as needed. □

There is also a formula for $\tan n\theta$ (generalizing the textbook formula for $\tan 2\theta$):

$$\tan n\theta = \frac{\binom{n}{1}\tan\theta - \binom{n}{3}\tan^3\theta + \binom{n}{5}\tan^5\theta - \dots}{1 - \binom{n}{2}\tan^2\theta + \binom{n}{4}\tan^4\theta - \binom{n}{6}\tan^6\theta + \dots}$$

(see Exercise 2.1).

These applications, however, do not represent the main goal of this lecture. We will be interested mainly in arithmetical properties of binomial coefficients, like divisibilities, remainders, and so on.

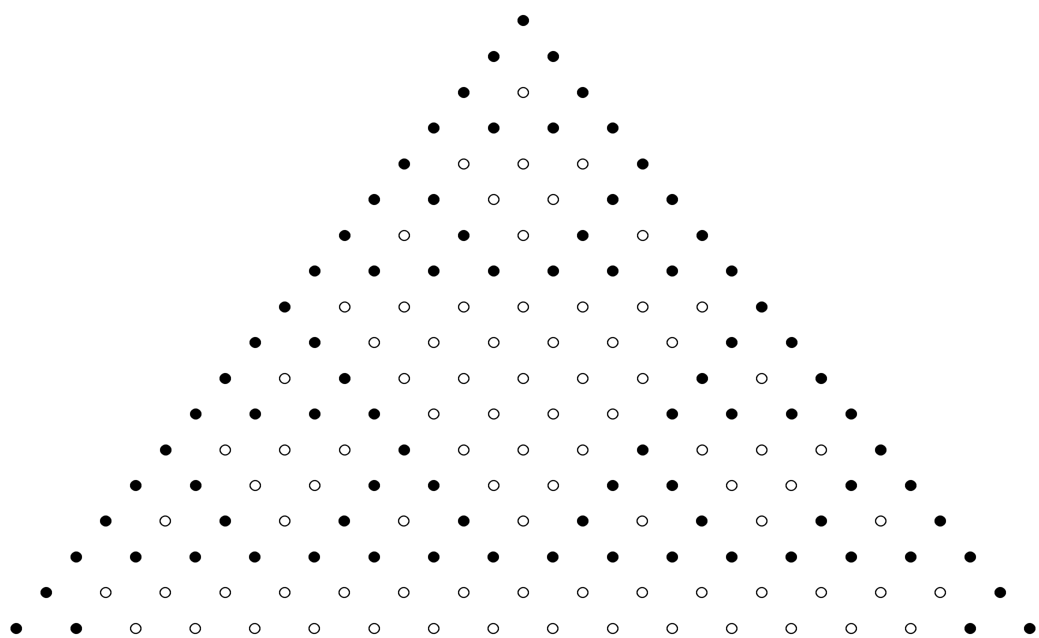

**2.4 Pascal triangle mod $p$.** Let us take the Pascal triangle and replace every odd number by a black dot, •, and every even number by a white dot, ∘. The resulting picture will remind the Sierpinski carpet (for those who know what the Sierpinski carpet – a.k.a. Sierpinski gasket – is).

A close look at this picture reveals the following. Let $2^r \le n < 2^{r+1}$. Then

(1) if $m \le n - 2^r$, then $\binom{n}{m}$ has the same parity as $\binom{n-2^r}{m}$;

(2) if $m \ge 2^r$, then $\binom{n}{m}$ has the same parity as $\binom{n-2^r}{m-2^r}$;

(3) if $n - 2^r < m < 2^r$, then $\binom{n}{m}$ is even.

The following result generalizes these observations to the case of an arbitrary prime $p$.

Theorem 2.1 (Lucas, 1872). *Let $p$ be a prime number, and let $n, m, q, r$ be non-negative numbers with $0 \leq q < p,\ 0 \leq r < p$. Then*

$$\binom{pn+q}{pm+r} \equiv \binom{n}{m}\binom{q}{r} \bmod p.$$

(We assume the reader is familiar with the symbol $\equiv$. The formula $A \equiv B \bmod N$, "$A$ is congruent to $B$ modulo $N$" means that $A - B$ is divisible by $N$, or $A$ and $B$ have equal remainders after division by $N$. We shall also use this symbol for polynomials with integral coefficients: $P \equiv Q \bmod N$ if all the coefficients of the polynomial $P - Q$ are divisible by $N$.)

To prove the theorem, we need a lemma.

Lemma 2.5. *If $0 < m < p$, then $\binom{p}{m}$ is divisible by $p$ (and not divisible by $p^2$; but we do not need this).*

Proof of Lemma.

$$\binom{p}{m} = \frac{p(p-1)\dots(p-m+1)}{1 \cdot 2 \cdot \dots \cdot m},$$

and no factor in the numerator and denominator, except $p$ in the numerator, is divisible by $p$. □

Proof of Theorem. The Lemma implies that $(a+b)^p \equiv a^p + b^p \bmod p$. Therefore,

$$(a+b)^{pn+q} = ((a+b)^p)^n (a+b)^q \equiv (a^p + b^p)^n (a+b)^q \bmod p,$$

$$(a^p + b^p)^n (a+b)^q = \left(a^{pn} + \dots + \binom{n}{m} a^{pm} b^{p(n-m)} + \dots + b^{pn}\right)$$

$$\cdot \left(a^q + \dots + \binom{q}{r} a^r b^{q-r} + \dots + b^q\right)$$

and it is clear that the term $a^{pm+r} b^{p(n-m)+(q-r)}$ appears in the last expression only once and with the coefficient $\binom{n}{m}\binom{q}{r}$, whence

$$\binom{pn+q}{pm+r} \equiv \binom{n}{m}\binom{q}{r} \bmod p,$$

and we are done.□

To state a nice corollary of Lucas' Theorem, recall that, whether $p$ is prime or not, every positive integer $n$ has a unique presentation as $n_r p^r + n_{r-1} p^{r-1} + \dots + n_1 p + n_0$ with $0 < n_r < p$ and $0 \leq n_i < p$ for $i = 0, 1, \dots, r-1$. We shall use the brief notation $n = (n_r n_{r-1} \dots n_1 n_0)_p$. The numbers $n_i$ are called *digits* of $n$ in the numerical system with base $p$. If $p = 10$, then these digits are usual ("decimal") digits. Examples: $321 = (321)_{10} = (2241)_5 = (101000001)_2$. Note that we can use the presentation of numbers in the numerical system with an arbitrary base to add, subtract (and multiply; and even divide) numbers, precisely as we do this using the decimal system.

Let us return to our assumption that $p$ is prime.

COROLLARY 2.2. *Let* $n = (n_r n_{r-1} \dots n_1 n_0)_p$, $m = (m_r m_{r-1} \dots m_1 m_0)_p$ *(we allow* $m_r$ *to be zero). Then*

$$\binom{n}{m} \equiv \binom{n_r}{m_r}\binom{n_{r-1}}{m_{r-1}} \dots \binom{n_1}{m_1}\binom{n_0}{m_0} \bmod p.$$

Proof. Induction on $r$. The case $r = 0$ is obvious; assume that our congruence holds if $r$ is replaced by $r-1$. Then $n = pn' + n_0$, $m = pm' + m_0$ where $n' = (n_r n_{r-1} \dots n_2 n_1)_p$, $m' = (m_r m_{r-1} \dots m_2 m_1)_p$. Lucas' Theorem and the induction hypothesis give, respectively,

$$\binom{n}{m} \equiv \binom{n'}{m'}\binom{n_0}{m_0} \bmod p,$$

$$\binom{n'}{m'} \equiv \binom{n_r}{m_r} \dots \binom{n_1}{m_1} \bmod p,$$

whence

$$\binom{n}{m} \equiv \binom{n_r}{m_r} \dots \binom{n_1}{m_1}\binom{n_0}{m_0} \bmod p,$$

and we are done. □

This result shows that binomial coefficients have a tendency to be divisible by prime numbers: if at least one $m_i$ exceeds the corresponding $n_i$ then the product on the right hand side of the last congruence is zero. Example: what is the remainder of $\binom{31241}{17101}$ modulo 3? Since $31241 = (1120212002)_3$ and $17101 = (0212110101)_3$,

$$\binom{31241}{17101} \equiv \binom{1}{0}\binom{1}{2}\binom{2}{1}\binom{0}{2}\binom{2}{1}\binom{1}{1}\binom{2}{0}\binom{0}{1}\binom{0}{0}\binom{2}{1}$$

$$= 1 \cdot 0 \cdot 2 \cdot 0 \cdot 2 \cdot 1 \cdot 1 \cdot 0 \cdot 1 \cdot 2 = 0 \bmod 3.$$

On the other hand, $31241 = (1444431)_5$, $17101 = (1021401)_5$, and

$$\binom{31241}{17101} \equiv \binom{1}{1}\binom{4}{0}\binom{4}{2}\binom{4}{1}\binom{4}{4}\binom{3}{0}\binom{1}{1}$$

$$= 1 \cdot 1 \cdot 6 \cdot 4 \cdot 1 \cdot 1 \cdot 1 = 24 \equiv 4 \bmod 5.$$

Note in conclusion that Corollary 2.2 explains the observations made in the beginning of this section. If $2^r \le n < 2^{r+1}$, then $n = (1n_{r-1} \dots n_1 n_0)_2$ ($n_i = 0$ or 1 for $i = 0, \dots, r-1$). If $m \le n - 2^r$, then $m = (0m_{r-1} \dots m_1 m_0)_2$ and

$$\binom{n}{m} \equiv \binom{1}{0}\binom{n_{r-1}}{m_{r-1}} \dots \binom{n_0}{m_0} = \binom{n_{r-1}}{m_{r-1}} \dots \binom{n_0}{m_0} \equiv \binom{n-2^r}{m} \bmod 2.$$

If $m \ge 2^r$, then $m = (1m_{r-1} \dots m_1 m_0)_2$ and

$$\binom{n}{m} \equiv \binom{1}{1}\binom{n_{r-1}}{m_{r-1}} \dots \binom{n_0}{m_0} = \binom{n_{r-1}}{m_{r-1}} \dots \binom{n_0}{m_0} \equiv \binom{n-2^r}{m-2^r} \bmod 2.$$

If $n - 2^r < m < 2^r$, then $m_i > n_i$ for at least one $i \le r-1$. In this case $\binom{n_i}{m_i} = 0$ and $\binom{n}{m} \equiv \dots \cdot 0 \cdot \dots = 0 \bmod 2$, and so $\binom{n}{m}$ is even.

**2.5 Prime factorizations.** Let us begin with the following simple, but beautiful, result.

THEOREM 2.3. *Let* $n = (n_r \dots n_1 n_0)_p$. *Then the number of factors* $p$ *in the prime factorization of* $n!$ *is*

$$\frac{n - (n_r + \cdots + n_1 + n_0)}{p-1}.$$

REMARK 2.6. The fact that the last fraction is a whole number is true whether $p$ is prime or not, and is well known if $p = 10$: any positive integer has the same remainder modulo 9 as the sum of its digits. It can be proved for an arbitrary $p$ precisely as it is proved for $p = 10$ in elementary textbooks.

Proof. Induction on $n$. Denote by $C_p(n)$ the number of factors $p$ in the prime factorization of $n$. If $C_p(n) = k$, then $n_{k-1} = \cdots = n_0 = 0,\ n_k \neq 0$ and $n - 1 = (n_r \dots n_{k+1}(n_k - 1)(p-1)(p-1)\dots(p-1))_p$. According to the induction hypothesis,

$$\begin{aligned} C_p((n-1)!) &= \frac{(n-1) - (n_r + \cdots + n_{k+1} + n_k - 1 + (p-1)k)}{p-1} \\ &= \frac{n - (n_r + \cdots + n_k)}{p-1} - k \end{aligned}$$

and hence

$$C_p(n!) = C_p((n-1)!) + C_p(n) = \frac{n - (n_r + \cdots + n_k)}{p-1}.$$

□

This Theorem provides a very efficient way of counting the number of prime factors in a binomial coefficient. For example,

$$\begin{aligned} \binom{31241}{17101} &= \frac{31241!}{17101! \cdot 14140!}; \\ 31241 &= (1120212002)_3, \qquad C_3(31241!) = \frac{31241 - 11}{2} = 15615, \\ 17101 &= (212110101)_3, \qquad C_3(17101!) = \frac{17101 - 9}{2} = 8546, \\ 14140 &= (201101201)_3, \qquad C_3(14140!) = \frac{14140 - 8}{2} = 7066, \\ C_3\binom{31241}{17101} &= C_3(31241!) - C_3(17101!) - C_3(14140!) \\ &= 15615 - 8546 - 7066 = 3. \end{aligned}$$

We established in the previous section that $\binom{31241}{17101}$ is divisible by 3; now we see that the number of factors 3 in the prime factorization of this number is 3, that is, it is divisible by 27, but not divisible by 81.

Our exposition would not have been complete if we had skipped a beautiful way to count the number of given factors in the prime factorizations of binomial coefficients due to one of the best number theorists of 19-th century.

Theorem 2.4 (Kummer, 1852). *$C_p\binom{n}{m}$ equals the number of carry-overs in the addition $m + (n - m) = n$ in the numerical system with base $p$.*

For example, $17101 = (212110101)_3,\ 14140 = (201101201)_3$. Perform the addition:

$$\begin{array}{ccccccccccc}
 & * & & * & & & * & & & & \\
 & & 2 & 1 & 2 & 1 & 1 & 0 & 1 & 0 & 1 \\
+ & & & & & & & & & & \\
 & & 2 & 0 & 1 & 1 & 0 & 1 & 2 & 0 & 1 \\
\hline
 & 1 & 1 & 2 & 0 & 2 & 1 & 2 & 0 & 0 & 2
\end{array}$$

There are 3 carry-overs (marked by asterisks), and the prime factorization of $\binom{31241}{17101}$ contains 3 factors 3.

We leave to the reader the pleasant work of deducing Kummer's Theorem from the previous results of this section (see Exercise 2.5).

**2.6 Congruences modulo $p^3$ in the Pascal Triangle.** It is much easier to formulate the results of Sections 2.6 and 2.7 than to prove them. Accordingly, we will give the statements of more or less all known results and almost no proofs. The reader may want to reconstruct some of the proofs (although they are not elementary) and to think about further results in this direction.

Lucas' Theorem (Section 2.4) implies that

$$\binom{pn}{pm} \equiv \binom{n}{m}\binom{0}{0} = \binom{n}{m} \bmod p.$$

But experiments show that, actually, there are "better" congruences. For example, $\binom{3\cdot 5}{3\cdot 2} - \binom{5}{2}$ should be divisible by 3; but, actually,

$$\binom{3\cdot 5}{3\cdot 2} - \binom{5}{2} = \binom{15}{6} - \binom{5}{2} = 5005 - 10 = 4995 = 185 \cdot 3^3.$$

Another example:

$$\binom{5\cdot 3}{5\cdot 1} - \binom{3}{1} = 3003 - 3 = 3000 = 24 \cdot 5^3.$$

And there is a theorem that states precisely what we see!

Theorem 2.5 (Jacobsthal, 1952, [**11**]). *If $p \geq 5$, then*

$$\binom{pn}{pm} - \binom{n}{m}$$

*is divisible by $p^3$.*

(This is also true for $p = 2$ and 3, but with some "exceptions". Indeed, $\binom{14}{6} - \binom{7}{3} = 3003 - 35 = 2968 = 371 \cdot 2^3$ and $\binom{12}{3} - \binom{4}{1} = 216 = 8 \cdot 3^3$. But $\binom{6}{2} - \binom{3}{1} = 15 - 3 = 12 = 3 \cdot 2^2$ and $\binom{6}{3} - \binom{2}{1} = 20 - 2 = 18 = 2 \cdot 3^2$. For further results see Exercises 2.6, 2.7.)

We shall not prove Jacobsthal's theorem here; we shall restrict ourselves to a more modest result.

PROPOSITION 2.7. *For any prime $p$ and any $m$ and $n$,*

$$\binom{pn}{pm} - \binom{n}{m}$$

*is divisible by $p^2$.*

Proof. We shall use the following fact following from Lucas' Theorem: if $n$ is divisible by $p$ and $m$ is not divisible by $p$, then $\binom{n}{m}$ is divisible by $p$. (Indeed, if $n = pr$ and $m = ps + t,\ 0 < t < p$, then $\binom{n}{m} \equiv \binom{r}{s}\binom{0}{t} = 0 \bmod p$.)

Now, we use induction on $n$ (for $n = 1$, we have nothing to prove). Assume that the statement with $n - 1$ in place of $n$ is true. Consider the equality

$$(a + b)^{pn} = (a + b)^{p(n-1)} \cdot (a + b)^p.$$

Equating the coefficients of $a^{pm}b^{p(n-m)}$, we get the following:

$$\binom{pn}{pm} = \binom{p(n-1)}{pm}\binom{p}{0} + \binom{p(n-1)}{pm-1}\binom{p}{1} + \dots$$
$$+ \binom{p(n-1)}{pm-p+1}\binom{p}{p-1} + \binom{p(n-1)}{pm-p}\binom{p}{p}.$$

On the right hand side of the last equality every summand, with the exception of the two extreme ones, is a product of two numbers divisible by $p$; hence, each of these summands is divisible by $p^2$ and

$$\binom{pn}{pm} \equiv \binom{p(n-1)}{pm} + \binom{p(n-1)}{p(m-1)} \bmod p^2.$$

By the induction hypothesis,

$$\binom{p(n-1)}{pm} + \binom{p(n-1)}{p(m-1)} \equiv \binom{n-1}{m} + \binom{n-1}{m-1} = \binom{n}{m} \bmod p^2,$$

whence our result.□

Is it possible to enhance Jacobsthal's result? In some special cases it is possible (see next section). In general, it is unlikely. Let us mention the following (unpublished) result.

THEOREM 2.6 (G. Kuperberg, 1999). *If*

$$\binom{2p}{p} \equiv \binom{2}{1} \bmod p^4,$$

*then*

$$\binom{pn}{pm} \equiv \binom{n}{m} \bmod p^4$$

*for every $m, n$.*

However, this property $\left(\binom{2p}{p} \equiv \binom{2}{1} \bmod p^4\right)$ does not hold too often. According to G. Kuperberg (who has a heuristic "proof" that it is true for infinitely many primes $p$), the smallest prime number for which it holds is 16,483.

Still, for some special $m$ and $n$, congruence modulo a much higher power of $p$ may hold. We shall consider some results of this kind in the next (last) section.

**2.7 Congruences modulo higher powers of $p$.** Let us consider numbers of the form $\binom{2^{n+1}}{2^n}$:

$$\binom{2}{1} = 2,\ \binom{4}{2} = 6,\ \binom{8}{4} = 70,\ \binom{16}{8} = 12870,\ \binom{32}{16} = 601080390$$

None of these numbers is divisible even by 4. But let us examine their successive differences:

$$\binom{4}{2} - \binom{2}{1} = 6 - 2 = 4 = 2^2$$

$$\binom{8}{4} - \binom{4}{2} = 70 - 4 = 64 = 2^6$$

$$\binom{16}{8} - \binom{8}{4} = 12870 - 70 = 12,800 = 25 \cdot 2^9$$

$$\binom{32}{16} - \binom{16}{8} = 601080390 - 12870 = 601067520 = 146745 \cdot 2^{12}.$$

Consider similar differences for bigger primes:

$$\binom{9}{3} - \binom{3}{1} = 84 - 3 = 81 = 3^4$$

$$\binom{27}{9} - \binom{9}{3} = 4686825 - 84 = 3143 \cdot 3^7$$

$$\binom{25}{5} - \binom{5}{1} = 53130 - 5 = 17 \cdot 5^5$$

$$\binom{49}{7} - \binom{7}{1} = 85900584 - 7 = 5111 \cdot 7^5$$

Let us try to explain these results.

THEOREM 2.7 (A. Schwarz, 1959). *If $p \geq 5$, then*

$$\binom{p^2}{p} \equiv \binom{p}{1} \bmod p^5.$$

REMARK 2.8. (1) This result was never published. A. Schwarz, who is now a prominent topologist and mathematical physicist, does not himself remember proving this theorem. However, one of the authors of this book (DF) was a witness to the event.

(2) We do not know whether the congruence holds modulo $p^6$ for any prime $p$. We realize that modern software can, possibly, resolve this problem in a split second.

To prove Schwarz's Theorem, we shall use the following extended notion of a congruence. We shall say that a *rational* number $r = \dfrac{m}{n}$ (where the fraction is assumed irreducible) is divisible by $p^k$, if $m$ is divisible by $p^k$ and $n$ is not divisible by $p$. For rational numbers $r, s$, the congruence $r \equiv s \bmod p^k$ means that $r - s$ is divisible by $p^k$. (For example, $\dfrac{1}{5} \equiv 2 \bmod 3^2$.) These congruences possess the usual properties of congruences: if $r \equiv s \bmod p^k$ and $s \equiv t \bmod p^k$, then $r \equiv t \bmod p^k$; if $r \equiv s \bmod p^k$ and the denominator of $t$ is not divisible by $t$, then $rt \equiv st \bmod p^k$; etc.

Lemma 2.9. *For a prime $p \geq 5$,*

$$1 + \frac{1}{2} + \cdots + \frac{1}{p-1}$$

*is divisible by $p^2$.*

Proof of Lemma. Let $p = 2q + 1$ (since $p \geq 5$, $p$ is odd). Then

$$\begin{aligned} 1 + \frac{1}{2} + \cdots + \frac{1}{p-1} &= \left(1 + \frac{1}{p-1}\right) + \left(\frac{1}{2} + \frac{1}{p-2}\right) + \cdots + \left(\frac{1}{q} + \frac{1}{p-q}\right) \\ &= p \cdot \left(\frac{1}{p-1} + \frac{1}{2(p-2)} + \cdots + \frac{1}{q(p-q)}\right) \end{aligned}$$

and all we need to prove is that

$$\frac{1}{p-1} + \frac{1}{2(p-2)} + \cdots + \frac{1}{q(p-q)}$$

is divisible by $p$.

Sublemma 2.9.1. *For every $i = 1, \ldots, p-1$ there exists a unique $s_i$, $1 \leq s_i \leq p-1$ such that $is_i \equiv 1 \bmod p$. Moreover,*

*(a) $s_{p-i} = p - s_i$;*

*(b) the numbers $s_1, s_2, \ldots, s_{p-1}$ form a permutation of the numbers $1, 2, \ldots, p-1$.*

Proof of Sublemma. For a given $i$, consider the numbers $i, 2i, \ldots, (p-1)i$. None of these numbers is divisible by $p$, and no two are congruent modulo $p$ (indeed, if $ji \equiv ki \bmod p$, then $ji - ki = (j-k)i$ is divisible by $p$, which is impossible, since neither $i$, nor $j - k$ is divisible by $p$). Hence, the numbers $i, 2i, \ldots, (p-1)i$ have different remainders mod $p$, and since there are precisely $p-1$ possible remainders, each remainder appears exactly once. In particular, there exists a unique $j$ such that $ji \equiv 1 \bmod p$; this $j$ is our $s_i$. Statements (a) and (b) are obvious: $(p-i)(p-s_i) = p^2 - p(i+s_i) + is_i \equiv 1 \bmod p$, and since the numbers $s_1, s_2, \ldots, s_{p-1}$ are all different, they form a permutation of $1, 2, \ldots, p-1$. $\square$

Example: if $p = 11$, then $s_1 = 1, s_2 = 6, s_3 = 4, s_4 = 3, s_5 = 9, s_6 = 2, s_7 = 8, s_8 = 7, s_9 = 5, s_{10} = 10$.

Back to the Lemma. Since $\frac{1}{i} \equiv s_i \bmod p$ (indeed, $s_i - \frac{1}{i} = \frac{is_i - 1}{i}$ which is divisible by $p$),

$$\frac{1}{p-1} + \frac{1}{2(p-1)} + \cdots + \frac{1}{q(p-q)} \equiv s_1 s_{p-1} + s_2 s_{p-2} + \cdots + s_q s_{p-q} \bmod p$$

(where, as before, $p = 2q+1$). Of the two numbers $s_i, s_{p-i} = p - s_i$, precisely one is less than $\frac{p}{2}$. Hence, the numbers $s_1 s_{p-1}, s_2 s_{p-2}, \ldots, s_q s_{p-q}$ form a permutation of the numbers $1(p-1), 2(q-2), \ldots, q(p-q)$, and

$$\begin{aligned} \frac{1}{p-1} + \frac{1}{2(p-1)} \quad + \ldots + \frac{1}{q(p-q)} &\equiv 1(p-1) + 2(p-2) + \cdots + q(p-q) \\ &= p(1 + 2 + \cdots + q) - (1^2 + 2^2 + \cdots + q^2) \\ &= \frac{pq(q+1)}{2} - \frac{q(q+1)(2q+1)}{6} = \frac{pq(q+1)}{3} \equiv 0 \bmod p, \end{aligned}$$

as needed. □

Proof of Schwarz's Theorem.

$$\begin{aligned} \binom{p^2}{p} - \binom{p}{1} \quad &= \frac{p^2(p^2-1)\ldots(p^2-(p-1))}{1 \cdot \cdots \cdot (p-1)p} - p \\ &= \frac{p}{(p-1)!}[(1-p^2)(2-p^2)\ldots((p-1)-p^2) - 1 \cdot 2 \cdot \cdots \cdot (p-1)], \end{aligned}$$

and all we need to prove is that

$$(1-p^2)(2-p^2)\ldots((p-1)-p^2) - 1 \cdot 2 \cdot \cdots \cdot (p-1) \equiv 0 \bmod p^4.$$

But

$$\begin{aligned} (1-p^2)(2-p^2)\ldots((p-1)-p^2) \quad &= 1 \cdot 2 \cdot \cdots \cdot (p-1) \\ &\quad -p^2\left(1 + \frac{1}{2} + \cdots + \frac{1}{p-1}\right)(p-1)! \\ &\quad + \text{terms divisible by } p^4, \end{aligned}$$

whence

$$\begin{aligned} &(1-p^2)(2-p^2)\ldots((p-1)-p^2) - 1 \cdot 2 \cdot \cdots \cdot (p-1) \equiv \\ &\qquad -p^2\left(1 + \frac{1}{2} + \cdots + \frac{1}{p-1}\right)(p-1)! \bmod p^4 \end{aligned}$$

which is divisible by $p^4$ by Lemma 2.9.□

Many of the congruences considered above are contained in the following (also unpublished) result.

THEOREM 2.8 (M. Zieve, 2000). *If $p \geq 5$ then, for any positive integers $k, m, n$,*

$$\binom{np^k}{mp^k} \equiv \binom{np^{k-1}}{mp^{k-1}} \bmod p^{3k}.$$

We shall not prove this theorem here, but will restrict ourselves (as we did in the case of Jacobsthal's Theorem) to a more modest result.

Proposition 2.10. *If $k \geq 2$ then $\binom{2^{k+1}}{2^k} - \binom{2^k}{2^{k-1}}$ is divisible by $2^{2k+2}$.*

Proof. We shall use the following fact: if $0 < m < 2^k$ then $\binom{2^k}{m}$ is divisible by $2^k$. (The following, more general, result follows from Kummer's Theorem, Section 2.5: if $n$ is divisible by $p^k$ and $m$ is not divisible by $p$, then $\binom{n}{m}$ is divisible by $p^k$.)

The difference $\binom{2^{k+1}}{2^k} - \binom{2^k}{2^{k-1}}$ in question is the coefficient of $x^{2^k}$ in the polynomial

$$(1+x)^{2^{k+1}} - (1-x^2)^{2^k} = (1+x)^{2^k}[(1+x)^{2^k} - (1-x)^{2^k}]$$
$$= \left[1 + \binom{2^k}{1}x + \binom{2^k}{2}x^2 + \cdots + x^{2^k}\right]$$
$$\cdot 2\left[\binom{2^k}{1}x + \binom{2^k}{3}x^3 + \cdots + \binom{2^k}{2^k-1}x^{2^k-1}\right].$$

Since the second polynomial in the last expression contains only odd degrees, the coefficient of $x^{2^k}$ in the product is

$$2\left[\binom{2^k}{1}\binom{2^k}{2^k-1} + \binom{2^k}{3}\binom{2^k}{2^k-3} + \cdots + \binom{2^k}{2^k-1}\binom{2^k}{1}\right].$$

Every binomial coefficient in the last expression is divisible by $2^k$ by the remark at the beginning of the proof; hence every summand in the last sum is divisible by $2^{2k}$. Also, every summand in this sum is repeated twice, and also there is a factor 2 before the sum. Thus the whole expression is divisible by $2^{2k+2}$. □

Let us mention, in conclusion, A. Granville's dynamic on-line survey of arithmetical properties of binomial coefficients [**37**].

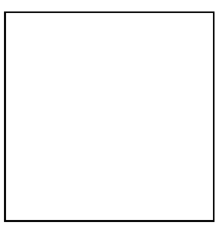

John Smith
January 23, 2010

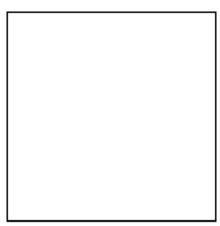

Martyn Green
August 2, 1936

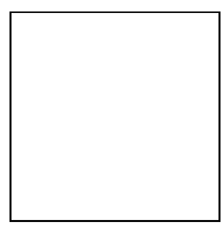

Henry Williams
June 6, 1944

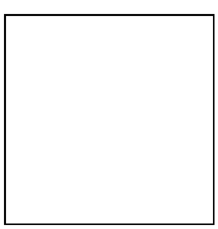

John Smith
January 23, 2010

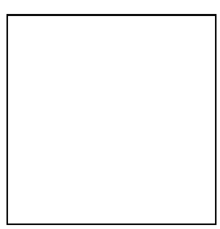

Martyn Green
August 2, 1936

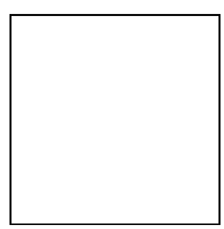

Henry Williams
June 6, 1944

## 2.8 Exercises.

2.1. Prove that

$$\tan(n\theta) = \frac{\binom{n}{1}\tan\theta - \binom{n}{3}\tan^3\theta + \binom{n}{5}\tan^5\theta - \dots}{1 - \binom{n}{2}\tan^2\theta + \binom{n}{4}\tan^4\theta - \binom{n}{6}\tan^6\theta + \dots}.$$

2.2. Prove that for the hyperbolic functions

$$\sinh(x) = \frac{e^x - e^{-x}}{2}, \ \cosh(x) = \frac{e^x + e^{-x}}{2}, \ \tanh(x) = \frac{\sinh(x)}{\cosh(x)}$$

formulas hold similar to those in Section 2.3with all the minuses replaced by pluses.

2.3. What percent of the numbers $\binom{m+n}{n}$ with $0 \le m < 2^{100}, \ 0 \le n < 2^{100}$ are odd?

2.4. What percent of the numbers $\binom{m+n}{n}$ with $0 \le m < 2^{100}, \ 0 \le n < 2^{100}$ are not divisible by 4?

2.5. Prove the Kummer Theorem 2.4 (deduce it from Theorem 2.3).

2.6. (a) Prove that $\binom{2n}{2m} - \binom{n}{m} \not\equiv 0 \bmod 2^3$ for infinitely many pairs $(m, n)$. Namely, prove that $\binom{2n}{2} - \binom{n}{1} \equiv 0 \bmod 2^3$ if and only if $\binom{n}{2}$ is even, that is, if $n \equiv 0$ or $1 \bmod 4$.

(b) Prove also that $\binom{2n}{4} - \binom{n}{2} \equiv 0 \bmod 2^3$ if and only if $n \not\equiv 3 \bmod 4$.

The reader is encouraged to consider the differences $\binom{2n}{6} - \binom{n}{3}$, $\binom{2n}{8} - \binom{n}{4}$ and so on.

2.7. (a) Prove that $\binom{3n}{3} - \binom{n}{1} \not\equiv 0 \bmod 3^3$ if and only if $n \equiv 2 \bmod 3$.

(b) Prove that $\binom{3n}{6} - \binom{n}{2} \equiv 0 \bmod 3^3$ for all $n$.

We do not know whether

$$\binom{3n}{3m} - \binom{n}{m} \equiv 0 \bmod 3^3$$

for all $m, n$ with $2 \le m \le n$.

2.8. (a) Prove that for $|x| < \frac{1}{4}$ the series $\sum_{n=0}^{\infty} \binom{2n}{n} x^n$ converges to $\frac{1}{\sqrt{1-4x}}$.

(b) Deduce from this (or prove directly) that for any $n$

$$1 \cdot \binom{2n}{n} + \binom{2}{1}\binom{2(n-1)}{n-1} + \binom{4}{2}\binom{2(n-2)}{n-2} + \dots + \binom{2n}{n} \cdot 1 = 4^n.$$

2.9. Let

$$C_n = \frac{(2n)!}{n!(n+1)!} = \frac{\binom{2n}{n}}{n+1};$$

these numbers are called the *Catalan numbers.*

(a) Prove that all the Catalan numbers are integers (the first 5 Catalan numbers are 1, 2, 5, 14, 42).

Let $C(x) = \sum_{n=0}^{\infty} C_n x^n$.

(b) Prove that

$$(xC(x))' = \sum_{n=0}^{\infty} \binom{2n}{n} x^n.$$

(c) Deduce from (b) and Exercise 2.8(a) that (for $0 < |x| < \frac{1}{4}$)

$$C(x) = \frac{1 - \sqrt{1-4x}}{2x}.$$

(d) It follows from (c) that $xC(x)^2 - c(x) + 1 = 0$. Deduce that for any $n \geq 1$

$$C_n = \sum_{p+q=n-1} C_p C_q.$$

The remaining parts of this exercise have solutions based on the last formula.

(e) Let $*$ be a non-associative multiplication operation. Then the expression $a*b*c$ may mean $(a*b)*c$ or $a*(b*c)$. Similarly, $a*b*c*d$ may have 5 different meanings $((a*b)*c)*d,\ (a*b)*(c*d),\ (a*(b*c)),\ a*((b*c)*d),\ a*(b*(c*d))$. Prove that the number of meanings which the expression $a_1 * \cdots * a_{n+1}$ may have, depending on the order of multiplication, is $C_n$.

(f) Let $P$ be a convex $n$-gon. A triangulation of $P$ is a partition of it into $n-2$ triangles whose vertices are those of $P$. For example, a convex quadrilateral $ABCD$ has 2 triangulations: $ABC \cup ACD$ and $ABD \cup BCD$. A convex pentagon has 5 triangulations (draw them!). Prove that the number of triangulation of a convex $n$-gon is $C_{n-2}$.

See exercise 6.19 in R. Stanleys book [**73**] for 66 different combinatorial interpretations of the Catalan numbers; see also an on-line addendum [**74**] for many more.

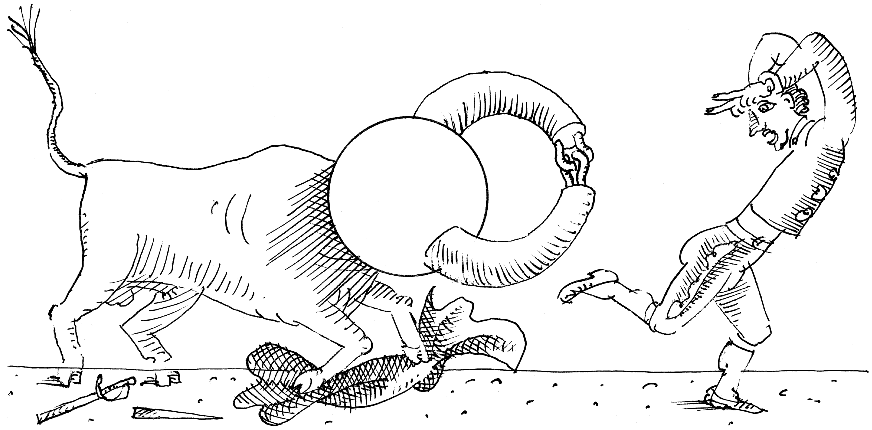

LECTURE 3

# On Collecting Like Terms, on Euler, Gauss and MacDonald, and on Missed Opportunities

**3.1 The Euler identity.** In the middle of 18-th century, Leonhard Euler became interested in the coefficients of the polynomial

$$\varphi_n(x) = (1-x)(1-x^2)(1-x^3)\dots(1-x^n).$$

He got rid of parentheses – and obtained the following amazing result:

| | | | | | | | | | |
|---|---|---|---|---|---|---|---|---|---|
| $\varphi_1(x) = 1 - x$ | | | | | | | | | |
| $\varphi_2(x) = 1 - x$ | $-x^2$ | $+x^3$ | | | | | | | |
| $\varphi_3(x) = 1 - x$ | $-x^2$ | | $+x^4$ | $+x^5$ | $-x^6$ | | | | |
| $\varphi_4(x) = 1 - x$ | $-x^2$ | | | $+2x^5$ | | | $-x^8$ | $-x^9$ | $+x^{10}$ |
| $\varphi_5(x) = 1 - x$ | $-x^2$ | | | $+x^5$ | $+x^6$ | $+x^7$ | $-x^8$ | $-x^9$ | $-x^{10}\dots$ |
| $\varphi_6(x) = 1 - x$ | $-x^2$ | | | $+x^5$ | | $+2x^7$ | | $-x^9$ | $-x^{10}\dots$ |
| $\varphi_7(x) = 1 - x$ | $-x^2$ | | | $+x^5$ | | $+x^7$ | $+x^8$ | | $-x^{10}\dots$ |
| $\varphi_8(x) = 1 - x$ | $-x^2$ | | | $+x^5$ | | $+x^7$ | | $+x^9$ | $\dots$ |
| $\varphi_9(x) = 1 - x$ | $-x^2$ | | | $+x^5$ | | $+x^7$ | | | $+x^{10}\dots$ |
| $\varphi_{10}(x) = 1 - x$ | $-x^2$ | | | $+x^5$ | | $+x^7$ | | | $\dots$ |

The dots mean the terms of the polynomials which have degrees $> 10$ (we have no room for them all: for example, the polynomial $\varphi_{10}(x)$ has degree 55).

Following Euler, let us make some observations. First (not surprisingly), the coefficients of every $x^m$ become stable when $n$ grows; more precisely, $\varphi_{m+1}(x), \varphi_{m+2}(x), \varphi_{m+3}(x), \dots$ all have the same coefficient of $x^m$. (It is obvious: $\varphi_{m+1}(x) = \varphi_m(x)(1-x^{m+1})$, $\varphi_{m+2}(x) = \varphi_{m+1}(1-x^{m+2})$, $\dots$; hence multiplication by $1-x^n$ with $n > m$ does not affect the coefficient of $x^m$.) Because of this, we can speak of the "stable" product

$$\varphi(x) = \varphi_\infty(x) = \prod_{n=1}^{\infty}(1-x^n);$$

it is not a polynomial any more, it is an infinite series containing arbitrarily high powers of $x$. We will sometimes call $\varphi(x)$ the *Euler function*.

The second observation (more surprising) is that when we collect terms in the product $(1-x)(1-x^2)\dots(1-x^n)$, many terms cancel. For example, when we multiply $(1-x)(1-x^2)\dots(1-x^{10})$, there will be 43 terms with $x$ to the powers 0 through 10, and only 5 of them $(1, -x, -x^2, x^5, x^7)$ survive the cancellations. This phenomenon becomes even more visible when we make further computations; here is, for example, the part of the series $\varphi(x)$ containing all the terms with $x$ to the power $\leq 100$:

$$\begin{aligned}\varphi(x) = 1 - x - x^2 + x^5 + x^7 \quad & -x^{12} - x^{15} + x^{22} + x^{26} - x^{35} - x^{40} \\ & +x^{51} + x^{57} - x^{70} - x^{77} + x^{92} + x^{100} + \dots\end{aligned}$$

Euler, who was extremely good with long computations, probably calculated almost this many terms. And after this he simply could not help noticing that all the non-zero coefficients of this series are ones and negative ones and that they go in a strictly predetermined order: two ones, two negative ones, two ones, two negative ones, and so on. If you look at the table below, you can guess (as Euler did) the powers of $x$ with non-zero coefficients:

| exponents | 0 | 1,2 | 5,7 | 12,15 | 22,26 | 35,40 | 51,57 | 70,77 | 92,100 |
|---|---|---|---|---|---|---|---|---|---|
| coefficients | 1 | −1 | 1 | −1 | 1 | −1 | 1 | −1 | 1 |

This table suggests that the term $x^{\frac{3n^2 \pm n}{2}}$ $(n \geq 0)$ appears with the coefficient $(-1)^n$, and there are no other non-zero terms. This conjecture may be stated in the form

$$\begin{aligned}(1-x)(1-x^2)(1-x^3)\dots \quad & = 1 - x - x^2 + x^5 + x^7 + \dots \\ & +(-1)^n x^{\frac{3n^2-n}{2}} + (-1)^n x^{\frac{3n^2+n}{2}} + \dots,\end{aligned}$$

or, shorter,

$$\prod_{n=1}^{\infty}(1-x^n) = 1 + \sum_{r=1}^{\infty}(-1)^r \left(x^{\frac{3r^2-r}{2}} + x^{\frac{3r^2+r}{2}}\right),$$

or, still shorter,

$$\prod_{n=1}^{\infty}(1-x^n) = \sum_{r=-\infty}^{\infty}(-1)^r x^{\frac{3r^2+r}{2}}.$$

By the way, the numbers $\dfrac{3n^2 \pm n}{2}$ arising in this formula are known as "pentagonal numbers" (or "Euler pentagonal numbers"). The reason for this name is clear from Figure 3.1 (the black-dotted pentagons have the same number of dots along each side).

It is quite interesting that although the proof of Euler's identity looks short and elementary (see Section 3.3), Euler, who did so many immensely harder things in mathematics, experienced difficulties with the proof. His "memoir" dedicated to this subject and published in 1751 under the title "Discovery of a most extraordinary law of the numbers concerning sums of their divisors" (the reader should wait until Section 3.5 for an explanation of this title) did not contain any proof of

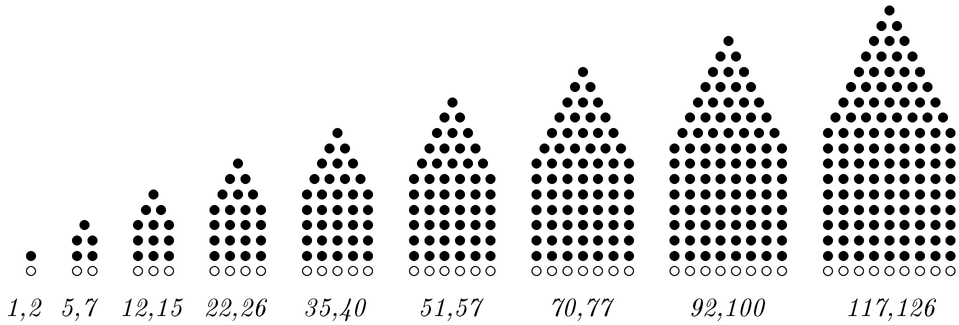


FIGURE 3.1. Pentagonal numbers

the identity. A relevant extract from the memoir (taken from the book of G. Polya [**62**]) is presented below.

**3.2 What Euler wrote about his identity.** "In considering the partitions of numbers, I examined, a long time ago, the expression

$$(1-x)(1-x^2)(1-x^3)(1-x^4)(1-x^5)(1-x^6)(1-x^7)(1-x^8)\dots,$$

in which the product is assumed to be infinite. In order to see what kind of series will result, I multiplied actually a great number of factors and found

$$1-x-x^2+x^5+x^7-x^{12}-x^{15}+x^{22}+x^{26}-x^{35}-x^{40}+\dots$$

The exponents of $x$ are the same which enter into the above formula; [1] also the signs $+$ and $-$ arise twice in succession. It suffices to undertake this multiplication and to continue it as far as it is deemed proper to become convinced of the truth of these series. Yet I have no other evidence for this, except a long induction which I have carried out so far that I cannot in any way doubt the law governing the formation of these terms and their exponents. I have long searched in vain for a rigorous demonstration of the equation between the series and the above infinite product $(1-x)(1-x^2)(1-x^3)\dots$, and I proposed the same question to some of my friends with whose ability in these matters I am familiar, but all have agreed with me on the truth of this transformation of the product into a series, without being able to unearth any clue of a demonstration."

**3.3 Proof of the Euler identity.** Let us collect terms in the product

$$(1-x)(1-x^2)(1-x^3)(1-x^4)\dots$$

We shall obtain the (infinite) sum of the terms

$$(-1)^k x^{n_1+\dots+n_k},\ k\geq 0,\ 0<n_1<\dots<n_k.$$

The total coefficient of $x^n$ will be

[1]This is a reference to a preceding part of the *Memoir* containing an explanation of the sequences $1,5,12,22,35,\dots$ and $2,7,15,26,40,\dots$.

$$\boxed{\begin{array}{c}\text{The number of partitions}\\ n = n_1 + \cdots + n_k\\ (0 < n_1 < \cdots < n_k)\\ \text{with even } k\end{array}} \quad - \quad \boxed{\begin{array}{c}\text{The number of partitions}\\ n = n_1 + \cdots + n_k\\ (0 < n_1 < \cdots < n_k)\\ \text{with odd } k\end{array}}$$

We want to prove that the two numbers in the boxes are usually the same, and in some exceptional cases differ by 1.

For a partition $n = n_1 + \cdots + n_k,\ 0 < n_1 < \cdots < n_k$ we denote by $s = s(n_1, \ldots, n_k)$ the maximal number of $n_i$'s, counting from $n_k$ to the left, which form a block of consecutive numbers (that is, of the form $a, a+1, \ldots, a+b$). In other words, $s$ is the maximal number satisfying the relation $n_{k-s+1} = n_k - s + 1$. (Thus, $1 \le s \le k$.)

We shall distinguish 3 types of partitions $n = n_1 + \cdots + n_k,\ 0 < n_1 < \cdots < n_k$

*Type 1*: $n_1 \le s$, excluding the case $n_1 = s = k$.

*Type 2*: $n_1 > s$, excluding the case $n_1 = s + 1 = k + 1$.

*Type 3*: the two excluded cases, $n_1 = s = k$ or $n_1 = s + 1 = k + 1$.

Here is a $1-1$ correspondence between partitions of $n$ of Type 1 and partitions of $n$ of Type 2:

$$\begin{array}{cccccc} n_1 n_2 \ldots \overbrace{\ldots\ldots\ldots n_{k-1} n_k}^{s \text{ consecutive numbers}} & \mapsto & & n_2 \ldots \overbrace{\ldots\ldots n_{k-1} n_k}^{s} & \mapsto & n_2 \ldots \underset{+1}{n_{k-n_1+1}} \ldots \underset{+1}{n_k} \\ & & \downarrow & \uparrow \ldots \uparrow \quad \uparrow & & \\ & & n_1 & \longrightarrow \underbrace{1 \ldots 1 \quad 1}_{n_1} & & \end{array}$$

In words: we remove the number $n_1$ from the partition, then split it into $n_1$ ones, and then add these ones to $n_1$ last (biggest) terms of the partition (it is important that if $s = n_1$, then $s < k$; otherwise we shall have to remove $n_1$ and then to add 1 to $n_1$, but it is not there anymore). In formulas:

$$(n_1, \ldots, n_k) \mapsto (m_1, \ldots, m_{k-1}),\ m_i = \begin{cases} n_{i+1}, & \text{if } i < k - n_1, \\ n_{i+1} + 1, & \text{if } i \ge k - n_1. \end{cases}$$

Examples:

$$13 = 1 + 3 + 4 + 5;\ (1, 3, 4, 5) \mapsto (\not{1}, 3, 4, \underset{+1}{5}) = (3, 4, 6)$$
$$37 = 2 + 5 + 9 + 10 + 11;\ (2, 5, 9, 10, 11) \mapsto (\not{2}, 5, 9, \underset{+1}{10}, \underset{+1}{11}) = (5, 9, 11, 12)$$

The partition $m_1, \ldots, m_{k-1}$ belongs to Type 2. Indeed, $m_1 \ge n_2 > n_1 = s(m_1, \ldots, m_{k-1})$ and if $m_1 = s(m_1, \ldots, m_{k-1}) + 1 = (k-1) + 1$, then, on one hand, $m_1 = n_1 + 1$, and on the other hand, $n_1 + 1 = k$, hence $m_i = n_{i+1} + 1$, if $i \ge k - n_1 = 1$, hence $m_1 = n_2 + 1$; this is not possible, since $n_2 > n_1$.

The fact that the above transformation is $1 - 1$ follows from the existence of an inverse transformation:

$$\begin{array}{cccccc} m_1 \ldots \overbrace{\ldots\ldots\ldots m_{k-1}}^{s \text{ consecutive numbers}} & \mapsto & & m_1 \ldots \underset{-1 \cdots -1}{\overbrace{\ldots\ldots m_{k-1}}^{s}} & \mapsto & s\, m_1 \ldots \underset{-1}{m_{k-s}} \ldots \underset{-1}{m_{k-1}} \\ & & \uparrow & \downarrow \ \ldots \ \downarrow & & \\ & & s & \longleftarrow 1 \ \ldots \ 1 & & \end{array}$$

(that is, we subtract 1 from each of the $s$ consecutive numbers in the right end, collect these ones into one number $s$ and place this $s$ before $m_1$) or, in formulas:

$$(m_1, \dots, m_{k-1}) \mapsto (n_1, \dots, n_k),\ n_i = \begin{cases} s, & \text{if } i = 1, \\ m_{i-1}, & \text{if } 2 \le i \le k-s, \\ m_{i-1} - 1, & \text{if } i > k-s. \end{cases}$$

Examples:

$$(3, 4, 6) \mapsto (3, 4, \underset{-1}{6}) \mapsto (1, 3, 4, 5)$$
$$(5, 9, 11, 12) \mapsto (5, 9, \underset{-1}{11}, \underset{-1}{12}) \mapsto (2, 5, 9, 10, 11)$$

The terms

$$(-1)^k x^{n_1+\dots+n_k} \qquad \text{and} \qquad (-1)^{k-1} x^{m_1+\dots+m_{k-1}}$$

corresponding to each other cancel in the product $(1-x)(1-x^2)(1-x^3)\dots$, and there remain only terms corresponding to partitions of Type 3. These are

$$k\, k+1 \, \dots \, 2k-1 \qquad \text{and} \qquad k+1\, k+2 \, \dots \, 2k,$$

and the corresponding terms in $(1-x)(1-x^2)(1-x^3)\dots$ are

$$(-1)^k x^{k+(k+1)+\dots+(2k-1)} = (-1)^k x^{\frac{k(3k-1)}{2}}$$

and

$$(-1)^k x^{(k+1)+(k+2)+\dots+2k} = (-1)^k x^{\frac{k(3k+1)}{2}}.$$

□

Next we shall show two applications of the Euler identity.

**3.4 First application: the partition function.** The word "partition" which we have been using before as a common English word, actually has a well established meaning in combinatorics. From now on, we will use this word according to the tradition: we call a partition of a number $n$ a sequence of integers $n_1, \dots, n_k$ such that $n = n_1 + \dots + n_k$ and $0 < n_1 \le \dots \le n_k$. We hope that this terminological shift will not cause any difficulties, but still want to mention that partitions considered in Section 3.3 are partitions of a special kind: with all parts $n_i$ different.

For a positive integer $n$, denote by $\mathbf{p}(n)$ the number of partitions $n = n_1 + \dots + n_k,\ k > 0,\ 0 < n_1 \le \dots \le n_k$. Compute $\mathbf{p}(n)$ for small values of $n$:

$$\begin{aligned} \mathbf{p}(1) &= 1 \\ \mathbf{p}(2) &= 2 \quad (2 = 1+1) \\ \mathbf{p}(3) &= 3 \quad (3 = 1+2 = 1+1+1) \\ \mathbf{p}(4) &= 5 \quad (4 = 1+3 = 2+2 = 1+1+2 = 1+1+1+1) \end{aligned}$$

Can you find $\mathbf{p}(10)$? It is not hard, although you might not be able to get the right result from the first try. The answer is $\mathbf{p}(10) = 42$. And what about $\mathbf{p}(20)$? $\mathbf{p}(50)$? $\mathbf{p}(100)$? It turns out that we can find these numbers relatively quickly if we use the Euler identity.

Consider the series

$$\mathbf{p}(x) = 1 + x + 2x^2 + 3x^3 + 5x^4 + \dots = 1 + \sum_{r=1}^{\infty} \mathbf{p}(r) x^r.$$

THEOREM 3.1. $\varphi(x)\mathbf{p}(x) = 1$.

Proof.

$$\frac{1}{\varphi(x)} = \frac{1}{\prod_{n=1}^{\infty}(1-x^n)} = \prod_{n=1}^{\infty}(1+x^n+x^{2n}+x^{3n}+\dots)$$

(thus, the series $\dfrac{1}{\varphi(x)}$ is itself a product of infinitely many series). What is the coefficient of $x^r$ in the product

$$(1+x+x^2+\dots)(1+x^2+x^4+\dots)(1+x^3+x^6+\dots)\dots ?$$

We need to take one summand from each factor (only finitely many of them should be different from 1) and multiply them up. We get:

$$x^{1\cdot k_1}\cdot x^{2\cdot k_2}\cdot\dots\cdot x^{m\cdot k_m} = x^{k_1+2k_2+\dots+mk_m}.$$

We want to count the number of such products with $k_1+2k_2+\dots+mk_m = r$, that is, the number of presentations

$$r = k_1+2k_2+\dots+mk_m = \underbrace{1+\dots+1}_{k_1}+\underbrace{2+\dots+2}_{k_2}+\dots+\underbrace{m+\dots+m}_{k_m},$$

that is, the number of partitions of $r$. Thus, the coefficient of $x^r$ in $\dfrac{1}{\varphi(x)}$ is equal to $\mathbf{p}(r)$. □

Now use the Euler identity:

$$(1-x-x^2+x^5+x^7-x^{12}-x^{15}\dots)(1+\mathbf{p}(1)x+\mathbf{p}(2)x^2+\mathbf{p}(3)x^3+\dots) = 1,$$

that is, the coefficient of $x^n$ with any $n>0$ in this product is equal to 0. We get a chain of equalities:

$$\begin{array}{ll}
\mathbf{p}(1) & -1 = 0\\
\mathbf{p}(2) & -\mathbf{p}(1)-1 = 0\\
\mathbf{p}(3) & -\mathbf{p}(2)-\mathbf{p}(1) = 0\\
\mathbf{p}(4) & -\mathbf{p}(3)-\mathbf{p}(2) = 0\\
\mathbf{p}(5) & -\mathbf{p}(4)-\mathbf{p}(3)+1 = 0\\
\mathbf{p}(6) & -\mathbf{p}(5)-\mathbf{p}(4)+\mathbf{p}(1) = 0\\
\mathbf{p}(7) & -\mathbf{p}(6)-\mathbf{p}(5)+\mathbf{p}(2)+1 = 0\\
\mathbf{p}(8) & -\mathbf{p}(7)-\mathbf{p}(6)+\mathbf{p}(3)+\mathbf{p}(1) = 0
\end{array}$$

or

$$\mathbf{p}(n) = \mathbf{p}(n-1)+\mathbf{p}(n-2)-\mathbf{p}(n-5)-\mathbf{p}(n-7)+\mathbf{p}(n-12)+\mathbf{p}(n-15)-\dots$$

where we count $\mathbf{p}(0)$ as 1 and $\mathbf{p}(m)$ with $m<0$ as 0. We can use this as a tool for an inductive computation of the numbers $\mathbf{p}(n)$:

$$\begin{array}{rl}
\mathbf{p}(5) & = \mathbf{p}(4)+\mathbf{p}(3)-1 = 5+3-1 = 7\\
\mathbf{p}(6) & = \mathbf{p}(5)+\mathbf{p}(4)-\mathbf{p}(1) = 7+5-1 = 11\\
\mathbf{p}(7) & = \mathbf{p}(6)+\mathbf{p}(5)-\mathbf{p}(2)-1 = 15+11-3-1 = 22\\
\mathbf{p}(8) & = \mathbf{p}(7)+\mathbf{p}(6)-\mathbf{p}(3)-\mathbf{p}(1) = 15+11-3-1 = 22\\
\mathbf{p}(9) & = \mathbf{p}(8)+\mathbf{p}(7)-\mathbf{p}(4)-\mathbf{p}(2) = 22+15-5-2 = 30\\
\mathbf{p}(10) & = \mathbf{p}(9)+\mathbf{p}(8)-\mathbf{p}(4)-\mathbf{p}(2) = 30+22-7-3 = 42
\end{array}$$

and further computations show that $\mathbf{p}(20) = 627$, $\mathbf{p}(50) = 204{,}226$, $\mathbf{p}(100) = 190{,}569{,}791$.

It is worth mentioning that our recursive formula for the function $\mathbf{p}$ may be used for constructing a very simple machine for computing the values of this function. This machine is shown in Figure 3.2. Take a sheet of graph paper and cut a long strip as shown in the left side of Figure 3.2 (the longer your strip is, the more values of the function $\mathbf{p}$ you will be able to compute). In the upper cell of the strip draw a (right) arrow. Then write the plus signs in the cells numbered 1,2,12,15,35,40,... (counting down from the arrow) and the minus sign in the cells numbered 5,7,22,26,... Write 1 (it is $\mathbf{p}(0)$) in the lower left corner of the sheet of graph paper. Attach the right edge of your strip to the left edge of the sheet in such a way that the arrow is against 1. Then move the strip upwards, and every time when the arrow is directed into an empty cell (in the left column of the sheet) write in this cell the sum of numbers against the pluses minus the sum of numbers against the minuses. The numbers written are consecutive values of the function $\mathbf{p}$. This procedure is shown in Figure 3.2, up to $\mathbf{p}(12)$.

In conclusion we display an asymptotic formula for $\mathbf{p}(n)$ due to Rademacher:

$$\mathbf{p}(n) \sim \frac{1}{4n\sqrt{3}}\, e^{\frac{2\pi}{\sqrt{6}}\sqrt{n}}.$$

This $\sim$ means that the ratio of the expression in the right hand side to $\mathbf{p}(n)$ approaches 1 when $n$ goes to infinity. Among other things, this formula reveals that $\mathbf{p}(n)$ has a property that is rare for the functions usually occurring in mathematics: it grows faster than any polynomial but slower than any exponential function $c^n$.

**3.5 Second application: the sum of divisors.** This application gave the name to Euler's *memoir*. In this section, we follow Euler's ideas.

For a positive integer $n$, denote by $\mathbf{d}(n)$ the sum of divisors of $n$. For example,

$$\begin{aligned}
\mathbf{d}(4) &= 1+2+4=7,\\
\mathbf{d}(1000) &= 1+2+4+5+8+10+20+25+40+50+100+125\\
&\qquad +200+250+500+1000=2340,\\
\mathbf{d}(1001) &= 1+7+11+13+77+91+143+1001=1344.
\end{aligned}$$

Unlike the numbers $\mathbf{p}(n)$, the numbers $\mathbf{d}(n)$ are easy to compute, there is a simple explicit formula for them. Namely, if $n = 2^{k_2}3^{k_3}\dots p^{k_p}$ is a prime factorization of $p$, then

$$\mathbf{d}(n) = (2^{k_2+1}-1)\cdot\frac{3^{k_3+1}-1}{2}\dots\frac{p^{k_p+1}-1}{p-1}$$

(see Exercise 3.3). Furthermore, it is interesting that there is a recursive formula for the numbers $\mathbf{d}(n)$, very similar to the formula for $\mathbf{p}(n)$ in Section 3.4 and relating the number $\mathbf{d}(n)$ to seemingly unrelated numbers $\mathbf{d}(n-1), \mathbf{d}(n-2), \mathbf{d}(n-5), \dots$. (For Euler, it was a step towards understanding the nature of the distribution of prime numbers.)

Let

$$\mathbf{d}(x) = \sum_{r=1}^{\infty}\mathbf{d}(r)x^r = x+3x^2+4x^3+7x^4+6x^5+12x^6+\dots$$

THEOREM 3.2. $\varphi(x)\mathbf{d}(x) + x\varphi'(x) = 0$.

Here $\varphi'(x)$ means the derivative of $\varphi(x)$. Thus,

$$x\varphi'(x) = -x-2x^2+5x^5+7x^7-12x^{12}-15x^{15}+\dots$$

Proof of Theorem. Consider the equality

$$\sum_{n=1}^{\infty} \frac{nx^n}{1-x^n} = \sum_{n=1}^{\infty} n(x^n + x^{2n} + x^{3n} + \dots).$$

If $d_1, d_2, \dots, d_m$ are divisors of $r$ (including 1 and $r$), then $x^r$ appears in the last sum as $d_i \cdot x^{d_i \cdot \frac{r}{d_i}}$ for every $d_i$, and the total coefficient of $x^r$ will be $d_1 + d_2 + \dots + d_m = \mathbf{d}(r)$. Thus, the sum is $\sum_{r=1}^{\infty} \mathbf{d}(r)x^r = \mathbf{d}(x)$, that is,

$$\mathbf{d}(x) = \sum_{n=1}^{\infty} \frac{nx^n}{1-x^n}.$$

But

$$\frac{nx^n}{1-x^n} = -x \cdot [\ln(1-x^n)]',$$

thus

$$\mathbf{d}(x) = -x \left( \sum_{n=1}^{\infty} \ln(1-x^n) \right)' = -x \left( \ln \prod_{n=1}^{\infty} (1-x^n) \right)'$$

$$= -x \cdot [\ln \varphi(x)]' = -\frac{x\varphi'(x)}{\varphi(x)}$$

which shows that $\mathbf{d}(x)\varphi(x) + x\varphi'(x) = 0$. □

Equating to 0 the coefficient of $x^n$, $n > 0$, on the left hand side of the last equality, we find that

$$\mathbf{d}(n) \quad -\mathbf{d}(n-1) - \mathbf{d}(n-2) + \mathbf{d}(n-5) + \mathbf{d}(n-7) - \dots$$

$$= \begin{cases} -(-1)^m \dfrac{3m^2 \pm m}{2}, & \text{if } n = \dfrac{3m^2 \pm m}{2}, \\ 0, & \text{if } n \text{ is not a pentagonal number.} \end{cases}$$

It is better to formulate this in the following form:

$$\mathbf{d}(n) = \mathbf{d}(n-1) + \mathbf{d}(n-2) - \mathbf{d}(n-5) - \mathbf{d}(n-7) + \mathbf{d}(n-12) + \mathbf{d}(n-15) - \dots$$

where $\mathbf{d}(k)$ with $k < 0$ is counted as 0, and $\mathbf{d}(0)$ (if it appears in this formula) is counted as $n$.

**3.6 The identities of Gauss and Jacobi.** About 70 years after Euler's discovery, another great mathematician, Carl-Friedrich Gauss, proved that the *cube* of the Euler function provides a series even more remarkable than the Euler series:

$$\varphi(x)^3 = (1-x)^3(1-x^2)^3(1-x^3)^3 \cdots = 1 - 3x + 5x^3 - 7x^6 + 9x^{10} - 11x^{15} \dots$$

or

$$\prod_{n=1}^{\infty} (1-x^n)^3 = \sum_{r=0}^{\infty} (-1)^r (2r+1) x^{\frac{r(r+1)}{2}}.$$

The Gauss identity appears even more remarkable, if we notice that the *square* of the Euler function does not reveal, at least at the first glance, any interesting properties:

$$\varphi(x)^2 = 1 - 2x - x^2 + 2x^3 + x^4 + 2x^5 - 2x^6 - 2x^8 - 2x^9 + x^{10} \dots$$

Several proof are known for the Gauss identity, and they belong to very different parts of mathematics, such as homological algebra, complex analysis, and hyperbolic geometry (this fact by itself may be regarded as an indication that the result is very deep). There exists also an elementary combinatorial proof (which we shall discuss in Section 3.7). Most of these proofs (including the proof in Section 3.7) yield, actually, a stronger result: the two-variable Jacobi identity:

$$\prod_{n=1}^{\infty}(1+y^{-1}z^{2n-1})(1+yz^{2n-1})(1-z^{2n}) = \sum_{r=-\infty}^{\infty} y^r z^{r^2}. \tag{3.1}$$

Before proving it, we shall show that it implies the Gauss identity.

Deducing the Gauss identity from the Jacobi identity. Differentiate the two sides of the Jacobi identity (3.1) with respect to $z$, then put $y=-z$, and then put $z^2=x$.

To differentiate a product (even infinite) we need to take the derivative of one factor, leaving all the rest unchanged, and then add up all the resulting products:

$$(f_1f_2f_3\dots)' = f_1'f_2f_3\dots + f_1f_2'f_3\dots + f_1f_2f_3'\dots + \dots$$

But the very first factor in the left hand side of the Jacobi identity, $(1+y^{-1}z)$, is annihilated by the substitution $y=-z$. Hence of all the summands in the derivative of the product, only one survives this substitution, and this is

$$(1+y^{-1}z)_z'(1+yz)(1-z^2)\prod_{n=2}^{\infty}(1+y^{-1}z^{2n-1})(1+yz^{2n-1})(1-z^{2n}).$$

After the substitution $y=-z$ we get (since $(1+y^{-1}z)_z' = y^{-1}$):

$$-z^{-1}(1-z^2)^2\prod_{n=2}^{\infty}(1-z^{2n-2})(1-z^{2n})^2 = -z^{-1}\prod_{n=1}^{\infty}(1-z^{2n})^3.$$

The whole identity (3.1) becomes (since $(y^r z^{r^2})_z' = r^2 y^r z^{r^2-1}$)

$$\prod_{n=1}^{\infty}(1-z^{2n})^3 = -z\sum_{r=-\infty}^{\infty} r^2(-1)^r z^r z^{r^2-1} = \sum_{r=-\infty}^{\infty}(-1)^{r+1}r^2 z^{r^2+r},$$

which becomes, after the substitution $z^2=x$,

$$\varphi(x)^3 = \sum_{r=-\infty}^{\infty}(-1)^{r+1}r^2x^{\frac{r^2+r}{2}}. \tag{3.2}$$

It remains to notice that the $r$-th and the $(-r-1)$-th terms on the right hand side of (3.2) are like terms: $\dfrac{(-r-1)^2+(-r-1)}{2} = \dfrac{r^2+r}{2}$. Hence,

$$\begin{aligned}\textstyle\sum_{r=-\infty}^{\infty}(-1)^{r+1}r^2x^{\frac{r^2+r}{2}} &= \textstyle\sum_{r=0}^{\infty}[(-1)^{r+1}r^2+(-1)^{-r}(-r-1)^2]x^{\frac{r^2+r}{2}}\\ &= \textstyle\sum_{r=0}^{\infty}(-1)^r(2r+1)x^{\frac{r^2+r}{2}}\end{aligned}$$

as required. □

We remark, in conclusion, that the Jacobi identity may be used to prove other one-variable identities. For example, if we simply plug $y=-1$ in the Jacobi identity

(3.1) (and then replace $z$ by $x$), we get a remarkable identity

$$(1-x)^2(1-x^2)(1-x^3)^2(1-x^4)\cdots = \sum_{r=-\infty}^{\infty}(-1)^r x^{r^2} = 1+2\sum_{r=1}^{\infty}(-1)^r x^{r^2}$$

also known to Gauss. By the way, the left hand side of this identity is $\dfrac{\varphi(x)^2}{\varphi(x^2)}$; hence, we can get from it also a formula for $\varphi(x)^2$;

$$\varphi(x)^2 = \sum_{r=-\infty}^{\infty}(-1)^r x^{r^2}\cdot\sum_{s=-\infty}^{\infty}(-1)^s x^{3s^2+s},$$

not as remarkable, however, as the formulas for $\varphi(x)$ and $\varphi(x)^3$.

For another identity involving $\varphi(x)$ and following from the Jacobi identity, see Exercise 3.4 .

**3.7 Proof of the Jacobi identity.** This proof is due to Zinovy Leibenzon; we follow his article [**50**] and use his terminology.

Rewrite the Jacobi identity as

$$\begin{aligned}\prod_{n=1}^{\infty}(1+yz^{2n-1})(1+y^{-1}z^{2n-1}) &= \prod_{n=1}^{\infty}(1-z^{2n})^{-1}\sum_{r=-\infty}^{\infty}y^r z^{r^2}\\ &= \mathbf{p}(z^2)\sum_{r=-\infty}^{\infty}y^r z^{r^2} = \sum_{n=0}^{\infty}\mathbf{p}(n)z^{2n}\sum_{r=-\infty}^{\infty}y^r z^{r^2}\end{aligned}$$

and compare the coefficients of $y^r z^{2n+r^2}$. On the right hand side, the coefficient is, obviously, $\mathbf{p}(n)$. On the left hand side, $y^r x^{2n+r^2}$ may appear as a product

$$yz^{2\alpha_1-1}\cdot\dots\cdot yz^{2\alpha_s-1}\cdot y^{-1}s^{2\beta_1-1}\cdot\dots\cdot y^{-1}z^{2\beta_t-1}$$

where $0<\alpha_1<\dots<\alpha_s,\ 0<\beta_1<\dots<\beta_t,\ s-t=r$, and

$$\sum_{i=1}^{s}(2\alpha_i-1)+\sum_{j=1}^{t}(2\beta_j-1)=2n+r^2.$$

Thus, the coefficient of $y^r x^{2n+r^2}$ is equal to the number of sets $((\alpha_1,\dots,\alpha_s),(\beta_1,\dots,\beta_t))$ with the properties indicated. We denote this number by $\mathbf{q}(n,r)$. To prove the Jacobi identity, we need to prove the following.

PROPOSITION 3.1. $\mathbf{q}(n,r)=\mathbf{p}(n)$ *(in particular,* $\mathbf{q}(n,r)$ *does not depend on* $r$*).*

To prove the proposition, we need the following construction.

By a *chain* we mean an infinite, in both directions, sequence of symbols of two types: ○ (*circles*) and | (*sticks*), such that to the left of some place only circles occur, and to the right of some place only sticks occur. Examples:

...... ○ ○ ○ | | ○ | ○ | ○ ○ | | | | ......

...... ○ ○ | | | | ○ ○ ○ | ○ | | | | ......

We do not distinguish between chains obtained from each other by translations to the left or to the right.

The *height* of a chain $A$, $h(A)$, is defined as the number of *inversions*, that is, pairs of symbols (not necessarily consecutive), of which the left one is a stick and the right one is a circle. For the two examples above, the heights are 13 and 17.

We shall assume that the distance between any two neighboring symbols in a chain is 2, and that between them, at distance 1 from each, there is a *lacuna*. The lacunas of a given chain can be naturally enumerated: we say that a lacuna $T$ has index $r$, if the number of sticks to the left of $T$ minus the number of circles to the right of $T$ is equal to $r$. It is clear that when we move from left to right the index of the lacuna increases by 1. Example:

$$\cdots\cdots \bigcirc\ {}^{-6}\ \bigcirc\ {}^{-5}\ \bigcirc\ {}^{-4}\ |\ {}^{-3}\ |\ {}^{-2}\ \bigcirc\ {}^{-1}\ |\ {}^{0}\ \bigcirc\ {}^{1}\ |\ {}^{2}\ \bigcirc\ {}^{3}\ \bigcirc\ {}^{4}\ |\ {}^{5}\ |\ {}^{6}\ |\cdots\cdots$$

Proof of Proposition. We shall compute, in two ways, the number of chains of height $n$.

*First way.* For a chain $A$ of height $n$, denote by $n_i$ the number of circles to the right of the $i$-th stick from the left. Obviously, $n_1 \geq n_2 \geq \dots$; $n_i = 0$ for $i$ large enough; and $n_1 + n_2 + \dots = n$. These numbers $n_1, n_2, \dots$ determine the chain and may take arbitrary values (if they satisfy the condition above). Thus, the number of chains of height $n$ is $\mathbf{p}(n)$.

*Second way.* Fix an integer $r$, and consider the lacuna $T$ number $r$. Let there be $s$ sticks to the left of $T$ and $t$ circles to the right of $T$; thus, $s-t=r$. Let the distances of the sticks to the left of $T$ to $T$ be (in the ascending order) $2\alpha_1 - 1, \dots, 2\alpha_s - 1$ and the distances of the circles to the right of $T$ to $T$, in the ascending order, be $2\beta_1 - 1, \dots, 2\beta_t - 1$. Example:

| | | | | | | | | | | | | | | | | | |
|---|---|---|---|---|---|---|---|---|---|---|---|---|---|---|---|---|---|
| | | | | $\alpha_4$ | | | | $\alpha_3$ | $\alpha_2$ | | $\alpha_1$ | $\beta_1$ | | | $\beta_2$ | | |
| | | | | 8 | | | | 4 | 3 | | 1 | 1 | | | 4 | | |
| $\cdots$ | $\bigcirc$ | $\bigcirc$ | $\bigcirc$ | $\vert$ | $\bigcirc$ | $\bigcirc$ | $\bigcirc$ | $\vert$ | $\vert$ | $\bigcirc$ | $\vert_T$ | $\bigcirc$ | $\vert$ | $\vert$ | $\bigcirc$ | $\vert$ | $\vert\cdots$ |

The numbers $s, t, \alpha_1, \dots, \alpha_s, \beta_1, \dots, \beta_t$ determine the chain. Let us prove that

$$2n + r^2 = \sum_{i=1}^{s} (2\alpha_i - 1) + \sum_{j=1}^{t} (2\beta_j - 1).$$

There are 3 kinds of inversions in the chain $A$: (1) both the circle and the stick are to the left of $T$; (2) both the circle and the stick are to the right of $T$, and (3) the circle is to the right of $T$ and the stick is to the left of $T$. Between a stick at distance $2\alpha_i - 1$ to the left of $T$ and $T$ (including this stick), there are $\alpha_i$ symbols, of which $i$ are sticks and $\alpha_i - i$ are circles; thus this stick participates in $\alpha_i - i$ inversions of the first kind, and the total number of inversions of the 1-st kind is $\sum_{i=1}^{s} (\alpha_i - i)$. Similarly, there are $\sum_{j=1}^{t} (\beta_j - j)$ inversions of 2-nd kind, and, obviously, the number of inversions of the 3-rd kind is $st$. Thus,

$$\begin{aligned} n &= \sum_{i=1}^{s}(\alpha_i - i) + \sum_{j=1}^{t}(\beta_j - j) + st \\ &= \sum_{i=1}^{s}\alpha_i + \sum_{j=1}^{t}\beta_j - \frac{s(s+1)}{2} + st - \frac{t(t+1)}{2} \\ &= \sum_{i=1}^{s}\alpha_i + \sum_{j=1}^{t}\beta_j - \frac{s^2+s-2st+t^2+t}{2} \\ &= \sum_{i=1}^{s}\alpha_i + \sum_{j=1}^{t}\beta_j - \frac{r^2+s+t}{2}, \end{aligned}$$

$$2n + r^2 = 2\sum_{i=1}^{s}\alpha_i + 2\sum_{j=1}^{t}\beta_j - s - t = \sum_{i=1}^{s}(2\alpha_i - 1) + \sum_{j=1}^{t}(2\beta_j - 1).$$

We see that the number of chains of height $n$ is $\mathbf{q}(n, r)$.

Thus, $\mathbf{p}(n) = \mathbf{q}(n, r)$ which proves the Proposition and the Jacobi identity. $\square$

**3.8 Powers of the Euler function.** Thus far, we know how the series for $\varphi(x)$ and $\varphi(x)^3$ look like, but we have nothing equally good for $\varphi(x)^2$. And what about the series $\varphi(x)^4, \varphi(x)^5$, etc.? In other words, for which $n$ is there a formula for the coefficients of the series $\varphi(x)^n$? To answer this informal (that is, not rigorously formulated) question, we shall use the following semi-formal criterion. If, for some $n$, there are many zeroes among the coefficients of the series $\varphi(x)^n$, this might mean that there is a formula for $\varphi(x)^n$ resembling the formulas of Euler and Gauss. (However, if there are only few zeroes, or no zeroes at all, this cannot be considered as a clear indication that a formula does not exist.) It is a matter of a simple computer program to find the number of zeroes among, say, the first 500 coefficients of $\varphi(x)^n$. We denote this number by $c(n)$, and here are the values of $c(n)$ for $n \leq 35$:

| $n$ | 1 | 2 | 3 | 4 | 5 | 6 | 7 | 8 |
|---|---|---|---|---|---|---|---|---|
| $c(n)$ | 464 | 243 | 469 | 158 | 0 | 212 | 0 | 250 |

| $n$ | 9 | 10 | 11-13 | 14 | 15 | 16-25 | 26 | 27-35 |
|---|---|---|---|---|---|---|---|---|
| $c(n)$ | 0 | 151 | 0 | 172 | 2 | 0 | 80 | 0 |

We can make the following observation. For $n = 1, 3$, there are very many zeroes (we already know this); for $n = 2, 4, 6, 8, 10, 14, 26$, the number of zeroes is substantial; for $n = 15$, there are 2 zeroes (which cannot be considered as a serious evidence of anything[2]); for $n = 5, 7, 9, 11-13, 16-25, 27-35$, there are

[2]Although a formula for $\varphi(x)^{15}$ exists, see below.

no zeroes at all. We should not be surprised by a substantial amount of zeroes for $n = 2, 4, 6$: the series for $\varphi(x)$ and $\varphi(x)^3$ are so sparse that their products $\varphi(x)^2 = \varphi(x) \cdot \varphi(x)$, $\varphi(x)^4 = \varphi(x) \cdot \varphi(x)^3$, $\varphi(x)^6 = \varphi(x)^3 \cdot \varphi(x)^3$ may lack some powers of $x$ even before collecting like terms. For example, the numbers $11, 18, 21$ (and many others) cannot be presented as sums of pairs of numbers of the form $\frac{3n^2 \pm n}{2}$, and for this reason there are no terms $x^{11}, x^{18}, x^{21}$ in the series for $\varphi(x)^2$. For a similar reason, there are no terms $x^9, x^{14}, x^{19}$ in the series for $\varphi(x)^4$, and no terms $x^5, x^8, x^{14}$ in the series for $\varphi(x)^6$. But why are there many zeroes in the series for $\varphi(x)^8, \varphi(x)^{10}, \varphi(x)^{14}$, and $\varphi(x)^{26}$?

It turns out that there are formulas for these powers of the Euler function, not so simple as the formulas of Euler and Gauss, but also deep and beautiful. (There are also formulas for some other powers of the Euler function, but this is not reflected in our table.) As an illustration, let us show a formula for $\varphi(x)^8$ due to Felix Klein:

$$\varphi(x)^8 = \sum \left[\frac{1}{3} + \frac{3}{2}(3klm - kl - km - lm)\right] x^{-(kl+km+lm)}$$

where the summation on the right hand side is taken over all triples $(k, l, m)$ of integers such that $k + l + m = 1$. One can see from the formula that if a number $r$ cannot be presented as $-(kl + km + lm)$ with $k + l + m = 1$, then the series for $\varphi(x)^8$ does not contain $x^r$. For example, it does not contain $x^r$ if $r = 4s + 3$ (with $s$ integral) or if $r = 13, 18, 28, 29$ (see Exercise 3.5).

We see from all this that there exist some "privileged exponents" $n$ for which a comprehensible formula for $\varphi(x)^n$ exists. The mystery of privileged exponents was resolved in 1972 by Ian MacDonald (see Section 3.9 for a partial statement of his results). An account of this discovery is contained in an emotionally written article of F. Dyson [**26**]. A couple of words should be said about Dyson and his article. Freeman Dyson is one of the most prominent physicists of our time. He started his career as a mathematician and has some well known works in classical combinatorics and number theory. The goal of his article was to show how lack of communication between physicists and mathematicians resulted in a catastrophic delay of some major discoveries in both disciplines. Below is an excerpt from Dyson's article related to our subject.

**3.9 Dyson's story.** "I begin with a trivial episode from my own experience, which illustrates vividly how the habit of specialization can cause us to miss opportunities. This episode is related to some recent and beautiful work by Ian MacDonald on the properties of affine root systems of the classical Lie algebras.

I started life as a number theorist and during my undergraduate days at Cambridge I sat at the feet of the already legendary figure G. H. Hardy. It was clear even to an undergraduate in those days that number theory in the style of Hardy and Ramanujan was old-fashioned and did not have a great and glorious future ahead of it. Indeed, Hardy in a published lecture on the $\tau$-function of Ramanujan had himself described this subject as "one of the backwaters of mathematics". The $\tau$-function is defined as the coefficient in the modular form

$$\sum_{n=1}^{\infty} \tau(n) x^{n-1} = \varphi(x)^{24} = \prod_{m=1}^{\infty} (1 - x^m)^{24}. \tag{3.3}$$

Ramanujan discovered a number of remarkable arithmetical properties of $\tau(n)$. The proof and generalization of these properties by Mordell, Hecke, and others played a significant part in the development of the theory of modular forms. But the $\tau$-function itself has remained a backwater, far from the mainstream of mathematics, where amateurs can dabble to their hearts' content undisturbed by competition from professionals.[3] Long after I became a physicist, I retained a sentimental attachment to the $\tau$-function, and as a relief from the serious business of physics I would from time to time go back to Ramanujan's papers and meditate on the many intriguing problems that he left unsolved. Four years ago, during one of these holidays from physics, I found a new formula for the $\tau$-function, so elegant that it is rather surprising that Ramanujan did not think of it himself. The formula is

$$\tau(n) = \sum \frac{\prod_{1\le i<j\le 5}(a_i - a_j)}{1!2!3!4!}, \tag{3.4}$$

summed over all sets of integers $a_1, \dots, a_5$ with $a_i \equiv i \bmod 5$, $a_1 + \dots + a_5 = 0, a_1^2 + \dots + a_5^2 = 10n^2$. This can also be written as a formula for the 24-th power of the Euler function $\varphi$ according to (3.3). I was led to it by a letter from Winquist who discovered a similar formula for the 10-th power of $\varphi$. Winquist also happens to be a physicist who dabbles in old-fashioned number theory in his spare time.

Pursuing these identities further by my pedestrian methods, I found that there exists a formula of the same degree of elegance as (3.4) for all $d$-th powers of $\varphi$ whenever $d$ belongs to the following sequence of integers:

$$d = 3, 8, 10, 14, 15, 21, 24, 26, 28, 35, 36, \dots \tag{3.5}$$

In fact, the case $d = 3$ was discovered by Jacobi, the case $d = 8$ by Klein and Fricke, and the cases $d = 14, 26$ by Atkin. There I stopped. I stared for a little while at this queer list of numbers (3.5). As I was, for the time being, a number theorist, they made no sense to me. My mind was so well compartmentalized that I did not remember that I had met these same numbers many times in my life as a physicist. If the numbers had appeared in the context of a problem in physics, I would certainly have recognized them as the dimensions of finite-dimensional simple Lie algebras. Except for 26. Why 26 is there I still do not know[4]. So I missed the opportunity of discovering a deeper connection between modular forms and Lie algebras, just because the number theorist Dyson and the physicist Dyson were not speaking to each other.

This story has a happy ending. Unknown to me the English geometer, Ian MacDonald, had discovered the same formulas as a special case of a much more general

[3] In a footnote to a Russian translation of Dyson's article (published in 1980), the translator noticed that it was difficult for him even to imagine that it could ever be so.

[4] Let us provide a short explanation. Rotations of the plane around a point depend on 1 parameter: the angle of rotation. Rotations of three-dimensional space depend on 3 parameters: the latitude and longitude of the axis of rotation and the angle of rotation. In general, rotation of an $n$-dimensional space depend on $\frac{n(n-1)}{2}$ parameters, and rotations of a complex $n$-dimensional space depend on $n^2 - 1$ parameters. To the numbers $\frac{n(n-1)}{2}$ and $n^2 - 1$, that is, $1, 3, 6, 10, 15, 21, 28, 36, \dots$ and $3, 8, 15, 24, 35, \dots$ one should add five "exceptional dimensions" $14, 52, 78, 133, 248$. If one also removes, as Dyson does, the number 1 and 6, and adds 26 (which appears here, according to a more modern explanation, as $52 \div 2$), then the sequence (3.5) arises; certainly, any theoretical physicist remembers this sequence very firmly.

theory. In his theory, the Lie algebras were incorporated from the beginning, and it was the connection with modular forms which came as a surprise. Anyhow, MacDonald established the connection and so picked the opportunity which I missed. It happened also that MacDonald was at the Institute for Advanced Study in Princeton while we were both working on the problem. Since we had daughters in the same class at school, we saw each other from time to time during his year in Princeton. But since he was a mathematician and I was a physicist, we did not discuss our work. The fact that we were thinking about the same problem while sitting so close to one another only emerged after he had gone back to Oxford. This was another missed opportunity, but not a tragic one, since MacDonald cleaned up the whole subject without any help from me."

**3.10 MacDonald's identities.** We finish this lecture with an infinite collection of identities which comprise a substantial part of MacDonald's work mentioned by Dyson. The first formula generalizes the Jacobi identity (which corresponds to the case $n = 2$):

$$\prod_{k=1}^{\infty}\left[(1-x_1^k\dots x_n^k)^{n-1}\prod_{1\le i<j\le n}\left(1-\frac{x_1^k\dots x_n^k}{x_i\dots x_{j-1}}\right)\left(1-\frac{x_1^k\dots x_n^k}{x_1\dots x_{i-1}x_j\dots x_n}\right)\right] = \sum\varepsilon(k_1,\dots,k_n)x_1^{k_1}\dots x_n^{k_n}$$

where the summation on the right hand side is taken over all $n$-tuples of non-negative integers $(k_1,\dots,k_n)$ satisfying the equation

$$k_1^2+\dots+k_n^2 = k_1+\dots+k_n+k_1k_2+\dots+k_{n-1}k_n+k_nk_1 \tag{3.6}$$

and $\varepsilon(k_1,\dots,k_n)=\pm1$ is defined in the following way. If the numbers $k_1,\dots,k_n$ satisfy equation (3.6), then so do the numbers $k_1,\dots,k_{i-1},k_i',k_{i+1},\dots,k_n$ where $k_i' = -k_i+k_{i-1}+k_{i+1}+1$ (here $1\le i\le n$; if $i=n$, we should take $x_1$ for $x_{i+1}$, and if $i=1$ then we should take $x_n$ for $x_{i-1}$). Moreover, any $n$-tuple $k_1,\dots,k_n$ of non-negative integers satisfying equation (3.6) can be obtained from $(0,\dots,0)$ by a finite sequence of such transformations. This may be done in many different ways; but the parity of the number of such transformations depend only on $k_1,\dots,k_n$. If this number is even, then $\varepsilon(k_1,\dots,k_n)=1$; otherwise, $\varepsilon(k_1,\dots,k_n)=-1$. There are some more explicit formulas for $\varepsilon(k_1,\dots,k_n)$. For example, if $n=2$, then equation (3.6) becomes $(k_1-k_2)^2=k_1+k_2$ and all integral solutions are

$$\left(\frac{n(n-1)}{2},\ \frac{n(n+1)}{2}\right), -\infty<n<\infty;$$

the corresponding $\varepsilon$ is $(-1)^n$. If $n=3$, then

$$\varepsilon(k_1,k_2,k_3)=\begin{cases}1, & \text{if } k_1+k_2+k_3\equiv 0 \bmod 3,\\ -1, & \text{if } k_1+k_2+k_3\equiv 1 \bmod 3\end{cases}$$

(the case $k_1+k_2+k_3\equiv 2 \bmod 3$ is not possible). If $n=4$, then

$$\varepsilon(k_1,k_2,k_3,k_4)=\begin{cases}1, & \text{if } k_1+k_2+k_3+k_4\equiv 0,2,3,7 \bmod 8,\\ -1, & \text{if } k_1+k_2+k_3+k_4\equiv 1,4,5,6 \bmod 8.\end{cases}$$

The second formula generalizes the Gauss identity (and also Klein's identity and Dyson's identity) to a formula for $\varphi(x)^{n^2-1}$:

$$\varphi(x)^{n^2-1}=(-1)^{n-1}\sum\varepsilon(k_1,\dots,k_n)\binom{k_1}{n-1}\binom{k_2}{n-2}\dots\binom{k_{n-1}}{1}x^{k_n}$$

where the summation is taken over the same $n$-tuples $(k_1, \ldots, k_n)$ as in the previous identity and $\varepsilon(k_1, \ldots, k_n)$ has the same meaning as before.

John Smith
January 23, 2010

Martyn Green
August 2, 1936

Henry Williams
June 6, 1944

John Smith
January 23, 2010

Martyn Green
August 2, 1936

Henry Williams
June 6, 1944

John Smith
January 23, 2010

Martyn Green
August 2, 1936

Henry Williams
June 6, 1944

### 3.11 Exercises.

3.1. Prove that

| | | |
|---|---|---|
| The number of partitions $n = n_1 + \cdots + n_k$ $(k > 0)$ with $0 < n_1 < \cdots < n_k$ | = | The number of partitions $n = n_1 + \cdots + n_k$ $(k > 0)$ with $0 < n_1 \leq \cdots \leq n_k$ and all $n_i$ odd |

*Hint.* There is a natural $1-1$ correspondence between the partitions in the left box and the partitions in the right box. The reader is encouraged to guess how it works from the following examples:

$$\begin{array}{rcl} 1+3+6+10 & \leftrightarrow & 1+3+3+3+5+5 \\ 1+4+7+11 & \leftrightarrow & 1+1+1+1+1+7+11 \\ 2+4+6 & \leftrightarrow & 1+1+1+1+1+1+1+3+3 \end{array}$$

3.2. Prove that for any real $s > 1$ (or a complex $s$ with the real part $\operatorname{Re} s > 1$),

$$1 + \frac{1}{2^s} + \frac{1}{3^s} + \frac{1}{4^s} + \frac{1}{5^s} + \cdots = \left(\frac{2^s}{2^s-1}\right)\left(\frac{3^s}{3^s-1}\right)\left(\frac{5^s}{5^s-1}\right)\left(\frac{7^s}{7^s-1}\right)\cdots$$

or, shorter,

$$\sum_{n=i}^{\infty} \frac{1}{n^s} = \prod_{p\in\{\text{primes}\}} \left(\frac{p^s}{p^s-1}\right).$$

*Remarks.* 1. This formula, also due to Euler, is not related directly to the subject of this lecture, but its proof strongly resembles the proof of Theorem 3.1, and we hope that the reader will appreciate it.

2. The expression on the left hand side (and hence the right hand side) of the last formula is denoted by $\zeta(s)$. This is the celebrated Riemann $\zeta$-function. A simple trick provides an extension of this function to all complex values of the argument (besides $s = 1$). It is well known that $\zeta(-2n) = 0$ for any positive integer $n$. The Riemann Hypothesis (which is, probably, currently the most famous unsolved problem in mathematics) states that if $\zeta(s) = 0$ and $s \neq 2n$ for any positive integer $n$, then $\operatorname{Re} s = \frac{1}{2}$.

3.3. Prove the formula from Section 3.5: if $n = 2^{k_2}3^{k_3}5^{k_5}\ldots$ is a prime factorization of $n$, then

$$\mathbf{d}(n) = \prod_{p\in\{\text{primes}\}} \frac{p^{k_p+1}-1}{p-1}.$$

3.4. Deduce from the Jacobi identity the following identity involving the Euler function $\varphi$:

$$\frac{\varphi(y)\varphi(y^4)}{\varphi(y^2)} = \sum_{n=-\infty}^{\infty} (-1)^n y^{2n^2+n}.$$

*Hint.* Try $z = -y^2$.

3.5. Prove that if $k, l, m$ are integers and $k + l + m = 1$, then $-(kl + km + lm)$ is a non-negative integer not congruent to 3 modulo 4.

*Remarks.* 1. This is related to the Klein identity for $\varphi(x)^8$.

2. According to the table in Section 3.8, 250 of the first 500 coefficients of the series for $\varphi(x)^8$ are zeroes. This exercise specifies 125 of them. The numbers which constitute the remaining 125 ones look chaotic. The reader may try to find some order in this chaos.

3.6. (a) Let $\mathbf{q}(n)$ be the number of partitions $n = n_1 + \cdots + n_k$ with $0 < n_1 \leq n_2 \leq \cdots \leq n_{k-1} < n_k$ (if $k = 1$, this means only that $0 < n$). Prove that $\mathbf{q}(n) = \mathbf{p}(n-1)$ for $n \geq 1$.

(b) Deduce from (a) that $\mathbf{p}(n) > \mathbf{p}(n-1)$ for $n \geq 2$.

3.7. Prove that $\mathbf{p}(n) < F_n$ where $F_n$ is the $n$-th Fibonacci number ($F_0 = F_1 = 1,\ F_n = F_{n-1} + F_{n-2}$ for $n \geq 2$).

*Hint.* Use the Euler identity and Exercise 3.6 (b.)

3.8. * Let $F_n$ ($k = 1, 2, \dots$) be the Fibonacci numbers ($F_1 = 1, F_2 = 2, F_n = F_{n-1} + F_{n-2}$ for $n \geq 3$; in contrast to Exercise 3.7, we do not consider $F_0$).

(a) Prove that every integer $n \geq 1$ can be represented as the sum of distinct Fibonacci numbers, $n = F_{k_1} + \dots + F_{k_s},\ 1 \leq k_1 < \dots < k_s$.

(b) Prove that a partition of $n$ as in Part (a) exists and is unique, if we impose the additional condition: $k_i - k_{i-1} \geq 2$ for $1 < i \leq s$.

(c) Prove that a partition of $n$ as in Part (a) also exists and is unique, if we impose the opposite condition: $k_1 \leq 2,\ k_i - k_{i-1} \leq 2$ for $1 < i \leq s$.

(d) Let $K_n$ be the number of partitions of $n$ as in Part (a) with $s$ even and $H_n$ be the same with $s$ odd. Prove that $|K_n - H_n| \leq 1$.

(e) (Equivalent to (d).) Let

$$(1-x)(1-x^2)(1-x^3)(1-x^5)(1-x^8)\cdots = 1 + g_1 x + g_2 x^2 + g_3 x^3 + \dots$$

(or, in the short notation, $\prod_{k=1}^{\infty}(1 - x^{F_k}) = 1 + \sum_{n=1}^{\infty} g_n x^n$). Prove that $|g_n| \leq 1$ for all $n$.

(f) (Generalization of (e).) Prove that for every $k, \ell > k$, all the coefficients of the polynomial $(1 - x^{F_k})(1 - x^{F_{k+1}})\dots(1 - x^{F_\ell})$ equal 0 or $\pm 1$.

(g) (An addition to (e).) Prove that, for any $k \geq 4$,

$$g_n = 0 \ \text{ for } \ 2F_k - 2 < n < 2F_k + F_{k-3}.$$

| | |
|---|---|
| $\rightarrow$ | |
| $+$ | |
| $+$ | |
| | |
| | |
| $-$ | |
| | |
| $-$ | |
| | |
| | |
| | |
| $+$ | |
| | |
| | |
| $+$ | |
| | |
| | |
| | |
| | |
| | |
| | |
| | |
| $-$ | |
| | |
| | |
| | |
| $-$ | |
| | |
| | |
| | |
| | |
| | |
| | |
| | |
| | |

| | |
|---|---|
| $\rightarrow$ | **1** |
| $+$ | $1 = \mathbf{p}(0)$ |

| | |
|---|---|
| $\rightarrow$ | **2** |
| $+$ | $1 = \mathbf{p}(1)$ |
| $+$ | $1 = \mathbf{p}(0)$ |

| | |
|---|---|
| $\rightarrow$ | **3** |
| $+$ | $2 = \mathbf{p}(2)$ |
| $+$ | $1 = \mathbf{p}(1)$ |
| | $1 = \mathbf{p}(0)$ |

| | |
|---|---|
| $\rightarrow$ | **5** |
| $+$ | $3 = \mathbf{p}(3)$ |
| $+$ | $2 = \mathbf{p}(2)$ |
| | $1 = \mathbf{p}(1)$ |
| | $1 = \mathbf{p}(0)$ |

| | |
|---|---|
| $\rightarrow$ | **7** |
| $+$ | $5 = \mathbf{p}(4)$ |
| $+$ | $3 = \mathbf{p}(3)$ |
| | $2 = \mathbf{p}(2)$ |
| | $1 = \mathbf{p}(1)$ |
| $-$ | $1 = \mathbf{p}(0)$ |

| | |
|---|---|
| $\rightarrow$ | **11** |
| $+$ | $7 = \mathbf{p}(5)$ |
| $+$ | $5 = \mathbf{p}(4)$ |
| | $3 = \mathbf{p}(3)$ |
| | $2 = \mathbf{p}(2)$ |
| $-$ | $1 = \mathbf{p}(1)$ |
| | $1 = \mathbf{p}(0)$ |

| | |
|---|---|
| $\rightarrow$ | **15** |
| $+$ | $11 = \mathbf{p}(6)$ |
| $+$ | $7 = \mathbf{p}(5)$ |
| | $5 = \mathbf{p}(4)$ |
| | $3 = \mathbf{p}(3)$ |
| $-$ | $2 = \mathbf{p}(2)$ |
| | $1 = \mathbf{p}(1)$ |
| $-$ | $1 = \mathbf{p}(0)$ |

| | |
|---|---|
| $\rightarrow$ | **22** |
| $+$ | $15 = \mathbf{p}(7)$ |
| $+$ | $11 = \mathbf{p}(6)$ |
| | $7 = \mathbf{p}(5)$ |
| | $5 = \mathbf{p}(4)$ |
| $-$ | $3 = \mathbf{p}(3)$ |
| | $2 = \mathbf{p}(2)$ |
| $-$ | $1 = \mathbf{p}(1)$ |
| | $1 = \mathbf{p}(0)$ |

| | |
|---|---|
| $\rightarrow$ | **30** |
| $+$ | $22 = \mathbf{p}(8)$ |
| $+$ | $15 = \mathbf{p}(7)$ |
| | $11 = \mathbf{p}(6)$ |
| | $7 = \mathbf{p}(5)$ |
| $-$ | $5 = \mathbf{p}(4)$ |
| | $3 = \mathbf{p}(3)$ |
| $-$ | $2 = \mathbf{p}(2)$ |
| | $1 = \mathbf{p}(1)$ |
| | $1 = \mathbf{p}(0)$ |

| | |
|---|---|
| $\rightarrow$ | **42** |
| $+$ | $30 = \mathbf{p}(9)$ |
| $+$ | $22 = \mathbf{p}(8)$ |
| | $15 = \mathbf{p}(7)$ |
| | $11 = \mathbf{p}(6)$ |
| $-$ | $7 = \mathbf{p}(5)$ |
| | $5 = \mathbf{p}(4)$ |
| $-$ | $3 = \mathbf{p}(3)$ |
| | $2 = \mathbf{p}(2)$ |
| | $1 = \mathbf{p}(1)$ |
| | $1 = \mathbf{p}(0)$ |

| | |
|---|---|
| $\rightarrow$ | **56** |
| $+$ | $42 = \mathbf{p}(10)$ |
| $+$ | $30 = \mathbf{p}(9)$ |
| | $22 = \mathbf{p}(8)$ |
| | $15 = \mathbf{p}(7)$ |
| $-$ | $11 = \mathbf{p}(6)$ |
| | $7 = \mathbf{p}(5)$ |
| $-$ | $5 = \mathbf{p}(4)$ |
| | $3 = \mathbf{p}(3)$ |
| | $2 = \mathbf{p}(2)$ |
| | $1 = \mathbf{p}(1)$ |
| | $1 = \mathbf{p}(0)$ |

| | |
|---|---|
| $\rightarrow$ | **77** |
| $+$ | $56 = \mathbf{p}(11)$ |
| $+$ | $42 = \mathbf{p}(10)$ |
| | $30 = \mathbf{p}(9)$ |
| | $22 = \mathbf{p}(8)$ |
| $-$ | $15 = \mathbf{p}(7)$ |
| | $11 = \mathbf{p}(6)$ |
| $-$ | $7 = \mathbf{p}(5)$ |
| | $5 = \mathbf{p}(4)$ |
| | $3 = \mathbf{p}(3)$ |
| | $2 = \mathbf{p}(2)$ |
| | $1 = \mathbf{p}(1)$ |
| $+$ | $1 = \mathbf{p}(0)$ |

FIGURE 3.2. A machine for computing $\mathbf{p}(n)$

# Chapter 2

## EQUATIONS

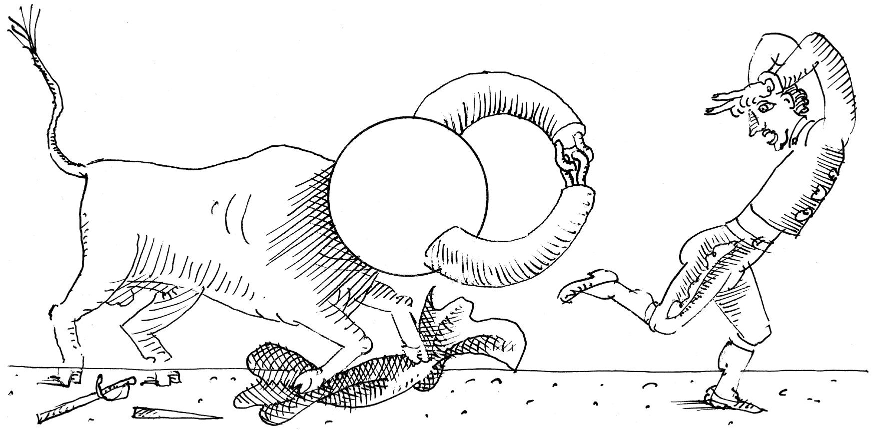

LECTURE 4

# Equations of Degree Three and Four

**4.1 Introduction.** The formula $x_{1,2} = \dfrac{-p \pm \sqrt{p^2 - 4q}}{2}$ for the roots of a quadratic equation $x^2+px+q=0$ is one of the most popular formulas in mathematics. It is short and convenient, it has a wide variety of applications, and everybody is urged to memorize it.

It is also widely known that there exists an explicit formula for solving cubic equation, but students are, in general, not encouraged to learn it. The usual explanation is that it is long, complicated and not convenient to use. These warnings, however, are not always sufficient to temper one's exploration mood, and some people are looking for this formula in various text books and reference books. Here is what they find there.

**4.2 The formula.** We shall consider the equation

$$x^3 + px + q = 0. \tag{4.1}$$

(The general equation $x^3 + ax^2 + bx + c$ can be reduced to an equation of this form by the substitution $x = y - \dfrac{a}{3}$:

$$x^3 + ax^2 + bx + c = \left(y - \frac{a}{3}\right)^3 + a\left(y - \frac{a}{3}\right)^2 + b\left(y - \frac{a}{3}\right) + c$$

$$= y^3 + \left(b - \frac{a^2}{3}\right)y + \left(\frac{2a^3}{27} - \frac{ab}{3} + c\right)$$

which is $y^3 + px + q$ with $p = b - \dfrac{a^2}{3},\ q = \dfrac{2a^3}{27} - \dfrac{ab}{3} + c$).

The formula is[1]

$$x = \sqrt[3]{-\frac{q}{2} + \sqrt{\frac{p^3}{27} + \frac{q^2}{4}}} + \sqrt[3]{-\frac{q}{2} - \sqrt{\frac{p^3}{27} + \frac{q^2}{4}}} \tag{4.2}$$

What we see is that this formula is not long and not complicated. The two cubic roots are very similar to each other: memorize one, and you will remember the other one. The denominators 2, 4, and 27 are also easy to memorize; moreover, it is possible to avoid them if you write the given equation as

$$x^3 + 3rx + 2s = 0;$$

then the formula becomes $x = \sqrt[3]{-s + \sqrt{r^3 + s^2}} + \sqrt[3]{-s - \sqrt{r^3 + s^2}}$. So, maybe, this formula is not as bad as most people think? To form our opinion, let us start with the most simple thing.

**4.3 The proof of the formula.**

THEOREM 4.1. *If* $\frac{p^3}{27} + \frac{q^2}{4} \geq 0$, *then (4.2) is a solution of the equation (4.1).*

Proof. Let

$$A = \sqrt[3]{-\frac{q}{2} + \sqrt{\frac{p^3}{27} + \frac{q^2}{4}}},\ B = \sqrt[3]{-\frac{q}{2} - \sqrt{\frac{p^3}{27} + \frac{q^2}{4}}}.$$

Then $A^3 + B^3 = -q$,

$$AB = \sqrt[3]{-\frac{q}{2} + \sqrt{\frac{p^3}{27} + \frac{q^2}{4}}} \cdot \sqrt[3]{-\frac{q}{2} - \sqrt{\frac{p^3}{27} + \frac{q^2}{4}}} = \sqrt[3]{-\frac{p^3}{27}} = -\frac{p}{3},$$

and

$$x^3 = (A+B)^3 = A^3 + 3AB(A+B) + B^3 = -px - q,\ x^3 + px + q = 0,$$

as required. □

**4.4 Let us try to use the formula.** If this formula is good, it should be useful. Let us try to apply it to solving equations.

EXAMPLE 4.1. Consider the equation

$$x^3 + 6x - 2 = 0.$$

According to the formula,

$$x = \sqrt[3]{1 + \sqrt{8+1}} + \sqrt[3]{1 - \sqrt{8+1}} = \sqrt[3]{4} - \sqrt[3]{2}.$$

This result is undoubtedly good: without the formula, we should have hardly been able to guess that this difference of cubic radicals is a root of our equation.

[1]This formula is usually called the Cardano Formula or the Cardano-Tartaglia Formula. The reader can find the dramatic history of its discovery in S. Gindikin's book [**35**].

Example 4.2. Consider the equation

$$x^3 + 3x - 4 = 0.$$

According to the formula,

$$x = \sqrt[3]{2 + \sqrt{1+4}} + \sqrt[3]{2 - \sqrt{1+4}} = \sqrt[3]{2+\sqrt{5}} + \sqrt[3]{2-\sqrt{5}}.$$

Not bad. But if you use your pocket calculator to approximate the answer, you will, probably, notice that $\sqrt[3]{2+\sqrt{5}} + \sqrt[3]{2-\sqrt{5}} = 1$. The best way to prove this is to plug the left hand side and the right hand side of the last equality into the equation $x^3 + 3x - 4 = 0$ to confirm that both are solutions, and then prove that the equation has at most one (real) solution (the function $x^3 + 3x - 4$ is monotone: if $x_1 < x_2$,then $x_1^3 + 3x_1 - 4 < x_2^3 + 3x_2 - 4$).

This casts the first doubt: the quadratic formula always shows whether the solution is rational; here the solution is rational (even integral), but the formula fails to show this.

Example 4.3. To resolve our doubts, let us consider an equation with the solutions known in advance. By the way, the coefficient $a$ of $x^2$ in the equation $x^3 + ax^2 + bx + c = 0$ equals minus the sum of the roots; so, for our equation (4.1) the sum of the roots should be zero. Let us take $x_1 = -3, x_2 = 2, x_3 = 1$. The equation with these roots is

$$(x+3)(x-2)(x-1) = x^3 - 7x + 6 = 0.$$

Solve it using our formula:

$$x = \sqrt[3]{-3 + \sqrt{\frac{-343}{27} + 9}} + \sqrt[3]{-3 - \sqrt{\frac{-343}{27} + 9}}$$

$$= \sqrt[3]{-3 + \sqrt{-\frac{100}{27}}} + \sqrt[3]{-3 - \sqrt{-\frac{100}{27}}} = \sqrt[3]{-3 + \frac{10}{3\sqrt{3}}i} + \sqrt[3]{-3 - \frac{10}{3\sqrt{3}}i}.$$

Nothing like $-3, 2$, or 1. Too bad.

Conclusions. The formula is simple and easy to memorize, but it is somewhat unreliable: sometimes it gives a solution in an unsatisfactory form, sometimes it does not give any solution. Let us try to locate the source of these difficulties.

**4.5 How many solutions?** The question is very natural. Our formula gives, at best, one solution, whereas a cubic equation may have as many as 3 (real) solutions (see Example 4.3 above).

Consider the graph of the function

$$y = x^3 + px + q.$$

The graph of $y = x^3$ is the well-known cubic parabola (Figure 4.1); when we add $px$, the graph will be transformed as shown on Figure 4.1, and it will look differently for $p > 0$ and $p < 0$. Finally, the graph of $y = x^3 + px + q$ may be obtained from one of the graphs of Figure 4.1 by a vertical upward or downward translation (Figure 4.2). We see the following. If $p \geq 0$, then the number of solutions is always 1. If $p < 0$, then the number of solutions is 1, 2, or 3. Let us learn how to distinguish between these cases.

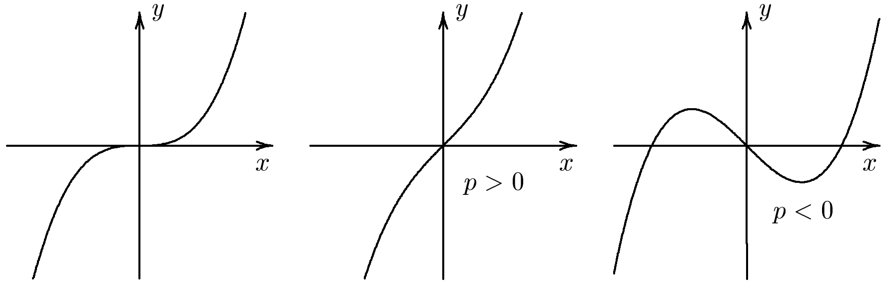


FIGURE 4.1. Cubic parabolas

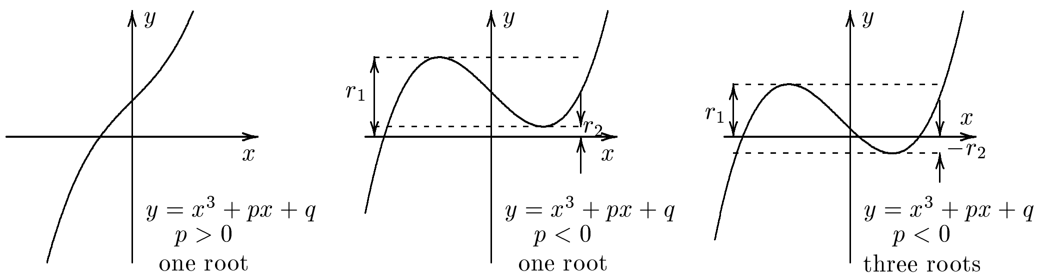


FIGURE 4.2. The number of roots

LEMMA 4.4. *The equation*

$$x^3 + px + q$$

*has precisely 2 solutions if and only if* $p < 0$ *and* $\dfrac{p^3}{27} + \dfrac{q^2}{4} = 0$.

REMARK 4.5. This result, with a proof different from the one below, is discussed in Lecture 8. Let us recall that the expression $\dfrac{p^3}{27} + \dfrac{q^2}{4}$, crucially important for our current purposes, is called the *discriminant* of the polynomial $x^3 + px + q$.

Proof of Lemma. To have two solutions, the equation has to have a multiple root. If this root is $a$, then the third root should be $-2a$, since the sum of the roots is 0. In particular, $a \neq 0$ (otherwise, there is only one root, 0). Hence

$$x^3 + px + q = (x - a)^2(x + 2a) = x^3 - 3a^2x + 2a^3,$$

$p = -3a^2, q = 2a^3$. In this case $p < 0$ and $\dfrac{p^3}{27} + \dfrac{q^2}{4} = -\dfrac{27a^6}{27} + \dfrac{4a^6}{4} = 0$. Conversely, if $p < 0$ and $\dfrac{p^3}{27} + \dfrac{q^2}{4} = 0$, then we take $a = \sqrt[3]{\dfrac{q}{2}}$ and deduce $q = 2a^3,\ p = \sqrt[3]{-\dfrac{27q^2}{4}} = \sqrt[3]{27a^6} = 3a^2$, hence

$$x^3 + px + q = x^3 - 3a^2x + 2a^3 = (x - a)^2(x + 2a)$$

which has a multiple root $a$. □

Consider now a general equation $x^3 + px + q = 0$ with $p < 0$ and without multiple roots. Obviously, there are two different numbers $r$ such that the equation

$x^3+px+q=r$ has a multiple root (see Figure 4.2). If these two $r$'s have the same sign (that is, their product is positive), then the equation $x^3+px+q=0$ has one solution; if they have opposite signs (their product is negative), then the number of solutions is three.

Let us make computations. According to the Lemma, $x^3+px+q=r$ has 2 solutions if and only if

$$\frac{p^3}{27}+\frac{(q-r)^2}{4}=0,$$

that is,

$$r=q\pm\sqrt{-\frac{4p^3}{27}}.$$

The product of the two values of $r$ is

$$q^2+\frac{4p^3}{27}=4\left(\frac{p^3}{27}+\frac{q^2}{4}\right).$$

We thus get the following result.

THEOREM 4.2. *The equation $x^3+px+q=0$ has*
*1 solution, if $\frac{p^3}{27}+\frac{q^2}{4}>0$ (or $p=q=0$);*
*2 solutions, if $\frac{p^3}{27}+\frac{q^2}{4}=0$ (and $p<0$);*
*3 solutions, if $\frac{p^3}{27}+\frac{q^2}{4}<0$.*

**4.6 Back to the formula.** Since the expression $\frac{p^3}{27}+\frac{q^2}{4}$ appears both in Theorem 4.2 and formula (4.2), there arises a link between these two results which explains fairly well the experimental observations of Section 4.4.

THEOREM 4.3. *If equation (4.1) has only one real root (or two real roots), then the right hand side of formula (4.2) is defined (is the sum of two cubic roots of real numbers). If the equation (4.1) has three (different) real roots, then the right hand sum of formula (4.2) is undefined: it is a sum of cubic roots of complex numbers.*

**4.7 The case of negative discriminant.** To apply formula (4.2) to this case, we need to learn how to extract cubic roots of complex numbers. Let us try to do it. Our problem: given $a$ and $b$, find $x$ and $y$ such that

$$(x+iy)^3=a+ib.$$

The last equation yields the system

$$\begin{aligned} x^3-3xy^2 &= a,\\ 3x^3y-y^3 &= b, \end{aligned}$$

which can be reduced to the equation

$$27b^3x^3=(x^3-a)(8x^3+a)^2.$$

The latter is a cubic equation with respect to $t=x^3$, and it must have three real solutions (since our initial problem has three solutions); thus, our formula will not help to solve it.

There is a different approach to extracting roots of complex numbers based on de Moivre's Formula

$$\sqrt[3]{r(\cos\theta + i\sin\theta)} = \sqrt[3]{r}\left(\cos\frac{\theta}{3} + i\sin\frac{\theta}{3}\right).$$

So, we can use trigonometry to solve cubic equations with the help of formula (4.2). Trigonometry, however, can be used for solving cubic equation without any formula like (4.2).

**4.8 Solving cubic equations using trigonometry.** In trigonometry, there is a formula for the sine of a triple angle:

$$\sin 3\theta = 3\sin\theta - 4\sin^3\theta.$$

Thus, if our equation is

$$4x^3 - 3x + \sin 3\theta = 0,$$

or

$$x^3 - \frac{3}{4}x + \frac{\sin 3\theta}{4} = 0,$$

then the solution is $x = \sin\theta$. In other words, if $p = -\frac{3}{4}$, then the solution of equation (4.1) is

$$x = \sin\left(\frac{1}{3}\sin^{-1}(4q)\right).$$

What if $p \neq -\frac{3}{4}$? In this case, we can make the substitution $x = ay$. The equation (4.1) becomes

$$a^3y^3 + apy + q = 0,$$

or

$$y^3 + \frac{p}{a^2}y + \frac{q}{a^3} = 0.$$

Thus, if $\frac{p}{a^2} = -\frac{3}{4}$, that is, $a = \sqrt{-\frac{4p}{3}}$, then the solution is

$$y = \sin\left(\frac{1}{3}\sin^{-1}\frac{4q}{\sqrt{(-\frac{4p}{3})^3}}\right),$$

$$x = ay = \sqrt{-\frac{4p}{3}}\sin\left(\frac{1}{3}\sin^{-1}\frac{9q}{4p^2}\sqrt{-\frac{4p}{3}}\right). \tag{4.3}$$

Isn't this a formula? Well, certainly, $p$ should be negative. But also the argument of $\sin^{-1}$ should be between $-1$ and 1:

$$\left|\frac{9q}{4p^2}\sqrt{-\frac{4p}{3}}\right| \leq 1,\ -\frac{81q^2\cdot 4p}{16p^4\cdot 3} \leq 1,$$

$$\frac{27q^2}{4p^3} \geq -1,\ 27q^2 \leq -4p^3,$$

$$27q^2 + 4p^3 \leq 0,\ \frac{p^3}{27} + \frac{q^2}{4} \leq 0.$$

We see that formula (4.3) works precisely when formula (4.2) does not work, so, together, formulas (4.2) and (4.3) cover the whole variety of cases. By the way, formula (4.3) always gives 3 solutions: if

$$\sin^{-1}\frac{9q}{4p^2}\sqrt{-\frac{4p}{3}}=\alpha,$$

then the 3 solutions are

$$x=\sqrt{-\frac{4p}{3}}\sin\left(\frac{1}{3}(\alpha+2k\pi)\right),\ k=0,1,2.$$

**4.9 Summary: how to solve cubic equations.** Formula (4.2) (together with formula (4.3)) always expresses the solutions of equation (4.1) in terms of $p$ and $q$. For practical purposes, this formula may be not very useful; approximate values of roots of cubic equations can be found by other methods (used, in particular, by pocket calculators); and it does not seem likely that one can use such a formula on the intermediate steps of calculations (plugging solutions of cubic equations into other equations). The significance of formula (4.2) is mainly theoretical, and we shall discuss this aspect below. Now we turn our attention to equations of degree four.

**4.10 Equations of degree 4: what is so special about the number 4?** Equations of degree 4 can be reduced to equations of degree 3. This phenomenon has no direct analogies for equations of degree greater than 4, and by this reason deserves a special consideration.

What is so special about the number 4? Of many possible answers to this question, we shall choose one which will be technically useful to us.

Among different mathematical problems, there are so-called "combinatorial problems". They look like this: "given such and such number of such and such things, in how many ways can we do such and such thing?"

For example: "In a class of 20 students, in how many ways can a president and two vice-presidents be selected?" Answer: $20\times\dfrac{19\cdot 18}{2}=3,420$.

Or: "In how many ways can one choose 2 green balls and 3 red balls from a box containing 10 balls of each color?" Answer: $\dfrac{10\cdot 9}{2}\cdot\dfrac{10\cdot 9\cdot 8}{6}=5,400$. And so on.

We can observe that the answers are relatively big, usually, substantially bigger than the number given in the statement of the problem. Do you know a combinatorial problem where the answer is less that the given number (and, say, greater than 1)? We know one such problem.

*Problem*: in how many ways can one break a set of 4 elements into 2 pairs? *Answer*: 3 (if the set is $\{ABCD\}$, then the solutions are $AB/CD,\ AC/BD,\ AD/BC$).

Surprisingly, this simple problem provides the main idea for solving equations of degree 4.

**4.11 The auxiliary cubic equation.** Let

$$x^4+px^2+qx+r=0 \tag{4.4}$$

be our equation (precisely as in the cubic case, we can get rid of the "second leading term" with $x^3$ by making a substitution of the form $x=y+\alpha$). Let $x_1,x_2,x_3,x_4$

be the solutions of equation (4.4). Then

$$x^4 + px^2 + qx + r = (x - x_1)(x - x_2)(x - x_3)(x - x_4),$$

whence

$$\begin{aligned} 0 &= x_1 + x_2 + x_3 + x_4, \\ p &= x_1x_2 + x_1x_3 + x_1x_4 + x_2x_3 + x_2x_4 + x_3x_4, \\ -q &= x_1x_2x_3 + x_1x_2x_4 + x_1x_3x_4 + x_2x_3x_4, \\ r &= x_1x_2x_3x_4. \end{aligned}$$

Now, let us look once more at our problem and set

$$\begin{aligned} y_1 &= (x_1 + x_2)(x_3 + x_4), \\ y_2 &= (x_1 + x_3)(x_2 + x_4), \\ y_3 &= (x_1 + x_4)(x_2 + x_3). \end{aligned}$$

Notice that, since $x_1 + x_2 + x_3 + x_4 = 0$, we can also write

$$\begin{aligned} y_1 &= -(x_1 + x_2)^2 = -(x_3 + x_4)^2, \\ y_2 &= -(x_1 + x_3)^2 = -(x_2 + x_4)^2, \\ y_3 &= -(x_1 + x_4)^2 = -(x_2 + x_3)^2. \end{aligned}$$

Let

$$y^3 + ay^2 + by + c = 0 \tag{4.5}$$

be the cubic equation with the roots $y_1, y_2, y_3$. Then

$$\begin{aligned} a &= -y_1 - y_2 - y_3, \\ b &= y_1y_2 + y_1y_3 + y_2y_3, \\ c &= -y_1y_2y_3. \end{aligned}$$

### 4.12 How to express $a, b, c$ via $p, q, r$?

THEOREM 4.4. $a = -2p,\ b = p^2 - 4r,\ c = q^2.$

Proof. (direct computation). It is slightly easier with $a$ and $c$ and longer with $b$.

$$\begin{aligned} a = -y_1 - y_2 - y_3 &= (x_1 + x_2)^2 + (x_1 + x_3)^2 + (x_2 + x_3)^2 \\ &= 2(x_1^2 + x_2^2 + x_3^2 + x_1x_2 + x_1x_3 + x_2x_3) \\ &= x_1^2 + x_2^2 + x_3^2 + (x_1 + x_2 + x_3)^2 = x_1^2 + x_2^2 + x_3^2 + (-x_4)^2 \\ &= (x_1 + x_2 + x_3 + x_4)^2 - 2p = -2p. \end{aligned}$$

$$\begin{aligned} c = -y_1y_2y_3 &= (x_1 + x_2)^2(x_1 + x_3)^2(x_1 + x_4)^2 \\ &= [(x_1 + x_2)(x_1 + x_3)(x_1 + x_4)]^2 \\ &= [x_1^3 + x_1^2(x_2 + x_3 + x_4) + x_1(x_2x_3 + x_2x_4 + x_3x_4) + x_2x_3x_4]^2 \\ &= (x_1^3 - x_1^3 - q)^2 = q^2. \end{aligned}$$

$$\begin{aligned} b = {} & y_1y_2 + y_1y_3 + y_2y_3 \\ = {} & (x_1 + x_2)^2(x_1 + x_3)^2 + (x_1 + x_2)^2(x_1 + x_4)^2 + (x_1 + x_3)^2(x_1 + x_4)^2 \\ = {} & x_1^4 + 2x_1^3(x_2 + x_3) + x_1^2(x_2^2 + x_3^2 + 4x_2x_3) + 2x_1x_2x_3(x_2 + x_3) + x_2^2x_3^2 + \\ & x_1^4 + 2x_1^3(x_2 + x_4) + x_1^2(x_2^2 + x_4^2 + 4x_2x_4) + 2x_1x_2x_4(x_2 + x_4) + x_2^2x_4^2 + \\ & x_1^4 + 2x_1^3(x_3 + x_4) + x_1^2(x_3^2 + x_4^2 + 4x_3x_4) + 2x_1x_3x_4(x_3 + x_4) + x_3^2x_4^2 \\ = {} & x_1^4 + 2x_1^3(x_2 + x_3) + x_1^2(x_2^2 + x_3^2 + 4x_2x_3) - 2x_1x_2x_3(x_1 + x_4) + x_2^2x_3^2 + \\ & x_1^4 + 2x_1^3(x_2 + x_4) + x_1^2(x_2^2 + x_4^2 + 4x_2x_4) - 2x_1x_2x_4(x_1 + x_3) + x_2^2x_4^2 + \\ & x_1^4 + 2x_1^3(x_3 + x_4) + x_1^2(x_3^2 + x_4^2 + 4x_3x_4) - 2x_1x_3x_4(x_1 + x_2) + x_3^2x_4^2 \\ = {} & 3x_1^4 + 4x_1^3(x_2 + x_3 + x_4) + 2x_1^2(x_2 + x_3 + x_4)^2 \\ & \quad -2x_1^2(x_2x_3 + x_2x_4 + x_3x_4) - 6x_1x_2x_3x_4 + x_2^2x_3^2 + x_2^2x_4^2 + x_3^2x_4^2 \\ = {} & x_1^4 - 2x_1^2(x_2x_3 + x_2x_4 + x_3x_4) - 6x_1x_2x_3x_4 + x_2^2x_3^2 + x_2^2x_4^2 + x_3^2x_4^2. \end{aligned}$$

$$\begin{aligned}
p &= -x_1^2 + x_2x_3 + x_2x_4 + x_3x_4;\\
p^2 &= x_1^4 - 2x_1^2(x_2x_3 + x_2x_4 + x_3x_4) + (x_2x_3 + x_2x_4 + x_3x_4)^2;\\
p^2 - b &= (x_2x_3 + x_2x_4 + x_3x_4)^2 - (x_2^2x_3^2 + x_2^2x_4^2 + x_3^2x_4^2) + 6x_1x_2x_3x_4\\
&= 2(x_2^2x_3x_4 + x_2x_3^2x_4 + x_2x_3x_4^2) + 6x_1x_2x_3x_4\\
&= 2x_2x_3x_4(x_2 + x_3 + x_4) + 6x_1x_2x_3x_4\\
&= -2x_1x_2x_3x_4 + 6x_1x_2x_3x_4 = 4x_1x_2x_3x_4 = 4r.
\end{aligned}$$

□

This proof is convincing but it does not reveal the reasons for the existence of an expression for $a, b, c$ via $p, q, r$. Let us try to explain these reasons. If we plug the (very first) formulas for $y_1, y_2, y_3$ into the definition of $a, b, c$, then $a, b, c$ will become polynomials in $x_1, x_2, x_3, x_4$ (of degrees 2, 4, 6). Moreover, these polynomials in $x_1, x_2, x_3, x_4$ are *symmetric* which means that if you switch any two variables $x_i, x_j$, the polynomial will remain the same. Indeed, if you, say, switch $x_1$ with $x_2$, then $y_1$ remains unchanged while $y_2$ will be switched with $y_3$; something similar will happen if you switch any two $x$'s. But $a, b, c$ remain unchanged, since they are, obviously, *symmetric with respect to the y's.*

There is a theorem in algebra (not difficult) stating that any symmetric polynomial in $x_1, x_2, x_3, x_4$ can be expressed as a polynomial in the "elementary symmetric polynomials"

$$\begin{aligned}
e_1 &= x_1 + x_2 + x_3 + x_4,\\
e_2 &= x_1x_2 + x_1x_3 + x_1x_4 + x_2x_3 + x_2x_4 + x_3x_4,\\
e_3 &= x_1x_2x_3 + x_1x_2x_4 + x_1x_3x_4 + x_2x_3x_4,\\
e_4 &= x_1x_2x_3x_4.
\end{aligned}$$

(A similar theorem holds for any number of variables.) Since $e_1 = 0$, $a, b, c$ are polynomials in $e_2, e_3, e_4$, that is, in $p, q, r$. Since the degrees of $p, q, r$ are $2, 3, 4$, one should have

$$\begin{aligned}
a &= Ap,\\
b &= Bp^2 + Cr,\\
c &= Dp^3 + Eq^2 + Fpr,
\end{aligned}$$

and we can find $A, \ldots, F$ by plugging particular values for $x_1, x_2, x_3, x_4$ (such that $x_1 + x_2 + x_3 + x_4 = 0$). For example, if $x_1 = 1, x_2 = -1, x_3 = x_4 = 0$, then $y_1 = 0, y_2 = y_3 = -1, p = -1, q = r = 0, a = -2, b = 1, c = 0$. Hence

$$\begin{aligned}
-2 &= A \cdot (-1),\\
1 &= B \cdot 1 + C \cdot 0,\\
0 &= D \cdot 1 + E \cdot 0 + F \cdot 0,
\end{aligned}$$

whence $A = 2, B = 1, D = 0$. Similarly, we can find $C, E$ and $F$.

**4.13 How to express $x_1, x_2, x_3, x_4$ via $y_1, y_2, y_3$?** Thus, given equation (4.4) of degree 4, we can compose the auxiliary equation (4.5) of degree 3, solve it, and find $y_1, y_2, y_3$. How to find our initial unknowns, $x_1, x_2, x_3, x_4$? It is easy: since

$$\begin{aligned}
y_1 &= -(x_1 + x_2)^2 = -(x_2 + x_3)^2,\\
y_2 &= -(x_1 + x_3)^2 = -(x_2 + x_4)^2,\\
y_3 &= -(x_1 + x_4)^2 = -(x_2 + x_3)^2,
\end{aligned}$$

and $x_1 + x_2 + x_3 + x_4 = 0$, we have

$$\begin{aligned} x_1 + x_4 = -(x_2 + x_3) &\quad = \pm\sqrt{-y_1}, \\ x_1 + x_3 = -(x_2 + x_4) &\quad = \pm\sqrt{-y_2}, \\ x_1 + x_4 = -(x_2 + x_3) &\quad = \pm\sqrt{-y_3}, \end{aligned}$$

$$3x_1 + x_2 + x_3 + x_4 = 2x_1 = \pm\sqrt{-y_1} \pm \sqrt{-y_2} \pm \sqrt{-y_3},$$

$$x_1 = \frac{\pm\sqrt{-y_1} \pm \sqrt{-y_2} \pm \sqrt{-y_3}}{2}.$$

Formulas for $x_2, x_3, x_4$ are *absolutely the same*. Varying the signs in the expression $\pm\sqrt{-y_1}, \pm\sqrt{-y_2}, \pm\sqrt{-y_3}$, we obtain 8 numbers, which are $\pm x_1, \pm x_2, \pm x_3, \pm x_4$. This completes solving equation (4.4). For the reader's convenience, we shall repeat the whole procedure, from the beginning to the end.

**4.14 Conclusion: solving equation (4.4).** 1. Given an equation

$$x^4 + px^2 + qx + r = 0.$$

2. Solve the auxiliary equation

$$y^3 - 2py + (p^2 - 4r)y + q^2 = 0;$$

let $y_1, y_2, y_3$ be the solutions.
3. Consider the eight numbers

$$\frac{\pm\sqrt{-y_1} \pm \sqrt{-y_2} \pm \sqrt{-}y_3}{2}.$$

Four of these numbers are solution of the given equation, the remaining are "minus solutions." Plug and select the solutions.

John Smith
January 23, 2010

Martyn Green
August 2, 1936

Henry Williams
June 6, 1944

**4.15 Exercises.**

4.1. The equation

$$x^3 + 9x + 26 = 0$$

can be solved explicitly by formula (4.2) with all square and cubic roots being integers:

$$\begin{aligned} x &= \sqrt[3]{-13 + \sqrt{27 + 169}} \\ &= \sqrt[3]{-13 + 14} + \sqrt[3]{-13 - 14} = \sqrt[3]{1} + \sqrt[3]{-27} = 1 - 3 = -2. \end{aligned}$$

Find infinitely many cubic equations with non-zero integral coefficients $p$ and $q$ with the same property.

4.2. Prove that the formula

$$x = r - \frac{p}{3r}$$

where $r$ is an arbitary value of the cubic root $\sqrt[3]{-\frac{q}{2}+s}$ where, in turn, $s$ is an arbitrary value of $\sqrt{\frac{p^3}{27}+\frac{q^2}{4}}$ gives precisely 3 complex solutions of a cubic equation $x^3+px+q=0$ with complex coefficients $p, q$ such that $p \neq 0$, $\frac{p^3}{27}+\frac{q^2}{4} \neq 0$.

4.3. Prove that if a cubic equation $x^3+px+q=0$ (with real coefficients) has a double (not triple!) root, then formula (4.2) gives the other (not double) root, and it is equal to $\sqrt[3]{-4q}$.

4.4. For the hyperbolic sine, $\sinh\alpha = \frac{e^{\alpha}-e^{-\alpha}}{2}$, there is a formula

$$\sinh 3\alpha = 3\sinh\alpha + 4\sinh^3\alpha.$$

Use this formula as in Section 4.8, and find a hyperbolic-trigonometric formula for the solutions of a cubic equation $x^3+px+q=0$ with real coefficients. For which $p, q$ does it work? How many solutions does it provide?

4.5. Solve, using the procedure in Section 4.14, the following equations of degree 4:

(a) $x^4+4x+3=0$;
(b) $x^4+2x^2+4x+2=0$;
(c) $x^4+480x+1924=0$.

*Remarks.* It is easy to solve the equation (a) by the usual high school method of guessing, plugging and dividing; it is given here because it also provides a good illustration to our method. However, it is permissible to apply the high school method described above to the auxiliary cubic equations arising from equations (b) and (c). In the latter case it is not easy to guess a root; for a desperate reader who fails to guess, we provide a clue: try $-100$.

4.6. Find the solutions of the equation

$$x^4+px^2+qx+r=0$$

following the lines of Sections 4.12, 4.13 with

$$\begin{aligned} y_1 &= x_1x_2+x_3x_4 \\ y_2 &= x_1x_3+x_2x_4 \\ y_3 &= x_1x_4+x_2x_3. \end{aligned}$$

4.7. Let $m, n, k$ be integers such that $mnk$ is an exact square. Find an equation $x^4+px^2+qx+r=0$ with rational $p, q, r$ for which $\sqrt{m}+\sqrt{n}+\sqrt{k}$ is a root.

*Hint.* Find an equation of degree 4 for which the auxiliary cubic equation is $(x+m)(x+n)(x+k)=0$.

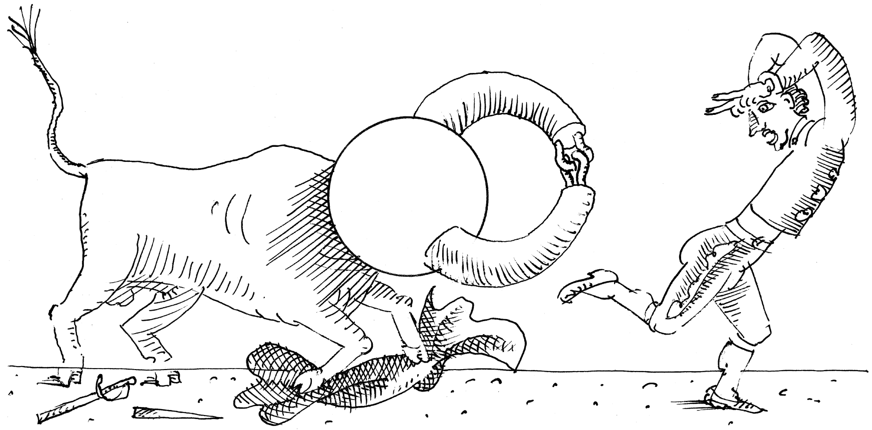

LECTURE 5

# Equations of Degree Five

**5.1 Introduction.** In Lecture 4 we presented "radical" formulas solving equations of degrees 3 and 4. These formulas express the roots of polynomials of degree 3 and 4 (plus, possibly, some extraneous roots) in terms of the coefficients of these polynomials. More precisely, the roots can be obtained from the coefficients by the operations of addition, subtraction, multiplication, and extracting roots of arbitrary positive integral degrees. Our goal in this lecture is to prove that no such formula can exist for polynomials of degree 5 and more.

The first result of this kind was obtained in 1828 by Niels Henrik Abel, who found an individual polynomial of degree 5 with integral coefficients such that no root of this polynomial can be obtained from rational numbers by the operations listed above. A general theory explaining such phenomena was created approximately at the same time by Evariste Galois. (Unfortunately, the work of Galois, who died at a very young age in 1832, became broadly known to the mathematical community only 50 years after his death.) The theorem which we shall prove here does not deal with any individual equation: it studies the dependence of the roots of a polynomial on the coefficients; in particular, we shall not care about the rationality or irrationality of the coefficients. The proof will be geometrical, although it is based (in an implicit way) on the ideas of Galois theory.

**5.2 What is a radical formula?** Let us start with a quadratic equation,

$$x^2 + px + q = 0. \tag{5.1}$$

The solutions are expressed by the formula

$$x = \frac{-p \pm \sqrt{p^2 - 4q}}{2}.$$

We can describe the procedure of finding roots avoiding the awkward symbol "$\sqrt{\phantom{x}}$". Instead, we write the sequence of formulas

$$\begin{aligned} x_1^2 &= p^2 - 4q, \\ x_2 &= -\frac{1}{2}p + \frac{1}{2}x_1 \end{aligned}$$

Starting with $p, q$, we find $x_1$, then $x_2$, and $x_2$ will be a solution. Since $x_1$ is not unique, $x_2$ is also not unique: we find *all* solutions of the equation (5.1).

Turn now to a cubic equation,

$$x^3 + px + q = 0. \tag{5.2}$$

Again, we write a chain of formulas,

$$\begin{aligned} x_1^2 &= \frac{p^3}{27} + \frac{q^2}{4}, \\ x_2^3 &= -\frac{q}{2} + x_1, \\ x_3^3 &= -\frac{q}{2} - x_1, \\ x_4 &= x_2 + x_3. \end{aligned}$$

We have two values for $x_1$, then three values for each of $x_2, x_3$. Seemingly, we have 36 values for $x_4$, but actually only 9 of them may be different. The solutions of equation (5.2) are three of them (the other 6 will be the roots of the polynomials $x^3 + \varepsilon_3 px + q,\ x^3 + \overline{\varepsilon}_3 px = 0$ where $\varepsilon_3 = -\frac{1}{2} + \frac{\sqrt{3}}{2}i$ is "the primitive cubic root of 1.")

In a similar way, we can present the solutions of equations of degree 4 (see Exercise 5.1). Now, we can give a precise definition of a "radical formula". We say that the equation

$$x^n + a_1 x^{n-1} + \cdots + a_{n-1}x + a_n = 0 \tag{5.3}$$

(with variable complex coefficients $a_1, \dots, a_n$) is *solvable in radicals* if there exist polynomials $p_1, \dots, p_N$ (in $n, n+1, \dots, n+N-1$ variables) and positive integers $k_1, \dots, k_N$ such that for any (complex) root $x = x_N$ of the polynomial (5.3) with given $a_1, \dots, a_n$ there are (complex) numbers $x_1, \dots, x_N$ satisfying the system

$$\begin{aligned} x_1^{k_1} &= p_1(a_1, \dots, a_n), \\ x_2^{k_2} &= p_2(a_1, \dots, a_n, x_1), \\ &\cdots\cdots\cdots\cdots\cdots\cdots \\ x_N^{k_N} &= p_N(a_1, \dots, a_n, x_1, \dots, x_{N-1}). \end{aligned}$$

We shall apply this definition also in the case when equation (5.3) contains (like equation (5.2)) fewer than $n$ variable coefficients.

### 5.3 Main result.

THEOREM 5.1. *The equation*

$$x^5 - x + a = 0 \tag{5.4}$$

*is not solvable in radicals.*

The goal of this lecture is to prove this theorem.

This theorem will imply that the general equation (5.3) with $n \geq 5$ is also not solvable in radicals. (Indeed, if equation (5.3) with some $n \geq 5$ is solvable in radicals, then the same is true for the equation $x^n - x^{n-4} + ax^{n-5} = x^{n-5}(x^5 - x + a) = 0$; then the equation $x^5 - x + a = 0$ is also solvable in radicals.)

Before we start proving Theorem 5.1, we shall make a general remark. The proof may seem unusual to many people. Instead of directly dealing with radical formulas, we shall analyze in some details things visibly unrelated to our goal. And when some readers may start feeling irritated with this abundant "preparatory work", we shall find out that the proof is over.

### 5.4 Number of roots.

PROPOSITION 5.1. *If equation* (5.4) *has multiple roots then* $a^4 = \dfrac{4^4}{5^5}$*, in other words,*

$$a = \pm\frac{4}{5\sqrt[4]{5}} \text{ or } \pm\frac{4i}{5\sqrt[4]{5}}.$$

LEMMA 5.2. *If $b$ is a multiple root of the equation* (5.4) *then* $5b^4 = 1$.

Proof of Lemma. . If $b$ is a multiple root of the polynomial $x^5 - x + a$, then $x^5 - x + a = (x-b)^2 p(x)$ where $p$ is a polynomial of degree 3. Take $x = b + \varepsilon$ where $\varepsilon$ is a very small number. Then

$$(b+\varepsilon)^5 - (b+\varepsilon) + a = \varepsilon^2 p(b+\varepsilon),$$

$$b^5 + 5\varepsilon b^4 + \varepsilon^2(10b^3 + 10b^2\varepsilon + 5b\varepsilon^2 + \varepsilon^3) - b - \varepsilon + a = \varepsilon^2 p(b+\varepsilon).$$

Delete $b^5 - b + a = 0$ and divide by $\varepsilon$:

$$5b^4 - 1 = \varepsilon(p(b+\varepsilon) - 10b^3 - 10b^2\varepsilon - 5b\varepsilon^2 - \varepsilon^3).$$

This is true for any $\varepsilon$, but the right hand side will be arbitrarily small (in absolute value) if $\varepsilon$ is small. Hence, $5b^4 - 1$ is "arbitrarily small," that is, $5b^4 - 1 = 0$. □

Proof of Proposition. . If $5b^4 = 1$, then $a^4 = (b - b^5)^4 = b^4(1 - b^4)^4 = \dfrac{1}{5} \cdot \dfrac{4}{5}^4 = \dfrac{4^4}{5^5}$. □

**5.5 Variation of $a$.** If $a = 0$ then the equation is $x^5 - x = 0$, and the solutions are $0, \pm 1, \pm i$. If we vary $a$ then the 5 roots will also vary, but they will not collide, if $a$ avoids the dangerous values $\pm\dfrac{4}{5\sqrt[4]{5}}, \pm\dfrac{4i}{5\sqrt[4]{5}}$ (Figure 5.1).

What happens, if $a$ traverses some closed path ("loop") starting and ending at 0 (and avoiding the dangerous values)? The five roots $0, \pm 1, \pm i$ of the equation $x^5 - x = 0$ will come back to $0, \pm 1, \pm i$; but will each individual root return to its initial seat? No! The roots, in general, will interchange their positions (Figure 5.2); moreover, they can do it in an *arbitrary way.* We will prove it below, but before we even make a rigorous statement we have to talk a little about *permutations.*

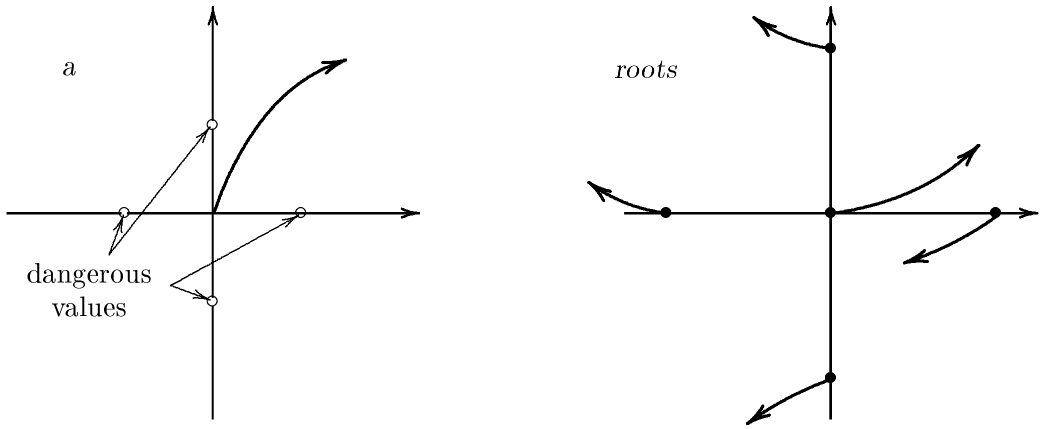


FIGURE 5.1. A variation of $a$ yields a variation of roots

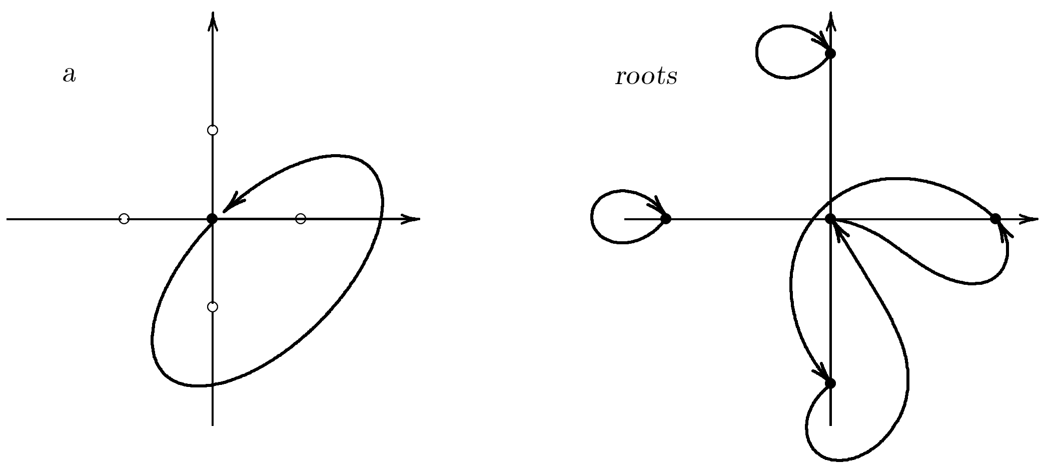


FIGURE 5.2. A loop variation of $a$ yields a permutation of roots

**5.6 Permutations.** We shall be interested only in permutations of the set of 5 elements which we will denote by $1, 2, 3, 4, 5$ (so the word "permutation" will always refer to a permutation of this set). A notation for a permutation is $(i_1 i_2 i_3 i_4 i_5)$ where $i_1, i_2, i_3, i_4, i_5$ are different integers between 1 and 5. The notation above means that the permutation acts as

$$1 \mapsto i_1,\ 2 \mapsto i_2,\ 3 \mapsto i_3,\ 4 \mapsto i_4, 5 \mapsto i_5.$$

We shall usually present the permutation by diagrams like the one in Figure 5.3 where the arrows indicate the images of $1, 2, 3, 4, 5$; for example, the permutation on Figure 5.3 is (41352). (The arrows on a figure like Figure 5.3 are usually assumed straight, but we may want to deform them a little to avoid triple intersections; for this reason, the arrow $3 \to 3$ on Figure 5.3 is not genuinely straight.)

The total number of permutations is 120.

If we successively perform two permutations, first $\alpha$ and then $\beta$, we get a new permutation, which is called the *product* of permutations $\alpha$ and $\beta$ and is denoted

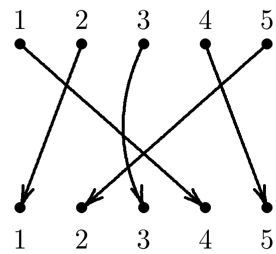


FIGURE 5.3. A permutation

by $\alpha\beta$. For example,

$$\begin{aligned}(21435)(13254) &= (31524),\\ (13254)(21435) &= (24153)\end{aligned}$$

(which shows that the product may depend on the order of the factors.) For every permutation, $\alpha$, there is the *inverse* permutation, $\alpha^{-1}$ which is obtained from $\alpha$ by reversing the arrows. The products $\alpha\alpha^{-1}$ and $\alpha^{-1}\alpha$ are both equal to the identity permutation $\varepsilon = (12345)$. Note that both products and inversions can be visualized by means of diagrams like Figure 5.3: to find a product, we need to draw the second factor under the first one, to find an inverse permutation, we need to reflect the diagram of the permutation in a horizontal line. This is illustrated by Figure 5.4 where the equalities $(41352)(21354) = (52341)$ and $(41532)^{-1} = (25413)$ are demonstrated.

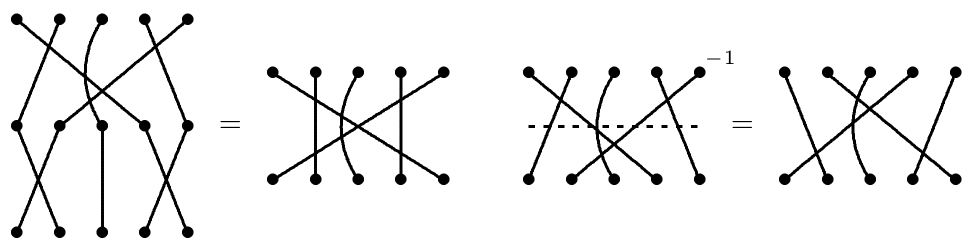


FIGURE 5.4. Operations on permutations

For a permutation $(i_1i_2i_3i_4i_5)$ one can count "the number of disorders," that is, the number of pairs $s, t$ with $1 \le s < t \le 5$, $i_s > i_t$. Thus the number of disorders varies from 0 (the identity permutation (12345) has 0 disorders) to 10 (the reversion permutation (54321) has 10 disorders). The permutation (41352) has 5 disorders ($4 > 1$, $4 > 3$, $4 > 2$, $3 > 2$, $5 > 2$). The best way to count disorders is to use a diagram like Figure 5.3: disorders correspond to crossings on this diagram (this is why we wanted to avoid triple crossings).

It is not the number of disorders, but rather its parity, that has a major significance in the theory of permutations. A permutation is called *even*, if the number of disorders is even, and is called *odd*, if the number of disorders is odd. For example, (12345) and (54321) are even permutations, while the permutation (41352) is odd.

PROPOSITION 5.3. *The product of two permutations of the same parity is even. The product of two permutations of the opposite parities is odd.*

Proof. We use the description of the product of two permutations as presented on Figure 5.4. For every $s = 1, 2, 3, 4, 5$, there is a two-edge polygonal paths starting at the point $s$ of the upper row and going downward (see Figure 5.5). For two such paths, starting at $s$ and $t$, there are 3 possibilities: (1) they do not cross each other either in the upper half of the diagram, or in the lower part; (2) they cross each other either in the upper half or in the lower part, but not in both; (3) they cross each other both in the upper half and in the lower part of the diagram. The total number of the crossings of the two paths in the two halves of the diagram is, respectively, 0, 1, and 2. The number of crossings of the same paths in the product diagram (where the paths are straightened) is, respectively, 0, 1, and 0. We see, that the parities before and after the paths being straightened are the same. □

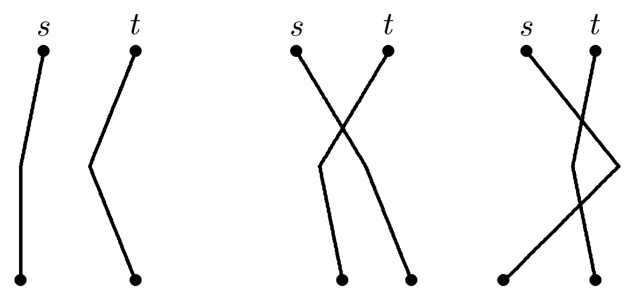


FIGURE 5.5. Proof of Proposition 5.3

COROLLARY 5.2. *For every permutation $\alpha$, the permutations $\alpha$ and $\alpha^{-1}$ have the same parity.*

Proof. This fact (obvious directly) follows from the equality $\alpha\alpha^{-1} = \varepsilon$.□

COROLLARY 5.3. *There are precisely 60 even permutations and 60 odd permutations.*

Proof. Let $\alpha_1, \ldots, \alpha_N$ be all even permutations, and let $\gamma$ be some odd permutation (say 12354)). Then the permutations $\beta_1 = \gamma\alpha_1, \ldots, \beta_n = \gamma\alpha_N$ are all odd and are all different: if $\gamma\alpha = \gamma\alpha'$, then $\gamma^{-1}\gamma\alpha = \gamma^{-1}\gamma\alpha'$, that is, $\alpha = \alpha'$. Moreover, every odd permutation is among the $\beta_i$'s: if $\beta$ is odd, then $\gamma^{-1}\beta$ is even and $\beta = \gamma\gamma^{-1}\beta$. Thus the number of even permutations is equal to the number of odd permutations, and since every permutation is either even or odd, and the total number of permutations is 120, the number of even permutation, as well as the number of odd permutations, equals 60. □

Now we shall prove two theorems about permutations which will be used in subsequent sections of this lecture. First, we shall prove that every permutation can be presented as a product involving only a few very special permutations. The special permutations are

$$\alpha_1 = (52341),\ \alpha_2 = (15342),\ \alpha_3 = (12543),\ \alpha_4 = (12354)$$

(briefly, $\alpha_i$ swaps $i$ with 5 and fixes the rest of the numbers).

THEOREM 5.4. *Any permutation can be presented as a product of $\alpha_i$'s.*

Proof. Consider a diagram (like Figure 5.3) of the given permutation. Assume that no two crossings belong to the same horizontal level, and cut the diagram by horizontal lines to pieces such that there is precisely one crossings within each piece (Figure 5.6). Then the permutation falls into a product of "elementary transpositions"

$$\beta_1 = (21345),\ \beta_2 = (13245),\ \beta_3 = (12435),\ \beta_4 = (12354)$$

($\beta_i$ swaps $i$ with $i+1$ and fixes the remaining numbers). It remains to notice that

$$\beta_1 = \alpha_2\alpha_1\alpha_2,\ \beta_2 = \alpha_3\alpha_2\alpha_3,\ \beta_3 = \alpha_4\alpha_3\alpha_4,\ \beta_4 = \alpha_4$$

(check this!). □

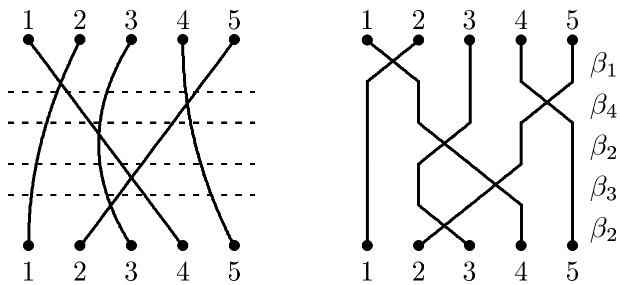


FIGURE 5.6. A decomposition of a permutation into a product of $\beta$s

For two permutations, $\alpha$ and $\beta$, their *commutator* $[\alpha, \beta]$ is defined as $\alpha\beta\alpha^{-1}\beta^{-1}$. Clearly, the commutator of any two permutations is an even permutation.

THEOREM 5.5. *Any even permutation is a product of commutators of even permutations.*

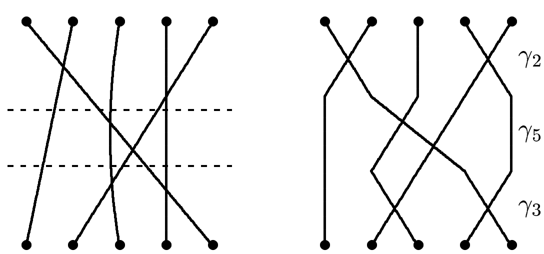


FIGURE 5.7. Proof of Theorem 5.5

Proof. Cut the diagram of the given even permutation by horizontal lines into pieces containing two crossings each (Figure 5.7). Then our permutation will become the product of two-crossing permutations. Obviously, there are precisely 9 such permutations (see Figure 5.8), $\gamma_1, \ldots, \gamma_9$.

Each of these permutations is a commutator of two even permutations:

$$\begin{array}{lll} \gamma_1 = [(42135), \gamma_5] & \gamma_4 = [\gamma_3, \gamma_2] & \gamma_7 = [\gamma_2, \gamma_3] \\ \gamma_2 = [(42351), (14352)] & \gamma_5 = [(52431), (53241)] & \gamma_8 = [(53241), (52431)] \\ \gamma_3 = [\gamma_9, (14352)] & \gamma_6 = [\gamma_2, \gamma_1] & \gamma_9 = [\gamma_1, \gamma_2] \end{array}$$

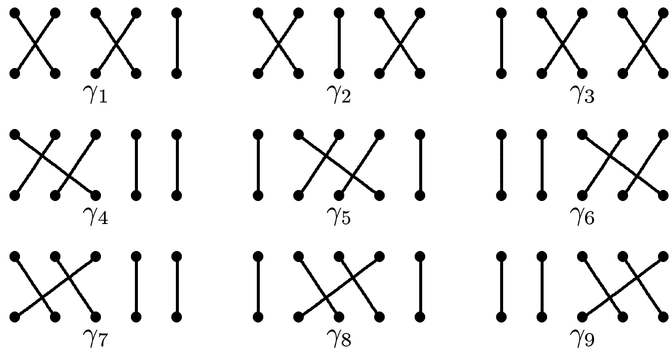


FIGURE 5.8. Permutations $\gamma$

(check this!). □

REMARK 5.4. Theorem 5.4 and its proof are valid for permutations of the set of $n$ elements for any $n \geq 2$ (certainly, in this case we shall have to consider $n-1$ permutations $\alpha_i$). However, the statement of Theorem 5.5 is not true for permutations of the set of $n$ elements, if $n < 5$. Actually, this is the reason why equations of degree less than 5 can be solved in radicals.

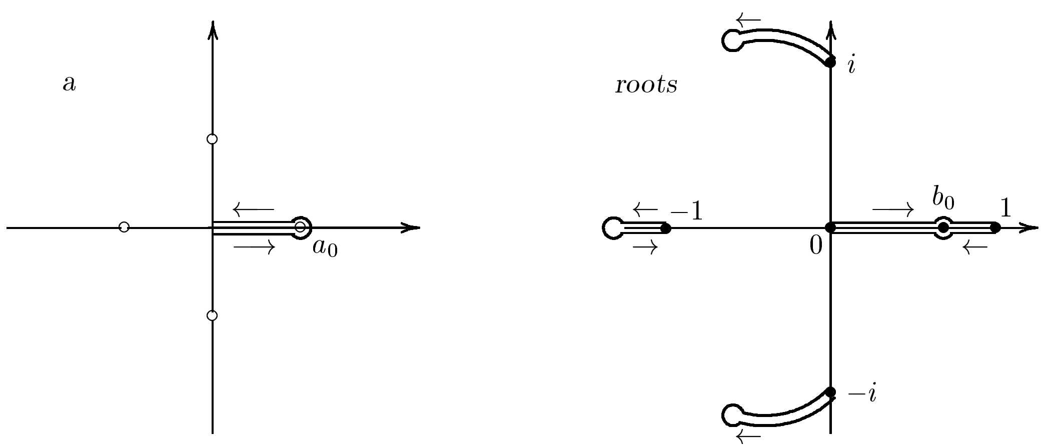


FIGURE 5.9. A special variation of $a$

**5.7 Variation of $a$ and permutations of roots.** Consider a closed path (a "loop") in the plane of $a$ that starts at 0, goes right along the real axis to a close proximity of the "dangerous point" $a_0 = \dfrac{4}{5\sqrt[4]{5}}$, then encircles this point counterclockwise along a circle of a very small radius, and then returns to 0 along the real axis.

It turns out that the roots of our polynomial $x^5 - x + a$ react to this variation of $a$ in the following way (see Figure 5.9). The roots $-1$ and $\pm i$ trace relatively small loops and return to their initial positions. On the contrary, the roots 0 and

1 approach the point $b_0 = \dfrac{1}{\sqrt[4]{5}}$ (and, hence, each other, then make clockwise half-rotations around $b_0$, and then move along the real axis, respectively, to 1 and 0. In particular, they swap their positions: 0 goes to 1 and 1 goes to 0.

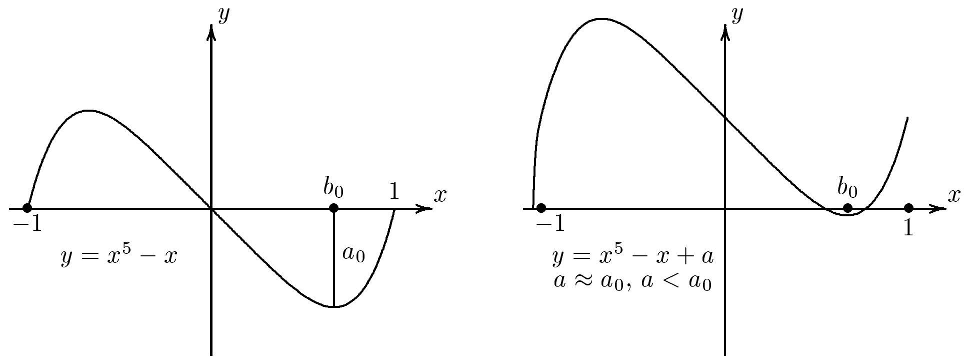


FIGURE 5.10. Two graphs

Let us explain why. The graph of the function $y = x^5 - x$ is shown on Figure 5.10, left (it is easy to draw it as the difference of the two well known graphs $y = x^5$ and $y = x$). If we add $a > 0$ to the function, then the graph goes up, the root $-1$ moves slightly to the left, the roots 0 and 1 move towards each other and almost collide (at the point $b_0$), when $a$ approaches $a_0$. The roots $\pm i$ remain complex conjugated, they never cross the real axis (because if they do, they reach the real axis simultaneously and become a double root therein).

When $a$ encircles $a_0$, the three roots originating from $-1$ and $\pm i$ stay almost unchanged; but what happens to the two other roots? Let us take a small (in absolute value) complex number $\varepsilon$ and look for which $a$ the polynomial $x^5 - x + a$ has the root $b_0 + \varepsilon$. This is a matter of an easy computation:

$$\begin{aligned} a &= (b_0+\varepsilon) - (b_0+\varepsilon)^5 \\ &= b_0 - b_0^5 + \varepsilon(1 - 5b_0^4) - \varepsilon^2(10b_0^3 + 10\varepsilon b_0^2 + 5\varepsilon^2 b_0 + \varepsilon^3) \\ &= a_0 - \varepsilon^2(10b_0^3 + 10\varepsilon b_0^2 + 5\varepsilon^2 b_0 + \varepsilon^3) \approx a_0 - 10b_0^3\varepsilon^2. \end{aligned}$$

(we used the fact that $b_0 - b_0^5 = a_0$ and $1 - 5b_0 = 0$; the symbol $\approx$ means an approximation with an error much less, in the absolute value, than $|\varepsilon|^2$). So, when $x$ makes a clockwise half-rotation around $b_0$, $a$ makes a full counterclockwise rotation around $a_0$. And vice versa: when $a$ makes a full rotation around $a_0$, $x$ makes a half-rotation around $b_0$; as a result, the two roots $x$ close to $b_0$ swap their positions. This justifies Figure 5.9.

Now, let us make one more simple observation. The roots of the polynomial $x^5 - x + ia$ are obtained from the roots of the polynomial $x^5 - x + a$ by multiplication by $i$. This means that if we turn the left Figure 5.9 counterclockwise by 90°, then the right Figure 5.9 will also turn counterclockwise by 90°. We see that the loops, similar to the loop on the left Figure 5.9, but encircling $ia_0$, $-a_0$, and $-ia_0$ (instead $a_0$), will swap the root 0, respectively, with $i, -1$, and $-i$ and keep the remaining three roots in their positions (see Figure 5.11).

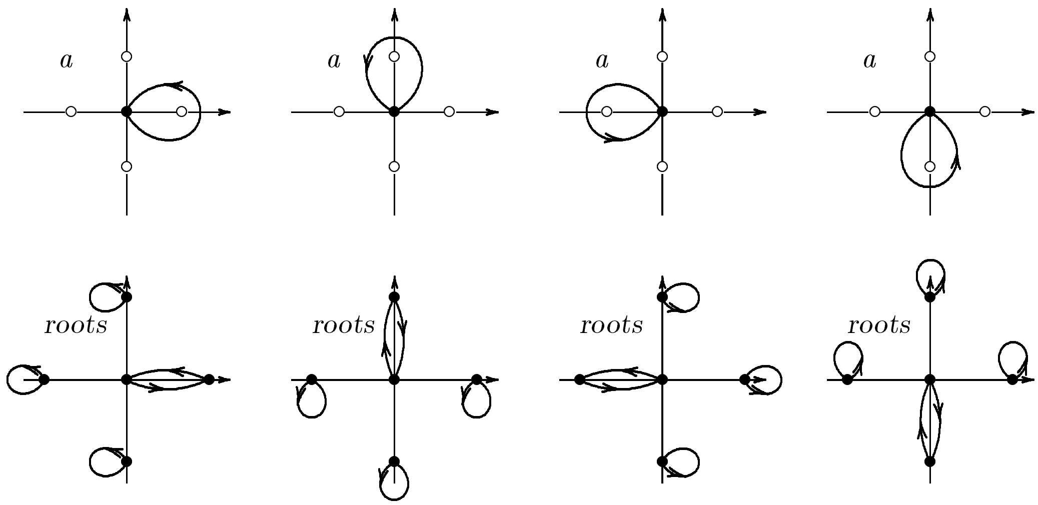


FIGURE 5.11. Swapping the roots

And one more remark. A composition of two loops (that is, a loop which first goes along the first loop and then along the second loop) leads to a permutation of roots which is the product of permutations corresponding to the two loops.

From all this, we can deduce the main result of this section (promised in Section 5.5).

THEOREM 5.6. *For any permutation of the 5 roots* $0, \pm 1, \pm i$, *there exists a loop starting and ending at* $0$ *and avoiding the points* $\pm\dfrac{4}{5\sqrt[4]{5}}, \pm\dfrac{4i}{5\sqrt[4]{5}}$, *which leads to this permutation.*

Proof. Enumerate the roots in the order $1, i, -1, -i, 0$. The construction above gives loops which induce the permutations $\alpha_1, \alpha_2, \alpha_3, \alpha_4$ (in the notations of Section 5.6). Hence, we can find a loop that induces any product of these permutations, that is, according to Theorem 5.4, an arbitrary permutation. □

**5.8 Variation of** $a$ **and permutations of intermediate radicals.** Suppose that equation (5.4) can be solved in radicals:

$$\begin{aligned} x_1^{k_1} &= p_1(a), \\ x_2^{k_2} &= p_2(a, x_1), \\ &\dots\dots\dots\dots\dots\dots \\ x_N^{k_N} &= p_n(a_1, x_1, \dots, x_{N-1}), \end{aligned}$$

and all the solutions of equation (5.4) are contained among the possible values of $x_N$. Theoretically, we can have as many as $k_1 k_2 \dots k_N$ values of $x_N$, but some of them may coincide for all values of $a$ (we observed this phenomenon in the case of a cubic equation). Thus we have a "tower" of values of $a, x_1, \dots, x_N$, see Figure 5.12. (Figure 5.12 presents a schematic picture, which cannot occur in reality: if two values of $x_2$ coincide as shown in this picture then there will be at least two other pairs of merging values). If we vary $a$ then the whole tower begins varying. What is important, the values of $x_N$, which are solutions of the equation (5.4), remain solutions of the equation (5.4), and their variation is the same as was studied in Section 5.7.

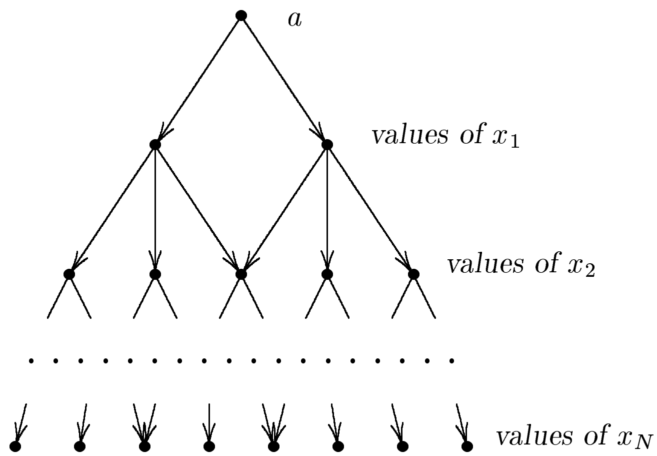


FIGURE 5.12. The tower of values of $x_i$

One more remark. As we observed earlier, some values of $x_M$ (for any $M$) may coincide for all values of $a$. But there might be also accidental coincidences which occur for isolated specific values of $a$. For example, the equation

$$x_1^{k_1} = p_1(a)$$

has $k_1$ solutions (for $x_1$), if $p_1(a) \neq 0$; if $p_1(a) = 0$, there is only one solution ($x_1 = 0$). So, the roots of the polynomial $p_1$ (but there are only finitely many of them) are sites of "accidental coincidences." We have to declare these roots "dangerous" (in addition to the 4 dangerous points (Section 5.5). A coincidence in the second row happens, if

$$p_2(a, x_1) = p_2(a, x_1')$$

for two different solutions $x_1, x_1'$ of the equation $x_1^{k_1} = p_1(a)$. The system

$$\begin{cases} x_1^{k_1} = p_1(a) \\ (x_1')^{k_1} = p_1(a) \\ p_2(a, x_1) = p_2(a, x_1') \end{cases}$$

either has finitely many solutions $(a, x_1, x_1')$ (in which case we declare the corresponding values of $a$ dangerous) or has solutions for all $a$ and also some isolated solutions $(a, x_1, x_1')$ (and we declare dangerous the values of $a$, corresponding to these solutions). Proceeding in this way, we declare dangerous a finite collection of values of $a$ and in the future consider only loops which avoid all dangerous values, old and new. (By the way, it may happen that 0 becomes a dangerous value. Then we should consider loops which start and end not at 0, but at some near-by non-dangerous point.)

**5.9 Commutators of loops.** Let $\ell_1, \ell_2$ be two loops in the plane of $a$. Consider the loop $[\ell_1, \ell_2] = \ell_1 \ell_2 \ell_1^{-1} \ell_2^{-1}$ which traverses the loop $\ell_1$, then $\ell_2$, then $\ell_1$ in the reverse direction, and then $\ell_2$ in the reverse direction (Figure 5.13). This loop is called the commutator of the loops $\ell_1$ and $\ell_2$.

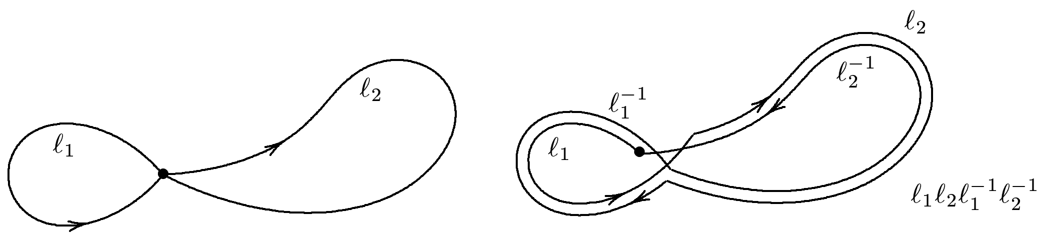


FIGURE 5.13. The commutator of loops.

LEMMA 5.5. *If a loop $\ell$ in the plane of variable $a$ is a product of commutators of loops (avoiding the dangerous points), then the variation of $a$ along $\ell$ returns each value of $x_1$ to its initial position.*

Proof. For any (non-dangerous) value of $a$, the $k_1$ values of $x_1$ can be obtained from one value as

$$x_1, x_1\varepsilon_{k_1}, x_1\varepsilon_{k_1}^2, \ldots, x_1\varepsilon_{k_1}^{k_1-1}$$

where $\varepsilon_{k_1} = \cos\dfrac{2\pi}{k_1} + i\sin\dfrac{2\pi}{k_1}$ is the "primitive $k_1$-th root of 1". The ratios of these values of $x_1$ remain constant in the process of the variation of $a$.

Let $\ell = \ell_1\ell_2\ell_1^{-1}\ell_2^{-1}$. Let the variation of $a$ along $\ell_1$ take $x_1$ to $x_1\varepsilon_{k_1}^{m_1}$ (and, hence, take $x_1\varepsilon_{k_1}^r$ to $x_1\varepsilon_{k_1}^{r+m_1}$) and the variation of $a$ along $\ell_2$ take $x_1$ to $x_1\varepsilon_{k_1}^{m_2}$ (and, hence, take $x_1\varepsilon_{k_1}^r$ to $x_1\varepsilon_{k_1}^{r+m_2}$). Then the successive variations of $a$ along $\ell_1, \ell_2, \ell_1^{-1}$, and $\ell_2^{-1}$ transforms $x_1$ according to the rule

$$x_1 \mapsto x_1\varepsilon_{k_1}^{m_1} \mapsto x_1\varepsilon_{k_1}^{m_1+m_2} \mapsto x_1\varepsilon_{k_1}^{m_1+m_2-m_1} \mapsto x_1\varepsilon_{k_1}^{m_1+m_2-m_1-m_1} = x_1.$$

Thus, the variation of $a$ along a commutator of loops takes every value of $x_1$ to itself, and the same is true for products of commutators. □

LEMMA 5.6. *If a loop $\ell$ in the plane of $a$ is*
*a product of commutators of*
*products of commutators of*
*loops (avoiding the dangerous points), then the variation of $a$ along $\ell$ returns each value of $x_1$ and $x_2$ to its initial position.*

Proof. Let $\ell$ be a commutator of loops $\ell_1, \ell_2$ which are, in turn, products of commutators. Then, according to Lemma 5.5, the variation of $a$ along each of the loops $\ell_1, \ell_2$ takes every value of $x_1$ to itself. Since

$$x_2^{k_2} = p_2(a, x_1),$$

$x_2$ must be taken to $x_2\varepsilon_{k_2}^m$ for some $m$. In this case, $x_2\varepsilon_{k_2}^r$ will be taken to $x_2\varepsilon_{k_2}^{r+m}$ (the ratios between $x_2's$ corresponding to the same – varying – value of $x_1$ remains constant during the variation). Thus, the successive variations along the loops $\ell_1, \ell_2, \ell_1^{-1}, \ell_2^{-1}$ transforms $x_2$ in the following way:

$$x_2 \mapsto x_2\varepsilon_{k_2}^{m_1} \mapsto x_2\varepsilon_{k_2}^{m_1+m_2} \mapsto x_2\varepsilon_{k_2}^{m_1+m_2-m_1} \mapsto x_2\varepsilon_{k_2}^{m_1+m_2-m_1-m_1} = x_2.$$

Thus, the variation of $a$ along the commutator of products of commutators of loops avoiding the dangerous points takes any value of $x_2$ (as well as any value of

$x_1$) to itself, and the same is true for any product of commutators of products of commutators. □

Proceeding in the same way, we prove a chain of lemmas ending with

LEMMA 5.7. *If a loop $\ell$ is*

$$N \left\{ \begin{array}{l} \textit{a product of commutators of} \\ \textit{products of commutators of} \\ \dots\dots\dots\dots\dots\dots \\ \textit{products of commutators of} \end{array} \right.$$

*loops (avoiding the dangerous points), then the variation of $a$ along $\ell$ returns any values of $x_1, \dots, x_N$ to its initial position.*

We are fully prepared now for the

**5.10 Proof of main theorem.** Suppose that the equation $x^5 - x + a = 0$ is solvable in radicals. Fix some non-identical even permutation $\alpha_0$ of roots. Present $\alpha_0$ as a product of commutators of even permutations,

$$\alpha_0 = [\alpha_1, \alpha_2][\alpha_3, \alpha_4] \dots [\alpha_{2s-1}, \alpha_{2s}].$$

Then present each $\alpha_i$ as a product of commutators of even permutations,

$$\begin{array}{l} \alpha_1 = [\alpha_{11}, \alpha_{12}] \dots [\alpha_{1,2t-1}, \alpha_{1,2t}] \\ \dots\dots\dots\dots\dots\dots\dots\dots \end{array}$$

And so on, $N$ times. For each permutation $\alpha_{i_1 \dots i_N}$ occurring in the last, $N$-th, step, find a loop $\ell_{i_1 \dots i_N}$ avoiding all the dangerous values of $a$ which induces this permutation. In the expression of $\alpha_0$ via $\alpha_{i_1 \dots i_N}$'s replace each permutation $\alpha_{i_1 \dots i_N}$ by the corresponding loop $\ell_{i_1 \dots i_N}$. We shall obtain a loop which is an $N$-fold product of commutators of loops (as in Lemma 5.7).

On the one hand, by Lemma 5.7, this loop returns every value of $x_N$ to its initial position, and hence returns each root of the equation (5.4) to its initial position. On the other hand, this loop induces the (non-identical) permutation $\alpha_0$ of the roots.

This contradiction proves the theorem. □

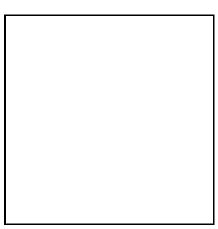

John Smith
January 23, 2010

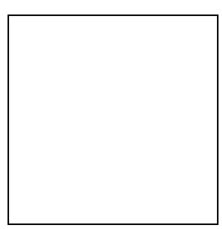

Martyn Green
August 2, 1936

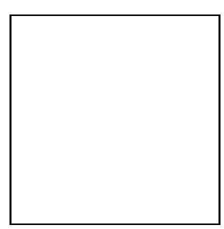

Henry Williams
June 6, 1944

### 5.11 Exercises.

5.1. Write a chain of formulas, as in the end of Section 5.2, solving the equation

$$x^4 + qx + r = 0.$$

How many solutions does it have? The extraneous solutions are the roots of some other equations. Which ones?

*Remark.* We suggest to consider a particular equation of degree 4 above, since for the general equation $x^4 + px^2 + qx + r = 0$, the solution is basically the same, but the formulas are much longer.

5.2. Prove that there are precisely 4 permutations $(i_1, i_2, i_3, i_4)$ of the set $\{1, 2, 3, 4\}$ which can be presented as products of commutators of even permutations (actually, they are just commutators of even permutations). Prove this and find these 4 permutations.

5.3. Consider the cubic equation

$$x^3 + ax - 1 = 0.$$

For $a = 0$, it has 3 roots: 1, $\varepsilon_3 = \dfrac{-1+\sqrt{3}i}{2}$, and $\overline{\varepsilon}_3$.

(a) For which values of $a$, does our equation have double roots (that is, what are the “dangerous values” of $a$)?

(b) One of these dangerous values of $a$ is real (and negative). If $a$ makes a loop around this dangerous value starting from 0 (as shown in the third diagram from the left in the upper row in Figure 5.11), then what is the resulting permutation of the roots?

(c) Show that any permutation of the roots can be obtained from a loop starting from $a = 0$, avoiding dangerous values of $a$ and returning to 0.

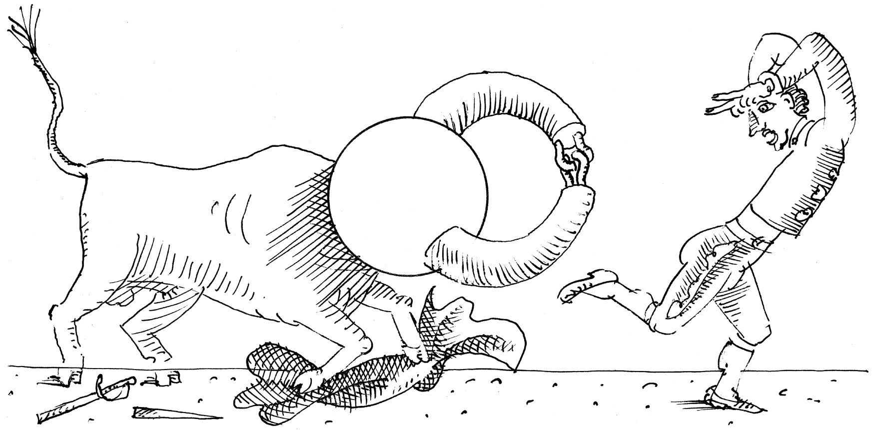

LECTURE 6

# How Many Roots Does a Polynomial Have?

Roots of polynomials are discussed more than once on these pages. The reaction of an average student of mathematics (or that of a practicing mathematician) to the question in the title of this lecture is that the number of roots of a polynomial of degree $n$ does not exceed $n$. Some would add that if one counts complex roots, and counts them with multiplicities, then this number is exactly $n$ (we shall prove this Fundamental Theorem of Algebra in Section 6.4).

The content of this lecture is different: we shall discuss two rather surprising facts. The first is that the number of real roots of a polynomial with real coefficients depends not on its degree but rather on the number of its non-zero coefficients. The second is that, although there are no explicit formulas for roots (see Lecture 5), one can determine exactly how many roots any polynomial has on a given segment.

**6.1 Fewnomials.** A fewnomial is not a mathematical term.[1] That is the name we give to a polynomial[2] of a large degree with only a few non-zero coefficients. A typical fewnomial is $x^{100} - 1$ or $ax^n + bx^m$. The main property of fewnomials is that they have only a few roots.

THEOREM 6.1. *A polynomial with $k$ non-zero coefficients has no more than $2k-1$ real roots.*

Proof. Induction on $k$. For $k = 1$, the result is obvious: $ax^n = 0$ has only one root, $x = 0$.

Let $f(x)$ be a polynomial with $k+1$ non-zero coefficients. Then, for some $r \geq 0$, $f(x) = x^r g(x)$ where $g(x)$ still has $k+1$ non-zero coefficients, and one of them is the constant term. Differentiation kills this constant term, and it follows that $g'(x)$ has $k$ non-zero coefficients. By the induction assumption, $g'(x)$ has at most $2k-1$ roots.

[1]The term was coined by A. Khovanskii.

[2]The polynomials in this lecture, except for the last section, are with real coefficients, and we are concerned only with their real roots.

Rolle's theorem implies that, between two consecutive roots of a polynomial (actually, any differentiable function, see Figure 6.1), there exists a root of its derivative. It follows that the number of roots of $g(x)$ does not exceed $2k$. As to $f(x)$, its roots are those of $g(x)$ and, possibly, $x = 0$. Therefore, $f(x)$ has at most $2k + 1$ roots, as claimed. □

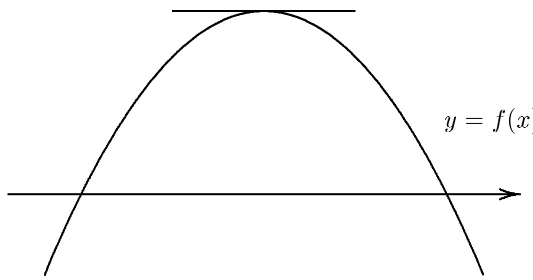


FIGURE 6.1. Rolle's theorem

The estimate of Theorem 6.1 is sharp: $x(x^2 - 1)(x^2 - 4) \cdots (x^2 - k^2)$ has $2k+1$ roots $0, \pm 1, \pm 2, \cdots, \pm k$ and $k + 1$ non-zero coefficients.

**6.2 Descartes' rule.** Theorem 6.1 becomes too weak if one is interested only in positive roots. For example, a polynomial with non-negative coefficients does not have positive roots at all! The next, more refined, theorem is called the Descartes rule.

THEOREM 6.2. *The number of positive roots of a polynomial does not exceed the number of sign changes in the sequence of its non-zero coefficients.*

In particular, Descartes' rule implies Theorem 6.1: one applies Descartes' rule twice, to the positive and the negative half-lines.

Proof. Let us examine what happens to the coefficients of a polynomial when a new positive root appears. Let $f(x) = (x - b)g(x)$ where $b > 0$ and $g(x) = a_0x^n + a_1x^{n-1} + \cdots + a_{n-1}x + a_n$. The coefficients of $f(x)$ are:

$$a_0, a_1 - ba_0, a_2 - ba_1, \cdots, a_n - ba_{n-1}, -ba_n. \tag{6.1}$$

The coefficients

$$a_0, a_1, \cdots, a_n \tag{6.2}$$

of the polynomial $g(x)$ are grouped into consecutive blocks of numbers having the same sign (we do not care about zeros); see Figure 6.2 where these blocks are represented by ovals. We see that in each place where the sequence $a_i$ changes sign, there arises the same sign as in the right oval. Namely, if $a_k < 0, a_{k+1} > 0$ then $a_{k+1} - ba_k > 0$, and if $a_k > 0, a_{k+1} < 0$ then $a_{k+1} - ba_k < 0$. Moreover, at the beginning of the sequence (6.1), we have the same sign as at the beginning of sequence (6.2), and at the end of (6.1), one has the sign opposite to that at the end of (6.2).

It follows that the number of sign changes in the sequence (6.1) is at least one greater than that in the sequence (6.2). That is, each new positive root of a

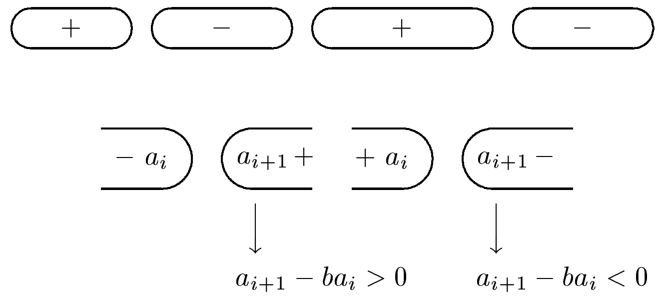


FIGURE 6.2. How a new root affects the coefficients of a polynomial

polynomial increases the number of sign changes in the sequence of its coefficients by at least one.

To finish the proof, write $f(x)$ as $(x - b_1)\cdots(x - b_k)g(x)$ where $g(x)$ does not have positive roots. Then the number of sign changes in the sequence of coefficients of $f(x)$ is at least that of $g(x)$ plus $k$, hence, not less than $k$. □

**6.3 Sturm's method.** In this section we shall explain how to determine the number of roots of a polynomial on a given segment. Let $f(x)$ be a polynomial without multiple roots. We shall construct a sequence of polynomials $p_0(x), p_1(x), p_2(x), \cdots, p_n(x)$ of decreasing degrees, called a Sturm sequence, that enjoys the properties:

(1) $p_0(x) = f(x), p_1(x) = f'(x)$;

(2) if $p_k(t) = 0$ then the numbers $p_{k-1}(t)$ and $p_{k+1}(t)$ are non-zero and have the opposite signs;

(3) the last polynomial $p_n(x)$ does not have any roots at all.[3]

Let us call such a sequence of polynomials a Sturm sequence. For a given $x$, let $S(x)$ be the number of sign changes in the sequence $p_0(x), \cdots, p_n(x)$ (again, ignoring zeros). For example, the sequence $2, 0, 1$ has no sign changes whereas $2, 0, -1$ has one.

To determine the number of roots of $f(x)$ on a segment $(a, b)$ (we do not exclude the case when either $a$, or $b$, or both are infinite) one computes $S(a) - S(b)$: *this is the number of roots of* $f(x)$ *on the interval* $(a, b)$.

Let us prove that this is indeed the case. As $x$ moves from $a$ to $b$, the number $S(x)$ may change only when $x$ is a root of one of the polynomials $p_i$. If $x$ is a root of $p_0 = f$ then either $f$ changes sign from $-$ to $+$, and then $f'(x) > 0$, or from $+$ to $-$, and then $f'(x) < 0$, see Figure 6.3. The first two terms in the Sturm sequence change as follows:

$$(- + \cdots) \mapsto (+ + \cdots) \quad \text{or} \quad (+ - \cdots) \mapsto (- - \cdots),$$

and in both cases, the number of sign changes decreases by 1.

If $x$ is a root of a polynomial $p_k$ with $0 < k < n$ then, according to the second property of Sturm sequences, the signs of $p_{k-1}(x)$ and $p_{k+1}(x)$ are opposite. This implies that, no matter how the sign of $p_k$ changes, the number of sign changes in

[3]Recall that we consider only real roots.

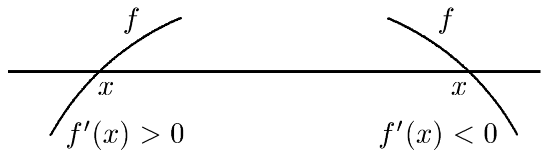


FIGURE 6.3. The number of sign changes decreases by 1

the Sturm sequence remains the same:

$$(\cdots - + + \cdots) \mapsto (\cdots - - + \cdots) \quad \text{or} \quad (\cdots + + - \cdots) \mapsto (\cdots + - - \cdots).$$

It remains to construct a Sturm sequence. This is done by long division of polynomials. We already know the terms $p_0$ and $p_1$. To construct $p_{k+1}$ from $p_k$ and $p_{k-1}$, divide the latter by the former and take the remainder with the opposite sign:

$$p_{k-1}(x) = q(x)p_k(x) - p_{k+1}(x). \tag{6.3}$$

Note that the degree of the next term, $p_{k+1}$, is smaller than that of $p_k$; thus, the division will terminate after finitely many steps.

This process is a version of the Euclidean algorithm for finding the greatest common divisor of two numbers, discussed in Section 1.9. And indeed, the last polynomial, $p_n(x)$, is the greatest common divisor of $f(x)$ and $f'(x)$. This implies that $p_n(x)$ has no roots: if such a root existed it would be also a common root of $f(x)$ and $f'(x)$, that is, $f(x)$ would have a multiple root[4] – the case that was excluded from the very beginning.

It remains to verify property (2) of Sturm sequences. Assume that $p_k(x) = 0$. We see from (6.3) that $p_{k+1}(x)$ and $p_{k-1}(x)$ have opposite signs, provided they are both non-zero. If $p_{k+1}(x) = 0$ then (6.3) implies that $p_{k-1}(x) = 0$ as well, and iterating the argument, eventually that $p_1(x) = p_0(x) = 0$. But this again means that $f$ has a multiple root at $x$ which is impossible.

To summarize, (6.3) is an algorithm for constructing a Sturm sequence. Let us work out an example.

Let $f(x) = x^5 - x + a$, the main character of Lecture 5. The Sturm sequence consists of four terms:

$$x^5 - x + a, \quad x^4 - \frac{1}{5}, \quad x - \frac{5}{4}a, \quad \left(\frac{5}{4}\right)^4 a^4 - \frac{1}{5}$$

(we scaled some terms by positive factors to keep the leading coefficient equal to 1). One immediately sees that the values of $a$ for which $a^4 = 4^4/5^5$ is "dangerous", hardly a new fact for those familiar with Lecture 5.

To fix ideas, assume that $a^4 > 4^4/5^5$. Let us determine the total number of real roots of $f(x)$. The signs of the Sturm sequence at $-\infty$ and $+\infty$ are

$$(-, +, -, +) \quad \text{and} \quad (+, +, +, +),$$

hence there are 3 roots (if $a^4 < 4^4/5^5$ this number is equal to 1).

[4]This fact is proved in Section 8.2.

What about the number of positive roots? To answer this question, we need to evaluate the polynomials of the Sturm sequence at $x = 0$. We get:

$$a, \quad -\frac{1}{5}, \quad \frac{5}{4}a, \quad \left(\frac{5}{4}\right)^4 a^4 - \frac{1}{5}.$$

Still assuming that the last number is positive, there are two cases: $a > 0$ and $a < 0$. In the former, we have the signs $(+, -, -, +)$, and in the latter $(-, -, +, +)$.

Comparing this to the signs at $+\infty$ (all pluses), we conclude that if $a > 0$ there are 2 positive roots, and if $a < 0$ there is a single one (this also holds for $a = 0$).

**6.4 Fundamental Theorem of Algebra.** We feel that this lecture would not be complete without a discussion of the Fundamental Theorem of Algebra.[5] The reader probably knows what it states: every complex polynomial of degree $n$ has exactly $n$ complex roots (counted with multiplicities). In fact, it suffices to show that there exists one: if $b$ is a root of $f(x)$ then $x - b$ divides $f(x)$. Then the quotient also has a root, etc., until all $n$ roots are found.

It has been noted that nearly every branch of mathematics tests its techniques and demonstrates its maturity by providing a proof of the Fundamental Theorem of Algebra. We shall give a proof that makes use of the notion of the rotation number of a closed curve about a point.[6] Given a polynomial $f(x) = x^n + a_1 x^{n-1} + \cdots + a_n$ with complex coefficients, assume that 0 is not its value for any complex $x$. We view $f$ as a continuous map from the complex plane to itself.

Consider the circle of radius $t$ about the origin and let $\gamma_t$ be the image of this circle under the map $f$. Then $\gamma_t$ is a closed curve that does not pass through the origin. Let $r(t)$ be the rotation number (total number of turns) of this curve about the origin. As $t$ varies from very small to very big values, the number $r(t)$ does not change: indeed, this is an integer, that continuously depends on $t$, and therefore constant.

Let us compute $r(t)$ for $t$ very small. The constant term $a_n$ of $f(x)$ is non-zero, otherwise $f(0) = 0$. If $t$ is small enough then the curve $\gamma_t$ lies in a small neighborhood of the point $a_n$ and does not go around the origin at all, see Figure 6.4. Thus $r(t) = 0$.

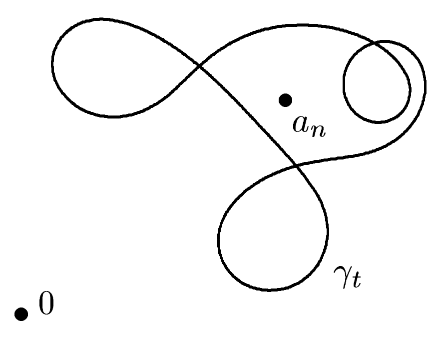


FIGURE 6.4. For $t$ small, the rotation number is zero

[5]Its first proof was published by d'Alembert in 1746.

[6]See Lecture 12 for a detailed discussion.

What about $r(t)$ for $t$ very large? Let us write

$$f(x) = x^n \left(1 + \frac{a_1}{x} + \frac{a_2}{x^2} + \cdots + \frac{a_n}{x^n}\right).$$

Now we deform this formula:

$$f_s(x) = x^n \left(1 + s\left(\frac{a_1}{x} + \frac{a_2}{x^2} + \cdots + \frac{a_n}{x^n}\right)\right) \tag{6.4}$$

where $s$ varies from 1 to 0. Let $\gamma_{t,s}$ be the image of the circle of radius $t$ under the map $f_s$.

If $|x|$ is sufficiently large then the complex number inside the inner parentheses in (6.4) is small, in particular, its absolute value is less than 1. Indeed, let $|x|^i > n|a_i|$ for all $i = 1, \ldots, n$. Then

$$\left|\frac{a_1}{x} + \frac{a_2}{x^2} + \cdots + \frac{a_n}{x^n}\right| \le \frac{|a_1|}{|x|} + \cdots + \frac{|a_n|}{|x^n|} < n \cdot \frac{1}{n} = 1.$$

It follows that the curves $\gamma_{t,s}$ do not pass through the origin for all $s$. Hence they all have the same rotation numbers about the origin. This rotation number is especially easy to find for $s = 0$: since $f_0(x) = x^n$, the curve $\gamma_{t,0}$ is a circle of radius $t^n$, making $n$ turns about the origin and hence having the rotation number $n$.

It follows that $r(t) = n$ for $t$ large enough, while $r(t) = 0$ for small values of $t$. This is a contradiction, which proves that $f(x)$ has a root.

In conclusion, let us outline a different argument, very much in the spirit of Lectures 8 and 5.

We considered in these lectures the space of polynomials of a certain type (such as $x^3 + px + q$ or $x^5 - x + a$) and saw that the set of polynomials with multiple roots separated the whole space into pieces, corresponding to the number of roots of a polynomial. The set of polynomials with multiple roots is a (very singular) hypersurface obtained by equating the discriminant of a polynomial to zero.

Unlike the real case, the set of zeros of a complex equation does not separate complex space. This is particularly obvious in dimension one: a finite set of points partitions the real line into a number of segments and two rays, but does not separate the complex plane, so that every two points can be connected by a path avoiding this set.

One starts with a polynomial $f_0(x)$ of degree $n$ that manifestly has $n$ roots, say, $(x-1)(x-2)\cdots(x-n)$. Any other polynomial, $f(x)$, without multiple roots can be connected with $f_0(x)$ by a path in the space of polynomials without multiple roots. When one "moves" $f_0$ to $f$, the roots also move, but never collide, until they become the roots of $f(x)$ (this process is described in detail in Lecture 5).

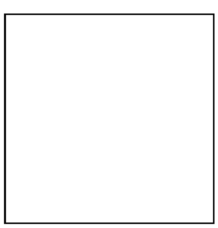

John Smith
January 23, 2010

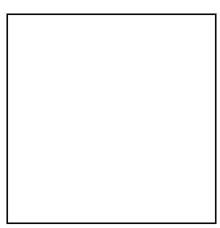

Martyn Green
August 2, 1936

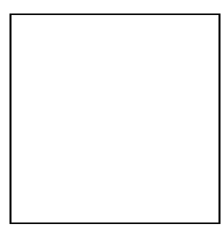

Henry Williams
June 6, 1944

### 6.5 Exercises.

6.1. A polynomial of degree $n$ is called hyperbolic if it has $n$ distinct real roots. Prove that if $f(x)$ is a hyperbolic polynomial then so is its derivative $f'(x)$.

6.2. Prove that between two roots of a polynomial $f(x)$ there is a root of the polynomial $f'(x) + af(x)$ where $a$ is an arbitrary real.

6.3. Let $f(x)$ be a polynomial without multiple roots. Consider the curve in the plane given by the equations $x = f(t),\ y = f'(t)$.

(a) This curve does not pass through the origin.

(b) The curve intersects the positive $y$-semiaxis from left to right, and the negative one from right to left.

(c) Conclude that between two roots of $f$ there lies a root of $f'$ (Rolle's theorem).

6.4. (a) If a graph $y = f(x)$ intersects a line in three distinct points then there is an inflection point of the graph between the two outermost intersections.

(b) If a function coincides at $n+1$ points with a polynomial of degree $n-1$ then its $n$th derivative has a root.

6.5. The polynomial

$$1 + \frac{x}{1!} + \frac{x^2}{2!} + \cdots + \frac{x^n}{n!}$$

has either no roots or one root according as $n$ is even or odd.

*Remark*. In contrast, as $n \to \infty$, the complex roots of this polynomial have an interesting distribution. More precisely, in the limit $n \to \infty$, the complex roots of the polynomial

$$1 + \frac{nx}{1!} + \frac{(nx)^2}{2!} + \cdots + \frac{(nx)^n}{n!}$$

tend to the curve $|ze^{1-z}| = 1$, a theorem by G. Szegö [**77**].

6.6. Prove that the number of positive roots of a polynomial has the same parity as the number of sign changes in the sequence of its coefficients.

6.7. Prove the Descartes rule for the function

$$f(x) = a_1 e^{\lambda_1 x} + a_2 e^{\lambda_2 x} + \cdots + a_n e^{\lambda_n x} :$$

if $\lambda_1 < \lambda_2 < \cdots < \lambda_n$ then the number of roots of the equation $f(x) = 0$ does not exceed the number of sign changes in the sequence $a_1, \ldots, a_n$.

6.8. Compute the Sturm sequence and determine the number of roots of the polynomial $x^3 - 3x + 1$ on the segments $[-3, 0]$ and $[0, 3]$.

6.9. * The following result is known as the Fourier-Budan theorem.

Let $f(x)$ be a polynomial of degree $n$. Let $S(x)$ be the number of sign changes in the sequence $f(x), f'(x), f''(x), \ldots, f^{(n)}(x)$. Then the number of roots of $f$ between $a$ and $b$, where $f(a) \neq 0, f(b) \neq 0$ and $a < b$, is not greater than and has the same parity as $S(a) - S(b)$.

6.10. The following approach to the Fundamental Theorem of Algebra is due to Gauss.

Let $f(x)$ be a generic complex polynomial of degree $n$. Consider the two curves, $\gamma_1$ and $\gamma_2$, given by the conditions that the real and the imaginary parts of $f(x)$ equal zero. One wants to prove that $\gamma_1$ and $\gamma_2$ intersect.

Prove that each curve $\gamma_1$ and $\gamma_2$ intersects the boundary $C$ of a sufficiently large disc $D$ at exactly $2n$ points, and the points $\gamma_1 \cap C$ alternate with the points $\gamma_2 \cap C$. Conclude that $\gamma_1 \cap D$ and $\gamma_2 \cap D$ consist of $n$ components each, and that every component of $\gamma_1 \cap D$ crosses some component of $\gamma_2 \cap D$.

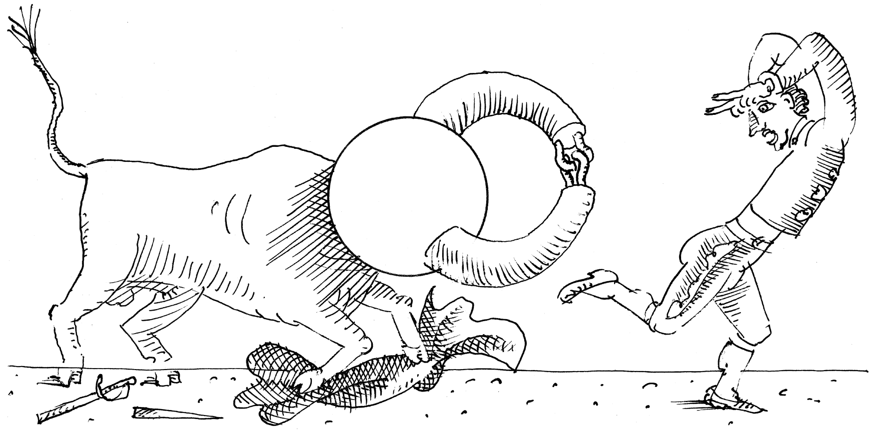

LECTURE 7

# Chebyshev Polynomials

**7.1 The problem.** The topic of this lecture is a very elegant problem on polynomials that goes back to P. Chebyshev, an outstanding Russian 19-th century mathematician (cf. Lecture 18).

Fix a segment of the real axis, say, $[-2, 2]$ (the formulas for this segment are the simplest possible; see Exercise 7.2 for the general case). Given a monic polynomial of degree $n$

$$P_n(x) = x^n + a_1 x^{n-1} + \cdots + a_n, \tag{7.1}$$

let $M$ and $m$ be its maximum and minimum on the segment $[-2, 2]$. The *deviation of $P_n(x)$ from zero* is the greatest of the numbers $|M|$ and $|m|$. If the deviation from zero is $c > 0$ then the graph of the polynomial is contained in the strip $|y| \le c$ and is not contained in any narrower strip symmetric with respect to the $x$-axis.

The problem is to find the monic polynomial of degree $n$ whose deviation from zero is as small as possible, and to find the value of this smallest deviation.

**7.2 Small degrees.** Let us experiment with polynomials of small degrees.

Example 7.1. If $P_1(x) = x + a$ then $M = a + 2, m = a - 2$. If $c$ is the deviation from zero then $|a + 2| \le c, |a - 2| \le c$. By the triangle inequality

$$2c \ge |a + 2| + |a - 2| \ge |(a + 2) - (a - 2)| = 4,$$

and hence $c \ge 2$. This deviation is attained by the polynomial $P_1(x) = x$.

Example 7.2. Let us consider polynomials of degree two, $P_2(x) = x^2 + px + q$. A little reflection suggests that the optimal position of the graph of a quadratic polynomial is the most symmetric one, as in Figure 7.1. This figure depicts the graph of the polynomial $x^2 - 2$ whose deviation from zero is 2.

Let us prove that this is indeed the answer for polynomials of degree 2. If $c$ is the deviation from zero of $P_2(x)$ then the moduli of its values at the end points $\pm 2$

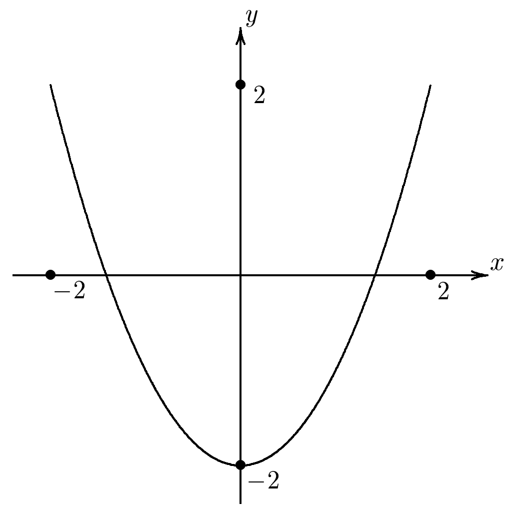


FIGURE 7.1. The "best" quadratic parabola

and point 0 do not exceed $c$:

$$\begin{aligned} c &\geq |4-2p+q|, \\ c &\geq |4+2p+q|, \\ c &\geq |q|. \end{aligned}$$

Using the triangle inequality again yields:

$$4c \geq |4-2p+q| + |4+2p+q| + 2|q| \geq |(4-2p+q)+(4+2p+q)-2q| = 8,$$

and hence $c \geq 2$.

EXAMPLE 7.3. Let us try our luck once again, for polynomials of degree three, $P_3(x) = x^3 + px^2 + qx + r$. If $c$ is the deviation from zero of $P_3(x)$ then the moduli of its values at the end points $\pm 2$ and points $\pm 1$ do not exceed $c$:

$$\begin{aligned} c &\geq |-8+4p-2q+r|, \\ c &\geq |8+4p+2q+r|, \\ c &\geq |-1+p-q+r|, \\ c &\geq |1+p+q+r|. \end{aligned}$$

The triangle inequality yields:

$$\begin{aligned} 2c \geq &\ |-8+4p-2q+r| + |8+4p+2q+r| \geq |16+4q|, \\ 4c \geq &\ 2|-1+p-q+r| + 2|1+p+q+r| \geq |4+4q|, \end{aligned}$$

and applying the triangle inequality again,

$$6c \geq |16+4q| + |4+4q| \geq |(16+4q)-(4+4q)| = 12,$$

which implies that $c \geq 2$. An example of a cubic polynomial with deviation from zero 2 is $x^3 - 3x$.

An adventurous reader may try to consider polynomials of degree 4 but this is not a very inviting task. One may conjecture that the least deviation from zero will be always 2, but to prove this, one needs more than just "brute force".

**7.3 Solution.** Suppose that, for some $c > 0$, we found a polynomial $P_n(x)$ of degree $n$ such that its graph (over the segment $[-2, 2]$) lies in the strip $|y| \leq c$ and contains $n+1$ points of its horizontal boundaries: the right-most on the upper boundary $y = c$, the next left on the lower boundary $y = -c$, the next left on $y = c$, etc. Thus the graph snakes between the lines $y = \pm c$, touching them alternatively $n + 1$ times.

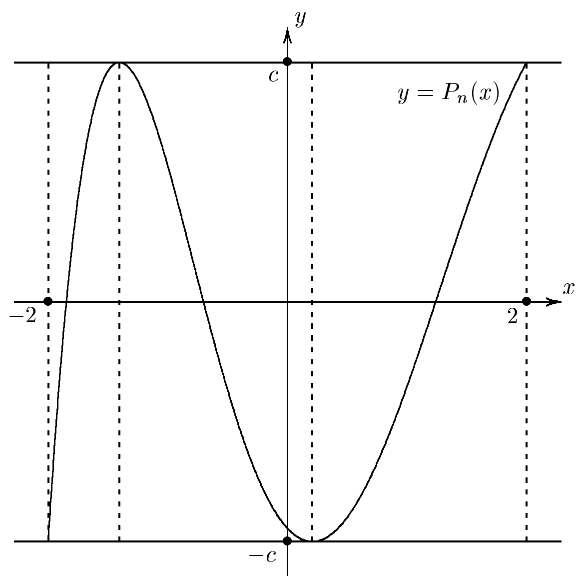


FIGURE 7.2. The graph of an optimal polynomial

THEOREM 7.1. *The deviation from zero of any monic polynomial of degree $n$ is not less than $c$, and $P_n(x)$ is the unique monic polynomial of degree $n$ with the deviation from zero equal to $c$.*

Proof. Let $Q_n(x)$ be another monic polynomial of degree $n$ whose deviation from zero is less than or equal to $c$. Then its graph also lies in the strip $|y| \leq c$.

Let us partition this strip into $n + 1$ rectangles by the vertical lines through the maxima and minima of $P_n(x)$, see Figure 7.2. The graph of $P_n(x)$ connects the diagonally opposite vertices of each rectangle, therefore the graph of $Q_n(x)$ interests that of $P_n(x)$ in each rectangle (see Figure 7.3). There are $n$ such rectangles, and therefore the equation $P_n(x) - Q_n(x) = 0$ has at least $n$ roots. But $P_n(x) - Q_n(x)$ is a polynomial of degree $n-1$, which has at most $n-1$ roots, unless it is identically zero. Conclusion: $P_n(x) \equiv Q_n(x)$, and we are done. □

We cannot claim yet "mission accomplished" because we still do not have the polynomials $P_n(x)$ satisfying the conditions of Theorem 7.3.

LEMMA 7.4. *There exists a monic polynomial $P_n(x)$ of degree $n$ such that*

$$2 \cos n\alpha = P_n(2 \cos \alpha). \tag{7.2}$$

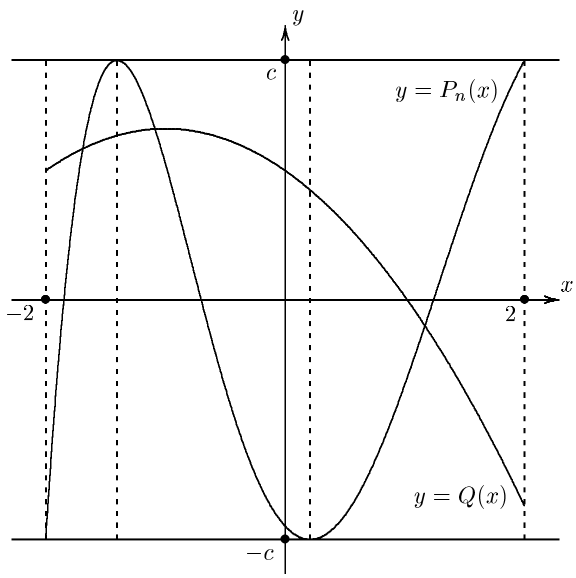


FIGURE 7.3. Proof of Theorem 7.1

For example,

$$\begin{aligned} 2\cos 2\alpha &= 4\cos^2\alpha - 2 = (2\cos^2\alpha)^2 - 2, \quad \text{thus} \quad P_2(x) = x^2 - 2, \\ 2\cos 3\alpha &= 8\cos^3\alpha - 6\cos\alpha = (2\cos^2\alpha)^3 - 3(2\cos\alpha), \quad \text{thus} \quad P_3(x) = x^3 - 3x. \end{aligned}$$

Proof. (cf. Proposition 2.4) Induction on $n$. Assume that (7.2) holds for $n-1$ and $n$. Then

$$\cos(n+1)\alpha + \cos(n-1)\alpha = 2\cos\alpha\cos n\alpha,$$

and hence

$$\begin{aligned} 2\cos(n+1)\alpha = 4\cos\alpha\cos n\alpha - 2\cos(n-1)\alpha &= (2\cos\alpha)(2\cos n\alpha) - 2\cos(n-1)\alpha \\ &= (2\cos\alpha)P_n(2\cos\alpha) - P_{n-1}(2\cos\alpha). \end{aligned}$$

Therefore

$$P_{n+1}(x) = xP_n(x) - P_{n-1}(x). \tag{7.3}$$

This recurrence relation defines the desired sequence of monic polynomials $P_n$ of degree $n$. □

The polynomials $P_n(x)$ are what we need. Indeed, let $\alpha$ vary over $[0, \pi]$. Then $n\alpha$ varies over $[0, n\pi]$, and the functions $x = 2\cos\alpha$ and $P_n(x) = 2\cos n\alpha$ range over the segment $[-2, 2]$. Moreover, $x$ covers this segment exactly once, while $P_n(x)$ covers it $n$ times, assuming alternating values $\pm 2$ for $x = \arccos(k\pi/n)$, $k = 0, \ldots, n$. This means that the graph of the polynomial $P_n(x)$ lies in the strip $|y| \leq 2$ and contains $n+1$ points of its alternating boundaries.

Let us summarize: *there is a unique monic polynomial of degree $n$, given by (7.2), whose deviation from zero on segment $[-2, 2]$ is 2, and the deviation from zero of any other monic polynomial of degree $n$ is greater.*

The polynomials $P_n(x)$ are called Chebyshev polynomials ; see Figure 7.4 for the graphs of the first Chebyshev polynomials.

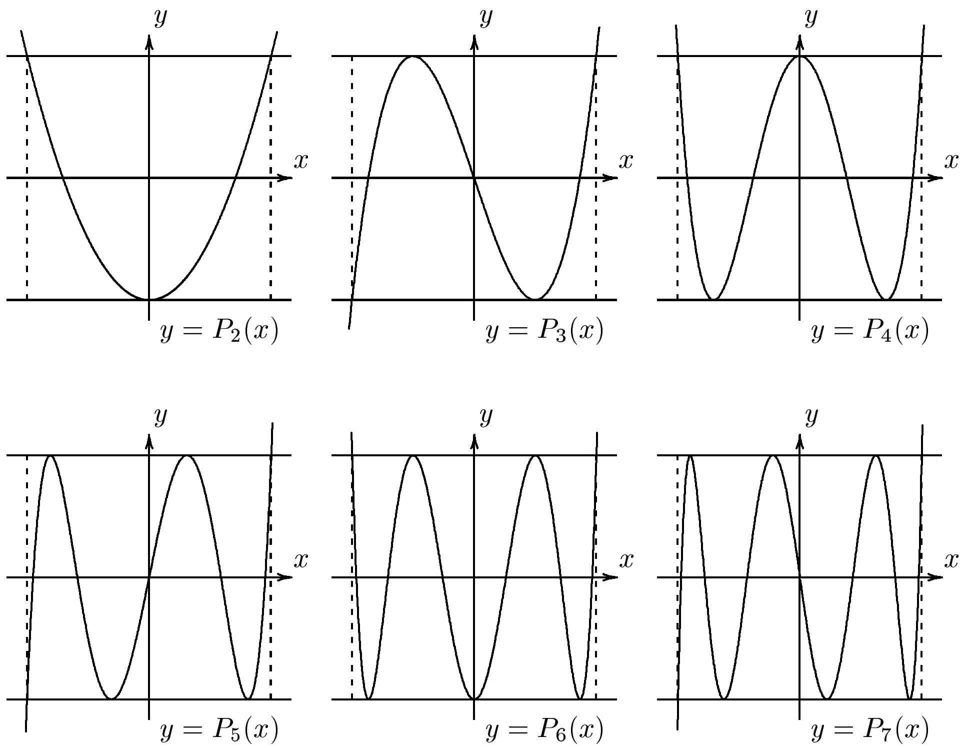


FIGURE 7.4. The graphs of the first seven Chebyshev polynomials

**7.4 Formulas.** The Chebyshev polynomials

$$P_0(x) = 2,\ P_1(x) = x,\ P_2(x) = x^2 - 2,\ P_3(x) = x^3 - 3x,\ P_4(x) = x^4 - 4x^2 + 2, \dots$$

can be described by a number of explicit formulas. For example, consider the continued fraction:

$$R_n = x - \cfrac{1}{x - \cfrac{1}{x - \cfrac{1}{\dots - \cfrac{1}{x - \cfrac{2}{x}}}}}.$$

Thus

$$R_1 = x, \quad R_2 = \frac{x^2 - 2}{x}, \quad R_3 = \frac{x^3 - 3x}{x^2 - 2},$$

and in general,

LEMMA 7.5.

$$R_n(x) = \frac{P_n(x)}{P_{n-1}(x)}.$$

Proof. Induction on $n$. One has:

$$R_{n+1} = x - \frac{1}{R_n} = x - \frac{P_{n-1}(x)}{P_n(x)} = \frac{xP_n(x) - P_{n-1}(x)}{P_n(x)} = \frac{P_{n+1}(x)}{P_n(x)},$$

the last equality due to the recurrence relation (7.3). □

Here is another formula which describes the coefficients of the Chebyshev polynomials via binomial coefficients.

THEOREM 7.2.

$$P_n(x) = x^n - \frac{n}{n-1}\binom{n-1}{1}x^{n-2} + \frac{n}{n-2}\binom{n-2}{2}x^{n-4} + \dots$$
$$+(-1)^j \frac{n}{n-j}\binom{n-j}{j}x^{n-2j} + \dots$$

*(with $j \le n/2$).*

Proof. One can encode Chebyshev polynomials in the *generating function*

$$\Phi(z) = 2 + xz + (x^2-2)z^2 + \dots + P_n(x)z^n + \dots.$$

Using the recurrence relation (7.3), one can replace each $P_n(x)$, starting with $n=2$, by a combination of $P_{n-1}(x)$ and $P_{n-2}(x)$:

$$\Phi(z) = 2+xz+(xP_1(x)-P_0(x))z^2+(xP_2(x)-P_1(x))z^3+(xP_3(x)-P_2(x))z^4+\dots$$
$$= 2+xz+xz(P_1(x)z+P_2(x)z^2+P_3(x)z^3\dots)-z^2(P_0(x)+P_1(x)z+P_2(x)z^2+\dots)$$
$$= 2+xz+xz(\Phi(z)-2)-z^2\Phi(z) = 2-xz+(xz-z^2)\Phi(z).$$

Hence

$$\Phi(z) = \frac{2-xz}{1-xz+z^2}.$$

This formula contains all the information about Chebyshev polynomials; it remains only to extract the information from there. The key is the formula for geometric progression:

$$\frac{1}{1-q} = 1+q+q^2+q^3+\dots.$$

Thus

$$\Phi(z) = (2-xz)[1+(xz-z^2)+(xz-z^2)^2+(xz-z^2)^3+\dots] \tag{7.4}$$

One has:

$$(xz-z^2)^k = x^kz^k - kx^{k-1}z^{k+1} + \dots + (-1)^j\binom{k}{j}x^{k-j}z^{k+j} + \dots.$$

Collecting terms on the right-hand side of (7.4) yields the following coefficient in front of $z^n$:

$$x^n + \dots + (-1)^j\left[2\binom{n-j}{j} - \binom{n-j-1}{j}\right]x^{n-2j} + \dots.$$

It remains to simplify the expression in the brackets:

$$2\binom{n-j}{j} - \binom{n-j-1}{j} = \frac{2(n-j)!}{j!(n-2j)!} - \frac{(n-j-1)!}{j!(n-2j-1)!}$$
$$= n\frac{(n-j-1)!}{j!(n-2j)!} = \frac{n}{n-j}\binom{n-j}{j},$$

and the result follows. □

John Smith
January 23, 2010

Martyn Green
August 2, 1936

Henry Williams
June 6, 1944

## 7.5 Exercises.

7.1. There is a shortcoming in the proof of Theorem 7.1: the graphs of the two polynomials may be tangent at the intersection point, see Figure 7.5. Adjust the argument to this case.

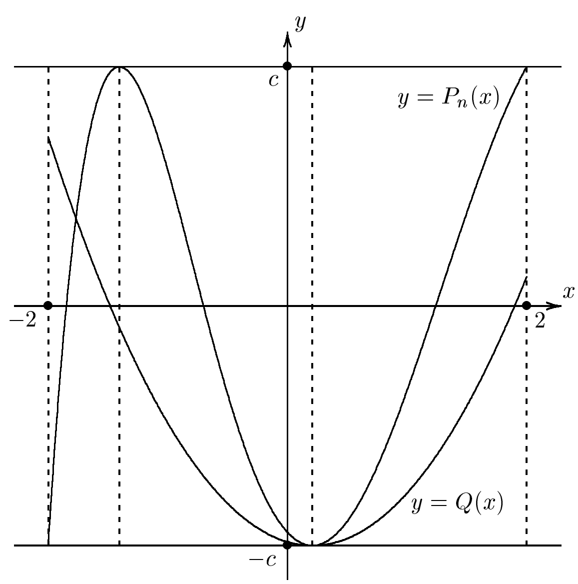


FIGURE 7.5. A difficulty with tangency

7.2. Prove that the least deviation from zero of a monic polynomial on a segment $[a, b]$ equals

$$2\left(\frac{b-a}{4}\right)^n.$$

7.3. Find the least deviation from the function $y = e^x$ of a linear function $y = ax + b$ on the segment $[0, 1]$.

7.4. Prove yet another formula for Chebyshev polynomials:

$$P_n(x) = \frac{(x+\sqrt{x^2-4})^n + (x-\sqrt{x^2-4})^n}{2^n}$$

(we assume here that $|x| \geq 2$).

7.5. Prove that

$$P_n(x) = \det \begin{vmatrix} x & 2 & 0 & 0 & \cdots & 0 \\ 1 & x & 1 & 0 & \cdots & 0 \\ 0 & 1 & x & 1 & \cdots & 0 \\ . & \cdots & \cdots & \cdots & \cdots & . \\ 0 & 0 & \cdots & 1 & x & 1 \\ 0 & 0 & \cdots & 0 & 1 & x \end{vmatrix}$$

7.6. Prove that the polynomials are orthogonal in the following sense:

$$\int_{-2}^{2} \frac{P_m(x)P_n(x)}{\sqrt{4-x^2}} dx = 0$$

for all $m \neq n$.

7.7. Prove that Chebyshev polynomials commute:

$$P_n(P_m(x)) = P_m(P_n(x)).$$

7.8. * Consider a family of pairwise commuting polynomials with positive leading coefficients and containing at least one polynomial of each positive degree. Prove that, up to linear substitution, it is the family of Chebyshev polynomials or the family $x^n$.

The next three exercises provide an alternative proof of 7.1.

7.9. Consider a trigonometric polynomial of degree $n$

$$f(\alpha) = a_0 + a_1 \cos\alpha + a_2 \cos 2\alpha + \cdots + a_n \cos n\alpha. \tag{7.5}$$

Prove that its "average" value

$$\frac{1}{2n}\left[f(0) - f\left(\frac{\pi}{n}\right) + f\left(\frac{2\pi}{n}\right) - f\left(\frac{3\pi}{n}\right) + \cdots - f\left(\frac{(2n-1)\pi}{n}\right)\right]$$

is equal to $a_n$.

7.10. Prove that the deviation from zero of the trigonometric polynomial (7.5) on the circle $[0, 2\pi]$ is not less than $|a_n|$.

*Hint*. The deviation from zero is not less than

$$\frac{1}{2n}\left[|f(0)| + \left|f\left(\frac{\pi}{n}\right)\right| + \cdots + \left|f\left(\frac{(2n-1)\pi}{n}\right)\right|\right].$$

Use Exercise 7.9 and the triangle inequality $|a| + |b| \geq |a+b|$.

7.11. Deduce Theorem 7.1 from Exercises 7.9 and 7.10.

*Hint*. After the substitution $x = \cos\alpha$, the polynomial $P_n(x)$ becomes a trigonometric polynomial (7.5) with the leading coefficient $1/2^{n-1}$. As $\alpha$ ranges over the circle, $x$ traverses the segment $[-1, 1]$.

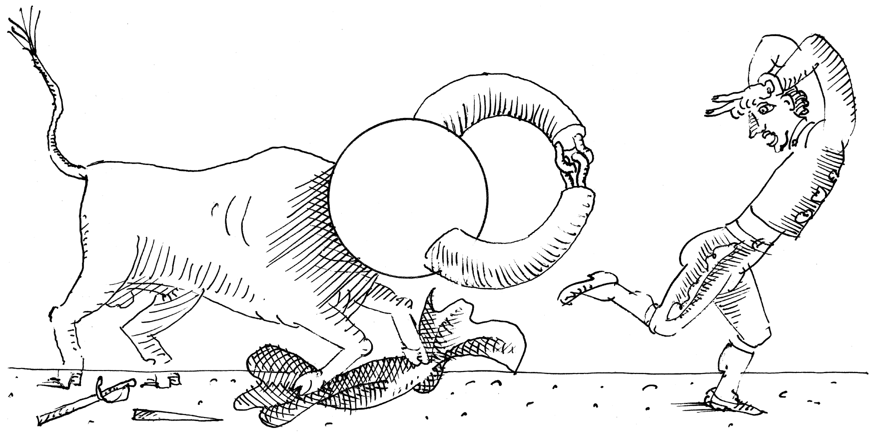

LECTURE 8

# Geometry of Equations

**8.1 The equation $x^2 + px + q = 0$.** Looking at the expression in the title of this section, we see a quadratic equation in the variable $x$ whose coefficients are the parameters $p$ and $q$. This is a matter of one's perspective: equally well one may view this expression as a linear equation in the variables $p$ and $q$ with coefficients depending on the parameter $x$. A linear equation $q = -xp - x^2$ describes a non-vertical line; thus one has a 1-parameter family of lines in the $(p, q)$-plane, one for each $x$.

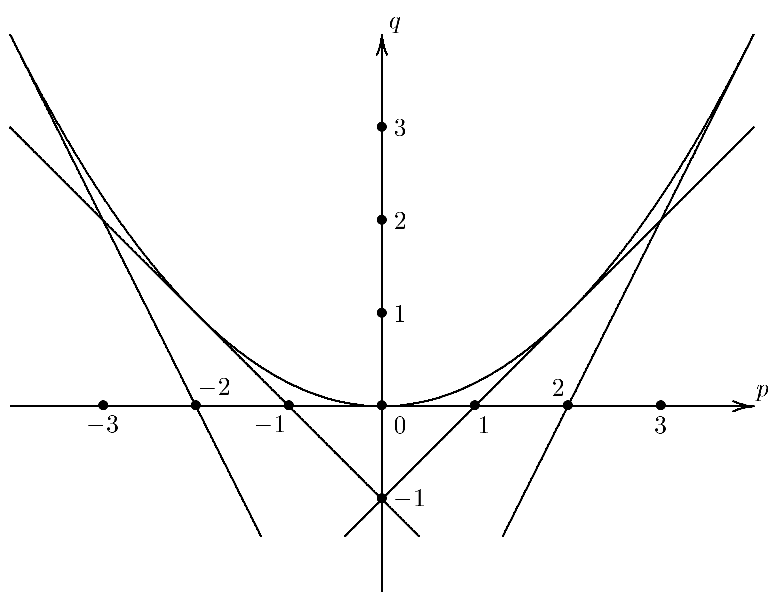


FIGURE 8.1. The envelope of the family of lines $q = -xp - x^2$

Let us draw a few lines from this family, see Figure 8.1. These lines are tangent to a curve that looks like a parabola. This *envelope* is the locus of intersection points of pairs of infinitesimally close lines from our family (the reader will find explicit formulas in Section 8.3). That our envelope is indeed a parabola, will become clear shortly. Each line in Figure 8.1 corresponds to a specific value of $x$. Let us write this value of $x$ at the tangency point of the respective line with the envelope. This makes the envelope into a measuring tape, like the $x$-axis, but bent – see Figure 8.2.

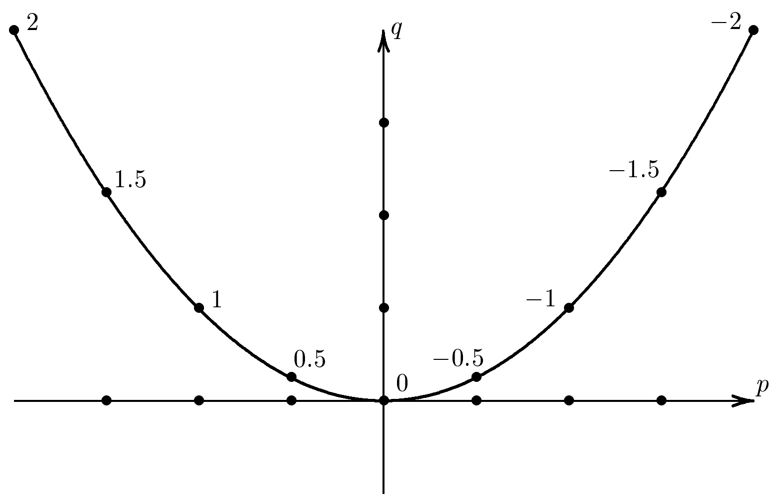


FIGURE 8.2. A bent "measure tape"

The curve in Figure 8.2 can be used to solve the equation $x^2 + px + q = 0$ graphically. Given a point in the $(p, q)$-plane, draw a tangent line from this point to the envelope. Then the $x$-value of the tangency point is a root of the equation $x^2 + px + q = 0$, see Figure 8.3. In particular, the number of roots is the number of tangent lines to the envelope from a point $(p, q)$. For the points below the envelope there are two tangent lines, and for the points above it – none.

What about the points on the envelope? For them, there is a unique tangent line to the envelope, that is, the two roots of the quadratic equation coincide. Thus the envelope is the locus of points $(p, q)$ for which the equation $x^2 + px + q = 0$ has a multiple root. This happens when $p^2 = 4q$, that is, the envelope is the parabola $q = p^2/4$.

**8.2 The equation $x^3 + px + q = 0$.** A simple quadratic equation probably does not deserve this relatively complicated treatment. Let us now consider the more interesting cubic equation $x^3 + px + q = 0$. Although this equation still can be solved explicitly in radicals (see Lecture 4), these formulas are not so simple and, in some situations, not very useful. Instead, let us treat this equation as a 1-parameter family of lines in the $(p, q)$-plane.

Figure 8.4 depicts several lines and features their envelope with a scale on it. This envelope is a cusp and it strongly resembles the semicubic parabola from Lecture 9. We shall find its equation in a minute.

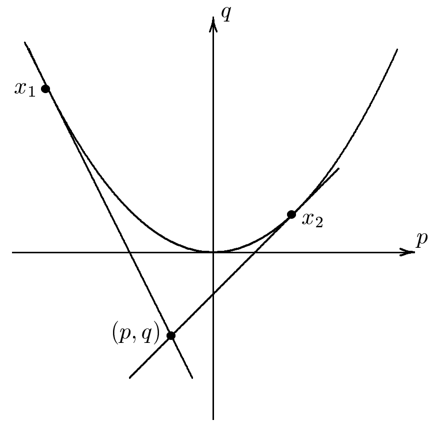


FIGURE 8.3. A machine for solving quadratic equations

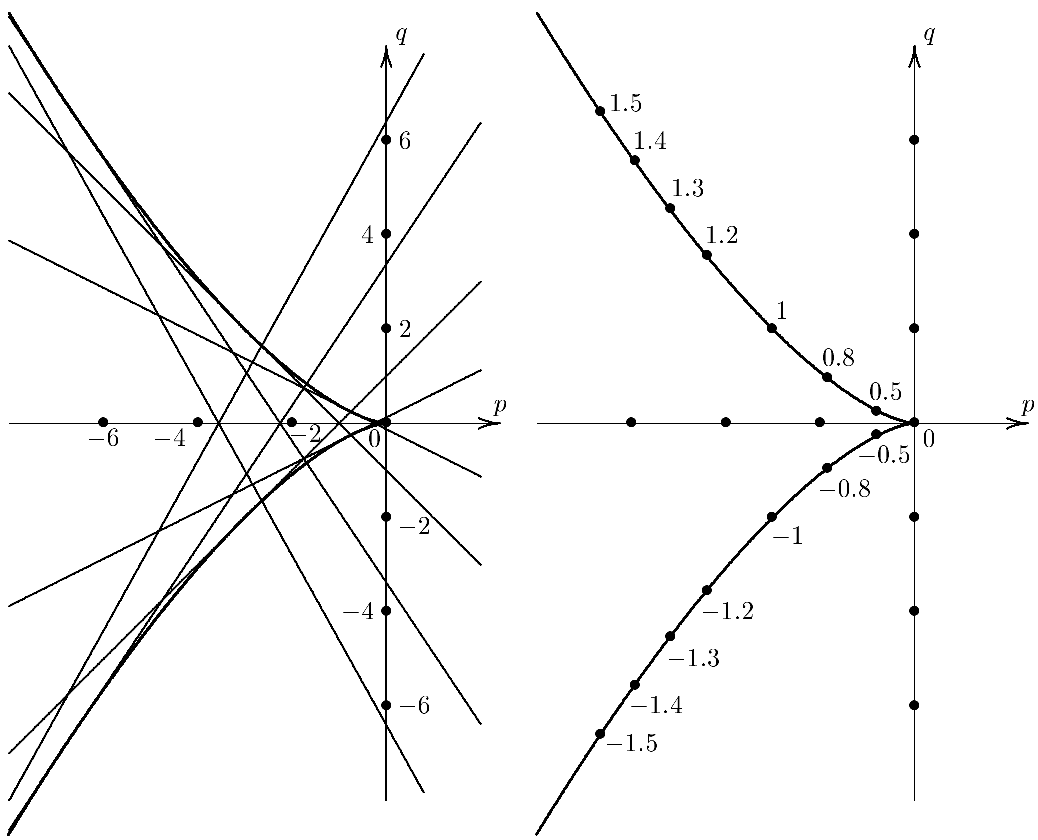


FIGURE 8.4. The envelope of the family of lines $x^3 + px + q = 0$ and a bent "measure tape"

As before, the curve in Figure 8.4 is a device for solving the equation $x^3 + px + q = 0$ graphically: draw a tangent line to the envelope from a point $(p, q)$ and read off a root as the $x$-coordinate of the tangency point. For points inside the cusp, there are three tangent lines, and for points outside it – only one, see Figure 8.5. The curve itself is the locus of points $(p, q)$ for which the equation has a multiple root, and the vertex of the cusp, the origin, corresponds to the equation $x^3 = 0$ whose roots are all equal.

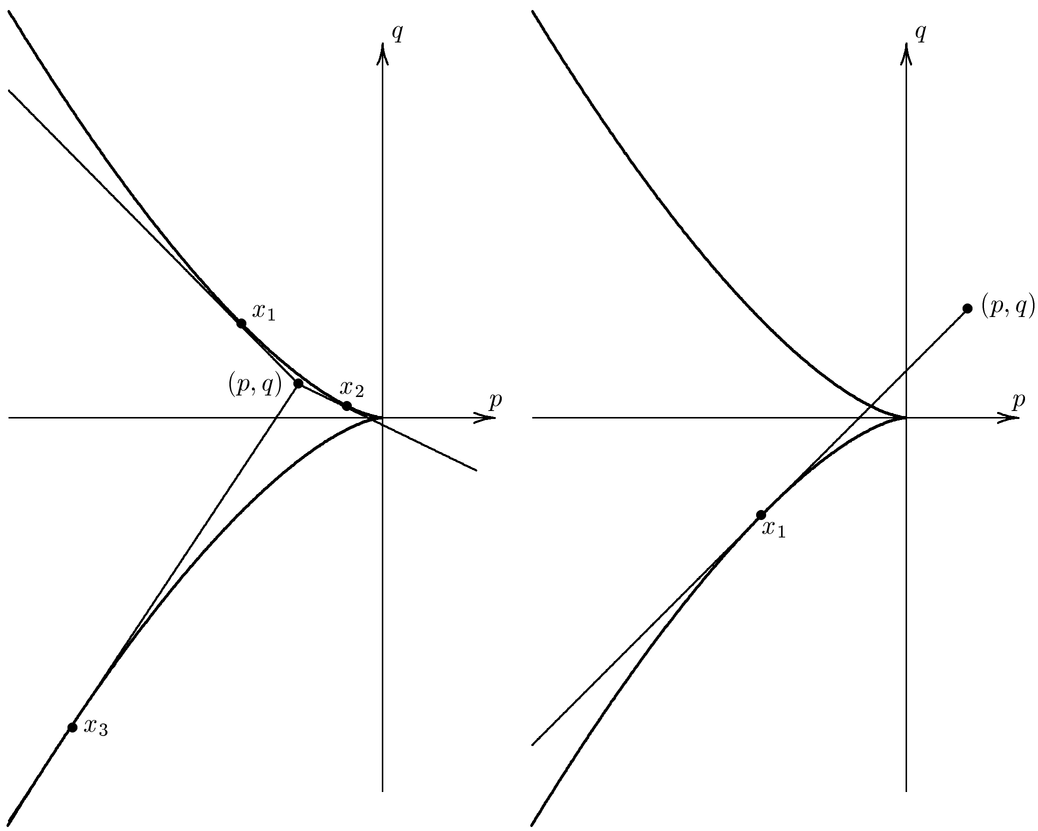


FIGURE 8.5. The number of roots of a cubic equation

To find an equation of the curve in Figures 8.4 and 8.5, one needs to know when the equation $x^3 + px + q = 0$ has a multiple root. A general criterion is as follows.

LEMMA 8.1. *A polynomial $f(x)$ has a multiple root if and only if it has a common root with its derivative $f'(x)$.*

Proof. If $a$ is a multiple root of $f(x)$ then $f(x) = (x - a)^2 g(x)$ where $g(x)$ is also a polynomial. Then $f'(x) = 2(x - a)g(x) + (x - a)^2 g'(x)$, hence $a$ is a root of $f'(x)$.

Conversely, let $a$ be a common root of $f$ and $f'$. Then $f(x) = (x - a)g(x)$ for some polynomial $g$, and hence $f'(x) = g(x) + (x - a)g'(x)$. Since $a$ is a root of $f'$, it is also a root of $g$. Thus $g(x) = (x - a)h(x)$ for some polynomial $h$, and therefore $f(x) = (x - a)^2 h(x)$. It follows that $a$ is a multiple root of the polynomial $f$. □

In our situation, $f(x) = x^3 + px + q$ and $f'(x) = 3x^2 + p$. If $a$ is a common root of these polynomials then $p = -3a^2$ and $q = -a^3 - pa = 2a^3$. These are parametric equations of the envelope in Figures 8.4 and 8.5. One may eliminate $a$ from these equations, and the result is

$$4p^3 + 27q^2 = 0.$$

This is a semicubic parabola.

The expression $D = -(4p^3 + 27q^2)$ is the discriminant of the polynomial $x^3 + px+q$; its sign determines the number of roots: if $D > 0$ there are three, and if $D < 0$ one real root. By the way, there is no loss of generality in considering polynomials $x^3 + px + q$ with zero second highest coefficient: one can always eliminate this coefficient by a substitution $x \mapsto x + c$ (this is discussed in detail in Lecture 4).

**8.3 Equation of the envelope.** An equation for the envelope of a 1-parameter family of curves, in particular, lines, is easy to find. Let us do this in the case of our cubic polynomial $f(x) = x^3 + px + q$.

A point of the envelope is a point of intersection of the line $x^3 + px + q = 0$ and the infinitesimally close line $(x + \varepsilon)^3 + p(x + \varepsilon) + q = 0$. The second equation can be written as

$$(x^3 + px + q) + \varepsilon(3x^2 + p) + O(\varepsilon^2) = 0$$

where, following the common calculus notation, $O(\varepsilon^2)$ denotes the terms of order 2 and higher in $\varepsilon$. Since $\varepsilon$ is an infinitesimal, we ignore its powers starting with $\varepsilon^2$, and the system of equations becomes $f(x) = 0, f(x) + \varepsilon f'(x) = 0$, which is of course equivalent to

$$f(x) = f'(x) = 0.$$

This is a parametric equation of the envelope ($x$ being the parameter), and this holds true for any 1-parameter family of curves in the $(p, q)$-plane given by the equation $f(x, p, q) = 0$. In view of Lemma 8.1, we see again that the envelope corresponds to the points $(p, q)$ for which the cubic polynomials $x^3 + px + q$ has a multiple root.

**8.4 Dual curves.** Consider the equation

$$l + kp + q = 0. \tag{8.1}$$

We are free to consider (8.1) as a linear equation in the variables $p, q$ depending on $k, l$ as parameters, or as a linear equation in the variables $k, l$ depending on $p, q$ as parameters. Thus every non-vertical straight line in the $(p, q)$-plane corresponds via (8.1) to a point of the $(k, l)$-plane, and vice versa. We have two planes, and points of one are the non-vertical lines of the other. These two planes are said to be *dual* to each other.

Let us use the following convention: points are denoted by upper-case letters and lines by lower-case ones. Given a point of one of the planes, denote the corresponding line of the dual plane by the same lower-case letter. We shall think of the $(k, l)$-plane as positioned on the left and the $(p, q)$-plane on the right.

The first observation is that the incidence relation is preserved by this duality: if $A \in l$ then $L \in a$. Indeed, let $A$ and $l$ lie in the left plane, $A = (k, l)$, and $L = (p, q)$ be the point dual to $l$. Then equation (8.1) says that $l$ passes through $A$ but, by the same token, that $a$ passes through $L$.

For example, a triangle is a figure made of three points and three lines. Duality interchanges points and lines but preserves their incidence, and the dual figure is again a triangle. Likewise, the figure dual to a quadrilateral with its two diagonals consists of four lines and their six pairwise intersection points, see Figure 8.6.

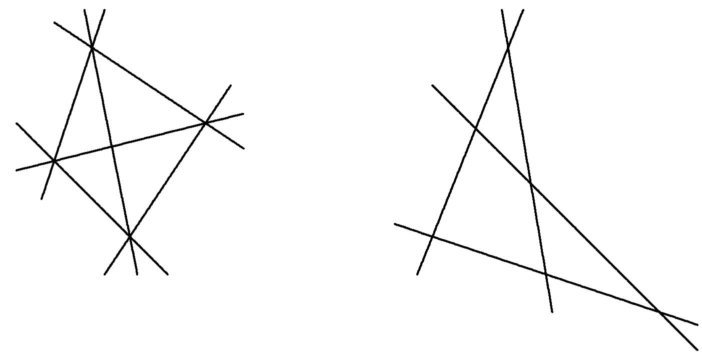

FIGURE 8.6. Dual figures

Duality extends to smooth curves. Let $\gamma$ be a curve in the left plane. The tangent lines to $\gamma$ correspond to points of the right plane (we assume that $\gamma$ has no vertical tangents). One obtains a 1-parameter family of points of the right plane, that is, a curve. This curve is said to be dual to $\gamma$ and we denote it by $\gamma^*$. The following example will clarify this construction.

EXAMPLE 8.2. Let $\gamma$ be a "parabola" of degree $\alpha$ given by the equation $l = k^\alpha$. The tangent line at the point $(t, t^\alpha)$ has the equation $l - \alpha t^{\alpha-1}k + (\alpha - 1)t^\alpha = 0$, that is, $l + kp + q = 0$ with $p = -\alpha t^{\alpha-1},\ q = (\alpha - 1)t^\alpha$. This is a parametric equation of another parabola of degree $\beta = \alpha/(\alpha - 1)$, and hence $\gamma^*$ is a parabola of degree $\beta$. A more symmetric way to write the relation between $\alpha$ and $\beta$ is

$$\frac{1}{\alpha} + \frac{1}{\beta} = 1.$$

In particular, if $\alpha = 2$ then $\beta = 2$, and if $\alpha = 3$ then $\beta = 3/2$.

Let us discuss how duality changes the shape of a curve. If $\gamma$ has a double tangent line then the dual curve $\gamma^*$ has a double point, see Figure 8.7.

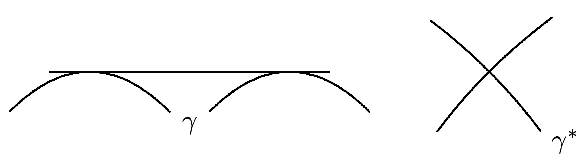


FIGURE 8.7. A double tangent is dual to a double point

Suppose now that $\gamma$ has an inflection point as in Figure 8.8. An inflection point is where a curve is abnormally well approximated by a line (at a generic point, one has first order tangency but at an inflection point the tangency is of at least second order). This implies that the dual curve is abnormally close to a point, that is, has a singularity, see Figure 8.8. This qualitative argument is confirmed by Example 8.2: if $\gamma$ is a cubic parabola then $\gamma^*$ is a semicubic cusp.

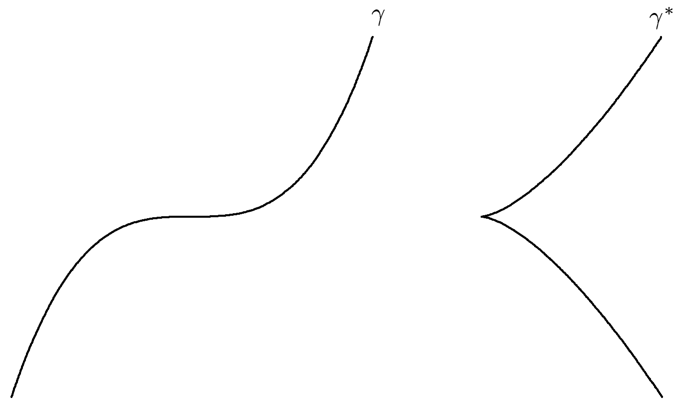


FIGURE 8.8. An inflection is dual to a cusp

Due to the symmetry between dual planes, one would expect duality to be a reflexive relation, that is, if $\gamma$ is dual to $\delta$ then $\delta$ is dual to $\gamma$. This is indeed the case.

THEOREM 8.1. *The curve* $(\gamma^*)^*$ *coincides with* $\gamma$.

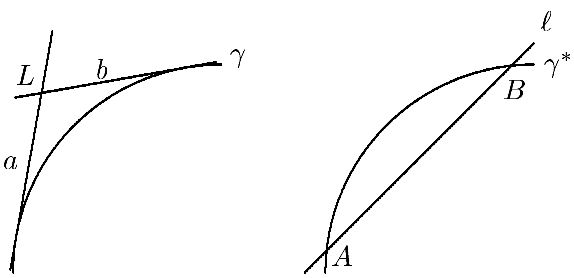


FIGURE 8.9. Proof of Theorem 8.1

Proof. Start with the curve $\gamma^*$. To construct its dual curve one needs to consider its tangent lines. Consider instead a secant line $l$ that intersects $\gamma^*$ at two close points $A$ and $B$. The dual picture consists of two close tangent lines $a$ and $b$ to $\gamma$ intersecting at the point $L$, dual to the line $l$ – see Figure 8.9. In the limit, as the points $A$ and $B$ tend to each other, the line $l$ becomes tangent to $\gamma^*$ and the point $L$ "falls" on $\gamma$. Thus $(\gamma^*)^* = \gamma$. □

This duality theorem makes it possible to read Figures 8.7 and 8.8 backwards: if a curve has a double point then its dual has a double tangent, and if a curve has a cusp then its dual has an inflection. For example, the curves in Figure 8.10 are dual to each other.

Let us relate this to what we did in Sections 8.1 and 8.2. For example, the equation $x^3+px+q=0$ is obtained from the equation $l+kp+q=0$ if $k=x, l=x^3$. The latter equations describe a cubic parabola in the $(k,l)$-plane. The dual curve in the $(p,q)$-plane is the envelope of the 1-parameter family of lines $x^3+px+q=0$, a semicubic parabola, as we discovered in Section 8.2.

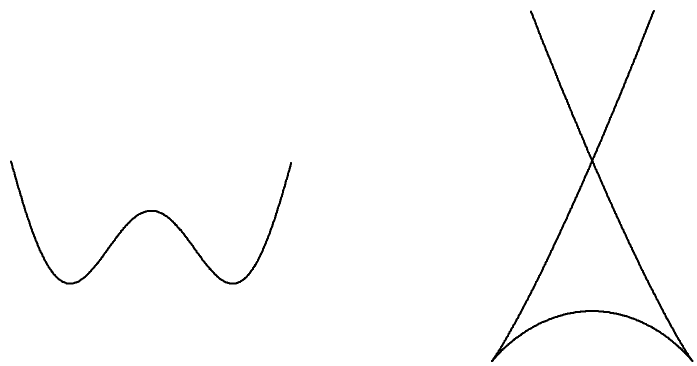

FIGURE 8.10. A pair of dual curves

We can also explain why the curves in Figures 8.2 and 8.4 do not have inflections. The 1-parameter families of lines $x^2 + px + q = 0$ and $x^3 + px + q = 0$ determine smooth curves in the $(k, l)$-plane (for example, $k = x, l = x^2$, in the first case). Therefore their dual curves in Figures 8.2 and 8.4 are free from inflections.

**8.5 The projective plane.** The self-imposed restriction not to consider vertical lines is somewhat embarrassing. Can one extend duality between points and lines to all lines? The way to go is to extend the plane to the projective plane.

The projective plane is defined as the set of lines in Euclidean three dimensional space passing through the origin. Since every line intersects the unit sphere at two antipodal points, the projective plane is the result of identifying pairs of antipodal points of the sphere. The (real) projective plane is denoted by $\mathbf{RP}^2$.

Given a line in $l$ through the origin, that is, a point of the projective space, choose a vector $(u, v, w)$ along $l$. This vector is not unique, it is defined up to multiplication by a non-zero number. The coordinates $(u, v, w)$, defined up to a factor, are called homogeneous coordinates of the point $l$.

By definition, a line in the projective plane consists of the lines in space that lie in one plane. Choose a plane $\pi$ in space not through the origin (a screen). Assign to every line its intersection point with this screen. Of course, some lines are parallel to the screen and we shall temporarily ignore them. This provides an identification of a part of the projective space with the plane $\pi$, and the lines in the projective plane identify with the lines in $\pi$. In other words, the plane $\pi$ can be considered as a (large) part of the projective plane, called an affine chart. Another choice of a screen would give another affine chart. If $\pi$ is given by the equation $z = 1$ (where $x, y, z$ are Cartesian coordinates) then one may choose homogeneous coordinates in the form $(u, v, 1)$ and drop the last component to obtain the usual Cartesian coordinates in the plane $\pi$.

Which part of the projective plane does not fit into an affine chart? These are the lines in space that are parallel to $\pi$. If a line makes a small angle with $\pi$ then its intersection point is located far away, and if this angle tends to zero, the respective point escapes to infinity. Thus the projective plane is obtained from the usual plane $\pi$ by adding "points at infinity". These points form a line, "the line at infinity". The homogeneous coordinates of these points are $(u, v, 0)$.

Given a line $l$ through the origin, consider the orthogonal plane $\beta$ passing through the origin. This defines a correspondence between points and lines of the projective plane, the projective duality. Let $(u, v, w)$ be homogeneous coordinates of $l$, and let the plane $\beta$ be given by the linear equation $ax + by + cz = 0$. The condition that $l$ is orthogonal to $\beta$ is

$$au + bv + cw = 0. \tag{8.2}$$

Assume that $w \neq 0$ and $a \neq 0$. Then one may rescale the homogeneous coordinates so that $w = a = 1$, and equation (8.2) can be written as $u + bv + c = 0$. This differs from equation (8.1) only by the names of the variables. The condition $w \neq 0$ means that we are restricted to an affine chart and the condition $a \neq 0$ that we consider non-vertical lines.

**8.6 The equation $x^4 + px^2 + qx + r = 0$.** This equation defines a 1-parameter family of planes in Euclidean 3-space with coordinates $p, q, r$. The envelope of this family is a surface depicted in Figure 8.11.

Consider two planes from our family corresponding to very close values of the parameter, $x$ and $x + \varepsilon$. These two planes intersect along a line, and this line has a limiting position as $\varepsilon \to 0$. One has a 1-parameter family of lines, $l(x)$, and they all lie on the surface. Thus this surface is ruled.

Now take three planes from our family, corresponding to the parameter values $x - \varepsilon, x$ and $x + \varepsilon$. These three planes intersect at a point, and again this point has a limiting position as $\varepsilon \to 0$. This point, $P(x)$, is also the intersection point of infinitesimally close lines $l(x)$ and $l(x + \varepsilon)$. Thus the lines $l(x)$ are tangent to the space curve $P(x)$ which they envelop. Note that, in general, a 1-parameter family of lines in space does not envelop a curve: two infinitesimally close lines will be skew; our situation is quite special! To summarize: the surface in Figure 8.11 consists of lines, tangent to a space curve.

In fact, it is easy to write down equations for this curve. Let $f(x) = x^4 + px^2 + qx + r$. Arguing as in Section 8.3, a parametric equation of the curve $P(x)$ is given by the system of equations $f(x) = f'(x) = f''(x) = 0$, that is,

$$x^4 + px^2 + qx + r = 0, \quad 4x^3 + 2px + q = 0, \quad 12x^2 + 2p = 0.$$

Hence

$$p = -6x^2, \quad q = 8x^3, \quad r = -3x^4,$$

a parametric equation of a spacial curve. This curve itself has a cusp at the origin. In Figure 8.11, this curve cosists of two smooth segments, $BA$ and $AC$; $A$ represents the origin. Besides the curviliunear triangle $BAC$, the surface has two "wings," $ABGF$ and $ACHE$, attached to the segments $BA$ and $AC$ and crossing each other along the curve $AD$. Figure 8.11 shows the surface as it was presented in the algebraic works of the 19-th century. In geometric works of the second half of the 20-th century, this surface reappeared under the name of *swallow tail*. We shall consider this surface in the context of Paper Sheet Geometry, and a (more comprehensible) picture of this surface will be presented in Lecture 13 (see Figure 13.17).

Figure 8.12 depicts the curve

$$p = -6x^2, \quad q = 8x^3, \quad r = -3x^4$$

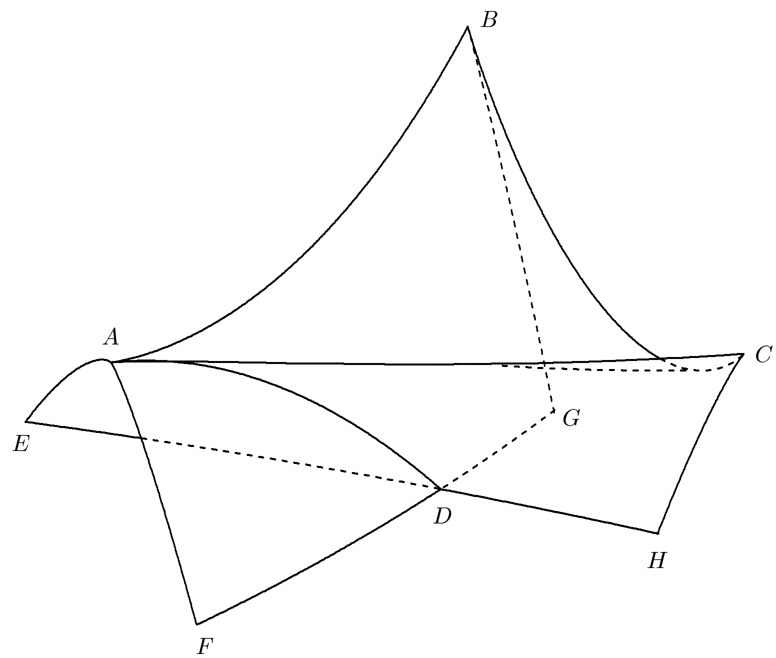


FIGURE 8.11. The envelope of the family of planes $x^4+px^2+qx+r=0$

separately from the surface. The side diagrams of Figure 8.12 show the projections of this curve onto the $pq$-, $pr$-, and $qr$-planes. Notice that in the projection onto the $pr$-plane, the curve folds into a half of a parabola.

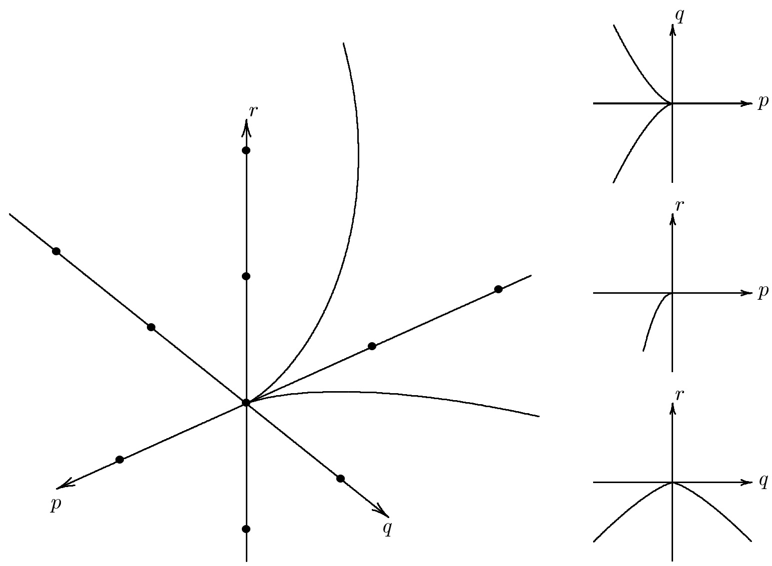


FIGURE 8.12. The curve itself has a cusp

The surface in Figure 8.11 is given by the system of equations $f(x) = f'(x) = 0$, that is,

$$x^4 + px^2 + qx + r = 0, \quad 4x^3 + 2px + q = 0.$$

If one eliminates $x$ from these equations, one obtains one relation on $p, q, r$, and this equation will be our goal in the next section.

Similarly to Sections 8.1 and 8.2, the number of roots of the equation $x^4 + px^2 + qx + r = 0$ equals the number of tangent planes to our surface from the point $(p, q, r)$. This number changes by 2 when the point crosses the surface. The set complement of the surface consists of three pieces, corresponding to 4, 2 and 0 roots.

**8.7 A formula for the discriminant.** The discriminant of a polynomial $f(x)$ of degree $n$ is a polynomial $D$ in the coefficients of $f(x)$ such that $D = 0$ if and only if $f(x)$ has a multiple root. Namely,

$$D = \Pi_{1 \le i < j \le n}(x_i - x_j)^2$$

where $x_1, ..., x_n$ are the roots. Recall that the coefficients of a polynomial are the elementary symmetric functions of its roots, see Lecture 4. The discriminant $D$ is also a symmetric function of the roots, and therefore it can be expressed as a polynomial in the coefficients of $f(x)$. The actual computation is a tedious task but it is doable "barehanded" for polynomials of small degrees.

Example 8.3. Let us make this computation for $f(x) = x^3 + px + q$ (we know the answer from Section 8.2). One has:

$$\begin{aligned} x_1 + x_2 + x_3 &= 0, \\ x_1x_2 + x_2x_3 + x_3x_1 &= p, \\ x_1x_2x_3 &= -q. \end{aligned}$$

Thus $p$ has degree 2 as a polynomial in the roots, and $q$ has degree 3. The discriminant has degree 6, and there are only two monomials in $p$ and $q$ of this degree: $p^3$ and $q^2$. Thus $D = ap^3 + bq^2$ with unknown coefficients $a$ and $b$.

To find these coefficients, let

$$x_1 = x_2 = t, \ x_3 = -2t.$$

Then

$$D = 0 \quad \text{and} \quad p = -3t^2, \ q = 2t^3.$$

This implies that $27a = 4b$. Next, let $x_1 = -x_2 = t, x_3 = 0$. Then

$$D = 4t^6 \quad \text{and} \quad p = -t^2, \ q = 0.$$

It follows that $a = -4, b = -27$ and $D = -4p^3 - 27q^2$.

A similar, but much more tedious, computation yields the rather formidable formula for the discriminant of the polynomial $f(x) = x^4 + px^2 + qx + r$:

$$D = 256r^3 - 128p^2r^2 - 27q^4 - 4p^3q^2 - 16p^4r - 144pq^2r. \tag{8.3}$$

Another method of computing the discriminant $D$ is as follows. We want to know when $f(x)$ and $f'(x)$ have a common root, say $a$. If this is the case then $f(x) = (x - a)g(x), f'(x) = (x - a)h(x)$ where $g$ and $h$ are polynomials of degree 3 and 2, respectively. It follows that

$$f(x)h(x) - f'(x)g(x) = 0. \tag{8.4}$$

One may consider the coefficients of $h$ and $g$ as unknowns (there are 7 of them), and then equating all the coefficients in (8.4) yields a system of seven linear equations in these variables. This system has a non-trivial solution if and only if its determinant vanishes. The reader will easily check that this determinant is

$$\begin{vmatrix} 1 & 0 & p & q & r & 0 & 0 \\ 0 & 1 & 0 & p & q & r & 0 \\ 0 & 0 & 1 & 0 & p & q & r \\ -4 & 0 & -2p & -q & 0 & 0 & 0 \\ 0 & -4 & 0 & -2p & -q & 0 & 0 \\ 0 & 0 & -4 & 0 & -2p & -q & 0 \\ 0 & 0 & 0 & -4 & 0 & -2p & -q \end{vmatrix}, \tag{8.5}$$

and equating it to zero yields another form of the equation of the surface in Figure 8.11. This might be a nicer way to present the answer but it is still a separate and not-so-pleasant task to check that this is the same as (8.3); nowadays we might delegate this task to a computer.

A final remark: the coefficients in formula (8.3) are rather large numbers, and one wonders whether these numbers have any combinatorial or geometrical meaning. A conceptual explanation of this and many other similar formulas is provided by the contemporary theory of discriminants and resultants, see the book by I. Gelfand, M. Kapranov and A. Zelevinsky [**33**]; in particular, the coefficients in (8.3) are interpreted as volumes of certain convex polytopes.

### 8.8 Exercises.

8.1. (a) Consider the 1-parameter family of lines

$$p \sin x + q \cos x = 1. \tag{8.6}$$

Draw its envelope and use it to solve equation (8.6) geometrically for different values of $(p, q)$.

(b) Same problem for the equation $\ln x = px + q$.

8.2. Draw the curve dual to the graph $y = e^x$.

8.3. (a) The equation $x^2 + y^2 = 1$ describes a circle in the affine chart $z = 1$ of the projective plane. Draw this curve in the affine chart $x = 1$.

(b) Same question for the equation $y = 1/(1 + x^2)$.

8.4. Draw the curves in the projective plane, dual to the curves from Exercise 8.3.

8.5. Take a unit disc and paste together every pair of antipodal points on its boundary. Prove that the resulting space is the projective plane.

8.6. (a) Prove that the projective plane with a deleted disc is a Möbius band.

(b) Prove that the set of all non-oriented lines in the plane (not necessarily passing through the origin) is a Möbius band.

8.7. (a) Prove formula (8.3).

(b) Prove that (8.3) is equal to (8.5).

# Geometry and Topology

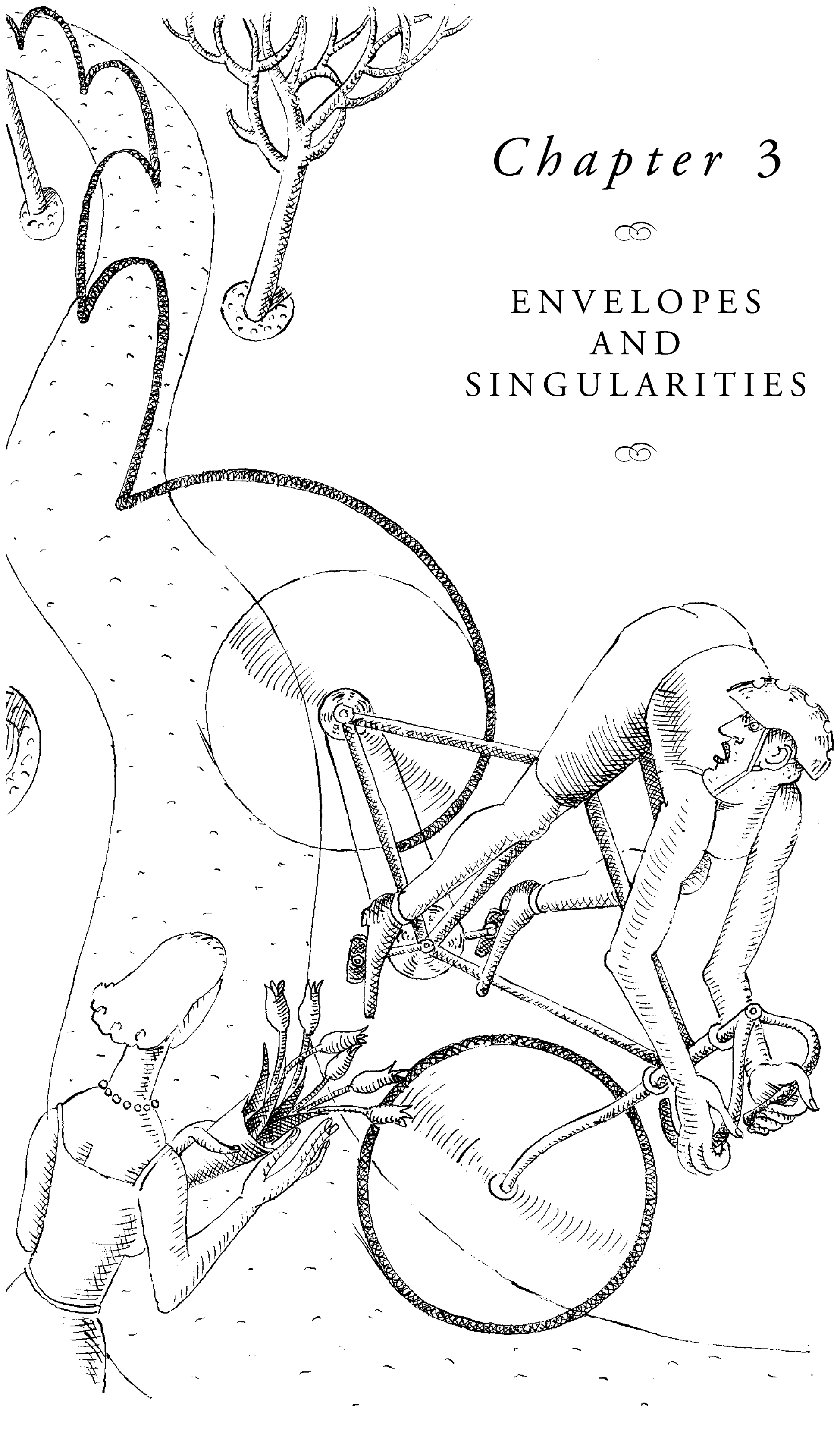

# *Chapter 3*

## ENVELOPES AND SINGULARITIES

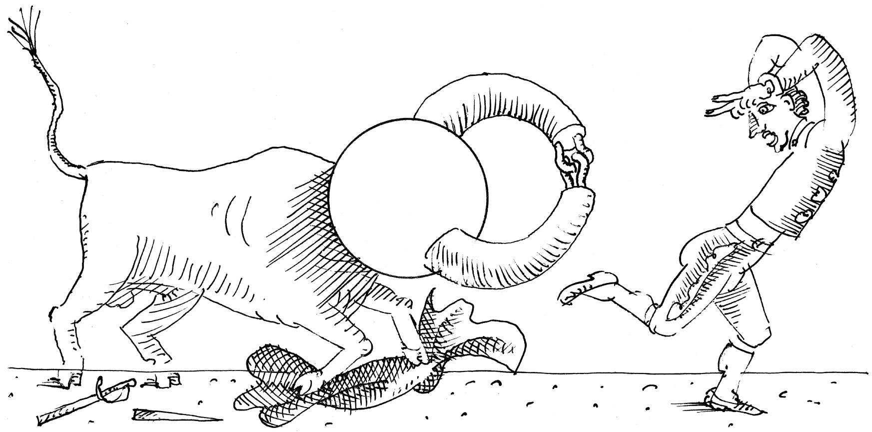

LECTURE 9

# Cusps

Among the graphs that calculus teachers love to assign their students, there are curves containing sharp turns, which mathematicians call *cusps*. A characteristic example given in Figure 9.1 below. This is a *semicubic parabola*, a curve given by the equation $y^2 = x^3$.

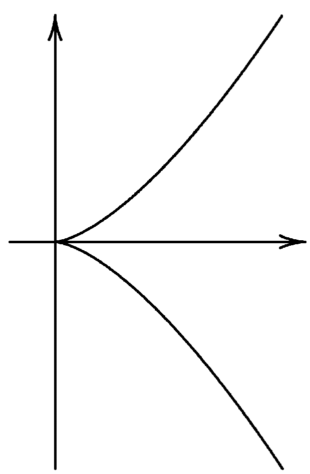

FIGURE 9.1. Semicubic parabola

The next example is the famous *cycloid* (Figure 9.2). You will observe it if you make a colored spot on the tire of your bike and then ask your friend to ride the bike. The spot will trace the cycloid.

Our last example is the so-called *cardioid* (Figure 9.3), a curve whose name reflects its resemblance to a drawing of a human heart. Mathematicians usually present this curve by the polar equation $\rho = 1 + \cos\theta$.

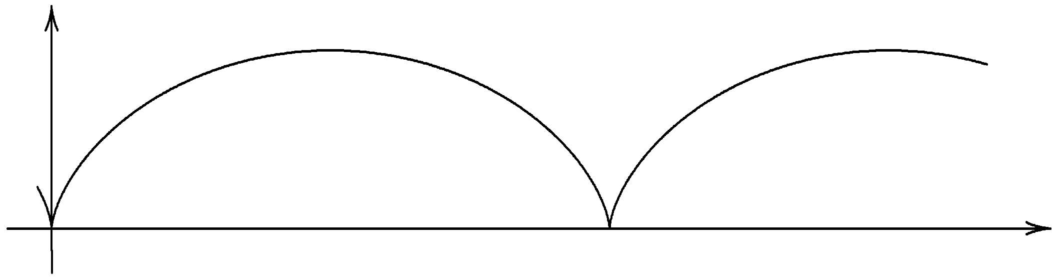

FIGURE 9.2. Cycloid

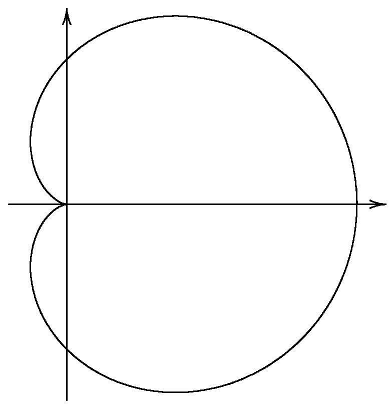

FIGURE 9.3. Cardioid

Certainly, the cusps on these graphs may seem something occasional, accidental: there are so many curves without cusps. But do not come to a premature conclusion. Our goal is to convince you that cusps appear naturally in so many geometric or analytic contexts, that we can justly say: *cusps are everywhere around!*

Let us draw an ellipse, the one given by the equation $\frac{x^2}{4} + y^2 = 1$ and a sufficiently dense family of *normals* to the ellipse (a normal is a line perpendicular to the tangent at the point of tangency, see Figure 9.4).

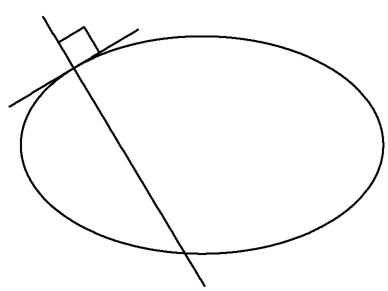

FIGURE 9.4. A tangent and a normal to an ellipse

A picture of the ellipse and 32 of its normals is shown in Figure 9.5. Although Figure 9.5 does not contain anything but an ellipse and 32 straight lines, we see one more curve on it: a diamond-shaped curve with four cusps. This phenomenon is not any special property of an ellipse. If we take a family of normals to a less symmetric egg-shaped curve, the diamond will also lose its perfect symmetry, but the cusps will still be there (see Figure 9.6).

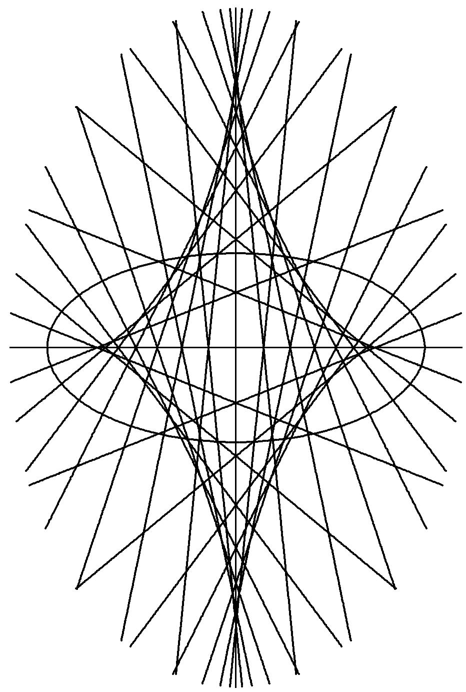

FIGURE 9.5. An ellipse with thirty two normals

The curve with cusps is called the *evolute* of the given curve (to which we have taken the normals). It has a simple geometric, or, better to say, mechanical description. If a particle is moving along a curve, at every single moment its movement may be regarded as a rotation around a certain center. This center changes its position at every moment, thus it also traces a curve. It is this curve that we see on Figures 9.5 and 9.6. Evolutes always have cusps. Moreover, the celebrated *Four Vertex Theorem*[1] (proved about 100 years ago, but still appearing mysterious) states that if the given curve is non-self-intersecting (like an ellipse or the egg-shaped curve of Figure 9.6), then the number of cusps on the evolute is at least four.

For self-intersecting curves this is no longer true; the next picture (Figure 9.7) shows a family of normals to a self-intersecting curve; the evolute is clearly visible on this picture, and it has only two cusps.

To be honest, this seemingly spontaneous appearance of a curve with cusps on a picture of a family of normals is not directly related to normals. You will see something very similar, if you take a "sufficiently arbitrary", or "sufficiently

[1]See Lecture 10.

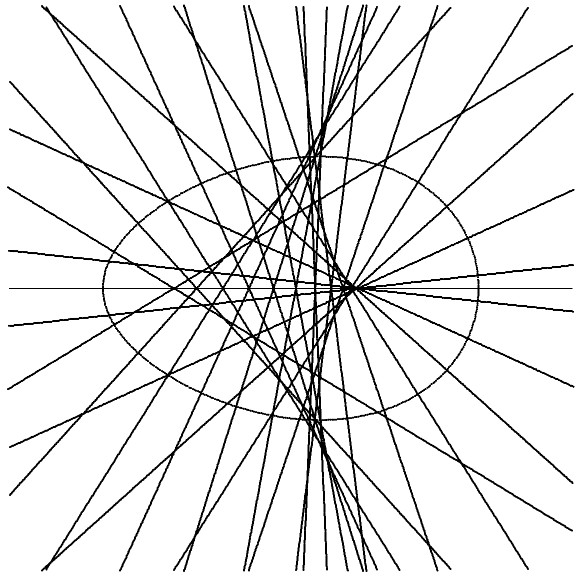

FIGURE 9.6. An egg-shaped curve with normals

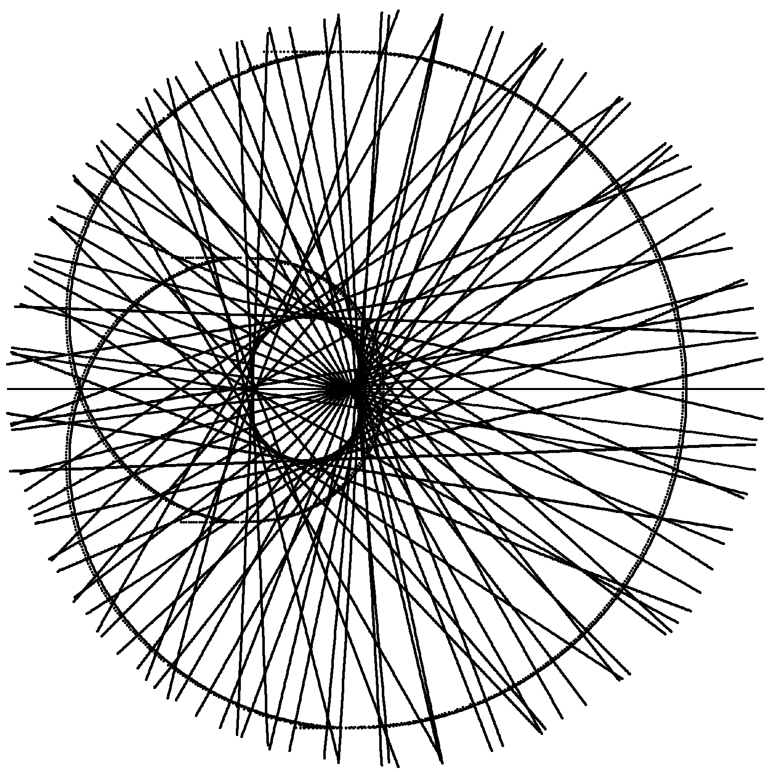

FIGURE 9.7. A self-intersecting curve with normals

random" family of lines. Imagine an angry professor who throws his cane at his students. The cane flies and rotates in its flight. If you draw a family of subsequent positions of the cane in the air, you will see something like Figure 9.8.

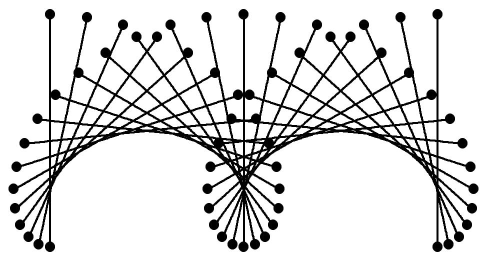

FIGURE 9.8. A flying cane (straight)

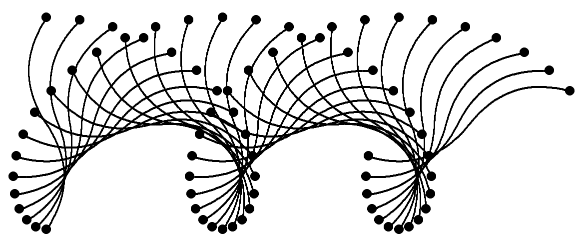

FIGURE 9.9. A flying cane (curvy)

You see here 32 subsequent positions of the cane, but also a curve looking a bit like the cycloid (Figure 9.2), with cusps (one of the cusps is clearly seen in the middle of the drawing). And straight lines do not play any special role, simply it is more convenient to draw them. If the professor is old and heavy, and his cane has long lost its linearity, then the picture of Figure 9.8 will look differently, but the cusps will remain (see Figure 9.9).

But let us turn to another geometric construction where cusps arise in an even more unexpected way. Let us again begin with an ellipse. Imagine that all point of our ellipse simultaneously begin moving at a constant speed, the same for all points, and that every point moves inside the ellipse along the normal to the ellipse. At first, the ellipse shrinks, but still retains its smooth oval shape (Figure 9.10).

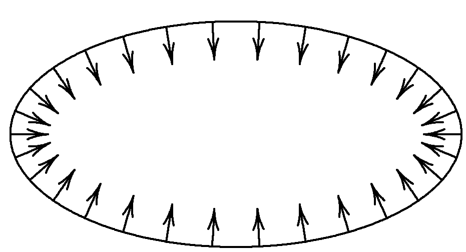

FIGURE 9.10. First, the ellipse retains its oval shape

But then the points begin forming sort of crowds at the left hand and right hand extremities of the curve (Figure 9.11), then the trajectories of the points cross each other (no collisions, they pass through each other), and, believe it or not, the curve acquires four cusps (Figure 9.12).

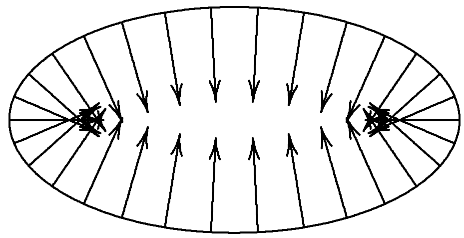

FIGURE 9.11. Then the points begin forming crowds

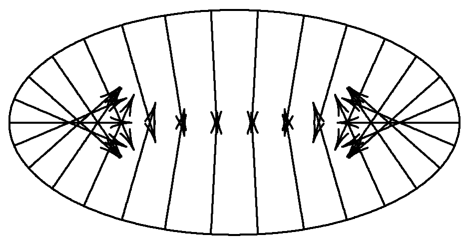

FIGURE 9.12. Eventually, the curve acquires cusps

The evolution of the moving curve, which is conveniently called a front, can be seen on Figure 9.13. We see that after the appearance of the four cusps, the curve consists of four sections between the cusps, two short and two long, and the long sections cross each other twice. Then the short sections become longer, and the long sections become shorter. At some moment, the "long" sections (which are not so long at this moment) go apart; then the "short" sections (which are quite long at this moment) meet and form two crossings. Then the cusps bump into each other and disappear, and the curve again becomes more or less elliptic.

It is interesting to draw all the fronts of Figure 9.13 on one picture. The cusps of the fronts form a curve themselves (Figure 9.14), and if you compare Figure 9.14 with Figure 9.5, you will see that our curve is nothing but the evolute of the ellipse.

Similarly, the movement of the fronts of the self-intersecting curve of Figure 9.7 is shown on Figure 9.15. The drawing on Figure 9.16 presents the whole family on one picture; if you trace, mentally, the curve of cusps, you will get the two-cusp evolute visible on Figure 9.7.

If you want to have more examples, observe the family of fronts of a sine wave (Figure 9.17); you can guess, what the evolute of a sine wave looks like (the evolute of a curve with *inflection points* always has asymptotes; these asymptotes are the normals to the curve at the inflection points; if the words "inflection points" and "asymptotes" do not mean much to you, forget about them).

Still, all these examples do not seem to justify the statement "*cusps are everywhere around*." One can argue, "if cusps are everywhere around, then why we don't see them?" But we do!

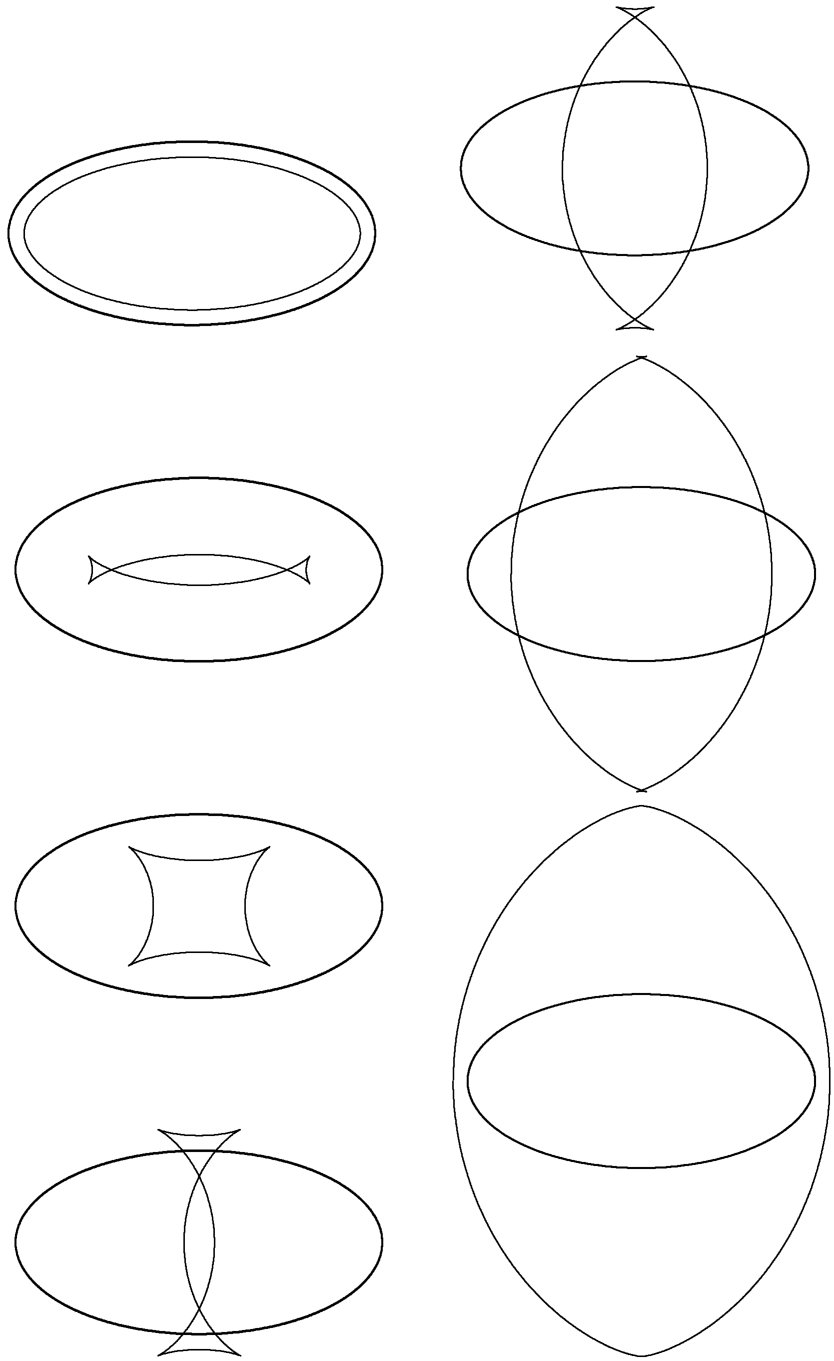

FIGURE 9.13. The evolution of a front

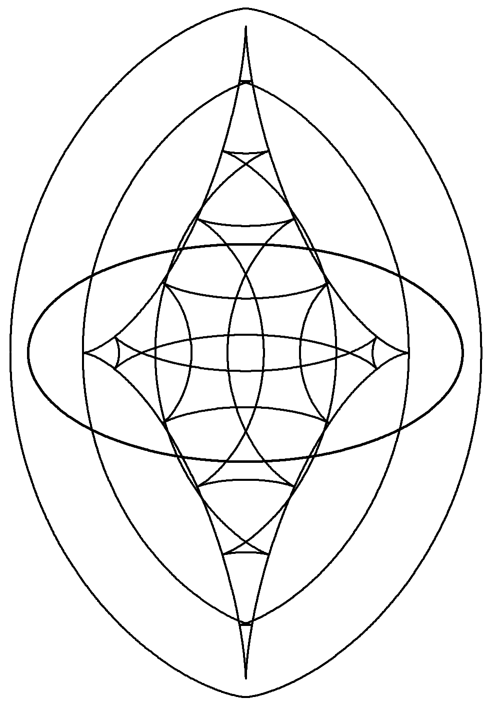

FIGURE 9.14. The fronts and the evolute

To be convinced, let us look around through the eyes of a great artist. Look at the famous portrait of Igor Stravinsky drawn in 1932 by Pablo Picasso (Figure 9.18). This picture of a great composer made by a great artist, which probably bears a notable resemblance to the original, is, actually, nothing but several dozens of pencil curves. But Igor Stravinsky's face was not made of curves! Then, what do these curves represent? And why do they stop abruptly without any visible reason?

Certainly, this drawing is too complicated to begin thinking of such things. Let us consider a more simple drawing. Imagine young Pablo Picasso first entering an art school in his native Malaga, or, maybe, later, in Barcelona. It is very probable that his teacher offered him a jug to draw (art students often begin their studies with jugs).

It is very unlikely that Pablo's picture of a jug, even if it ever existed, can be still found anywhere. But maybe it looked like one of the drawings on Figure 9.19.

Or, maybe, the art teacher was a geometry lover, and Pablo's first assignment was a torus (the surface of a bagel, if you do not know what a torus is). Then Pablo's first drawing could look like Figure 9.20.

On these simple drawings, we see the same things as on the masterpiece: there are curves, some of them end abruptly, either when they meet other curves, or without any visible reasons.

Let us think about the reasons. The curves we see (and draw) are boundaries of visible shapes, or, in other words, they are made of points of tangency of the rays from our eyes to the surface we are looking at. Let us denote this surface by $S$ and the curve made of tangency points by $C$ (see Figure 9.21). If we place,

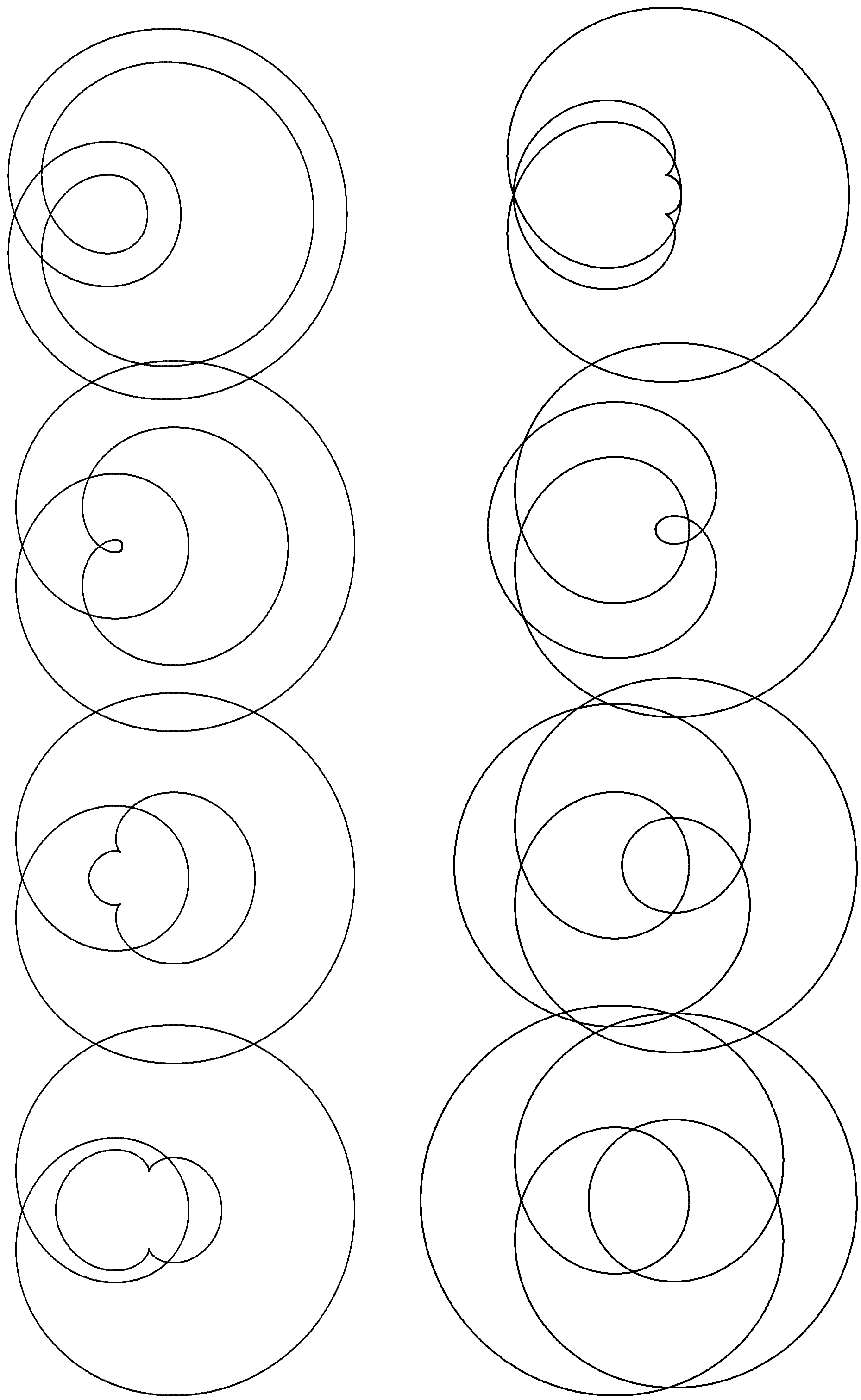

FIGURE 9.15. Evolution of fronts for a self-intersecting curve

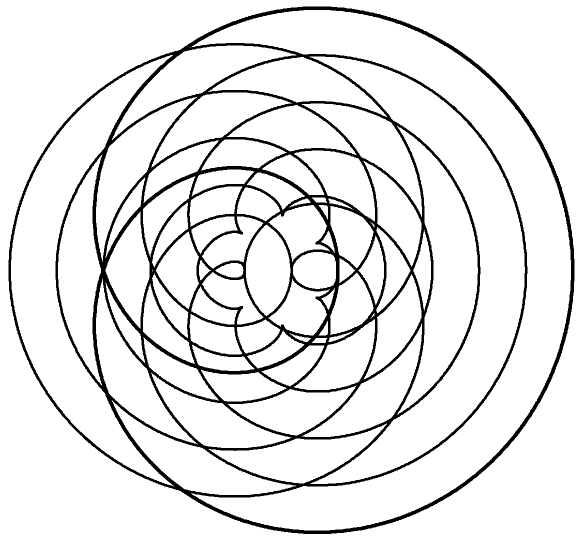

FIGURE 9.16. The fronts of a self-intersecting curve

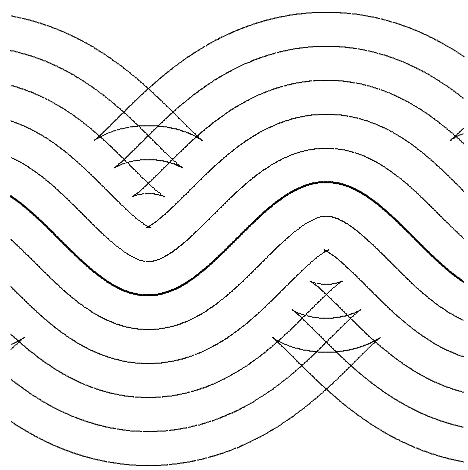

FIGURE 9.17. The fronts of a sine wave

mentally, a screen behind the surface, then our rays will trace a curve on the screen, and this curve $C'$ looks precisely like the contour of the surface that we see. If the shape of the surface $S$ is more complicated, then some parts of the curve $C$ may be hidden from our eye by the surface (geometrically this means that the ray crosses the surface, maybe more than one time, before the tangency). This is what happens where a curve stops when meeting another curve: if the things we are drawing were transparent, the curve would not have stopped, it would have gone further as a smooth curve.

The second case, when the curve stops without meeting another curve is more interesting. As we have said before, the tangency points of the rays of our vision form a curve $C$ on our surface $S$. A simple analytic argument, which we skip here,

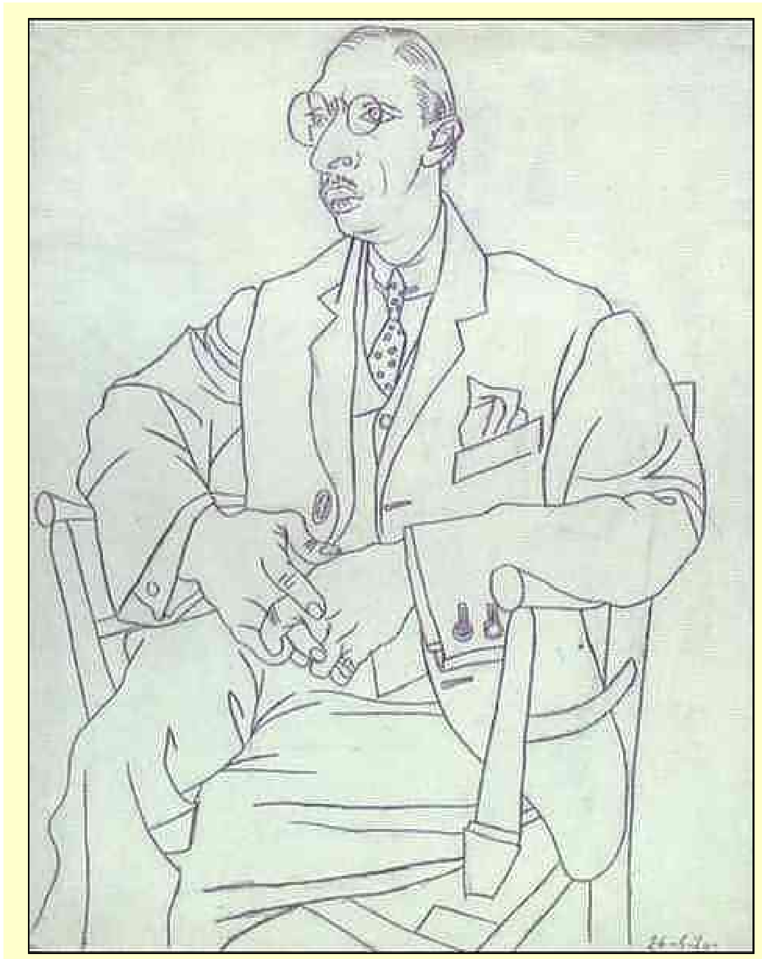

FIGURE 9.18. *Pablo Picasso.* Portrait of Igor Stravinsky (1932)

shows that this curve $C$ is always smooth. However, the ray may be tangent not only to the surface $S$, but also to the curve $C$. In this case, the image of this curve on the screen, and, hence, inside our eye, or on our drawing, forms a cusp (see Figure 9.22). But we see only a half of this cusp, while the second half is hidden behind the shape. Thus, if the things around us were transparent (sounds Nabokovian!), we would never have seen stopping curves; we would rather have seen a lot of cusps, which in real life are visible only by half.

For, example, if Pablo's jugs and torus were transparent, he would have supplemented his drawing by the curves shown (dotted) on Figure 9.23.

In conclusion, let us look at the projections of a transparent torus. To make it transparent, we replace it by a dense family of circles in parallel planes. More precisely, a torus is a surface of revolution of a circle around an axis not crossing the circle (see Figure 9.24 a). We replace the circle by a dense set of points, in our example by the set of vertices of an inscribed regular 32-gon (Figure 9.24 b).

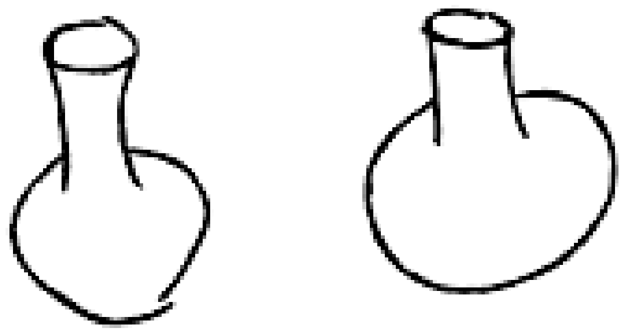

FIGURE 9.19. *Pablo ??.* Two jugs

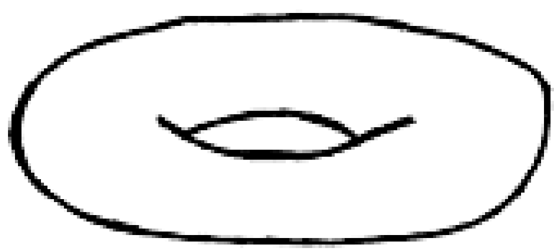

FIGURE 9.20. *Pablo ???.* A torus

Four projections (under slightly different angles) along with magnifications of the central fragments of these projections are shown on Figures 9.25, 9.26, 9.27, and 9.28. The curve with four cusps is seen on each of these projections.

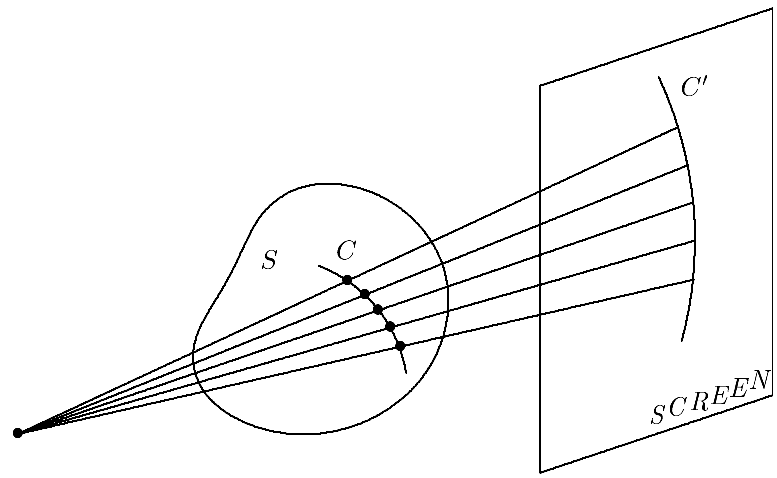


FIGURE 9.21. A visible (apparent) contour of a simple shape

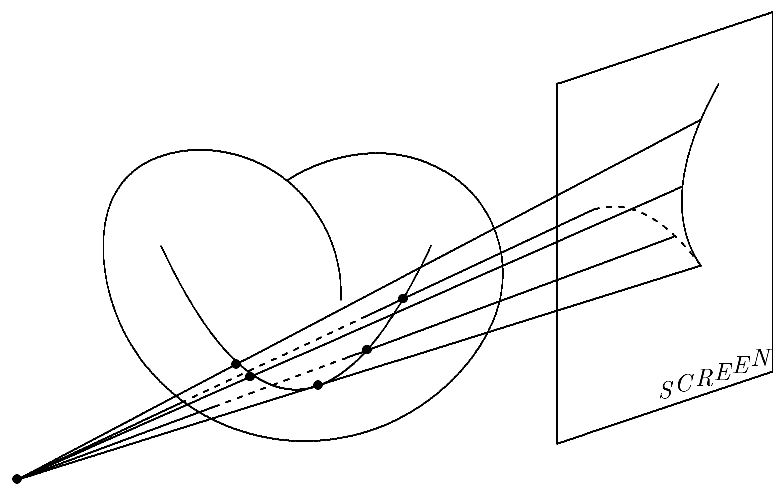


FIGURE 9.22. A visible contour of a complicated shape

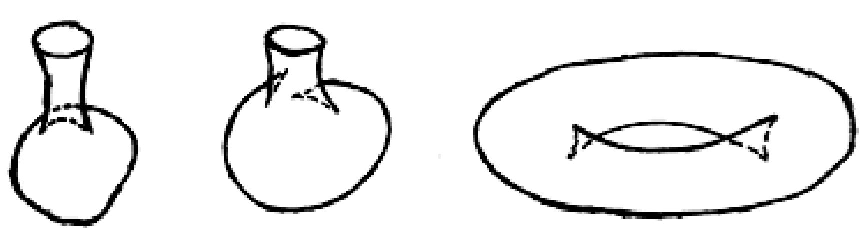

FIGURE 9.23. Transparent things

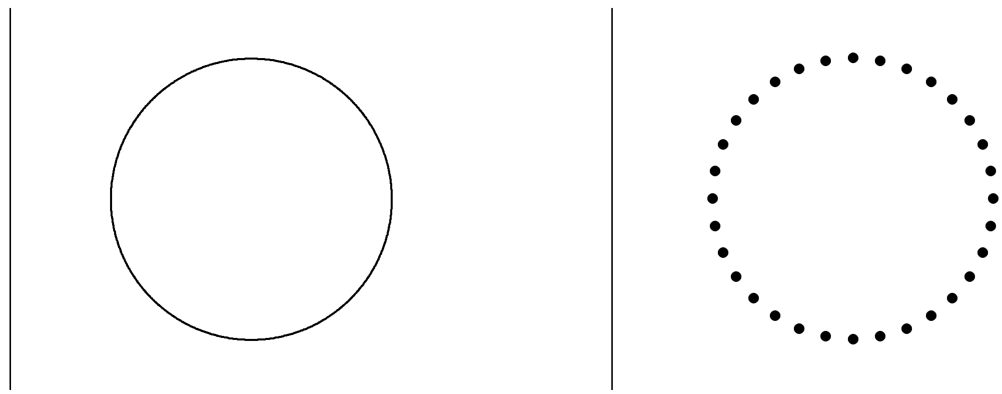

FIGURE 9.24. Replace a circle by a set of 32 points

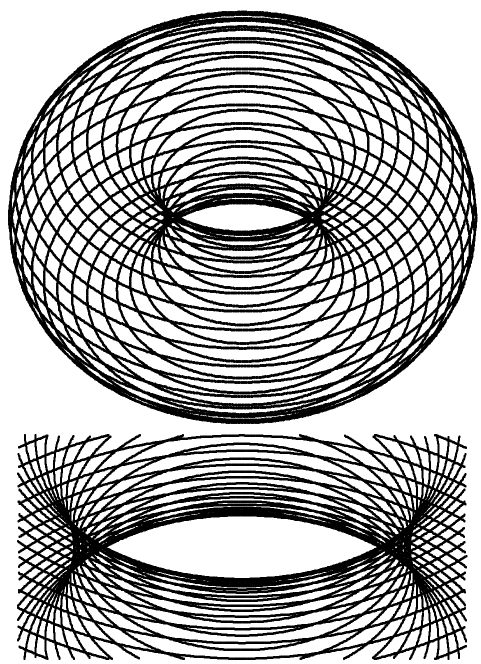

FIGURE 9.25. A projection of a torus

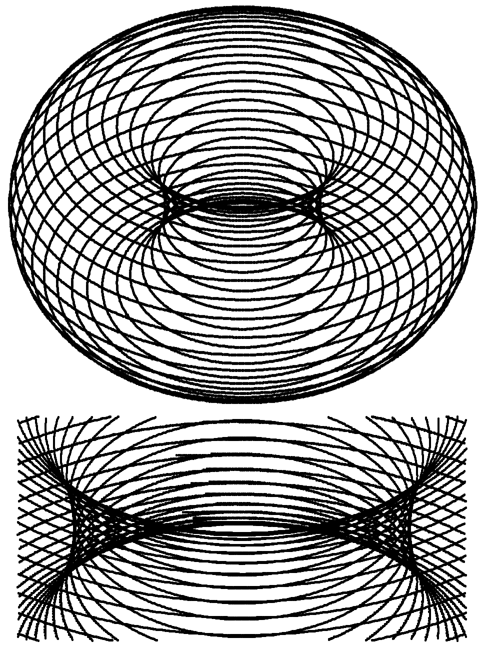

FIGURE 9.26. Another projection of a torus

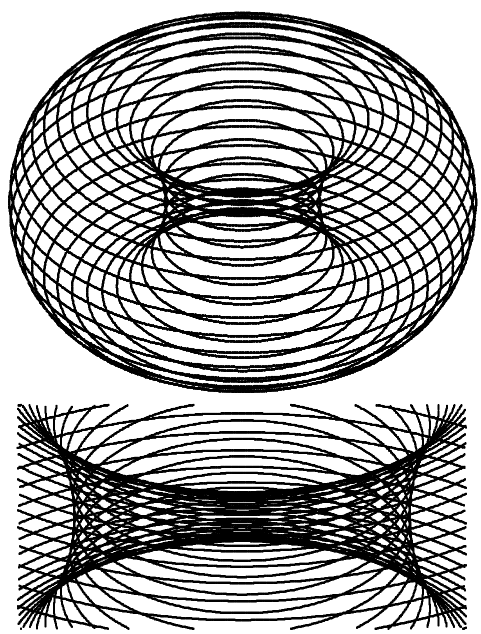

FIGURE 9.27. One more projection of a torus

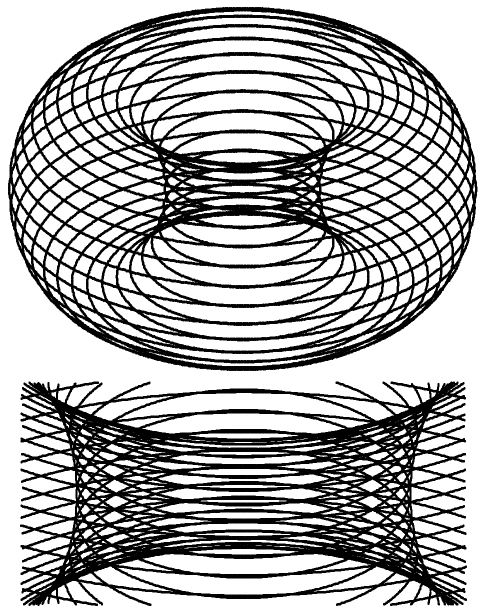

FIGURE 9.28. The last projection of a torus

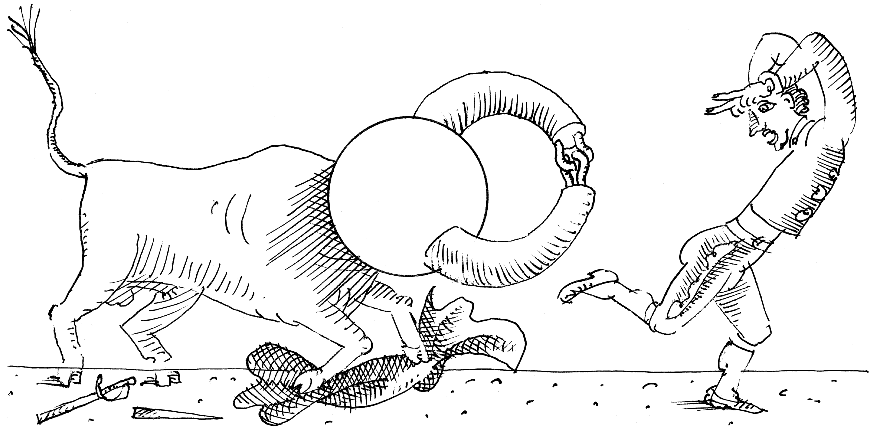

LECTURE 10

# Around Four Vertices

**10.1 The theorem.** There are results in mathematics that could have been easily discovered much earlier than they actually were. One example that comes to mind is Pick's formula from Exercise 1.1 that could have been known to the Ancient Greeks, but it was discovered by Georg Pick only in 1899.

The subject of this lecture is the four vertex theorem, and the reader will agree with us that it also could have been discovered much earlier, say, by Huygens or Newton. However, the vertex theorem was published by an Indian mathematician S. Mukhopadhyaya only in 1909.

The four vertex theorem states that *a plane oval has at least 4 vertices.* An oval for us will always be a closed smooth curve with positive curvature.[1] A *vertex* of a curve is a local maximum or minimum of its curvature. That a closed curve has at least two vertices is obvious: the curvature attains a maximum and a minimum at least once.

**10.2 Caustics, evolutes, involutes and osculating circles.** Consider a smooth curve $\gamma$ in the plane. At every point $x \in \gamma$, one has a family of circles tangent to the curve at this point, see Figure 10.1. Of these circles, one is "more tangent" than the others; it is called the *osculating circle*.

The definition of the osculating circle is as follows. Let two points start moving in the same direction from point $x$ with unit speed, one along the curve $\gamma$ and another along a tangent circle. For all tangent circles, but one, the distance between the points will grow quadratically with time, and only for one exceptional circle the rate of growth will be cubic. This is the osculating circle.

The osculating circle can be constructed as follows. Give $\gamma$ some parameterization so that $x = \gamma(t)$. Consider three close points $\gamma(t-\varepsilon), \gamma(t), \gamma(t-\varepsilon)$. There is a unique circle through these three points (we do not exclude the case of a line, a circle of infinite radius). As $\varepsilon \to 0$, the limiting position of this circle is the

[1]Ovum is an egg in Latin.

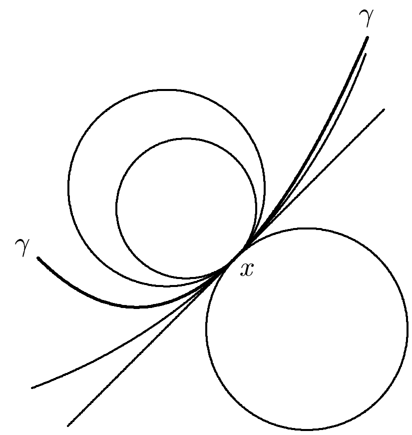


FIGURE 10.1. The osculating circle of a curve

osculating circle of $\gamma$ at the point $x$. One can say that the osculating circle has 3-point contact with the curve or that it is second order tangent to the curve.

The radius of the osculating circle is called the *curvature radius* and its reciprocal the *curvature* of the curve at the given point; the center of the osculating circle is called the *center of curvature* of the curve. If the curve is given an arc length parameterization, that is, one moves along the curve with unit speed, then the curvature is the magnitude of the acceleration vector.[2]

The order of tangency of the osculating circle at a vertex of a curve is higher than at an ordinary point: the circle has 4-point contact with the curve at a vertex, that is, the osculating circle *hyperosculates*.

Imagine that our curve is a source of light: rays of light emanate from $\gamma$ in the perpendicular direction (in the plane of $\gamma$). The envelope $\Gamma$ of this 1-parameter family of normals will be especially bright; this envelope is called the *caustic*,[3] or the *evolute*, of the curve. See Figure 10.2 and the figures in Lecture 9. The curve $\gamma$ is called an *involute* of the curve $\Gamma$. Evolutes and involutes are the main characters of this lecture.

LEMMA 10.1. *The evolute of a curve is the locus of centers of curvature. A vertex of the curve corresponds to a singularity of the evolute, generically, a cusp.*

Proof. Let $\gamma(t)$ be a parameterization of the curve. The equation of the normal line to $\gamma$ at the point $\gamma(t)$ involves the first derivative, $\gamma'(t)$, and the coordinates of the intersection point of two infinitesimally close normals, that is, the center of curvature, involve the first two derivatives, $\gamma'(t)$ and $\gamma''(t)$ (see the equation of an envelope in Section 8.3).

This means that, computing the center of curvature of the curve at point $x$, one may replace the curve by its osculating circle which is second order tangent with the curve at this point. The normals of a circle intersect at its center. Hence the infinitesimally close normals to the curve at $x$ intersect at the center of this circle.

Likewise, the velocity vector of the evolute involves the first three derivatives of the vector valued function $\gamma(t)$. At a vertex, the curve is approximated by the

[2]This is known to every driver: the sharper a turn, the the harder to negotiate it.

[3]From Greek *kaustikos* via Latin *causticus*, “burning”.

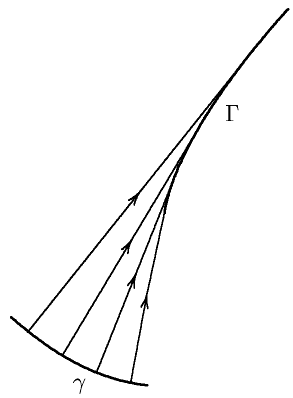


FIGURE 10.2. The evolute of a curve

osculating circle up to three derivatives. Therefore the evolute of the curve at a vertex has the same velocity vector as the evolute of a circle. But the latter is a point! This means that the velocity of the evolute vanishes and it has a singular point. □

Let us add that, at a local maximum of curvature, the cusp of the evolute points toward the curve, while at a local minimum of curvature it points from the curve.

It follows from Lemma 10.1 that the four vertex theorem can be reformulated as a four cusp theorem for the evolute. Note however that, unlike the four vertices, the singular points of the evolute may merge together: for example, the evolute of a circle is just one (*very* singular) point.

Orient the normals to $\gamma$ inward. Then the smooth arcs of the evolute also get oriented. What happens to this orientation at a cusp is shown in Figure 10.3. It follows that the cusps partition the evolute into arcs with opposite orientations. Hence, if $\gamma$ is closed, *the evolute has an even number of cusps.*

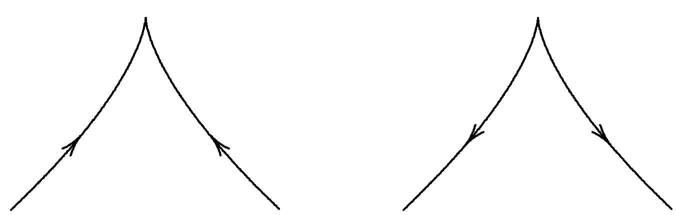

FIGURE 10.3. Orientations of cusps

Evolutes may have cusps but they do not have inflection points. The reason was explained in Lecture 8. The normals to a smooth curve determine a smooth curve in the dual plane, and the envelope is dual to this smooth curve. An inflection is dual to a cusp, so *the evolute is inflection-free.*

The reader who finds this argument too high-brow, may consider a more down-to-earth approach: should $\Gamma$ have an inflection point, at some point of $\gamma$ there would be two different inward normals to $\gamma$ – see Figure 10.4.

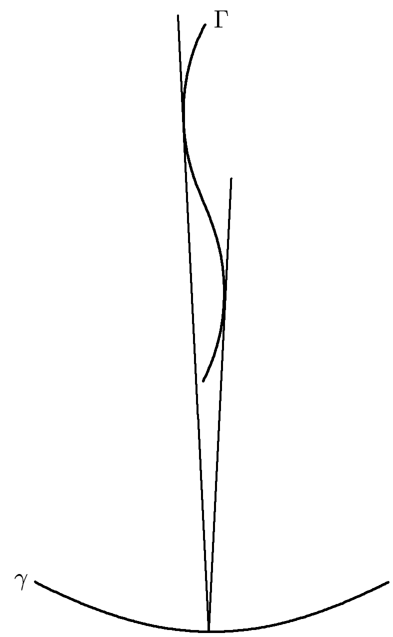


FIGURE 10.4. Evolutes have no inflections

Given the evolute Γ, can one reconstruct the initial curve? In other words, how to construct an involute of a curve? The answer is given by the following *string construction.* Choose a point $y$ on Γ and wrap a non-stretchable string around Γ starting at $y$. Then the free end of the string, $x$, will draw an involute of Γ, see Figure 10.5.

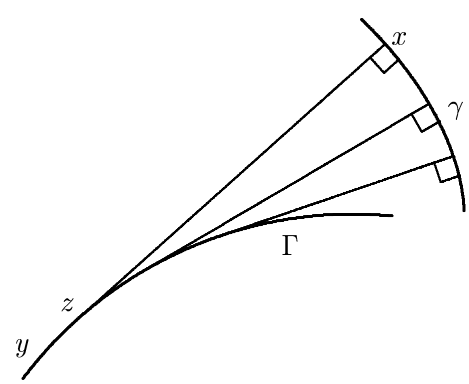


FIGURE 10.5. The string construction of the involute

Proof of the string construction. We need to see that the velocity of the point $x$ is perpendicular to the segment $zx$. Physically, this is obvious: the radial component of the velocity of $x$ would stretch the string.

The reader suspicious of this argument, will probably be satisfied by the following calculus proof. Give Γ the arc-length parameterization $\Gamma(t)$ so that $y = \Gamma(0)$, and let $c$ be the length of the string. Then $z(t) = \Gamma(t)$ and $x(t) = \Gamma(t) + (c-t)\Gamma'(t)$. Hence

$$x'(t) = \Gamma'(t) - \Gamma'(t) + (c-t)\Gamma''(t) = (c-t)\Gamma''(t),$$

and the acceleration vector $\Gamma''(t)$ is orthogonal to the velocity $\Gamma'(t)$ since $t$ is an arc-length parameter. □

Note that the string construction yields not just one but a whole 1-parameter family of involutes: the parameter is the length of the string. Every two involutes are equidistant: the distance between them along their common normals is constant. The relation between involutes and evolutes resembles the one between functions and their derivatives: recovering a function from its derivative involves a constant of integration.

The string construction implies the following property.

COROLLARY 10.1. *The length of an arc of the evolute $\Gamma$ equals the difference of its tangent segments to the involute $\gamma$, that is, the increment of the radii of curvature of $\gamma$.*

Consider the evolute of a plane oval. Let us adapt the convention that the sign of the length of the evolute changes after each cusp; this convention makes sense because the number of cusps is even.

LEMMA 10.2. *The total length of the evolute is zero.*

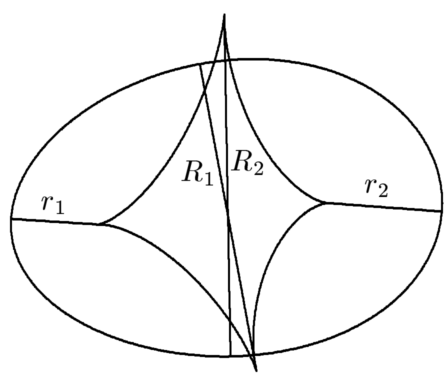


FIGURE 10.6. The total length of the evolute is zero

Proof. Consider Figure 10.6. If the radii of curvature are $r_1, R_1, r_2, R_2$ then, according to Corollary 10.1, the arcs of the evolute have lengths $R_1 - r_1, R_1 - r_2, R_2 - r_2$ and $R_2 - r_1$, and their alternating sum vanishes. The general case is similar. □

The zero length property, of course, again implies the existence of cusps of the caustic of an oval, but this is hardly new to us.

Consider an arc $\gamma$ with monotonic positive curvature and draw a few osculating circles to it. Most likely, your picture looks somewhat like Figure 10.7. This is wrong! A correct picture is shown in Figure 10.8, as the next Tait-Kneser's theorem shows.

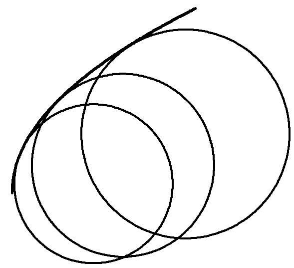

FIGURE 10.7. A wrong picture of osculating circles

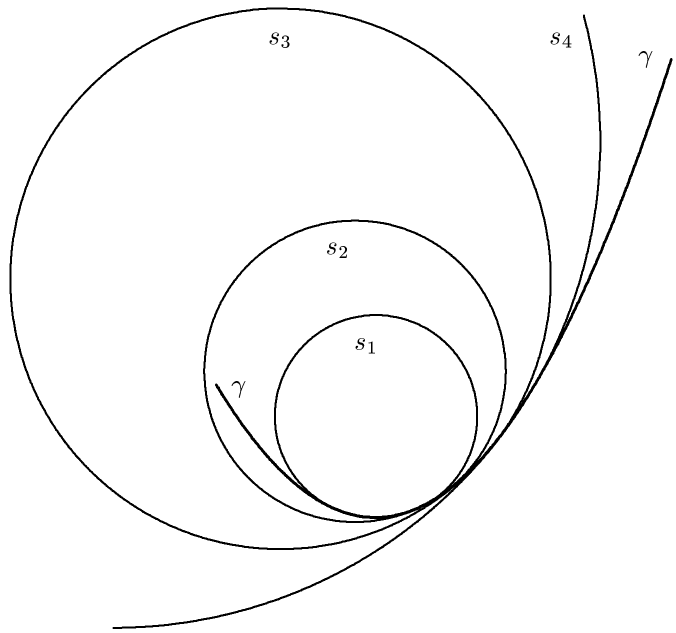


FIGURE 10.8. Osculating circles $s_1, s_2, s_3, s_4$ to a curve $\gamma$ are shown. Although the circles $s_1, s_2, s_3, s_4$ are all disjoint, they seem tangent to each other. No wonder: the shortest distance between the circles $s_1$ and $s_2$ is approximately 0.2% of the radius of $s_1$, and the shortest distance between the circles $s_1$ and $s_4$ is approximately 5% of the radius of $s_1$.

THEOREM 10.2. *The osculating circles of an arc with monotonic positive curvature are nested.*

Proof. Consider Figure 10.9. The length of the arc $z_1z_2$ equals $r_1 - r_2$, hence $|z_1z_2| \leq r_1 - r_2$. Therefore the circle with center $z_1$ and radius $r_1$ contains the circle with center $z_2$ and radius $r_2$. $\square$

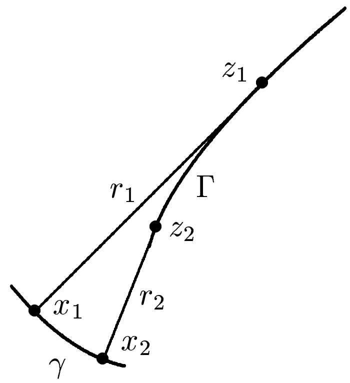


FIGURE 10.9. Proof of the Tait-Kneser theorem 10.2

Consider Figure 10.10 featuring a spiral $\gamma$ and a 1-parameter family of its osculating circles. The circles are disjoint and their union is an annulus.[4] This figure is quite amazing (although this may not be obvious from the first glance)!

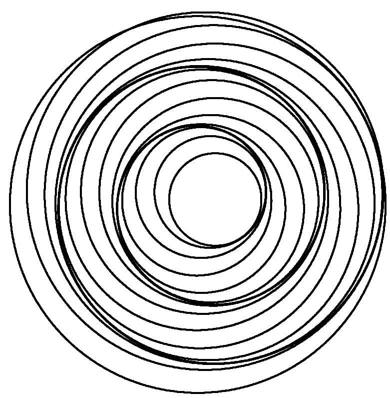

FIGURE 10.10. An annulus filled with disjoint osculating circles

First of all, Figure 10.10 depicts 16 circles; the curve which you see "snaking" between the circles is not drawn – but you clearly see it as the envelope of the circles. Secondly, the partition of the annulus into disjoint circles is quite paradoxical, in the following sense.

PROPOSITION 10.3. *If a differentiable function in the annulus is constant on each circle then this is a constant function.*[5]

Thinking about what this proposition claims, the reader is likely to conclude that it cannot be true. For example, there is an obviously non-constant function on the annulus assiging to each point the radius of the circle passing through this point. This function is clearly constant on the circles and non-constant on the annulus. This function is so natural that it is hard to believe that it is not differentiable. But differentiable it is not!

[4]In technical terms, the annulus is foliated by circles.

[5]In technical terms, the foliation is not differentiable – although its leaves are perfect circles.

Proof. If a function $f$ is constant on the circles, its differential vanishes on the tangent vectors to these circles. Since the curve $\gamma$ is tangent to some circle at every point, the differential $df$ vanishes on $\gamma$. Hence $f$ is constant on $\gamma$. But $\gamma$ intersects all the circles that form the annulus, so $f$ is constant everywhere. □

REMARK 10.4. Most mathematicians are brought up to believe that things like non-differentiable functions do not appear in "real life", they are invented as counterexamples to reckless formulations of mathematical theorems and belong to books with titles such as "Counterexamples in analysis" or "Counterexamples in topology". Proposition 10.3 provides a perfectly natural example of such a situation, and there is nothing artificial about it at all.

**10.3 Proof of the four vertex theorem.** A plane oval $\gamma$ can be described by its *support function*. Choose the origin $O$, preferably inside $\gamma$. Given a direction $\phi$, consider the tangent line to $\gamma$ perpendicular to this direction, and denote by $p(\phi)$ the distance from this tangent line to the origin, see Figure 10.11. If the origin is outside of the oval, this distance will be signed.

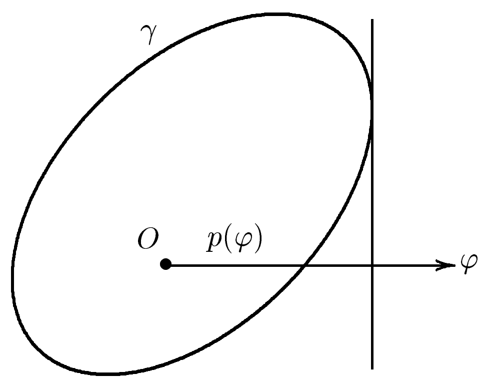


FIGURE 10.11. The support function of an oval

The support function uniquely determines the family of tangent lines to $\gamma$, and therefore the curve itself, as the envelope of this family. One can express all the interesting characteristics of $\gamma$, such as the perimeter length or the area bounded by it, in terms of $p(\phi)$, but we do not need these formulas.

What we need to know is how the support function depends on the choice of the origin. Let $O' = O + (a, b)$ be a different origin.

LEMMA 10.5. *The new support function is given by the formula*

$$p' = p - a\cos\phi - b\sin\phi. \tag{10.1}$$

Proof. Every parallel translation can be decomposed into one in the direction of $\phi$ and one in the orthogonal direction. For a translation distance $r$ in the former direction, $a = r\cos\phi, b = r\sin\phi$, and (10.1) gives $p' = p - r$, as required. For a translation in the orthogonal direction, $a = -r\sin\phi, b = r\cos\phi$, and (10.1) gives $p' = p$, as required. □

What are the support functions of circles? If a circle is centered at the origin, its support function is constant. By the previous lemma, the support functions of circles are linear harmonics, the functions

$$p(\phi) = c + a\cos\phi + b\sin\phi.$$

We can now characterize vertices in terms of the support function.

LEMMA 10.6. *The vertices of a curve correspond to the values of $\phi$ for which*

$$p'''(\phi) + p'(\phi) = 0. \tag{10.2}$$

Proof. Vertices are the points where the curve has the third-order contact with a circle. In terms of the support functions, this means that $p(\phi)$ coincides with $a\cos\phi + b\sin\phi + c$ up to the third derivative. It remains to note that linear harmonics satisfy (10.2) identically. □

Thus the four vertex theorem can be reformulated as follows.

THEOREM 10.3. *Let $p(\phi)$ be a smooth $2\pi$-periodic function. Then the equation $p'''(\phi) + p'(\phi) = 0$ has at least 4 distinct roots.*

Proof. A function on the circle changes sign an even number of times. The mean value of the function $f = p''' + p'$ is zero since it is the derivative of $p'' + p$, hence $f$ changes sign at least twice. Assume that $f$ changes sign exactly twice, at points $\phi = \alpha$ and $\phi = \beta$.

On can find constants $a, b, c$ such that the linear harmonic $g(\phi) = c + a\cos\phi + b\sin\phi$ changes sign exactly at the same points, $\alpha$ and $\beta$, and so that $f$ and $g$ have the same signs everywhere. For example,

$$\pm g(\phi) = \cos\left(\frac{\beta - \alpha}{2}\right) - \cos\left(\phi - \frac{\beta + \alpha}{2}\right).$$

Then

$$\int_0^{2\pi} f(\phi)g(\phi)\ d\phi > 0.$$

On the other hand, integration by parts yields:

$$\int_0^{2\pi} (p''' + p')g\ d\phi = -\int_0^{2\pi} (p'' + p)g'\ d\phi = \int_0^{2\pi} (p'g'' - pg')\ d\phi$$
$$= -\int_0^{2\pi} p(g''' + g')d\phi = 0$$

since $g''' + g' = 0$. This is a contradiction. □

REMARK 10.7. Theorem 10.3 has generalizations. A smooth $2\pi$-periodic function has a Fourier expansion

$$f(\phi) = \sum_{k\geq 0} (a_k \cos k\phi + b_k \sin k\phi).$$

The Fourier series of the function $f = p''' + p'$ does not contain linear harmonics. The Sturm-Hurwitz theorem states that if the Fourier expansion of a function starts with $n$-th harmonics, that is, $k \geq n$ in the sum above, then this function has at least $2n$ distinct zeroes on the circle $[0, 2\pi)$. The above proof can be adjusted to this more general set-up; other proofs are known as well, see, e.g., [**57**] and Exercise 10.6.

**10.4 Two other proofs.** Like almost every good mathematical result, the four vertex theorem has a number of different proofs. We present two geometrical ones in this section. We know many other proofs, using different ideas and generalizing in different directions; one would be hard pressed to choose "proof from the Book"[6] for the four vertex theorem.

First proof. [**79**]. Consider the evolute $\Gamma$ of an oval $\gamma$. According to Lemma 10.2, the length of $\Gamma$ is zero, and hence it has at least two cusps. Assume that the (even) number of cusps is exactly two.

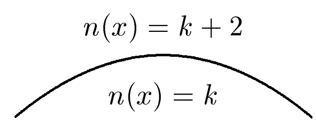


FIGURE 10.12. The number of tangents to a curve

Given a point $x$ in the plane, let $n(x)$ be the number of normals to $\gamma$ that pass through this point. In other words, $n(x)$ equals the number of tangent lines from $x$ to $\Gamma$. This function is locally constant in the complement of the evolute. When $x$ crosses $\Gamma$ from the concave to the convex side, the value of $n(x)$ increases by 2, see Figure 10.12.

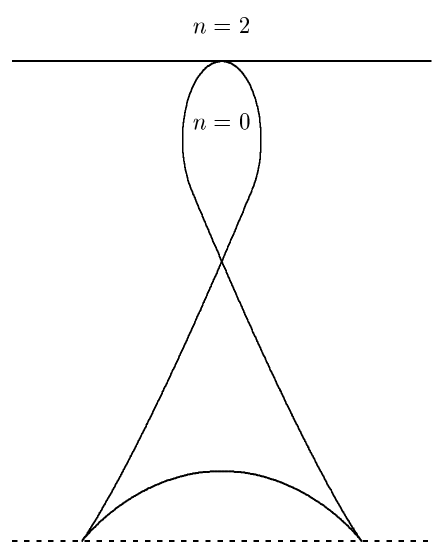


FIGURE 10.13. Proof of the four vertex theorem

For every point $x$, the distance to $\gamma$ has a minimum and a maximum. Therefore there are at least two perpendiculars from $x$ to the oval, and hence $n(x) \geq 2$ for every $x$. Since the normals to $\gamma$ turn monotonically and make one complete turn, $n(x) = 2$ for all points $x$, sufficiently far away from the oval.

Consider the line through two cusps of the evolute; assume it is horizontal, see Figure 10.13. Then the height function, restricted to $\Gamma$, attains either minimum, or

[6]Paul Erdös used to refer to "The Book" in which God keeps the most elegant proofs of mathematical theorems, see [**2**].

maximum, or both, not in a cusp. Assume it is a maximum (as in Figure 10.13); draw the horizontal line $l$ through it. Since the evolute lies below this line, $n(x) = 2$ above it. Therefore $n(x) = 0$ immediately below $l$. This is a contradiction proving the four vertex theorem. □

Outline of the second proof. This follows ideas of the famous French mathematician R. Thom. This is a beautiful argument indeeed!

For every point $x$ inside the oval $\gamma$, consider the closest point $y$ on the oval. Of course, for some points $x$, the closest point is not unique. The locus of such points is called the *symmetry set*; denote it by $\Delta$. For example, for a circle, $\Delta$ is its center, and for an ellipse, $\Delta$ is the segment between the two centers of maximal curvature. For a generic oval, $\Delta$ is a graph (with curved edges), and its vertices of valence 1 are the centers of local maximal curvature of $\gamma$, see Figure 10.14.

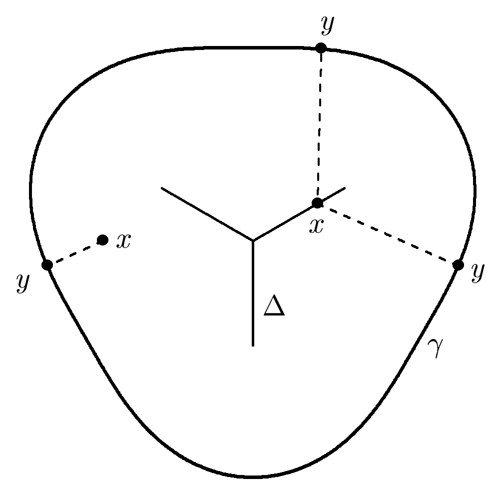


FIGURE 10.14. The symmetry set of an oval

The last claim needs an explanation. It is clear that the vertices of $\Delta$ of valence 1 are the centers of extremal curvature (where two points labeled $y$ in Figure 10.14 merge together). But why not centers of minimal curvature? This is because an osculating circle of minimal curvature locally lies outside of the curve $\gamma$. Therefore the distance from the center of such a circle to the curve is less than its radius and hence its center does not belong to the symmetry set $\Delta$.

Delete the symmetry set from the interior of $\gamma$. What remains can be continuously deformed to the boundary oval by moving every point $x$ toward the closest point $y$. Hence the complement of $\Delta$ is an annulus, and therefore $\Delta$ has no loops (and consists of only one component). Thus $\Delta$ is a tree which necessarily has at least two vertices of valence 1. It follows that the curvature of the oval has at least two local maxima, and we are done. □

**10.5 Sundry other results.** Since its discovery about a century ago, the four vertex theorem and its numerous generalizations keep attracting the attention of mathematicians. In this last section we describe, without proofs, a few results around four vertices (see, e.g., [**57**]).

One way to generalize the four vertex theorem is to approximate a smooth plane curve not by its osculating circles but by some other type of curves, for instance, conics. There exists a unique conic through every generic 5 points in the plane. Taking these points infinitesimally close to each other on an oval, one obtains its osculating conic. Just like an osculating circle, this conic may hyperosculate: such a point of the curve is called *sextactic* (or, for reasons that we will not discuss here, an affine vertex). What is the least number of sextactic points of a plane oval? The answer is six, and this was proved by Mukhopadhyaya in his 1909 paper.

One can also approximate a curve by its tangent lines. Then we are interested in inflections, the points where the tangent line is second-order tangent to a curve. Of course, an oval does not have inflections. However, consider a simple closed curve in the projective plane. Recall from Lecture 8 that the projective plane is the result of pasting together pairs of antipodal points of the sphere. A closed curve in the projective plane can be drawn on the sphere, either as a closed curve or as a curve whose endpoints are antipodal, and an inflection is its abnormal tangency with a great circle.

Assume that our curve belongs to the latter type, that is, its endpoints are antipodal. Then a Möbius theorem (1852) states that the curve has at least three inflections. See Figure 10.15 where the sphere is projected on a plane from its center, and so the curves appear to escape to infinity; this figure features a simple curve with 3 inflections and a self-intersecting curve with only 1 inflection.

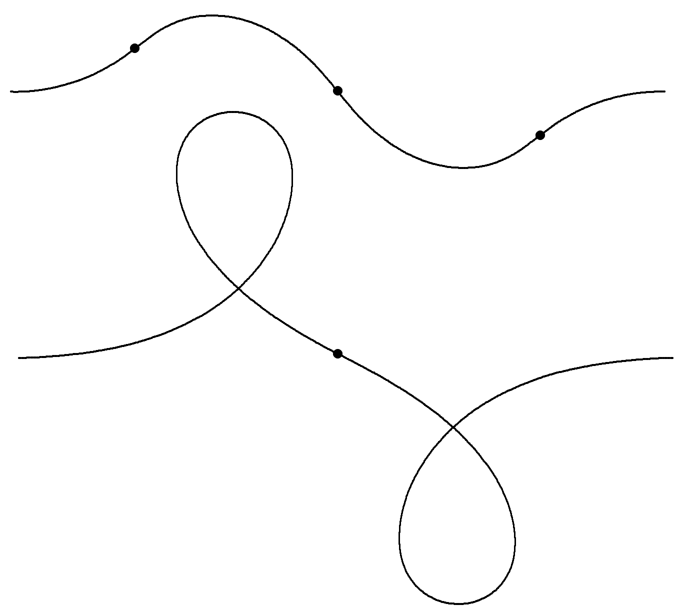

FIGURE 10.15. Inflection points of a curve in the projective plane

By the way, there is another, much more recent, result about spherical curves. Assume that a smooth closed simple curve bisects the area of the sphere. Then it has at least 4 inflection points. This result, which V. Arnold called the “tennis ball theorem",[7] was discovered by B. Segre (1968) and rediscovered by Arnold in the late 1980s.

One may also approximate a smooth curve by a cubic curve. An algebraic curve of degree 3 is determined by 9 of its points, and the osculating cubic of a smooth curve passes through 9 infinitesimally close points. A cubic is hyperosculating if it passes through 10 such points, and the respective point of the curve is called 3-extactic (in this, somewhat cumbersome, terminology, 2-extactic=sextactic and 1-extactic=inflection).

A typical cubic curve looks like one of the curves in Figure 10.16; in the latter case, its bounded component is called an oval. Recently V. Arnold discovered the following theorem: *a smooth curve, obtained by a small perturbation of the oval of a cubic curve, has at least ten 3-extactic points.* It is tempting to continue by increasing the degree of approximating algebraic curves but, to the best of our knowledge, no further results in this direction are available.

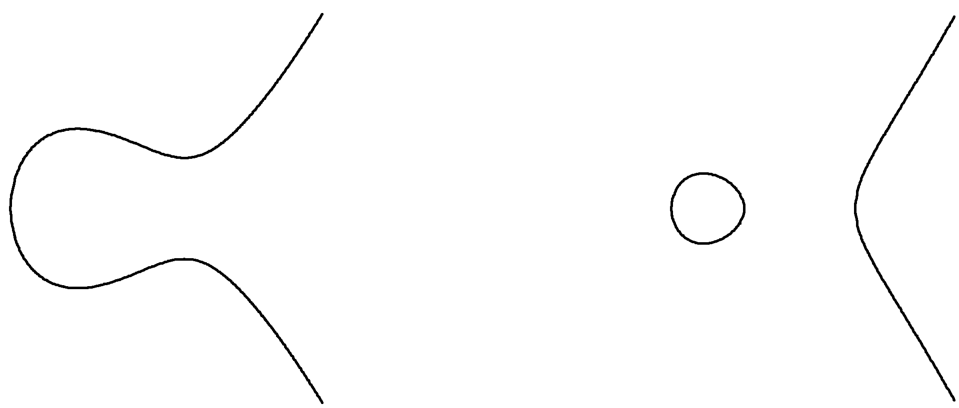

FIGURE 10.16. Cubic curves

In the early 1990s, E. Ghys discovered the following beautiful theorem. The real projective line is obtained from the real line by adding one point "at infinity". This extension has clear advantages. For example, a fractional-linear function

$$f(x) = \frac{ax+b}{cx+d}, \quad ad - bc \neq 0,$$

is not a well-defined function of the real variable: if $x = -d/c$ then $f(x) = \infty$; but $f$ regains its status of a well-defined and invertible function from the real projective line to itself ($f(\infty) = a/c$).

Let $f(x)$ be a smooth invertible function from the real projective line to itself. At every point $x$, one can find a fractional-linear function whose value, whose first and whose second derivatives coincide with those of $f$ at the point $x$. It is natural to call this the osculating fractional-linear function. A fractional-linear function is hyperosculating at $x$ if its third derivative there equals $f'''(x)$ as well. How many hyperosculating fractional-linear functions are there for an arbitrary $f$? According to the Ghys theorem, at least four. In terms of the function $f$, these points are the

[7]Every tennis ball has a clearly visible curve on it surface which has exactly four inflections.

roots of a rather intimidating expression

$$\frac{f'''(x)}{f'(x)} - \frac{3}{2}\left(\frac{f''(x)}{f'(x)}\right)^2,$$

called the *Schwarzian derivative* of $f$.

Another direction of generalizing the four vertex theorem is to replace a smooth curve by a polygon. This discretization may be performed in different ways, leading to different results. We mention only one, probably the oldest. This is the Cauchy lemma (1813) which plays the central role in Cauchy's celebrated proof of the rigidity of convex polyhedra, described in Lecture 24: *given two convex polygons whose respective sides are congruent, the cyclic sequence of the differences of their respective angles changes sign at least four times.*

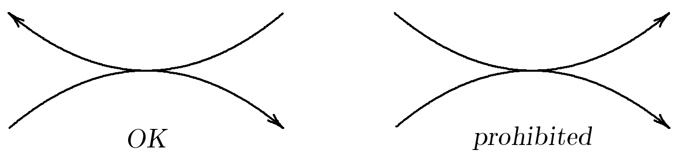


FIGURE 10.17. Positive and negative self-tangencies

Finally, back to vertices. It has been known for a long time that the four vertex theorem holds for non-convex simple closed curves as well. V. Arnold conjectured that one could extend it much further. Starting with an oval, one is allowed to deform the curve smoothly and even to intersect itself; the only prohibited event is when the curve touches itself so that the touching pieces have the same orientations as in Figure 10.17. According to Arnold's conjecture, the four vertex theorem holds for every curve that can be obtained from an oval as a result of such a deformation; see Figure 10.18 for a sample.

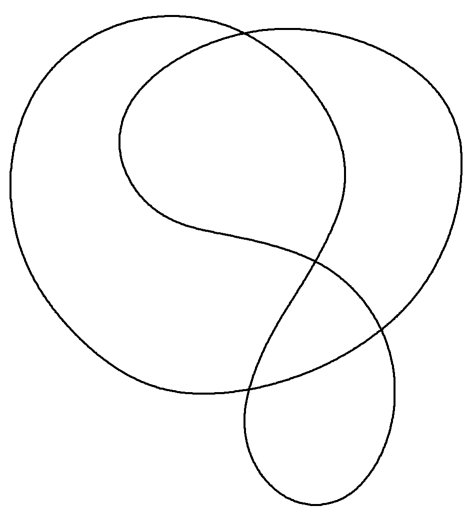

FIGURE 10.18. An allowed deformation of an oval

Recently Yu. Chekanov and P. Pushkar' proved this conjecture using ideas from contemporary symplectic topology and knot theory [**15**].

John Smith
January 23, 2010

Martyn Green
August 2, 1936

Henry Williams
June 6, 1944

John Smith
January 23, 2010

Martyn Green
August 2, 1936

Henry Williams
June 6, 1944

John Smith
January 23, 2010

Martyn Green
August 2, 1936

Henry Williams
June 6, 1944

### 10.6 Exercises.

10.1. (a) Draw involutes of a cubic parabola.
(b) Draw involutes of the curve in Figure 10.19.

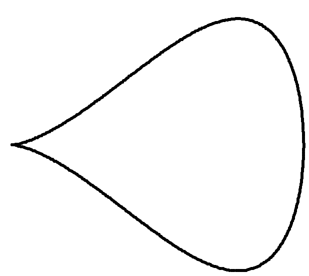

FIGURE 10.19

10.2. A cycloid is the curve traversed by a point of a circle that rolls without sliding along a horizontal line. Describe the evolute of a cycloid.

10.3. Compute the curvature of a semi-cubic parabola at the cusp.

10.4. (a) Express the perimeter length and the area of an oval in terms of its support function.

(b) Parameterize an oval $\gamma$ by the angle $\phi$ made by its tangent with a fixed direction, and let $p(\phi)$ be the support function. Prove that

$$\gamma(\phi) = (p(\phi)\sin\phi + p'(\phi)\cos\phi, -p(\phi)\cos\phi + p'(\phi)\sin\phi).$$

(c) Show that the radius of curvature of $\gamma(\phi)$ equals $p''(\phi) + p(\phi)$.

10.5. Let $f$ be a smooth function of one real variable. The osculating (Taylor) polynomial $g_t(x)$ of degree $n$ of the function $f(x)$ at point $t$ is the polynomial, whose value and the values of whose first $n$ derivatives at point $t$ coincide with those of $f$:

$$g_t(x) = \sum_{i=0}^{n} \frac{f^{(i)}(t)}{i!}(x-t)^i.$$

Assume that $n$ is even and $f^{(n+1)}(t) \neq 0$ on some interval $I$ (possibly, infinite). Prove that for any distinct $a$ and $b$ from the interval $I$, the graphs of the osculating polynomials $g_a(x)$ and $g_b(x)$ are disjoint.

*Comment*: this theorem strongly resembles the Tait-Kneser theorem 10.2.

10.6. * Consider a trigonometric polynomial

$$f(x) = a_k \cos kx + b_k \sin kx + a_{k+1}\cos(k+1)x + b_{k+1}\sin(k+1)x + \dots$$
$$+ a_n \cos nx + b_n \sin nx$$

where $k < n$. Prove that $f$ has at least $2k$ roots on the circle $[0, 2\pi]$.

*Hint.* Let $I$ be the inverse derivative of a periodic function with the integration constant chosen so that the average value of the function is zero. Denote the number of sign changes of a function $f$ by $Z(f)$. Then Rolle's theorem states that $Z(f) \geq Z(I(f))$. Iterate this inequality many times and investigate how $f$ changes under the action of $I$.

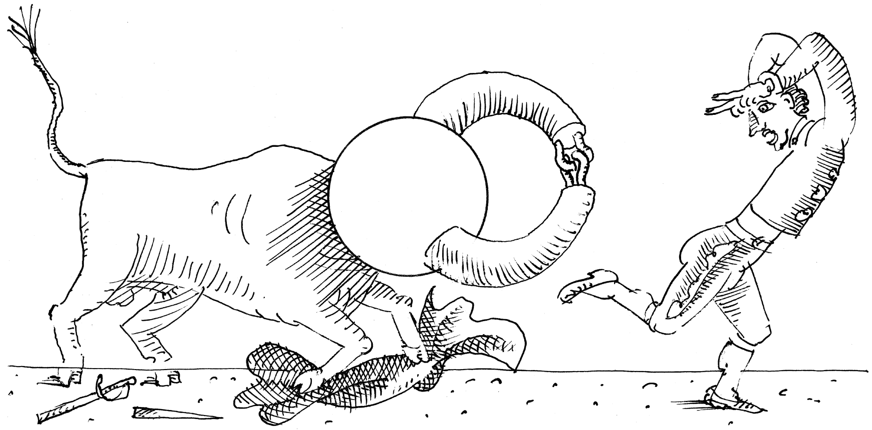

LECTURE 11

# Segments of Equal Areas

**11.1 The problem.** The main "message" of Lecture 9 was that cusps are ubiquitous: every generic 1-parameter family of curves has an envelope, and this envelope usually has cusps. This lecture is a case study: we investigate, in detail, one concrete family of lines in the plane.

Let $\gamma$ be a closed convex plane curve. Fix a number $0 \le t \le 1$. Consider the family of oriented lines that divide the area inside $\gamma$ in the ratio $t : (1-t)$, the $t$-th portion on the left, and the $(1-t)$-th on the right of the line. This 1-parameter family of lines has an envelope, the curve $\Gamma_t$.

Let us make an immediate observation: the curves $\Gamma_t$ and $\Gamma_{1-t}$ coincide. Thus we may restrict ourselves to $0 \le t \le 1/2$. The curves $\Gamma_t$ are our main objects of study.

**11.2 An example.** Let us start with a simple example (which still might be familiar to some of the readers from high school[1]). Consider the family of lines that cut off a fixed area $A$ from a plane wedge, and let $\Gamma$ be the envelope of this family of lines.

THEOREM 11.1. *The curve $\Gamma$ is a hyperbola.*

Proof. Apply an area preserving linear transformation that takes the given wedge to a right angle. We consider the sides of the angle as the coordinate axes. It suffices to prove the theorem in this case.

Let $f(x)$ be a differentiable function. The tangent line to the graph $y = f(x)$ at point $(a, f(a))$ has the equation $y = f'(a)(x-a) + f(a)$. The $x$- and $y$-intercepts of this line are

$$a - \frac{f(a)}{f'(a)} \quad \text{and} \quad f(a) - af'(a).$$

[1]Admittedly, an over-optimistic statement.

Consider the hyperbola $y = c/x$. In this case, the $x$- and $y$-intercepts of the tangent line at point $(a, c/a)$ are $2a$ and $2c/a$. Therefore the area of the triangle bounded by the coordinate axis and this tangent line is $2c$, a constant.

This proves that the tangent lines to a hyperbola cut off triangles of constant areas from the coordinate "cross". Formally, this is not yet what the theorem claims. To finish the proof, choose the constant $c$ in the equation of the hyperbola $y = c/x$ so that the areas in question equals $A$. Then this hyperbola is the curve $\Gamma$ from the formulation of the theorem, the envelope of the lines that cut off triangles of area $A$ from the coordinate axes. □

**11.3 The envelope of segments of equal areas is the locus of their midpoints.** The title of this section is a formulation of a theorem. The theorem asserts that the curve $\Gamma_t$ is tangent to the segments that cut off $t$-th portion of the total area in their midpoints.

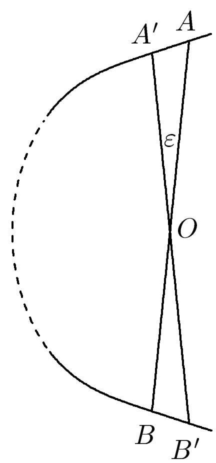


FIGURE 11.1. Proving that the envelope of segments of equal areas is the locus of their midpoints

Proof of Theorem. Consider Figure 11.1. Let $AB$ and $A'B'$ be two close segments from our family and $\varepsilon$ the angle between them. Since both segments cut off equal areas from the curve $\gamma$, the areas of the sectors $AOA'$ and $BOB'$ are equal. The areas of these sectors are approximately equal to $(1/2)|AO|^2\varepsilon$ and $(1/2)|BO|^2\varepsilon$, with error of order $\varepsilon^2$. Therefore $|AO| - |BO|$ tends to zero as $\varepsilon \to 0$. □

As an application, let us solve the following problem: *given two nested ovals, is there a chord of the outer one, tangent to the inner one and bisected by the tangency point?* See Figure 11.2. Simple as it sounds, this problem is not easy to solve, unless one uses the above theorem.

Solution to the problem. Let $\ell$ be the tangent segment to the inner curve that cuts off the smallest area from the outer one. Denote by $S$ be the value of this area. Consider two close segments $\ell'$ and $\ell''$ that cut off area $S$ from the outer oval. Let $A$ be the tangency point of $\ell$ with the inner oval, and $B$ and $C$ the intersections of $\ell$ with $\ell'$ and $\ell''$, see Figure 11.3.

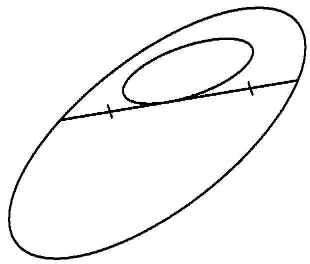

FIGURE 11.2. A problem on two ovals

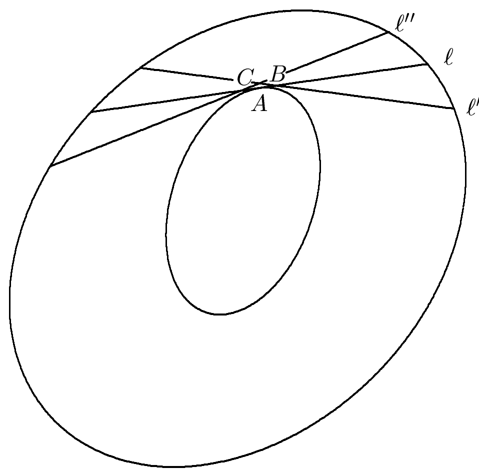


FIGURE 11.3. Solving the problem on two ovals

Since $S$ is the minimal area, segments $\ell'$ with $\ell''$ do not contain points inside the inner oval. Hence point $A$ lies between points $B$ and $C$. As $\ell'$ and $\ell''$ tend to $\ell$, points $B$ and $C$ tend to $A$. Thus $A$ is the tangency point of segment $\ell$ with the envelope of the segments that cut off area $S$ from the outer oval. By the above theorem, $A$ bisects $\ell$.

Of course, one can repeat the argument, replacing the minimal area by the maximal one. As a result, there are at least two chords, tangent to the inner oval at their midpoints.

**11.4 Digression: outer billiards.** One is naturally led to the definition of an interesting dynamical system, called the outer (or dual) billiard. Unlike the usual billiards, discussed in Lecture 28, the game of outer billiard is played outside the billiard table.

Let $C$ be a plane oval. From a point $x$ outside $C$, there exist two tangent lines to $C$. Choose the right one, as viewed from $x$, and reflect $x$ in the tangency point. One obtains a new point, $y$, and the transformation that takes $x$ to $y$ is the outer billiard map, see Figure 11.4.

There are many interesting things one can say about outer billiards, see [**23, 78, 83**] for surveys. We will establish but a few fundamental properties of outer billiards.

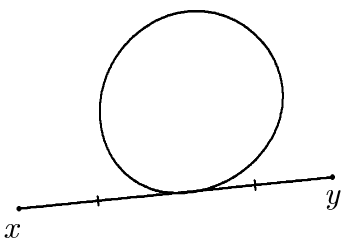


FIGURE 11.4. Outer billiard transformation

THEOREM 11.2. *For every oval $C$, the outer billiard map is area preserving.*

Proof. Consider two close tangent lines to the curve $C$, pick points $x_1, x_2$ and $x_1', x_2'$ on these lines, and let $y_1, y_2, y_1', y_2'$ be their images under the outer billiard map, see Figure 11.5. The outer billiard map takes the quadrilateral $x_1x_2x_2'x_1'$ to $y_1y_2y_2'y_1'$.

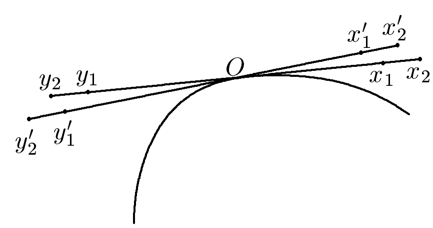


FIGURE 11.5. Area preserving property of outer billiards

Denote by $O$ the intersection point of the lines and let $\varepsilon$ be the angle between them. Arguing as in Section 11.3, the areas of the triangles $x_1Ox_1'$ and $y_1Oy_1'$ are equal, up to error of order $\varepsilon^2$, and likewise for the triangles $x_2Ox_2'$ and $y_2Oy_2'$. Hence, up to the same error, the areas of the quadrilaterals $x_1x_2x_2'x_1'$ and $y_1y_2y_2'y_1'$ are equal. In the limit $\varepsilon \to 0$, we obtain the area preserving property. □

Here is another question about outer billiards. Given a plane oval $C$, is there an $n$-gon, circumscribed about $C$, whose sides are bisected by the tangency points? Such a polygon corresponds to an $n$-periodic orbit of the outer billiard about $C$.

The answer to this question is affirmative. Indeed, consider the circumscribed $n$-gon of the minimal area. Then, arguing as in the solution to the problem in Section 11.3, each side of this polygon is bisected by its tangency points to $C$. The same argument applies to star-shaped $n$-gons, see Figure 11.6 for three types of septagons.[2]

**11.5 What the envelope has and what it has not.** The envelopes $\Gamma_t$ do not have double tangent lines and inflection points. Indeed, if a curve has a double tangent line or an inflection point then it has two close parallel tangents, see Figure 11.7, and these parallel tangents cannot cut off the same areas from the curve $\gamma$.

[2]In fact, for every $n \geq 3$ and every $1 \leq r \leq n/2$, coprime with $n$, there are at least *two* circumscribed $n$-gons, making $r$ turns around the oval $C$, whose sides are bisected by the tangency points, see [**78, 83**].

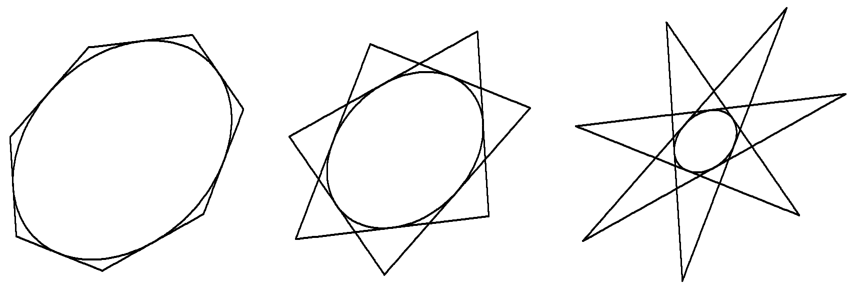

FIGURE 11.6. Three types of circumscribed septagons

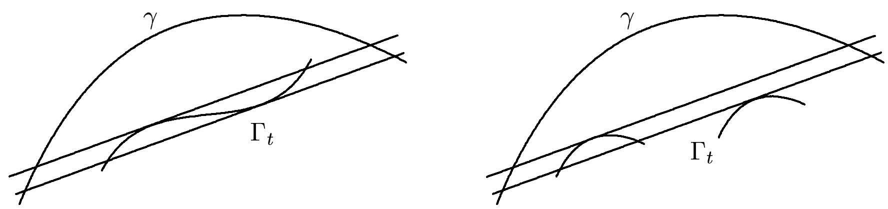


FIGURE 11.7. The envelope does not have double tangents

What the envelope of segments of equal areas may have are cusps. The following theorem tells us when $\Gamma_t$ has a cusp. We assume that $\gamma$ is an oval.

THEOREM 11.3. *If the midpoint of a chord $AB$ of the curve $\gamma$ is a cusp of the envelope of segments of equal areas then the tangent lines to $\gamma$ at points $A$ and $B$ are parallel.*

Proof. Let $O$ be the midpoint of $AB$. Since $O$ is a cusp of the envelope of segments of equal areas, the velocity of point $O$ is zero, and the instantaneous motion of the line $AB$ is revolution about point $O$. Since $O$ is the midpoint of the segment $AB$, the velocity vectors of points $A$ and $B$ are symmetric with respect to point $O$, and hence the tangent lines to $\gamma$ at the points $A$ and $B$ are parallel. □

Suppose that the tangent lines to $\gamma$ at points $A$ and $B$ are parallel. To describe the behavior of the envelope of segments of equal areas $\Gamma_t$ we need additional information about the curvature of the curve $\gamma$ at points $A$ and $B$. Assume that the curvature at $B$ is greater.

THEOREM 11.4. *The envelope $\Gamma_t$ has a cusp pointing toward $B$.*

Proof. Consider Figure 11.8, left: $\gamma_1$ and $\gamma_2$ are pieces of the curve $\gamma$ near points $A$ and $B$; $O$ is the midpoint of segment $AB$; and $\bar{\gamma}_1$ is symmetric to $\gamma_1$ with respect to $O$.

Draw a chord $C'D'$ through point $O$, close to $AB$. Since the curvature of $\gamma_2$ is greater than that of $\gamma_1$, the area of the sector $AOC'$ is greater than that of $BOD'$ (it is equal to the area of the sector $BOM$, symmetric to $AOC'$). Therefore the segment $CD$, that divides the area of $\gamma$ in the same ratio as $AB$, lies to the right of $C'D'$. The midpoint of $CD$ is close to point $O'$, the intersection of the segments $AB$ and $CD$. Similar observations can be made concerning the segments $E'F'$ and

$EF$. Thus, the envelope $\Gamma_t$ tangent to $AB$, $CD$, and $EF$ and passing through $O$, must have a cusp at $O$, pointing toward point $B$ (see Figure 11.8, right). □

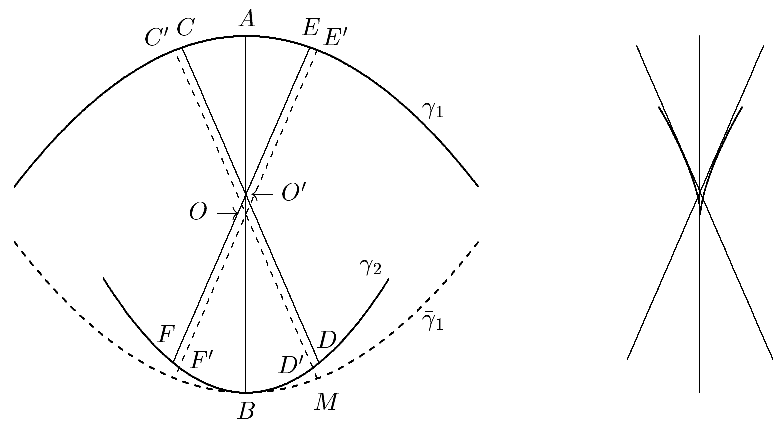


FIGURE 11.8. Cusp of the envelope

And what if the curvatures at points $A$ and $B$ are equal? This event will not happen for a generic curve $\gamma$. Indeed, we assume three conditions to hold: the segment $AB$ divides the area in the ratio $t : (1-t)$, the tangent lines at $A$ and $B$ are parallel, and the curvatures at $A$ and $B$ are equal. But a pair of points $A$ and $B$ on the curve $\gamma$ have only two degrees of freedom, so for three conditions to hold is too much to expect.

However, if one allows the parameter $t$ to vary, then one may encounter a chord $AB$ of $\gamma$ with parallel tangent lines and equal curvatures at the endpoints. We will refer to this situation as the *case of maximal degeneracy.* In fact, cases of maximal degeneracy are bound to happen.

LEMMA 11.1. *Any oval $\gamma$ has a chord with parallel tangent lines and equal curvatures at the endpoints; the number of such chords is odd.*

Proof. For every point $A$ of $\gamma$ there exists a unique "antipodal" point $B$ such that the tangents at $A$ and $B$ are parallel. Assume that the curvature at $A$ is greater than that at $B$. Let us move point $A$ continuously toward $B$; its antipodal point will move toward $A$. After the points $A$ and $B$ have switched, the curvature at the first point is smaller than that at the second. Therefore the curvatures at the two points were equal somewhere in-between. Furthermore, the total number of sign changes of the difference between the curvatures at points $A$ and $B$ is odd, as claimed. □

**11.6 How many cusps are there?** How many cusps does the envelope $\Gamma_t$ have? The answer depends on whether $t = 1/2$ or not.

THEOREM 11.5. *The number of cusps of $\Gamma_{1/2}$ is odd and not less than 3.*[3]

[3]Compare with the Möbius theorem mentioned in Lecture 10

Proof. For every direction, there is a unique *non-oriented* line that bisects the area bounded by the curve $\gamma$. Hence, after traversing $\Gamma_{1/2}$, its tangent line makes a turn through 180°. How can this be? Each time one passes a cusp, the tangent direction switches to the opposite, see Figure 11.9. This means that the total number of cusps is odd.

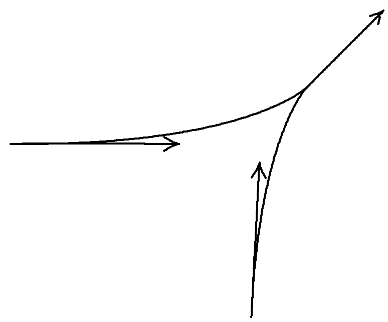

FIGURE 11.9. A cusp reverses the direction

The number of cusps of $\Gamma_{1/2}$ is not one. Arguing by contradiction, assume there is a single cusp with a vertical tangent line. Then $\Gamma_{1/2}$ has no other vertical tangent lines. Left of the cusp, the smooth curve $\Gamma_{1/2}$ moves to the left, and right of the cusp – to the right. Such a curve cannot close up, see Figure 11.10; a contradiction. □

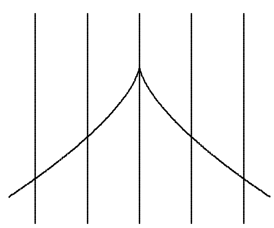

FIGURE 11.10. Proving that there are at least 3 cusps

If $t \neq 1/2$ then, for every direction, there is a unique *oriented* line that divides the area bounded by the curve $\gamma$ in the ratio $t : (1-t)$. Hence, after traversing $\Gamma_t$, its tangent line makes a turn through 360°. It follows that the number of cusps is even.

**11.7 All in one figure.** Figure 11.11 depicts the family of envelopes $\Gamma_t$ as $t$ varies from 0 to 1/2. The delta-shaped curve at the center is $\Gamma_{1/2}$.

The main new observation is that the cusps of the curves $\Gamma_t$ lie on a new curve, $\Delta$ (shown as a dashed curve in Figure 11.11), the locus of midpoints of the chords with parallel tangents at the endpoints.

The curve $\Delta$ also has cusps! These are the points where cusps of the envelopes $\Gamma_t$ appear or disappear in pairs, and these are precisely the points of maximal degeneracy, introduced in Section 11.5.

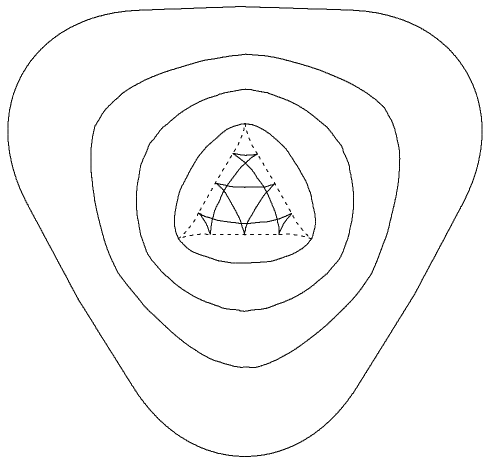

FIGURE 11.11. The family of envelopes $\Gamma_t$

How many cusps does the curve $\Delta$ have? Asking this question, we assume, as we always do when dealing with cusps, that our curves are sufficiently generic: otherwise $\Delta$ might degenerate even to a single point – this is the case when the original oval is a circle or an ellipse.

THEOREM 11.6. *The number of cusps of $\Delta$ is odd and not less than 3.*

Proof. That the number of cusps is odd, follows from Lemma 11.1. We claim that the number of cusps of $\Delta$ is not less than that of $\Gamma_{1/2}$, that is, by Theorem 11.5, not less than 3.

Let $k$ be the number of cusps of $\Gamma_{1/2}$. Then, for $\varepsilon$ small enough, the curve $\Gamma_{1/2-\varepsilon}$ has $2k$ cusps – see Figure 11.11. On the other hand, for $\varepsilon$ small enough, the curve $\Gamma_\varepsilon$ is smooth. Therefore, as $t$ varies from $1/2-\varepsilon$ to $\varepsilon$, all $2k$ cusps must pairwise vanish at points of maximal degeneracy, that is, cusps of $\Delta$. Thus $\Delta$ has at least $k$ cusps, and since $k \geq 3$, the result follows. $\Box$

**11.8 Polygons.** Of course, a convex polygon is not an oval, but one can approximate it by a smooth strictly convex curve: almost flat arcs along sides and sharp turns at the vertices.

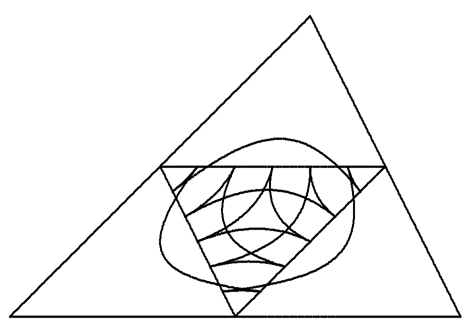

FIGURE 11.12. For a triangle, the curve $\Delta$ is a homothetic triangle

Let us start with a triangle. A pair of points $A, B$ with parallel tangents is a vertex of the triangle and any point of the opposite side. The locus $\Delta$ of midpoints of such segments $AB$ is a triangle, similar to the given one with coefficient -1/2, see Figure 11.12. The vertices of $\Delta$ lie in the middles of the sides of the original triangle, therefore *all* the envelopes $\Gamma_t$ have cusps (even for very small values of $t$). The curves $\Gamma_t$ are made of arcs of hyperbolas: this follows from Theorem 11.1.

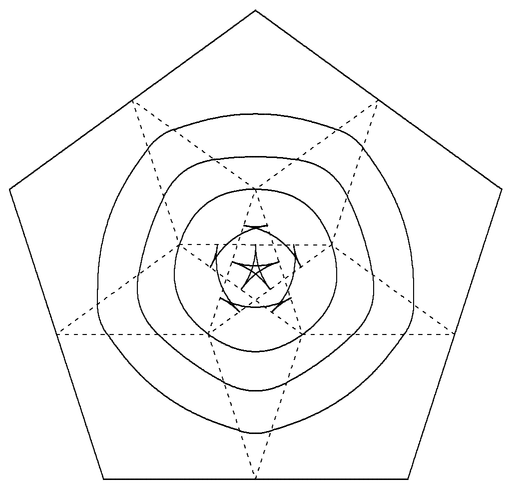

FIGURE 11.13. The envelopes $\Gamma_t$ for a regular pentagon

The latter holds for every convex polygon: the envelopes $\Gamma_t$ are piece-wise smooth curves, made of arcs of hyperbolas. Notice that at the conjunction points between different hyperbolas, the two hyperbolas have the same tangent line. The directions of the two hyperbolas may be either opposite (in which case the conjunction point looks like a cusp) or the same (in which case the curve looks smooth, although the two hyperbolas have, in general, different curvatures).

Let us call a vertex $A$ of a convex polygon *opposite* to a side $a$ if the line through $A$, parallel to $a$, lies outside of the polygon. Every side is opposite to a unique vertex (we assume that the polygon has no parallel sides), but a vertex may be opposite to a number of sides, or to none, for that matter.

Similarly to triangles, a pair of points $A, B$ with parallel tangents is a vertex $A$ of the polygon and points $B$ of the opposite side; the locus of midpoints of such segments $AB$ is a segment, parallel to the side at half the distance to $A$. The union of these segments is a (possibly, self-intersecting) polygon $\Delta$, and this is the locus of cusps of all the envelopes $\Gamma_t$. The vertices of the polygon $\Delta$ are points of maximal degeneracy. See Figure 11.13 for the case of a regular pentagon. The curve $\Delta$ in this case is a star-like selfintersecting pentagon; it is shown in Figure 11.13 dashed. The loci of other conjunctions of hyperbolas making the curves $\Gamma_t$ are also shown dashed. A magnified version of the central part of Figure 11.13 is shown on Figure 11.14.

Let us finish with a comment on the curious difference between odd- and even-gons. For an $n$-gon with odd $n$ and close to a regular one, the envelope $\Gamma_{1/2}$ of lines that bisect the area has $n$ cusps and resembles a regular $n$-pronged star. A regular $n$-gon with $n$ even is centrally symmetric, and the curve $\Gamma_{1/2}$ degenerates

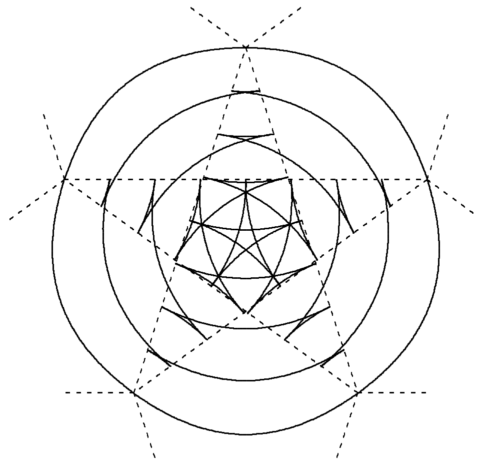

FIGURE 11.14. The central part of Figure 11.13

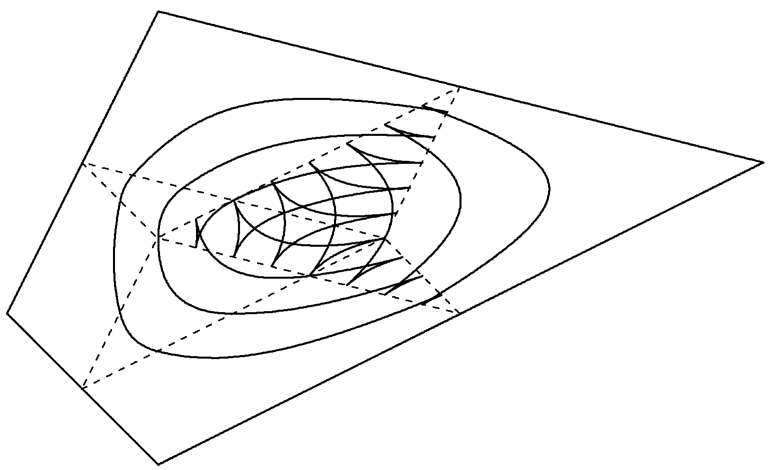

FIGURE 11.15. The envelopes $\Gamma_t$ for a quadrilateral

to a point, the center of the polygon. After a small perturbation, one obtains an "honest" curve $\Gamma_{1/2}$ with fewer than $n$ cusps (the number of cusps is odd by Theorem 11.5). For example, for a quadrilateral, this curve is a "triangle" made of three arcs of hyperbolas, making cusps at the vertices (see Figure 11.15 for the family of curves $\Gamma_t$ in the case of a generic quadrilateral).

**11.9 Exercises.**

11.1. Given an oval, show that there exists a line that bisects its area and its perimeter length.

11.2. Consider two nested convex bodies with smooth boundaries (ovaloids) in space. Prove that there exist at least two planes, tangent to the inner body and such that the tangency point is the center of mass of the intersection of the plane with the outer body.

*Hint*. Consider the plane that cuts off the maximal volume.

11.3. Given an oval $\gamma$, prove that there exists at least 3 pairs of points on $\gamma$ at which the tangent lines are parallel and the curvatures are equal.

*Hint*: Show that the number of such pairs is odd. Show that, in terms of the support function $p(\alpha)$, we are interested in those $\alpha$ for which

$$p(\alpha) + p''(\alpha) - p(\alpha + \pi) - p''(\alpha + \pi) = 0.$$

Then argue as in Section 10.3.

11.4. The *center symmetry set* of an oval is the envelope of the family of chords connecting pairs of points where the tangents to the oval are parallel, see [**34**].

(a) Prove that the center symmetry set of a generic oval has no inflections or double tangents but has an odd number of, and not fewer than three, cusps.

(b) Consider a chord $A_1A_2$ connecting two points of an oval with parallel tangents. Let $k_1$ and $k_2$ be the curvatures of the oval at points $A_1$ and $A_2$. Prove that $A_1A_2$ is divided by the tangency point with the center symmetry set in the ratio $k_2 : k_1$.

(c) Show that the cusps of the center symmetry set correspond to the case when $k_1 = k_2$.

(d) If an oval has constant width then the center symmetry set coincides with its evolute.

11.5. Prove that, for a quadrilateral which is not a parallelogram, all the curves $\Gamma_t$ have cusps.

11.6. (a) How many lines can there pass through a given point that bisect the area of a given triangle?

(b) Same question for a quadrilateral without parallel sides.

11.7. Let $P$ be a convex $n$-gon without parallel sides. Prove that if $n$ is even then the correspondence *side* $\mapsto$ *opposite vertex* is not one-to-one.

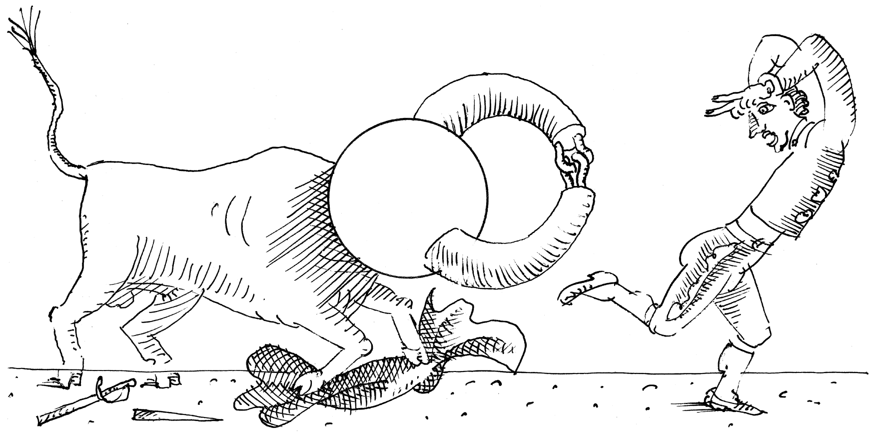

LECTURE 12

# On Plane Curves

**12.1 Double points, double tangents and inflections.** The topic of this lecture is smooth plane curves, like the one in Figure 12.1. Points of self-intersection are called *double points*; the curve in Figure 12.1 has three.

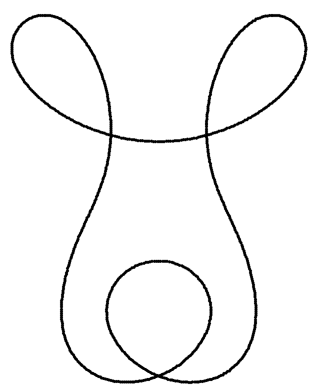

FIGURE 12.1. A plane curve

A *double tangent* is a line that touches the curve at two differrent points. We distinguish between *outer* and *inner* double tangents: for the former, the two small pieces of the curve lie on one side of the tangent line, and for the latter – on opposite sides, see Figure 12.2. It may be not immediately clear, but the curve in Figure 12.1 has 8 outer and 4 inner double tangents.

We shall be also interested in *inflection points*. Give a curve an orientation. When moving along the curve, one is turning either left or right. The inflection points are the points where the direction of this rotation changes to the opposite. The "left" and "right" segments of the curve alternate, hence the total number of inflection points of a closed curve is even. The curve in Figure 12.1 has two inflections.

FIGURE 12.2. Two kinds of double tangent lines

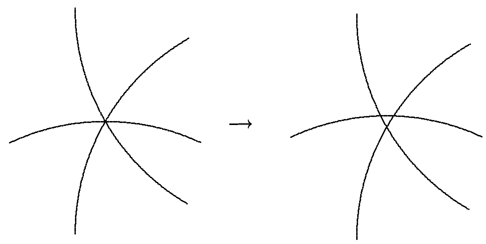

FIGURE 12.3. Eliminating a triple point by a small perturbation

We are interested in typical properties of curves which are not destroyable by small perturbations. For example, a curve may pass though the same point thrice, but this event is not typical: a small perturbation replaces the triple point by three double points, see Figure 12.3. Likewise, a double tangent may touch the curve a third time, but this is not typical either, see Figure 12.4.

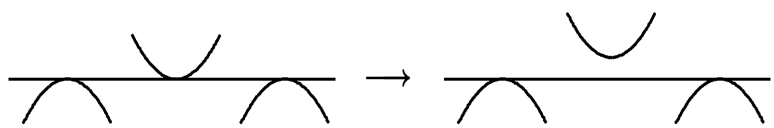

FIGURE 12.4. Eliminating a triple tangent line by a small perturbation

There are many other non-typical events that we exclude, such as a double tangent line passing through a double point, or a self-tangency of the curve, etc. We always assume our curves to be generic.

**12.2 Drawing doodles: the Fabricius-Bjerre formula.** Let $T_+$ and $T_-$ be the number of outer and inner double tangents of a smooth closed curve, $I$ its (even) number of inflections and $D$ the number of double points. These numbers are not independent: there is a universal relation between them described in the following theorem.

THEOREM 12.1. *For every generic smooth closed curve, one has:*

$$T_+ - T_- - \frac{1}{2}I = D. \tag{12.1}$$

For example, for the curve in Figure 12.5, $T_+ = 5, T_- = 2, I = 2, D = 2$.

Formula (12.1) was found by the Danish mathematician Fabricius-Bjerre in 1962 [**28**]. Drawing doodles is a natural human activity, enjoyed by millions of children around the world, and this beautiful result could easily have been discovered much earlier!

**Proof**. Orient the curve and consider its positive tangent half-line at point $x$. The number of intersection points $N$ of this half-line with the curve depends on the

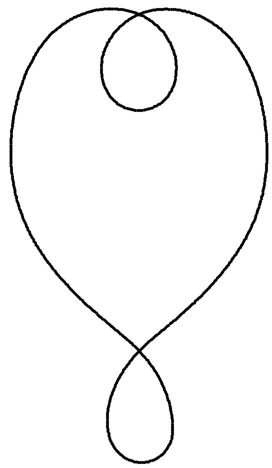

FIGURE 12.5. An example of the Fabricius-Bjerre formula: $T_+ = 5, T_- = 2, I = 2, D = 2$

point. As $x$ traverses the curve, this number changes, and when $x$ returns to the initial position, this number $N$ assumes the original value.

When does $N$ change? When $x$ passes a double point, $N$ decreases by 1. Since each double point is visited twice, the total contribution of double point to the increment of $N$ is $-2D$. When $x$ passes an inflection point, $N$ also decreases by 1, hence the total contribution of inflections is $-I$, see Figure 12.6.

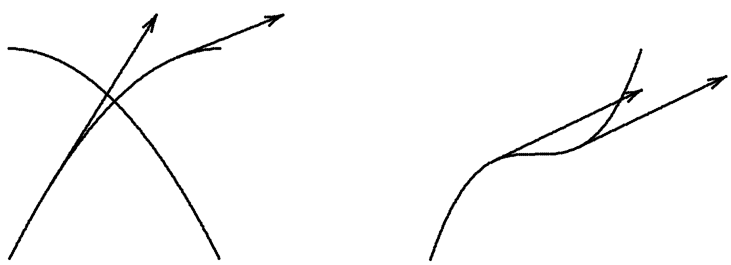

FIGURE 12.6. Two cases when $N$ changes

A double tangent contributes $\pm 2$, depending on whether it is outer or inner. More precisely, there are 6 cases, depending on the orientations, shown in Figure 12.7. Their total contributions to $N$ is $2T'_+ + 4T''_+ - 2T'_- - 4T''_-$.

Thus

$$2T'_+ + 4T''_+ - 2T'_- - 4T''_- - 2D - I = 0. \tag{12.2}$$

Now change the orientation of the curve. The numbers $T''_\pm$ and $T'''_\pm$ will interchange and the other number involved in formula (12.2) will remain the same. Therefore

$$2T'_+ + 4T'''_+ - 2T'_- - 4T'''_- - 2D - I = 0. \tag{12.3}$$

It remains to add (12.2) and (12.3) and to divide by 4:

$$T'_+ + T''_+ + T'''_+ - T'_- - T''_- - T'''_- - D - \frac{1}{2}I = 0,$$

which is the same as (12.1). □

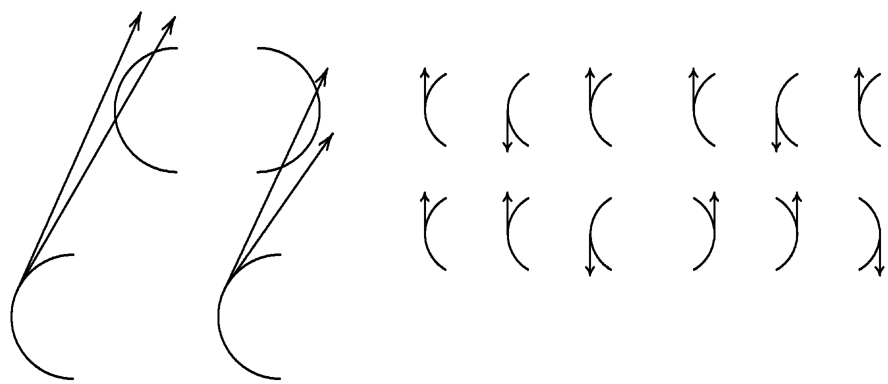

FIGURE 12.7. Bookkeeping of double tangent lines

Relation (12.1) is a necessary condition on $T_{\pm}, I, D$ to be the numbers of outer and inner tangents, inflections and double points of a closed plane curve. Is it also sufficient? See Exercise 12.5 for a partial answer.

A generalization of the Fabricius-Bjerre formula (12.1), due to Weiner [**89**], concerns smooth closed curves on the sphere. Of course, in this case, "lines" are understood as great circles. There is one more ingredient that goes into the formula, the number $A$ of pairs of antipodal points of the curve. Weiner's formula states:

$$T_{+} - T_{-} - \frac{1}{2}I = D - A. \tag{12.4}$$

If the curve lies in a hemisphere, it has no antipodal points. One may centrally project the hemisphere, along with the curve, to the plane, and then (12.4) will coincide with (12.1).

REMARK 12.1. To the reader familiar with algebraic geometry, formula (12.1) resembles the *Plucker formulas*. These formulas concern algebraic curves in the projective plane; everything is considered with complex coefficients. As before, let $T, D, I$ and $C$ denote the number of double tangents, double points, inflections and cusps of the curve (no signs are involved when working with complex numbers).

Two other numbers contribute to the Plucker formulas: the number of intersections of the curve with a general line, $N$ (the degree of the curve) and the number of tangent lines to the curve from a generic point, $N^*$ (the class of the curve). The number $N$ is the degree of the polynomial equation that defines the curve, and $N^*$ is the degree of the polynomial equation that defines the projectively dual curve. For example, for an ellipse, $N = N^* = 2$.

The Plucker formulas are:

$$N^* = N(N-1) - 2D - 3C, \quad N = N^*(N^*-1) - 2T - 3I,$$

and

$$3N(N-2) = I + 6D + 8C, \quad 3N^*(N^*-2) = C + 6T + 8I.$$

The formulas in each pair are interchanged by the projective duality, described in Lecture 8.

For example, for a smooth curve of degree $N = 4$, one has $C = D = 0$, and therefore $N^* = 12, I = 24$ and $T = 28$; this will be of critical importance in Lecture 17.

Note the difference between algebraic curves and smooth curves, the "doodles" of this lecture: the former are "rigid" objects, depending on a finite number of parameters, the coefficients of their polynomial equations, whereas the latter are extremely "soft" and can be deformed with much greater freedom. One manifestation off this flexibility will be discussed in Section 12.4.

**12.3 Doodles with cusps: Ferrand's formula.** Another, quite recent, formula for curves with cusps is due to E. Ferrand [**29**]. Consider a plane curve with an even number of cusps and color the smooth arcs between the cusps alternatively red and blue. We assign signs to double points: a double point is positive if it is the intersection of two arcs of the same color, and it is negative if it is the intersection of two arcs of the opposite colors. Denote by $D_{\pm}$ the number of positive and negative double points.

We also redefine the signs of double tangents. There are three attributes to a double tangent: whether the orientations of the two arcs are the same or opposite; whether the arcs lie on the same or opposite sides of the tangent line; and whether the two arcs are of the same or opposite colors. The sign of a double tangent is shown in Figure 12.8.

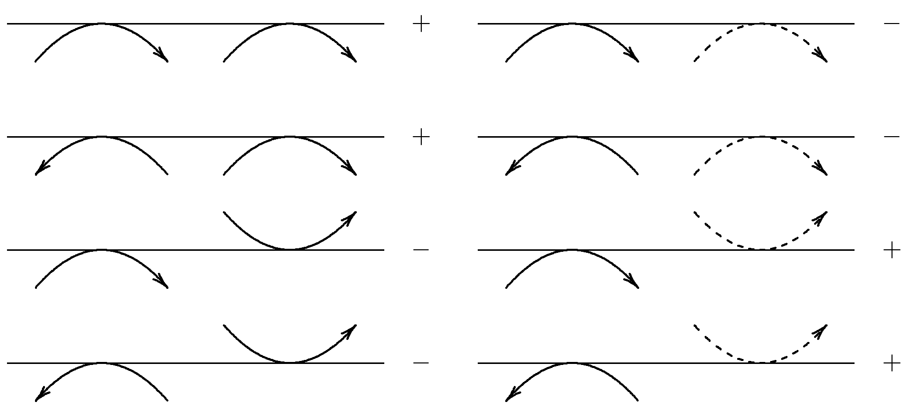


FIGURE 12.8. The signs of double tangents

Let $T_{\pm}$ be the number of positive and negative double tangent lines. With this preparation, Ferrand's generalization of Fabricius-Bjerre formula to curves with cusps is as follows.

THEOREM 12.2. *For every generic plane curve with cusps, one has:*

$$T_+ - T_- - \frac{1}{2}I = D_+ - D_- - \frac{1}{2}C. \tag{12.5}$$

We shall not prove Ferrand's theorem: we do not know a proof as simple as the one given to the Fabricius-Bjerre theorem (but the reader is welcome to try to find such a proof, see Exercise 12.8). Formula (12.5) is illustrated in Figure 12.9; the first curve has

$$T_+ = 4,\ T_- = 3,\ I = 6,\ D_+ = 0,\ D_- = 1,\ C = 2,$$

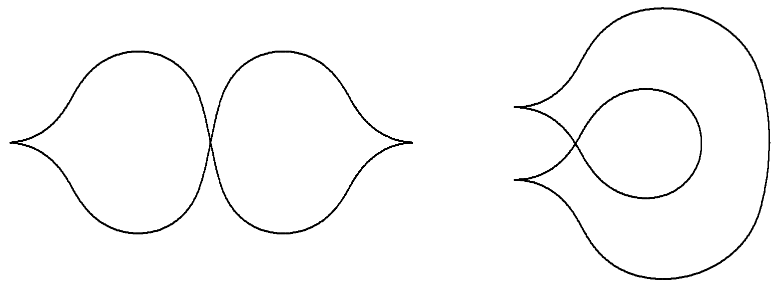

FIGURE 12.9. An illustration of Ferrand's formula

and the second

$$T_+ = 2,\ T_- = 0,\ I = 4,\ D_+ = 1,\ D_- = 0,\ C = 2.$$

REMARK 12.2. Projective duality interchanges the numbers involved in the Fabricius-Bjerre and Ferrand formulas: the numbers of double tangents and of inflections of a curve equals the numbers of double points and of cusps of the dual curve – see Figures 8.7 and 8.8.

**12.4 Winding number and Whitney's theorem.** The *winding number* of a closed smooth curve is the total number of turns made by the tangent vector as one traverses the curve. If the curve is oriented, the winding number has a sign, otherwise it is a non-negative integer. For example, the winding numbers of the curves in Figure 12.10 are equal to 1 and 3, respectively.

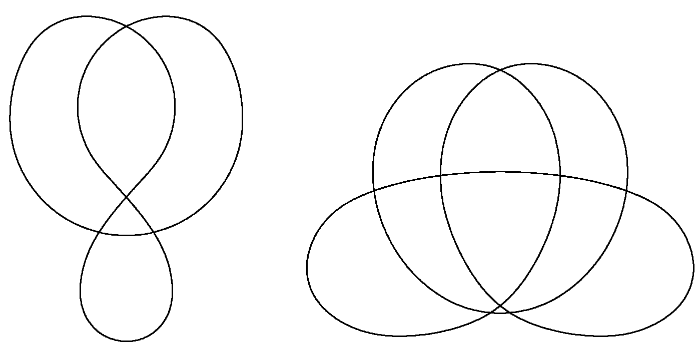

FIGURE 12.10. Winding numbers 1 and 3

Let us continuously deform a smooth curve. We do not exclude self-tangency or multiple self-intersections, as in Figure 12.11. In such a deformation,[1] the winding number remains the same. Indeed, a small perturbation of a curve leads to a small change in the winding number; being an integer, it must remain constant.

The converse statement is Whitney's theorem.

THEOREM 12.3. *If two closed smooth curves have the same winding numbers then one can be continuously deformed to the other.*

For example, the left curve in Figure 12.10 can be deformed to a circle, as the reader has probably already noticed.

[1]The technical term for such deformation is *regular homotopy.*

FIGURE 12.11. A continuous deformation of a smooth curve

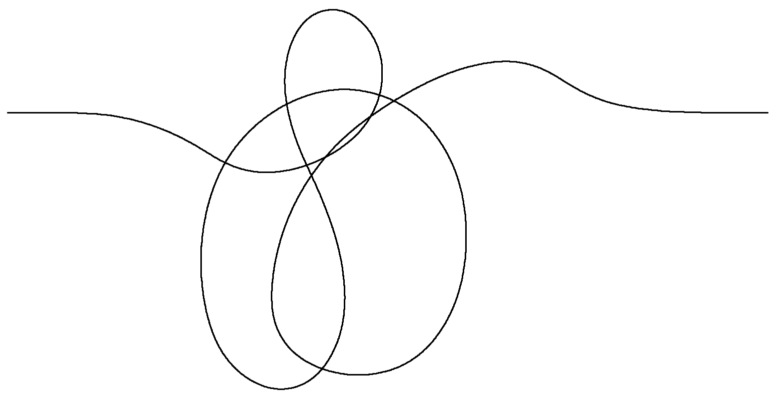

FIGURE 12.12. A long curve

We shall prove Whitney's theorem for another class of curves, the *long curves.* A long curve is a smooth plane curve that, outside some disc, coincides with the horizontal axis, see Figure 12.12. Long curves are a little easier to work with, whence our choice.

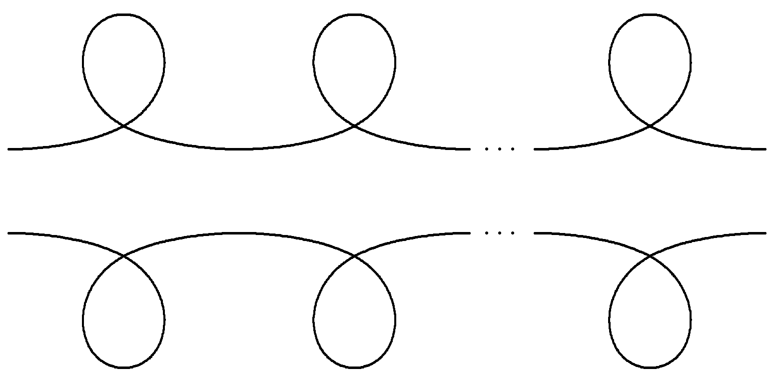

FIGURE 12.13. Model long curves

Proof of Whitney's theorem for long curves. Long curves are oriented from left to right. A model long curve with winding number $n$ is the horizontal line with $|n|$ consecutive kinks, clock- or counter clock-wise, depending on the sign of $n$, see Figure 12.13. We want to prove that a long curve with winding number $n$ can be deformed to one of these model curves.

Figure 12.14 features a deformation that adds (or cancels) a pair of kinks with opposite orientations. Using this trick, one can always add $|n|$ such pairs to a given curve so that one obtains a curve with winding number zero, followed by $n$ kinks. Therefore, it suffices to prove that a long curve $\gamma$ with zero winding number can be deformed to the horizontal axis.

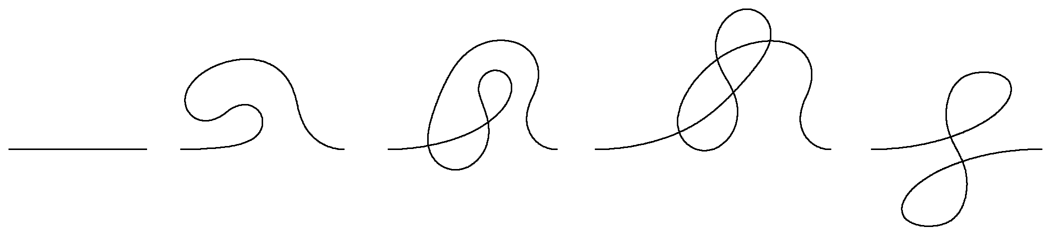

FIGURE 12.14. Adding or canceling a pair of opposite kinks

Let $\gamma(t)$ be a parameterization of our curve. Consider the angle $\alpha(t)$ made by the positive tangent vector to $\gamma(t)$ with the horizontal direction. The graph of the function $\alpha(t)$ may look like Figure 12.15.

In fact, the angle $\alpha(t)$ is defined only up to addition of a multiple of $2\pi$. We choose $\alpha(t) = 0$ on the left horizontal part of the curve and extend it continuously to an "honest" function of $t$. Since the winding number is zero, $\alpha(t) = 0$ on the right horizontal part of the curve as well.

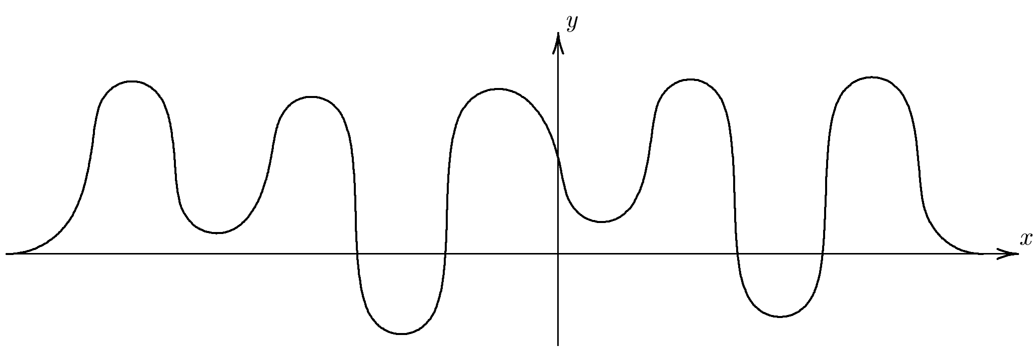


FIGURE 12.15. A graph of the function $\alpha(t)$

Let us squeeze this graph toward the horizontal axis: $\alpha_s(t) = s\alpha(t)$ where $s$ varies from 1 to 0. For every value of $s$, one has a unique curve $\gamma_s$ whose direction at point $\gamma_s(t)$ is $\alpha_s(t)$. In particular, $\alpha_0(t) = 0$, hence $\gamma_0$ is the horizontal axis.

What do the curves $\gamma_s$ look like? They start as the horizontal axis and end as horizontal lines, since $\alpha(t) = 0$ for sufficiently large $|t|$. The only problem is that the right end of $\gamma_s$ may be on a different height, see Figure 12.16. This problem is addressed by smoothly adjusting the curve on its horizontal right part, see the same figure, and one obtains a long curve $\gamma_s$.

To wit: we have constructed a continuous family of long curves, from $\gamma = \gamma_1$ to $\gamma_0$, the horizontal axis. This is a desired deformation. $\Box$

Let us mention a version of Whitney's theorem for curves on the sphere. The result is even simpler than in the plane. A generic smooth closed spherical curve

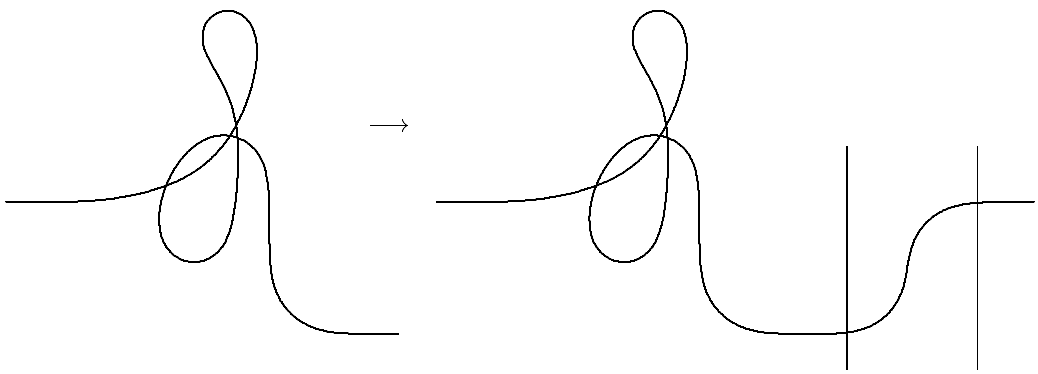

FIGURE 12.16. Adjusting the height of the right end

has a single invariant that assumes values 0 or 1: this is the parity of the number of double points.

THEOREM 12.4. *Two generic smooth spherical curves can be continuously deformed to each other if and only if their numbers of double points are either both even or both odd.*

Sketch of Proof. That the parity of the number of double points does not change under a generic deformation is clear from Figure 12.11.

Let us show that two curves with the same parity of the number of double points can be deformed to each other. The sphere becomes the plane after deletion of a point. One obtains a plane curve that, by the Whitney theorem, can be deformed to (the closure of) a model curve in Figure 12.13. For these curves, the number of double points is one less than the winding number. It remains to show that, on the sphere, the model curves with winding numbers that differ by 2 can be deformed to each other. Such a deformation (for the winding numbers 0 and 2) is shown in Figure 12.17. □

REMARK 12.3. Whitney's theorem has far reaching generalizations in which the circle and the plane are replaced by arbitrary smooth manifolds. This area is known as the Smale-Hirsch theory. One of the most striking results of this theory is the sphere eversion, a deformation of the sphere in 3-dimensional space in the class of smooth, but possibly self-intersecting, surfaces that ends with the same sphere, turned inside out. A number of explicit constructions of such sphere eversions are known; one, due to W. Thurston, is shown in the movie "Outside in" [**94**] which we recommend to the reader.[2]

**12.5 Combinatorial formulas for the winding number.** To find the winding number of a closed or long curve, one may just traverse the curve and count the total number of turns made. However, there are better ways of counting spins without getting dizzy, and we shall discuss a few in this section.

The first formula is shown in Figure 12.18. This formula is, more-or-less, obvious. To count the number of total turns, it suffices to count how many times the

[2]A more recent movie, "The Optiverse", features a different sphere eversion based on minimizing an elastic bending energy for surfaces in space.

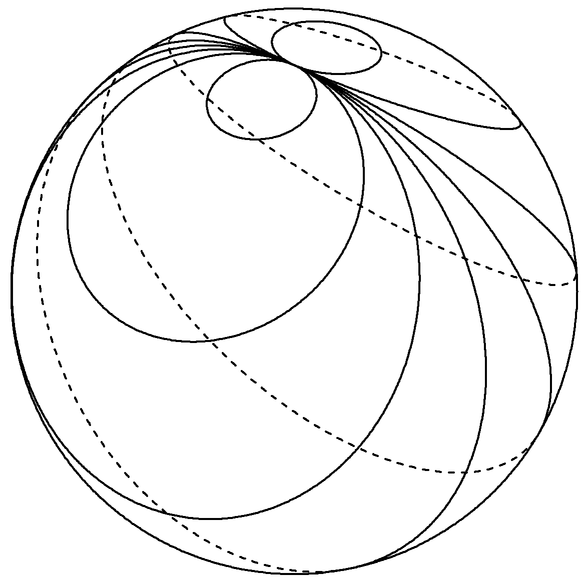

FIGURE 12.17. A deformation of a spherical curve

tangent line to the curve is horizontal. There are four possibilities shown in Figure 12.18. The first two contribute to rotation in the positive, counter clock-wise direction, and the second two, to rotation in the negative direction. This proves the formula.


FIGURE 12.18. A formula for the winding number

Another formula for the winding number was given by Whitney in the same paper where he proved the theorem discussed in the preceding section. Let us first describe this formula for long curves. Traverse a curve from left to right. Each double point is visited twice and looks as shown in Figure 12.19. Call the first a positive and the second a negative double point. Let $D_\pm$ be the number of positive and negative double points of the curve. The formula for the winding number is:

$$w = D_+ - D_-. \tag{12.6}$$

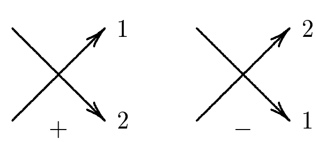


FIGURE 12.19. The signs of double points

**Proof of formula 12.6**. If the curve is a model one, as in Figure 12.13, the result clearly holds. Since every curve can be deformed to a model one, we shall be done if we show that $D_+ - D_-$ does not change under deformations.

During a generic deformation, one may encounter two "singular" events depicted in Figure 12.11. The first introduces (or eliminates) a pair of double points of the opposite signs, and hence does not affect $D_+ - D_-$, while the second does not change the number or the signs of the double points involved. This proves (12.6). □

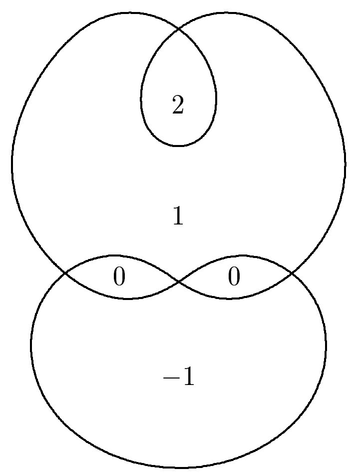


FIGURE 12.20. Rotation numbers

For a closed oriented curve $\gamma$, formula (12.6) is modified as follows. First of all, to assign signs to double points, one chooses a starting point $x$ on $\gamma$.

Let $y$ be a point not on the curve $\gamma$. Denote by $r(y)$ the rotation number of the curve about $y$, that is, the number of times $\gamma$ goes about $y$ (cf. Section 6.4). In other words, $r(y)$ is the number of complete turns made by the position vector $yx$ as the point $x$ traverses the curve. See for example Figure 12.20, where the rotation numbers are assigned to the components of the complement of the curve.

When the point $y$ crosses the curve, $r(y)$ changes by 1, as in Figure 12.21. If $y$ is a point on the curve (but not a double point), the rotation number $r(y)$ is defined as the half-integer, equal to the average of the two values obtained by pushing $y$ slightly on both sides of the curve.

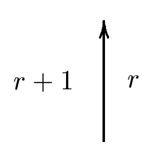


FIGURE 12.21. How the rotation number changes upon crossing the curve

The formula for the winding number of a closed curve is:

$$w = D_+ - D_- + 2r(x). \tag{12.7}$$

Still another way to find the winding number $w$ of an oriented curve is to resolve each double point as shown in Figure 12.22. After this is done everywhere, our curve decomposes into a collection of simple curves, some oriented clock-wise and some counter clock-wise. Let $I_-$ and $I_+$ be the numbers of these simple curves.

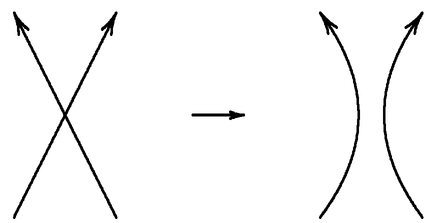

FIGURE 12.22. The resolution of a double point

THEOREM 12.5. *One has: $w = I_+ - I_-$, see Figure 12.23.*

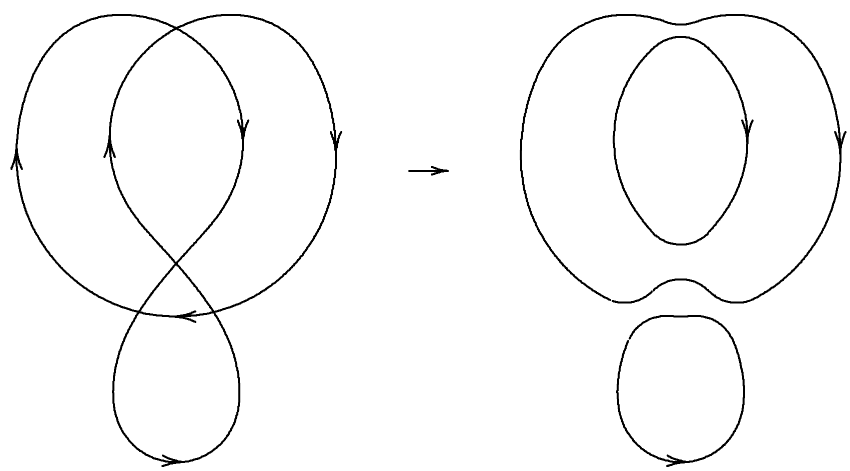

FIGURE 12.23. Computation of the winding number by resolving a curve

Proof. Traverse a curve $\gamma$, starting at a double point, say, $x$. Upon the first return to $x$, one traverses a closed curve (with corner) $\gamma_1$; let $\alpha_1$ be the total turn of its tangent vector. Likewise, continuing along $\gamma$ until the second return at $x$, one traverses another closed curve, $\gamma_2$; let $\alpha_2$ be the total turn of its tangent vector. Clearly the total turn of the tangent vector of $\gamma$ is $\alpha_1 + \alpha_2$. Resolving the double point $x$, as in Figure 12.22, we make both curves smooth, adding the same amount (say, $\pi/2$) to $\alpha_1$ and subtracting from $\alpha_2$. Thus the winding number of $\gamma$ is the sum of the winding numbers of the rounded curves $\gamma_1$ and $\gamma_2$. Applying this argument to every double point yields the result. □

REMARK 12.4. The subject of this lecture is closely related with knot theory (see [**1, 72**] for expositions). The Fabricius-Bjerre (12.1) and Ferrand (12.5) formulas have natural interpretations as self-linking numbers, and this stimulated recent interest in them. The combinatorial formulas for the winding number in Section 12.5 resemble some formulas for finite order knot invariants in contemporary knot theory.

| | | |
|---|---|---|
| John Smith<br>January 23, 2010 | Martyn Green<br>August 2, 1936 | Henry Williams<br>June 6, 1944 |
| John Smith<br>January 23, 2010 | Martyn Green<br>August 2, 1936 | Henry Williams<br>June 6, 1944 |
| John Smith<br>January 23, 2010 | Martyn Green<br>August 2, 1936 | Henry Williams<br>June 6, 1944 |

### 12.6 Exercises.

12.1. Prove that the complement to a closed plane curve has a chess-board coloring (so that the adjacent domains have different colors).

12.2. Prove that the number of intersection points of two closed curves is even.

12.3. Consider two plane curves (as usual, in general position). Let $t_+$ and $t_-$ be the number of their outer and inner common tangent lines and $d$ the number of their intersection points (thus we are not concerned with double tangents or double points of either curve). Show that $t_+ = t_- + d$.

12.4. Draw curves with
(a) $T_+ = 2, T_- = 0, I = 2, D = 1$;
(b) $T_+ = 3, T_- = 0, I = 2, D = 2$;
(c) $T_+ = 4, T_- = 2, I = 0, D = 2$.

12.5. * (a) If $I$ is a positive even number and $T_+ - T_- - I/2 = D$ then there exists a curve with the respective number of double tangents, inflections and double points.

(b) If $I = 0$, prove that $T_-$ is even and $T_- \leq (2D+1)(D-1)$.

(c) If $T_-$ is even and $T_- \leq D(D-1)$ then there exists a curve without inflections and with the respective number of double tangents and double points.

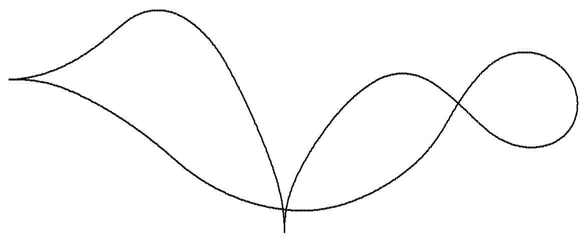

FIGURE 12.24. A curve with cusps

12.6. Consider a curve with cusps, such as in Figure 12.24, and extend the notion of double tangents to include the lines that touch the curve in cusps, see Figure 12.25. Let $C$ be the number of cusps. Prove that

$$T_+ - T_- - \frac{1}{2}I = D + C.$$

*Hint.* Round up cusps, trading each for two inflections, see Figure 12.26.

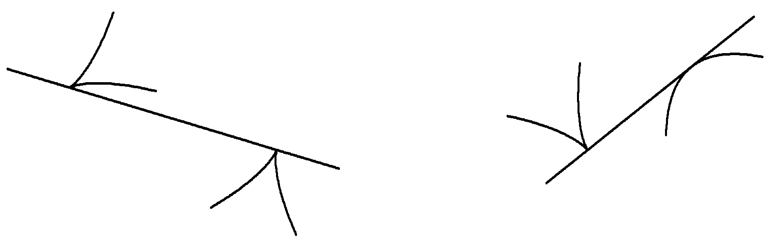

FIGURE 12.25. Generalized double tangent lines

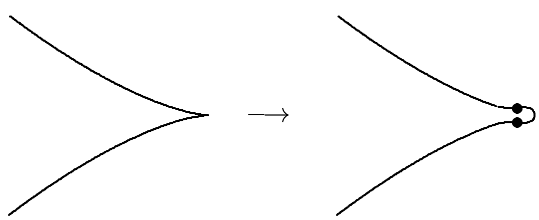

FIGURE 12.26. Rounding up a cusp

12.7. * Prove the Weiner formula (12.4).

12.8. * Prove the Ferrand formula (12.5).

12.9. Prove formula (12.7).
*Hint.* Check that the right hand side of (12.7) does not depend on the choice of $x$, see Figure 12.27.

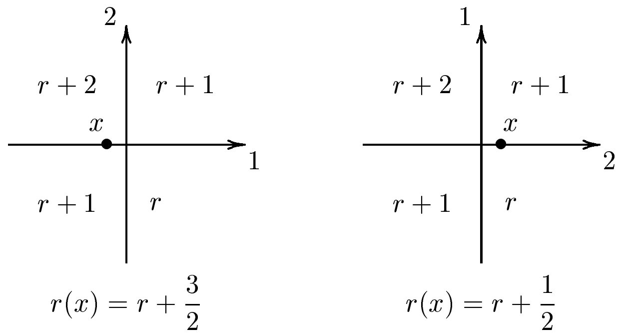


FIGURE 12.27. The effect of changing the base point

12.10. Prove that the rotation number $r(y)$ of the curve about a point $y$ can be computed as follows: resolving all double points as in Figure 12.22, $y$ gets surrounded by a number of clock-wise and counter clock-wise oriented curves. Then $r(y)$ is the number of the latter minus the number of the former.

12.11. Show that the winding number of a closed curve is at most one greater than the number of its double points and has the parity, opposite to it.

12.12. Assume that a closed curve has $n$ double points, labeled 1 through $n$. Traverse the curve and write down the labels of the double points in the order they are encountered. One obtains a cyclic sequence in which each number $1, \dots, n$ appears twice. Prove that, for any $i$, between two occurrences of symbol $i$, there is an even number of symbols in this sequence (theorem of Gauss).

*Hint.* Resolve the $i$-th double point, as in Figure 12.22, and use the fact that the resulting two curves intersect an even number of times.

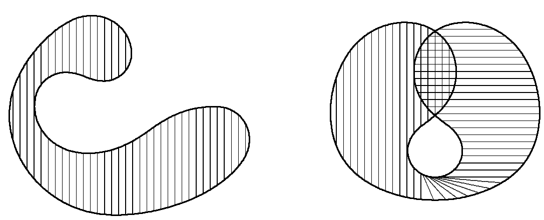

FIGURE 12.28. Embedded and immersed discs

12.13. The left Figure 12.28 shows a disc embedded in the plane, whereas the right one is an *immersed* disc which overlaps itself. Such an immersion is a smooth map of a disc in the plane that is locally an embedding. The boundary of an embedded disc is a simple closed curve; the boundary of an immersed disc may be much more complex.

(a) Does the curve in Figure 12.29 bound an immersed disc?
(b) Prove that the boundary of an immersed disc has winding number 1.
(c) Show that the curve in Figure 12.30 bounds two different immersed discs.

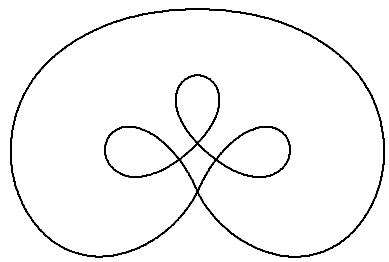

FIGURE 12.29. Does this curve bound an immersed disc?

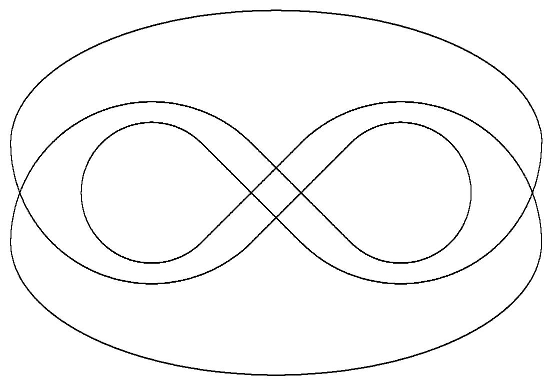

FIGURE 12.30. This curve bounds two different immersed discs

# *Chapter* 4

# DEVELOPABLE SURFACES

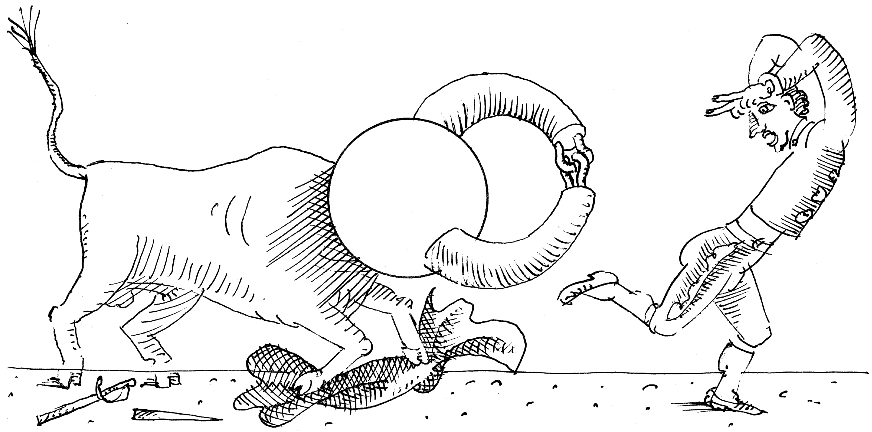

LECTURE 13

# Paper Sheet Geometry

**13.1 Developable surfaces: surfaces made of a sheet of paper.** Take a sheet of paper and bend it without folding. You will have in your hands a piece of surface whose shape will depend on how you bend. Samples of surfaces which you can get are shown on Figure 13.1.

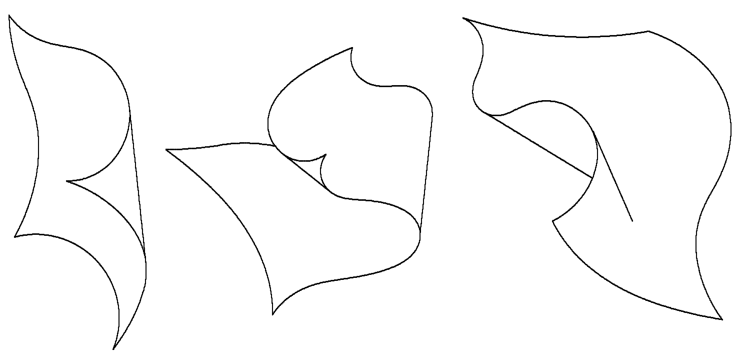

FIGURE 13.1. Paper sheet surfaces

However, not every surface can be obtained by bending a sheet of paper. Everybody knows, for example, that it is impossible to make even a small piece of a sphere out of a sheet of paper: if you press a piece of paper to a globe, some folds will appear on your sheet. It is possible to make a cylinder or a cone, but you cannot bend a sheet of paper like a handkerchief without making fold lines (Figure 13.2).

In geometry, surfaces which can be made out of a sheet of paper, in the way described above are called *developable*. We shall not even try to make this definition more rigorous, but still we shall specify the two physical properties of paper which are essential for our geometric purposes: paper is not compressible or stretchable

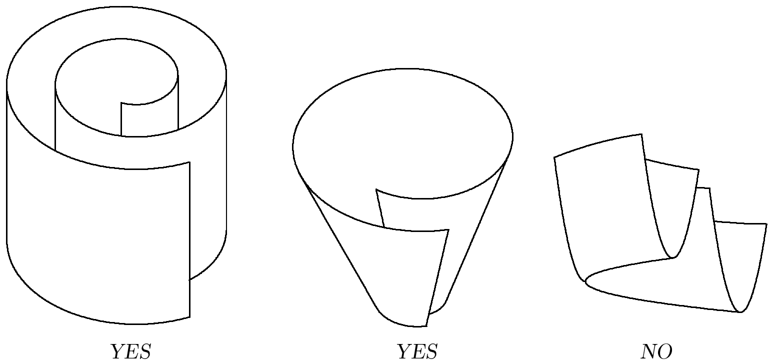


Figure 13.2. Cylinder and cone, but not a handkerchief

and is absolutely elastic. The first means that, after bending, all curves drawn on the paper retain their lengths. The second means that there are no other restrictions on bending paper. "Without folding" means that the surface remains smooth, which means, in turn, that the surface has a tangent plane at every point.

We shall see that not all surfaces are developable from the simplest property of developable surfaces (this property, as well as all other major results of the theory of developable surfaces, was proved by Euler).

**13.2 Every developable surface is ruled.** The latter means that for every point of a developable surface there exists a straight interval which is contained in the surface and contains the point in its interior. In terms of our everyday experience, we can say, that at every point $A$ of the bent sheet of paper, we can attach a bicycle spoke to the paper in such a way that some piece of it on both sides from the point $A$ will touch the paper (Figure 13.3). We shall not prove this fact (the proofs known to us operate with formulas rather than geometric images) and shall regard it as an experimental, but firmly established, property of developable surfaces.

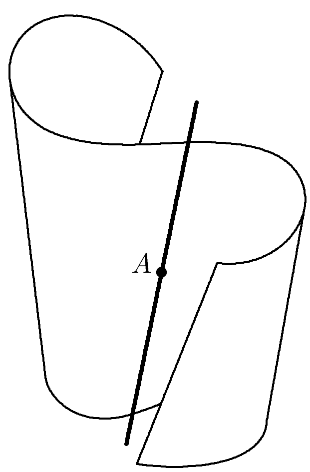


Figure 13.3. A straight ruling

If some point of a developable surfaces belongs to two different straight intervals, then some piece of the surface around this point is planar (Figure 13.4). To avoid this possibility we shall simply restrict our attention to surfaces which have no planar pieces. This assumption implies that for every point of the surface there is a unique line belonging to the surface and passing through this point.

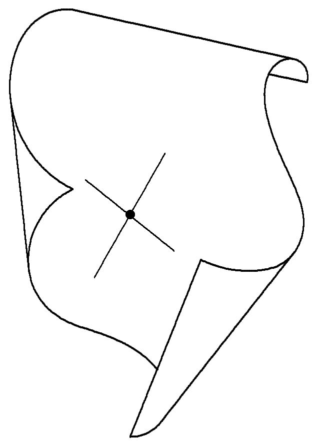

FIGURE 13.4. A planar point of a developable surface

We must add that no real life sheet of paper is infinite. So, our surfaces will have boundaries. Every point of the surface belongs to a unique straight interval which starts and ends on the boundary. These straight intervals form a continuous family which sweeps the whole surface (Figure 13.5).

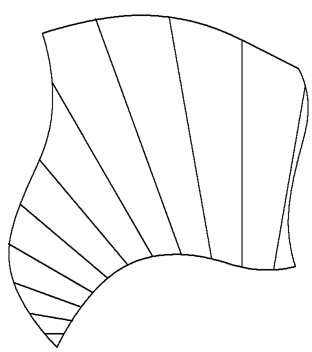

FIGURE 13.5. A family of rulings

**13.3 Not only a spoke, but also a ruler.** There are too many ruled surfaces: a moving straight line in space sweeps one. Some ruled surfaces are well known: we shall discuss, in detail, the properties of two of them in Lecture 16: a one-sheeted hyperboloid and a hyperbolic paraboloid. Now we can state that developable surfaces are much rarer than ruled surfaces; in particular, the doubly ruled surfaces of Lecture 16 are not developable (which is seen already from the properties of developable surfaces listed in Section 13.2.) We are going to formulate another experimental fact which characterizes the difference between ruled surfaces and developable surfaces.

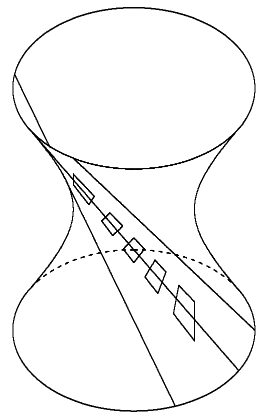

FIGURE 13.6. The tangent planes along a ruling revolve

Take an arbitrary ruled surface $S$, take a line $\ell$ on $S$, and consider the tangent plane $T_A$ to $S$ at some point $A$ of $\ell$. This plane will contain $\ell$, but the planes $T_A$ will be, in general, different for different points $A$ of $\ell$; that is, when we move point $A$ along $\ell$, the plane $T_A$ will rotate about $\ell$. For example, if $S$ is a one-sheeted hyperboloid (see Figure 13.6), then $T_A$ will contain, besides $\ell$, the line of the second family of lines (see Lecture 16), and hence these planes will be different for different points $A$; when $A$ moves along $\ell$, $T_A$ makes almost half a turn about $\ell$. Such things, however, never happen on a developable surface:

*All tangent planes tangent to a developable surface $S$ at points of a straight line on this surface coincide. In other words, one can attach to a developable surface not only a (one-dimensional) bicycle spoke, but also a (two-dimensional) ruler* (Figure 13.7).

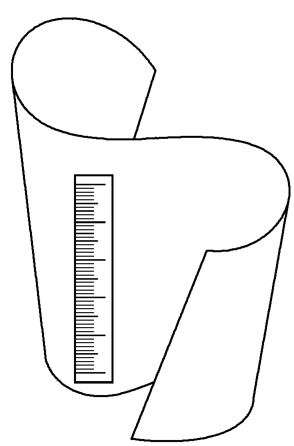

FIGURE 13.7. The tangent planes along a ruling are the same

This criterion (which we also do not prove) provides not only a necessary, but also a sufficient condition for a ruled surface to be developable.

**13.4 Let us expand the lines on a developable surface.** Look again at Figure 13.5. Since our surface $S$ is not infinite (a sheet of paper cannot be infinite!) the straight lines on $S$ are not infinite: they begin and end on the boundary of the surface. Let us expand these lines, in one of the two possible directions. What will happen?

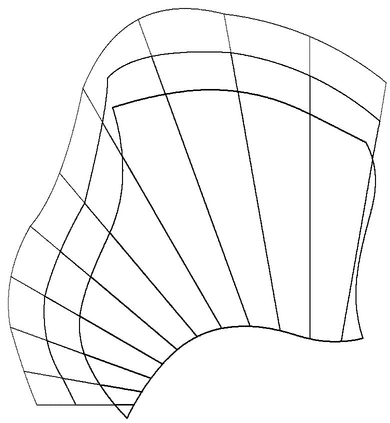

FIGURE 13.8. Expanding the rulings upwards

This question seems innocent, at the first glance. Let us expand the lines shown on Figure 13.5 upwards, in the direction where they diverge. We see that nothing extraordinary will happen: the surface will grow, eventually becoming less and less curved, more and more resembling a plane (Figure 13.8).

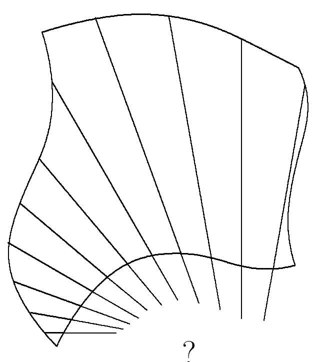


FIGURE 13.9. Expanding the rulings downwards

But what if we expand the lines in the opposite direction (Figure 13.9)? The reader can pause here and think of this question. The lines converge, but they do not, in general, come to one point, we can expect that they are pairwise skew. We can expect that they will first converge and then diverge, forming a surface resembling a hyperboloid – but the hyperboloid is not a developable surface, so this is also not likely. It is not easy to guess what will happen. And what happens is the following:

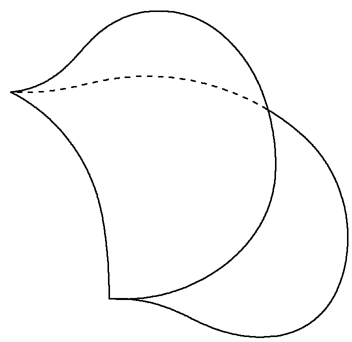

FIGURE 13.10. Cuspidal edge

*The surface will not be smooth, it will gain a cuspidal edge. This is a curve such that the section of the surface by a plane, perpendicular to this curve, looks like a semi-cubic parabola* (Figure 13.10). *Moreover, all the lines on the surface S will be tangent to this curve.*

**13.5 Why a cuspidal edge?** Let us try, if not to prove this statement, then, at least, to explain, why it should hold. Let us try to make an actual drawing of the expanded lines on our Figure 13.5 (see Figure 13.11). You can see the cuspidal edge on Figure 13.11 with your own eyes!

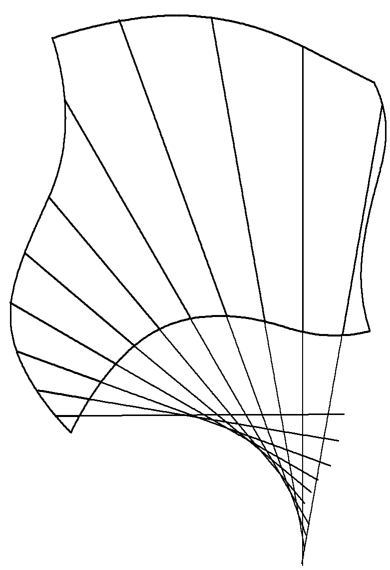

FIGURE 13.11. The envelope of the rulings

But no, this is not convincing. The drawing of a hyperboloid (Figure 13.12) looks precisely the same: there is a curve on the drawing (the side hyperbola) to which all the lines on the hyperboloid are visibly tangent.

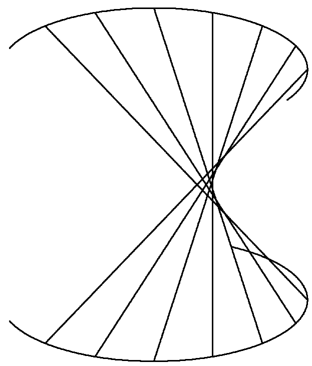

FIGURE 13.12. The tangent plane of the hyperboloid is perpendicular to the drawing

We say "visibly," since the lines which we see on the drawing are the *projections* of the lines on the surface onto a planar page of the book. No tangency occurs on the surface; it is simply that the tangent planes to the hyperboloid at the point corresponding to the points of the side hyperbola are perpendicular to our drawing and their projections are lines. But this is not possible on a developable surface – because of the rule formulated in Section 13.3. Indeed, the tangent plane to the surface at the points of our line, not belonging to the proposed cuspidal edge, are not perpendicular to the plane of the drawing. But the tangent plane is the same at all points of the line (remember our ruler rule?); hence it is not perpendicular to the drawing at the points of tangency to the edge.

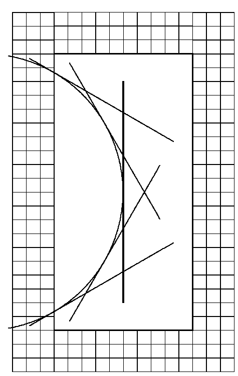

FIGURE 13.13. The tangent plane of a developable surface is not perpendicular to the drawing

Thus, the tangent plane looks like it is shown on Figure 13.13, which shows that the curve, the cuspidal edge, is indeed tangent to the straight lines on the surface.

**13.6 Backward construction: from the cuspidal edge to a developable surface.** Since our surface consists of lines tangent to the cuspidal edge, we can look at our construction from the opposite end. Let us begin with a space curve (which should be nowhere planar). Take all the tangent lines to our curve; they sweep out a surface. This surface is a developable surface, and the initial curve is its cuspidal edge. What is really surprising, is that an arbitrary nowhere planar developable surface (including the sheet of paper which you are holding in your hands) can be obtained in this way.

Well, not quite arbitrary. There are two exceptional, degenerate, cases. Your surface may be *cylindrical* which means that all the lines on it are parallel to each other; it has no cuspidal edge (one can say that its cuspidal edge *escapes to infinity*). Or it can be *conical* which means that all the lines pass through one point (one can say in this case that the cuspidal edge *collapses to a point*). But a "generic," randomly bent sheet of paper always consists of tangent lines to an invisible cuspidal edge (invisible, because it always lies not on the sheet, but on the expanded surface).

It is no less surprising that an arbitrary non-planar curve is a cuspidal edge of the surface formed by its tangent lines. For an illustration, the reader may look at the picture of the surface formed by tangent lines to the most usual helix (Figure 13.14).

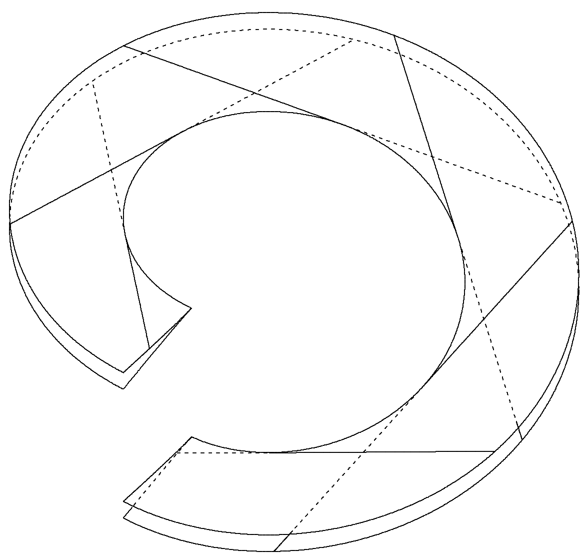

FIGURE 13.14. This surface is made of the tangent lines to a helix

A handy reader may even make a model of this surface of a helical piece of wire and a bunch of bicycle spokes. The spokes should be attached to the wire as tangents to the curve.

**13.7 Is the cuspidal edge smooth?** Is this all that one can say? Actually, no, as we shall see in a moment. Magnify, mentally, your surface to such a size that you can walk on it, and then walk across the straight lines on the surface. Since the lines are tangent to the cuspidal edge, the distance from you to the tangency point will rapidly decrease or rapidly increase, and both are possible. What happens at the moment of a transition from one mode to the other one? Figure 13.15 presents a sheet of paper with straight lines on it and two segments of the cuspidal edge. And what is between them? A smooth curve like the flash insert on this drawing?

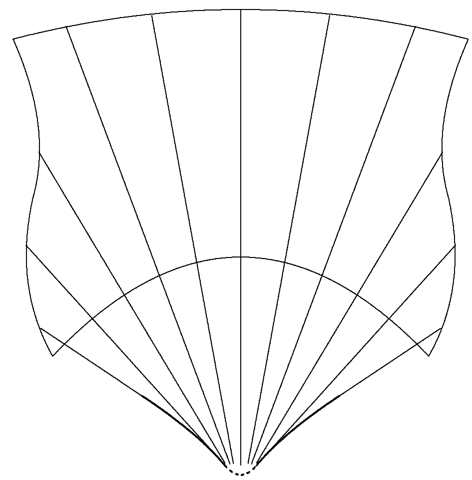


FIGURE 13.15. Is the cuspidal edge everywhere smooth?

No, this curve cannot be tangent to all straight lines. Thus, only one possibility remains:

*The cuspidal edge itself must have cusps at some points* (see Figure 13.16).

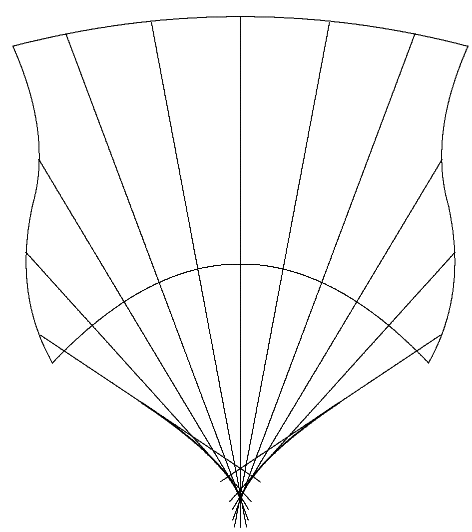

FIGURE 13.16. The cuspidal edge has a cusp

Let us try to understand what the surface looks like in the proximity of these incredible points.

**13.8 The swallow tail.** Let us begin with a picture. The surface shown on Figure 13.17 is called a *swallow tail* (we let the reader judge how much is resembles the actual tail of a swallow). Besides the cuspidal edge it also has a curve of self-intersection. The left hand side drawing shows a family of straight lines on the

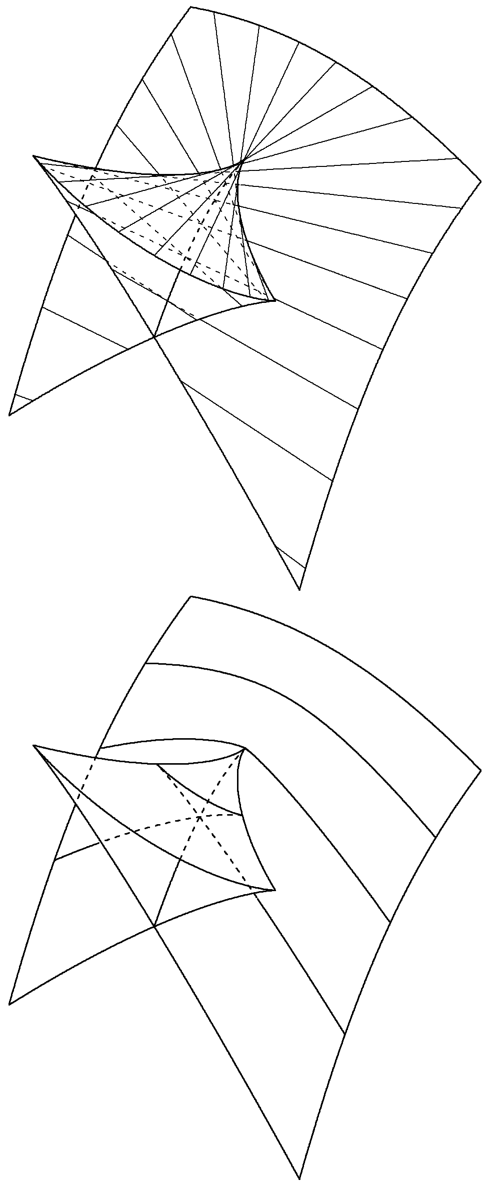

FIGURE 13.17. The swallow tail: straight rulings and plane sections

surface; the right hand side drawing (of the same surface) presents several relevant plane sections.

To convince ourselves that the surface indeed looks as shown on Figure 13.17, let us act as in Section 13.6: start with a cuspidal edge and construct a surface as the union of the tangent lines.

The "typical" space curve with a cusp can be obtained from a (planar) semicubic parabola by slightly bending its plane. This curve may be described, in a rectangular coordinate system, by parametric equations $x = at^2$, $y = bt^3$, $z = ct^4$.

Look at this curve from above (so you will see a semi-cubic parabola) and draw its tangent lines. Break every line into three parts by the tangency point and the intersection point with the line of symmetry of the semi-cubic parabola as shown on Figure 13.18.

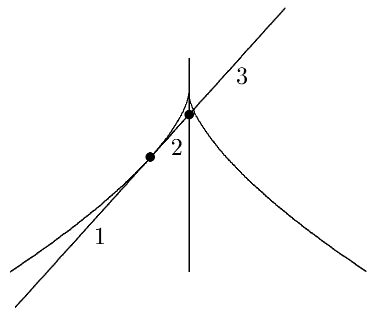


FIGURE 13.18. Tangent line to a semi-cubic parabola

Then draw separately the first, the second, and the third parts of the tangent lines (Figure 13.19, a–c); these are three parts of the swallow tail. Figure 13.19 a shows the piece of the surface between the two branches of the cuspidal edge; it is slightly concave up. Figure 13.19 b presents the two pieces of the swallow tail and the self-intersection curve, and Figure 13.19 c shows the rest of the surface. Notice that the parts of the surface presented on Figures 13.19 b and 13.19 c have edges along the self-intersection curve, and that this curve is a half of a usual planar parabola.

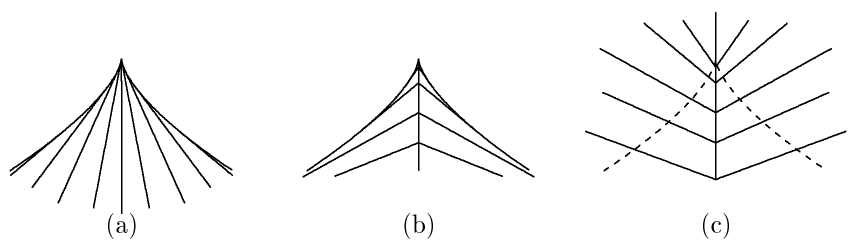


FIGURE 13.19. Three parts of the swallow tail

Thus a surface obtained by a most natural expansion of a randomly bent sheet of paper has a cuspidal edge with cusps and looks like a swallow tail in a neighborhood of the cusps of the cuspidal edge. This is the answer to an innocently looking question which we asked in the beginning of Section 13.4.

**13.9 There are swallow tails all around.** You may remember that in another part of this book (Lecture 9) we were trying to convince the reader that there are cusps all around us. This was true for planar geometry; in space, we have to admit that there are swallow tails all around. The spatial constructions similar to those of Lecture 9, including fronts of surfaces and visible contours of four-dimensional bodies, lead to surfaces with swallow tails. For instance, if you take a surface looking like an ellipsoid (for example, an ellipsoid) and then move every point along a normal line inside the ellipsoid, then, at some moment, the moving surface will acquire cuspidal edges, self-intersections and swallow tails which will pass through each other and finally disappear.

But, historically, the first picture of the swallow tail (not the name: it was given to the surface in the 1960s by René Thom) appeared in the middle of 19-th century in algebra books. We discussed this aspect of the swallow tail in Lecture 8. Recall that if we are interested in the number of (real) solutions of the equation

$$x^4 + px^2 + qx + r = 0, \tag{13.1}$$

then we need to consider a swallow tail in space with coordinates $p, q, r$ (the cuspidal edge of this swallow tail should be $p = -6t^2$, $q = 8t^3$, $r = -3t^4$).

Inside the triangular pocket of the swallow tail, there will be points $(p, q, r)$ for which the equation (13.1) will have 4 real solutions. Above the surface there will be points $(p, q, r)$ corresponding to the equations with 2 real (and 2 complex conjugated) solutions. Below the surface, there will not be real solutions at all. On the surface, besides the boundary of the pocket (in other words, on the part of the surface corresponding to Figure 13.19 c), there will be one real solution (repeated twice) and a pair of complex conjugated solutions. On the boundary of the pocket, there will be 3 real solutions: two simple and one repeated; the difference between the top part of this boundary (Figure 13.19 a) and the side parts (Figure 13.19 b) is in the order of the solutions: on the top part, the repeated root lies between the simple roots, on the two side parts it is, respectively, less than each simple roots and greater than each simple root. On the cuspidal edge, there are two roots: one triple and one simple; the two branches of the cuspidal edge distinguish between the two possible inequalities between these roots. On the self-intersection curve, there are two pairs of double roots (by the way, the second half of the parabola of self-intersection lies in the "no real roots" domain; it corresponds to equations with repeated complex conjugated roots). Finally, the most singular point, the cusp of the cuspidal edge, corresponds to the equation $x^4 = 0$ with four equal roots.

Note that the first picture of the swallow tail looks very different from Figure 13.17 (see Figure 8.11 in Lecture 8).

John Smith
January 23, 2010

Martyn Green
August 2, 1936

Henry Williams
June 6, 1944

**13.10 Exercises.** For solving the exercises below the reader may use all theorems provided in this lecture, with or without complete proofs.

Let $\gamma = \{x = x(t), y = y(t), z = z(t)\}$ be a curve and $P = (x(t_0), y(t_0), z(t_0)$ be a non-inflection point (which means that the velocity vector $\gamma'(t_0) = (x'(t_0), y'(t_0), z'(t_0))$ and the acceleration vector $\gamma''(t_0) = (x''(t_0), y''(t_0), z''(t_0))$ are not collinear. The plane spanned by these two vectors at $P$ is called the *osculating plane* of $\gamma$ at the point $P$.

13.1. Prove that if a plane $\Pi$ contains the tangent line to the curve $\gamma$ at $P$ and in any neighborhood of $P$ the curve $\gamma$ does not lie at one side of $\Pi$, then $\Pi$ is the osculating plane.

13.2. Prove that the tangent planes of a generic (non-planar, non-cylindrical and non-conical) developable surface are osculating planes to the cuspidal edge, and vice versa. (There are tangent planes to the surface passing through cusps of the cuspidal edge; these planes may be regarded as osculating planes of the cuspidal edge, although this case is not covered by the definition above.)

13.3. Prove that a generic family of planes in space is the family of tangent planes to a developable surface, and hence, by Exercise 13.2, also a family of osculating planes to a curve.

*Comment.* Thus, a family of planes has two "envelopes": a developable surface and a curve; the latter is the cuspidal edge of the former.

13.4. (Exercise 13.3 in formulas.)

(a) Let

$$A(t)x + B(t)y + C(t)z + D(t) = 0$$

(where $t$ is a parameter) be a family of planes. Prove that to get parametric equations of the enveloping developable surface, one needs to take, as parameters, $t$ and one of the coordinates and then to solve the system

$$\begin{cases} A(t)x + B(t)y + C(t)z + D(t) = 0 \\ A'(t)x + B'(t)y + C'(t)z + D'(t) = 0 \end{cases}$$

with respect to the remaining two coordinates. To get parametric equations of the enveloping curve, one needs to solve with respect to $x, y, z$ the system

$$\begin{cases} A(t)x + B(t)y + C(t)z + D(t) = 0 \\ A'(t)x + B'(t)y + C'(t)z + D'(t) = 0 \\ A''(t)x + B''(t)y + C''(t)z + D''(t) = 0 \end{cases}$$

(b) Apply these formulas to the family of planes obtained from the plane $x+z = 0$ by rotating about the $z$ axis with simultaneous parallel shift in the direction of the same axis:

$$x \cos t - y \sin t + z - t = 0.$$

13.5. Take a spatial curve with an inflection point, $x = t, y = t^3, z = t^4$, and consider the developable surface formed by tangents to this curve. Investigate all singularities (cuspidal edges and self-intersections) of this surface.

13.6. * (a) Consider a ruled developable disc $D$ and let $\gamma$ be a smooth closed curve on $D$. Prove that there are two points of $\gamma$ that lie on the same ruling of $D$ and such that the tangent lines to $\gamma$ at these points are parallel.

(b) Construct a developable disc and a smooth closed curve on it that has no parallel tangents.

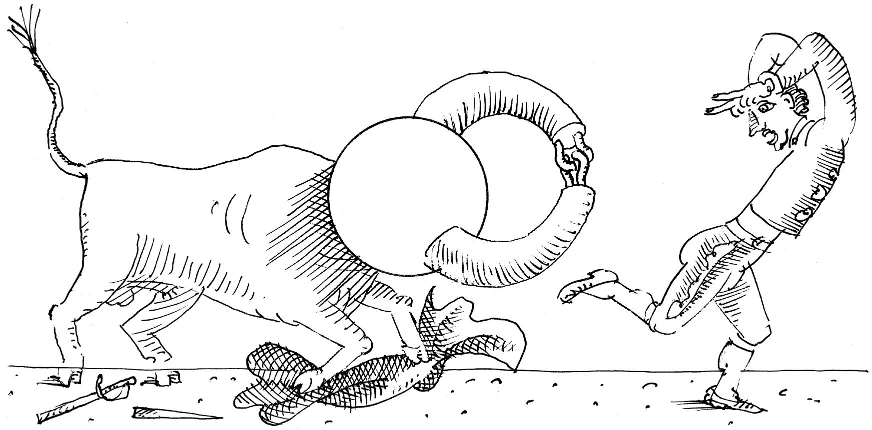

LECTURE 14

# Paper Möbius Band

**14.1 Introduction: it is not about ants or scissors.** The Möbius band is an immensely popular geometrical object. Even small children can make it: take a paper strip, twist it through 180 degrees (by half a turn), and then attach the ends to each other by glue or tape. By the way, one of us is still grateful to his analysis professor who taught his students how to draw a Möbius band: draw a standard trefoil, then add the three double tangents, then erase three segments of the curve between self-intersections and tangency points (Figure 14.1). You can see the drawing, it is beautiful.

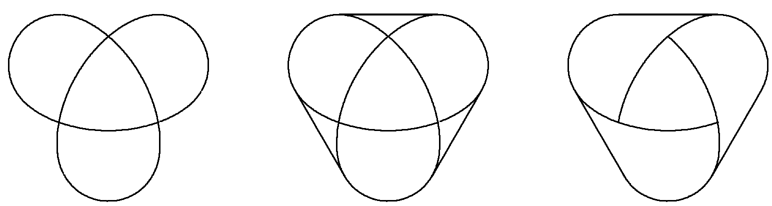

FIGURE 14.1. How to draw a Möbius band

There is a number of familiar tricks involving the Möbius band. You can cut it along the middle circle, and – check for yourself what happens. Or you can let a stupid ant crawl from one side to another without crossing the border. But we shall consider a totally different problem: if it is so easy to make a Möbius band out of a paper strip, then what shape of strip should one take? More precisely: there should be a real number $\lambda$ such that with a rectangular strip of paper of width 1 and length $\ell$ one can make a Möbius band for $\ell > \lambda$, but it is impossible if $\ell < \lambda$.

Question: what is $\lambda$?

Answer: not known.

We could have stopped here, but we shall not. Let us discuss, what is known about this problem, and what the perspectives are.

**14.2 Do not fold paper.** Our readers who are familiar with Lecture 13 on paper sheet geometry know that the condition of *smoothness* is crucial in problems of this kind. Indeed, if it is allowed to, say, fold the paper, then a Möbius band can be made of an arbitrary paper rectangle, even when its width exceeds its length. How to do it, is shown in Figure 14.2: take a rectangular piece of paper (of any dimensions), pleat it, then twist and glue. The condition of smoothness of our surface, that is, in more mathematical terms, of the existence of a unique tangent plane at every point of the surface, should play a role in our problem.

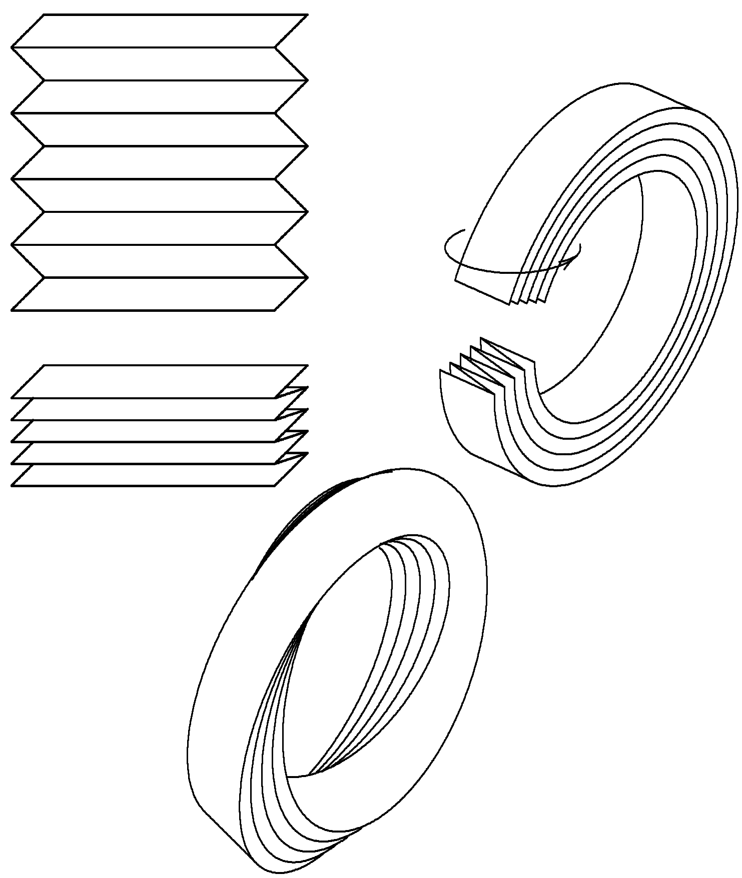

FIGURE 14.2. Making a Möbius band of folded paper

Now we are prepared to formulate our main result.

**14.3 Main Theorem.** Let $\lambda$ be a real number such that a smooth Möbius band can be made of a paper rectangle of dimensions $1 \times \ell$ if $\ell > \lambda$ and cannot, if $\ell < \lambda$.

THEOREM 14.1. $\frac{\pi}{2} \leq \lambda \leq \sqrt{3}$.

Thus, the interval between $\pi/2 \approx 1.57$ and $\sqrt{3} \approx 1.73$ remains a grey zone for our problem. Later, we shall discuss the situation within this zone, but first let us prove this theorem.

We shall need some general properties of surfaces made of paper.

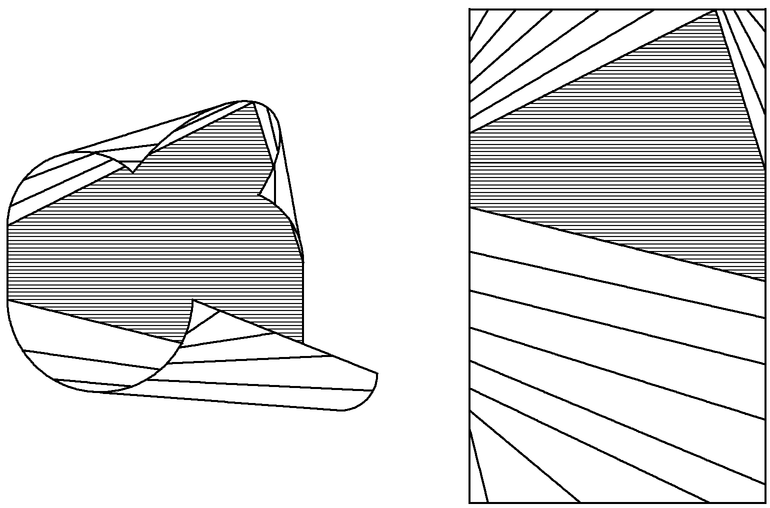

FIGURE 14.3. A ruling of a paper surface

**14.4 Surfaces made of paper.** We discussed these properties in Lecture 13 mentioned above. Not every surface can be made of paper. Restriction come from physical properties of (ideal) paper: it is flexible but not stretchable. The latter means that any curve drawn on a sheet of paper retains its length after we bend the sheet into a surface. As we know from Lecture 13, any paper surface is *ruled* which means that every point belongs to a straight interval lying on the surface. The line containing this interval is unique, unless a piece of the surface around the chosen point is planar. Thus, any paper surface consists of planar domains and straight intervals. If we draw these intervals and shadow these domains on the surface and then unfold the surface into a planar sheet, we will get a picture like the one shown in Figure 14.3.

**14.5 Proof of the inequality $\lambda \geq \frac{\pi}{2}$.** Let a Möbius band be made of a paper strip of width 1 and length $\ell$. If we take a very long (infinite) strip of width 1, we can wind it onto our Möbius band, so that every rectangle of length $\ell$ will assume the shape of our Möbius band (and these rectangles will be located alternatively on two sides of the core band). Mark on the strip the straight intervals and the planar domains (the latter will have the shape of trapezoids which may degenerate into triangles, they are shaded in the upper Figure 14.4). The picture is periodic: it repeats itself with period $2\ell$, and the successive rectangles of length $\ell$ repeat each other but turning upside down. We fill the planar domains with straight intervals, so that the whole strip will be covered by a continuous family of intervals (pairwise disjoint) with the same periodicity property as above (see lower Figure 14.4). All the intervals have lengths $\geq 1$, their ends lie on the boundary lines of the strip, and all of them remain straight when we bend our strip into a Möbius band.

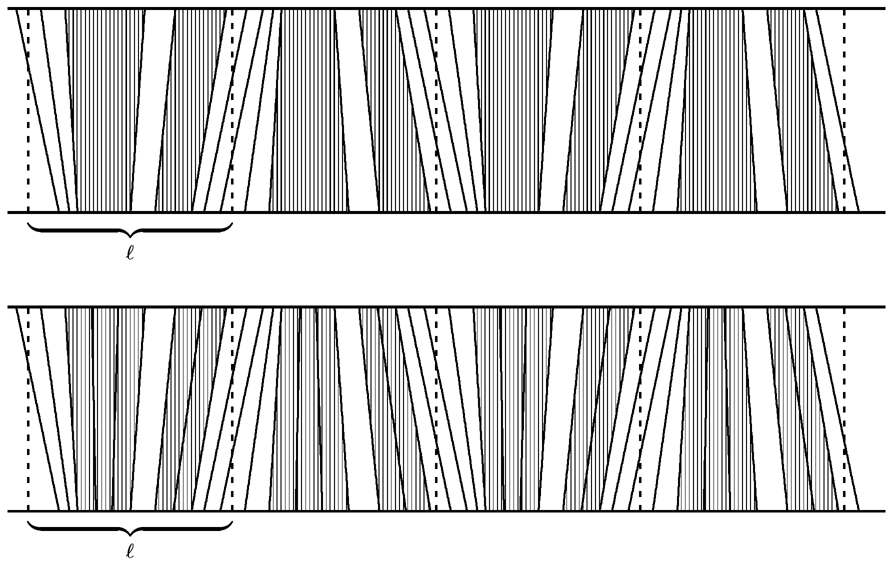


FIGURE 14.4. Filing planar domains on the strip with straight segments

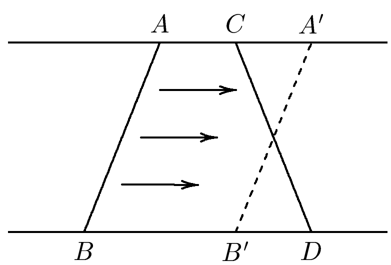


FIGURE 14.5. $AB$ and $CD$.

Take any interval of our family, say, $AB$. Shift it to the right by $\ell$ to the position $A'B'$ and then reflect the interval $A'B'$ in the middle line of the strip (Figure 14.5). The resulting interval $CD$ also belongs to our family (because of the periodicity properties described above).

Two things are obvious. First, $AC+BD = 2\ell$; second, on the Möbius band the point $C$ coincides with $B$ and the point $D$ coincides with $A$. The second statement means that on our paper model the angle between the intervals $AB$ and $CD$ is 180°. Thus, in space, the intervals of our family between $AB$ and $CD$ form the angle with the interval $AB$ which continuously varies from 0 to 180°. Take some (big) number $n$ and choose intervals $A_0B_0 = AB,\ A_1B_1, \ldots, A_{n-1}B_{n-1},\ A_nB_n = CD$ of our family (Figure 14.6) such that the angle between $AB$ and $A_kB_k$ (on the Möbius band) is equal to $k \cdot \dfrac{180^\circ}{n}$ (for $k = 0, 1, \ldots, n-1$). This implies that the angle between $A_kB_k$ and $A_{k+1}B_{k+1}$ is at least $\dfrac{180^\circ}{n}$.

LEMMA 14.1. *Let $a_n$ be the side of the regular $n$-gon inscribed into a circle of diameter 1. Then (on our paper strip) $A_kA_{k+1} + B_kB_{k+1} > a_n$ (for any $k$).*

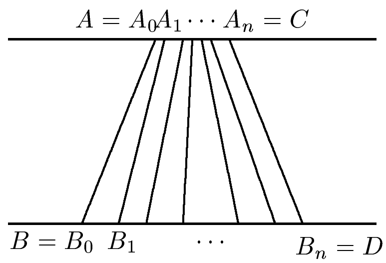


FIGURE 14.6. The family $A_kB_k$.

Proof. Consider a piece of our paper Möbius band containing the (images of) the intervals $A_kB_k$ and $A_{k+1}B_{k+1}$. The lengths of segments $A_kA_{k+1}$, $B_kB_{k+1}$ in space do not exceed the length of the same intervals on the strip (the latters are equal to the lengths of arcs $A_kA_{k+1}, B_kB_{k+1}$ on the boundary curve of the Möbius band). So, it is sufficient to prove our inequality for the points $A_k, A_{k+1}, B_k, B_{k+1}$ in space. Take point $E$ such that $A_kE$ has the same length and direction as $A_{k+1}B_{k+1}$ (see Figure 14.7, left). Then $B_{k+1}E = A_{k+1}A_k$ and $B_kE \le B_kB_{k+1} + B_{k+1}E = A_kA_{k+1} + B_kB_{k+1}$.

But $B_kE > a_n$. To prove this, consider an isosceles triangle $KLM$ inscribed into a circle of diameter 1 whose base $LM$ is a side of a regular $n$-gon inscribed into the same circle and which contains the center of the circle (Figure 14.7, right). In this triangle, $\angle MKL = 180°/n$ and $KL = KM = b_n < 1$. In the triangle $A_kB_kE$, denote by $F$ and $G$ the points on the sides $A_kB_k$ and $A_kE$ at distance $b_n$ from $A_k$ (these points exist since $A_kB_k \ge 1 > b_n$ and $A_kE = A_{k+1}B_{k+1} \ge 1 > b_n$). Then $B_kE > FH \ge FG \ge a_n$ (the latter is true since $\angle B_kA_kE \ge 180°/n$). □

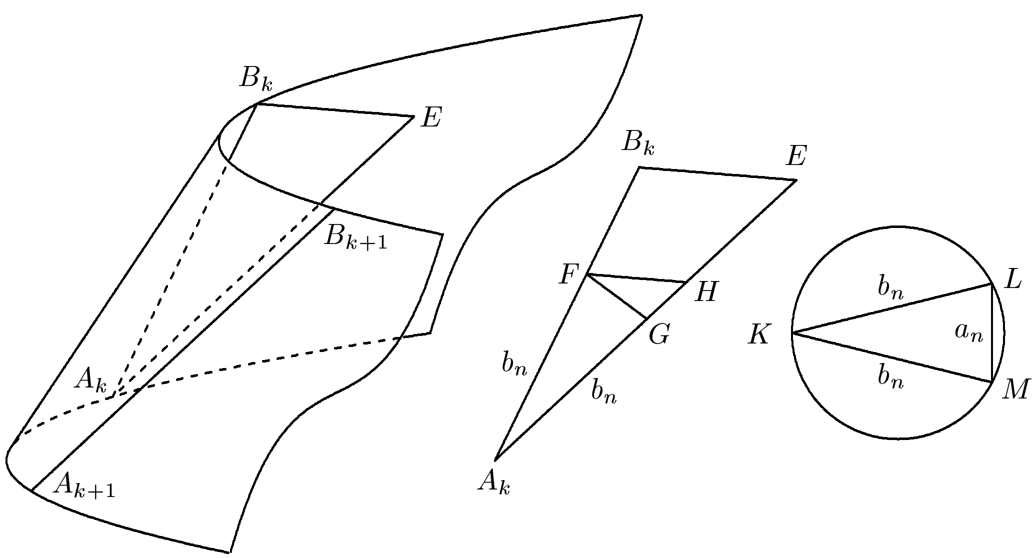


FIGURE 14.7. Proof of Lemma 14.1

Back to the inequality $\lambda \geq \dfrac{\pi}{2}$. We have:

$$\begin{aligned} 2\lambda \geq 2\ell &= AC + BD \\ &= (A_0A_1 + \cdots + A_{n-1}A_n) + (B_0B_1 + \cdots + B_{n-1}B_n) \\ &= (A_0A_1 + B_0B_1) + \cdots + (A_{n-1}A_n + B_{n-1}B_n) > na_n \end{aligned}$$

Since this is true for every $n$, and $na_n$ approaches $\pi$ when $n$ grows, we have $2\lambda \geq \pi$. □

**14.6 Proof of the inequality $\lambda \leq \sqrt{3}$.** To prove this inequality, it is sufficient to show how a Möbius band can be made of a $1 \times \ell$ strip for an arbitrary $\ell > \sqrt{3}$. We shall show how a Möbius band can be made of a strip of length precisely $\sqrt{3}$, but this will require several folds. We have a commitment to avoid folds, but it is clear that disjoint folds can be smoothened at the expense of an arbitrarily slight elongation of the strip (see Figure 14.8).

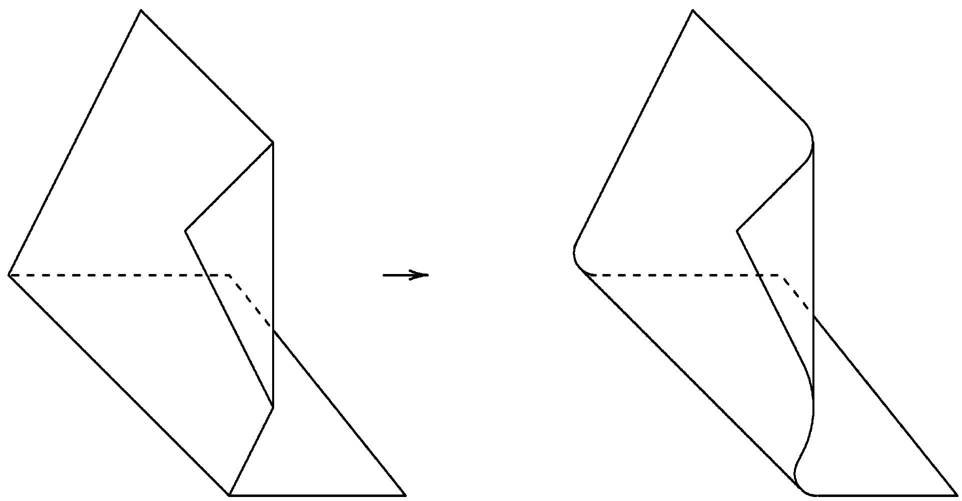

FIGURE 14.8. Rounding folds.

The construction is shown in Figure 14.9: we take a rectangle $ABCD$ with $AB = 1$, $AD = \sqrt{3}$, draw equilateral triangles $AKL$ and $KLC$ with $K$ on $BC$ and $L$ on $AD$. Notice that the right triangles $ABK$ and $CDL$ are two halves of one more equilateral triangle. (This construction is possible, since the side of an equilateral triangle with altitude 1 is $2\tan 30^\circ = \dfrac{2}{3}\sqrt{3}$, and $\sqrt{3} = \dfrac{2}{3}\sqrt{3} + \dfrac{1}{3}\sqrt{3}$). Then we fold the strip along the lines $AK$, $KL$, and $LC$, as shown in Figure 14.9. □

Notice that a "Möbius band" we constructed does not look like a Möbius band. It is rather the union of three identical equilateral paper triangles $AKL$, the top one attached to the middle one along the side $AL$, the middle one attached to the bottom one along the side $KL$ and the top one and the bottom one attached to each other along the side $AK$. If we take a strip slightly longer than $\sqrt{3}$ and round the folds, we shall get a smooth Möbius band which will still look more like an equilateral triangle than a Möbius band.

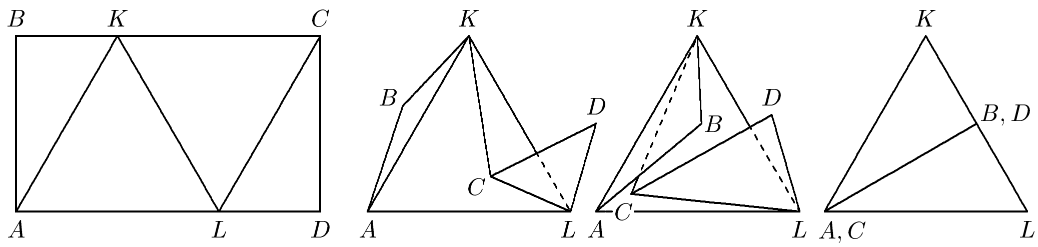


FIGURE 14.9. Constructing a Möbius band of a rectangle $1 \times \sqrt{3}$.

**14.7 Why is a more precise value of $\lambda$ not known?** Until a problem is solved, it is difficult to say why it is not solved. Still sometimes it is possible to detect common difficulties in different unsolved problems, which, in turn, may help to predict success or failure in solving some problems, or even to guess a solution. In previous sections we proved that $\lambda$ is a point of the segment $\left[\pi/2, \sqrt{3}\right]$. Which point? Is there, at least, a plausible conjecture? Yes: we think that $\lambda = \sqrt{3}$ and we are not surprised that a proof has not been found yet.

To justify this, let us notice that our proof of the inequality $\lambda \geq \pi/2$ does not use one important property of a paper Möbius band: it has no self-intersections. One cannot make a self-intersecting Möbius band of a real-life paper sheet, but it is not hard to imagine it: like a self-intersecting curve, it passes "through itself" but consists of non-self-intersecting pieces.

Suppose that, from the very beginning, speaking of a paper Möbius band, we do not exclude the possibility of self-intersections. Then the number $\lambda$ acquires a new sense, and the new value of $\lambda$ will be less than or equal to the old one. Moreover, the inequality $\lambda \geq \pi/2$ will remain valid, and we shall not need to change a single word in its proof: the absence of self-intersections is not used in it at all. As to the inequality $\lambda \leq \sqrt{3}$, it may be considerably improved.

THEOREM 14.2. *A smooth self-intersecting Möbius band can be made of a paper rectangle* $1 \times \ell$ *for any* $\ell > \pi/2$.

Proof. Take an arbitrarily big odd $n$, and consider a regular $n$-gon such that the distance from a vertex to the opposite side equals 1. Let $p_n$ be the perimeter of this $n$-gon; it is clear that when $n$ grows, the $n$-gon becomes indistinguishable from a circle of diameter 1 and $p_n$ approaches $\pi$.

Take a rectangle $ABCD$ of dimensions $1 \times \dfrac{p_n}{2}$ and inscribe in it $n-1$ isosceles triangles $AKQ, KQL, \ldots, MNC$, equal to the triangle formed by a side and two of the longest diagonals of our regular $n$-gon (see Figure 14.10 where $n = 7$). The triangles $ABK$ and $NCD$ are two halves of such triangle. Then fold the rectangle along the lines $AK, KQ, \ldots, NC$ (in alternating directions). The process of this folding is shown in Figure 14.10.

In the end we shall obtain a paper figure, indistinguishable from a regular $n$-gon (a regular heptagon in our picture), with the segments $AB$ and $CD$ almost merging together: they will be separated only by several layers of folded paper. If we make the folds smooth (this will require a slightly longer strip) and then connect $AB$ with $CD$ by a very short paper strip (which will create severe self-intersections), we shall

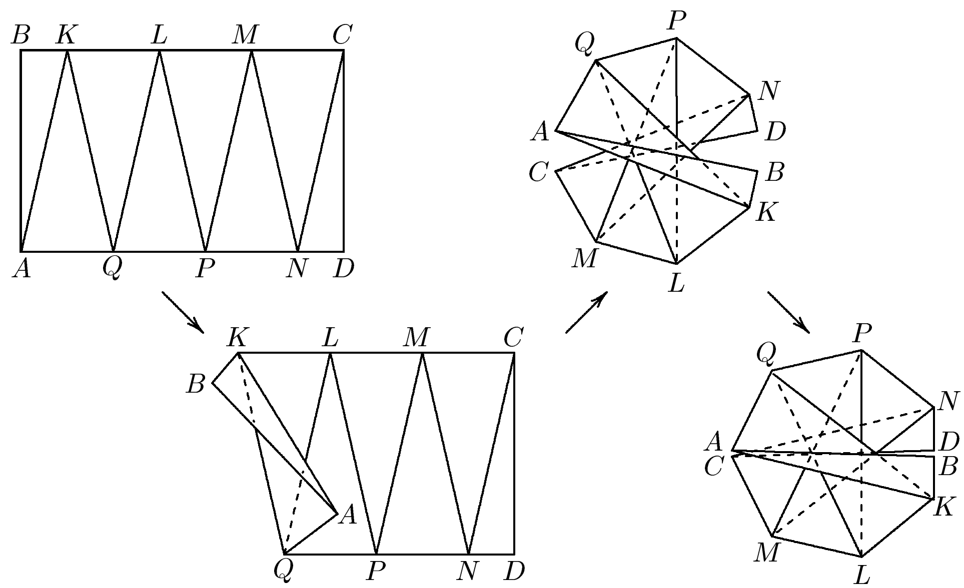


FIGURE 14.10. A heptagonal model of a self-intersecting Möbius band.

get a smooth self-intersecting Möbius band with the ratio between the length and the width of the strip arbitrarily close to $\pi/2$. □

Thus, if we want to prove that $\lambda > \pi/2$, our proof should have to use the absence of self-intersections. The question whether a surface has self-intersections, belongs to three-dimensional "position geometry". The whole experience of mathematics shows that this part of geometry is especially hard: there are almost no technical means to approach its problems. Thus, if an improvement of the inequality $\lambda \geq \pi/2$ exists, it is difficult to find a proof. On the contrary, an improvement of the inequality $\lambda \leq \sqrt{3}$ would have involved a construction better than that of Section 14.5. But one can expect this construction to be natural and beautiful; the fact that we do not know it may be regarded as an indication that it does not exists. By this reason it seems plausible to us that $\lambda = \sqrt{3}$, but the proof is hardly easy.

**14.8 Exercise.** Suppose that we have a paper cylinder, made of a paper strip of dimensions $1 \times \ell$. Is it possible to turn it inside out (without violating its smoothness)? Clearly, if the cylinder is short and wide ($\ell$ is big), then it is possible, but if the cylinder is long and narrow ($\ell$ is small), it is impossible. Where is the boundary between short and wide cylinders and long and narrow ones? The following statements due to B. Halpern and K Weaver [**41**] give a partial answer to this problem. (Nothing else is known, so far.)

14.1. * (a) If $\ell > \pi + 2$, then it is possible to turn the cylinder inside out.

(b) If $\ell > \pi$, then the cylinder can be turned inside out with self-intersections.

(c) If $\ell < \pi$, then the cylinder cannot be turned inside out, with or without self-intersections.

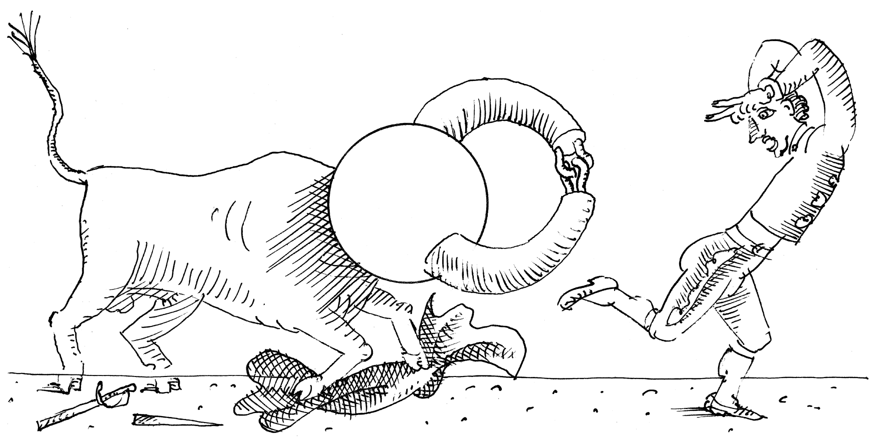

LECTURE 15

# More on Paper Folding

**15.1 The fold line is straight.** Take a sheet of paper and fold it: the fold line is straight, see Figure 15.1. We start our discussion of paper folding with a mathematical explanation of this phenomenon.

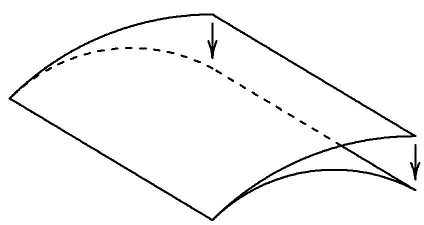

FIGURE 15.1. Folding a sheet of paper yields a straight line

The model for a paper sheet is a piece of the plane. The fold curve partitions the plane into two parts. Performing folding, we establish a one-to-one correspondence between these parts, and this correspondence is an isometry: the distances between points do not change. The last property means that paper is not stretchable; this is our standing assumption, made in Lecture 13.

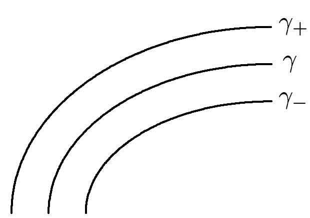


FIGURE 15.2. Proving that the fold line cannot be curved

Call the fold line $\gamma$, and let us prove that it is straight. If not, $\gamma$ has a sub-arc with non-zero curvature. Let $\gamma_+$ be the curve $\gamma$ translated (small) distance $\varepsilon$ from $\gamma$ on the concave side, and $\gamma_-$ – that on the convex side. Then

$$\text{length } \gamma_+ > \text{length } \gamma > \text{length } \gamma_-,$$

see Figure 15.2 (the difference is of order $\varepsilon \cdot \text{length } \gamma \cdot \text{curvature } \gamma$). On the other hand, the isometry takes $\gamma_+$ to $\gamma_-$, so length $\gamma_+$ and length $\gamma_-$ must be equal. This is a contradiction.

**15.2 And still, the fold line can be curved.** In spite of what has just been said, one can fold paper along an arbitrary smooth curve! The reader is invited to try an experiment: draw a curve on a sheet of paper and slightly fold the paper along the curve.[1] The result is shown in Figure 15.3 on the left.

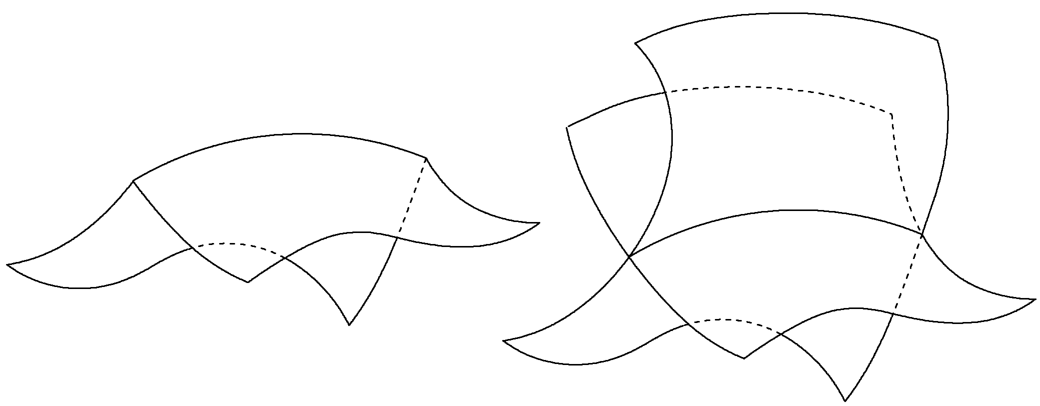

FIGURE 15.3. A sheet of paper folded along a curve

One may even start with a closed curve drawn on paper. To be able to fold, one must cut a hole inside the curve, see Figure 15.4.

It goes without saying that there is no contradiction to the argument in Section 15.1: the two sheets in Figure 15.3, left, do not come close to each other, they meet at a non-zero angle (varying from point to point).

To fix terminology, call the curve drawn on paper the *fold* and the curve in space, obtained as the result of folding, the *ridge*. Experiments with paper reveal the following:

(1) It is possible to start with an arbitrary smooth fold and obtain an arbitrary ridge, provided the ridge is "more curved" than the fold.
(2) At every point of the ridge, the two sheets of the folded paper make equal angles with the osculating plane[2] of the ridge.
(3) If the fold has an inflection point (where it looks like a cubic parabola) then the corresponding point of the ridge is also an inflection point, that is, has zero curvature.

[1] A word of practical advice: press hard when drawing the curve. It also helps to cut a neighborhood of the curve not to mess with too large a sheet. A more serious reason for restricting to a neighborhood is that this way one avoids self-intersections of the sheets, unavoidable otherwise.

[2] See Section 15.3 for definition.

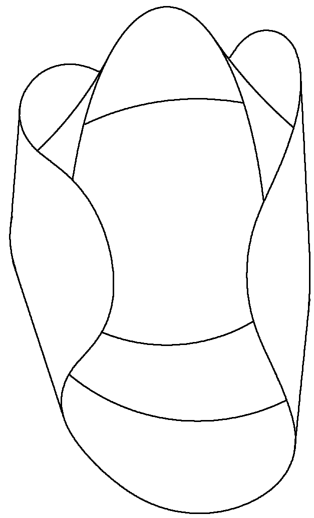

FIGURE 15.4. Closed fold line

(4) If the fold is closed and strictly convex then the ridge cannot be a planar curve.

In the next sections we shall explain these experimental observations.

**15.3 Geometry of space curves.** We need to say a few words about curvature of plane and space curves.

Let $\gamma$ be a smooth plane curve. To define curvature, give the curve arc length parameterization, $\gamma(t)$. Then the velocity vector, $\gamma'(t)$, is unit, and the acceleration vector $\gamma''(t)$ is always orthogonal to the curve. The magnitude of the acceleration, $|\gamma''(t)|$, is the curvature of the curve. That is, the curvature is the rate of change of the direction of the curve per unit of length.

Equivalently, one may consider the osculating circle of the curve at a given point; this is the circle through three infinitesimally close points of the curve (see Lecture 10). Curvature is the reciprocal to the radius of the osculating circle.

Still another way to measure curvature is as follows. Let every point of the curve move, with unit speed, in the direction, orthogonal to the curve (cf. Lecture 9). In this process, the length of the curve changes. The absolute value of the relative rate of change of the length at a point equals the curvature of the curve (this is easy to check for a circle; for an arbitrary curve, approximate by its osculating circle). This characterization of curvature was used in the argument at the end of Section 15.1.

We now turn to curves in space. Let $\gamma(t)$ be an arc length parameterized spatial curve. Similarly to the planar case, its curvature is the magnitude of the acceleration vector, $|\gamma''(t)|$.

Note the following important difference with the planar case. A typical plane curve has inflection points (points of zero curvature) where it looks like Figure 15.5. The word "typical" means that if one perturbs the curve slightly then the inflection point will move a little but will not disappear. In space, *typical curves have no points of zero curvature.*

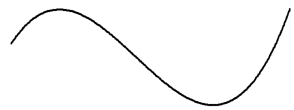

FIGURE 15.5. A typical plane curve has inflections

(An accurate proof of this claim is rather tedious, but here is a plausible explanation. The acceleration vector $\gamma''(t)$ is orthogonal to the curve and has two degrees of freedom. For this vector to vanish, two independent conditions must hold. But a point of a curve has only one degree of freedom, so we have more equations than variables, and hence a typical curve has no points of zero curvature.)

Suppose our space curve has no points of zero curvature. The plane spanned by the velocity and acceleration vectors $\gamma'(t)$ and $\gamma''(t)$ is called the *osculating plane* of the curve. This plane approximates the curve at point $\gamma(t)$ better than any other plane: up to infinitesimals of second order, the curve lies in its osculating plane. Equivalently, the osculating plane is the plane through three infinitesimally close points of the curve.

The unit vector, orthogonal to the osculating plane, is called the binormal. The binormal vector changes from point to point, and the magnitude of its derivative (with respect to arc length parameter) is called torsion. Torsion measures how the osculating plane rotates along the curve.

Suppose that an arc length parameterized curve $\gamma(t)$ lies on a surface $M$. The acceleration vector $\gamma''(t)$ can be decomposed into two components: the component orthogonal to $M$ and the tangential one. The magnitude of the latter is called the *geodesic curvature* of the curve (cf. Lecture 20); it can be again interpreted as the relative rate of change of the length as every point of $\gamma$ moves on $M$, with unit speed, in the direction perpendicular to the curve.

**15.4 Explaining paper folding experiments.** Recall that our mathematical models for paper sheets are developable surfaces. Extend the two sheets of the developable surfaces in Figure 15.3, left, beyond their intersection curve, the ridge, as in Figure 15.3, right. One sees two developable surfaces intersecting along a space curve $\gamma$. Unfolding either of the surfaces to the plane transforms $\gamma$ to the same plane curve $\delta$, the fold. Reverse the situation and pose the following question: given a plane curve $\delta$, a space curve $\gamma$ and an isometry (distance preserving correspondence) $f$ between $\delta$ and $\gamma$, is it possible to extend $f$ to a planar neighborhood of $\delta$ to obtain a developable surface, containing $\gamma$? Said differently, can one bend a sheet of paper, with a curve $\delta$ drawn on it, so that $\delta$ bends to a given space curve $\gamma$?

THEOREM 15.1. *Assume that for every point $x$ of $\delta$ the curvature of $\gamma$ at the respective point $f(x)$ is greater than the curvature of $\delta$ at $x$. Then there exist exactly two extensions of $f$ to a plane neighborhood of $\delta$ yielding developable surfaces, containing $\gamma$.*

Proof. Parametrize the curves $\gamma$ and $\delta$ by an arc length parameter $t$ so that $\gamma(t) = f(\delta(t))$. Let the desired developable surface $M$ make the angle $\alpha(t)$ with the osculating plane of the curve $\gamma(t)$ (well defined since, by assumption, the curvature of $\gamma$ never vanishes). Denote by $\kappa(t)$ the curvature of the space curve $\gamma$ and by $k(t)$ that of the plane curve $\delta$.

The magnitude of the curvature vector of $\gamma$ is $\kappa$, and its projection on $M$ has magnitude $\kappa(t)\cos\alpha(t)$; thus the geodesic curvature of $\gamma$ equals $\kappa(t)\cos\alpha(t)$. The geodesic curvature of a curve on a surface depends only on the inner geometry of the surface and does not change when this surface is bent without stretching. Therefore the geodesic curvature of $\gamma$ equals the curvature of the plane curve $\delta$:

$$\kappa(t)\cos\alpha(t) = k(t). \tag{15.1}$$

This equation uniquely determines the function $\alpha(t)$. Since $k < \kappa$, the angle $\alpha$ never vanishes.

To construct the developable surface $M$ from the function $\alpha(t)$, consider a one-parameter family of planes through points $\gamma(t)$, containing the tangent vector $\gamma'(t)$ and making angle $\alpha(t)$ with the osculating plane of $\gamma$ (there are two such planes, see Figure 15.6). According to the discussion of developable surfaces in Lecture 13, a one-parameter family of planes envelop a developable surface, and we obtain our two surfaces through the curve $\gamma$. □

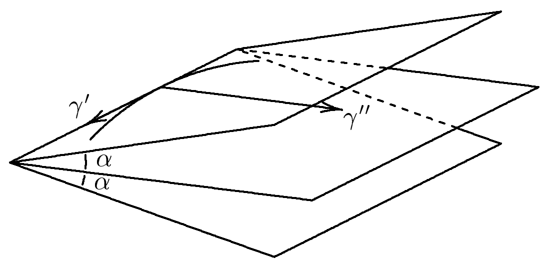


FIGURE 15.6. Construction of the developable surface from the function $\alpha(t)$

The two developable surfaces of Theorem 15.1 are the sheets, intersecting along the ridge in Figure 15.3. Extending the sheets beyond the ridge one obtains another configuration of sheets that meet along the curve $\gamma$. Thus there are exactly two ways to fold paper along curve $\delta$ to produce the space curve $\gamma$. This explains and extends the first observation made in Section 15.2.

In the particular case when $\gamma$ is a planar curve, one of the sheets is obtained from another by reflection in this plane. In the general case of a nonplanar curve $\gamma$, the tangent planes of the two sheets are symmetric with respect to the osculating plane of $\gamma$ at every point: indeed, the angles between the osculating plane and the two sheets are equal to $\alpha$. This justifies the second observation in Section 15.2.

Proceed to the third observation. Let $\delta(t_0)$ be an inflection point where the fold looks like a cubic parabola. Thus $k(t_0) = 0$, and the curvature does not vanish immediately before and after the inflection point. According to formula (15.1), either $\alpha(t_0) = \pi/2$ or $\kappa(t_0) = 0$. We want to show that, indeed, the latter possibility holds.

Suppose not; then both sheets are perpendicular to the osculating plane of $\gamma$ at point $\gamma(t_0)$, and therefore their tangent planes coincide. Moreover, if $\kappa(t_0) \neq 0$ then the projection of the curvature vector of the space curve $\gamma$ onto each sheet is the vector of the geodesic curvature therein. This vector lies on one side of $\gamma$ on the surface at points $\gamma(t_0 - \varepsilon)$ just before the inflection point and on the other side at points $\gamma(t_0+\varepsilon)$ just after it. Therefore the function $\alpha(t)-\pi/2$ changes sign at $t=t_0$. This means that the two sheets pass through each other at $t=t_0$. Impossible for real paper, this implies that $\kappa(t_0)=0$, that is, the ridge has an inflection point.

Now, to the fourth observation. Assume that both the ridge $\gamma$ and the fold $\delta$ are closed planar curves and $\delta$ is strictly convex. The relation (15.1) between the curvatures still holds: $\kappa\cos\alpha=k$, and $k$ does not vanish anywhere. Hence $\kappa$ does not vanish either, and $\gamma$ is a convex planar curve. In addition, $\kappa(t)\ge k(t)$ for all $t$ and $\int\kappa(t)\ dt>\int k(t)\ dt$ since $\alpha(t)$ does not vanish. On the other hand, the integral curvature of a simple closed planar curve equals $2\pi$, see Exercise 15.1. Therefore the two integrals must be equal, a contradiction.

**15.5 More formulas and further observations.** According to Theorem 15.1, the fold $\delta$ and the ridge $\gamma$ determine the developable surface, the result of extending the isometry between $\delta$ and $\gamma$ to a neighborhood of $\delta$. Recall from Lecture 13 that developable surfaces are ruled. Denote by $\beta(t)$ the angle made by the rulings with $\gamma(t)$.

One should be able to express the angles $\beta(t)$ in terms of geometric characteristics of the fold and the ridge. Indeed, such a formula exists:

$$\cot\beta(t)=\frac{\alpha'(t)-\tau(t)}{\kappa(t)\sin\alpha(t)}, \tag{15.2}$$

where $\tau$ is the torsion of the curve $\gamma$ and $\alpha$ is the angle between the surface and the osculating plane of the curve $\gamma$, given by equation (15.1). We do not deduce this formula here: this is a relatively straightforward exercise on the Frenet formulas in differential geometry of space curves; if the reader is familiar with the Frenet formulas, he will do this as Exercise 15.3, and if not, he will trust us.

Back to the folded paper depicted in Figure 15.3. We see two developable surfaces intersecting along the ridge $\gamma$, and each carries a family of rulings. Thus we have two functions, $\beta_1(t)$ and $\beta_2(t)$. Unfolding the surfaces back in the plane yields a planar curve, the fold $\delta$, with two families of rulings along it, one on each side, see Figure 15.7.

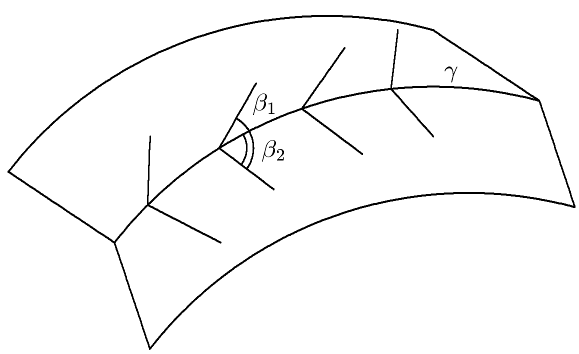


FIGURE 15.7. Unfolding the folded paper

The angles $\beta_1$ and $\beta_2$ are given by the formulas

$$\cot\beta_1(t)=\frac{\alpha'(t)-\tau(t)}{\kappa(t)\sin\alpha(t)},\quad \cot\beta_2(t)=\frac{-\alpha'(t)-\tau(t)}{\kappa(t)\sin\alpha(t)},$$

the first being (15.2), and the second obtained from the first by replacing $\alpha$ by $\pi - \alpha$. It follows that

$$\cot\beta_1(t) + \cot\beta_2(t) = \frac{-2\tau(t)}{\kappa(t)\sin\alpha(t)},\quad \cot\beta_1(t) - \cot\beta_2(t) = \frac{2\alpha'(t)}{\kappa(t)\sin\alpha(t)}. \tag{15.3}$$

Formulas (15.3) have two interesting consequences. Suppose that the ridge is a planar curve. Then $\tau = 0$, and therefore $\beta_1 + \beta_2 = \pi$. In this case unfolding the two sheets in the plane yields the straight rulings that extend each other on both sides of the fold, see Figure 15.8. Suppose now that the dihedral angle between two sheets along the ridge is constant. Then $\alpha' = 0$, and therefore $\beta_1 = \beta_2$. In this case the rulings make equal angles with the fold.

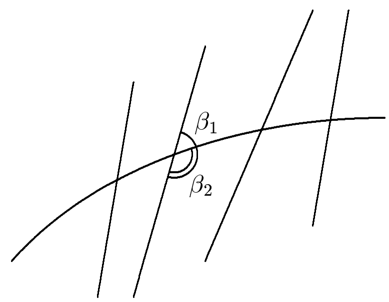


FIGURE 15.8. Rulings on both sides of the fold may extend each other

And again we may reverse the situation: start with the fold $\delta$ and prescribe the angles $\beta_1$ and $\beta_2$. The reader with a taste for further experimentation may paste, with scotch tape, a number of pins or needles on both sides of the fold (thus fixing the angles $\beta_1$ and $\beta_2$.) Now fold!

**15.6 Two examples.** As the first example, let the fold be an arc of a circle, and let the rulings on both sides be radial lines, orthogonal to the fold. Then $\beta_1 = \beta_2 = \pi/2$. Therefore the ridge is planar and the dihedral angle between the sheets is constant. The rulings on each sheet intersect at one point, hence both sheets are cones, see Figure 15.9.

In the second example, we utilize the optical property of the parabola: the family of rays from the focus reflects to the family of rays, parallel to the axis of the parabola, see Figure 15.10 (the reader not familiar with this property should either solve Exercise 15.4 or wait for a discussion in Lecture 28).

Let the fold be a parabola, let the rulings on the convex side be parallel to the axis and let the extensions of the rulings on the concave side all pass through the focus. By the optical property, these rulings make equal angles with the parabola, hence the dihedral angle between the sheets is constant. One of the sheets is again a cone; the rulings on the other being parallel, it is a cylinder, see Figure 15.11.

**15.7 Historical notes.** We learned that paper can be folded along curves from M. Kontsevich in 1994; he discovered this as an undergraduate student a long time ago. Among other things, Kontsevich noticed that the ridge tends to be a planar curve; this cannot be proved, unless some assumptions on elasticity of the folded material are made (our mathematical model of paper folding completely

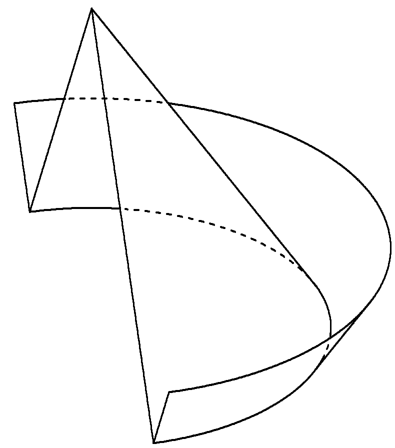

FIGURE 15.9. Both sheets are cones

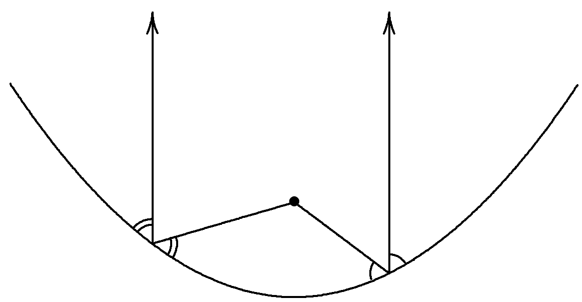

FIGURE 15.10. Optical property of parabola

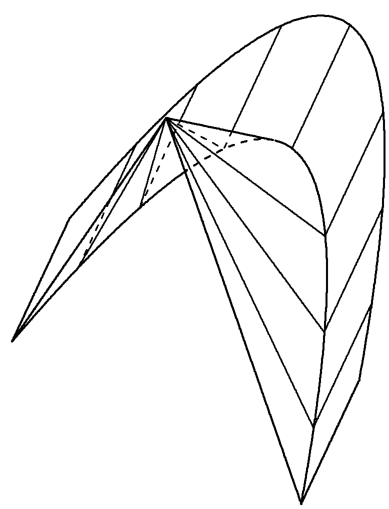

FIGURE 15.11. One sheet is a cone, another a cylinder

ignored these issues). We published the results of our reflections on paper folding in [**32**]. We discovered that Theorem 15.1 was quite old: it was mentioned in [**6**].

Later we found that folding of non-stretchable material along curves was considered before [**24**]. Duncan and Duncan studied the problem with an eye on engineering products made by folding and bending of a single sheet (such as sheet-metal duct-work or cardboard containers).

We wonder whether this interesting subject has further antecedents. It remains for us to quote M. Berry's Law (posted on his web site[3]): *Nothing is ever discovered for the first time*.

### 15.8 Exercises.

15.1. Let $\gamma(t)$ be a smooth arc length parameterized closed curve of length $L$ and winding number $w$. Let $k(t)$ be the curvature of $\gamma(t)$. Find

$$\int_0^L k(t)\ dt.$$

15.2. Let $\gamma$ be a smooth closed curve of length $L$ and winding number $w$. Move every point of $\gamma$ in the normal direction a small distance $\varepsilon$ to obtain a curve $\gamma_\varepsilon$. Find the length of $\gamma_\varepsilon$.

15.3. Prove formula (15.2).

15.4. Prove the optical property of the parabola.

15.5. Let the fold line be an arc of an ellipse, and let the rulings on one side of the fold line pass through one focus and on the other side though another focus. Prove that folding yields two cones making a constant angle along the ridge.

*Hint*. Use the optical property of ellipses, Lecture 28.

15.6. Why does one need to make a hole in a piece of paper when folding along a closed curve?

[3]www.phy.bris.ac.uk/people/berry_mv/quotations.html

# *Chapter 5*

# STRAIGHT LINES

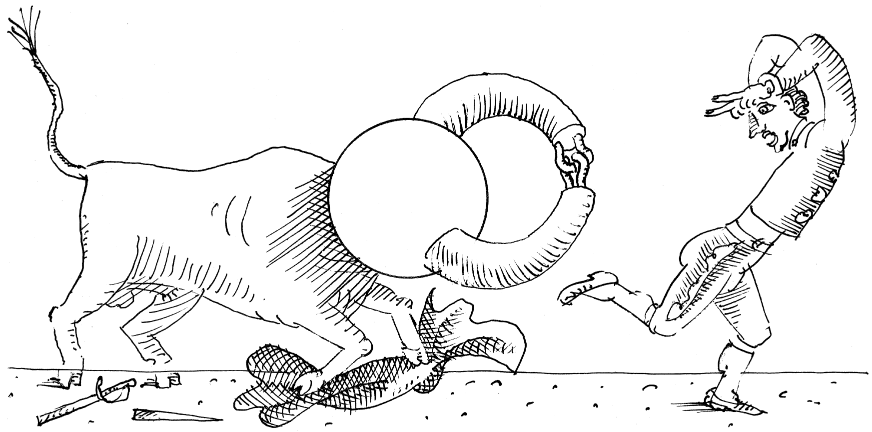

LECTURE 16

# Straight Lines on Curved Surfaces

**16.1 What is a surface?** We would prefer to avoid answering this question honestly, but to prove theorems we need precise definitions.

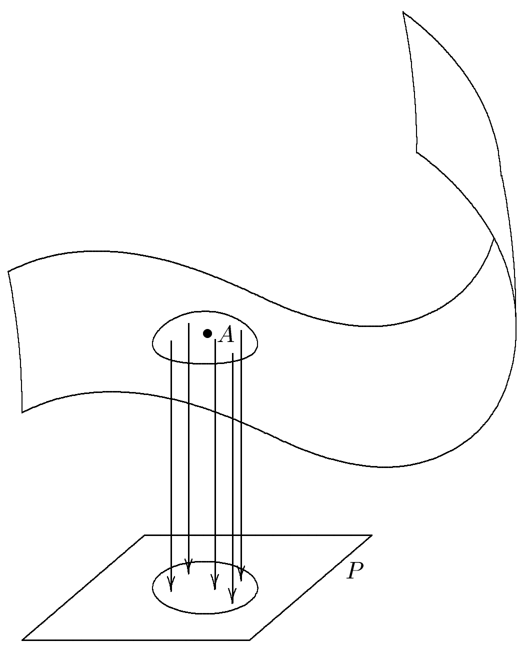


FIGURE 16.1. Definition of a surface

A set $S$ in space is called a surface if for every point $A$ in $S$ there exists a plane $P$ and a positive number $r$ such that the intersection of $S$ with any ball of radius $< r$ centered at $A$ has a $1-1$ projection onto the plane $P$ (Figure 16.1). Planes, spheres, cylinders, paraboloids, etc., are all surfaces.

Some surfaces, however curved they look, contain whole straight line (like the one shown in Figure 16.2).

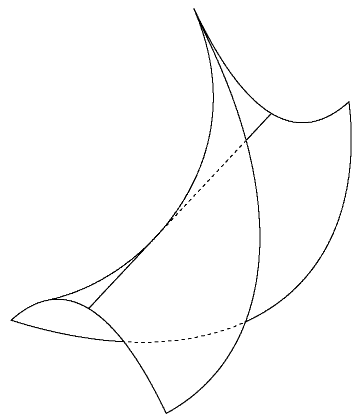

FIGURE 16.2. This surface contains a straight line

In this lecture, we shall consider surfaces which contain very many straight lines.

**16.2 Ruled surfaces.** A surface $S$ is called ruled, if for every point $A$ in $S$, there exists a straight line $\ell$ through $A$ contained in $S$.

There are many ruled surfaces. A plane is a ruled surface, but this is not interesting. Some other ruled surfaces, like cylinders, readily display their rulings. Some surfaces are also ruled, but this is less visible; for example, if you bend (without folding) a piece of paper, you will obtain a ruled surface – see Lecture 13. Here we shall be interested in a different class of surfaces.

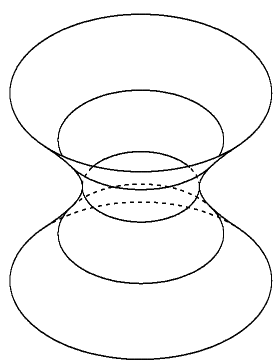

FIGURE 16.3. A one-sheeted hyperboloid

**16.3 Two key examples.** A *one-sheeted hyperboloid* is described in space by the equation

$$x^2 + y^2 - z^2 = 1.$$

It may be also described as a surface of revolution of the hyperbola $x^2 - z^2 = 1$ in the $xz$ plane about the $z$ axis (Figure 16.3).

Do you think, this surface is ruled? It is. To see it, make a cylinder of vertical threads joining two identical horizontal hoops, and then rotate the upper hoop about the vertical axis keeping the threads tight. Your cylinder will become a hyperboloid, and you will see the ruling (Figure 16.4).

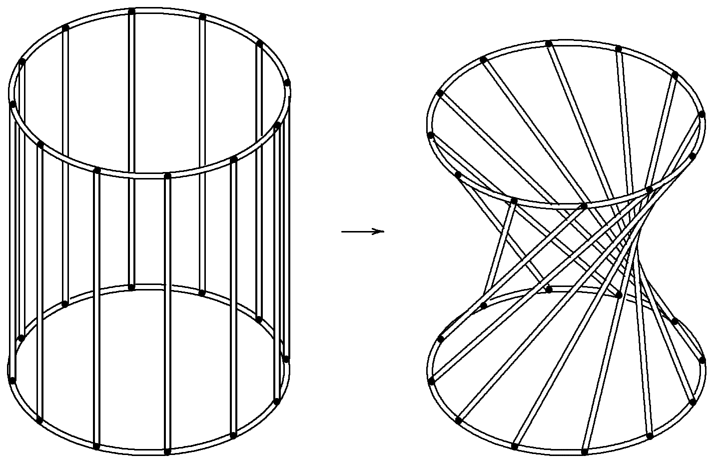

FIGURE 16.4. Twisting a cylinder provides a ruling of a hyperboloid

Moreover, there exists a *second ruling* of the same surface: just rotate the hoop by the same angle in the opposite direction, see Figure 16.5 for a picture of both rulings (in fact, we shall get the mirror image of our hyperboloid, but being a surface of revolution, it is symmetric in any plane through the axis, and hence coincides with its mirror image). To obtain the hyperboloid described by the equation above one needs to make a special choice of the size of the cylinder and the angle of rotation; we leave details to the reader.

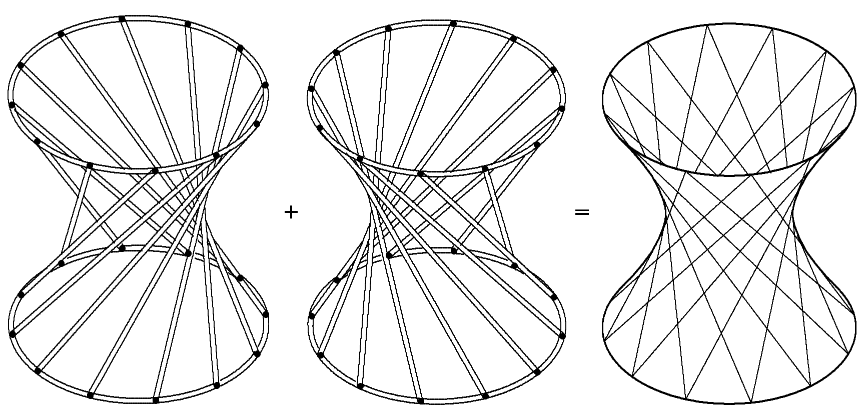


FIGURE 16.5. A one-sheeted hyperboloid is doubly ruled

One more example: a *hyperbolic paraboloid*. This can be described by a very simple equation:

$$z = xy$$

(Figure 16.6, left). It resembles a horse saddle, or a landscape near a mountain pass. The easiest way to construct a ruling of this surface is to take its intersections with planes $x = c$ parallel to the $yz$ plane. The intersection is given (in the coordinates $y, z$ in the plane $x = c$) by the equation $z = cy$; it is a straight line. Again, this surface has another ruling: take its intersections with the planes $y = c$ (Figure 16.6, right).

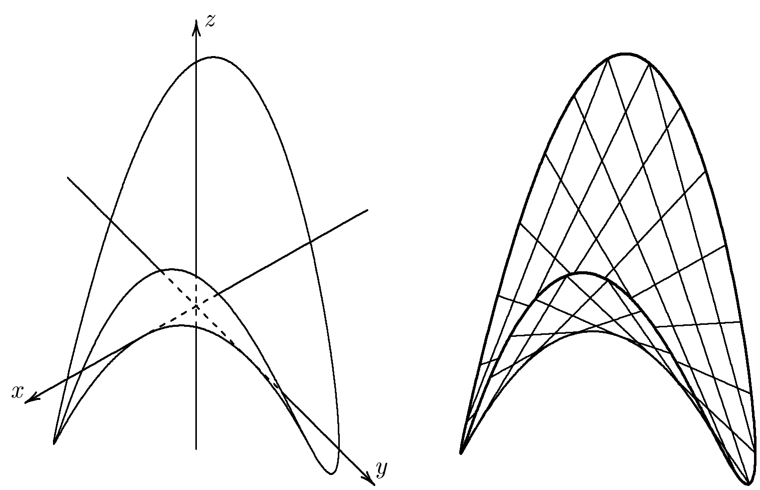


FIGURE 16.6. A hyperbolic paraboloid

**16.4 Doubly ruled surfaces.** The two surfaces described above are *doubly ruled* which means that for every point $A$ of any of these surfaces, there are two different lines, $\ell_1$ and $\ell_2$, through $A$ contained in the surface. One can obtain further examples of doubly ruled surfaces by compressing the previous surfaces toward planes, or stretching them from planes. Speaking more formally, there are doubly ruled surfaces described by the equations $x^2 + y^2 - z^2 = 1,\ z = xy$ in arbitrary, not necessarily rectangular, coordinate systems. What is amazing, is that *there are no other doubly ruled surfaces* (we shall give a more precise statement below). But we shall begin with a proposition which more or less rules out triply ruled surfaces.

**16.5 There are no non-planar triply ruled surfaces.** A triply ruled surface should be defined as a surface such that for any point there exist three different lines through this point contained in the surface. We want to prove that, essentially, a triply ruled surface should be a plane. We begin with a statement that a much milder condition imposes a devastating restriction on the geometry of a surface.

THEOREM 16.1. *Let $S$ be a ruled surface, and let $A \in S$ be a point such that there are three different lines $\ell_1, \ell_2, \ell_3$ through $A$ contained in $S$. Then either $S$ contains a planar disc centered at $A$, or $S$ consists of straight lines passing through $A$.*

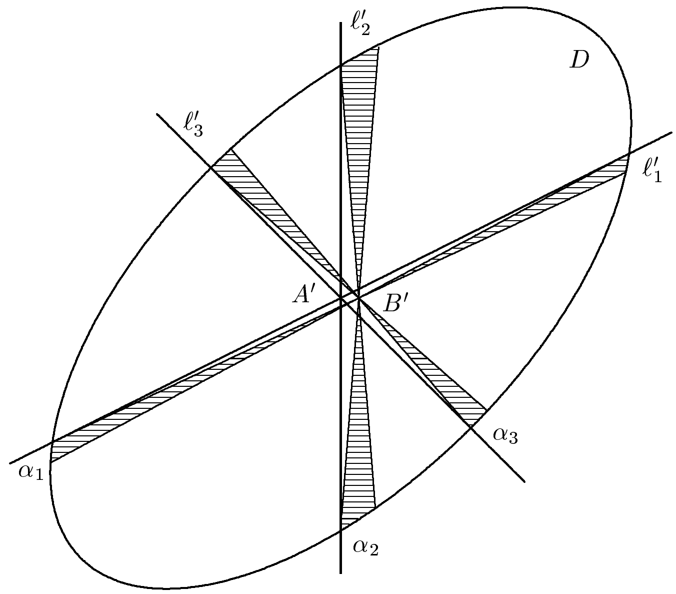


FIGURE 16.7. The angles $\alpha_1, \alpha_2, \alpha_3$ are disjoint

Proof. According to the definition of a surface, a piece of $S$ around $A$ has a $1-1$ projection onto a domain $D$ in a plane $P$. Denote by $A', \ell'_1, \ell'_2, \ell'_3$ the projections of $A, \ell_1, \ell_2, \ell_3$ onto $D$. Take a point $B$ in $S$, sufficiently close to $A$ and such that the line $BA$ does not belong to the surface (if no such point exists, then the surface $S$ consists of lines passing through $A$). Let $\ell$ be a line through $B$ (not passing through $A$) contained in $S$. Let $B', \ell'$ be projections of $B, \ell$ onto the plane $P$. Then, if $B$ is sufficiently close to $A$, the line $\ell'$ must intersect, within our domain $D$, at least two of the lines $\ell'_1, \ell'_2, \ell'_3$. (Indeed, if $B'$ is sufficiently close to $A'$, then lines through $B'$ which do not intersect $\ell'_1$ in $D$ form a small angle $\alpha_1$ at $B'$, and similar small angles, $\alpha_2$ and $\alpha_3$, arise for $\ell'_2$ and $\ell'_3$ – see Figure 16.7. These three angles are disjoint, so a line through $B'$ can miss, in $D$, at most one of the lines $\ell'_1, \ell'_2, \ell'_3$.) Let $\ell'$ cross $\ell'_1$ and $\ell'_2$. Then $\ell, \ell_1, \ell_2$ also cross each other in three different points and, in particular belong to some plane, $Q$. Moreover, for every point $C \in S$ sufficiently close to $A$, the line in the surface through $C$ must cross, in two different points, at least two of the lines $\ell, \ell_1, \ell_2$ (the proof is identical to the previous proof), and, hence $C$ also belongs to $Q$. □

COROLLARY 16.2. *Locally, a triply ruled surface is a plane; that is, for every point of a triply ruled surface, there is a planar disc centered at this point and contained in the surface.*

Proof. According to Theorem 16.1, the surface, in a proximity of $A$, is either planar, or conical. But it is obvious that if a conical surface with the vertex at $A$ contains a line not passing through $A$, then it is planar. □

(A better looking statement, which we leave to the reader to understand and to prove, says that every *connected* triply ruled surface is a plane.)

Our next goal is to describe all doubly ruled surfaces in space. For this purpose, we have to consider one very special class of surfaces.

**16.6 Surfaces generated by triples of lines.** Imagine that you have a job of writing problem sections for textbooks in mathematics. Imagine further that your assignment is to compose problems for a chapter dealing with equations of lines and planes in space. Say, you write: find an equation of a plane passing through three given points. It is a "good" problem: it always has a solution, and this solution is usually unique (it is unique, unless, by accident, the three point are "collinear", that is, belong to one line). The problem, however, will not be good, if you give four points (the problem, usually, will have no solutions) or two points (there will be infinitely many solutions). Or a problem requires to find an equation of a plane through a given point parallel to – how many? – given lines. The answer to "how many?" is two: you take lines parallel to the given lines through the given point, and if there are two lines, they determine (if they do not coincide) a unique plane. Just for fun, think about the following problem: find a line (in space) crossing – how many? – given lines. How many lines should we give to make the problem good? We shall give the answer in the end of Section 16.7, so that you have time to think about it. And for the time being, we shall consider a simpler problem.

PROPOSITION 16.1. *Let $A, \ell_1, \ell_2$ be a point and two lines in space such that $A$ does not belong to either $\ell_1$ or $\ell_2$ and all three do not belong to one plane. Then there exists a unique line through $A$ which is coplanar with (that is, crossing or parallel to) both $\ell_1$ and $\ell_2$.*

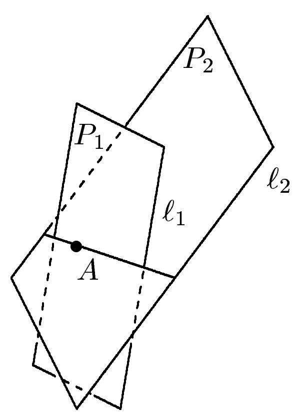


FIGURE 16.8. Proof of Proposition 16.1

Proof. (See Figure 16.8.) Let $P_1$ be the plane containing $A$ and $\ell_1$ and $P_2$ be the plane containing $A$ and $\ell_2$. The assumptions in the Proposition imply that such planes $P_1, P_2$ exist, are unique and different. Since they are not parallel (both contain $A$), their intersection is a line. This line $\ell$ satisfies the conditions of the proposition, and such a line is unique, because it must belong to both $P_1$ and $P_2$. □

As an immediate application, we single out a property of the two doubly ruled surfaces considered in Section 16.3. Obviously, a line belonging to the first family of lines (first ruling) of the one-sheeted hyperboloid is coplanar with any line of the second family. Take any three lines, $\ell_1, \ell_2, \ell_3$, from the first family. Then the second family consists precisely of the lines coplanar with all three. Indeed, all the lines of the second family have this property, so we only need to show that any line $\ell$ with this property belongs to this family. Let $\ell$ cross the line, say, $\ell_1$ at a point $A$ (it cannot be parallel to all three). There is a line of the second family through $A$. It must be coplanar with $\ell_2$ and $\ell_3$, so it must be $\ell$, since a line with this property is unique. Thus, the one-sheeted hyperboloid is the union of all lines coplanar to any three pairwise skew lines contained in the hyperboloid. Precisely the same is true (and is proved in the same way) for the hyperbolic paraboloid (with an additional remark that no two lines on the hyperbolic paraboloid are parallel).

**16.7 Equations for surfaces generated by triples of lines.** Let $\ell_1, \ell_2, \ell_3$ be three pairwise skew (not coplanar) lines in space. Consider straight lines coplanar to all these three lines. Actually, according to Proposition 16.1, there is one such line passing through every point of $\ell_3$, and there is one more line, parallel to $\ell_3$ and crossing $\ell_1$ and $\ell_2$. The union $S$ of all such lines is a ruled surface (we shall not check that it is a surface, since it will follow from further results). We shall call $S$ a surface generated by the lines $\ell_1, \ell_2, \ell_3$.

THEOREM 16.3. *Let $S$ be a surface generated by pairwise skew lines $\ell_1, \ell_2, \ell_3$.*
(1) *If the lines $\ell_1, \ell_2, \ell_3$ are not parallel to one plane, then $S$ is described in some (possibly, skew) coordinate system by the equation $x^2 + y^2 - z^2 = 1$.*
(2) *Otherwise, $S$ is described in some coordinate system by the equation $z = xy$.*

Proof. Let us begin with Part (1). Let the lines $\ell_1, \ell_2, \ell_3$ be not parallel to one plane.

LEMMA 16.2. *There exists a coordinate system with respect to which the lines are described by the equations*

$$\begin{array}{ll}(\ell_1) & x = -z, y = 1,\\ (\ell_2) & x = z, y = -1,\\ (\ell_3) & x = 1, y = z\end{array}$$

*(that is, consist of points $(t, 1, -t), (t, -1, t), (1, t, t)$).*

Proof of Lemma. Let $\ell_i', i = 1, 2, 3$, be a line parallel to $\ell_i$ and crossing the two remaining lines $\ell_j, j \neq i$. (This line exists and is unique. Indeed, choose $j \neq i$ and take the plane $P$ formed by lines, parallel to $\ell_i$ and crossing $\ell_j$. This plane is not parallel to the third line, $\ell_k$, otherwise it is parallel to all three lines. Let $C$ be the intersection point of $P$ and $\ell_k$. The line through $C$ parallel to $\ell_i$ crosses both $\ell_i$ and $\ell_j$; it is $\ell_i'$.) The lines $\ell_1, \ell_2', \ell_3, \ell_1', \ell_2, \ell_3'$ form a spatial hexagon with parallel opposite sides. We denote its vertices by $ABCDEF$ (where $A$ is the intersection point of $\ell_1$ and $\ell_2'$, $B$ is the intersection point of $\ell_2'$ and $\ell_3$, etc. – see Figure 16.9, left). The opposite sides of this hexagon are parallel (as we already mentioned), but also have equal lengths: we have

$$\overrightarrow{AD} = \overrightarrow{AB} + \overrightarrow{BC} + \overrightarrow{CD} = \overrightarrow{AF} + \overrightarrow{FE} + \overrightarrow{ED},$$

and, since a presentation of a vector as a sum of vectors collinear to $\ell_1, \ell_2, \ell_3$ is unique, one must have $\overrightarrow{AF} = \overrightarrow{CD}, \overrightarrow{AB} = \overrightarrow{ED}, \overrightarrow{BC} = \overrightarrow{FE}$.

This implies that the hexagon $ABCDEF$ is centrally symmetric; take its center of symmetry, $O$, for the origin of a coordinate system. For $\mathbf{e}_1$, take the vector from $O$ to the midpoint of $BC$; for $\mathbf{e}_2$ the vector $\overrightarrow{OA}$; for $\mathbf{e}_3$ the vector $\overrightarrow{OB} - \mathbf{e}_1 - \mathbf{e}_2$. In the coordinate system with the origin $O$ and coordinate vectors $\mathbf{e}_1, \mathbf{e}_2, \mathbf{e}_3$ the points $A, B, C, D, E, F$ will have coordinates as shown in Figure 16.9, right. We see that the points $F, A$ have coordinates satisfying the equations $x = -z, y = 1$, and hence the latter are the equations of the line $\ell_1$. Similarly the coordinates of $D, E$ satisfy the equations $x = z, y = -1$ and the coordinates of $B, C$ satisfy the equations $x = 1, y = z$, so these equations are those of lines $\ell_2$ and $\ell_3$. □

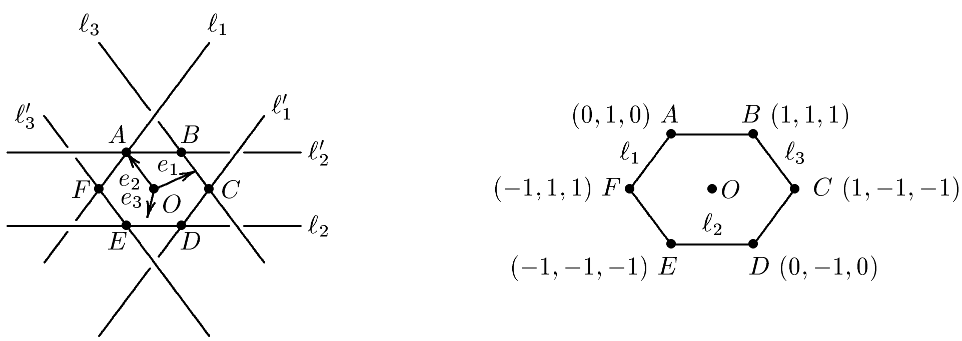


FIGURE 16.9. Proof of Lemma 16.2

Lemma 16.2 implies Part (1) of Theorem 16.3. Indeed, the lines in the Lemma obviously belong to the surface $S'$ presented (in our coordinate system) by the equation $x^2 + y^2 - z^2 = 1$; The points of $S'$ correspond to points of the one-sheeted hyperboloid (presented by the same equation in the standard coordinate system), and this correspondence takes lines into lines. Since the hyperboloid is the union of lines coplanar with any three pairwise skew lines on it, the same is true for $S'$, that is, $S'$ is the union of lines coplanar with $\ell_1, \ell_2, \ell_3$. Thus, $S'$ is $S$.

Turn now to Part (2). Let the lines $\ell_1, \ell_2, \ell_3$ lie in parallel planes, $P_1, P_2, P_3$. Assume also that $P_2$ lies between $P_1$ and $P_3$, and that the ratio of the distances from $P_1$ to $P_2$ and from $P_2$ to $P_3$ equals $a$.

LEMMA 16.3. *There exists a coordinate system in which the lines are described by the equations*

$$\begin{array}{ll} (\ell_1) & y = -a, z = -ax, \\ (\ell_2) & y = 0, z = 0, \\ (\ell_3) & y = 1, z = x. \end{array}$$

Proof of Lemma. Fix two lines, $m_1, m_2$, crossing the lines $\ell_1, \ell_2, \ell_3$ in the points $A_1, A_2; B_1, B_2; C_1, C_2$ respectively (see Figure 16.10, left). Take $B_1$ for the origin of the coordinate system and define coordinate vectors as $\mathbf{e}_1 = \overrightarrow{B_1B_2}, \mathbf{e}_2 = \overrightarrow{B_1C_1}, \mathbf{e}_3 = \overrightarrow{B_1C_2} - \mathbf{e}_1 - \mathbf{e}_2$. Then the coordinates of the points $B_1, B_2, C_1, C_2$ are as shown in Figure 16.10, right. Furthermore, since the lines $\ell_1, \ell_2, \ell_3$ lie in parallel planes,

$$\frac{|A_1B_1|}{|B_1C_1|} = \frac{|A_2B_2|}{|B_2C_2|} = a,$$

and hence the coordinates of the points $A_1, A_2$ are $(0,0,0) - a((0,1,0) - (0,0,0)) = (0,-a,0)$ and $(1,0,0) - a((1,1,1) - (1,0,0)) = (1,-a,-a)$. This implies that the lines $\ell_1, \ell_2, \ell_3$ have equations as stated. □

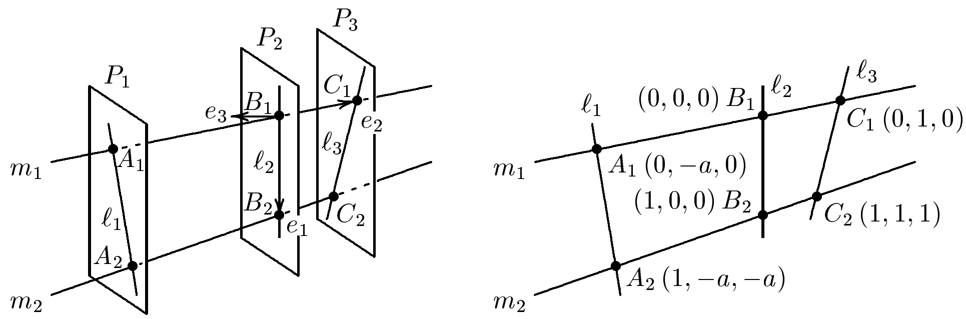


FIGURE 16.10. Proof of Lemma 16.3

Lemma 16.3 implies Part (2) of Theorem 16.3 precisely as Lemma 16.2 implies Part (1). □

In conclusion, let us answer the question left unanswered in the beginning of Section 16.6. If we want the problem of constructing a line coplanar with a certain number of skew lines to be good, the number of lines should be four. Indeed, the lines coplanar with the first three form a surface presented by an equation of degree 2. The fourth line intersects this surface in 2, or 1, or 0 points, and each of these points is contained in a line coplanar with the first three lines. Thus, the number of solution is 2, 1, or 0: just as for a quadratic equation.

### 16.8 There are no other doubly ruled surfaces.

THEOREM 16.4. *Let $S$ be a doubly ruled surface containing no planar discs. Then for every point $A$ in $S$ there exists a surface $S_0$ generated by three lines such that within some ball around $A$ the surfaces $S$ and $S_0$ coincide.*

REMARK 16.4. It may be deduced from Theorem 16.4 that any connected non-planar doubly ruled surface is generated by three skew lines, and hence, according to the previous theorem, is described, in some coordinate system by one of the equations $x^2 + y^2 - z^2 = 1$ or $z = xy$. We leave a proof of this statement to the reader.

Proof of Theorem 16.4. Since the surface is not planar, there are only two lines passing through $A$ and contained in $S$; let $\ell_1, \ell_2$ be these two lines.

A piece of the surface around $A$ has a $1-1$ projection onto a domain $D$ in a plane. Let $A', \ell_1', \ell_2'$ be the projections of $A, \ell_1, \ell_2$ (Figure 16.11, left). For a point $B$ in $S$, sufficiently close to $A$, any line through its image $B'$ in $D$ crosses either $\ell_1'$ or $\ell_2'$. Let $m_1, m_2$ be the two lines in $S$ through point $B$, and let $m_1', m_2'$ be their images in $D$. Then each of $m_1', m_2'$ crosses in $D$ one of $\ell_1', \ell_2'$. But neither of then can cross both: if, say, $m_1'$ crosses both $\ell_1', \ell_2'$, then the lines $m_1, \ell_1, \ell_2$ form a triangle, and the planar interior of this triangle should be contained in $S$ (any line through any point $C$ inside this triangle crosses the contour of this triangle in two points, and, hence, is contained in the plane of the triangle). For the same reason, the two lines $m_1', m_2'$ cannot cross the same line, $\ell_1'$ or $\ell_2'$. Thus, in some proximity of $A$, every line in $S$ through any point of $S$, not on $\ell_1$ and $\ell_2$, crosses precisely one of these lines.

This enables us to speak of two families of lines in $S$: lines crossing $\ell_2$ (including $\ell_1$) form "the first family", while lines crossing $\ell_1$ (including $\ell_2$) form "the second family". Obviously: (1) within each family, the lines do not cross each other; (2) every line of each family crosses every line of the other family; (3) the lines of each family cover the whole surface (a whole piece around $A$) – see Figure 16.11, right. This shows that the surface is generated (in a proximity of $A$) by any three lines of any of the two families. □

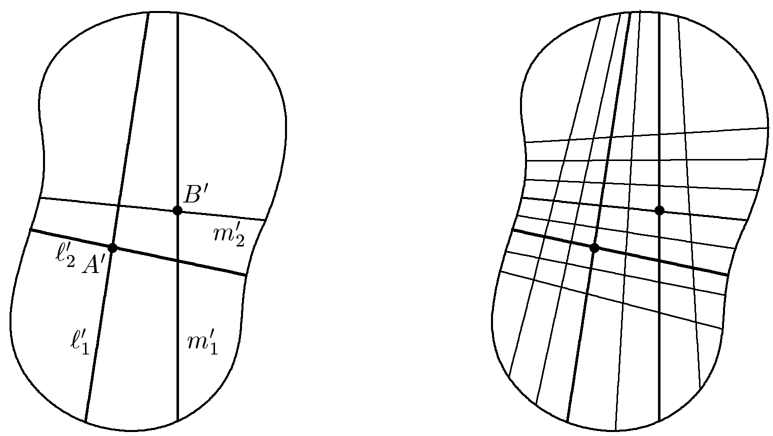


FIGURE 16.11. Proof of Theorem 16.4

Thus, at least locally, every non-planar doubly ruled surface is either a one-sheeted hyperboloid, or a hyperbolic paraboloid.

**16.9 Shadow theater.** In conclusion, we shall consider configurations of shadows of rulings of a doubly ruled surface on a flat screen. We shall restrict ourselves to the case of a one-sheeted hyperboloid made of two identical round hoops and a couple of dozens of identical rods representing the two rulings (see Figure 16.5). (See Exercise 16.6 for the case of a hyperbolic paraboloid.)

First assume that the rays of light are all parallel to each other (that is, the source of light is at infinity) and to one of the lines, say, $\ell$, on the hyperboloid. First ignore the hoops (that is, assume the lines very long and the distance from the screen very big). The shadow of $\ell$ will be one point (let it be $A$). One of the lines of the second family (say, $\ell'$) is parallel to $\ell$; its shadow will be also one point (say, $A'$). Any line from the first family, with the exception of $\ell$, will cross $\ell'$; hence its shadow will pass through $A'$. Similarly, the shadows of all the lines from the second family will pass through $A$. Hence, the shadows of all lines on the hyperboloid will be the lines on the screen passing through one of the points $A$ or $A'$ (but not through both) – see Figure 16.12.

Now, add the hoops. Their shadows will be equal ellipses $E_1, E_2$ (or circles, if we make them parallel to the screen; certainly, in this case the rays of light will not be perpendicular to the screen). Since both $\ell$ and $\ell'$ cross the hoops, the ellipses

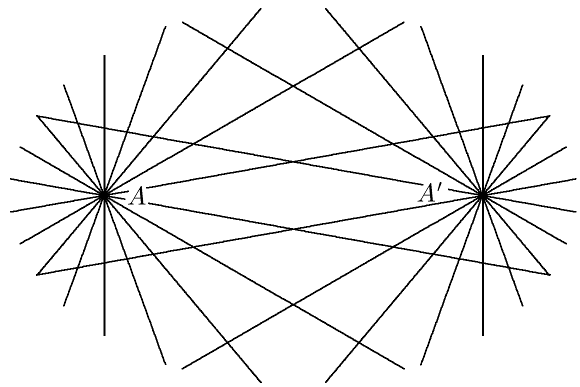


FIGURE 16.12. Shadows of rulings

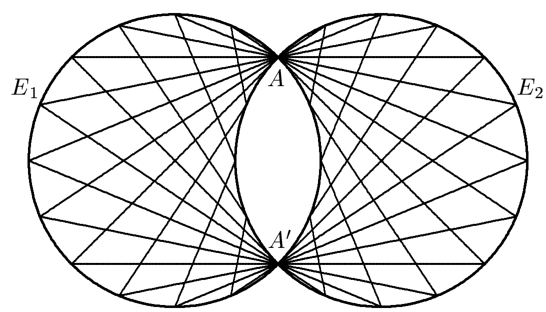


FIGURE 16.13. Shadows of hoops and rods

$E_1, E_2$ both pass through $A$ and $A'$. If $s$ is the shadow of the line $m$ of the second family, that is, $s$ passes through $A$, then $s$ crosses $E_1$ in two points, $A$ and $B$, and crosses $E_2$ in two points, $A$ and $B'$; the segment $BB'$ will be the shadow of the line $m$ between the hoops. In the same way, one can draw the shadows of the lines of the first family (between the hoops). See Figure 16.13.

Consider now a different configuration. Place a one point light source at a point $L$ on the hyperboloid, denote by $\ell$ and $\ell'$ the two lines through $L$ and make the screen parallel to $\ell$ and $\ell'$ (so the hyperboloid lies between the light source and the screen – see Figure 16.14).

The lines $\ell$ and $\ell'$ cast no shadow. Let $m \neq \ell$ be a line on the hyperboloid from the same family as $\ell$; it crosses $\ell'$ at some point $M$ (or is parallel to $\ell'$). The shadow of $m$ is the intersection line of the screen and the plane of $\ell'$ and $m$; in particular, it is parallel to $\ell'$. Similarly, the shadows of the lines of the second family are parallel to $\ell$. Thus, if we ignore the hoops, the configuration of the shadows will be that of two families of parallel lines (see Figure 16.15, left).

Now, let $A, A'$ be the intersection points of the lines $\ell, \ell'$ with the first hoop, and $B, B'$ be the intersection points of these lines with the second hoop. Of the two arcs $AA'$ of the first hoop, one does not produce any shadow; the shadow of the second (bigger) arc is one branch of a hyperbola with asymptotes parallel to $\ell$ and $\ell'$. The shadow of the big arc $BB'$ of the second hoop is one branch of a different

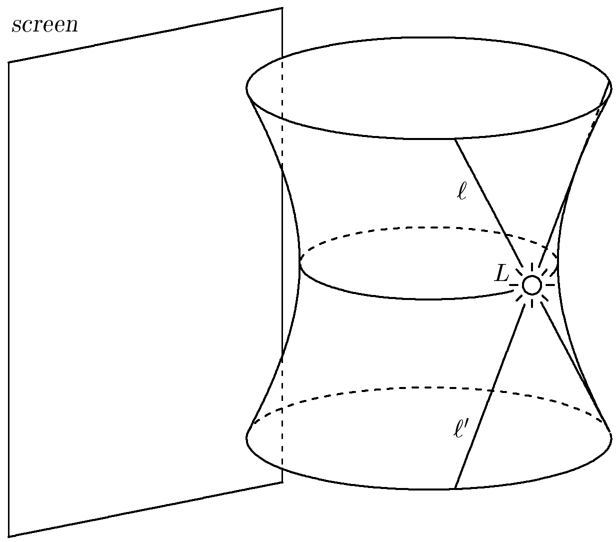


FIGURE 16.14. A projection from a point on the hyperboloid

hyperbola, also with asymptotes parallel to $\ell, \ell'$. The whole picture is presented on Figure 16.15, right. Notice that it is centrally symmetric: the center of symmetry is the shadow of the point $L'$ opposite to $L$ (in other words, the intersection point of the lines on the hyperboloid parallel to $\ell$ and $\ell'$.

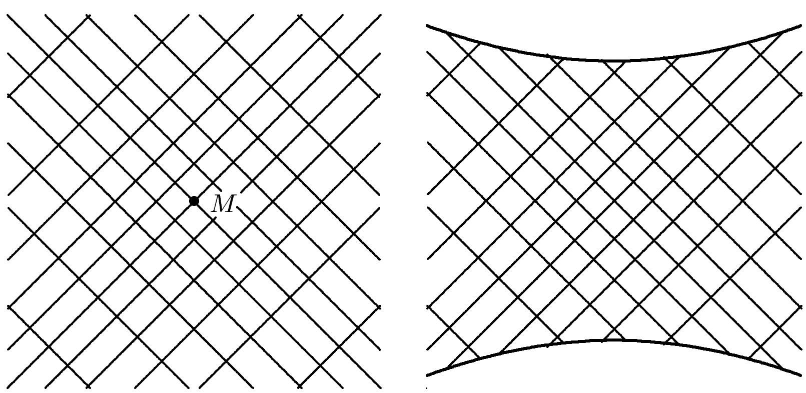


FIGURE 16.15. Shadows at the screen

### 16.10 Exercises.

16.1. Two points, $A$ and $B$ are moving at constant speeds along two skew lines in space. Which surface does the line $AB$ sweep?

16.2. Prove that any non-planar quadrilateral is contained in a unique hyperbolic paraboloid.

16.3. Let $ABCD$ be a spatial quadrilateral. Consider points $K, L, M, N$ on the sides $AB, BC, CD, DA$ such that $\dfrac{AK}{AB} = \dfrac{MD}{CD}$ and $\dfrac{BL}{BC} = \dfrac{NA}{DA}$. Prove that the segments $KM$ and $LN$ have a common point.

16.4. Let $\ell_1, \ell_2, \ell_3$ be three lines such that $\ell_1$ and $\ell_2$ are coplanar (but different) and $\ell_3$ is skew to both of them. What surface do the lines $\ell_1, \ell_2, \ell_3$ generate? (In other words, what is the union of all lines coplanar with all the three lines?)

*Hint*. Consider separately the cases when the line $\ell_3$ is parallel to the plane of the lines $\ell_1, \ell_2$ or crosses this plane.

16.5. Find all lines coplanar with the four lines

$$\begin{array}{ll} x = 1, & z = y; \\ x = 0, & z = 0; \\ x = -1, & z = -y; \\ x = y, & z = 4. \end{array}$$

16.6. A hyperbolic paraboloid is projected onto a screen in the direction parallel

(a) to one of the rulings;

(b) to the two planes to which all rulings are parallel.

How will the projections of all the rulings look like?

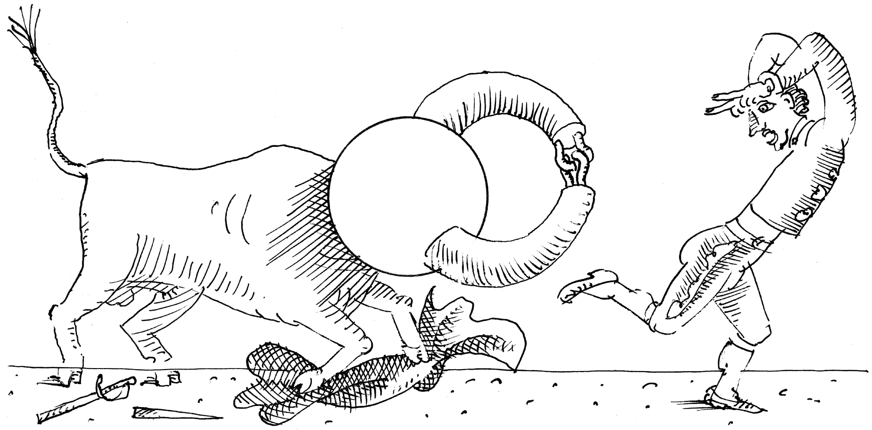

LECTURE 17

# Twenty Seven Lines

**17.1 Introduction.** We saw in Lecture 16 that some surfaces of degree 2 are totally made up of straight lines; moreover, they are *doubly ruled*. We remarked there that if we count not only real but also complex lines, then *all* surfaces of degree two, even spheres and paraboloids, become doubly ruled.

If we adopt an algebraic approach to geometry, then the next step after surfaces of degree 2 should be surfaces of degree 3. But while the geometry of surfaces (and, certainly, curves) of degree 2 was well understood by the Greeks millennia ago, the systematic study of surfaces (and curves) of degree 3 was not started before the 19-th century.

Now there are books dedicated to the "cubic geometry" (let us mention "The non-singular cubic surfaces" by B. Segre [**71**] and "Cubic forms" by Yu. Manin [**53**]). Cubic geometry is very much different from classical "quadratic geometry". In particular, cubic surfaces are not ruled, in general. But still they contain abundant, although finite, families of straight lines. (By the way, surfaces of degree $> 3$ usually do not contain any straight lines.) Geometers of the 19-th century, like Salmon and Cayley, found an answer to a natural question:

*How many straight lines does a surface of degree 3 contain?*

The answer is: twenty seven.

**17.2 "How many?" – is this a good question to ask?** The question makes sense in *algebraic geometry*, that is, in the geometry of curves and surfaces given by algebraic (polynomial) equations. Such curves and surfaces have *degrees*, which are the degrees of the polynomials.

For example, how many common points do two lines in the plane have? The right answer is 1, although it may be also 0 (if the lines are parallel) or $\infty$ (if they coincide). In the first case we may say that the point is "infinite" and still count it. So the result is 1 or $\infty$.

Consider now a curve of degree two. It may be an ellipse, a hyperbola, a parabola, or something more degenerate, like a pair of lines. We can say that a curve of degree 2 and a line have 2, 1, 0, or $\infty$ common points. But the cases of 1 or 0 are disputable. If there is only one point, this means that either we have a tangent, or two colliding points, or a line parallel to an asymptote of a hyperbola or the axis of a parabola; in these cases the "second point" is infinite. 0 means that we have complex points (points with complex coordinates satisfying the equations of both the line and of the curve), or both points at the infinity (this happens if our line is an asymptote of a hyperbola). But if we count each point as many times as it warrants and do not neglect complex or infinite solutions, then our answer is: 2 or $\infty$.

Similarly, curves of degrees $m$ and $n$ must have $mn$ or $\infty$ common points (the Bézout theorem).

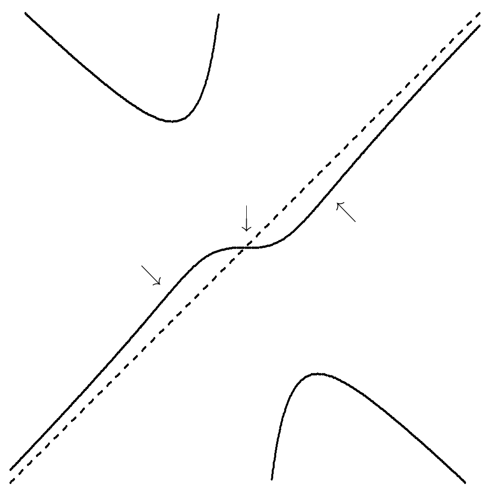

FIGURE 17.1. The curve $x^3 = x^2y + y^2$ with inflection points shown

Informally speaking, if a problem of algebraic geometry has finitely many solutions, then the number of solutions depends only on the degrees of curves and surfaces involved. Certainly, this becomes false if we are interested only in *real* solutions. What is worse, for some problems, it is never possible that all the solutions are real. For example, it is known that a curve of degree 3, not containing a straight line, has precisely 9 inflection points. But no more than 3 of them are real. A curve of degree 3 with 3 real inflection points is shown in Figure 17.1. (Another curve of degree 3 with 3 real inflection points is shown on Figure 18.6.) For the reader's convenience, we marked an asymptote of the curve and indicated the three inflection points by arrows.

**17.3 Main result.**

THEOREM 17.1. *A surface of degree* 3 *contains* 27 *or* $\infty$ *straight lines.*

**17.4 An auxiliary problem: double tangents.** A double tangent to a curve, or a surface, is a straight line that is tangent to the curve or surface at two different points. A point of tangency is counted as two (or more) intersection points of a line and a curve or a surface. Hence, curves or surfaces of degree $< 4$ never have double tangents that are not contained in them.

Important Observation. A double tangent to a surface of degree 3 is contained in this surface.

Consider now curves of degree 4 in the plane.

Question. How many double tangents does a curve of degree 4 have?

Answer: 28

We refrain from giving a full proof of this.[1] We restrict ourselves to constructing a curve of degree 4 with 28 *real, finite, different* double tangents. Consider the polynomial

$$p(x, y) = (4x^2 + y^2 - 1)(x^2 + 4y^2 - 1).$$

It has degree 4. The equation $p(x, y) = 0$ defines in the plane an "elliptic cross" (see Figure 17.2, left). The cross divides the plane into 6 domains. The function $p(x, y)$ is positive in the outer (unbounded) domain and in the central domain, and is negative in the petals. Choose a very small positive $\varepsilon$ and consider the curve $p(x, y) + \varepsilon = 0$, also of degree 4. It consists of four ovals within the petals of the previous cross.[2] These ovals are very close to the boundaries of the petals.

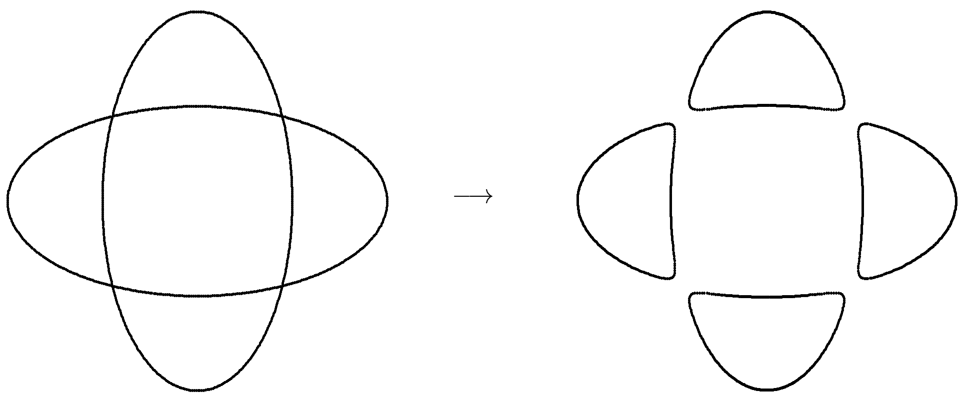

FIGURE 17.2. Construction of a curve

Every two ovals have (at least, but, actually, precisely) 4 common tangents: two exterior and two interior. Also the ovals are not convex (their shape is close to that of the petals), and each of them has a double tangent of its own. Total:

$$\binom{4}{2} \cdot 4 + 4 = 28.$$

**17.5 Surfaces of degree 3 and curves of degree 4.** Let $S$ be a surface of degree 3 given by the equation

$$p_3(x, y, z) + p_2(x, y, z) + p_1(x, y, z) + c = 0$$

where $p_1, p_2, p_3$ are homogeneous polynomials of degrees 1,2,3. Suppose that $0 = (0, 0, 0) \in S$, which means that $c = 0$. Consider a line passing through 0; it consists

[1] This can be deduced from the Plücker formulas, see Lecture 12.

[2] The term "oval" is used elsewhere in this book as synonymous to closed strictly convex smooth curve. In real algebraic geometry, an oval of an algebraic curve is its component that bounds a topological disc.

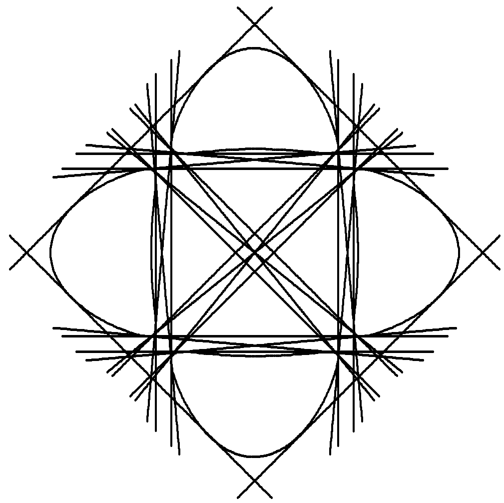

FIGURE 17.3. 28 double tangents

of points with proportional coordinates, say,

$$x = \alpha t, y = \beta t, z = \gamma t \qquad (\alpha, \beta, \gamma) \neq (0, 0, 0). \tag{17.1}$$

This line crosses $S$ at 0, and at two other points. Mark our line, if these two points coincide, that is, each marked line crosses $S$ at 0, tangent to $S$ at some point $T$, and has no common points with $S$, besides 0 and $T$. Consider intersections of the marked lines with a screen. We get a curve in the screen, denote it by $L$.

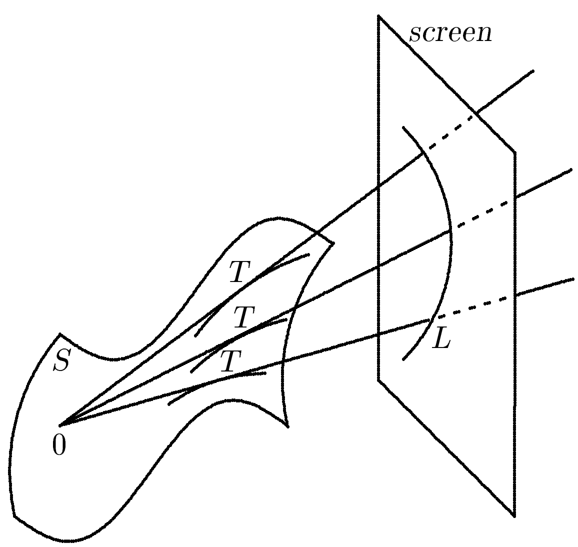


FIGURE 17.4. A projection of the surface on a screen

Thus, if $P \in L$, then the line through 0 and $P$ is tangent to $S$ at some point, $T(P) \in S$. Note that if $l$ is a tangent line to $L$ at $P$, then the plane $p$ containing 0 and $l$, is tangent to $S$ at $T(P)$.

Let us show now that the curve $L$ has degree 4. To find the intersection of the line (17.1) with $S$, plug (17.1) into the equation of $S$:

$$p_3(\alpha,\beta,\gamma)t^3 + p_2(\alpha,\beta,\gamma)t^2 + p_1(\alpha,\beta,\gamma)t = 0.$$

One solution of this equation is 0, the other two coincide if and only if

$$D(\alpha,\beta,\gamma) = p_2(\alpha,\beta,\gamma)^2 - 4p_3(\alpha,\beta,\gamma)p_1(\alpha,\beta,\gamma) = 0.$$

The intersection of the line (17.1) and the plane $z = 1$ corresponds to $t = \gamma^{-1}$ (if $\gamma = 0$, then there is no intersection; this possibility corresponds to the points of $L$ "at infinity"; there must be 4 such points). This intersection has the coordinates $(x, y, 1)$ where $x = \alpha/\gamma$, $y = \beta/\gamma$. The equation $D(\alpha,\beta,\gamma) = 0$ may be rewritten as $D(x, y, 1)\gamma^4 = 0$, that is, $D(x, y, 1) = 0$. This is an equation of degree 4.

Let now $l$ be one of the 28 double tangents to $L$, with the tangency points $P_1$ and $P_2$. The plane $p$ containing 0 and $l$ is tangent to $S$ at $T(P_1)$ and at $T(P_2)$. Hence, the line through $T(P_1)$ and $T(P_2)$ is tangent to $S$ at $T(P_1)$ and at $T(P_2)$, which is possible only if it is contained in $S$ (see Important Observation in Section 17.4). This proves our theorem modulo the last, and rather unexpected, question.

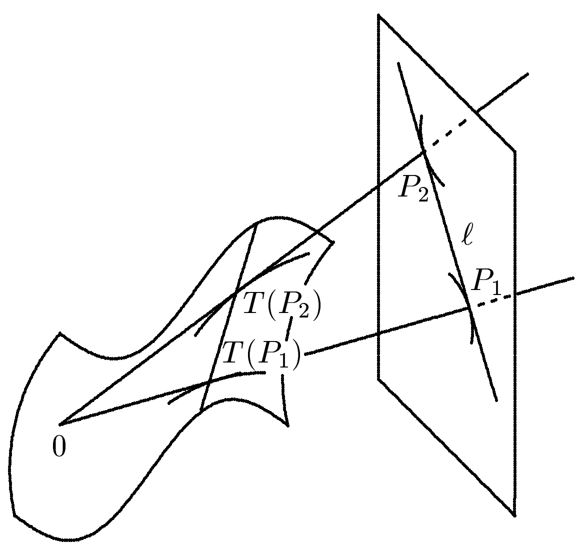


FIGURE 17.5. From double tangents to lines on the surface

**17.6 Twenty eight or twenty seven?** Seemingly, we have constructed 28 straight lines within $S$. Let us show that one of them is a mirage.

Who can swear that if $P = (x, y, 1) \in L$, then $T(P) \neq 0$? The equality $T(P) = 0$ holds, if and only if the line (17.1) has a triple intersection with $S$. This means that the equation

$$p_3(x, y, 1)t^3 + p_2(x, y, 1)t^2 + p_1(x, y, 1)t = 0$$

has three coinciding solutions, $t_1 = t_2 = t_3 = 0$, which happens if and only if $p_2(x, y, 1) = 0$ and $p_1(x, y, 1) = 0$. These two equations describe a line and a curve of degree two in the plane with coordinates $x, y$; so it has two solutions. Geometrically, this means that there are two lines intersecting $S$ only at 0: all the three intersection points merge. These two lines generate the tangent plane $p_0$ to $S$ at 0; they intersect the plane $z = 1$ at two points of the curve $L$, and the plane $p_0$ intersect the plane $z = 1$ in a line tangent to $L$ at these two points. This double tangent to $L$ does not correspond to any line in $S$. Thus, we have "only" $28-1 = 27$ lines in $S$.

**17.7 All these lines can be real.** Consider the surface

$$4(x^3 + y^3 + z^3) = (x + y + z)^3 + 3(x + y + z). \tag{17.2}$$

It is shown in Figure 17.6; the vertical axis in this picture is the "diagonal" $x = y = z$.

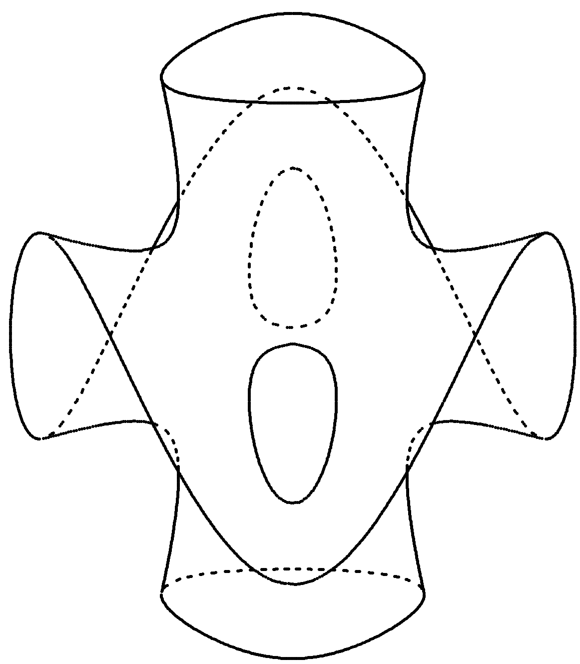

FIGURE 17.6. A cubic surface (17.2)

THEOREM 17.2. *The surface* (17.2) *contains* 27 *real straight lines.*

All 27 lines on the surface (17.2) are shown in Figure 17.7 – you can try to count them. Still this figure looks rather messy, but the proof of Theorem 17.2 given below may shed some light on the construction of the lines and their behavior.

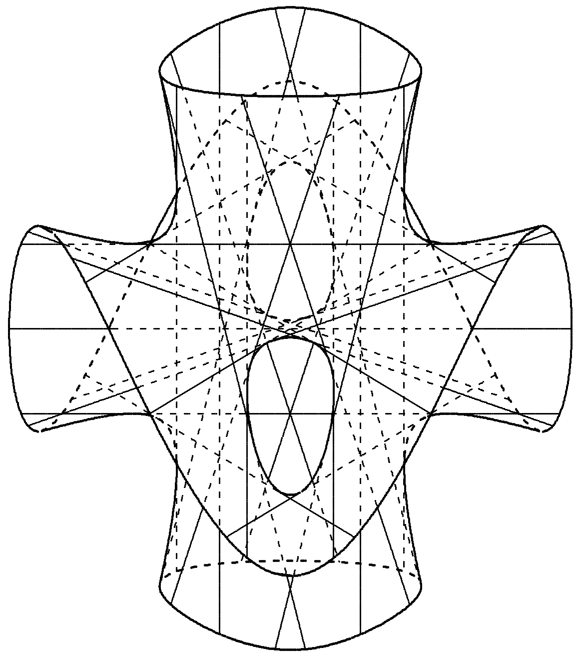

FIGURE 17.7. The surface with 27 lines

Proof. Nine of the lines are obvious:

$$(\mathbf{1})\begin{cases}x=0\\y=-z\end{cases}\quad(\mathbf{2})\begin{cases}y=0\\z=-x\end{cases}\quad(\mathbf{3})\begin{cases}z=0\\x=-y\end{cases}$$
$$(\mathbf{4})\begin{cases}x=1\\y=-z\end{cases}\quad(\mathbf{5})\begin{cases}y=1\\z=-x\end{cases}\quad(\mathbf{6})\begin{cases}z=1\\x=-y\end{cases}$$
$$(\mathbf{7})\begin{cases}x=-1\\y=-z\end{cases}\quad(\mathbf{8})\begin{cases}y=-1\\z=-x\end{cases}\quad(\mathbf{9})\begin{cases}z=-1\\x=-y\end{cases}$$

(each of these equations implies $x^3+y^3+z^3=x+y+z=(x+y+z)^3$). These lines lie in three parallel planes: $x+y+z=0,\ x+y+z=1,\ x+y+z=-1$; in the first of these planes the lines all meet at the point $(0,0,0)$, in the other two planes the lines form equilateral triangles.

For the remaining 18 lines we introduce, for further convenience, letter notation: $\mathbf{a},\mathbf{b},\dots,\mathbf{r}$. Six of these lines have simple equations:

$$(\mathbf{f})\begin{cases}x=0\\y=z+1\end{cases}\quad(\mathbf{j})\begin{cases}y=0\\z=x+1\end{cases}\quad(\mathbf{b})\begin{cases}z=0\\x=y+1\end{cases}$$
$$(\mathbf{g})\begin{cases}x=0\\y=z-1\end{cases}\quad(\mathbf{k})\begin{cases}y=0\\z=x-1\end{cases}\quad(\mathbf{c})\begin{cases}z=0\\x=y-1\end{cases}$$

(To find these equation, we consider the intersections of the surface (17.2) with the planes $x=0,\ y=0$ and $z=0$. Say, plug $x=0$ into the equation (2): $4(y^3+z^3)=(y+z)^3+3(y+z)$, hence $3x^3+3y^3=3yz(y+z)+3(y+z)$, hence either $y+z=0$, or $y^2=yz+z^2=yz+1$, that is $(y-z)^2=1,\ y-z=\pm1$. One of the three equation obtained is that of the line ($\mathbf{1}$), the other two are ($\mathbf{f}$) and ($\mathbf{g}$). The cases $y=0,z=0$ are treated in a similar way.)

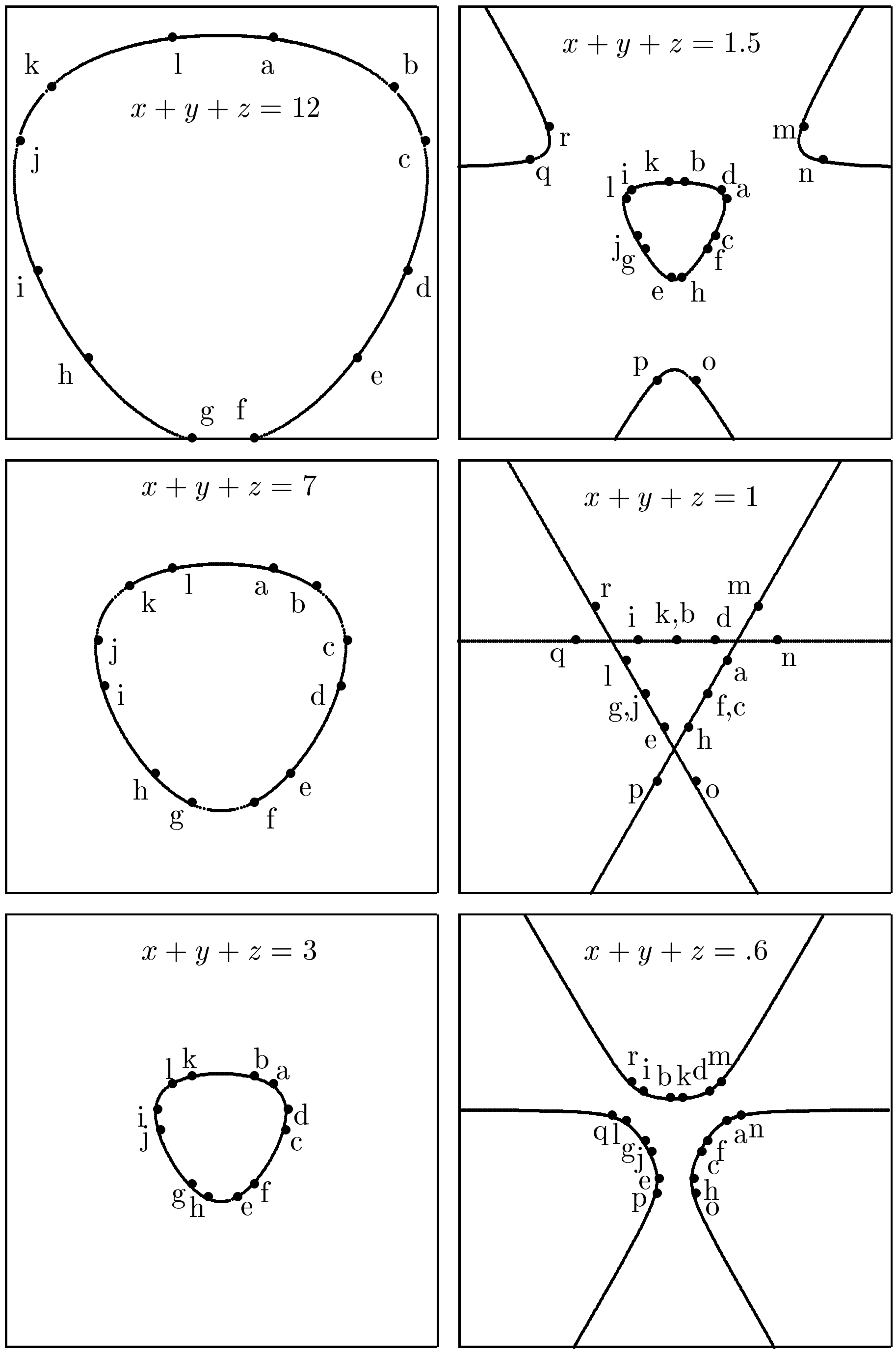


Figure 17.8. Sections of the surface (17.2)

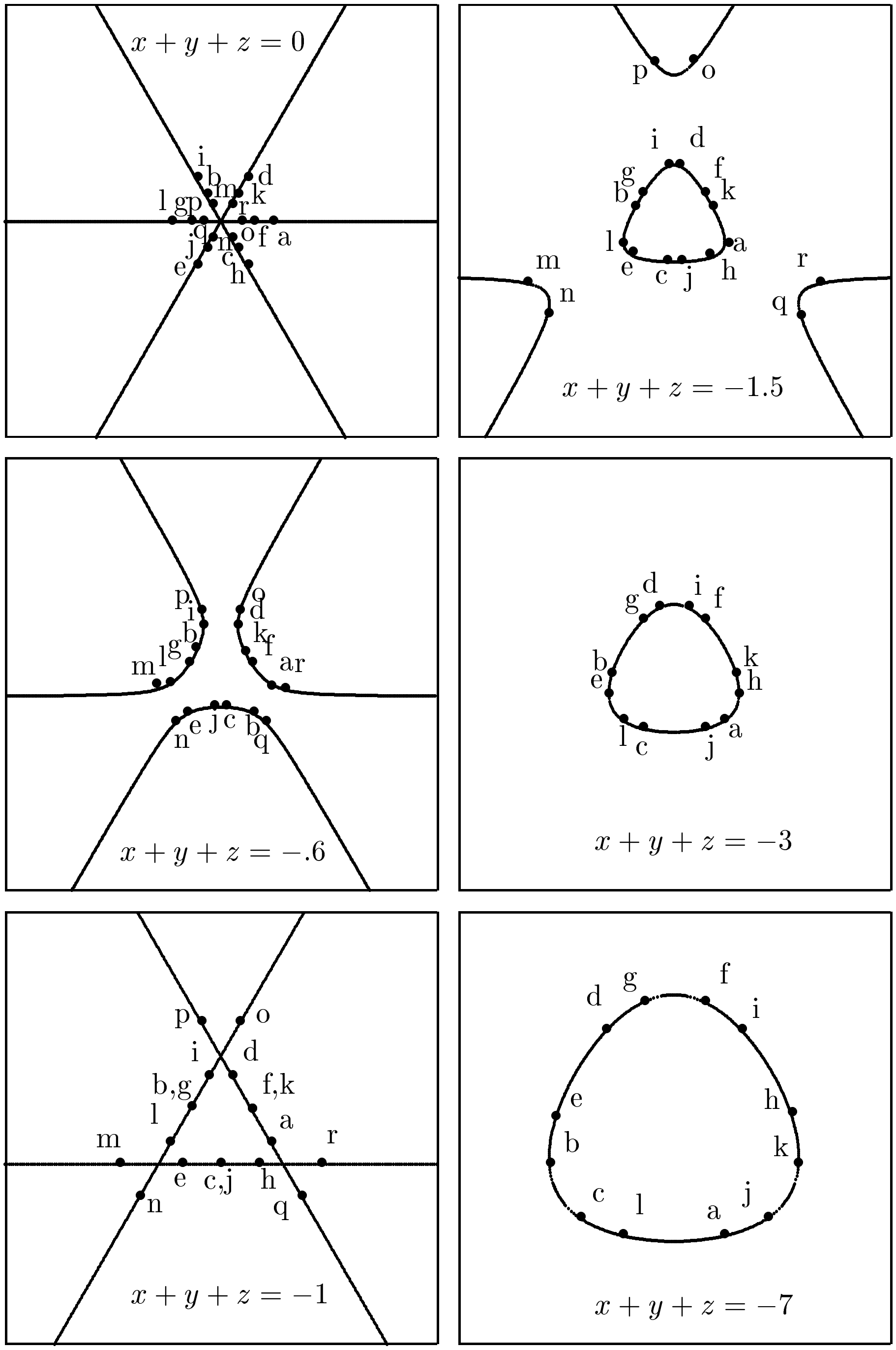


FIGURE 17.9. Sections of the surface (17.2), continued

The equations of the remaining 12 lines involve the "golden ratio" $\varphi = \dfrac{1+\sqrt{5}}{2}$. The equations are:

$$(\mathbf{a}) \begin{cases} x = \varphi(y+z) \\ y = z+\varphi \end{cases} \quad (\mathbf{e}) \begin{cases} y = \varphi(z+x) \\ z = x+\varphi \end{cases} \quad (\mathbf{i}) \begin{cases} z = \varphi(x+y) \\ x = y+\varphi \end{cases}$$
$$(\mathbf{l}) \begin{cases} x = \varphi(y+z) \\ y = z-\varphi \end{cases} \quad (\mathbf{d}) \begin{cases} y = \varphi(z+x) \\ z = x-\varphi \end{cases} \quad (\mathbf{h}) \begin{cases} z = \varphi(x+y) \\ x = y-\varphi \end{cases}$$

and

$$(\mathbf{o}) \begin{cases} x = -\varphi^{-1}(y+z) \\ y = z+\varphi^{-1} \end{cases} \quad (\mathbf{q}) \begin{cases} y = -\varphi^{-1}(z+x) \\ z = x+\varphi^{-1} \end{cases} \quad (\mathbf{m}) \begin{cases} z = -\varphi^{-1}(x+y) \\ x = y+\varphi^{-1} \end{cases}$$
$$(\mathbf{p}) \begin{cases} x = -\varphi^{-1}(y+z) \\ y = z-\varphi^{-1} \end{cases} \quad (\mathbf{r}) \begin{cases} y = -\varphi^{-1}(z+x) \\ z = x-\varphi^{-1} \end{cases} \quad (\mathbf{n}) \begin{cases} z = -\varphi^{-1}(x+y) \\ x = y-\varphi^{-1} \end{cases}$$

(we leave plugging these 12 equations into the equation (17.2) and verifying that these lines lie on the surface to the reader).

The diagrams in Figures 17.8, 17.9 show the sections of our surface by 12 different planes of the form $x+y+z = \text{const}$ (centered at the point with $x = y = z$). The traces of the lines (**a**) − (**r**) are also shown. You can see that in each of the domains $x+y+z > 1$ and $x+y+z < 1$ the surface consists of a "central tube" and three "wings". In the domain $-1 \le x+y+z \le 1$ these wings and the tube merge together; there are 9 lines, (**1**) − (**9**), contained in this domain. Of the remaining 18 lines, 6 (three pairs of parallel lines, (**m**) − (**r**)) lie on the wings, and 12 (six pairs of parallel lines, (**a**) − (**l**)) lie on the central tube. The configuration of these lines is shown in Figure 17.10. □

**17.8 Some other surfaces.** There are other cubic surfaces with ample families of real lines. We will briefly discuss some of them.

Consider the family of surfaces

$$x^3 + y^3 + z^3 - 1 = \alpha(x+y+z-1)^3. \tag{17.3}$$

Theorem 17.3. *If $\alpha > \dfrac{1}{4}$ and $\alpha \neq 1$, then the surface* (17.3) *contains 27 real lines.*

Proof. Three lines are obvious: $\{x = 1, y = -z\}$ and two more obtained by switching $x$ with $y$ and $z$. Four more are $\{x = u, y+z = 0\}$, $\{x = 1, y+uz = 0\}$ where $u$ is one of the solutions of the quadratic equation

$$(\alpha-1)(u-1)^2 = 3u$$

and eight more are again obtained by switching $x$ with $y$ and $z$. Finally, four more are $x + v^2(y+z) = 0, y - z = 2v - v^3(y+z)\}$ where $v$ is one of four solutions of the equation

$$(4\alpha-1)(v^2-1)^2 = 3v^2$$

and, once again, eight more are obtained by switching $x$ with $y$ and $z$. The total is 27. □

In the case $\alpha = 1/4$, the equation (17.3) determines a surface with "singular points $(1,1,1), (1,-1,-1), (-1,1,-1), (-1,-1,1)$ (in a neighborhood of each of these points the surface looks like a cone; by the way, this "surface" is not a surface in the sense of definition given in Lecture 15.2). There are only 9 lines on this

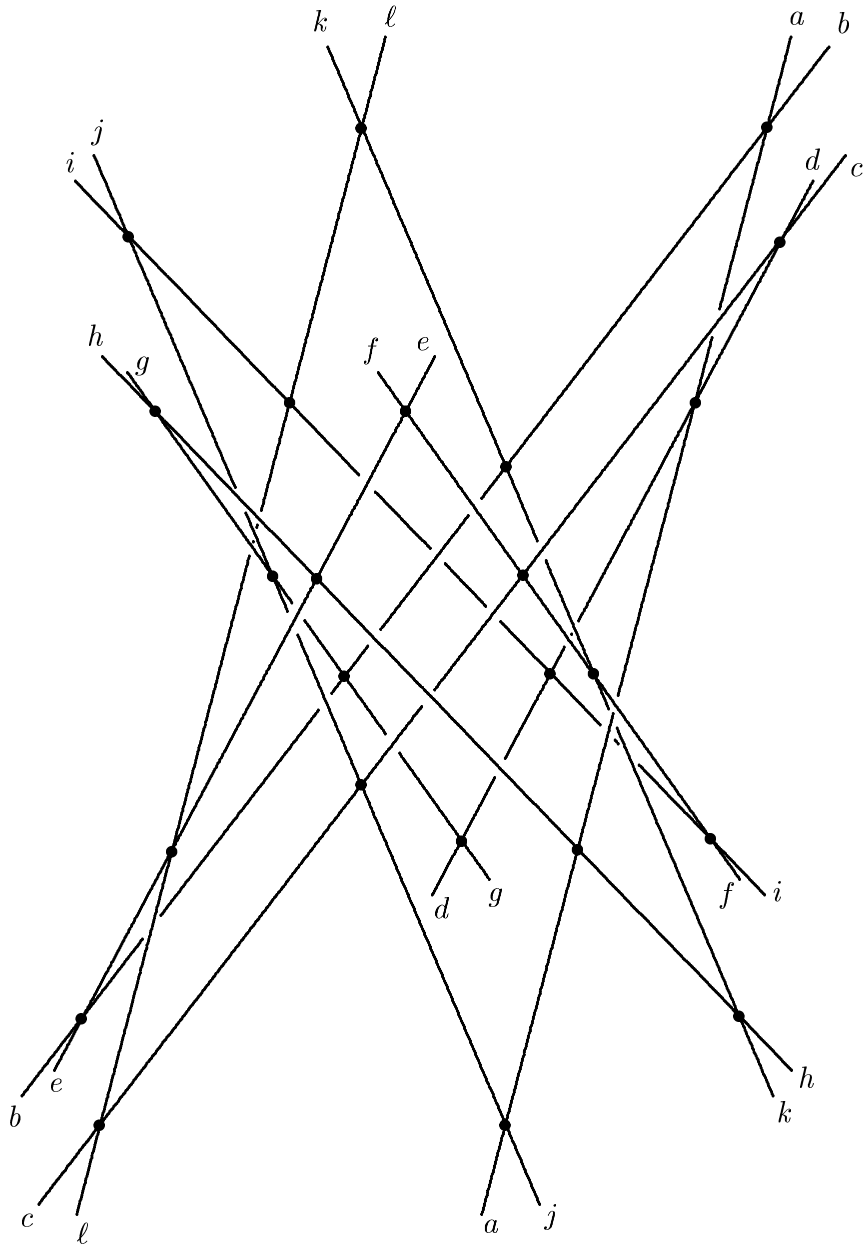


FIGURE 17.10. Lines on the tube

surface: $\{x = 1, y = z\}$, $\{x = 1, y = -z\}$, $\{x = -1, y = -z\}$, and 6 more can be obtained by switching $x$ with $y$ and $z$.

The case $\alpha = 1$ is especially interesting. To make this surface more attractive, it is reasonable to take a (non-rectangular) coordinate system such that the points $(0, 0, 0), (1, 0, 0), (0, 1, 0), (0, 0, 1)$ (belonging to the surface) are vertices of a regular tetrahedron. Then all the symmetries of space which take the tetrahedron into itself also take the surface into itself. We leave the work of finding the equations of the lines in this surface to the reader (see Exercise 17.1).

**17.9 The configuration of the 27 lines.** One can easily see in Figures 17.8, 17.9, and still better, in Figure 17.10, that there are many crossings between the 27 lines. Actually, these crossings obey very strict rules, the same for all cubic surfaces. As usual, we shall not make a difference between crossing and parallel lines, so we shall speak rather of coplanar, than crossing, lines. The first property is obvious.

THEOREM 17.4. *If some two of the lines in our surface are coplanar then there exists a unique third line in our surface belonging to the same plane.*

Proof. The intersection of a cubic surface with a plane is a cubic curve in the plane, that is, it may be presented by an equation of degree three. If this intersection contains two different lines, then the equation of the curve is divisible by the equations of the lines, and, after division, we obtain an equation of degree one, which is the equation of the third line. □

The following theorem characterizes the coplanarity properties between the lines completely.

THEOREM 17.5. *Let $\ell_1$ be any of the* 27 *lines in a cubic surface $S$.*

(1) *There exists precisely* 10 *lines in $S$ coplanar with $\ell_1$; let us denote them by $\ell_2, \dots, \ell_{11}$. These* 10 *lines can be arranged into* 5 *pairs of mutually coplanar lines, $\ell_2, \ell_3;\ \ell_4, \ell_5; \dots; \ell_{10}, \ell_{11}$. No other two lines among $\ell_2, \dots, \ell_{11}$ are coplanar.*

(2) *Each of the remaining* 16 *lines, $\ell_{12}, \dots, \ell_{27}$, is coplanar with precisely one line of each of the pairs in* (1). *For any two of the lines $\ell_{12}, \dots, \ell_{27}$, the number of lines from $\ell_2$ to $\ell_{11}$, coplanar with both, is odd.*

(3) *Two of the lines $\ell_{12}, \dots, \ell_{27}$ are coplanar if and only if there is precisely one of the lines $\ell_2, \dots, \ell_{11}$ coplanar to both (that is, the odd number mentioned in Part* (2) *is one).*

It is remarkable that all these statements are true whichever of the 27 lines one takes for $\ell_1$.

We shall not prove this theorem, but for the surface in Section 17.7 it can be checked with the help of the diagrams (Figures 17.8, 17.9, 17.10) and/or equations. For example, the line **a** is coplanar to each of the lines

$$(1), \mathbf{l};\ (5), \mathbf{h};\ (9), \mathbf{d};\ \mathbf{b}, \mathbf{r};\ \mathbf{j}, \mathbf{n}.$$

The 5 pairs in this formula are also shown. Any of the other lines is coplanar with one line from each pairs. For example:

the line **c** is coplanar with $\mathbf{l}, (5), \mathbf{d}, \mathbf{b}, \mathbf{j}$;
the line **f** is coplanar with $(1), (5), (9), \mathbf{r}, \mathbf{n}$;
the line **m** is coplanar with $\mathbf{l}, (5), \mathbf{d}, \mathbf{r}, \mathbf{n}$.

The quintuples for the lines **c** and **f** contain only one common line, (5), and the lines **c** and **f** are coplanar. On the contrary, the quintuples for the lines **c** and **m** contain 3 common lines, **l**, (5), and **d**, and the lines **c** and **m** are not coplanar.

Some other properties of the lines follow from Theorem 17.5. We leave them to the reader as exercises.

**17.10 Conclusion. Other enumerative problems in algebraic geometry.** Problems of computing the number of algebraic curves of a given degree (say, straight lines) intersecting some other curves and/or tangent to some other curves became very popular recently because of their importance in modern theoretical physics (more specifically, in the quantum field theory, see [**18, 44**]). We will discuss here briefly one such problem, interesting by an unexpected result and a dramatic 200 year long history.

**Question.** Given 5 conics (= ellipses, hyperbolas, parabolas), how many conics are tangent to all of them?

(Why 5? Because for 4 conics the number of conics tangent to them is infinite, and for a generic set of 6 conics, there are no conics tangent to all of them at all.)

This problem was first considered by Steiner (whose theorem is mentioned in Section 29.5), who published, in the beginning of 19-th century, his result: there are 7736 such conics. This result, however, seemed doubtful to many people. Several decades after Steiner's work, De Jonquières repeated Steiner's computations, and got a different result. But Steiner's reputation in the mathematical community was so high that De Jonquières did not dare to publish his work. Finally, the right answer was found, in 1864, by Chasles (whose other result is proved in Section 28.6); there are 3264 conics tangent to 5 given conics.

However, Chasles counted complex conics, and it remained unclear how many of them could be real. In 1997, Ronga, Tognoli and Vust found a family of 5 ellipses for which all 3264 tangent conics were real. And in 2005 Welschinger proved that for a family of 5 real conics whose interiors are pairwise disjoint at least 32 of the 3264 conics tangent to them are real.

John Smith
January 23, 2010

Martyn Green
August 2, 1936

Henry Williams
June 6, 1944

John Smith
January 23, 2010

Martyn Green
August 2, 1936

Henry Williams
June 6, 1944

**17.11 Exercises.**

17.1. Find the equations of all lines in the surface

$$x^3 + y^3 + z^3 - 1 = (x + y + z - 1)^3$$

*Hints.* (a) There are only 24 lines; the remaining three escape to infinity.

(b) There are three lines through each of the vertices of the tetrahedron described in Section 17.8; they are parallel to the three sides of the face, opposite to this vertex. This gives 12 lines.

(c) The equations of the remaining 12 lines involve the golden ratio.

17.2. Find straight lines on the surface

$$xyz + \beta(x^2 + y^2 + z^2) = \gamma.$$

17.3. Among the 27 lines on a cubic surface, there are precisely 45 coplanar triples of lines.

*Remark.* Some coplanar triples in Section 17.7 consist of lines passing through one point (there are 7 such triples) or mutually parallel (there are two such triples). These properties should be regarded as accidental, on a general cubic surface, these events do not happen.

17.4. The maximal number of mutually non-coplanar lines is 6. There are precisely 72 such 6-tuples.

17.5. The number of permutations of the 27 lines taking coplanar lines into coplanar lines is $51,840 = 2^7 \cdot 3^4 \cdot 5$. (These permutations form a group known in group theory as the group $E_6$.)

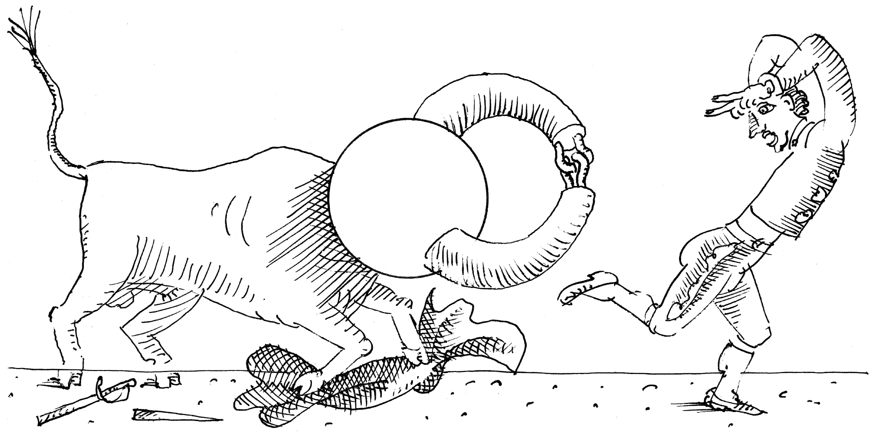

LECTURE 18

# Web Geometry

**18.1 Introduction.** This lecture concerns web geometry, a relatively recent chapter of differential geometry. Web geometry was created mostly by an outstanding German geometer W. Blaschke and his collaborators in the 1920s. Web geometry is connected by many threads with other parts of geometry, in particular, with the Pappus theorem discovered by Pappus of Alexandria in the 4th century A.D. A nice introduction to web geometry is a small book [**8**] by Blaschke (which unfortunately was never translated into English) and an article by his student, a great geometer of the 20-th century, S.-S. Chern [**14**].

In differential geometry, one is often concerned with local properties of geometrical objects. For example, we mentioned in Lecture 13 that a sheet of paper, no matter how small, cannot be bent so that it becomes part of a sphere. The invariant that distinguishes between the plane and the sphere is curvature, zero for the plane and positive for the sphere (cf. Lecture 20), and the allowed transformations are isometries (paper is not compressible or stretchable). In web geometry, the supply of allowed deformations is even greater: one does not insist on preserving the distances and considers all differentiable and invertible deformations of the plane.

**18.2 Definition and a few examples.** A $d$-web in a plane domain consists of $d$ families of smooth curves so that no two curves are tangent and through every point there passes exactly one curve from each family. We always assume that each family consists of level curves of a smooth function (this is a meaningful condition: see the example of osculating circles of a plane curve discussed in Lecture 10); note however that this function is not at all unique.

Two $d$-webs are considered the same if there is a smooth deformation of the domain that takes one to another.

For $d = 1$, there is nothing to study: one can deform the curves into horizontal lines. Likewise, if $d = 2$, one can deform both families so that they become horizontal and vertical lines. (Proof: if the families consist of the level curves of functions $f(x, y)$ and $g(x, y)$ then, in the new coordinates $X = f(x, y)$, $Y = g(x, y)$, the curves are horizontal and vertical lines.) Interesting things start to happen when $d = 3$.

Let us consider a few examples. The simplest 3-web consists of three families of lines

$$x = const, \quad y = const, \quad x + y = const.$$

This 3-web is called trivial.

Every 3-web consists of the level curves of three smooth functions $f(x, y)$, $g(x, y)$ and $h(x, y)$; since no two curves in the web are tangent, the gradients of any two of these functions are linearly independent. One has a simple triviality criterion for a 3-web.

LEMMA 18.1. *If functions $f, g, h$ can be chosen in such a way that*

$$f + g + h = 0 \tag{18.1}$$

*then the 3-web is trivial.*

Proof. As before, consider the new coordinates $X = f(x, y)$, $Y = g(x, y)$ in which the first two families consist of horizontal and vertical lines. Since $h = -f - g$, the third family has the equation $X + Y = const$. □

Our next example is a 3-web in the interior of triangle $A_1A_2A_3$. The curves of the $i$-th family ($i = 1, 2, 3$) consist of the circles that pass through vertices $A_i$ and $A_{i+1}$, see Figure 18.1 (we consider the indices mod 3: this convention makes sense of the notation, such as $A_{i+1}$, for $i = 3$).

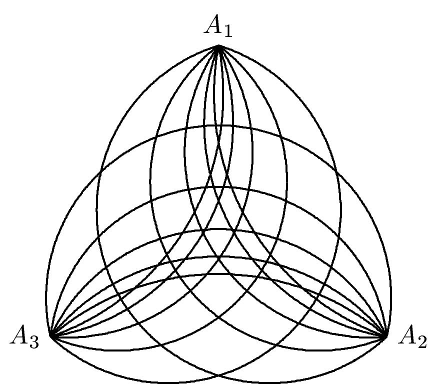


FIGURE 18.1. A 3-web consisting of circles passing through pairs of vertices of a triangle

A point $P$ inside a triangle is uniquely characterized by the angles $\alpha = A_1PA_2, \beta = A_2PA_3$ and $\gamma = A_3PA_1$. Since an angle supported by a fixed chord of a circle has a fixed measure, the three families of circles have the equations:

$$\alpha = const, \quad \beta = const, \quad \gamma = const.$$

Since $\alpha + \beta + \gamma = 2\pi$, one may take the functions

$$f = \alpha - 2\pi/3, \quad g = \beta - 2\pi/3, \quad h = \gamma - 2\pi/3$$

as defining the 3-web. These functions satisfy (18.1), and hence this 3-web is trivial.

Next example: the 3-web in the interior of the first quadrant that consists of horizontal lines, vertical lines and lines through the origin, see Figure 18.2. This web has the equations

$$x = const, \quad y = const, \quad y/x = const.$$

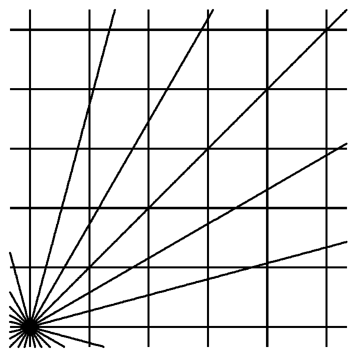

FIGURE 18.2. A 3-web consisting of the horizontal lines, the vertical lines and the lines through the origin

Another choice of defining functions is $\ln x, -\ln y$ and $\ln y - \ln x$. These three functions satisfy (18.1), and hence this 3-web is trivial as well.

Our next example is a modification of the previous one, see Figure 18.3. This 3-web inside a triangle $A_1A_2A_3$ is made of the families of lines through the vertices of the triangle. Is this web trivial?

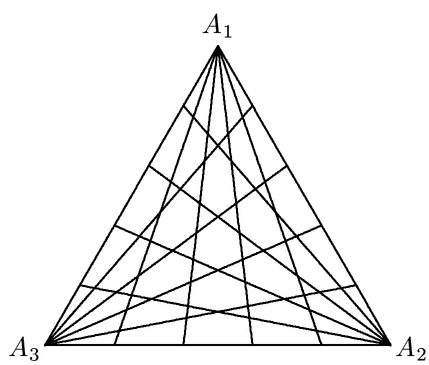


FIGURE 18.3. A 3-web consisting of the lines though the vertices of a triangle

Project the plane of the triangle $A_1A_2A_3$ on another plane, a screen, from a point $O$ so that the lines $OA_2$ and $OA_3$ are parallel to the screen. Then the lines through point $A_2$ project to parallel lines, and likewise for $A_3$. Hence the projection of the 3-web in Figure 18.3 is the one in Figure 18.2, and therefore trivial.

**18.3 Hexagonal webs.** The reader might have developed an illusion that all 3-webs are trivial. The truth is, a generic 3-web is not.

To see this, consider the configuration in Figure 18.4. Pick a point $O$ and draw the curves of the three families through it. Choose a point $A$ on the first curve, draw the curve from the second family through it until its intersection with the third curve through $O$ at point $B$, draw the curve from the first family through $B$ until its intersection with the second curve through $O$ at point $C$, etc. The final result of this spider-like activity is the point $G$ on the first curve. For a trivial 3-web, $G = A$; in general, not necessarily so.

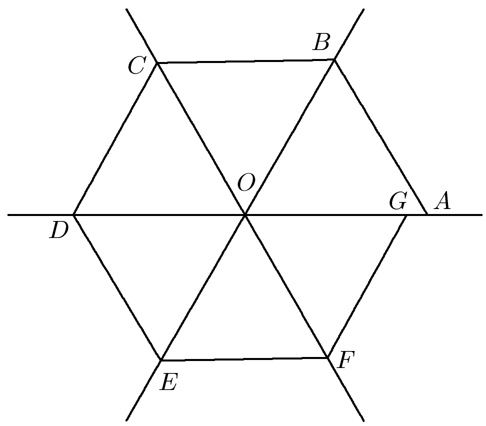


FIGURE 18.4. A hexagon in a 3-web

A 3-web for which the hexagon in Figure 18.4 always closes up is called *hexagonal*. A trivial 3-web is hexagonal. The converse is also true, see Exercise 18.5.

**18.4 Hexagonal rectilinear webs and cubic curves.** A *rectilinear* web is a web whose curves are straight lines, see the examples in Figures 18.2 and 18.3. In this section we shall describe hexagonal rectilinear 3-webs. This subject is closely related, somewhat unexpectedly, with a classical result in geometry, the Pappus theorem.

A generic 1-parameter family of lines consists of lines tangent to a curve; this was discussed in detail in Lectures 8 and 9. We have three such families, and they consist of lines tangent to three curves, say $\gamma_1, \gamma_2$ and $\gamma_3$.

Our web is assumed to be hexagonal, see Figure 18.5. Consider the dual configuration of points and lines (see Lecture 8 for a discussion of projective duality). This configuration is shown in Figure 18.5, right, where the points, dual to lines $AB, BC$, etc., are marked $AB, BC$, etc., and lines, dual to points $A, B, \ldots$ are marked $a, b, \ldots$. Points $AD, FE, BC$ lie on the dual curve $\gamma_1^*$, points $AF, CD, BE$ on the curve $\gamma_2^*$ and points $FC, AB, DE$ on the curve $\gamma_3^*$. Let us call a configuration of 6 lines and their 9 intersection points, as in Figure 18.5, a Pappus configuration.

We should like to know for which triples of curves $\gamma_1^*, \gamma_2^*$ and $\gamma_3^*$ one has a Pappus configuration inscribed into these three curves. A sufficient (and necessary – but we shall not prove it) condition is that $\gamma_1^*, \gamma_2^*$ and $\gamma_3^*$ are all parts of the same cubic curve.

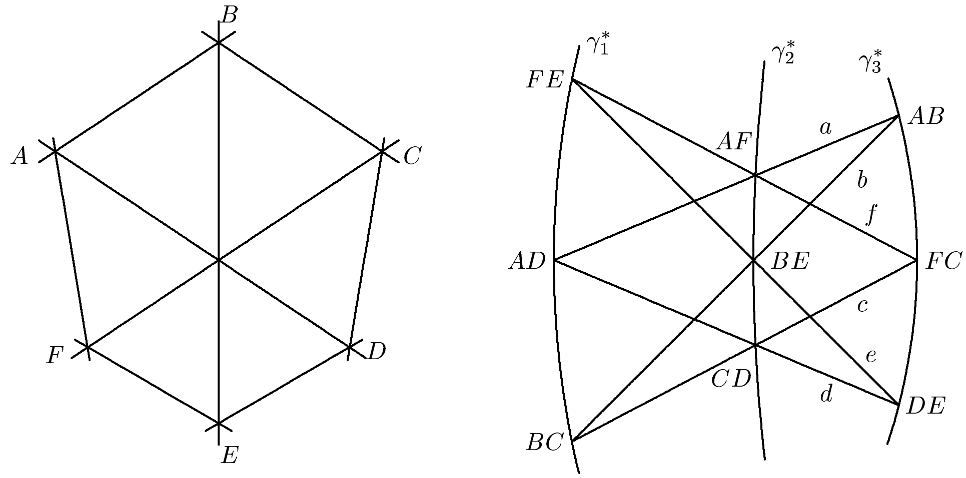


FIGURE 18.5. A closed hexagon and the projectively dual configuration

Cubic curves are given by equations of degree 3

$$P(x, y) = ax^3 + bx^2y + \cdots + j = 0$$

(all in all, 10 terms). Multiplying all the coefficients by the same factor, yields the same curve. There is a unique cubic curve through a generic collection of 9 points. Cubic curves have numerous interesting properties. The one that we need is as follows.

THEOREM 18.1. *Consider two triples of lines intersecting at 9 points. If a cubic curve $\Gamma$ passes through 8 out of these points then it also passes through the 9-th point (see Figure 18.6).*

Proof. Denote the intersection point of line $L_i = 0$ with $R_j = 0$ by $A_{ij}$; here $L_i$ and $R_j$ are linear equations of the lines. Assume that all points, except possibly $A_{22}$, lie on $\Gamma$. Let $P(x, y) = 0$ be an equation of $\Gamma$ and set: $\mathcal{L} = L_0L_1L_2, \mathcal{R} = R_0R_1R_2$.

We claim that $P = \lambda\mathcal{L} + \mu\mathcal{R}$ for some coefficients $\lambda$ and $\mu$. This would imply that $P = 0$ at point $A_{22}$ since $L_2$ and $R_2$ both vanish at this point.

Choose coordinates so that $L_0(x, y) = x$ and $R_0(x, y) = y$ (this involves only an affine change of coordinates, so a cubic curve remains cubic). Then $\mathcal{L} = x(x - a_1 - b_1y)(x - a_2 - b_2y)$ where $a_1$ and $a_2$ are the $x$-coordinates of the points $A_{10}$ and $A_{20}$. Since $P = 0$ at points $A_{00}, A_{10}$ and $A_{20}$, one has $P(x, 0) = \lambda x(x - a_1)(x - a_2)$ for some constant $\lambda$, that is, $P(x, 0) = \lambda\mathcal{L}(x, y)$. Likewise, $P(0, y) = \mu\mathcal{R}(0, y)$.

Consider now the polynomial $Q = P - \lambda\mathcal{L} - \mu\mathcal{R}$. One has: $Q(x, 0) = Q(0, y) = 0$, hence $Q(x, y) = xyH(x, y)$ where $H$ is a linear function. Note that $Q$ vanishes at points $A_{11}, A_{12}$ and $A_{21}$ but $xy$ does not vanish at these points. Therefore $H = 0$ at these three non-collinear points. This implies that $H = 0$ identically, and so is $Q$. Therefore $P = \lambda\mathcal{L} + \mu\mathcal{R}$. $\Box$

Let us summarize: a rectilinear 3-web is hexagonal if it consists of three families of tangent lines to a curve whose dual is a cubic.

For example, consider the semicubic parabola $y^2 = x^3$. The dual curve is a cubic parabola (see Lecture 8), and hence the 3-web in Figure 18.7 is hexagonal.

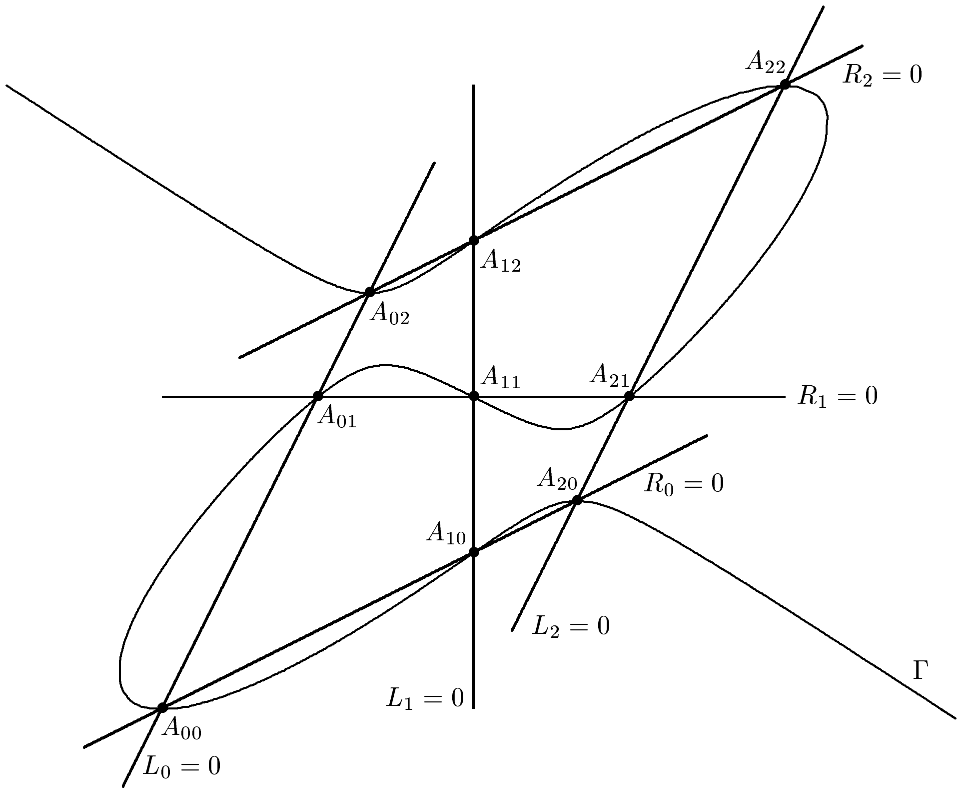


FIGURE 18.6. Illustration of Theorem 18.1

**18.5 Pappus and Pascal.** Two particular cases of Theorem 18.1 are especially worthwhile to mention. The first concerns the case when a cubic curve Γ consists of three lines. Then we obtain the celebrated Pappus theorem depicted in Figure 18.8.

The dual curve to the union of three lines is degenerate and consists of three points. The respective 3-web is the one in Figure 18.3. Our earlier proof that this web is hexagonal implies, via duality, the Pappus theorem.

Another particular case is when Γ consists of a line and a conic. We obtain the celebrated theorem of Pascal (1640) illustrated in Figure 18.9.

**18.6 Addition of points on a cubic curve.** Theorem 18.1 is intimately related to a remarkable operation of addition of points on a cubic curve. This operation is defined geometrically, based on the property that a line that intersects a cubic curve twice will intersect it once again.

Here is the definition. Let Γ be a non-singular cubic curve. Choose a point $E$ that will play the role of the zero element. Given two points, $A$ and $B$, construct the third intersection point $D$ of the line $AB$ with Γ; connect $D$ to $E$ and let $C$ be the third intersection point of this line with Γ. By definition, $A + B = C$.

Let us work out an example: Γ is the graph $y = x^3$ and $E$ is the origin. Let points $A, B$ and $D$ have the first coordinates $x_1, x_2$ and $x_3$, see Figure 18.10. These

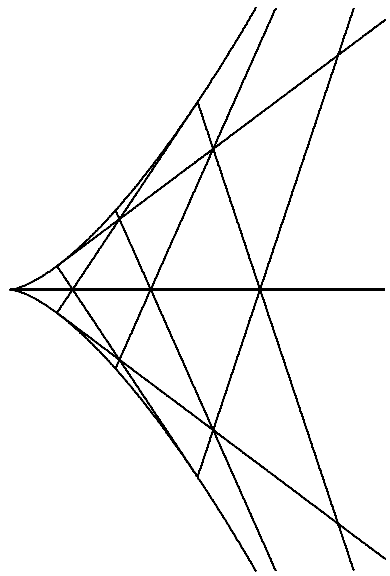

FIGURE 18.7. A hexagonal 3-web consisting of the tangent lines to a semicubic parabola

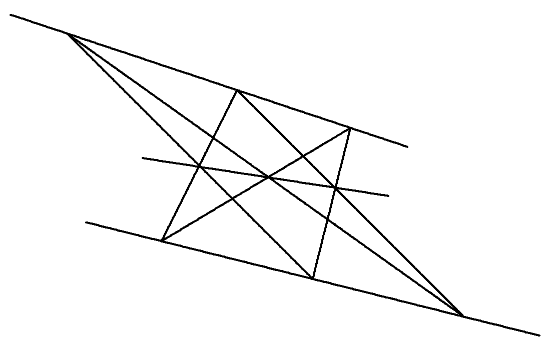

FIGURE 18.8. The Pappus theorem

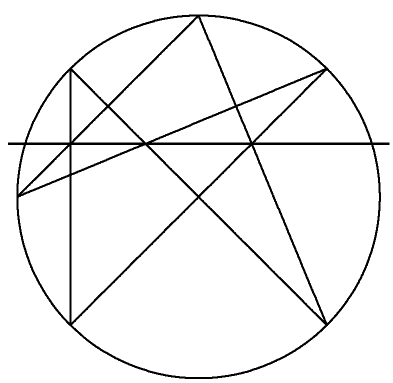

FIGURE 18.9. The Pascal theorem

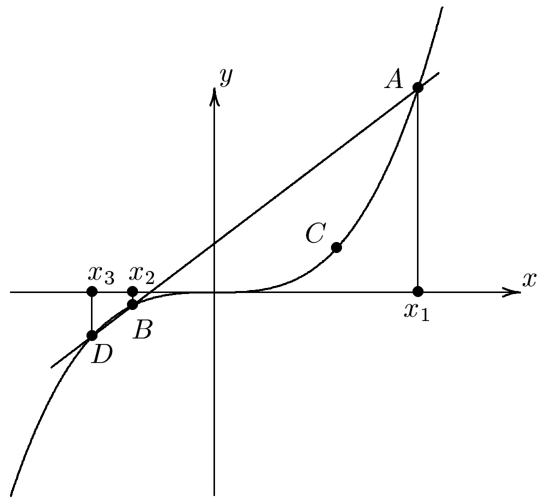


FIGURE 18.10. An example of addition of points on a cubic curve

points are collinear, therefore

$$\frac{x_1^3 - x_3^3}{x_1 - x_3} = \frac{x_2^3 - x_3^3}{x_2 - x_3},$$

which implies $x_1^2 + x_1x_3 + x_3^2 = x_2^2 + x_2x_3 + x_3^2$ or $(x_1 - x_2)(x_1 + x_2 + x_3) = 0$, and finally, $x_1 + x_2 + x_3 = 0$. Point $C$ is centrally symmetic to $D$, so its first coordinate is $-x_3 = x_1 + x_2$. Thus the addition of points on this cubic curve amounts to the usual addition of the first coordinates.

The addition of points on a cubic curve is commutative and associative. The former is obvious: the line $AB$ coincides with the line $BA$. The latter follows from (and is equivalent to) Theorem 18.1, as illustrated in Figure 18.11. This theorem implies that the intersection point of the lines connecting $A$ to $B + C$, and $A + B$ to $C$, lies on $\Gamma$ (this is point $X$ in the figure). It follows that

$$A + (B + C) = (A + B) + C = Y,$$

the desired associativity.

**18.7 In space.** We mentioned in Section 18.2 that every 2-web in the plane is trivial. Not so in space![1] A trivial 2-web in space is the one made of two families of lines, parallel to the $x$ and $y$ axes, and every 2-web that can be deformed to this one.

To construct an obstruction to triviality of a 2-web in space is even easier than in the plane. Take a point $A$, draw through it the curve from the first family, choose a point $B$ on this curve, draw through it the curve from the second family, choose a point $C$ on this curve. Now draw through $C$ the curve from the first family and through $A$ the curve from the second family, see Figure 18.12. Will these curves intersect? Yes, if the web is trivial, and no, in general.

Here is an example of a non-trivial 2-web. The first family consists of the vertical lines and the second of horizontal ones. The horizontal lines in the plane at

[1] Every 1-web in space is trivial.

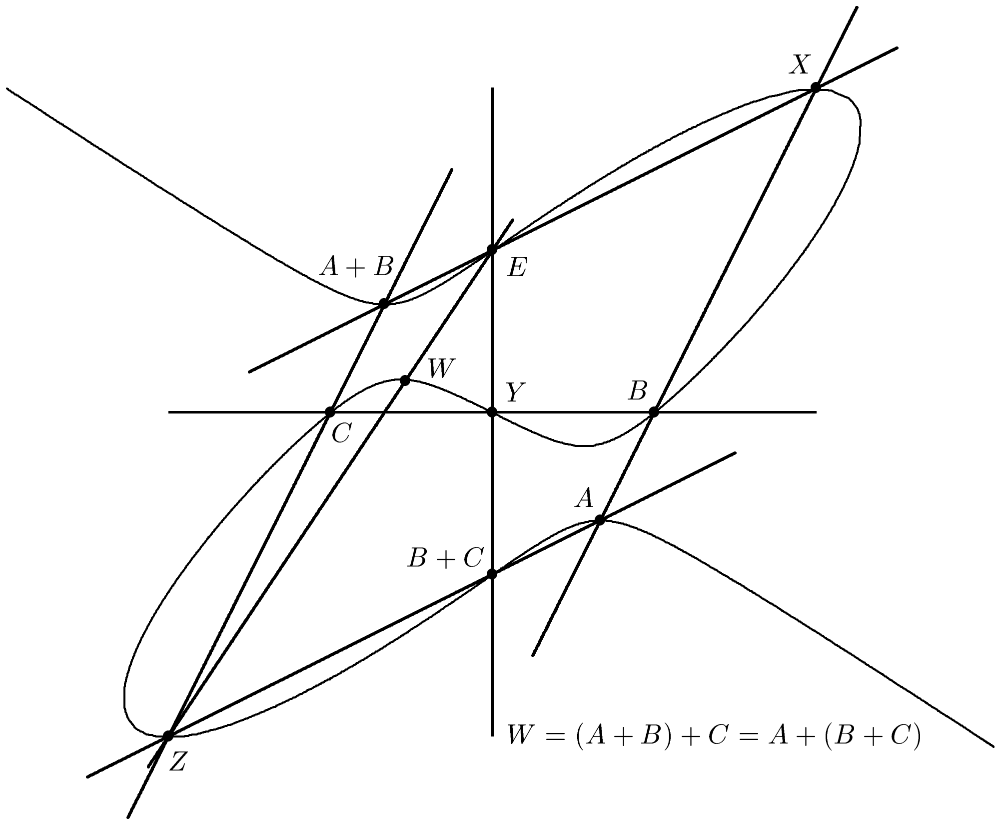


FIGURE 18.11. Associativity of addition

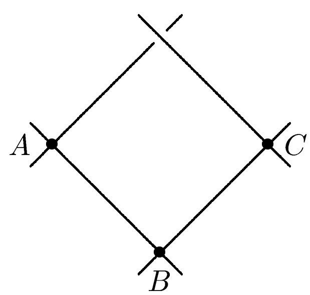


FIGURE 18.12. This quadrilateral may fail to close up

height $h$ are parallel to each other and have slope $h$ in this plane. In other words, take a horizontal plane with a family of parallel lines on it and move it along the vertical axis, revolving about this axis with a positive angular speed. This screw driver motion yields the web depicted in Figure 18.13.

Non-triviality of this 2-web has an interesting consequence. The two lines through point $x$ span a plane, say, $\pi(x)$. We obtain a family of planes in space. These planes enjoy the property called *complete non-integrability*: there does not

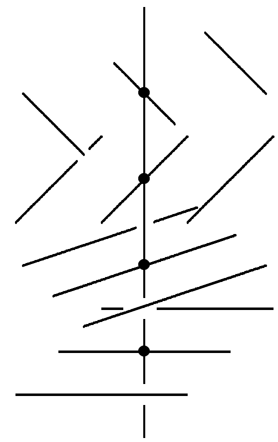

FIGURE 18.13. A non-trivial 2-web in space

exist a surface (no matter how small) for which $\pi(x)$ would be the tangent plane at every point $x$. Indeed, if such a surface existed then the quadrilateral in Figure 18.12 would lie on it and be closed.

At first glance, this non-integrability is rather surprising: it contradicts our intuition developed in the plane case. In the plane (and in space of any dimension), if one has a direction at every point, smoothly depending on the point, then there exists a family of smooth curves, everywhere tangent to these directions – see Figure 18.14 (this is the Fundamental Theorem of Ordinary Differential Equations). A completely non-integrable field of planes in space is called a *contact structure*, this a very popular object of study in contemporary mathematics.

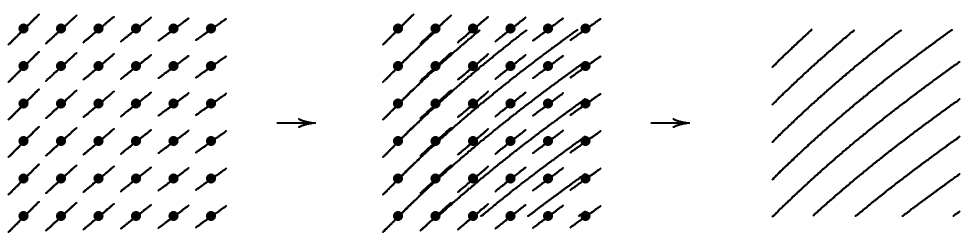

FIGURE 18.14. A family of directions integrates to a family of curves

**18.8 Chebyshev nets.** Can one model fabric by a web?

A flat piece of fabric is woven of two families of non-stretchable threads making a rectangular grid. Drape this piece of fabric over a curved surface, and the rectangles will get distorted to elementary parallelograms, see Figure 18.15.

A *Chebyshev net* is a 2-web such that the lengths of the opposite sides of every quadrilateral, made by a pair of curves from each family, are equal, see Figure 18.16.

Pafnuty Chebyshev, a prominent Russian mathematician of the 19-th century,[2] was motivated by an applied problem: how to cut fabric more economically (he

[2]The reader of Lecture 7 is familiar with some other works of Chebyshev.

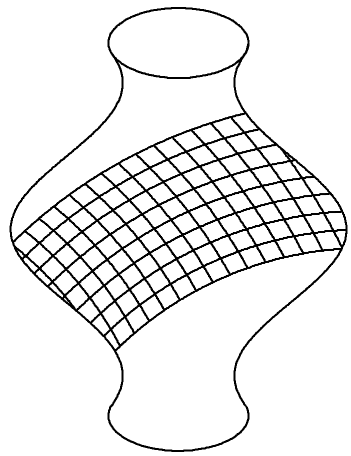

FIGURE 18.15. A piece of fabric

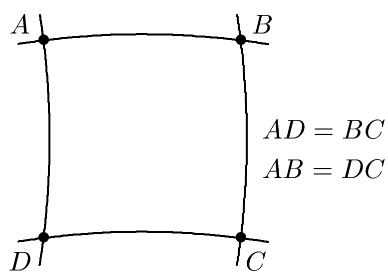


FIGURE 18.16. Chebyshev net

was working for a private client, an owner of a textile business). This was an acute problem: with the onset of the Crimean War, there was a huge demand for army uniforms.

Here is a construction of a Chebyshev net in the plane. Start with two curves, $a$ and $b$, intersecting at the origin $O$. For every point $A$ on curve $a$, parallel translate curve $b$ through vector $OA$. Likewise, for every point $B$ on $b$, translate $a$ through vector $OB$. The result is a 2-web, and this is a Chebyshev net. Indeed, the quadrilateral $OBCA$ in Figure 18.17 is a parallelogram. Therefore the curve $BC$ is a parallel translate of the curve $OA$, and likewise for the curves $AC$ and $OB$. Hence the opposite sides of the curvilinear quadrilateral $OBCA$ are equal.

One can say more: the curves $a$ and $b$ uniquely determine a Chebyshev net. To see this, let us approximate the curves $a$ and $b$ by polygonal lines, say, with sides of length $\varepsilon$. If an elementary quadrilateral of a Chebyshev net has rectilinear sides then it is a parallelogram. It follows that the polygonal lines $a$ and $b$ uniquely determine a family of parallelograms, see Figure 18.18. In the limit $\varepsilon \to 0$, one obtains a Chebyshev net generated by the curves $a$ and $b$.

To obtain a Chebyshev net on a curved surface, one can draw a planar Chebyshev net on a sheet of paper and then bend the sheet into a "developable" surface

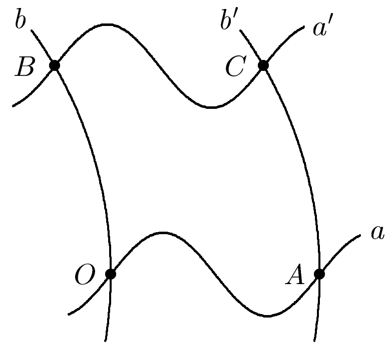


FIGURE 18.17. A construction of a Chebyshev net in the plane

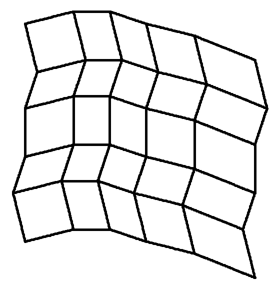

FIGURE 18.18. A Chebyshev net made of parallelograms

(see Lecture 13); for example, one can consider a surface made of a sheet of a graph paper. However, Chebyshev nets exist not only on developable surfaces.

Here is a more general construction of a Chebyshev net, this time, on a curved surface. Let $a$ and $b$ be two curves in space. For every pair of points, $A$ on $a$ and $B$ on $b$, let $C$ be the midpoint of the segment $AB$. The locus of points $C$ is a surface. This surface is made of two families of curves: these curves are obtained by fixing, in the above construction, point $A$ (first family) or point $B$ (second family). This is a Chebyshev net.

Indeed, consider two pairs of points: $A$ and $A'$ on curve $a$, and $B$ and $B'$ on curve $b$, see Figure 18.19. The midpoints of the four segments, $K, L, M, N$, lie on the surface. The pairs $K, L$ and $M, N$ lie on two curves from one family, and the pairs $K, N$ and $L, M$ on two curves from another family. One has:

$$KL = \frac{1}{2}AA' = NM, \quad KN = \frac{1}{2}BB' = LM,$$

and hence curve $NM$ is obtained from curve $KL$ by parallel translation through vector $KN$; and likewise for curves $LM$ and $KN$. It follows that the lengths of the opposite sides of the curvilinear quadrilateral $KLMN$ are equal.

The surface itself (the locus of midpoints $C$) is the result of parallel translation of curve $a$ along curve $b$. Such surfaces are called *translation surfaces.* If curves $a$ and $b$ lie in one plane, the translation surface coincides with this plane, and the constructed Chebyshev net is the one in Figure 18.17.

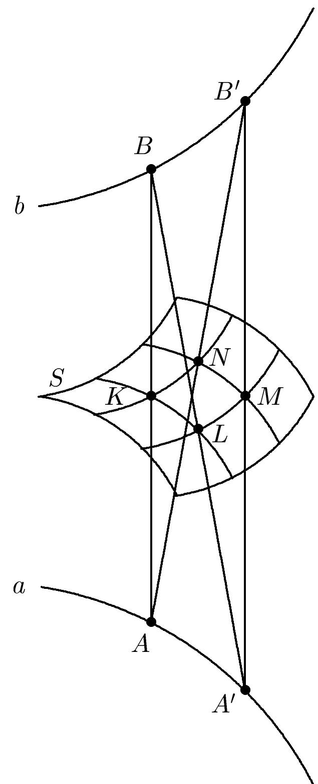


FIGURE 18.19. A construction of a Chebyshev net in space

A familiar example of a translation surface is a hyperbolic paraboloid $z = x^2 - y^2$; the respective curves are the parabolas $(2x, 0, 2x^2)$ and $(0, 2y, -2y^2)$ (see Figure 18.20, left); a circular paraboloid $z = x^2 + y^2$ provides one more example (see Figure 18.20, right).

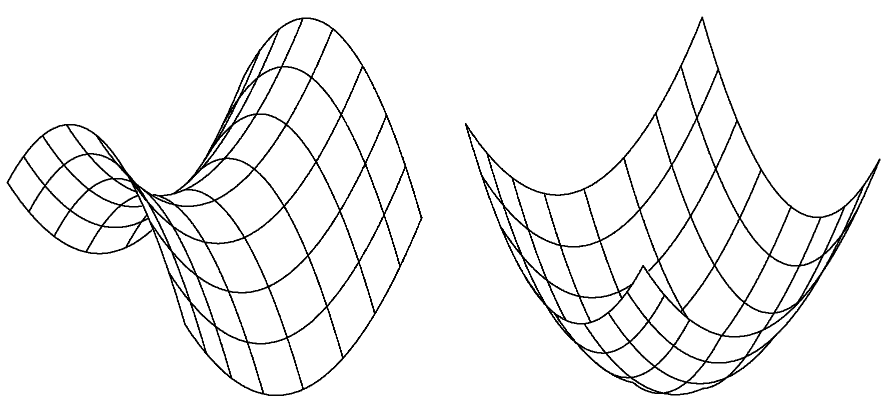

FIGURE 18.20. Quadratic surfaces as translation surfaces

Returning to the difference between developable surfaces and surfaces with Chebyshev nets, one can notice that while the former are images of maps of the plane to space preserving lengths of all smooth curves, the latter are described by maps which preserve only the lengths of vertical and horizontal lines. Less formally, one can say that a surface is developable if one can tightly attach to it a piece of paper, while it admits a Chebyshev net, if one can tightly attach to it a fishing net. For example, the paraboloids of Figure 18.20 are not developable, but admit Chebyshev nets.

John Smith
January 23, 2010

Martyn Green
August 2, 1936

Henry Williams
June 6, 1944

John Smith
January 23, 2010

Martyn Green
August 2, 1936

Henry Williams
June 6, 1944

### 18.9 Exercises.

18.1. (a) Prove that the web made of horizontal lines, vertical lines and hyperbolas $xy = const$ is trivial.

(b) Same for the web made of horizontal lines, vertical lines and the graphs $y = f(x) + const$ where $f(x)$ is any function with positive derivative.

18.2. Consider the 3-web made of the lines through one fixed point, the lines through another fixed point and of tangent half-lines to a fixed circle. Is this web trivial?

18.3. Prove that the 3-web made of the tangent lines to a fixed circle and the lines through a fixed point is hexagonal.

18.4. Consider a triangle made of curves of a 3-web. Show that there exists a unique inscribed triangle, made of curves of this web.

18.5. * Prove that a hexagonal 3-web is trivial.

*Hint.* Extend the hexagon to a "honeycomb" as in Figure 18.21. One can change coordinates so that the honeycomb is made of three families of parallel lines. Making the original hexagon smaller and smaller, one deforms, in the limit, a hexagonal 3-web into a trivial one.

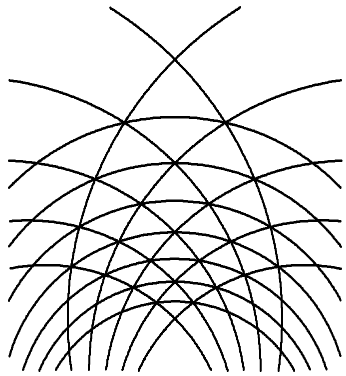

FIGURE 18.21. A hexagonal 3-web is trivial

18.6. * Prove that the three inflection points of a smooth cubic curve lie on a straight line (this is clearly seen in Figure 18.6).

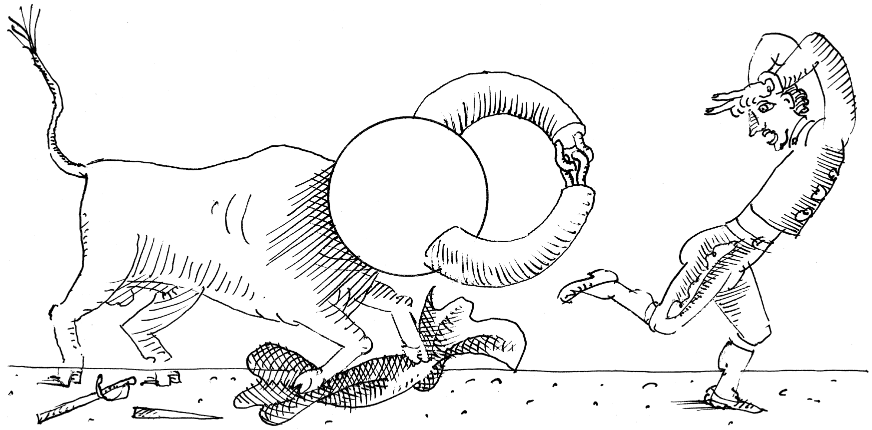

LECTURE 19

# The Crofton Formula

**19.1 The space of rays and the area form.** The Crofton formula concerns the set of oriented lines in the plane. Sometimes, as in geometrical optics, we shall think of oriented lines as rays of light and call them rays.

An oriented line is characterized by its direction $\varphi$ and its distance $p$ from the origin $O$. This distance is signed, see Figure 19.1. Thus the space of rays is a cylinder with coordinates $(\varphi, p)$ (which we visualize as the vertical unit circular cylinder in space).

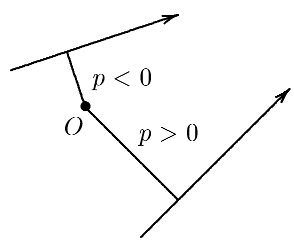


FIGURE 19.1. Coordinates in the space of oriented lines

Changing the orientation of a line is the central symmetry of the cylinder: $(\varphi, p) \mapsto (\varphi + \pi, -p)$. It follows that the set of non-oriented lines identifies with the quotient of the cylinder by this central symmetry, that is, the Möbius band.

Translating the origin changes the coordinates of a line. Namely, if $O' = O + (a, b)$ is a different choice of the origin then the new coordinates depend on the old ones as follows:

$$\varphi' = \varphi, \quad p' = p - a \sin \varphi + b \cos \varphi. \tag{19.1}$$

The reader may look up a proof of this formula in Lecture 10 or do Exercise 19.1. In particular, the set of rays through point $(a, b)$ is given by the equation $p = -a \sin \varphi + b \cos \varphi$. This is a plane section of our cylinder.

The cylinder has the area element $d\varphi dp$; this area form is the main character of this lecture. It does not change under isometries of the plane. Indeed, an isometry is a composition of a rotation about the origin and a parallel translation. A rotation through angle $\alpha$ acts on the space of rays as follows:

$$\varphi' = \varphi + \alpha, \quad p' = p.$$

This is a rotation of the cylinder that does not distort the area. A parallel translation acts according to formulas (19.1). This does not change the area either, see Figure 19.2.

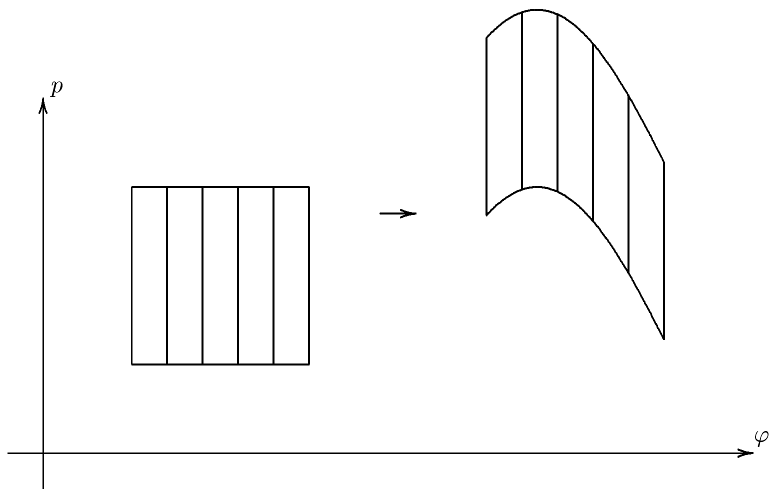


FIGURE 19.2. Parallel translation preserves the area form in the space of oriented lines

It is worth mentioning a fact known to Archimedes. Inscribe a unit sphere into the cylinder and consider the axial projection from the sphere to the cylinder (which is not defined at the poles). This projection is area-preserving: *the areas of any domain on the sphere and the cylinder are equal*, see Exercise 19.2. This fact makes it possible to immediately find the area of the sphere.

The axial projections are used in cartography where they are known under a number of names: Gall-Peters, Behrmann, Lambert, Balthasart, etc. They do not distort areas, so Greenland appears approximately 13 times as small as Africa (unlike the Mercator projection where they appear roughly of the same areas) but they severely distort distances, especially, near the poles. See [**90**] for the history of cartography.

The fact that the axial projection from the unit sphere to the cylinder is area-preserving implies that the area of a spherical belt (the domain of the sphere between two parallel planes) depends only on the height $h$ of the belt (that is, $h$ is the distance between the planes); namely, this area equals $2\pi h$. This high school geometry fact has a curious consequence.

Let the unit disc be covered by a collection of strips with parallel sides ("planks").

THEOREM 19.1. *The sum of the widths of the strips is not less than 2.*

This is the Tarski plank theorem (its statement is of course obvious if the strips are parallel).

Proof. Consider the disc covered by strips as the vertical projection of the unit sphere covered by spherical belts. The total area of the belts is $2\pi$ times the sum of their widths, and this is not less than the area of the sphere, $4\pi$. Thus the sum of the widths is not less than 2. □

**19.2 Relation to geometrical optics.** The area form $d\varphi dp$ on the space of rays plays a role in geometrical optics. An ideal mirror, in dimension 2, is represented by a plane curve; the law of reflection is "the angle of incidence equals the angle of reflection".

Thus a mirror determines a (partially defined) transformation of the space of rays: an incoming ray is sent to the reflected, outgoing one. This is a transformation of the cylinder, and its crucial property is that it is area-preserving. The same holds for more complicated optical systems involving a number of mirrors and lenses. See Lecture 28 for a detailed discussion of this area preserving property in the framework of billiards.

By the way, the existence of an area form on the space of rays, invariant under mirror reflection, is not specific to the plane. Consider, for example, the unit sphere. The role of lines is played by great circles. An oriented great circle is uniquely characterized by its pole, a center of this great circle in the spherical metric (it is a matter of convention which of the two poles to choose, but once made, this choice should be consistent; in particular, changing the orientation of a great circle, one chooses the opposite pole).

Thus the space of rays on the sphere is identified with the sphere itself (this construction almost coincides with the projective duality discussed in Lecture 8). The sphere has a standard area element, and this provides an area element on the space of rays. This area form is invariant under the motions of the sphere (Exercise 19.3) and does not change under a reflection in any mirror, represented by a smooth spherical curve.

**19.3 The formula.** Consider a smooth plane curve $\gamma$ (not necessarily closed or simple), and define a function $n_\gamma$ on the space of oriented lines as the number of intersections of a line with the curve. There are some problems with this definition: for example, if $\gamma$ is a straight segment then $n_\gamma$ will have an infinite value for the two oriented lines that contain this segment. Not to worry: we are going to integrate $n_\gamma$ over the cylinder, and these "abnormalities" will not contribute to the integral.

Generically, the value of $n_\gamma$ changes by 2 when the lines becomes tangent to the curve $\gamma$, see Figure 19.3. If $(\varphi, p)$ are the coordinates of the line we write the function as $n_\gamma(\varphi, p)$.

Crofton's formula is the following statement.

THEOREM 19.2.

$$\text{length } (\gamma) = \frac{1}{4} \int\int n_\gamma(\varphi, p)\ d\varphi\ dp. \tag{19.2}$$

If the curve $\gamma$ is bounded, that is, lies in a disc of some radius $r$, centered at the origin, then $n_\gamma(\varphi, p) = 0$ for $|p| > r$, and hence the integral has a finite value.

Proof of Crofton's formula. The curve $\gamma$ can be approximated by a polygonal line, and it suffices to prove (19.2) for such a line. Suppose that a polygonal line is the concatenation of two, $\gamma_1$ and $\gamma_2$. Both sides of (19.2) are additive, and the

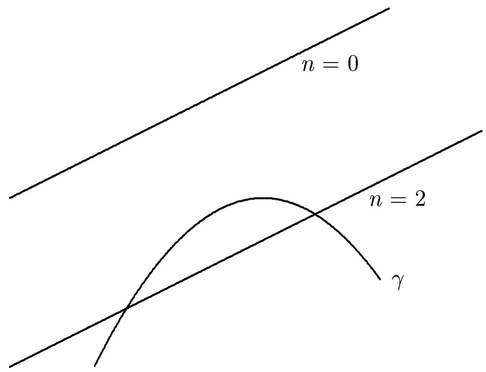


FIGURE 19.3. The function $n_\gamma$

formula for $\gamma$ would follow from those for $\gamma_1$ and $\gamma_2$. Hence it suffices to establish (19.2) for a segment.

Let $C$ be the value of the integral (19.2) for a unit segment; the constant does not depend on the position of the segment because the area form on the space of lines is isometry invariant. A dilation by a factor $r$ multiples the area form by $r$, therefore

$$\int\int n_\gamma(\varphi, p)\ d\varphi\ dp = C|\gamma|$$

for every segment $\gamma$.

It remains to check that $C = 4$. This is most easily seen when $\gamma$ is the unit circle centered at the origin: the length is $2\pi$, while $n_\gamma(\varphi, p) = 2$ for all $\varphi$ and $-1 \leq p \leq 1$, and zero otherwise. □

An analog of Crofton's formula holds for curves on the sphere: of course, the integral is taken with respect to the area element, discussed at the end of Section 19.2, see Exercise 19.5.

**19.4 First applications.** The Crofton formula has numerous applications. In this section, we shall discuss four.

1). Consider two nested closed convex curves, $\gamma$ and $\Gamma$, see Figure 19.4, and let $l$ and $L$ be their lengths. We claim that $L \geq l$. Indeed, a line intersects a convex curve at two points, and every line that intersects the inner curve intersects the outer one as well. Hence $n_\Gamma \geq n_\gamma$, and the result follows from the Crofton formula.

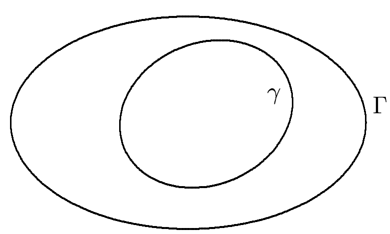


FIGURE 19.4. Nested ovals

2). The width of a convex figure in a given direction is the distance between two lines in this direction, tangent to the figure on the opposite sides. A figure of constant width has the same width in all directions. An example is a circle.

There are many other figures of constant width, see Figure 19.5. What they have in common is their perimeter length, equal to $\pi d$, where $d$ is the width. Let us prove this claim.

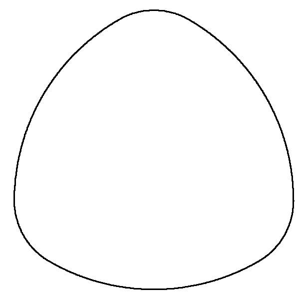

FIGURE 19.5. A figure of constant width

Let $\gamma$ be a closed convex curve of constant width $d$. Choose an origin inside $\gamma$. Consider the tangent line to $\gamma$ in the direction $\varphi$ and let $p(\varphi)$ be its distance from the origin. The periodic function $p(\varphi)$ is called the support function of the curve, see Lecture 10.

The constant width condition is: $p(\varphi)+p(\varphi+\pi)=d$. By the Crofton formula,

$$\text{length } (\gamma)=\frac{1}{4}\int_0^{2\pi}\int_{-p(\varphi+\pi)}^{p(\varphi)} 2\ dp\ d\varphi=\frac{d}{2}\int_0^{2\pi} d\varphi=\pi d,$$

as claimed.

3). The distance between the lines on a ruled paper is 1. What is the probability that a unit length needle, randomly dropped on the paper, intersects a line? This is the celebrated *Buffon's needle problem.*

Assume that the unit segment, $\gamma$, is horizontal and centered at the origin, while the ruled paper may assume all possible positions. Now, instead of the ruled paper, consider just one line at distance at most $1/2$ from the origin. Then all possible positions of the line is the rectangle $0 \le \varphi \le 2\pi,\ -1/2 \le p \le 1/2$ whose area is $2\pi$.

If a line intersects $\gamma$ then $n_\gamma = 1$, otherwise $n_\gamma = 0$. Therefore the desired probability equals

$$\left(\int\int n_\gamma(\varphi,p)\ d\varphi\ dp\right)/2\pi.$$

By Crofton's formula, the integral is 4 times the length of $\gamma$, and the probability equals $2/\pi$.

4). The curvature of a smooth space curve is the magnitude of the acceleration vector if the curve is given an arc length parameterization, see Lecture 15.

THEOREM 19.3. *The total curvature of a closed space curve is at least $2\pi$.*

Proof. Let $\gamma(t)$ be the curve. As the parameter $t$ varies, the velocity vector $\Gamma(t) = \gamma'(t)$ describes a closed curve on the unit sphere (sometimes called the *tangent indicatrix*, or simply the *tantrix*). The length of the tantrix is

$$\int |\Gamma'(t)|dt = \int |\gamma''(t)|dt,$$

that is, the total curvature of $\gamma$. We want to show that the length of $\Gamma$ is not less than $2\pi$.

We claim that the tantrix intersects every great circle at least twice. All great circles being equal, take the equator. Consider the highest and the lowest points of $\gamma$. At these points, the velocity $\gamma'$ is horizontal, and hence $\Gamma$ intersects the equator.

Finally, apply the spherical Crofton formula: $n_\Gamma \geq 2$ everywhere and the total area of the sphere is $4\pi$, therefore length $(\Gamma) \geq 2\pi$. $\square$

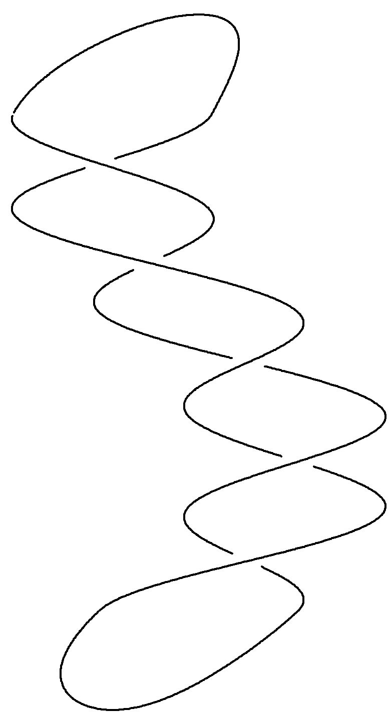

FIGURE 19.6. A curve with one local maximum and one local minimum cannot be knotted

The celebrated Fary-Milnor theorem says more:

THEOREM 19.4. *If a closed spacial curve is knotted then its total curvature is greater than $4\pi$.*

That the total curvature is not less than $4\pi$ follows from the more-or-less obvious fact that a knot must have at least two local maxima and two local minima, see Figure 19.6. We do not dwell on how to make this inequality strict.

**19.5 The DNA geometric inequality.** Consider again two plane closed smooth nested curves: the outer one, $\Gamma$, is convex and the inner one, $\gamma$, is not necessarily convex and may have self-intersections. The picture resembles DNA inside a cell, see Figure 19.7.

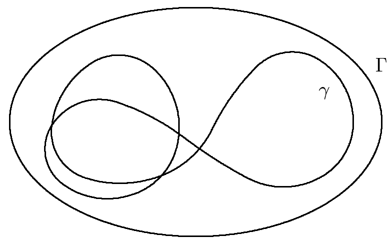


FIGURE 19.7. DNA inside a cell

Define the *total absolute curvature* of a closed curve as the integral of the absolute value of the curvature with respect to the arc length parameter. Total absolute curvature is the "total turn" of the curve. The *average absolute curvature* of a curve is the total absolute curvature divided by the length.

One has the following geometrical inequality.

THEOREM 19.5. *The average absolute curvature of* $\Gamma$ *is not greater than the average absolute curvature of* $\gamma$.

We call this the DNA geometric inequality. This theorem was proved only recently [**49, 54**], and the proof is surprisingly hard. We shall prove a weaker result, due to Fary (of the Fary-Milnor theorem fame; this theorem was mentioned in Section 19.4). Namely, we assume that the outer curve, $\Gamma$, has a constant width (for example, a circle).

Proof. We already know that the length of $\Gamma$ is $\pi d$, where $d$ is the diameter, and its total curvature is $2\pi$. Denote the total curvature of $\gamma$ by $C$, and let $L$ be its length. We want to prove that

$$\frac{C}{L} \geq \frac{2}{d}. \tag{19.3}$$

Give $\gamma$ an orientation and define a locally constant function $q(\varphi)$ on the circle as the number of oriented tangent lines to $\gamma$ having direction $\varphi$. One has the following integral formula for the total absolute curvature:

$$C = \int_0^{2\pi} q(\varphi)\ d\varphi. \tag{19.4}$$

Indeed, if $t$ is the arc length parameter on $\gamma$ and $\varphi$ the direction of its tangent line then the curvature is $k = d\varphi/dt$. The total curvature

$$\int_0^L |k| dt = \int_0^L \left|\frac{d\varphi}{dt}\right| dt,$$

is the total variation of $\varphi$. Let $I$ be an interval of $\varphi$ for which the function $q(\varphi)$ has a constant value, say, $m$. Then $I$ has $m$ pre-images under the function $\varphi(t)$, and the value of the integral

$$\int \left| \frac{d\varphi}{dt} \right| dt$$

over each of these $m$ intervals is the length of $I$. This implies formula (19.4).

Let us use Crofton's formula to evaluate $L$. The crucial observation is that

$$n_\gamma(\varphi, p) \le q(\varphi) + q(\varphi + \pi) \tag{19.5}$$

for all $p, \varphi$. Indeed, between two consecutive intersections of $\gamma$ with a line whose coordinate are $(\varphi, p)$, the tangent line to $\gamma$ at least once has the direction of $\varphi$ or $\varphi + \pi$ (this is, essentially, Rolle's theorem), see Figure 19.8.

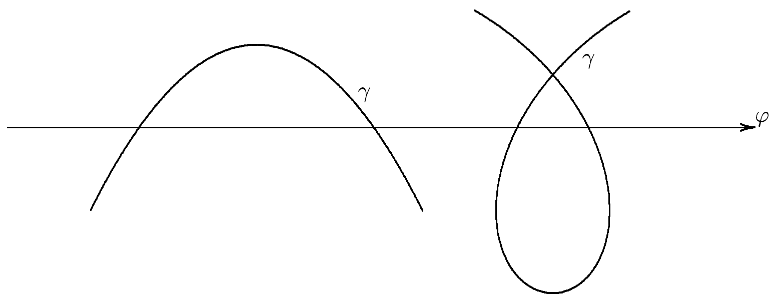


FIGURE 19.8. A version of Rolle's theorem

Denote the support function of $\Gamma$ by $p(\varphi)$. It remains to integrate (19.5), taking into account (19.4) and that $p(\varphi) + p(\varphi + \pi) = d$:

$$L = \frac{1}{4} \int\int n_\gamma(\varphi, p)\ dp\ d\varphi \le \frac{1}{4} \int_0^{2\pi} \int_{-p(\varphi+\pi)}^{p(\varphi)} (q(\varphi) + q(\varphi + \pi))\ dp\ d\varphi$$

$$= \frac{d}{4} \int_0^{2\pi} (q(\varphi) + q(\varphi + \pi))\ d\varphi = \frac{d}{2} \int_0^{2\pi} q(\varphi)\ d\varphi = \frac{Cd}{2}.$$

This implies the desired inequality (19.3). □

We can add that equality in (19.3) implies that $\gamma$ coincides with $\Gamma$, possibly traversed more than once. This follows from our proof as well.

It is interesting to investigate the spatial version of the DNA inequality when the cell is a convex body containing a closed curve. If the cell is a ball one has essentially the same result, but nothing is known for cells of more general shapes.

**19.6 Hilbert's Fourth problem.** In his famous talk at the International Congress of Mathematicians in 1900, D. Hilbert formulated 23 problems that would greatly influence the development of mathematics in the 20-th century and are likely to continue to inspire mathematicians. The Fourth problem asks to "construct and study the geometries in which the straight line segment is the shortest connection between two points". In this section, we shall show how Crofton's formula yields a solution to Hilbert's Fourth problem in dimension two.

First of all, what does one means by "geometry"? Geometrical optics suggests the following answer. Consider propagation of light in an inhomogeneous and anisotropic medium. This means that the speed of light depends on the point and the direction. One may define "distance" between points $A$ and $B$ as the shortest time it takes light to get from $A$ to $B$. This defines geometry, called *Finsler geometry*, and the trajectories of light will be the analogs of straight lines (they are called geodesics). We want these geodesics to be straight lines.

The speed of light at every point $x$ can be described by the "unit circle" at $x$ consisting of unit velocity vectors at this point. This "unit circle", called the *indicatrix*, is a smooth convex centrally symmetric curve, centered at $x$. For example, in the standard Euclidean plane, all indicatrices are unit circles. If all indicatrices are ellipses, the geometry is called Riemannian (this is the most important and thoroughly studied class of geometries).

Let us start with examples satisfying Hilbert's requirement. The very first one, of course, is the Euclidean metric in the plane. Next, consider the unit sphere with its standard geometry in which the geodesics are great circles. Project the sphere on some plane from the center; this central projection identifies the plane with a hemisphere, and it takes great circles to straight lines. This gives the plane a geometry, different from Euclidean, whose geodesics are straight lines (for the reader, familiar with differential geometry, this is a Riemannian metric of constant positive curvature).

The next example features hyperbolic geometry whose discovery was one of the major achievements of 19-th century mathematics. Consider the unit disc in the plane and define the distance between points $x$ and $y$ by the formula:

$$d(x, y) = \ln[a, x, y, b] \tag{19.6}$$

where $a$ and $b$ are the intersection points of the line $xy$ with the boundary circle, see Figure 19.9, and $[a, x, y, b]$ is the *cross-ratio of four points* defined as

$$[a, x, y, b] = \frac{(a - y)(x - b)}{(a - x)(y - b)}.$$

This is the so-called Beltrami-Klein (or projective) model of the hyperbolic plane.

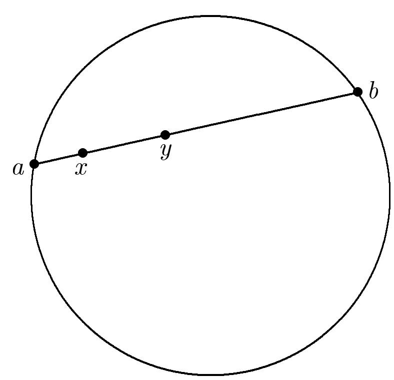


FIGURE 19.9. The Beltrami-Klein model of the hyperbolic plane

In fact, it was well known by the time of Hilbert's talk that the only Riemannian geometries whose geodesics are straight lines are the Euclidean, spherical and hyperbolic ones (Beltrami's theorem).

Posing his problem, Hilbert was motivated by two other examples. One was discovered by Hilbert in 1894, and it is called the *Hilbert metric*. The Hilbert metric is a generalization of the Klein-Beltrami model with the unit disc replaced by an arbitrary convex domain. The distance is given by the same formula (19.6) but, unless the boundary curve is an ellipse, this Finsler metric is not Riemannian anymore. Another example was studied by H. Minkowski in the framework of number theory. In Minkowski geometry, the indicatrices at different points are identified by parallel translations. This is a homogeneous but, generally, anisotropic geometry.

The solution to Hilbert's Fourth problem is based on the Crofton formula. Let $f(p,\varphi)$ be a positive continuous function on the space of rays, and even with respect to the orientation reversion of a line: $f(-p,\varphi+\pi) = f(p,\varphi)$. Then one has a new area form on the space of rays $f(p,\varphi)\ d\varphi\ dp$. Define the length of a curve by the formula

$$\text{length } (\gamma) = \frac{1}{4} \int\int n_\gamma(\varphi,p) f(p,\varphi)\ d\varphi\ dp. \tag{19.7}$$

We obtain a geometry in the plane, and we claim that its geodesics are straight lines. To see that this is the case one needs to check the triangle inequality: the sum of the lengths of two sides of a triangle is greater than the length of the third side. Indeed, every line intersecting the third side also intersects the first or the second, and integration (19.7) yields the desired triangle inequality.

In fact, every Finsler metric whose geodesics are straight lines is given by formula (19.7), but we do not prove this fact here. This means that in each such geometry one has a version of the Crofton formula. In higher dimensions, Hilbert's Fourth problem has a similar solution; instead of the space of lines one utilizes the space of hyperplanes and a version of Crofton's formula therein.

To conclude our brief discussion of Hilbert's Fourth problem, let us mention an elegant description of metrics whose geodesics are straight lines. This is due to Hilbert's student, Hamel, and was obtained in 1901, shortly after Hilbert's talk.

One may characterize a Finsler metric by a function which, following the tradition in physics, we call the Lagrangian and denote by $L$. Given a velocity vector $v$ at point $x$, the value of the Lagrangian $L(x,v)$ is the magnitude of the vector $v$ in units of the speed of light, that is, the ratio of $v$ to the speed of light at this point and in this direction. Said differently, the indicatrix at point $x$ consists of the velocity vectors $v$ satisfying the equation $L(x,v) = 1$. Clearly, $L(x,v)$ is homogeneous in the velocity: $L(x,tv) = tL(x,v)$ for all positive $t$.

For example, in Euclidean geometry, $L(x,v) = |v|$, the Euclidean length of the vector. In Minkowski geometry, the Lagrangian $L(x,v)$ does not depend on $x$.

For a smooth curve $\gamma(t)$, its length is given, in terms of the Lagrangian, by the formula

$$\int L(\gamma(t),\gamma'(t))\ dt.$$

Due to the fact that the Lagrangian is homogeneous of degree one, this integral does not depend on the parameterization (as every student of calculus learns when studying line integrals).

One may recover the Lagrangian from formula (19.7) by applying it to an infinitesimal segment $\gamma = [x, x+\varepsilon v]$. The result is the following formula:

$$L(x_1,x_2,v_1,v_2) = \frac{1}{4}\int_0^{2\pi} |v_1\cos\alpha + v_2\sin\alpha|\ f(x_1\cos\alpha + x_2\sin\alpha,\alpha)\ d\alpha, \tag{19.8}$$

see Exercise 19.11.

We are ready to formulate Hamel's theorem.

THEOREM 19.6. *A Lagrangian $L(x_1, x_2, v_1, v_2)$ defines a Finsler metric whose geodesics are straight lines if and only if*

$$\frac{\partial^2 L}{\partial x_1 \partial v_2} = \frac{\partial^2 L}{\partial x_2 \partial v_1}.$$

The explicit formula (19.8) provides a solution to this partial differential equation.

For more on Hilbert's Fourth problem, see Busemann's contribution in [**93**], the books [**61, 91**] and the article [**3**].

| | | |
|---|---|---|
| John Smith<br>January 23, 2010 | Martyn Green<br>August 2, 1936 | Henry Williams<br>June 6, 1944 |
| John Smith<br>January 23, 2010 | Martyn Green<br>August 2, 1936 | Henry Williams<br>June 6, 1944 |
| John Smith<br>January 23, 2010 | Martyn Green<br>August 2, 1936 | Henry Williams<br>June 6, 1944 |
| John Smith<br>January 23, 2010 | Martyn Green<br>August 2, 1936 | Henry Williams<br>June 6, 1944 |

### 19.7 Exercises.

19.1. Prove formula (19.1).

19.2. Prove that the axial projection from a sphere to the circumscribed cylinder is area-preserving (Archimedes).

19.3. Prove that the area element on the space of oriented great circles on the sphere, defined in Section 19.2, is invariant under the rotations of the sphere.

19.4. Make an explicit computation to verify Crofton's formula (19.2) for a unit segment.

19.5. Prove Crofton's formula for the sphere.

19.6. Let $\Gamma$ be a closed convex curve and $\gamma$ a closed, possibly self-intersecting, curve inside $\Gamma$; let $L$ and $l$ be their lengths. Prove that there exists a line that intersects $\gamma$ at least $[2l/L]$ times.

19.7. (a) Replace each side of an equilateral triangle with the arc of a circle centered at the opposite vertex. Prove that the resulting convex curve has constant width (Reuleaux triangle).

(b) Construct a similar figure of constant width based on a regular $n$-gon with odd $n$.

(c) Prove that one can circumscribe a regular hexagon about a curve of constant width.

*Hint*. Circumscribe a hexagon with angles 120° and show that the sum of any two consecutive sides is the same. Rotate this hexagon 60° and show that some intermediate hexagon is regular.

(d)* Prove that the Reuleaux triangle has the smallest area among the figures of constant width.

*Hint*. Circumscribe a regular hexagon about the curve of constant width $\gamma$ and inscribe a Reuleaux triangle into this hexagon as well. Show that the support function of the Reuleaux triangle is not greater than that of $\gamma$ and use Exercise 10.4 (a).

19.8. Prove that if one randomly drops a curve of length $l$ on the ruled paper then the average number of intersections with a line equals $2l/\pi$.

19.9. Let $\gamma$ be a not necessarily closed curve inside a unit circle, $C$ its total absolute curvature and $L$ its length. Prove that $L \le C + 2$.

19.10. Formulate and prove a version of the DNA theorem for a curve inside a ball in space.

19.11. * Let $\gamma$ be a closed curve in space and $C$ its total curvature. For a unit vector $v$, consider the orthogonal projection on the plane along $v$. Let $C_v$ be the total absolute curvature of the plane projection of $\gamma$. Prove that

$$C = \frac{1}{4\pi} \int C_v \, dv$$

where $v$ is considered as a point of the unit sphere and the integration is with respect to the standard area element on the sphere.

*Hint*: assume that $\gamma$ is a polygonal line and reduce to the case of a single angle.

19.12. Prove the triangle inequality for Hilbert metric.

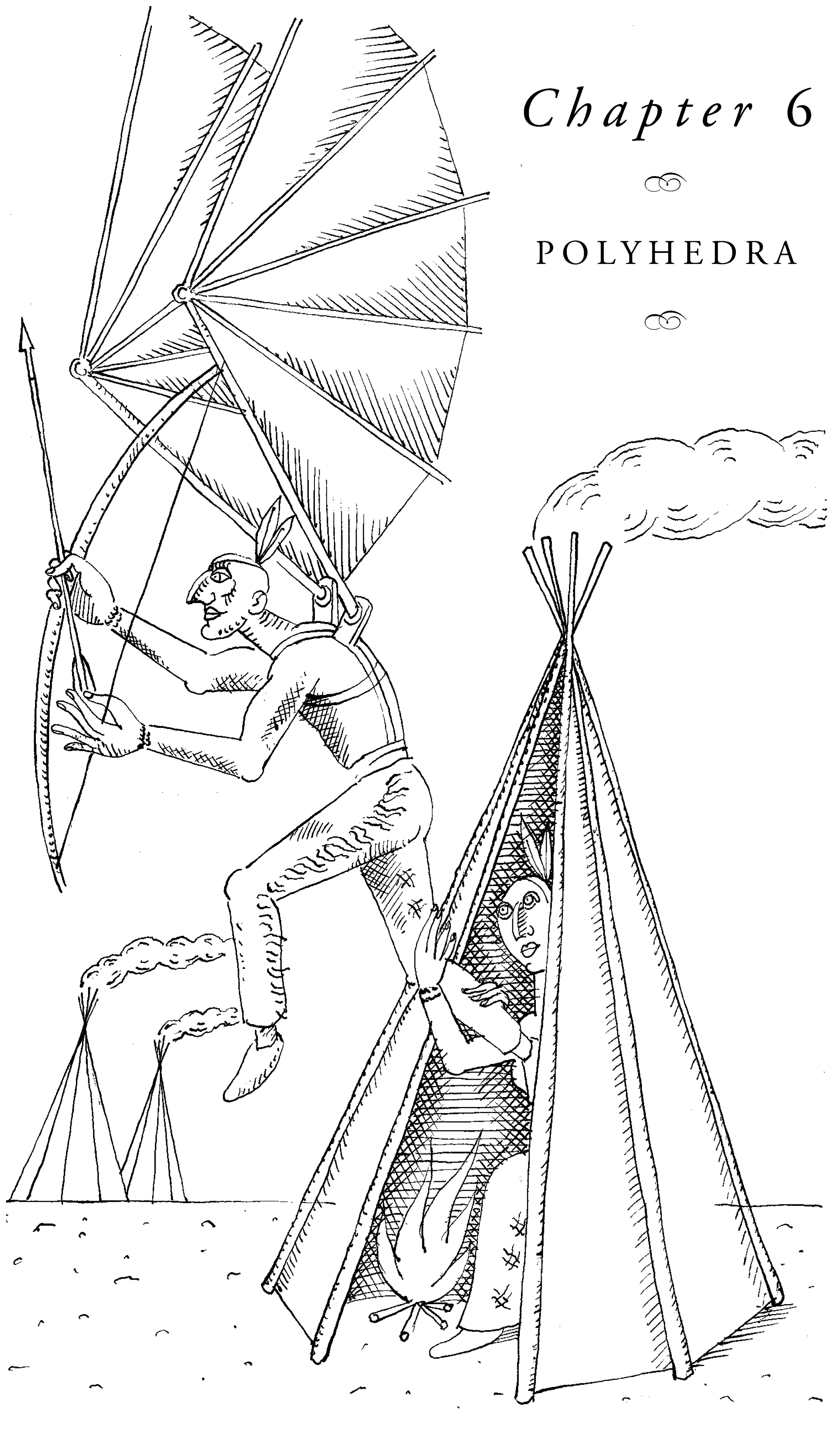

# *Chapter 6*

# POLYHEDRA

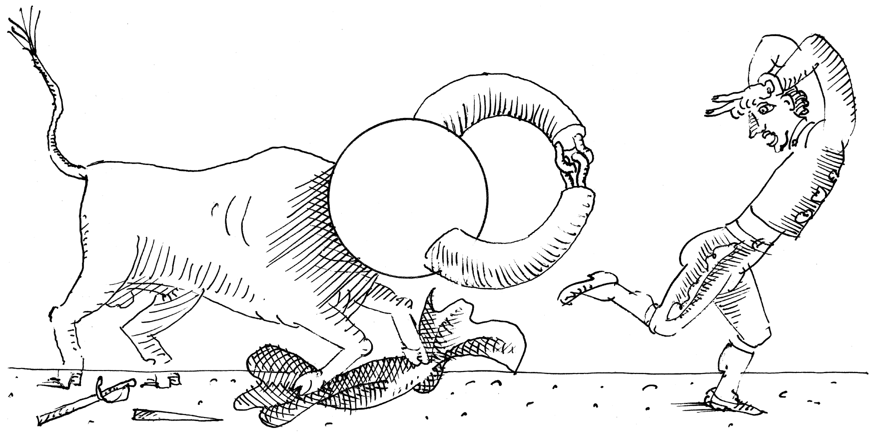

LECTURE 20

# Curvature and Polyhedra

**20.1 In the plane.** The curvature of a smooth plane curve is the rate with which the tangent line turns as one moves along the curve with unit speed. How does one define the curvature of a polygonal line?

The curvature of a plane wedge $\alpha$ is defined as its *defect*, $\pi - \alpha$, the angular measure of the complementary angle. The more acute the angle is, the greater its curvature. The curvature of a polygonal line is the sum of the curvatures of its angles.

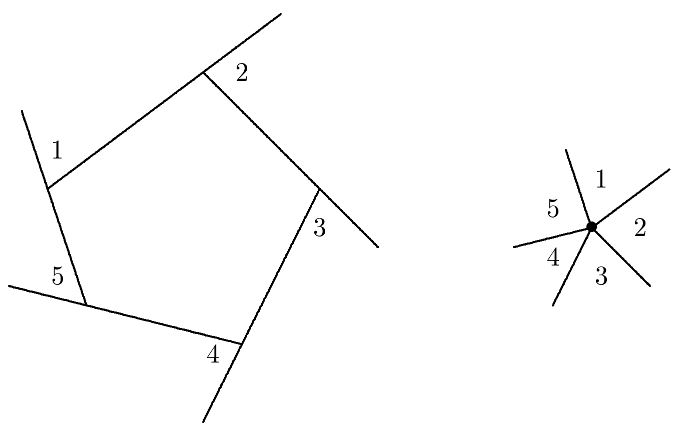


FIGURE 20.1. Sum of exterior angles of a convex polygon

The sum of curvatures of a convex polygon is $2\pi$, see Figure 20.1. The sum of curvatures of the two 7-pronged stars in Figure 20.2 are $4\pi$ and $6\pi$.

**20.2 Curvature of a polyhedral cone.** Each face of a polyhedral cone has an angle subtended at the vertex; we call this angle a *flat angle*. Consider

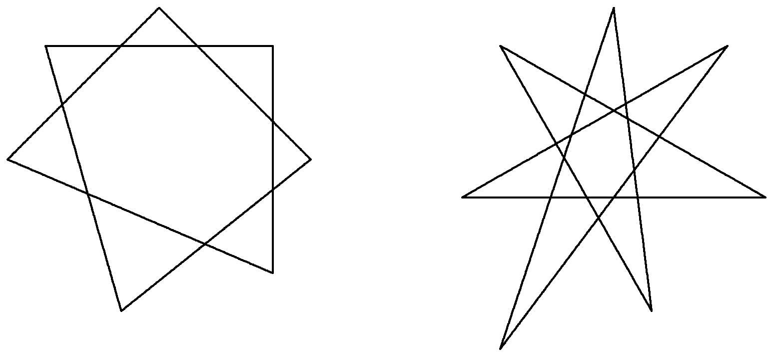

FIGURE 20.2. Two 7-pronged stars

a polyhedral cone with flat angles $\alpha_1, \dots, \alpha_n$. Define its curvature as the defect, $2\pi - (\alpha_1 + \cdots + \alpha_n)$. Note that curvature can be positive or negative; if the cone is flat then its curvature is zero.

If the cone has more than three faces, it is flexible. Imagine that the faces, which are rigid plane wedges, are connected at the edges by hinges. Then one can deform the cone in such a way that each face is not stretched or compressed, but the dihedral angles vary. Under such a deformation, the curvature remains constant.

Let $P$ be a convex polyhedron.

LEMMA 20.1. *The sum of curvatures of all vertices of $P$ equals $4\pi$.*

Proof. Let $v, e, f$ be the number of vertices, edges and faces of $P$. These numbers satisfy the Euler formula: $v - e + f = 2$ (see Lecture 24 for a proof).

Let us compute the sum $S$ of all angles of the faces of $P$. At a vertex, the sum of angles is $2\pi$ minus the curvature of this vertex. Summing up over the vertices gives:

$$S = 2\pi v - K$$

where $K$ is the total curvature. On the other hand, one may sum over the faces. The sum of the angles of the $i$-th face is $\pi(n_i - 2)$, where $n_i$ is the number of sides of this face. Hence

$$S = \pi(n_1 + \cdots + n_f) - 2\pi f.$$

Since every edge is adjacent to two faces, $n_1 + \cdots + n_f = 2e$; therefore

$$S = 2\pi e - 2\pi f.$$

Thus $2\pi v - K = 2\pi e - 2\pi f$, which, combined with the Euler formula, yields the result. □

An analog of Lemma 20.1, along with its proof, holds for non-convex polyhedra as well and even for other polyhedral surfaces not necessarily topologically equivalent to the sphere (for example, a torus): the total curvature equals $2\pi\chi$ where $\chi = v - e + f$ is the *Euler characteristic.*

**20.3 Dual cones and spherical polygons.** Given a convex polyhedral cone $C$ with vertex $V$, consider outward normal lines to its faces through $V$. These lines are the edges of a new convex polyhedral cone $C^*$ called *dual* to $C$. A similar construction in the plane yields an angle which complements the original angle to $\pi$.

The relation between a cone and its dual in space is more complex and is described in the next lemma.

LEMMA 20.2. *The angles between the edges of $C^*$ are complementary to $\pi$ of the dihedral angles of $C$, and the dihedral angles of $C^*$ are complementary to $\pi$ of the angles between the edges of $C$.*

Proof. The first claim is clear from Figure 20.3 and the second from the symmetry of the relation between $C$ and $C^*$. □

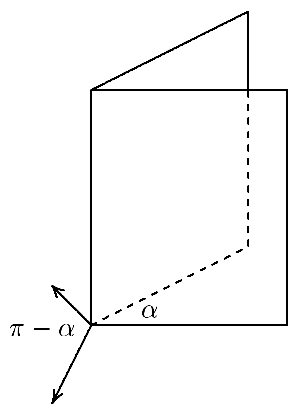


FIGURE 20.3. Proving Lemma 20.2

From this point on, our arguments involve spherical geometry. It is natural to replace the Euclidean plane by the (unit) sphere – after all, the surface of the Earth is (approximately) a sphere.[1] The role of straight lines is played by great circles (unlike the plane, any two such "lines" intersect at two points); a spherical polygon is bounded by arcs of great circles. The reader who wants to learn what are the counterparts of straight lines on arbitrary surfaces should wait until Section 20.8. The angle between two great circles, intersecting at point $X$, is defined as the angle between their tangent lines in the tangent plane to the sphere at $X$.

A peculiar property of spherical geometry is the absence of similarities; in particular, one cannot dilate a polygon so that its angles remain the same but the area changes. More precisely, the area of a spherical polygon is determined by its angles.

THEOREM 20.1. *Let $P$ be a convex $n$-gon on the unit sphere, $A$ its area and $\alpha_1, \dots, \alpha_n$ its angles. Then*

$$A = \alpha_1 + \cdots + \alpha_n - (n-2)\pi. \tag{20.1}$$

Note that, for a plane $n$-gon, the right-hand side of (20.1) vanishes.

Proof. Let us start with $n = 2$. A 2-gon is a domain bounded by two meridians connecting the poles. If $\alpha$ is the angle between the meridians, then the area of the 2-gon is the $(\alpha/2\pi)$-th part of the total area $4\pi$ of the sphere, that is, $2\alpha$.

[1]Spherical geometry was already known to the Ancient Greeks. Many results of plane geometry have spherical analogs, for example, there are spherical Laws of Sines and Cosines.

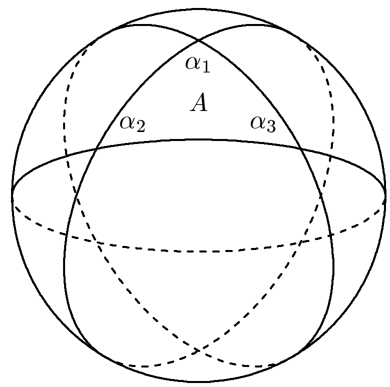


FIGURE 20.4. Area of a spherical triangle

Next, consider a spherical triangle; see Figure 20.4. The three great circles form six 2-gons that cover the sphere. The original triangle and its antipodal triangle are covered three times, and the rest of the sphere is covered once. The total area of the six 2-gons equals $2(2\alpha_1 + 2\alpha_2 + 2\alpha_3)$; hence

$$4(\alpha_1 + \alpha_2 + \alpha_3) = 4\pi + 4A.$$

This implies the statement for $n = 3$.

Finally, every convex $n$-gon with $n \geq 4$ can be cut by its diagonals into $n - 2$ triangles. The area and the sum of angles are additive under cutting, and (20.1) follows. □

As a consequence, we interpret the curvature of a convex polyhedral cone $C$ as the area of a spherical polygon. Let $C^*$ be the dual cone and consider the unit sphere centered at its vertex. The intersection of $C^*$ with the sphere is a convex spherical polygon $P$. The area of $P$ measures the solid angle of the cone $C^*$.

COROLLARY 20.2. *The area $A$ of the spherical polygon $P$ equals the curvature of the cone $C$.*

Proof. Assume that $P$ is $n$-sided and let $\alpha_i$ be its angles. The area of $P$ is given by formula (20.1).

The angles $\alpha_i$ are the dihedral angles of $C^*$. Let $\beta_i$ be the angles between the edges of the cone $C$. By Lemma 20.2, $\alpha_i = \pi - \beta_i$. Substitute into (20.1) to obtain:

$$A = 2\pi - (\beta_1 + \cdots + \beta_n).$$

The right hand side is the curvature of the cone $C$, as claimed. □

Corollary 20.2 provides an alternative proof of Lemma 20.1: one may translate the dual cones at all the vertices of $P$ to the origin, and then the cones will cover the whole space, see Figure 20.5. It follows that the sum of the areas of the respective spherical polygons is $4\pi$, and Lemma 20.1 follows. This alternative proof, combined with the argument of Lemma 20.1, implies Euler's formula as well.

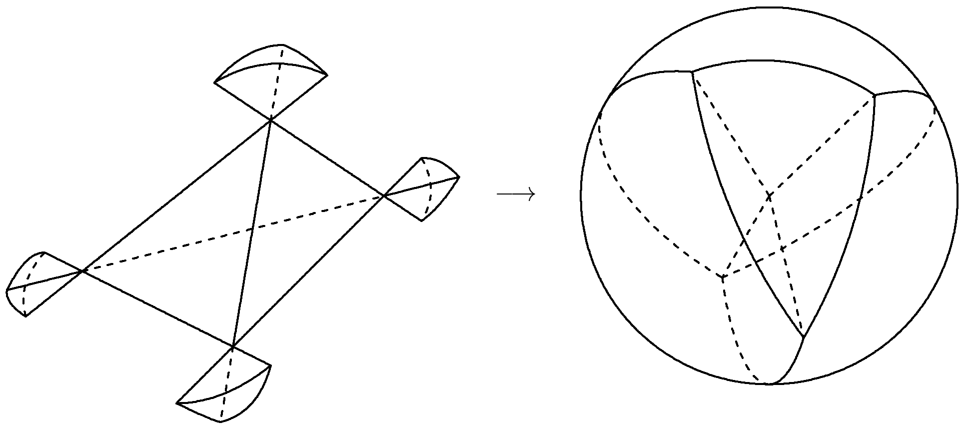

FIGURE 20.5. Sum of curvatures of a convex polyhedron

**20.4 Parallel translation and rolling.** Let us define *parallel translation* on a polyhedral surface $P$. What we want to translate is a vector, say, $v$, that lies in one of the faces of the polyhedron. As long as one stays within one face, one parallel translates $v$, just as in the plane. The question arises when one wants to carry the vector over an edge.

Let $F_1$ and $F_2$ be adjacent faces that share an edge $E$. Identify the planes of the two faces by revolution about $E$ (as if they were connected by hinges). Let a tangent vector $v$ be parallel translated inside $F_1$. When the foot point of $v$ reaches $E$, apply this rotation to obtain a vector $u$ that lies in $F_2$. Vector $u$ is the result of parallel translating $v$ across edge $E$.

Said differently, under the parallel translation of $v$ across edge $E$, the tangential component of $v$ along $E$ and its normal component remain the same. See Figure 20.6, featuring parallel translation of a vector across three adjacent edges of a cube.

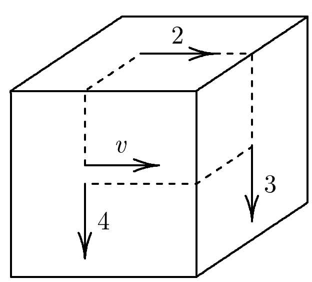


FIGURE 20.6. Parallel translation on a cube

Equivalently, position $P$ so that the face $F_1$ is on the horizontal plane and roll it across edge $E$. Now the face $F_2$ is on the horizontal plane. The prints of the vectors $v$ and $u$ on the horizontal plane are parallel. Thus parallel translation on the surface of a polyhedron is the same as rolling this polyhedron on the horizontal plane.

A *geodesic* $\gamma$ is defined as a curve on a polyhedral surface which is straight within each face and whose tangent vectors are parallel translated across each edge intersected by $\gamma$. We assume that geodesics do not pass through vertices. A realistic image of a geodesic is a ribbon wrapped around a box of chocolate. When rolling a polyhedron in the plane, a geodesic leaves a straight trace.

Geodesics minimize the distance between their sufficiently close points.

LEMMA 20.3. *Consider two planes in space, $F_1$ and $F_2$, intersecting along a line $E$, and let $A_1$ and $A_2$ be points in $F_1$ and $F_2$. Let $\gamma$ be the shortest path from $A_1$ to $A_2$ across the edge $E$ on the surface made by two half-planes, separated by $E$ . Then $\gamma$ is a geodesic.*

Proof. Turn the plane $F_2$ around the edge $E$ until it coincides with the plane $F_1$. The shortest curve $\gamma$ from $A_1$ to $A_2$ unfolds to a straight segment, therefore the unit tangent vector to $\gamma$ is parallel translated across $E$. □

**20.5 Gauss-Bonnet theorem.** Let $V$ be a vertex of a polyhedral cone $C$. Consider a vector that lies in one of the faces of the cone. Choose a closed path on the surface of the cone, starting at the foot point of the vector and going around $V$ once counterclockwise, and parallel translate the vector along the path. What happens? The foot point returns to the initial position, and the vector turns through some angle $\alpha$. This angle depends neither on the choice of the vector nor on the path. What is this angle?

LEMMA 20.4. *The angle $\alpha$ equals the curvature of $C$.*

Proof. Instead of parallel translating, put $C$ on the horizontal plane and roll it across consecutive edges. The resulting unfolding of the cone is a plane wedge whose measure is the sum of flat angles of $C$. The angle in question complements this sum to $2\pi$, and the result follows; see Figures 20.6 and 20.7. □

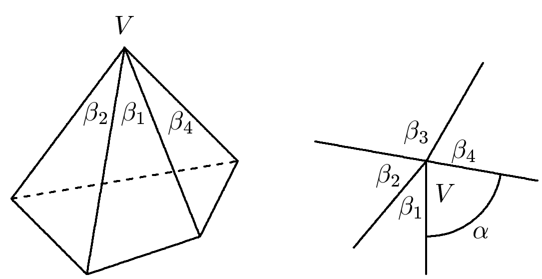


FIGURE 20.7. Proving Lemma 20.4

More generally, let $\gamma$ be an oriented simple closed path on a polyhedral surface $P$; we assume that $\gamma$ intersects the edges transversally and avoids the vertices. The curve $\gamma$ partitions $P$ into two components, one on the left and one on the right of the curve. We refer to the former as the domain bounded by $\gamma$. Choose a tangent vector $v$ with foot point on $\gamma$ and parallel translate it along $\gamma$. Let $u$ be the final vector, whose foot point coincides with that of $v$; denote by $\alpha(\gamma)$ the angle between $v$ and $u$. The next result is (a polyhedral version of) the celebrated *Gauss-Bonnet theorem.*

THEOREM 20.3. *The angle $\alpha(\gamma)$ equals the sum of curvatures of the vertices of $P$ that lie in the domain bounded by $\gamma$.*

Proof. Let us argue inductively on the number $n$ of vertices inside $\gamma$. If $n = 1$, this is Lemma 20.4.

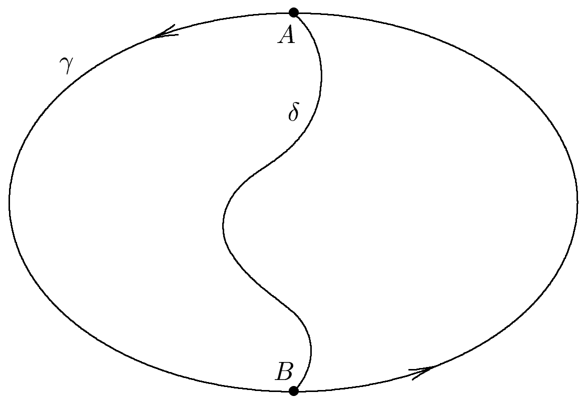


FIGURE 20.8. Proving the Gauss-Bonnet theorem

If $n > 1$, one may cut the domain bounded by $\gamma$ by an arc $\delta$ into two domains, each with fewer than $n$ vertices; see Figure 20.8. Let $\gamma_1$ be the path that follows $\gamma$ from $A$ to $B$ and then $\delta$ from $B$ to $A$. Likewise, $\gamma_2$ is the path that follows $\delta$ from $A$ to $B$ and then $\gamma$ from $B$ to $A$. The concatenation of $\gamma_1$ and $\gamma_2$ differs from $\gamma$ by the arc $\delta$, traversed back and forth. Hence the contribution of $\delta$ cancels, $\alpha(\gamma) = \alpha(\gamma_1) + \alpha(\gamma_2)$, and the result follows by induction. □

**20.6 Closed geodesics on generic polyhedra.** Figure 20.9 depicts simple closed geodesics on a regular tetrahedron and a cube. The former is the section of the tetrahedron by a plane parallel to a pair of pairwise skew edges, and the latter is the section of the cube by a plane perpendicular to its great diagonal.

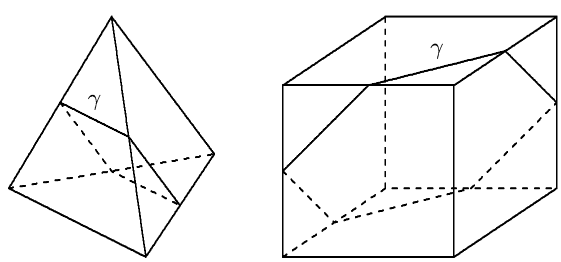


FIGURE 20.9. Closed geodesics on polyhedra

Can one find such a geodesic on a generic closed convex polyhedron $P$? What we mean by "generic" is that the only linear relation, with rational coefficients, between the curvatures of the vertices and $\pi$ is the one given by Lemma 20.1.

THEOREM 20.4. *There exist no simple closed geodesics on $P$.*

Proof. Assume there is such a geodesic $\gamma$. Then the unit tangent vector to $\gamma$ is parallel translated along $\gamma$. In particular, this tangent vector returns, without rotation, to the initial point.

On the other hand, by the Gauss-Bonnet theorem, parallel translation along $\gamma$ results in rotation through the angle equal to the sum of curvatures of the vertices inside $\gamma$. This set of vertices is a proper and non-empty subset of the set of vertices of $P$. Since $P$ is generic, the sum of curvatures cannot be a multiple of $2\pi$, a contradiction. □

In particular, the geodesics in Figure 20.9 will disappear after a generic small perturbation of the tetrahedron or the cube.

**20.7 Closed geodesics on regular polyhedra.** The discussion in the preceding section suggests that more symmetric polyhedra are more amenable for constructing closed geodesics. From this point of view, it is reasonable to investigate the case of regular polyhedra (see [**16, 31**] for such a study).

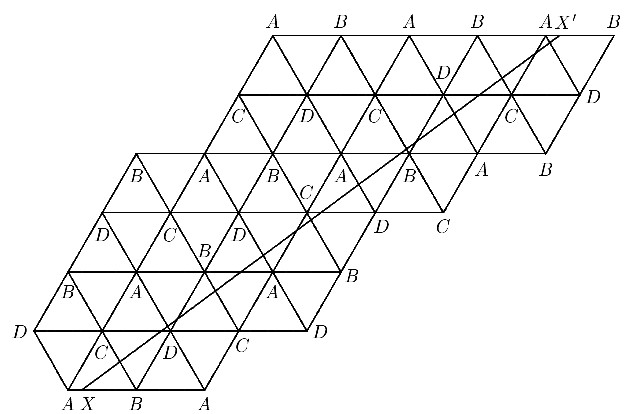


FIGURE 20.10. Triangular tiling of the plane

The simplest case is that of a regular tetrahedron. Denote a regular tetrahedron with the edge 1 by $T$ and its vertices by $A, B, C, D$. Consider the standard tiling of the plane by equilateral triangles with the unit edge and label vertices by letters $A, B, C, D$ as shown in Figure 20.10. There is a natural map $\pi$ of the plane onto the tetrahedron $T$ taking the vertices of the tiling into the vertices of $T$ labeled by the same letters, edges into edges and triangles (tiles) into the faces.

Take the coordinate system in the plane with the origin at a point labeled $A$ and coordinate vectors $\overrightarrow{AB}, \overrightarrow{AC}$ where $B$ is the next right to $A$ and $C$ is immediately above $AB$. Take points $X = (\alpha, 0),\ 0 < \alpha < 1$, on $AB$ and $X' = (\alpha + 2p, 2q), q \geq p \geq 0,\ q > 0$ on another side labeled $AB$. If $(p, q) = 1$ and $q\alpha \notin \mathbb{Z}$, then the map $\pi$ takes $XX'$ into a simple (not repeating itself) closed geodesic on $T$ of length $\sqrt{p^2 + pq + q^2}$. Moreover, this geodesic is non-self-intersecting and all closed geodesics on $T$ are given by this construction; in particular, all closed geodesics on $T$ are non-self-intersecting (see Exercise 20.8). The geodesic corresponding to $p = 2, q = 3$ is shown in Figure 20.11. It cuts the tetrahedron into two pieces also shown in Figure 20.11. (In accordance with the Gauss-Bonnet Theorem, each of the two pieces contains two vertices.)

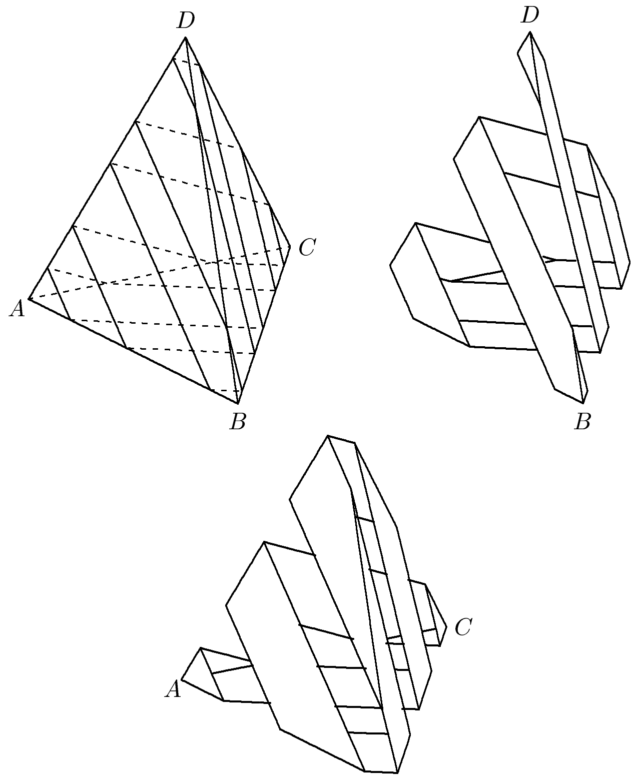


FIGURE 20.11. A closed geodesic on the tetrahedron

A full description of closed geodesics on the regular octahedron is given in Exercise 20.9. Up to a parallelism and symmetries of the octahedron, there are only two non-self-intersecting closed geodesics, of lengths 3 and $2\sqrt{3}$ (where the edge of the octahedron is unit); one of them is planar, one is not. There are also infinitely many non-parallel self-intersecting geodesics. The two non-self-intersecting closed geodesics and one self-intersecting closed geodesic are shown in Figure 20.12.

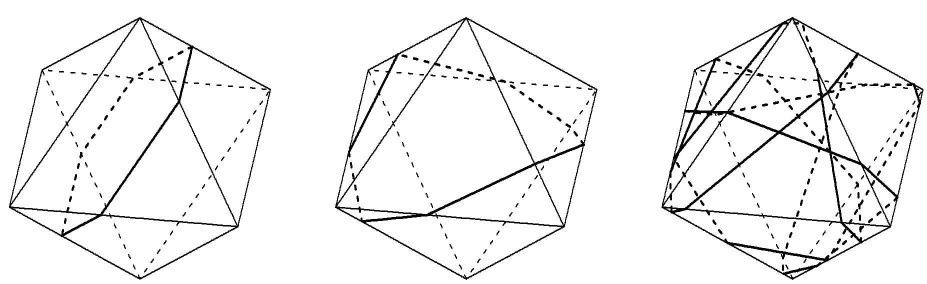

FIGURE 20.12. Three closed geodesics on the octahedron

An almost full description of closed geodesics in the cube is given in Exercise 20.10. There are three types of non-self-intersecting closed geodesics (their lengths are $4, 3\sqrt{2}, 2\sqrt{5}$), and infinitely many types of self-intersecting closed geodesics. The three non-self-intersecting and three self-intersecting closed geodesics are shown, respectively, in Figures 20.13, 20.14.

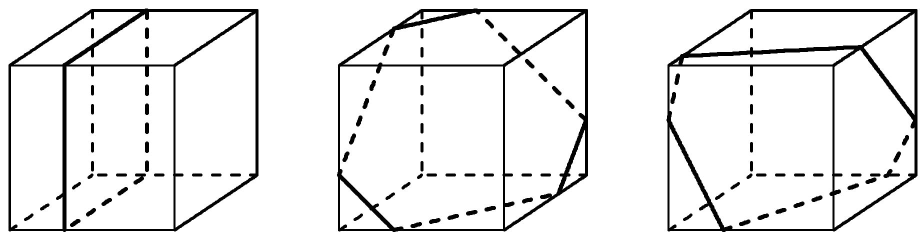

FIGURE 20.13. Simple closed geodesics on the cube

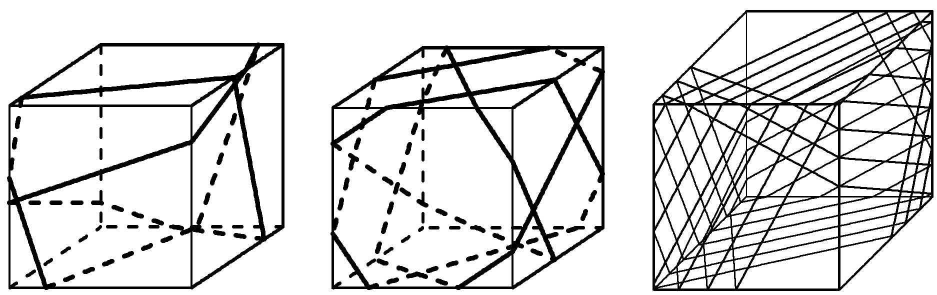

FIGURE 20.14. Self-intersecting closed geodesics on the cube

On a regular icosahedron, there are 3 (up to parallelism and symmetries of the icosahedron) non-self-intersecting closed geodesics (of lengths $5, 3\sqrt{3}$ and $2\sqrt{7}$), and only one of them is planar. They are shown in Figure 20.15. Also, there are infinitely many self-intersecting closed geodesics. (See the details in [**31**].)

**20.8 Smooth surfaces: a panorama.** In differential geometry, all the notions that we have discussed so far, are defined for smooth surfaces. The relation between the polyhedral and smooth cases is, roughly, the same as between polygonal lines and smooth curves in the plane discussed in Section 20.1.

The definition of curvature is modeled on the statement of Corollary 20.2. Let $X$ be a point of a surface. Consider a small neighborhood of point $X$ of area $A$. At every point of this neighborhood consider the unit normal vector to the surface (so the surface looks like a porcupine). Translate the foot points of these normal vectors to the origin to obtain a piece of the unit sphere. Let $A'$ be its area. The curvature of the surface at point $X$ is the limit value of the ratio $A'/A$ as the neighborhood shrinks to point $X$.

For example, the curvature of a cylinder or a cone is zero: the end points of the unit normal vectors lie on a curve, whose area is zero. The curvature of a sphere of radius $r$ is $1/r^2$.

The relation of this definition to the definition of the curvature of a polyhedral cone in Section 20.3 is straightforward. Let $C$ be a polyhedral cone. One can smooth its edges and its vertex to obtain a smooth surface, approximating the cone. The unit normal vectors to this surface describe a domain on the unit sphere.

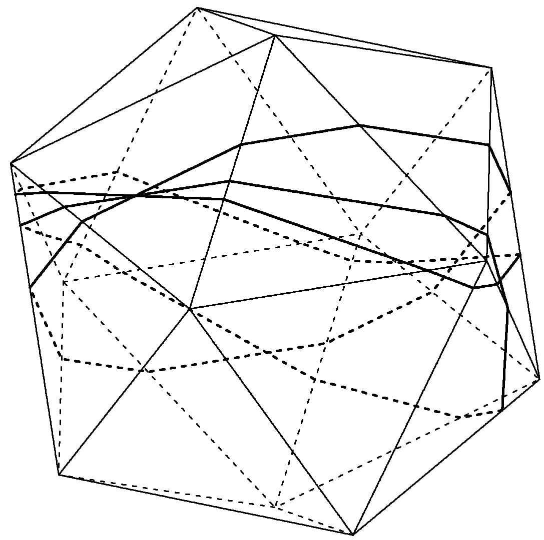

FIGURE 20.15. Closed geodesics on the icosahedron

For the cone, this domain becomes a spherical polygon $P$, the intersection of the sphere with the dual cone $C^*$. The area of $P$ is the curvature of $C$, as we know from Corollary 20.2.

The curvature has sign. This is because the area $A'$ is signed. Specifically, traverse the boundary of a neighborhood of point $X$ counter clock-wise. The end points of the unit normal vectors traverse a curve on the unit sphere; if this curve is oriented counter clock-wise, the curvature is positive, and if clock-wise – negative. See Figure 20.16 for the case of a torus.

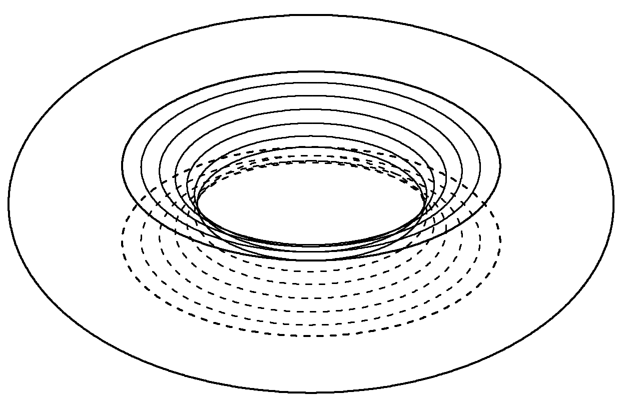

FIGURE 20.16. Positive and negative curvature

Similarly to Lemma 20.1, the total curvature of a closed convex surface is $4\pi$. For more general closed surfaces, the answer is $2\pi\chi$ where $\chi$ is the Euler characteristic.

The curvature of a polyhedral cone does not change under deformations that preserve flat angles. Likewise, the curvature of a smooth surface remains constant under isometric deformations, the deformation that do not change the inner geometry of the surface.[2] For example, a wide variety of developable surfaces are obtained by bending, without stretching, a sheet of paper (piece of plane), and they all have zero curvature; see Lecture 13.

Let $\gamma$ be an oriented smooth curve on a smooth surface $S$. Parallel translation along $\gamma$ is defined as rolling, without sliding, of the tangent plane to $S$ along $\gamma$. Equivalently, one may put $S$ on the plane and roll the surface along the curve $\gamma$.

The Gauss-Bonnet theorem holds in the smooth setting: *parallel translation of the tangent plane to a surface $S$ along an oriented simple closed curve $\gamma$ results in the rotation of the tangent plane through the angle, equal to the total curvature of $S$ inside $\gamma$.*

A *geodesic curve* on a smooth surface $S$ is defined as a curve $\gamma$ whose tangent vector is parallel translated along $\gamma$. If one rolls a surface along a geodesic curve, the trace on the horizontal plane is straight. Geodesics are trajectories of a free particle confined to $S$: their speed remains constant and their acceleration is orthogonal to the surface (that is, the only force acting on the particle is the normal reaction force). For example, the geodesics on a sphere are great circles. Just as in the polyhedral case, geodesics minimize the distance between pairs of their sufficiently close points.

Unlike Theorem 20.4, every closed smooth convex surface carries a simple closed geodesic, in fact, even three: this was conjectured by Poincaré; a proof was published by Lyusternik and Shnirelman in 1930. These three closed geodesics are manifest for an ellipsoid, they are its sections by the three planes of symmetry.

Finally, define the *geodesic curvature* of an oriented curve on a smooth surface. Approximate a curve by a geodesic polygonal line, $\gamma$. The geodesic curvature is concentrated at the corners, and its value is the angular measure of the complementary angle, positive if $\gamma$ turns left and negative if it turns right. The geodesic curvature of a geodesic line is zero.

Let $\gamma$ be an oriented simple geodesic polygon. Parallel translation along $\gamma$ results in rotation of the tangent plane, and the angle of this rotation complements the total geodesic curvature of $\gamma$ to $2\pi$, see Figure 20.17. This yields another version of the Gauss-Bonnet theorem: *the total geodesic curvature of an oriented simple closed curve $\gamma$ plus the total curvature of the surface inside $\gamma$ equals $2\pi$.*

**20.9 Three examples: tennis ball, Foucault pendulum, and bicycle wheel.** Every tennis ball has an indented closed curve on its surface. Mark a point of this curve and put the ball on the floor so that it is touching the floor at the marked point. Now roll the ball without sliding along the curve until it again touches the floor at the marked point. From the initial to the final positions of the ball, it has made a certain revolution about the vertical axis. What is the angle of this revolution?

The Gauss-Bonnet theorem provides an answer. The angle in question is the total curvature bounded by the curve. Although the curve has a complicated shape, a glance at a tennis ball reveals that this curve is symmetric and bounds exactly one half of the total curvature of the ball, that is, $2\pi$. Hence the angle of revolution is zero.

[2]This is the Teorema Egregium of C.-F. Gauss.

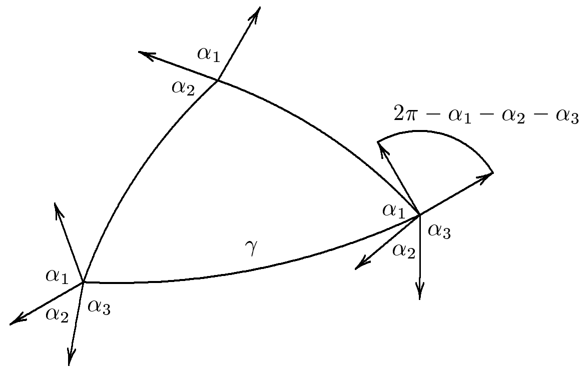


FIGURE 20.17. Parallel translation on a surface

Our second example concerns the Foucault pendulum demonstrating rotation of the earth. The original pendulum was constructed by Léon Foucault for the 1850 Paris Exhibition: this was a 67 meter, 28 kilogram pendulum suspended from the dome of the Panthéon in Paris; the plane of its motion, with respect to the earth, rotated slowly clockwise.[3] Now almost every science museum exhibits a Foucault pendulum.

Imagine that the pendulum is suspended at the North Pole. The plane of its motion remains the same while the earth rotates eastward. Thus the plane of motion of the pendulum rotates, with respect to the earth, with angular speed of $360°/24 = 15°$ per hour. The closer to the equator, the weaker the effect, and on the equator, the plane of motion of the pendulum does not rotate relative to the earth (by symmetry!)

The Foucault pendulum is a purely geometric phenomenon. Its behavior is due to the motion of the suspension point. Let us imagine that the earth is not rotating, and only the suspension point of the pendulum is moving along a curve $\gamma$ on the surface of the earth. Assume further that $\gamma$ is a spherical polygon. As long as we are moving along a geodesic segment, the plane of motion of the pendulum does not rotate relative to the direction of the geodesic. At a corner, the plane of motion of the pendulum remains the same but the direction of motion of the suspension point changes by the exterior angle $\gamma$. Thus the plane of motion of the pendulum turns relative to the direction of $\gamma$ by the exterior angle at the corner.

Conclusion: the total rotation of the plane of motion of the pendulum equals the total geodesic curvature of the trajectory of its suspension point. By the Gauss-Bonnet theorem, this is $2\pi$ minus the total curvature inside this trajectory.

Consider Foucault pendulum at latitude $\psi$. The trajectory of the suspension point is a latitude circle. The total curvature of the polar cap of the sphere bounded by this circle equals the area of the polar cap of latitude $\psi$ on the unit sphere; it is easily computed – see Exercise 20.3 – and the answer is $2\pi(1 - \sin\psi)$. Thus the total rotation of the plane of motion of the pendulum is $2\pi \sin\psi$.

For Paris, $\psi$ is about $48°$, and the angular speed of the Foucault pendulum in the Panthéon equals $11°$ per hour.

[3]The reader is recommended to the novel "Foucault's Pendulum" by Umberto Eco.

In physics, the rotation of the plane of motion of the pendulum is attributed to an inertia, Coriolis, force. The same force is accountable for the direction of the major circulations of air and wind on earth. It is observed that rivers of the Northern Hemisphere tend to erode chiefly on the right bank; those of the Southern hemisphere chiefly on the left bank. This is especially manifest for the great North flowing rivers in Russia, such as the Ob, Lena and Yenisey. This phenomenon is also often attributed to the Coriolis force although the issue remains somewhat controversial (and the Coriolis force is not responsible for rotation of water in bathtubs!)

Finally, following M. Levi [**51**], one can use a bicycle wheel with frictionless bearings for physical realization of parallel translation. Keep the plane of the wheel tangent to the surface, and set the angular velocity of the wheel relative to its axis to zero. Guiding the center of the wheel along a curve on the surface, each spoke, considered as a tangent vector, undergoes parallel translation along the curve. (The explanation of this phenomenon is essentially the same as for the Foucault pendulum.)

John Smith
January 23, 2010

Martyn Green
August 2, 1936

Henry Williams
June 6, 1944

John Smith
January 23, 2010

Martyn Green
August 2, 1936

Henry Williams
June 6, 1944

### 20.10 Exercises.

20.1. Find the sum of curvatures of an $(n, k)$-star, that is, an $n$-pronged star making $k$ turns; the numbers $n$ and $k$ are relatively prime.

20.2. Let $C$ be a convex cone and $C^*$ its dual cone. Show that $(C^*)^* = C$.

20.3. Compute the area of the polar cap of latitude $\psi$ on the unit sphere.

20.4. One throws a loop on a cone and pulls it down. If the cone is sharp, the loop will stay but if the cone angle is sufficiently obtuse the loop will slide off (of course, we assume that there is no friction). Find the critical cone angle separating the two cases.

20.5. A closed smooth simple curve is drawn in the plane. One places a convex body on the plane at some point of the curve and rolls the body, without sliding, all around the curve. Prove that the trace of the curve on the surface of the body cannot be a closed simple curve.

*Hint.* Use the Gauss-Bonnet theorem and the fact that the total curvature of a closed simple plane curve is $2\pi$.

The next problem concerns geometry of curves on the unit sphere and has much to do with the material of Section 10.2.

20.6. Let $\gamma$ be a simple convex curve on the unit sphere. Move each point of $\gamma$ distance $\pi/2$ along the outer normal (that is, the orthogonal great circle). Denote the resulting curve $\gamma^*$ and call it *dual* to $\gamma$.

(a) Show that $((\gamma)^*)^*$ is the curve antipodal to $\gamma$.

(b) Prove that the length of $\gamma^*$ equals $2\pi$ minus the area bounded by $\gamma$.

(c) Let $\gamma_\varepsilon$ be the curve obtained from $\gamma$ by moving each point distance $\varepsilon$ along the outer normal. Find the length of $\gamma_\varepsilon$ and the area bounded by it.

Denote by $\gamma'$ the curve obtained from $\gamma$ by moving each point distance $\pi/2$ along the tangent great circle to $\gamma$. The curve $\gamma'$ is called the *derivative* of $\gamma$.

(d) Let $\gamma$ be a circle of latitude $\phi$. Find $\gamma'$.

(e) Prove that $\gamma'$ bisect the area of the sphere.

20.7. Given a convex polytope $P$, denote by $S(P)$ the sum of the solid angles at its vertices and by $D(P)$ the sum of its dihedral angles.

(a) If $P$ is a tetrahedron, prove that $S(P) - 2D(P) + 4\pi = 0$.

*Hint.* Parallel translate the faces of $P$ to the origin and consider the partition of the unit sphere by the respective half-spaces. Use the inclusion-exclusion formula.

(b) In general, prove that $S(P) - 2D(P) + 2\pi f - 4\pi = 0$ where $f$ is the number of faces of $P$ (Gram's theorem).

*Hint.* Cut $P$ into tetrahedra and use additivity of the desired relation.

20.8. (a) Prove that the construction given in Section 20.7 gives all closed geodesics on a regular tetrahedron.

(b) Prove that all closed geodesics on a regular tetrahedron are non-self-intersecting.

20.9. A straight interval in the plane equipped with the standard triangular tiling as in Figure 20.10 (but without letter notations for the vertices) not passing through the vertices yields a geodesic on a octahedron, once the trianlge containing the initial point is identified with a face of the octahedron. Consider an interval with the endpoints $(\alpha, 0)$, $(\alpha + k, \ell)$ with $0 < \alpha < 1$, $k, \ell \in \mathbb{Z}$, $\ell \geq k \geq 0$, $\ell > 0$, $\frac{\ell}{(k,\ell)}\alpha \notin \mathbb{Z}$, as in Figure 20.10. Call $(k, \ell)$ a *good pair*, if this interval corresponds to a closed, non-self-repeating geodesic.

(a) Let $(p, q) = 1$, $q \geq p \geq 0, q > 0$. If $p \equiv q \bmod 3$, then $(2p, 2q)$ is a good pair. If $p \not\equiv q \bmod 3$, then $(3p, 3q)$ is a good pair.

(b) Up to parallelism and symmetries of the octahedron, the pairs from Part (a) yield all closed geodesics on the regular octahedron.

(c) Only geodesics corresponding to the good pairs $(0, 3)$ and $(2, 2)$ are non-self-intersecting.

20.10. A straight interval in the plane not passing through the vertices of the standard square tiling yields a geodesic on a cube, once the square containing the initial point is identified with a face of the cube. We use the natural coordinate system in which the vertices of the tiling are the points with integral coordinates. Consider an interval with the endpoints $(\alpha, 0)$, $(\alpha + k, \ell)$ with $0 < \alpha < 1$, $k, \ell \in \mathbb{Z}$, $\ell \geq k \geq 0$, $\ell > 0$, $\frac{\ell}{(k,\ell)}\alpha \notin \mathbb{Z}$. Once again, $(k, \ell)$ is a *good pair* if this interval corresponds to a closed, non-self-repeating geodesic.

(a) Let $(p, q) = 1$. If $p$ and $q$ are both odd, then $(3p, 3q)$ is a good pair. If one of $p, q$ is even, then either $(2p, 2q)$ or $(4p, 4q)$ is a good pair. (We do not know which one.)

(b) Up to parallelism and symmetries of the cube, the pairs from Part (a) yield all closed geodesics on the cube.

(c) Only the geodesics corresponding to the good pairs $(0, 4), (3, 3)$ and $(2, 4)$ are non-self-intersecting.

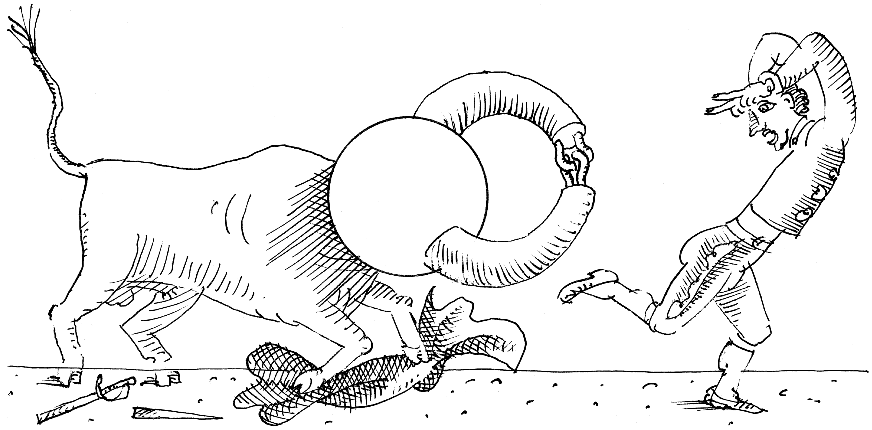

LECTURE 21

# Non-inscribable Polyhedra

**21.1 Main theorem.** The vertices of a randomly chosen convex polyhedron are not likely to lie on a sphere. For example, the pyramid in Figure 21.1 is not inscribed into a sphere if its quadrilateral base is not inscribed into a circle. But one can easily adjust the shape of the base so that it becomes an inscribed quadrilateral, and then the pyramid becomes an inscribed polyhedron. One is tempted to think that every convex polyhedron can be adjusted to get inscribed into a sphere.

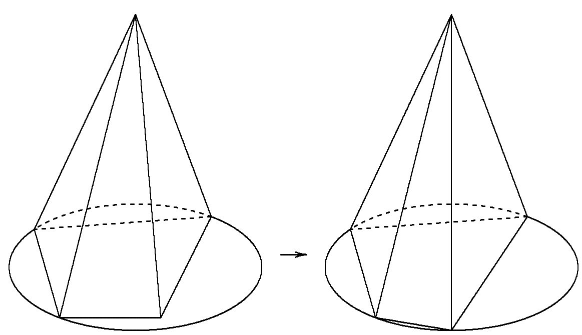

FIGURE 21.1. Deforming a pyramid to inscribe it into a sphere

This is not at all so! In 1928, E. Steinitz proved the following theorem.

THEOREM 21.1. *Let $P$ be a convex polyhedron whose vertices are colored black and white so that there are more black vertices and no two black vertices are adjacent. Then $P$ cannot be inscribed into a sphere.*

The condition is purely combinatorial, so no deformation can make $P$ inscribed. Thus $P$ is a *non-inscribable polyhedron.*

Here is an example of a polyhedron satisfying this condition. Consider an octahedron and color its vertices white. Attach a tetrahedron to every face (with sufficiently small altitude, not to violate convexity) and color these new vertices black. We have 8 black and 6 white vertices, and no two black ones are connected by an edge, see Figure 21.2. Equally well, one may start with an icosahedron instead of an octahedron.

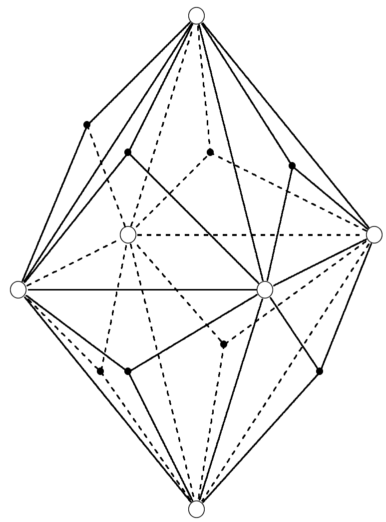

FIGURE 21.2. A non-inscribable polyhedron

At first glance, the situation appears paradoxical. A regular octahedron is already inscribed into a sphere. One can easily choose the sizes of the tetrahedra, attached to its faces, so that their new vertices lie on the same sphere, and we obtain an inscribed polyhedron. What goes wrong is that this new polyhedron is not convex!

Proof. Consider a sphere $S$ and a wedge (formed by two planes) whose edge intersects $S$ at points $A$ and $B$. The intersection of the two planes, that make the wedge, with the sphere are two circles. Let $\alpha$ be the angle between the circles evaluated at point $A$. We shall call $\alpha$ the dihedral angle relative to the sphere or, for short, the relative dihedral angle. Clearly, one may equally well choose the point $B$: this yields a congruent angle, see Figure 21.3. An exterior relative dihedral angle is $\pi - \alpha$ where $\alpha$ is a relative dihedral angle.

Consider now a convex polyhedral cone whose vertex $A$ lies on the sphere $S$ and whose edges intersect the sphere. Then the sum of its exterior relative dihedral angles is $2\pi$. Indeed, one can use the tangent plane to $S$ at $A$ to evaluate the relative dihedral angles as follows. Move this plane parallel to itself inside the sphere so that it intersects all the edges of the cone. The intersection is a convex polygon whose angles are equal to the relative dihedral angles. But the sum of the exterior angles of any convex polygon is $2\pi$, and this proves our claim – see Figure 21.4.

After this preparation, consider an inscribed polyhedron $P$ satisfying the condition of the theorem. For every vertex, the sum of the exterior relative dihedral angles is $2\pi$. Let $\Sigma$ be the sum of these angles, taken with positive signs for the white vertices, and negative signs for the black vertices. On the one hand, there are more black vertices, so $\Sigma < 0$.

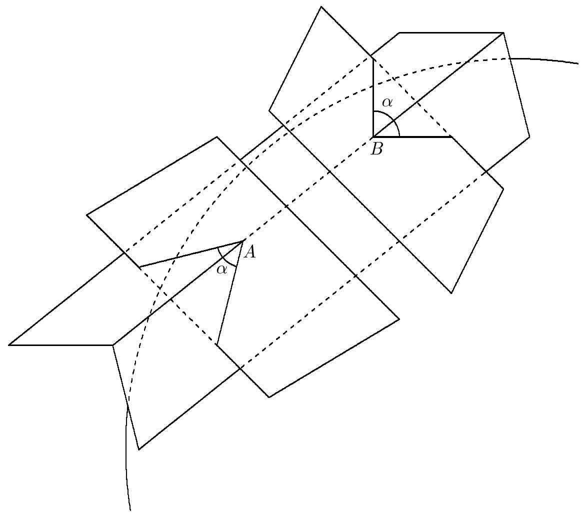


FIGURE 21.3. Relative dihedral angles

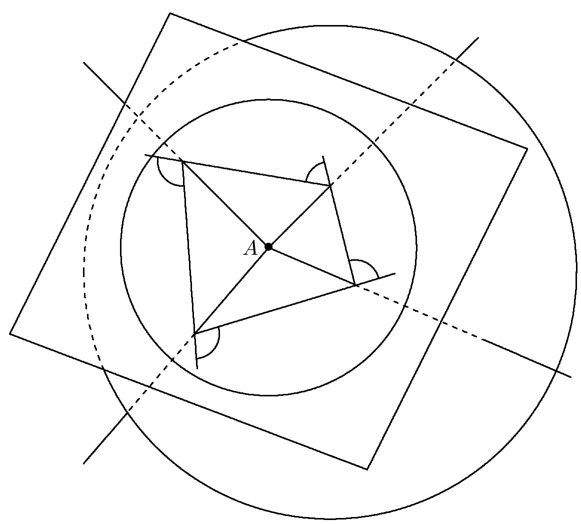


FIGURE 21.4. Proof of Theorem 21.1

On the other hand, there are two kinds of edges: with two white vertices and with one white and one black vertex. The exterior relative dihedral angles at the end points of an edge are equal. For a white–white edge, the two contributions to $\Sigma$ are positive, and for a white–black edge the contributions cancel. Thus $\Sigma \geq 0$, a contradiction. □

**21.2 Another example.** Theorem 21.1 is a sufficient condition for convex polyhedron not to be inscribable, but by no means it is necessary. Consider the example shown in Figure 21.5. This truncated cube $P$ does not satisfy the conditions of Theorem (21.1). Let us prove that $P$ is not inscribable.

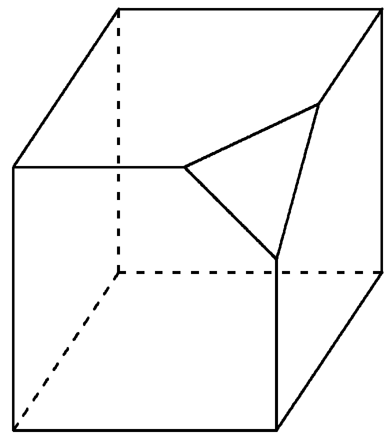

FIGURE 21.5. Truncated cube

Consider a polyhedral cone with three faces and vertex $A$ whose edges intersect a sphere $S$.

LEMMA 21.1. *The sum of the relative dihedral angles is less, equal or greater than $\pi$ depending on whether $A$ lies outside, on or inside $S$.*

Proof. The faces of the cone intersect the sphere along three circles, and the angles between these circles are the relative dihedral angles. Pick a point of the sphere not on the circles and project $S$ stereographically from this point. We obtain three circles in the plane, and the angles between the circles are the same as on the sphere (this is because stereographic projection preserves angles and takes circles to circles).

If $A$ lies on $S$ then the three circles intersect at one point, and the sum of the angles is $\pi$, see Figure 21.6. If $A$ lies off $S$, there are two cases, shown in Figure 21.6, depending on whether $A$ is outside or inside. In the former, the sum of angles is less than $\pi$, and in the latter greater than $\pi$. □

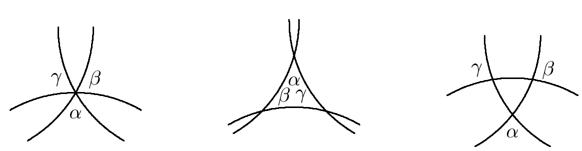


FIGURE 21.6. Mutual position of three circles

Let us return to the truncated cube $P$, and assume that it is inscribed into a sphere $S$. Denote by $Q$ the initial cube, that is, the polyhedron whose truncation is $P$. Let us color the vertices of $Q$ black and white so that the end points of each edge have opposite colors. Call the truncated vertex $A$ and assume that it was white.

Assign to each edge of $Q$ the exterior relative dihedral angle of the respective edge of $P$. For each vertex of $Q$, except $A$, the sum of these angles is $2\pi$. The vertex $A$ clearly lies outside of $S$ so, by Lemma 21.1, the sum of the relative dihedral angles at $A$ is less than $\pi$, and therefore, the sum of the exterior relative dihedral angles is greater than $2\pi$.

Now, as in the proof of Theorem 21.1, sum up, with signs, these sums of relative angles over all vertices of $Q$. On the one hand, we get zero: every edge has one black and white end point. On the other hand, this sum is positive: the seven vertices of $Q$, 3 white and 4 black, contribute $-2\pi$ to the total, and the contribution of $A$ is greater than $2\pi$. A contradiction. □

In conclusion, let us mention that there is a third type of mutual position of a sphere and convex polyhedron: when all the edges are tangent to the sphere. P. Koebe proved in 1936 that such polyhedra realize all combinatorial types of a convex polyhedra. Much later, in 1992, O. Schramm proved in the paper titled “How to cage an egg” [**69**] that the sphere can be replaced by an arbitrary ovaloid.

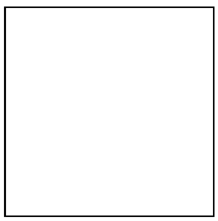

John Smith
January 23, 2010

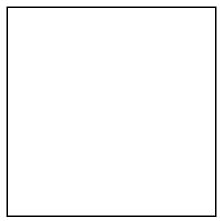

Martyn Green
August 2, 1936

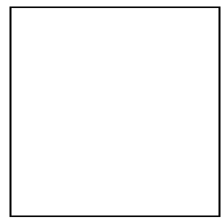

Henry Williams
June 6, 1944

### 21.3 Exercises.

21.1. Make an explicit computation to check that if one attaches tetrahedra to the faces of an octahedron so that their vertices lie on the circumscribed sphere of the octahedron then the resulting polyhedron is not convex, see Figure 21.2.

21.2. Prove that the stereographic projection from the sphere to the plane takes circles to circles and preserves the angles between them.

21.3. * Let $P$ be a polyhedron whose faces are colored black and white so that there are more black faces and no two black faces are adjacent. Then $P$ is not circumscribed about a sphere.

A simple example of such a polyhedron is obtained by cutting off all the vertices of a cube, see Figure 21.7.

21.4. Consider a polyhedron such that every vertex is adjacent to the same number of faces. Prove that if the vertices are colored black and white in such a way that no two vertices of the same color are adjacent then the number of black vertices equals the number of white ones.

21.5. Prove that the vertices of a polyhedron can be colored black and white in such a way that no two vertices of the same color are adjacent if and only if each face has an even number of edges.

*Hint.* Color one vertex, then the adjacent vertices, then their adjacent ones, etc. This process either results in the desired coloring or there is a closed path made of an odd number of edges of the polyhedron.

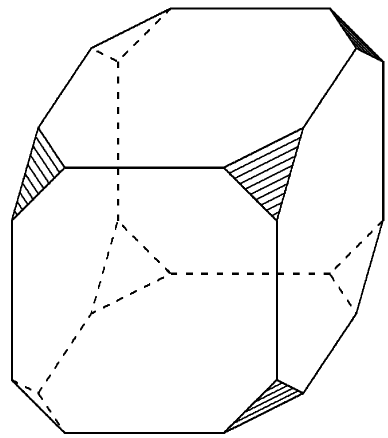

FIGURE 21.7. A non-circumscribable polyhedron

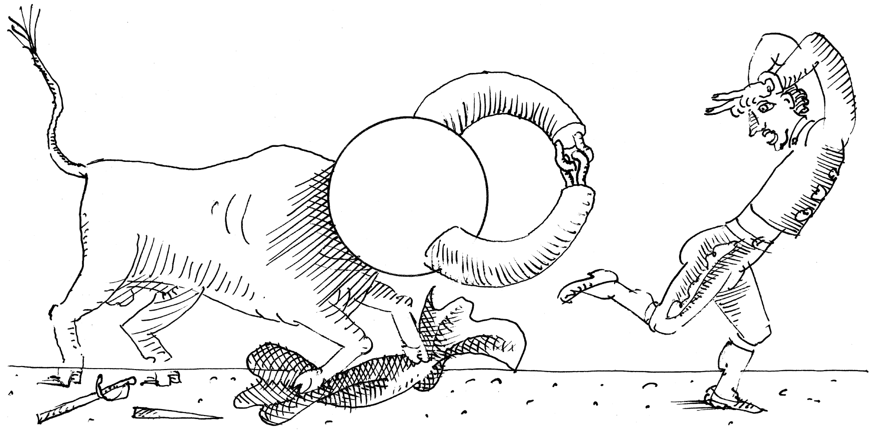

LECTURE 22

# Can One Make a Tetrahedron out of a Cube?

**22.1 Hilbert's Third Problem.** *Is it possible to cut a cube by finitely many planes and assemble, out of the polyhedral pieces obtained, a regular tetrahedron of the same volume?*

This is a slight modification of one of the 23 problems presented by David Hilbert in his famous talk at the Congress of Mathematicians in Paris, on August 8, 1900; it goes under the number 3. Hilbert's problems had a tremendous impact on mathematics. Most of them were solved during the 20-th century, and each has a very special history. Still, the Third Problem remains exceptional in many respects.

First, this was the first of Hilbert's problems to be solved. The solution belonged to a 23 year old German geometer, Hilbert's student Max Dehn [**20**]. His article appeared two years after the Paris Congress, but the solution was found earlier, maybe, even before Hilbert stated the problem.

Dehn's proof (more or less the same as the one presented below) was short and clear, and it became one of the favorite subjects for popular lectures, articles, and books in geometry, like the one you are holding in your hands. But among working mathematicians, it was almost forgotten.

Certainly, the name of Dehn was not forgotten. He became one of the few top experts in the topology of three-dimensional manifolds, and his work of 1902 has been never regarded as his main achievement.

In 1976, the American Mathematical Society published a two-volume collection of articles under the title "Mathematical Developments Arising from Hilbert Problems" [**93**]. It was a very solid account of the three quarters of century history of the problems: solutions, full and partial, generalizations, similar problems, and so on. This edition contains a thorough analysis of 22 of 23 Hilbert's problems. And only the Third Problem is not discussed there. The opinion of the editors is obvious: no developments, no influence on mathematics; nothing to discuss.

How strange it seemed just a couple of years later! Dehn's theorem, Dehn's theory, Dehn's invariant became one of the hottest subjects in geometry. This was stimulated by then new-born K-theory, an exciting domain developed on the borderline between algebra and topology. We shall not follow this development, but shall just present the theorem and its proof.

**22.2 For a similar problem in the plane the answer is yes.**

THEOREM 22.1 (Wallace, Bolyai, Gerwien). *Let $P_1$ and $P_2$ be two plane polygons of the same area. Then it is possible to cut $P_1$ into pieces by straight lines and to reassemble these pieces as $P_2$.*

Proof. First, it is clear that it is sufficient to consider the case when $P_2$ is a rectangle with one side of length 1 and with area $P_1$; in doing this, we can shorten the notation of $P_1$ to just $P$.

Second, since any polygonal domain can be cut into triangles, we can reduce the general case to that of a triangle (see Figure 22.1).

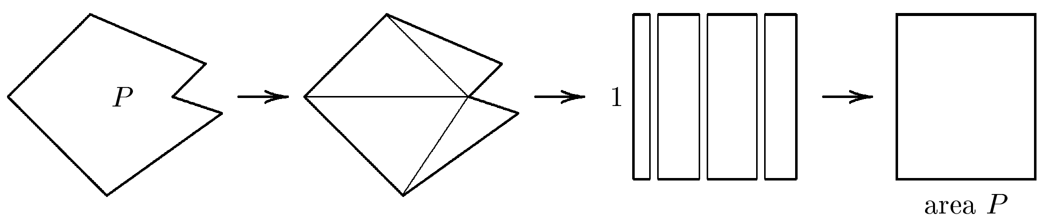


FIGURE 22.1. Reducing the general polygonal case to that of a triangle

Third, we need to transform, by cutting and pasting, a triangle into a rectangle with one of the sides having length one. This is done, in four steps, in Figure 22.2.

First, we make a parallelogram out of our triangle (Step 1). Then we cut a small triangle on one side of the parallelogram and attach it to the other side in such a way that the length of one of the sides of the parallelogram becomes rational, $p/q$ (Step 2). On Step 3, we make this parallelogram a rectangle (the number of horizontal cuts needed depends on the shape of the parallelogram). On the final step, we cut the rectangle into $pq$ equal pieces by $p-1$ horizontal lines and $q-1$ vertical lines (with the understanding that it is the vertical side of the rectangle that has the length $p/q$); then we rearrange these $pq$ pieces into a rectangle with the length of the vertical side being 1.

**22.3 A planar problem which does not look similar to Hilbert's Third Problem, but has a similar solution.** *Is it possible to cut a $1 \times 2$ rectangle into finitely many smaller rectangles with sides parallel to the sides of the given rectangle and to assemble a $\sqrt{2} \times \sqrt{2}$ square?*

The answer is *NO*. The proof is more algebraic than geometric, but still, unlike the Hilbert Problem, it requires a small geometric preparation.

*22.3.1 A geometric preparation.* Let us be given two rectangles with vertical and horizontal sides (below, we shall call such rectangles briefly $VH$-rectangles), and suppose that it is possible to cut them into smaller $VH$-rectangles such that the pieces of the first are equal (congruent) to the pieces of the second.

Then there exists a collection of $N$ (still smaller) $VH$-rectangles such that each of the given rectangles can be obtained by a sequence of $N-1$ *admissible moves*. An admissible move is: we take two of our small rectangles having equal widths or

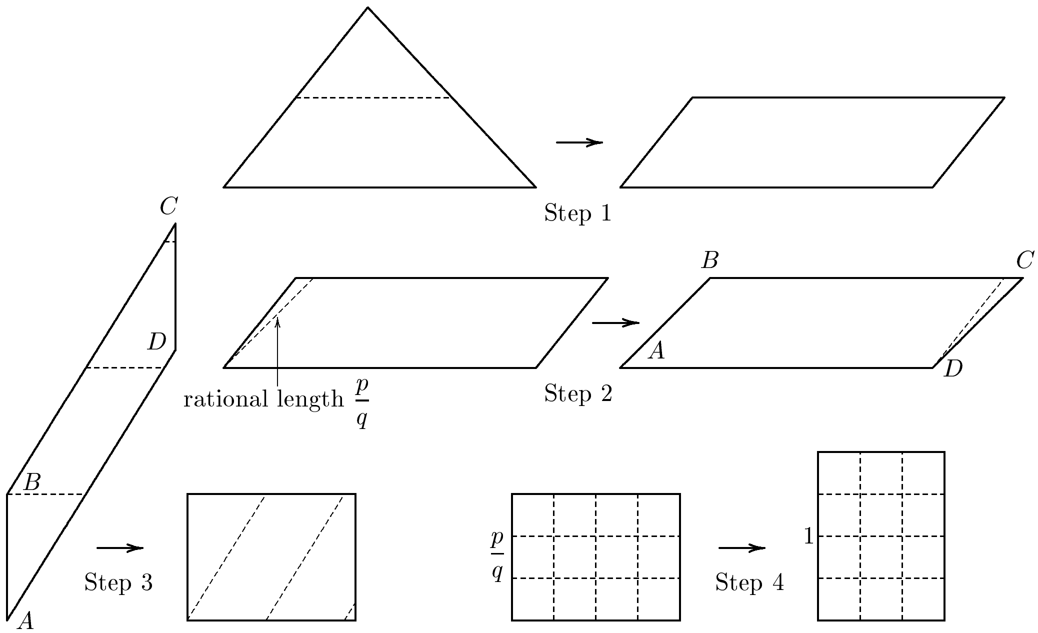


FIGURE 22.2. Making a triangle into a rectangle

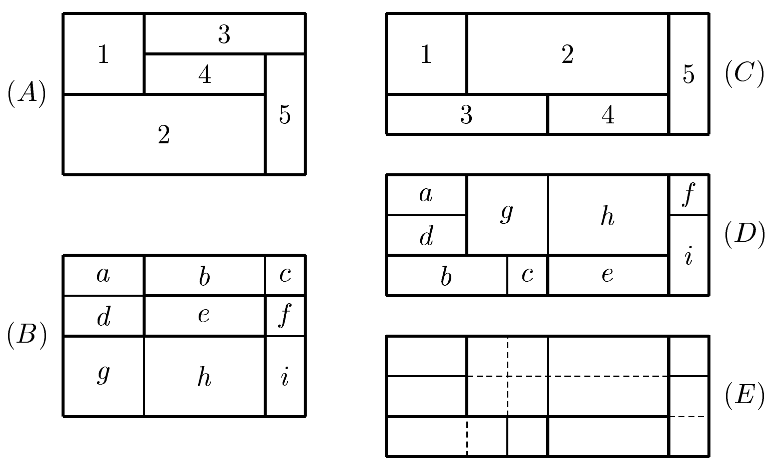


FIGURE 22.3. Creating rectangles by admissible moves

equal heights and attach them to each other vertically or horizontally, creating one rectangle of the same width or height. Thus our process of cutting is replaced by the process of attaching rectangles. How to do this, is shown on Figure 22.3.

Suppose that two rectangles are cut into equal pieces as requested by the Problem (the rectangles $(A)$ and $(C)$ in Figure 22.3; equal pieces are marked there by the same Arabic numbers). Then we extend the sides of the pieces of the rectangle $(A)$ to the whole width or length of this rectangle (see the rectangle $(B)$ in Figure 22.3). Some of the pieces of the division are cut into smaller pieces (marked by

Roman letters in the rectangle ($B$): so **1** becomes a union of $a$ and $d$, **2** becomes a union of $g$ and $h$, etc.) Then we divide in the same way the pieces of the second given rectangle (see the rectangle ($D$) in Figure 22.3; we break the rectangle **1** of the rectangle ($C$) into pieces congruent to $a$ and $d$, the rectangle **2** into pieces $g, h$, and so on). We obtain a new division of the second given rectangle, $C$, into smaller rectangles, and again extend the sides of these smaller pieces to the whole width or length of the rectangle (see the rectangle ($E$) of Figure 22.3). These last pieces form our collection. Obviously we can assemble the rectangle ($C$) from these pieces using the admissible moves. Other admissible moves produce, out of our small rectangles, the parts of the finer division of the rectangle ($A$) (that is, $a, b, c, \dots, i$), and out of these parts we can assemble, using admissible moves, the rectangle ($A$). The geometric preparation is over.

*22.3.2 An algebraic proof. Let us have a finite collection of $VH$-rectangles with total area 2. Suppose that one can compose out of these rectangles, using only admissible moves, a $(1 \times 2)$-rectangle. Then it is impossible to compose out of these rectangles, using only admissible moves, a $(\sqrt{2} \times \sqrt{2})$-square.*

This is what we need to prove that the answer to the question of this section is negative.

Let $w_1, \dots, w_N$ be the widths of the rectangles of our collection ($N$ being the number of these rectangles), and $h_1, \dots, h_N$ be their heights.

Consider the sequence

$$1, \sqrt{2}, w_1, \dots, w_N; \tag{22.1}$$

remove all terms in this sequence that are linear combinations of the preceding terms with rational coefficients. (Thus, we do not remove 1; we do not remove $\sqrt{2}$, since it is irrational; we remove $w_1$, if and only if $w_1 = r_1 + r_2\sqrt{2}$, with rational $r_1, r_2$, and so on.) Let $a_1, \dots, a_m$ be the remaining numbers (thus, $a_1 = 1, a_2 = \sqrt{2}$). It is important that each of the numbers (22.1) can be presented as a rational linear combination of the numbers $a_1, \dots, a_m$ in a unique way.

(This is a standard theorem from linear algebra, but for the sake of completeness, let us give a proof. $1 = a_1$ is a rational linear combination of $a_1, \dots, a_m$, and so is $\sqrt{2} = a_2$. Assume, by induction, that all the numbers (22.1) preceding $w_k$ are rational linear combinations of $a_1, \dots, a_m$. If $w_k$ is not a rational linear combination of preceding numbers, then it is one of $a_j$'s, and hence is a rational linear combination of $a_1, \dots, a_m$; if $w_k$ is a rational linear combination of preceding numbers, then it is a rational linear combination of $a_1, \dots, a_m$, since all the preceding numbers are rational linear combinations of $a_1, \dots, a_m$. It remains to prove uniqueness. If two different rational linear combinations of $a_1, \dots, a_m$ are equal, $\sum_{i=1}^m r_i' a_i = \sum_{j=1}^m r_j'' a_j$, and $s$ is the largest of $1, \dots, m$, for which $r_s' \neq r_s''$, then $a_s = \displaystyle\sum_{i=1}^{s-1} \frac{r_i' - r_i''}{r_s'' - r_s'} a_i$ which shows that $a_s$ is a rational linear combination of preceding $a_j$'s, in contradiction to the choice of $a_1, \dots, a_m$.)

Now, do the same with the sequence

$$1, \sqrt{2}, h_1, \dots, h_N. \tag{22.2}$$

We shall get the numbers $b_1, \dots, b_n$ with $b_1 = 1, b_2 = \sqrt{2}$ such that each of the numbers (22.2) can be presented as a rational linear combination of the numbers $b_1, \dots, b_n$ in a unique way.

Call a rectangle admissible, if its width is a rational linear combination of $a_1, \dots, a_m$ and its height is a rational linear combination of $b_1, \dots, b_n$. Let $P$ be an admissible rectangle of the width $w$ and the length $h$, and let $w = \sum_{i=1}^m r_i a_i$ and $h = \sum_{j=1}^n s_j b_j$ with rational $r_i$'s an d $s_j$'s. We define the *symbol* Symb$(P)$ of the rectangle $P$ as the rational $m \times n$ matrix $\|S_{ij}\|$ with $S_{ij} = r_i s_j$. We shall use the notation $\text{Symb}(P) = \sum_{i,j} r_i s_j \, a_i \otimes b_j$ for the symbols (which is simply an alternative notation for the matrix above). Thus, we regard the symbols as "formal rational linear combination" of the "expressions" $a_i \otimes b_j$. Such formal linear combinations can be added in the obvious way; we consider two formal rational linear combinations $\sum_{i,j} t'_{ij} a_i \otimes b_j,\ \sum_{i,j} t''_{ij} a_i \otimes b_j$ equal if $t'_{ij} = t''_{ij}$ for all $i, j$.

Let $P'$ and $P''$ be two admissible rectangles of equal heights or equal widths. Then we can merge these two rectangles into one rectangle, $P$, using an admissible move. Obviously, $P$ is also an admissible rectangle, and $\text{Symb}(P) = \text{Symb}(P') + \text{Symb}(P'')$. Indeed, if $P'$ and $P''$ have widths $w' = \sum_{i=1}^m r'_i a_i$ and $w'' = \sum_{i=1}^m r''_i a_i$ and the same height $h = \sum_{j=1}^n s_j b_j$, then $P$ has the width $w' + w'' = \sum_{i=1}^m (r'_i + r''_i) a_i$ and the height $h$, and

$$\begin{aligned}\text{Symb}(P) &= \textstyle\sum_{i,j} (r'_i + r''_i) s_j \ a_i \otimes b_j \\ &= \textstyle\sum_{i,j} r'_i s_j \ a_i \otimes b_j + \sum_{i,j} r''_i s_j \ a_i \otimes b_j \\ &= \text{Symb}(P') + \text{Symb}(P'').\end{aligned}$$

Thus, if we have a collection of admissible rectangles, $P_1, \dots, P_N$, and can assemble out of them, by $N - 1$ admissible moves, a rectangle $P$, then $\text{Symb}(P) = \sum_{i=1}^N \text{Symb}(P_i)$. If we can assemble in this way two different rectangles, $P$ and $P'$, then $\text{Symb}(P') = \text{Symb}(P)$. This proves our theorem, since the symbol of a $1 \times 2$ rectangle is $2(a_1 \otimes b_1)$, and the symbol of a $\sqrt{2} \times \sqrt{2}$ square is $a_2 \otimes b_2$ which is different. □

## 22.4 Proof of Dehn's Theorem.

We want to prove the following.

THEOREM 22.2. *Let $C$ and $T$ be a cube and a regular tetrahedron of the same volume. Suppose that each of them is cut into the same number of pieces by planes. (That is, we cut our polyhedron into two pieces, then cut one of the two pieces into two pieces, then cut one of the three pieces into two pieces, and so on.) It is not possible that the two collections of (polyhedral) pieces are the same.*

Proof. Let $\ell_1, \dots, \ell_N$ be the lengths of all edges of all polyhedra involved in the two cutting processes. Let $\varphi_1, \dots, \varphi_N$ be the corresponding dihedral angles (we suppose that $0 < \varphi_i < \pi$ for all $i$). Take the sequence $\ell_1, \dots, \ell_N$ and remove from it any term which is a rational linear combination of the previous terms; we obtain a sequence $a_1, \dots, a_m$ such that each of the $\ell_k$'s is equal to a unique rational linear combination of $a_i$'s. Then do the same with the sequence $\pi, \varphi_1, \dots, \varphi_N$; the resulting sequence is denoted by $\alpha_0 = \pi, \alpha_1, \dots, \alpha_n$, and each of the $\varphi_k$'s is equal to a unique linear combination of $\alpha_j$'s. Call a convex polyhedron admissible, if the length of every edge is a rational linear combination of $a_1, \dots, a_m$ and each dihedral angle is a rational linear combination of $\alpha_0, \alpha_1, \dots, \alpha_n$.

Let $m_1, \dots, m_q$ be the lengths of edges of an admissible convex polyhedron $P$, and let $\psi_1, \dots, \psi_q$ be the corresponding dihedral angles. Let $m_k = \sum_{i=1}^m r_{ki} a_i$ and $\psi_k = \sum_{j=0}^n s_{kj} \alpha_j$. Similarly to the symbol considered in the previous section, we define the *Dehn invariant* of $P$ by the formula

$$\mathrm{Dehn}(P) = \sum_{i=1}^{m} \sum_{j=1}^{n} \left( \sum_{k=1}^{q} r_{ki} s_{kj} \right) a_i \otimes \alpha_j.$$

*Important remark*: it is not a misprint that the second summation is taken from $j = 1$ to $n$, not from $j = 0$ to $n$; we do not include into the Dehn invariant the summand $s_{k0}\pi$. Thus, if one changes an angle by a rational multiple of $\pi$, then the Dehn invariant is not affected; if some dihedral angle *is* a rational multiple of $\pi$, then the corresponding edge does not appear in the expression for the Denh invariant at all.

EXAMPLE 22.1. The Dehn invariant of a cube (or of a rectangular box) is zero. Indeed, all the angles are $\pi/2$.

LEMMA 22.2. *Let $P$ be a convex polyhedron. Suppose that it is cut by a plane $L$ into two pieces, $P'$ and $P''$. Then (provided that $P, P'$, and $P''$ are admissible)*

$$\mathrm{Dehn}(P) = \mathrm{Dehn}(P') + \mathrm{Dehn}(P'').$$

Proof. Let $S = \{e_1, \dots, e_q\}$ be the set of all edges of $P$, let $\ell_k$ be the length of the edge $e_k$ and $\psi_k$ be the corresponding dihedral angle. We divide the set $S$ into four subsets: $S_1$ consists of edges which have no interior points in $L$ and lie on the $P'$ side of $L$; $S_2$ is the similar set with $P''$ instead of $P'$; $S_3$ consists of edges $e_k$ cut by $L$ into an edge $e'_k$ of $P'$ and an edge $e''_k$ of $P''$; and $S_4$ consists of edges which are totally contained in $L$; for each $e_k \in S_4$, the dihedral angle $\psi_k$ is divided by $L$ into two parts: $\psi'_k$ and $\psi''_k$. Consider also the intersection $L \cap P$. This is a convex polygon; each $e_k \in S_4$ is its side; let $T = \{f_1, \dots, f_p\}$ be the set of the other sides. Each $f_k$ is a side of both $P'$ and $P''$; let $m_k$ be the length of $f_k$ and $\chi'_k, \chi''_k$ be the corresponding dihedral angles in $P'$ and $P''$. Obviously, $\chi'_k + \chi''_k = \pi$.

The edges of $P'$ are:
– the edges $e_k \in S_1$; the lengths are $\ell_k$, the angles are $\psi_k$;
– the edges $e'_k$ for $e_k \in S_3$; the lengths are $\ell'_k$, the angles are $\psi_k$;
– the edges $e_k \in S_4$; the lengths are $\ell_k$, the angles are $\psi'_k$;
– the edges $f_k \in T$; the lengths are $m_k$, the angles are $\chi'_k$.

The edges of $P''$ are:
– the edges $e_k \in S_2$; the lengths are $\ell_k$, the angles are $\psi_k$;
– the edges $e''_k$ for $e_k \in S_3$; the lengths are $\ell''_k$, the angles are $\psi_k$;
– the edges $e_k \in S_4$; the lengths are $\ell_k$, the angles are $\psi''_k$;
– the edges $f_k \in T$; the lengths are $m_k$, the angles are $\chi''_k$.

The Dehn invariant of each of the polyhedra $P', P''$, and $P$ consists of four groups of summands; for $P'$ and $P''$ these groups correspond to the four groups of edges as listed above; for $P$ they correspond to the sets $S_1, S_2, S_3, S_4$. The first group of summands in $\mathrm{Dehn}(P')$ is the same as the first group of summands in $\mathrm{Dehn}(P)$. The first group of summands in $\mathrm{Dehn}(P'')$ is the same as the second group of summands in $\mathrm{Dehn}(P)$. The sum of the second groups of summands in $\mathrm{Dehn}(P')$ and $\mathrm{Dehn}(P'')$ is the third group of summands in $\mathrm{Dehn}(P)$ because $\ell'_k + \ell''_k = \ell_k$. The sum of the third groups of summands in $\mathrm{Dehn}(P')$ and $\mathrm{Dehn}(P'')$ is the fourth group of summands in $\mathrm{Dehn}(P)$ because $\psi'_k + \psi''_k = \psi_k$. Finally, the sum of the fourth groups of summands in $\mathrm{Dehn}(P')$ and $\mathrm{Dehn}(P'')$ is zero, since $\chi'_k + \chi''_k = \pi$. Thus, $\mathrm{Dehn}(P) = \mathrm{Dehn}(P') + \mathrm{Dehn}(P'')$ as stated in the Lemma. □

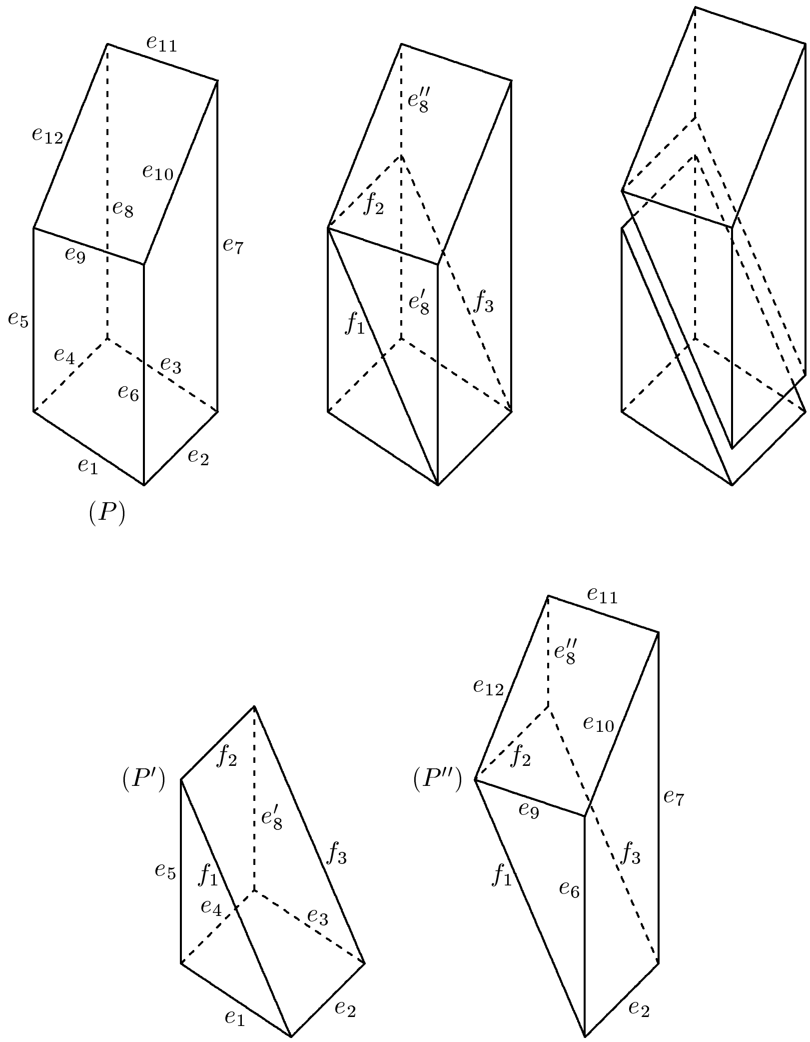


FIGURE 22.4. Proof of Lemma 22.2

An example is shown in Figure 22.4. A polyhedron $P$ (a four-gonal prism with non-parallel bases, shown at the left of the first row) is cut into two polyhedra by a plane (the cut is shown in the first row, the polyhedra $P'$ and $P''$ are shown in the second row). The edges of $P$ are $e_1, \dots e_{12}$; the sets $S_i$ are: $S_1 = \{e_1, e_3, e_4, e_5\}, S_2 = \{e_6, e_7, e_9, e_{10}, e_{11}, e_{12}\}, S_3 = \{e_8\}, S_4 = \{e_2\}$.

Back to Theorem 22.2. If two polyhedra can be cut into the same collection of polyhedral parts, then their Dehn invariants are both equal to the sum of the Dehn invariants of the parts, and, hence, the Dehn invariants of the given two polyhedra are equal to each other. But the Dehn invariant of a cube is equal to zero, since all the angles are $\pi/2$ (see Example 22.1). The Dehn invariant of a regular tetrahedron is equal to $6(\ell \otimes \alpha)$ where $\ell$ is the length of the edge and $\alpha$ is the dihedral angle. All we need to check is that $\alpha$ is not a rational multiple of $\pi$.

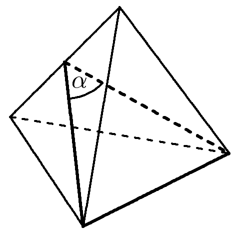


FIGURE 22.5. The dihedral angle of a regular tetrahedron

The dihedral angle of a regular tetrahedron is the largest angle of an isosceles triangle whose sides are $\ell, \ell\frac{\sqrt{3}}{2}, \ell\frac{\sqrt{3}}{2}$ (see Figure 22.5). The cosine theorem shows that

$$\cos\alpha = \frac{\left(\ell\frac{\sqrt{3}}{2}\right)^2 + \left(\ell\frac{\sqrt{3}}{2}\right)^2 - \ell^2}{2\left(\ell\frac{\sqrt{3}}{2}\right)\left(\ell\frac{\sqrt{3}}{2}\right)} = \frac{1}{3}$$

LEMMA 22.3. *If* $\cos\alpha = \frac{1}{3}$, *then* $\frac{\alpha}{\pi}$ *is irrational.*

Proof. Otherwise, $\cos n\alpha = 1$ for some $n$. However, it is known from trigonometry that

$$\cos n\alpha = P_n(\cos\alpha)$$

where $P_n$ is a polynomial of degree $n$ with the leading coefficient $2^{n-1}$ (cf. Lecture 7).

This is proved by induction. Statement: for all $n$,

$$\cos n\alpha = P_n(\cos\alpha),\ \sin n\alpha = Q_n(\cos\alpha)\cdot\sin\alpha$$

where $\deg P_n = n$, $\deg Q_n = n-1$, and the leading coefficients of both $P_n$ and $Q_n$ are equal to $2^{n-1}$. For $n = 1$, this is true $(P_1(t) = t, Q_1(t) = 1)$; assume that the statement is true for some $n$. Then

$$\begin{aligned} \cos(n+1)\alpha &= \cos n\alpha\sin\alpha - \sin n\alpha\sin\alpha \\ &= P_n(cos\alpha)\cos\alpha - Q_n(cos\alpha)\sin^2\alpha \\ &= P_n(cos\alpha)\cos\alpha + Q_n(cos\alpha)(\cos^2\alpha - 1); \end{aligned}$$

$$\begin{aligned} \sin(n+1)\alpha &= \sin n\alpha\cos\alpha + \cos n\alpha\sin\alpha \\ &= Q_n(\cos\alpha)\sin\alpha\cos\alpha + P_n(\cos\alpha)\sin\alpha \\ &= (Q_n(\cos\alpha)\cos\alpha + P_n(\cos\alpha))\sin\alpha \end{aligned}$$

Hence,

$$\begin{aligned} P_{n+1}(t) &= P_n(t)t + Q_n(t)(t^2-1), \\ Q_{n+1}(t) &= Q_n(t)t + P_n(t), \end{aligned}$$

and the statement for the degrees and the leading terms follows.

This shows that

$$\cos n\alpha = P_n\left(\frac{1}{3}\right) = \frac{2^{n-1}}{3^n} + \frac{\text{an integer}}{3^{n-1}}$$

which cannot be an integer, in particular, 1. □

This proves Lemma 22.3 and completes the proof of Dehn's theorem. □

**22.5 Further results.** In the language of algebra (which may be technically unfamiliar to the reader, but the formulas below seem to us self-explanatory), the construction of the previous section assigns to every convex (actually, not necessarily convex) polyhedron a certain invariant,

$$\text{Dehn}(P) \in \mathbf{R} \otimes_{\mathbf{Q}} (\mathbf{R}/\pi\mathbf{Q}),$$

and Dehn's theorem states that if two polyhedra, $P_1$ and $P_2$, are equipartite (that is, can be cut by planes into identical collections of parts), then

$$\text{Dehn}(P_1) = \text{Dehn}(P_2).$$

This is precisely the result of the previous section.

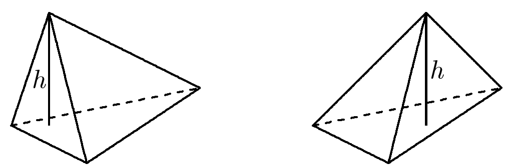


FIGURE 22.6. These tetrahedra do not have to be equipartite

Certainly, this may be applied not only to cubes and tetrahedra. The initial Hilbert's problem, by the way, dealt with a different example; Hilbert conjectured that two tetrahedra with equal bases and equal heights (like those on Figure 22.6) are not equipartite.

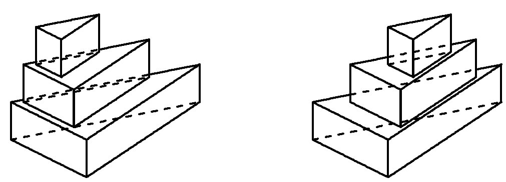

FIGURE 22.7. Computing the volume of a tetrahedron by a limiting process

The origin of this question belongs to the foundations of geometry. The whole theory of volumes of solids is based on the lemma stating that the volumes of the tetrahedra in Figure 22.6 are the same. The similar planar lemma (involving areas of triangles) has a direct geometric proof based on cutting and pasting. But the three-dimensional fact requires a limit "stair construction" involving pictures like Figure 22.7 (you can find a figure like this in textbooks on spatial geometry). The question is, is this really necessary, and the answer is "yes": Dehn's theorem easily implies that the tetrahedra like those in Figure 22.6 are not, in general, equipartite.

More than 60 years after Dehn's work, Sydler proved that polyhedra with equal volumes and equal Dehn invariants are equipartite [**76**]. There are similar results in spherical and hyperbolic geometries.

Dehn's invariant may be generalized to polyhedra of any dimension: for an $n$-dimensional polyhedron $P$,

$$\mathrm{Dehn}(P) = \sum_{\substack{(n-2)\text{-dimensional} \\ \text{faces } s \text{ of } P}} \text{volume(s)} \otimes \begin{bmatrix} \text{dihedral} \\ \text{angle at } s \end{bmatrix} \in \mathbf{R} \otimes_{\mathbf{Q}} (\mathbf{R}/\pi\mathbf{Q})$$

(the angle is formed by the two $(n-1)$-dimensional faces of $P$ adjacent to $s$). In dimension 4, as in dimension 3, two polyhedra are equipartite, if and only if their volumes and their Dehn invariants are the same. But in dimension 5 it is not true any longer: there arises a new invariant, a "secondary Dehn invariant" involving a summation over the edges (for an $n$-dimensional polyhedron, over $(n-4)$-dimensional faces) of $P$. There is a conjecture that an "equipartite type" of an $n$-dimensional polyhedron is characterized by a sequence of $\left[\frac{n+1}{2}\right]$ invariants: the volume, Dehn invariant, secondary Dehn invariant, and so on, taking values in more and more complicated tensor products ($k$-th Dehn invariant involves a summation over $(n-2k)$-dimensional faces. In particular, for one- and two-dimensional polyhedra (segments and polygons) only the "volume" (the length and the area) matters; in dimensions 3 and 4 we also have Dehn invariant, and so on).

For more information about this subject, we recommend the popular book of Boltianskii [**9**], the talk of Cartier at the Bourbaki Seminar [**13**] and the books [**25, 67, 91**].

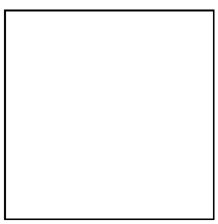

John Smith
January 23, 2010

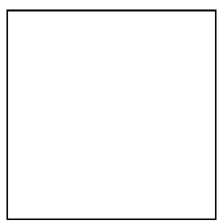

Martyn Green
August 2, 1936

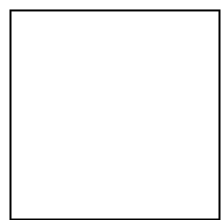

Henry Williams
June 6, 1944

**22.6 Exercises.**

22.1. Prove that the Dehn invariant of any rectangular prism with a polygonal base is zero.

Exercises 22.2–22.4 are particular cases of Sydler's theorem (see Section 22.5). Since we did not prove this theorem, we suggest to solve these exercises by direct constructions.

22.2. Prove that two collections of parallelepipeds of equal total volumes are equipartite.

22.3. A regular octahedron $O$ with the edge 1 can be obtained from the regular tetrahedron $\widetilde{T}$ with the edge 2 by cutting off 4 regular tetrahedra $T$ with the edge 1 contained in $\widetilde{T}$ and containing the 4 vertices of $\widetilde{T}$. Since, obviously, $\mathrm{Dehn}(\widetilde{T}) = 2\,\mathrm{Dehn}(T)$,

$$\mathrm{Dehn}(O) = \mathrm{Dehn}(\widetilde{T}) - 4\,\mathrm{Dehn}(T) = -2\,\mathrm{Dehn}(T).$$

Prove that the collection of the octahedron $O$ and two tetrahedra $T$ is equipartite to a cube of the appropriate volume $(6\,\mathrm{Vol}(T))$.

22.4. (a)Let $\widetilde{T}$ and $T$ denote the same as in Exercise 22.3. Prove that $\widetilde{T}$ is equipartite to a collection of two copies of $T$ and a cube.

(b) Generalization. Let $P$ be an arbitrary polyhedron and $\widetilde{P}$ is its double magnification (of the volume $8\,\mathrm{Vol}(P)$). Prove that $\widetilde{P}$ is equipartite to a collection of two copies of $P$ and a cube of the volume $6\,\mathrm{Vol}(P)$.

*Hint*. (a) follows from Exercise 22.3; to prove (b), observe that (a) holds for any (not necessarily regular) tetrahedra, and then cut $P$ into the union of tetrahedra.

22.5. A polyhedron $P$ is called a *crystal* if there exist a tiling of whole space by polyhedra congruent to $P$. Prove that the Dehn invariant of a crystal is 0.

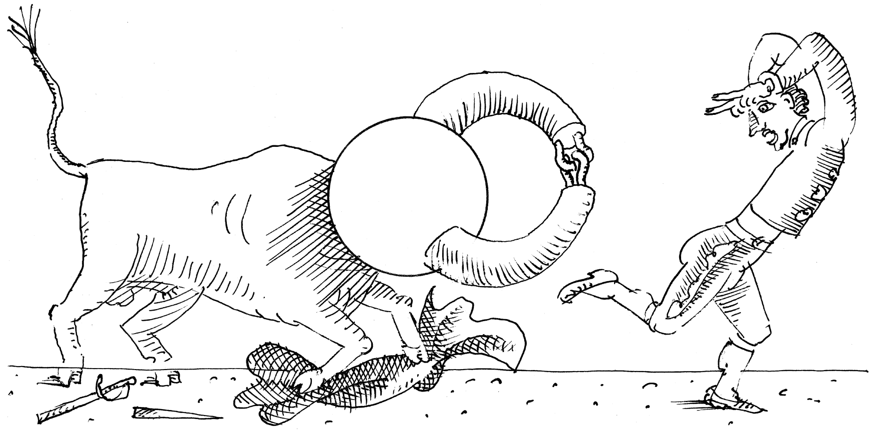

LECTURE 23

# Impossible Tilings

**23.1 Introduction.** This lecture is about tilings of plane polygons by other plane polygons. An example of such a problem is probably known to the reader:

Two diagonally opposite squares (A1 and H8) are deleted from a chess board. Can one tile this truncated board by $2 \times 1$ "dominos"? See Figure 23.1.

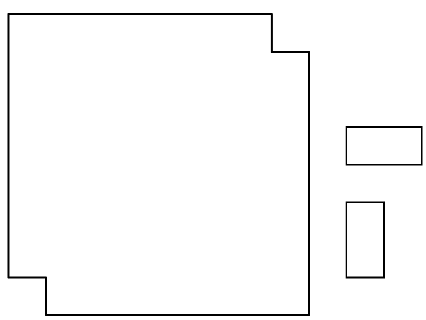

FIGURE 23.1. Can one tile this truncated chess board by dominos?

A typical fragment of a tiling by dominos is shown in Figure 23.2. The tiles do not overlap (they touch each other along parts of their boundaries), and every point of the board belongs to a tile. Note two things: we allow both horizontal and vertical positions of the tiles, and we do not assume that adjacent tiles necessarily share a full side. In general, a tiling problem is formulated as follows: given a polygon $P$ and a collection of polygons $Q_1, Q_2, \ldots$, is it possible to tile $P$ by isometric copies of the tiles $Q_i$?

In case the reader failed to solve the truncated chess board problem, its (negative) solution appears in the next section. In what follows, we shall see many more examples of impossible tilings but the proofs will get more and more involved.

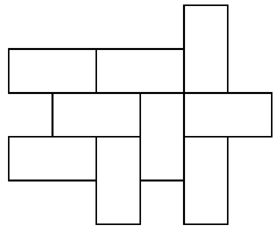

FIGURE 23.2. A fragment of tiling

**23.2 Coloring.** To solve the truncated chess board tiling problem, recall that the chess board has a black-and-white coloring. The diagonally opposite squares are both black, and the truncated board has 30 black and 32 white squares. On the other hand, every $2 \times 1$ domino covers one black and one white square. Hence the tiling is impossible, see Figure 23.3.

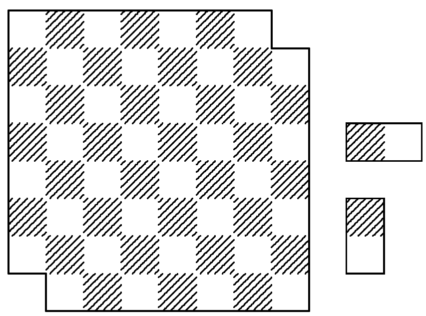

FIGURE 23.3. Coloring argument

There is an alternative way to present the black-and-white coloring argument. Write 0 in each white square and 1 in each black one. The total sum of these numbers on the truncated board is 30. But every domino has a 0 and a 1 written on it, and 31 dominos will make the total sum equal to 31, not to 30. Thus no tiling exists.

Here is a variation on this argument. *Can one tile a* $10 \times 10$ *square by L-shaped tiles as shown in Figure 23.4?* Note that a tile may now have 8 different orientations!

The answer again is in the negative. Write 1s and 5s in the squares as depicted in Figure 23.4. Each tile covers either three 1s and one 5, or three 5s and one 1. In either case, the sum on a tile is a multiple of 8. On the other hand, the total sum of the numbers on the board is 300, which is not divisible by 8. Hence the tiling does not exist.

**23.3 What a coloring argument cannot do.** Imagine that we have two kinds of tiles: the usual, positive, ones and the negative ones, made of "anti-matter". We are allowed to superimpose tiles so that the common parts of the positive and negative ones annihilate each other, see Figure 23.5. It is convenient to write 1 on each positive tile and $-1$ on each anti-tile. The *multiplicity* of a point is the sum of these $\pm 1$s, taken over all tiles that cover this point. We say that a polygon $P$

| | | | | | | | | | |
|---|---|---|---|---|---|---|---|---|---|
| 1 | 1 | 1 | 1 | 1 | 1 | 1 | 1 | 1 | 1 |
| 5 | 5 | 5 | 5 | 5 | 5 | 5 | 5 | 5 | 5 |
| 1 | 1 | 1 | 1 | 1 | 1 | 1 | 1 | 1 | 1 |
| 5 | 5 | 5 | 5 | 5 | 5 | 5 | 5 | 5 | 5 |
| 1 | 1 | 1 | 1 | 1 | 1 | 1 | 1 | 1 | 1 |
| 5 | 5 | 5 | 5 | 5 | 5 | 5 | 5 | 5 | 5 |
| 1 | 1 | 1 | 1 | 1 | 1 | 1 | 1 | 1 | 1 |
| 5 | 5 | 5 | 5 | 5 | 5 | 5 | 5 | 5 | 5 |
| 1 | 1 | 1 | 1 | 1 | 1 | 1 | 1 | 1 | 1 |
| 5 | 5 | 5 | 5 | 5 | 5 | 5 | 5 | 5 | 5 |

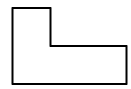

FIGURE 23.4. Coloring modulo 8

admits a *signed* tiling if one can superimpose negative and positive tiles so that the multiplicity of every point inside $P$ equals 1.

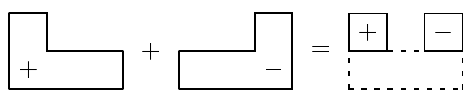


FIGURE 23.5. Tiles and anti-tiles

It is clear that if a coloring argument, like the ones discussed in Section 23.2, proves that a polygon cannot be tiled by a certain collection of tiles, then this proof implies that a signed tiling does not exist either. There are, however, tiling problems that have solutions in signed tiles and no solutions in positive tiles only.

Consider a triangular array of dots as in Figure 23.6. We want to cover this triangle by "tribones" consisting of three dots; a tribone may have one of the three indicated orientations. *For which values of* $n$ *does such a tiling exist?*

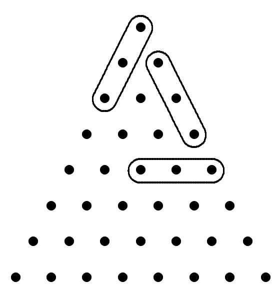

FIGURE 23.6. Can one color a triangle by tribones?

First of all, for a tiling to exit, the number of dots must be a multiple of 3. This number is $n(n+1)/2$, and hence $n \equiv 0$ or 2 mod 3.

Let us now "color" the dots as shown in Figure 23.7. The sum of numbers covered by each tile is divisible by 3. The total sum depends on $n$ periodically with period 9, and its value mod 3 is as follows:

$$0, 2, 2, 2, 1, 1, 1, 0, 0.$$

Therefore $n$ mod 9 should be either 1, or 8, or 0. We already know that $n \equiv 0$ or 2 mod 3, so only the latter two cases "remain on the table".

0<br>
1 1<br>
2 2 2<br>
0 0 0 0<br>
1 1 1 1 1<br>
2 2 2 2 2 2<br>
0 0 0 0 0 0 0<br>
1 1 1 1 1 1 1 1<br>
2 2 2 2 2 2 2 2 2<br>
0 0 0 0 0 0 0 0 0 0

FIGURE 23.7. Coloring modulo 3

Let us show that if $n \equiv 8$ or 0 mod 9 then there exists a signed tiling of the triangular array by tribones. Figure 23.8 depicts such a tiling for $n = 8$, and Figure 23.9 shows how to build bigger arrays from triangles of size 8 and rows of tribones.

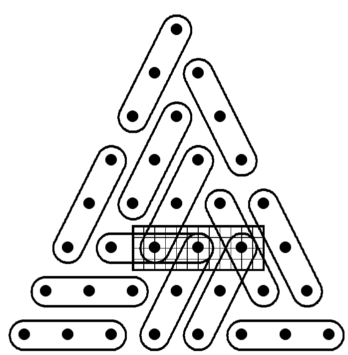

FIGURE 23.8. Signed tiling for $n = 8$

We conclude that the following surprising theorem is beyond the reach of any coloring argument.

THEOREM 23.1. *For every $n$, a triangular array of size $n$ cannot be tiled by tribones.*

**23.4 Conway's tiling group.** To prove Theorem 23.1, we need to do some preparatory work. To fix ideas, assume that all the polygons, the region to be tiled and the tiles, are drawn on graph paper, that is, are composed of unit squares. We assume that every polygon involved does not have holes: its boundary consists of a single closed curve.

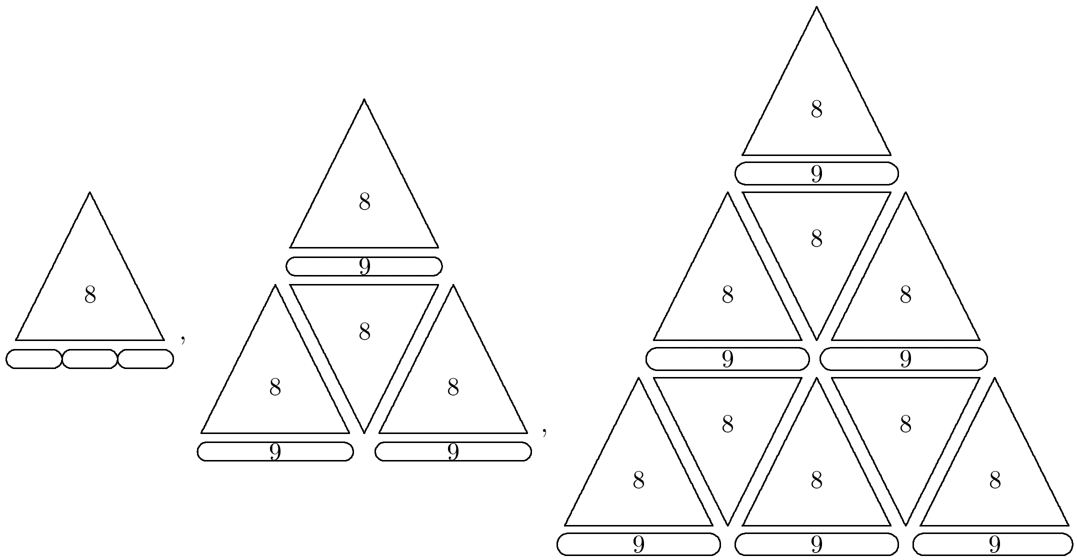


FIGURE 23.9. Building larger signed tilings from smaller ones

A path on the square grid will be described by a word in four symbols $x, x^{-1}, y$ and $y^{-1}$: a step right by $x$, a step left by $x^{-1}$, a step up by $y$ and a step down by $y^{-1}$. See Figure 23.10, for example. We write $k$ consecutive symbols $x$ or $x^{-1}$ as $x^{\pm k}$, and likewise for $y$, and denote by $e$ a trivial path. We also cancel consecutive $x$ and $x^{-1}$ or $y$ and $y^{-1}$; for example, $xyy^{-1}x^{-1} = e$.

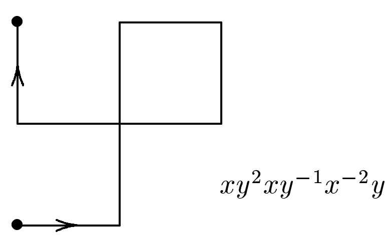


FIGURE 23.10. A path and the respective word

To compose two words $a$ and $b$, consider their concatenation and reduce it by canceling all consecutive pairs of $x$ and $x^{-1}$ or $y$ and $y^{-1}$. The resulting word is denoted by $ab$.

The composition satisfies the associativity law: $(ab)c = a(bc)$, where $a, b$ and $c$ stand for any words. Given a word $w$, the word $w^{-1}$ is obtained from $w$ by reading its letters from right to left and changing their exponents to the opposite. For example, $(xy^{-1})^{-1} = yx^{-1}$. Clearly, $ww^{-1} = e$.

Let $T_1, \ldots, T_n$ be a complete list of tiles, positioned on the grid in all possible orientations (so that a domino has two, and an $L$-shaped tile eight different orientations). Choose a starting point on the boundary of $T_i$ and traverse this boundary counter clock-wise. This closed path is encoded by a word $W_i$ in $x, x^{-1}, y$ and $y^{-1}$. This word depends, of course, on the choice of the starting point.

So far, the only rule for manipulating with words was

$$xx^{-1} = x^{-1}x = e = yy^{-1} = y^{-1}y.$$

Let us add to this rule the new ones: $W_1 = W_2 = \cdots = e$. These rules mean that whenever one of the words $W_i$ appears in a longer word, we may replace it by $e$, and conversely, we may insert either of the words $W_i$ anywhere. If a word $V_1$ can be obtained from another word $V_2$ by consecutive applications of these rules, we call them equivalent and write simply $V_1 = V_2$.

We need to address an ambiguity in the choice of the words $W_i$, namely, their dependence on the starting point. Let $p'$ be another starting point on the boundary of the tile $T_i$, and let $W_i'$ be the word obtained by traversing the boundary starting at $p'$.

Lemma 23.1. *One has:* $W_i' = e$.

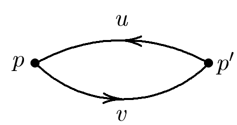


Figure 23.11. Proving Lemma 23.1

Proof. Let $u$ be (the code of) the path from $p$ to $p'$, and $v$ the path from $p'$ to $p$, see Figure 23.11. Then $W_i = uv$ and $W_i' = vu$. Since $W_i = e$, we have $uv = e$. Then $vu = (u^{-1}u)(vu) = u^{-1}(uv)u = u^{-1}u = e$, as claimed. □

Let $P$ be a polygon. Traverse its boundary to obtain a word $U$ (again depending on the starting point). The following proposition provides a necessary condition for tiling.

Proposition 23.2. *If $P$ is tiled by $T_1, \dots, T_n$ then $U = e$.*

Proof. Induction on the number of tiles. If this number is one then $P$ is itself a tile, say, $T_i$. The word $U$ is then what we called $W_i'$ above, and the claim follows from Lemma 23.1.

Now suppose there are several tiles. Then we can cut the polygon $P$ into two polygons, $P_1$ and $P_2$, by a path inside $P$, going from a boundary point $p$ to a boundary point $p'$ and traveling only on the boundaries of the tiles, see Figure 23.12. Let $w$ be the word corresponding to this path $pp'$ inside $P$, and let $v_1$ and $v_2$ be the boundary words of $P$ from $p$ to $p'$ and from $p'$ to $p$, respectively.

A closed counter clock-wise path along the boundary of $P$, starting at point $p'$, is encoded by the word $v_1v_2$. We have: $v_1v_2 = (v_1w^{-1})(wv_2)$. The words in the parentheses are the boundary words of the polygons $P_1$ and $P_2$. By our choice of the cutting path $pp'$, these two polygons are tiled by a smaller number of tiles. By the induction assumption, $v_1w^{-1} = e$ and $wv_2 = e$. Therefore $v_1v_2 = e$ as well. [1]

Finally, the boundary word $U$ may differ from $v_1v_2$ by the choice of the starting point. We already know from Lemma 23.1 that if one of these words is equivalent to $e$ then so is the other. This completes the proof. □

[1]Note similarity of this argument to the one from the proof of the polyhedral Gauss-Bonnet theorem 20.3.

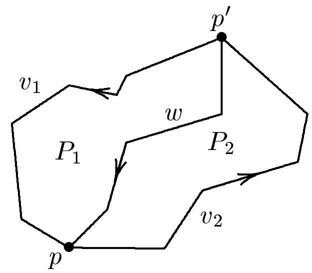


FIGURE 23.12. Induction step in the proof of Proposition 23.2

It is convenient to summarize the constructions of this section in terms of groups. The collection of tiles $T_1, \dots, T_n$ determines a group with two generators $x$ and $y$ and the relations $W_1, \dots, W_n$. This group is called *Conway's tiling group.* The boundary word of the polygon $P$ is an element of Conway's tiling group, and if $P$ is tiled by $T_1, \dots, T_n$ then this is the unit element.

EXAMPLE 23.3. Let us revisit the truncated chess board problem from the very beginning of this lecture.

The two positions of the $2 \times 1$ dominos have the boundary words $W_1 = x^2yx^{-2}y^{-1}$ and $W_2 = xy^2x^{-1}y^{-2}$, and the truncated chess board has the boundary word $U = x^7y^7x^{-1}yx^{-7}y^{-7}xy^{-1}$, see Figure 23.13. We want to show that the equalities $W_1 = W_2 = e$ do not imply that $U = e$; then, by Proposition 23.2, the board cannot be tiled.

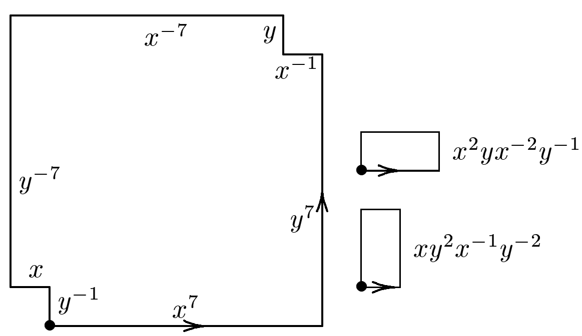


FIGURE 23.13. Truncated chess board revisited

Replace $x$ by the permutation (213) and $y$ by (132). Then $x^2$ and $y^2$ both become equal to the trivial permutation (123), and hence both words $W_1$ and $W_2$ become trivial as well. It follows that if $U = e$ then, after $x$ and $y$ are replaced by the permutations (213) and (132), we must obtain a trivial permutation.

But this is not the case! The reader will easily verify that $U = (312)$, a non-trivial permutation.[2]

[2]In group theoretical terms, we constructed a homomorphism from Conway's tiling group to the group of permutations of three elements; this homomorphism takes the boundary word of the truncated chess board to a non-trivial permutation.

**23.5 Proof of Theorem 23.1.** It should not come as a surprise that Theorem 23.1 will take more work compared to Example 23.3: after all, the truncated chess board problem has an easy coloring solution.

First of all, we know from Section 23.3 that a necessary condition for a tiling is that $n \equiv 8$ or $0 \bmod 9$. If a tiling exists for $n \equiv 8 \bmod 9$ then, as Figure 23.9 shows, it also exists for $n \equiv 0 \bmod 9$. Thus it suffices to prove that the tilings do not exist for $n$ a multiple of 9.

Redraw the triangular array of dots as a staircase-like polygon on graph paper: one square in the first row, two in the second, etc. Then the tribones become the kinds of tiles, depicted in Figure 23.14. The figure also indicates the boundary words of these polygons. We want to prove that, for every $n$, the equalities $W_1 = W_2 = W_3 = e$ do not imply that $U_n = e$.

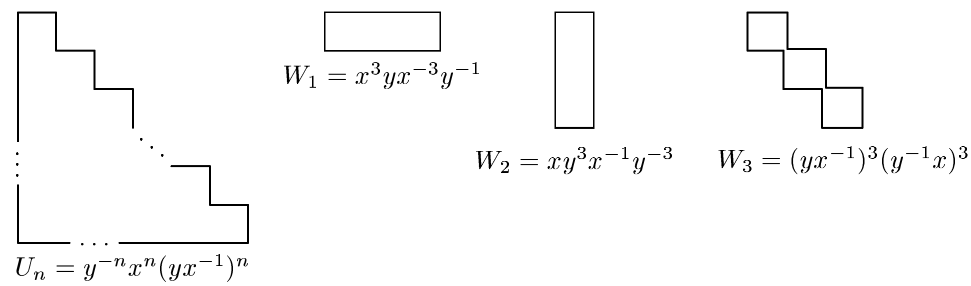


FIGURE 23.14. Tiles and the corresponding words

Consider three families of evenly spaced oriented parallel lines, see Figure 23.15. These lines intersect at angles of 60° and form a tessellation of the plane by equilateral triangles and regular hexagons. Write letters $x$ and $y$ in the triangles as shown in Figure 23.15. We shall refer to this pattern of lines and letters as the hexagonal grid.

The hexagonal grid is very symmetric. For its every two vertices, there exists a motion of the plane that takes one to another and preserves the grid. For example, a parallel translation takes vertex $B$ to $D$ in Figure 23.16, and the rotation through 120° about point $A$, the center of a triangle marked $x$, takes vertex $B$ to $C$.

A path on the square grid can be shadowed on the hexagonal grid. A path on the square grid is encoded by a word in $x, x^{-1}, y, y^{-1}$. At every vertex of the hexagonal grid, two oriented lines meet, and two of the four angles are labeled $x$ and $y$, see Figure 23.15. We interpret the symbols $x, x^{-1}, y, y^{-1}$ as instructions to build the shadow path: $x^{\pm 1}$ means "move one step on the boundary of the angle labeled $x$, along or against the orientation, respectively", and likewise for $y^{\pm 1}$. Thus, once one chooses a starting point, a path on the square grid determines a path on the hexagonal grid.

Figure 23.15 shows shadows, on the hexagonal grid, of the boundary paths of the three tiles from Figure 23.14. Note that all three shadow paths are closed; this fact holds true for any choice of the starting point of a shadow path, due to the symmetries of the hexagonal grid. In contrast, the path $xyx^{-1}y^{-1}$, that is, the boundary of a single square, has a non-closed shadow.

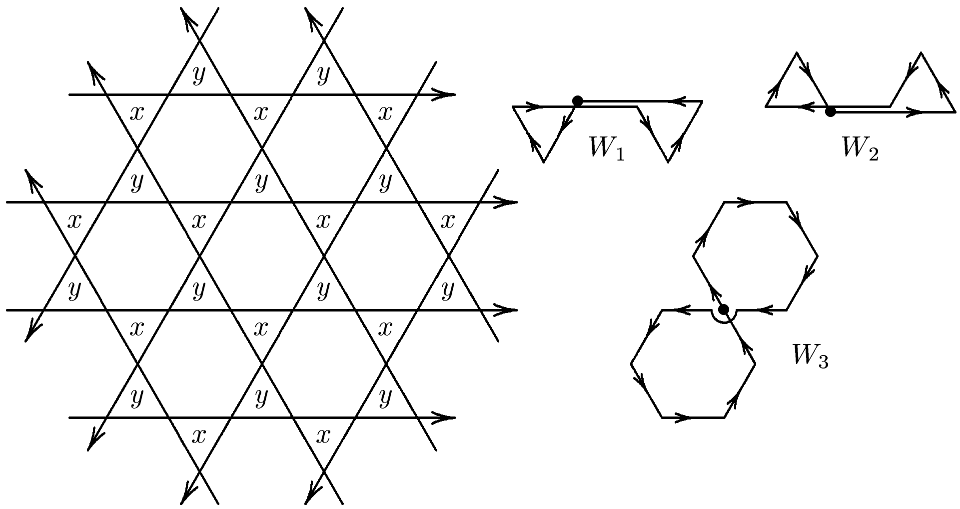


FIGURE 23.15. The hexagonal grid: the shadows of the three tiles

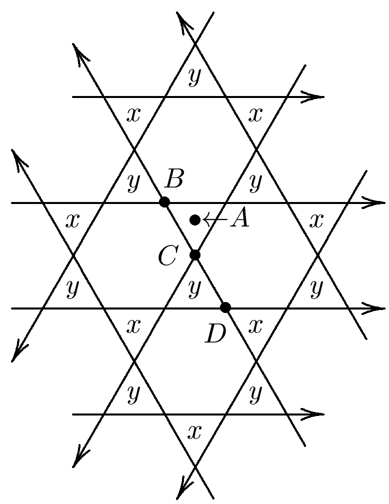


FIGURE 23.16. Symmetries of the hexagonal grid

Let us consider only those paths on the square grid whose shadows on the hexagonal grid are closed. The boundary paths of the three tiles satisfy this property, and so does the boundary path of the staircase region in Figure 23.14; its shadow is shown in Figure 23.17 (we use the assumption that $n$ is a multiple of 3).

An oriented closed curve partitions the plane into a number of components. To each component, there corresponds the rotation number of the curve about any point of this component. We discussed this notion in Lecture 12, see Figure 12.20. The signed area, bounded by a closed curve, is the sum of areas of the components, multiplied by the respective rotation numbers. For example, a counter clock-wise oriented unit circle has signed area $\pi$, and a clock-wise oriented one has signed

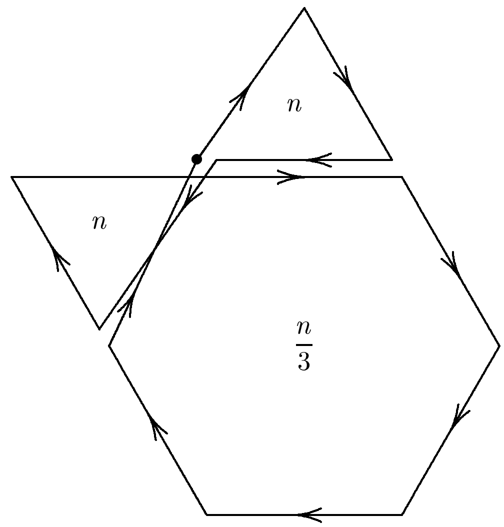


FIGURE 23.17. The shadow of the staircase region

area $-\pi$. In Calculus, signed area is defined as the integral, over the curve, of the differential form $xdy$.

Assign to a path on a square grid the signed area, bounded by its shadow on the hexagonal grid. For the boundary paths of the three tiles, this signed area is zero, see Figure 23.15. And for the boundary path of the staircase region, this signed area is negative, see Figure 23.17.

This implies that $U_n \neq e$. Indeed, when we replace one of the words $W_1, W_2$ or $W_3$ by $e$, or vice versa, the signed area of the shadow path is not affected. This area is zero for the trivial word $e$ but it is non-zero for the word $U_n$. This completes the proof of Theorem 23.1. $\square$

In conclusion of this section, here is another theorem that can be proved similarly to Theorem 23.1. Start with the same triangular array of dots but now we want to tile it by triangles made of three dots, see Figure 23.18.

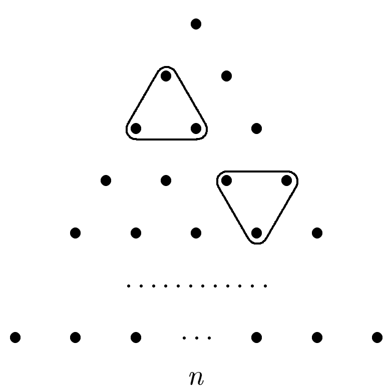


FIGURE 23.18. Can one tile the large triangle with small ones?

THEOREM 23.2. *Such a tiling exists if and only if* $n \equiv 0, 2, 9,$ or 11 mod 12.

For more information on Conway's tiling group, see [**17, 65, 85**].

**23.6 Back to Max Dehn.** After solving Hilbert's Third problem, M. Dehn [**21**] proved in 1903 the following theorem.

THEOREM 23.3. *If a rectangle is tiled by squares then the ratio of its side lengths is a rational number.*

The converse is obviously true, see Figure 23.19. The following proof is quite similar to what we did in Section 22.3.[3]

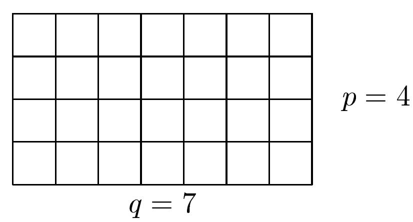


FIGURE 23.19. If the ratio of the sides of a rectangle is rational then it can be tiled by squares

Proof. Let us argue by contradiction. We can scale the rectangle so that its width is 1; let $x$ be its height, an irrational number.

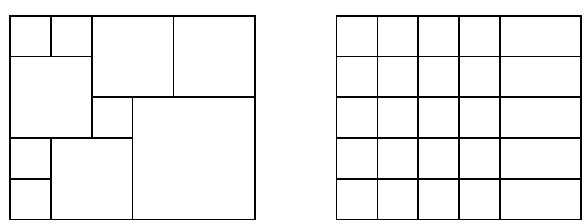

FIGURE 23.20. Extending the sides of the tiles

Assume that there is a tiling by squares. Extend the sides of the squares to the full width or height of the rectangle, see Figure 23.20. Now we have a tiling of our $x \times 1$ rectangle and of all the squares by a number of smaller rectangles; let $a_1, \dots, a_N$ be their side lengths (in any order). Consider the sequence

$$1, x, a_1, \dots, a_N; \qquad (23.1)$$

remove a term if it is a linear combination, with rational coefficients, of the preceding terms. Since $x$ is irrational, it will stay in the sequence. Let $b_1 = 1, b_2 = x, b_3, \dots, b_m$ be the remaining numbers. As in Section 22.3, each of the numbers (23.1) is a unique rational linear combination of $b_1, \dots, b_m$.

Let $f$ be the following function on the numbers $b_1, \dots, b_m$:

$$f(1) = 1, \ f(x) = -1, \ f(b_3) = \cdots = f(b_m) = 0;$$

[3]And this similarity is the reason for a lecture on tiling problems to be included into a chapter devoted to polyhedra.

extend $f$ to rational linear combinations of the numbers $b_1, \dots, b_m$ by linearity:

$$f(r_1 b_1 + \cdots + r_m b_m) = r_1 f(b_1) + \cdots + r_m f(b_m).$$

Thus, if $u$ and $v$ are rational linear combinations of the numbers $b_1, \dots, b_m$, then

$$f(u+v) = f(u) + f(v), \tag{23.2}$$

that is, the function $f$ is additive.

Consider a rectangle with side lengths $u$ and $v$, both rational linear combinations of the numbers $b_1, \dots, b_m$. Define the "area" of this rectangle as $f(u)f(v)$. If two such rectangles share either a horizontal or a vertical side, they can merge together to form a bigger rectangle. Due to the additivity of the function $f$, equation (23.2), the "area" of the bigger rectangle is the sum of "areas" of the two smaller ones.

It follows that the "area" of the $x \times 1$ rectangle is the sum of the "areas" of the squares that tile it. The former is $f(x)f(1) = -1$, while the area of a $u \times u$ square is $f(u)^2$, a non-negative number. This is a contradiction. □

**23.7 Tilings by squares and electrical circuits.** Consider a tiling of a rectangle by squares, such as in Figure 23.21. Let $x_1, \dots, x_9$ be the side lengths of the squares. For each segment in this figure, horizontal or vertical, we have a linear relation between the variables $x_i$: these relations express the length of a segment as the sum of the sides of the squares, adjacent to this segment on its two sides. For the tiling in Figure 23.21, these equations are:

$$x_2 = x_4 + x_5,\ x_3 + x_5 = x_6,\ x_1 + x_4 = x_7 + x_8,\ x_6 + x_8 = x_9 \tag{23.3}$$

(horizontal segments), and

$$x_1 = x_2 + x_4,\ x_7 = x_8 + x_9,\ x_4 + x_8 = x_5 + x_6 \tag{23.4}$$

(vertical segments). For a tiling to exist, this system of linear equation should have a solution in positive numbers. The tiling in Figure 23.21 corresponds to the following solution:

$$x_1 = 15,\ x_2 = 8,\ x_3 = 9,\ x_4 = 7,\ x_5 = 1,\ x_6 = 10,\ x_7 = 18,\ x_8 = 4,\ x_9 = 14;$$

of course, one can multiply these numbers by any factor.

Equations (23.3) and (23.4) can be interpreted at Kirchhoff laws for electrical circuits. An example of a circuit is shown in Figure 23.22. We assume that all the resistors are unit, and that the currents are given by the numbers $x_i$. There are two Kirchhoff laws: the vertex equations state that the flow of current into every vertex equals the flow out of it, and the mesh equations state that the voltage drop around any closed path is zero. Since the resistors are unit, by Ohm's law, the voltage drop on the $i$-th resistor equals $x_i$, the current. The vertex equations for the circuit in Figure 23.22 are precisely the equations (23.3), and the mesh equations are the equations (23.4).

The circuit in Figure 23.22 is constructed from the tiling in Figure 23.21 as follows: to every horizontal segment there corresponds a vertex in the electric circuit, and each square in the tiling corresponds to a resistor. A resistor connects two vertices if the respective square is adjacent to the two corresponding horizontal lines. This construction works for any tiling of a rectangle by squares and provides an electrical circuit.

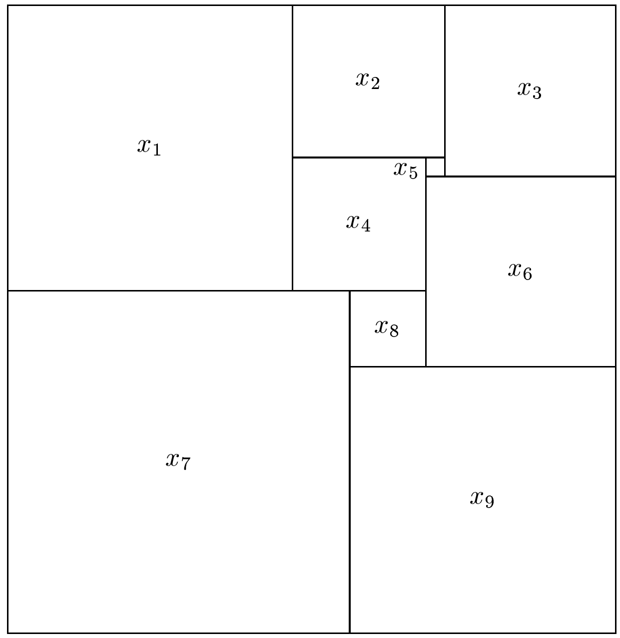


FIGURE 23.21. Tiling by squares

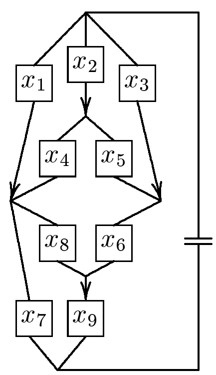


FIGURE 23.22. The circuit corresponding to the tiling in Figure 23.21

A choice of a voltage drop between the upper and lower vertices uniquely determines the currents in all resistors, and we obtain a solution of the system (23.3)-(23.4). In particular, the system (23.3)-(23.4) has a unique solution, up to a common factor. The same conclusion holds for any tiling of a rectangle by squares. The downside of this method is that we have no control on the signs of the currents: some of them may be zero or negative, and then the circuit will not correspond to a tiling by squares.

**23.8 Tilings by rectangles with an integer side.**

THEOREM 23.4. *A rectangle $R$ is tiled by rectangles each of which has an integer side. Then $R$ has an integer side.*

This tiling theorem has a record number of different proofs (14 given in [**87**], and more are known). We choose one of the most elegant.

Proof. The integral $\int \sin 2\pi x \ dx$ over an interval of integer length is zero. It follows that the double integral

$$\int\int \sin 2\pi x \sin 2\pi y \ dxdy$$

over each tile is zero. Hence this double integral, evaluated over $R$, vanishes as well. Assume that the lower left corner of $R$ is the origin and its sides have lengths $a$ and $b$. Then

$$0 = \int_0^a \int_0^b \sin 2\pi x \sin 2\pi y \ dxdy = \frac{1}{(2\pi)^2}(1 - \cos 2\pi a)(1 - \cos 2\pi b).$$

It follows that either $\cos 2\pi a = 1$ or $\cos 2\pi b = 1$, that is, either $a$ or $b$ is an integer. $\Box$

Theorem 23.4 has an interesting consequence. Suppose that an $m \times n$ rectangle is tiles by $p \times q$ rectangles (the numbers $m, n, p$ and $q$ are integers). Of course, this implies that $pq$ divides $mn$. We can say more:

Corollary 23.5. *The number $p$ divides either $m$ or $n$, and so does $q$.*

Proof. Rescale by the factor $1/p$: now an $(m/p) \times (n/p)$ rectangle is tiled by $1 \times (q/p)$ rectangles. By Theorem 23.4, either $m/p$ or $n/p$ is an integer, that is, $p$ divides either $m$ or $n$. Similarly for $q$. $\Box$

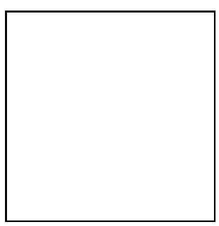

John Smith
January 23, 2010

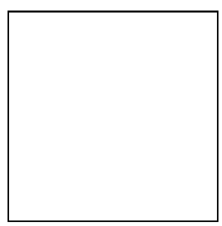

Martyn Green
August 2, 1936

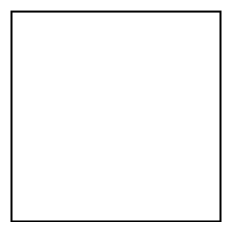

Henry Williams
June 6, 1944

**23.9 Tilings by triangles of equal areas, briefly mentioned.** In conclusion, we cannot help mentioning one more, extremely intriguing, "impossible tiling" result: *one cannot tile a square by an odd number of triangles of equal areas* (for any even number of tiles, see Figure 23.23). This theorem is relatively new (1970) and has a very surprising proof. Perhaps, even more surprisingly, there are quadrilaterals that cannot be tiled by any number of triangles of equal areas. See chapter 5 of [**75**] for an exposition.

**23.10 Exercises.**

23.1. Can one tile the polygon in Figure 23.24 by dominos?

23.2. Delete one black and one white square from the chess board. Prove that the truncated board can be tiled by dominos.

*Hint.* Consider a closed path that covers all all the squares of the chess board and place the dominos along it.

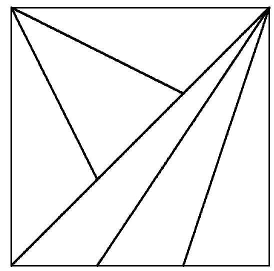

FIGURE 23.23. Tiling by triangles of equal areas

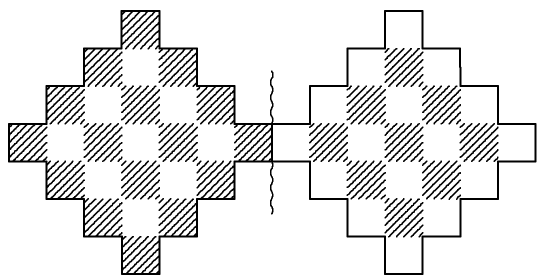

FIGURE 23.24. Variation on the coloring argument

23.3. Show that a $10 \times 10$ square cannot be tiled by $1 \times 4$ rectangles.
*Hint*. Use 4-coloring.

23.4. ** Prove Theorem 23.2.

23.5. Prove that the polygon in Figure 23.25 cannot be tiled by squares (it clearly can if we allow anti-tiles!).

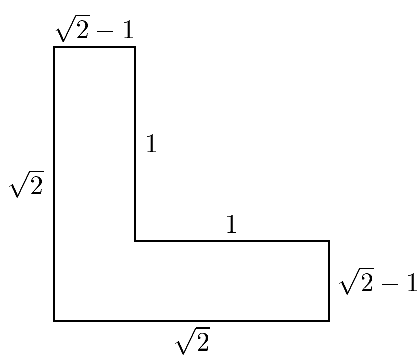


FIGURE 23.25. This region cannot be tiled by squares

23.6. Let $x = 2 - \sqrt[3]{5}$. Tile a square by three rectangles similar to the $1 \times x$ rectangle.

*Comment.* A square can be tiled by rectangles similar to the $1 \times x$ rectangle if and only if $x$ is a root of a polynomial with integer coefficients and, for a polynomial of least degree satisfied by $x$, every root $a + ib$ satisfies $a > 0$, see [**30**].

23.7. Show that Theorem 23.3 still holds true if one is allowed to use tiles made of "anti-matter".

*Hint.* Redefine the "area" of a $u \times v$ rectangle as $uf(v) - vf(u)$. This area is again additive and it vanishes for all squares.

23.8. Give a coloring proof of Theorem 23.4 considering an infinite chess board with $(1/2) \times (1/2)$ squares.

*Comment.* This is the same as to replace the function $\sin 2\pi x \sin 2\pi y$ by the function $(-1)^{[2x]}(-1)^{[2y]}$.

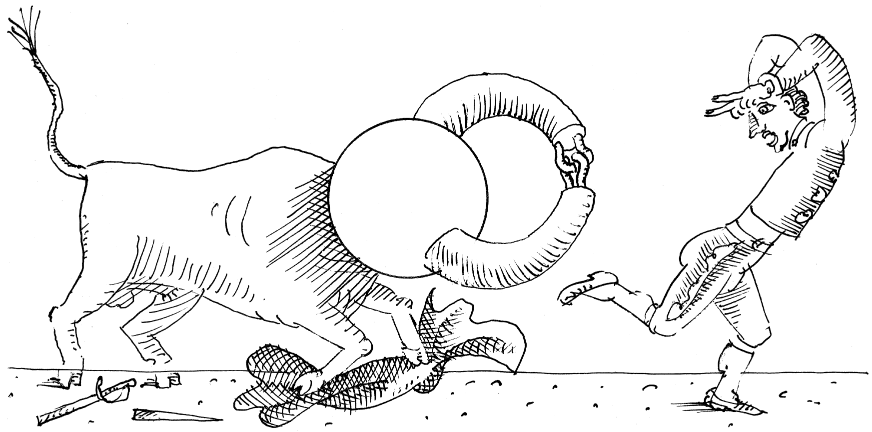

LECTURE 24

# Rigidity of Polyhedra

**24.1 Cauchy Theorem.** A cardboard model of a convex polyhedron $P$ is cut along its edges into a number of polygons, the faces of $P$. One has a complete list of adjacencies: when faces $F_i$ and $F_j$ shared an edge $E_k$. Following this list, one assembles a polyhedron $P'$ by pasting the faces along the same edges as in $P$. Is $P'$ necessarily congruent to $P$?

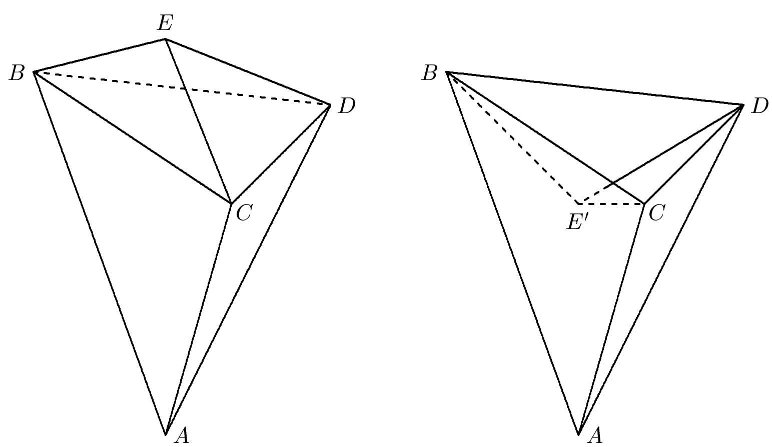


FIGURE 24.1. These polyhedra are combinatorially the same and have congruent faces

The answer depends on whether $P'$ is a convex polyhedron. Without the convexity assumption, the polyhedron is not uniquely determined, see Figure 24.1. However, for convex polyhedra, one has the following Cauchy theorem (1813).

THEOREM 24.1. *If the corresponding faces of two convex polyhedra are congruent and adjacent in the same way then the polyhedra are congruent as well.*

In the plane, a similar statement clearly fails: every polygon, except a triangle, admits deformations so that the lengths of the edges remain the same but he the angles change, see Figure 24.2.

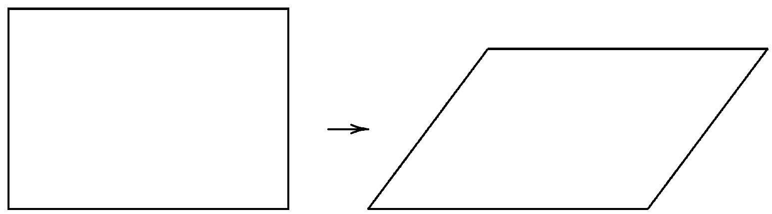

FIGURE 24.2. Plane polygons are flexible

A consequence of Theorem 24.1 is the Cauchy rigidity theorem: a convex polyhedron cannot be deformed. A more precise formulation is as follows.

COROLLARY 24.2. *If a convex polyhedron is continuously deformed so that all its faces remain congruent to themselves then the polyhedron also remains congruent to itself.*

This result is in stark contrast with the constructions of flexible (non-convex!) polyhedra described in Lecture 25.

A continuous version of Cauchy's theorem, due to Cohn-Vossen, states that smooth closed convex surfaces (ovaloids) are rigid: an isometric deformation is a rigid motion. It is not known whether smooth non-convex closed surfaces admit non-trivial isometric deformations.

**24.2 Proof of Cauchy's theorem.** The proof is based on two lemmas. The first is combinatorial (or, one may say, topological).

Suppose that some of the edges adjacent to a vertex of a convex polyhedron are marked + or − (and some edges are not marked at all). Let us make a full circuit around the vertex keeping track of the signs of the edges. We say that a sign change occurs if a positive edge follows a negative one, or a negative edge follows a positive one; the unmarked edges are ignored. For example, there are 4 sign changes in Figure 24.3.

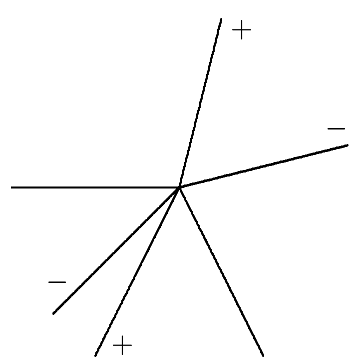


FIGURE 24.3. Four sign changes

LEMMA 24.1. *Assume that some edges of a convex polyhedron are labeled + or −. Let us mark the vertices adjacent to at least one labeled edge. Then there exists a marked vertex such that, going around this vertex, one encounters at most two sign changes.*

The second lemma is geometrical. Consider two convex spherical (or plane) $n$-gons $P_1$ and $P_2$ whose corresponding sides have equal lengths. Mark by + or − the vertices of $P_1$ according to whether the corresponding angle of $P_1$ is greater or smaller than that of $P_2$; if the angles are equal, the vertex is not marked.

LEMMA 24.2. *If there are marked vertices at all, that is, the polygons are not congruent, then, going around polygon $P_1$, one encounters at least four sign changes.*

An explanation is in order. In spherical geometry, the role of straight lines is played by great circles. The shortest segment between two points is the smaller arc of the great circle through these points. With this convention, the definition of convexity is the same as in the plane.

Probably Lemma 24.2 is historically the first in a long series of geometrical theorems involving the number four (four vertex theorems); quite a few are discussed in Lecture 10.

The rest of this lecture is devoted to proofs of Lemmas 24.1 and 24.2. But first we deduce Cauchy's theorem from them.

Proof of Cauchy's theorem. Assume that the faces of two convex polyhedra $S_1$ and $S_2$ are congruent and adjacent in the same way. If the polyhedra are not congruent then some of their corresponding dihedral angles are not equal. Label the edges of $S_1$ by + or − sign according to whether the corresponding dihedral angle of $S_1$ is greater or smaller than that of $S_2$; if the angles are equal, the edge is not labeled.

By Lemma 24.1, there is a vertex $V_1$ of the polyhedron $S_1$, adjacent to some labeled edges and with no more than two sign changes around it. Let $V_2$ be the corresponding vertex of $S_2$. Consider the unit spheres centered at $V_1$ and $V_2$. The faces of the polyhedra $S_1$ and $S_2$, adjacent to $V_1$ and $V_2$, intersect the spheres along convex spherical polygons, $P_1$ and $P_2$. The lengths of the sides of these polygons equal the angles of the respective faces of the polyhedra $S_1$ and $S_2$. Therefore $P_1$ and $P_2$ have equal corresponding edges.

The vertices of the spherical polygons $P_1$ and $P_2$ are the intersections of the respective edges of $S_1$ and $S_2$ with the spheres, and the angles of $P_1$ and $P_2$ are equal to the respective dihedral angles of $S_1$ and $S_2$. Hence the marking of the vertices of the polygon $P_1$, as described in Lemma 24.2, coincides with the labels of the edges of the polyhedron $S_1$ according to the dihedral angles. In particular, the number of sign changes around $P_1$ is not greater than two. But by Lemma 24.2, this number is at least four, a contradiction. □

**24.3 Euler's theorem and the proof of Lemma 24.1.** The classical Euler theorem relates the number of vertices $v$, edges $e$ and faces $f$ of a convex polyhedron: $v - e + f = 2$. For example, a dodecahedron has 20 vertices, 30 edges and 12 faces: $20 - 30 + 12 = 2$.

We need a little more general result concerning graphs on the sphere (central projection of a a convex polyhedron on a sphere whose center lies inside the polyhedron yields such a graph). Denote by $v, e, f$ the number of nodes, edges and faces and by $c$ the number of components of the graph.

THEOREM 24.3. *One has:*

$$v - e + f = c + 1. \tag{24.1}$$

Proof. The argument goes by induction on the number of edges.

Assume that the graph has a vertex $V$ of valence 1, that is, a vertex adjacent to exactly one edge, say, $E$. Delete $V$ and $E$ (but do not delete the other end point of $E$). Then the numbers $v$ and $e$ decrease by 1. Since the edge $E$ does not separate faces, the number $f$ remains intact, and so does $c$, the number of components of the graph. Therefore the number $v - e + f - c$ does not change.

Next assume that all vertices have valences 2 or higher. Then there exists a closed non self-intersecting path in the graph. Indeed, choose a vertex, say, $V_1$. There is an edge going from this vertex. Go to the other end-point of this edge, $V_2$. The valence of $V_2$ is not less than 2, so there is another edge going from $V_2$. Let $V_3$ be the other end-point of this edge, etc. We continue until we return, for the first time, to an already visited vertex. This yields a closed non self-intersecting path.

This path separates the sphere into two components (see Lecture 26 for a discussion of the Jordan Theorem). Delete one edge from this path (but do not delete its end points). Then the number $f$ decreases by 1, and so does $e$, while $v$ and $c$ remain the same. Again $v - e + f - c$ does not change.

Continue in this way until all edges are deleted. Then the graph consists of $v$ isolated vertices, has $f = 1$ face and $c = v$ components, and the relation (24.1) holds. □

Now we proceed to the proof of Lemma 24.1. The labeled edges of a convex polyhedron form a graph which we think of as drawn on the sphere. Let $v, e, f$ and $c$ have the same meaning as before, and let $s$ be the sum of the numbers of sign changes over all vertices of the graph. The number of sign changes around a vertex is even. Hence Lemma 24.1 will follow if we show that the average number of sign changes per vertex is less than 4, that is, $s < 4v$. Following Cauchy, one has a stronger estimate.

PROPOSITION 24.3. *One has:*

$$s \leq 4v - 8. \tag{24.2}$$

Proof. Instead of going around the vertices of the graph let us traverse the boundaries of all the faces. The total number of sign changes $s$ will be the same: indeed, two edges are neighbors when going around a vertex if and only if they are neighbors when traversing the boundary of a face, see Figure 24.4.

When traversing the boundaries, we make the following conventions:
a) if the boundary of a face has many components, we traverse them all and add the number of sign changes;
b) if a segment is adjacent to the face on both sides, we treat this segment as two-sided, both sides carrying the same sign; such a segment will be traversed twice, once on each side.

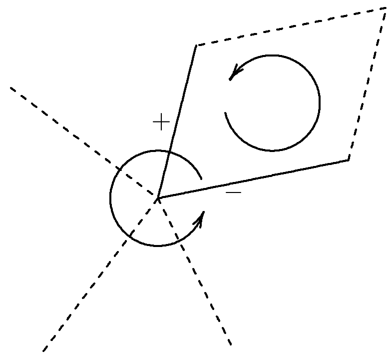


FIGURE 24.4. Counting the number of sign changes in two ways

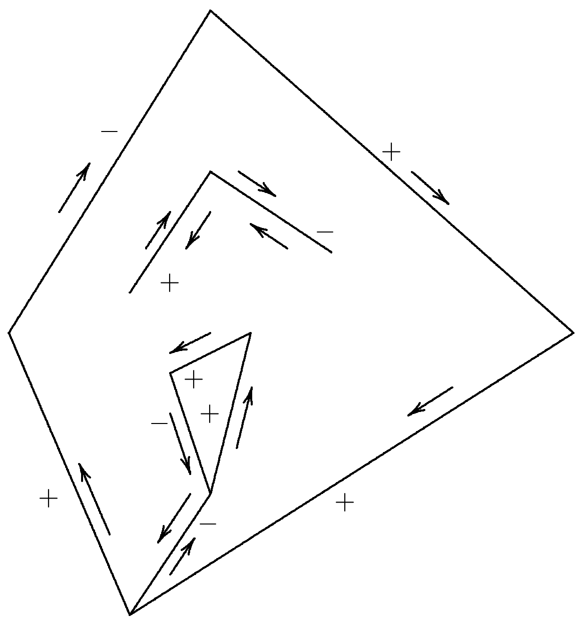


FIGURE 24.5. There are 8 sign changes on one of the boundary components and 2 on the other

This is illustrated in Figure 24.5: the total number of sign changes, contributed by the quadrilateral face, is 8.

Denote by $f_i$ the number of faces whose boundary consists of $i$ edges. Here $i \geq 3$, and an edge is counted twice if it is adjacent to the face on both sides. For example, the boundary of the face in Figure 24.5 has 13 edges. Thus

$$f = f_3 + f_4 + f_5 + \dots . \tag{24.3}$$

When one traverses the boundary of a domain with $i$ edges, one encounters at most $i$ sign changes, and if $i$ is odd, at most $i-1$ ones. Therefore

$$s \leq 2f_3 + 4f_4 + 4f_5 + 6f_6 + 6f_7 + \dots . \tag{24.4}$$

Each edge either belongs to the boundary of two faces or is counted twice in the boundary of one face, hence

$$2e = 3f_3 + 4f_4 + 5f_5 + \dots. \tag{24.5}$$

It follows from Euler's formula (24.1) that $v - e + f \geq 2$, or $4v - 8 \geq 4e - 4f$. Substitute $f$ and $e$ from (24.3) and (24.5):

$$4v-8 \geq (6f_3+8f_4+10f_5+\dots)-(4f_3+4f_4+4f_5+\dots) = 2f_3+4f_4+6f_5+8f_6+\dots$$

and the right hand side is not less than that of (24.4). This completes the proof. □

**24.4 Arm Lemma and proof of Lemma 24.2.** The following statement is known as the Cauchy Arm Lemma.[1]

LEMMA 24.4. *Let $P_1 \dots P_n$ and $P'_1 \dots P'_n$ be two convex spherical or plane polygons. Assume that $|P_iP_{i+1}| = |P'_iP'_{i+1}|$ for $i = 1, 2, \dots, n-1$ and $\angle P_iP_{i+1}P_{i+2} \leq \angle P'_iP'_{i+1}P'_{i+2}$ for $i = 1, \dots, n-2$. Then $|P_1P_n| \leq |P'_1P'_n|$ with equality only if all the corresponding angles are equal, see Figure 24.6.*

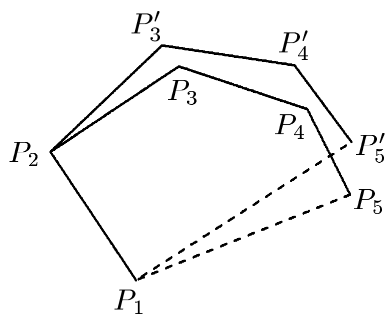


FIGURE 24.6. The Cauchy Arm Lemma

One may view $P_1 \dots P_n$ as robot's arm: when the arm opens the distance between the "shoulder" and "tips of the fingers" increases. This fact is intuitively quite clear; it is interesting that Cauchy's proof contained an error that went undetected for about 100 years. The proof below is due to I. Schoenberg.

Proof of the Arm Lemma. Induction on $n$. When $n = 3$, the result is obvious: if two triangles have two pairs of congruent corresponding sides then the third side opposite the greater angle is greater; see Figure 24.7.

Let $n \geq 4$. If the two polygons have equal angles, say, at vertices $P_i$ and $P'_i$, then one may cut off these vertices by the diagonals $P_{i-1}P_{i+1}$ and $P'_{i-1}P'_{i+1}$. Since these diagonals are equal, we are reduced to the same statement but with $n$ one less.

Thus we assume that each angle of the first polygon is smaller than the respective angle of the second one. Let us start increasing the angle $P_{n-2}P_{n-1}P_n$ by rotating the side $P_{n-1}P_n$ about the vertex $P_{n-1}$, keeping the polygon convex, until one of the two things happens: either $\angle P_{n-2}P_{n-1}P_n$ becomes equal to $\angle P'_{n-2}P'_{n-1}P'_n$ or we reach the situation when the vertices $P_1, P_2$ and $P_n$ lie on one

[1] This lemma was stated and proved, in different terms, by Legendre in 1794. Legendre also conjectured that convex polyhedra were rigid.

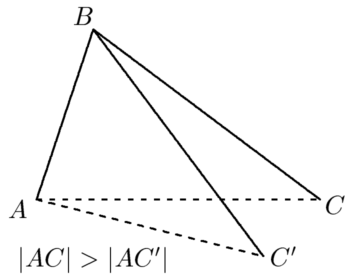


FIGURE 24.7. The side, opposite the greater angle, is greater

line, see Figure 24.8. We obtain a new polygon $P_1 \dots P_n$, and in both cases, the side $P_1P_n$ has increased – see the first paragraph of the proof applied to the triangle $P_1P_{n-1}P_n$.

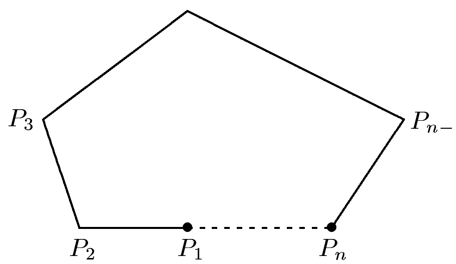


FIGURE 24.8. Inductive proof of the Cauchy Arm Lemma

In the first case, we obtain two $n$-gons satisfying the conditions of the Arm Lemma having a pair of equal corresponding angles. This case was already dealt with in the second paragraph of the proof.

In the second case, we ignore the first vertices in both polygons and apply the induction assumption to the polygons $P_2 \dots P_n$ and $P'_2 \dots P'_n$ to conclude that $|P'_2P'_n| \geq |P_2P_n|$. Then

$$|P'_1P'_n| \geq |P'_2P'_n| - |P'_1P'_2| \geq |P_2P_n| - |P_1P_2| = |P_1P_n|,$$

where the first inequality is the triangle inequality. This concludes the proof. □

It remains to prove Lemma 24.2. This is not hard, given the Arm Lemma.

Proof of Lemma 24.2. The number of sign changes being even, assume first that there are two sign changes. Then we can number the vertices of the polygon $P$ consecutively so that the first $k$ vertices $A_1, \dots, A_k$ are all positive or unmarked and the remaining $n - k$ vertices $A_{k+1}, \dots, A_n$ are all negative or unmarked. Let $B_1, \dots, B_n$ be the respective vertices of $P_2$.

Choose points $C$ and $D$ on the sides $A_kA_{k+1}$ and $A_nA_1$, and let $E$ and $F$ be points on the sides $B_kB_{k+1}$ and $B_nB_1$ so that $|A_kC| = |B_kE|$ and $|A_nD| = |B_nF|$, see Figure 24.9.

Apply the Arm Lemma to polygons $DA_1 \dots A_kD$ and $FB_1 \dots B_kE$ to conclude that $|CD| > |FE|$. Similarly, applied to polygons $CA_{k+1} \dots A_nD$ and $EB_{k+1} \dots B_nF$, the Arm Lemma yields: $|CD| < |FE|$, a contradiction.

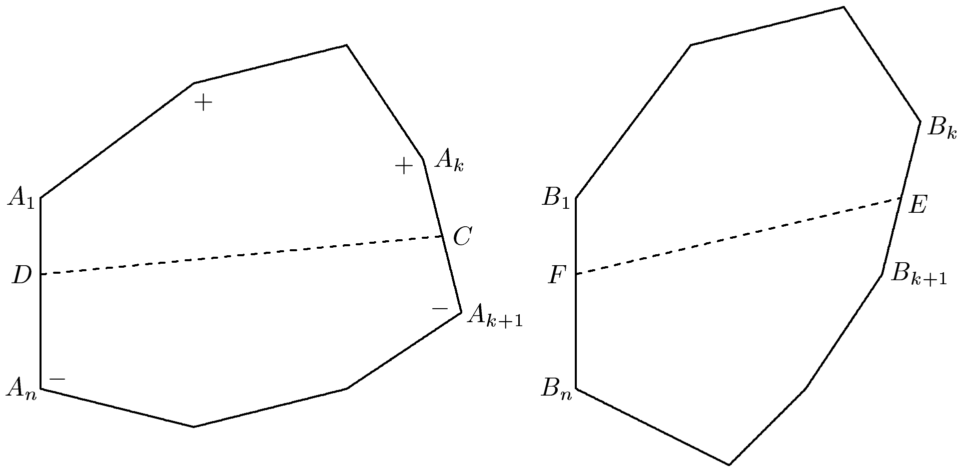


FIGURE 24.9. Proof of Lemma 24.2

Finally, if there are no sign changes at all, let us assume that all signs are positive. Then, by the Arm Lemma, $|A_1A_n| > |B_1B_n|$, again a contradiction. □

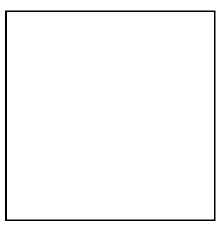

John Smith
January 23, 2010

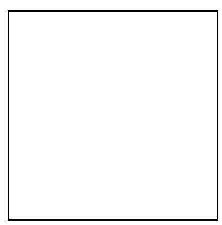

Martyn Green
August 2, 1936

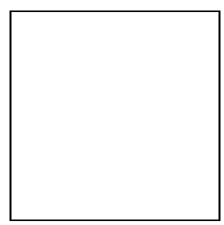

Henry Williams
June 6, 1944

**24.5 Exercises.**

24.1. Prove that every polyhedron has two faces with the same number of sides.

24.2. Prove that every convex polyhedron has either a triangular face or a vertex incident to three faces (or both).

24.3. * Prove the following continuous analog of Lemma 24.2: given two plane ovals, let $ds$ and $ds_1$ be the arc length elements at points with parallel and equally oriented exterior normals. Then the ratio $ds_1/ds$ has at least four extrema.

24.4. * Let $P$ and $P'$ be plane convex $n$-gons, $n \geq 4$, whose sides have lengths $\ell_1, \ldots, \ell_n$ and $\ell'_1, \ldots, \ell'_n$. Assume that the corresponding sides of the polygons are parallel to each other. Consider the cyclic sequence

$$a_i = \left(\frac{\ell'_{i+1}}{\ell_{i+1}} - \frac{\ell'_i}{\ell_i}\right)\left(\frac{\ell'_{i-1}}{\ell_{i-1}} - \frac{\ell'_i}{\ell_i}\right).$$

Prove that either $a_i = 0$ for all $i$ or $a_i > 0$ for at least four values of $i$.

24.5. * Prove a continuous analog of the Arm Lemma: given two smooth convex arcs $\gamma_1(s)$ and $\gamma_2(s)$ of equal lengths and parameterized by arc length, if their curvatures satisfy the inequality $k_1(s) \geq k_2(s)$ for all $s$ then the chord subtended by $\gamma_2$ is not less than that subtended by $\gamma_1$.

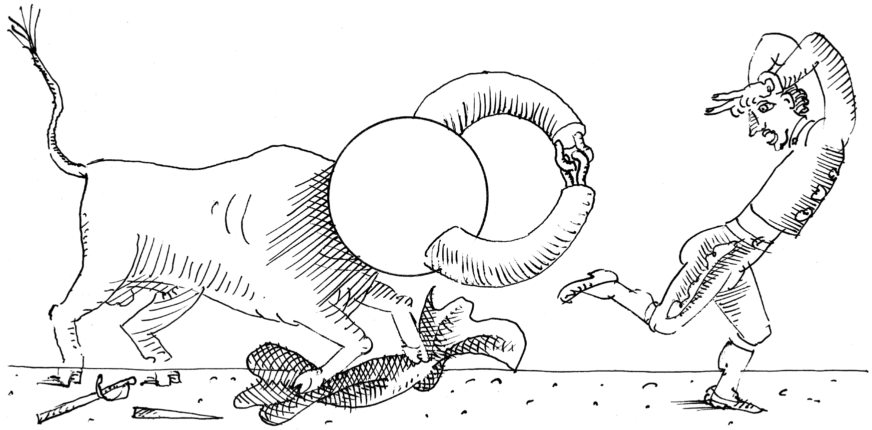

LECTURE 25

# Flexible Polyhedra

**25.1 Introduction.** This lecture is closely related to the previous one (Lecture 24), but they can be read independently, in particular, in either order. Again, we consider polyhedra made of rigid (say, metallic) faces attached to each other along edges of equal lengths by hinges which do not obstruct changing angles between faces. Except several clearly specified cases, polyhedra are assumed "complete" which means that every edge belongs to precisely two faces. Our problem is: *is it possible to bend the polyhedron without deforming its faces* (Figure 25.1). The readers of the previous lecture are familiar with the following theorem.

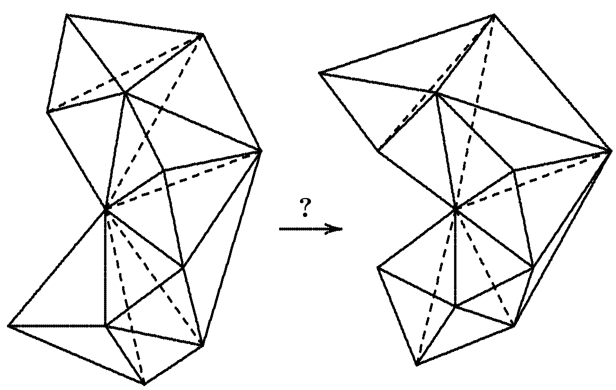


FIGURE 25.1. Can a polyhedron be flexible?

THEOREM 25.1 (Cauchy, 1813). *Any convex polyhedron is rigid (cannot be bent).*

Here we shall prove the following, quite unexpected result.

THEOREM 25.2 (Connelly, 1978). *There exists a (non-convex) flexible polyhedron.*

Unlike Cauchy's theorem, the theorem of Connelly can be proved by providing one single example of a flexible polyhedron. We shall construct such a polyhedron quite explicitly, and if you have appropriate materials (rigid cardboard and tape), you will be able to make a model of such polyhedron and to feel its flexibility with your own fingers.

**25.2 Bricard's octahedron.** One can ask why it took so long (more than 150 years) after the Cauchy theorem to find the Connelly example. Of course, questions like that can never be answered with certainty, but we can try to guess. The rigidity problem was well known and respected among geometers, but almost all of them believed and tried to prove that the answer is positive: all polyhedra, convex or not, are rigid. (By the way, the efforts of these geometers were not totally fruitless: the rigidity of polyhedra was established under conditions much milder than convexity.) Connelly, on the other hand, had the courage to doubt. And then he noticed that almost all necessary mathematical work was done in the 1890s by a French mathematician and architect Raoul Bricard. Bricard was able to construct a flexible polyhedron which, however, not only fails to be convex, but also has a self-intersection. So, Connelly looked for a tool to make the Bricard polyhedron free of self-intersections, and he found such tools – again in Bricard's construction.

Bricard's polyhedron is an octahedron, in the sense that it consists of eight triangular faces attached to each other precisely in the same way as the faces of Plato's regular octahedron. To construct the Bricard octahedron, we need two simple observations. The first is that a pyramid without bottom (this is an "incomplete" polyhedron) is flexible if and only if the number of its (triangular) faces is more than 3, see Figure 25.2.[1] Note that the (missing) bottom of this pyramid is not supposed to be flat (the points $A, B, C, D$ are not assumed to belong to one plane for either of the 4-gonal pyramids of Figure 25.2).

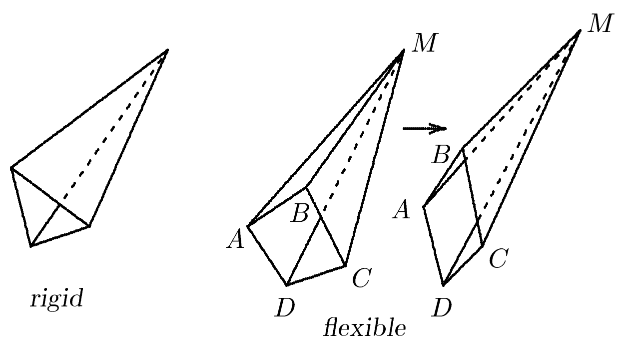


FIGURE 25.2. Rigid and flexible pyramids

The second observation is the following lemma.

LEMMA 25.1. *Let $ABCD$ be a non-planar spatial quadrilateral such that $AB = CD$ and $BC = AD$. Let $E, F$ be the midpoints of "diagonals" $AC$ and $BD$. Then $EF \perp AC$ and $EF \perp BD$.*

[1]This observation was also made in Lecture 20.

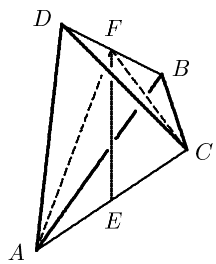


Figure 25.3. Proof of Lemma 25.1

Proof. (Figure 25.3). Draw the segments $AF$ and $CF$. Since $\triangle ABD = \triangle CBD$ (their sides are equal), $\angle ADB = \angle CBD$. Hence, $\triangle ADF = \triangle CBF$ (they have two pairs of equal sides forming equal angles). Thus, $AF = CF$, hence $\triangle ACF$ is isosceles and its median $FE$ is also its altitude. So, $EF \perp AC$, and we can establish, in the same way, that $EF \perp BD$. □

Lemma 25.1 can be reformulated in the following way: a spatial quadrilateral with equal opposite sides is symmetric with respect to the line joining the midpoints of its diagonals. In this form, it can be regarded as a spatial version of the well-known theorem stating that the diagonals of a parallelogram bisect each other.

Now we are prepared for Bricard's construction. Take a spatial quadrilateral $ABCD$ with equal opposite sides, $AB = CD, BC = AD$. Lemma 25.1 provides for this quadrilateral an axis of symmetry; denote it by $\ell$. Take two points, $M$ and $N$, different from each other and from each of $A, B, C, D$, and also symmetric with respect to $\ell$. (To visualize the construction better, you may choose the point $M$ and $N$ sufficiently far away from the quadrilateral $ABCD$). Bricard's octahedron is the union of 8 triangles: $ABM, BCM, CDM, DAM, ABN, BCN, CDN, DAN$ (see Figure 25.4). Some faces intersect each other: in Figure 25.4, $EF$ is the intersection line of the faces $ABN$ and $CDM$, the faces $ABN$ and $BCM$ meet at $BE$, and the faces $CDM$ and $ADN$ meet at $FD$.

Theorem 25.3 (Bricard, 1897). *The Bricard octahedron is flexible.*

Proof. We shall consider the Bricard octahedron as the union of two 4-gonal pyramids: $ABCDM$ and $ABCDN$. According to the first observation above, the (bottomless) pyramid $ABCDM$ is flexible. Its deformation retains the relations $AB = CD$ and $BC = AD$, thus the "base" $ABCD$ of the pyramid has a line of symmetry at every moment of the deformation. If we reflect the varying pyramid $ABCDM$ in this line, we shall get a deformation of the pyramid $ABCDN$, and together these two deformations form a deformation of the Bricard octahedron. □

**25.3 Geometry of Bricard's octahedron.** Of the geometric observations we are going to make in this section only the last one will be needed later. Still the fascinating properties of the Bricard octahedron deserve a detailed consideration.

First, the Bricard octahedron has axial symmetry: the midpoints of the "diagonals" $AC, BD$, and $MN$ lie on one line, and the whole octahedron is symmetric in this line. This gives the simplest construction of the Bricard octahedron: take a line in space, take three pairs of points, symmetric with respect to this line (no

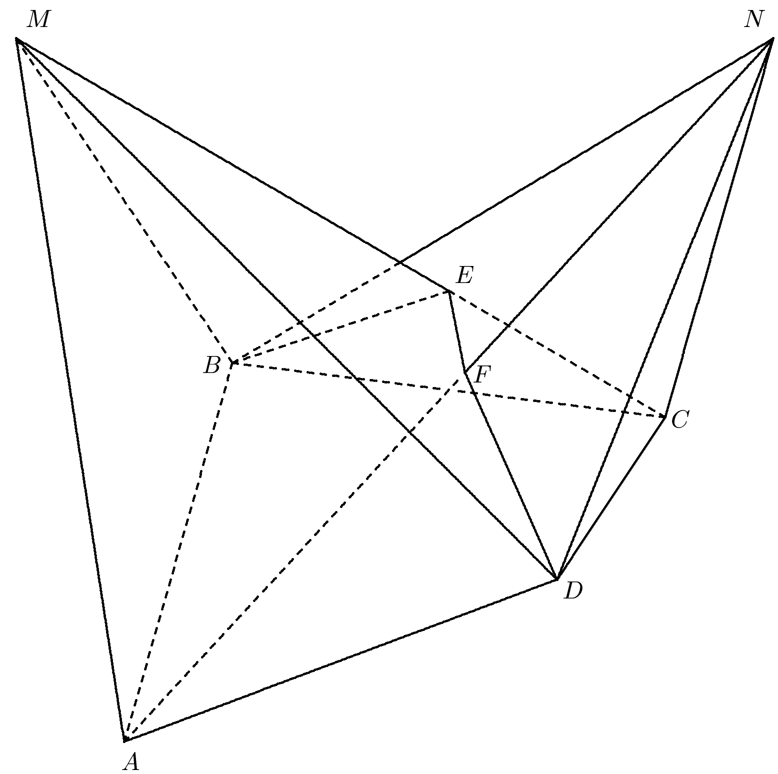


FIGURE 25.4. Bricard's octahedron

four of them should lie in one plane), denote these pairs of points by $A$ and $C$, $B$ and $D$, and $M$ and $N$, and you are done.

Since the Bricard octahedron is always self-intersecting, you cannot make a good model of it. But it is possible to make a model including 6 of 8 faces of the octahedron. (Notice that the octahedron in Figure 25.4 will be free of self-intersections, if you remove the faces $ABN$ and $CDN$.) To create your model, you can use a 6-triangle development like the one shown in Figure 25.5.

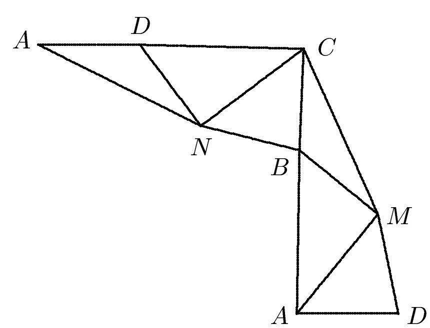


FIGURE 25.5. A development of the Bricard octahedron less two faces

You need to cut a polygon $ABMCBAKD$ out of a thin and rigid cardboard, then fold it along the segments $AM, MB, BC, CN$, and $ND$ in such a way that the two segments $AD$ come together ($A$ to $A$ and $D$ to $D$); attach them to each other by a tape. The whole "strip" should be twisted twice (twice as many times as we twist a strip to make a Möbius band). You can make a development of your own, but it is important that

$$\begin{array}{l} AB = CD, BC = AD, AM = CN, \\ AN = CM, BM = DN, BN = DM; \end{array} \qquad (*)$$

in particular, the two pentagons $ADMCB$ and $CBNAD$ are identical (with their decompositions into triples of triangles), but opposedly oriented. The figure obtained will be bounded by two triangles, $NAB$ and $MCD$, which will be linked (as they are linked in Figure 25.4).

You will be surprised how flexible your model is (with the triangular faces remaining rigid!). It can be deformed to look as shown in Figure 25.6, left, or Figure 25.6, right.

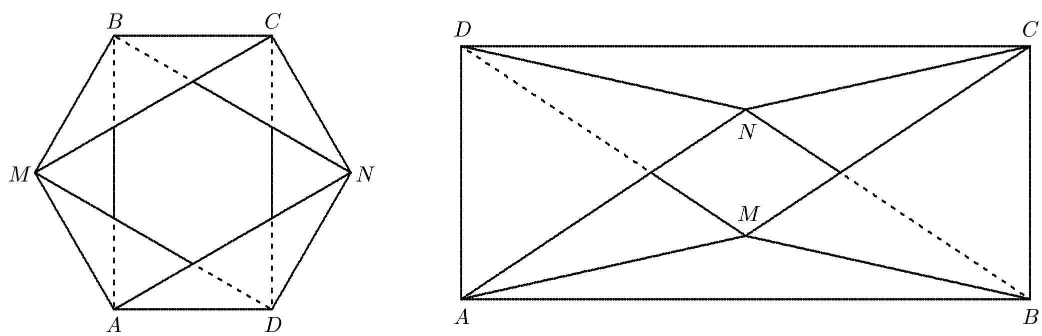


FIGURE 25.6. What the flexible model can look like

It is interesting that to be flexible, Bricard's octahedron needs to be symmetric. If you slightly distort the sizes of the triangles in Figure 25.5 in such a way that the equalities $(*)$ fail to hold (still the two segments $AD$ should be equal), you can make a model indistinguishable by sight from the previous model, but it will be rigid, and you will be able to feel the difference with your fingers. (How slightly the sizes should be varied, depends on the quality of your materials, the cardboard and the tape.)

Another way to make a non-self-intersecting incomplete Bricard's octahedron is to remove two faces which share an edge, say, $AMB$ and $ANB$. You can cut the 6-triangle development which is shown in Figure 25.7, left, and then attach to each other the two segments $AD$ above the plane $CMDN$ and the two segments $BC$ below this plane. (Actually, this figure is too symmetric, all we need is the equalities $(*)$; but it is more convenient to deal with an excessively symmetric octahedron.) You will get a flexible polyhedral surface with a 4-gonal edge ($AMBN$) as shown in Figure 25.7, right; note that the distance $AB$ does not change in the process of deformation.

You cannot add to this model either of the missing faces $AMB$ or $ANB$, because of self-intersections. But still you can make your polyhedron complete,

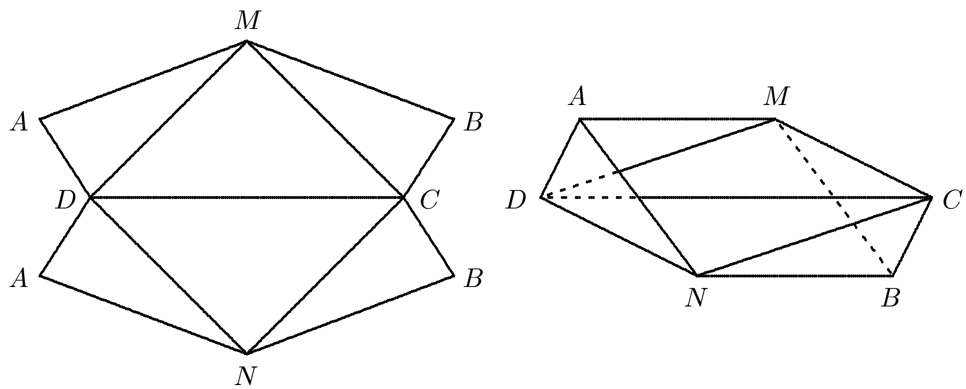


FIGURE 25.7. Another model of Bricard's octahedron

although infinite. Namely, replace the face $AMB$ by the complement of it in the half-plane bounded by $AB$ (see Figure 25.8) and do the same with the face $ANB$.

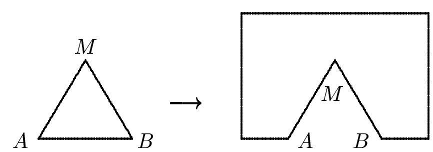


FIGURE 25.8. A replacement for a face

You will get a complete flexible polyhedron (resembling an open book) with 6 finite faces and 2 infinite faces. It is shown in Figure 25.9, left, and its side view, important for the next section, is shown in Figure 25.9, right. (The meaning of the arrow in this figure will be also explained in the next section.)

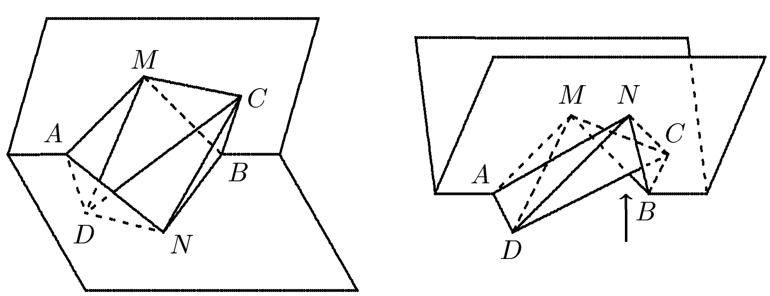


FIGURE 25.9. Bricard's octahedron as an open book

**25.4 Connelly's construction.** We start with a very degenerate Bricard octahedron. Take a (planar) rectangle $ABCD$ ($AB < CD$) and a point $M$ inside this rectangle such that $MA = MB < MC = MD$. Break the rectangle into 4 triangles: $AMB, BMC$, $CMD, DMA$. Take another copy of this rectangle and a point $N$ symmetric to $M$ with respect to the center of the rectangle. Then break

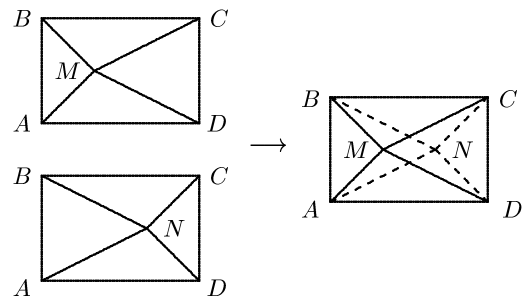


FIGURE 25.10. Starting point of the construction: a degenerate Bricard octahedron

the second rectangle into the triangles $ANB, BNC, CND, DNA$. After this, put the first copy of the rectangle onto the second one as shown in Figure 25.10.

The 8 triangles $AMB, \dots, DNA$, although they all lie in one plane, form a Bricard octahedron, which is flexible within the class of self-intersecting polyhedra. (Figure 25.6, right, may serve as a right picture of this deformation.)

We can make the self-intersections less dramatic if we erect pyramids on some of the faces of this octahedron. It should be noticed that we shall not destroy the flexibility of a polyhedron if we replace some faces by pyramids based on these faces (see Figure 25.11); the pyramids will stay rigid during the deformation.

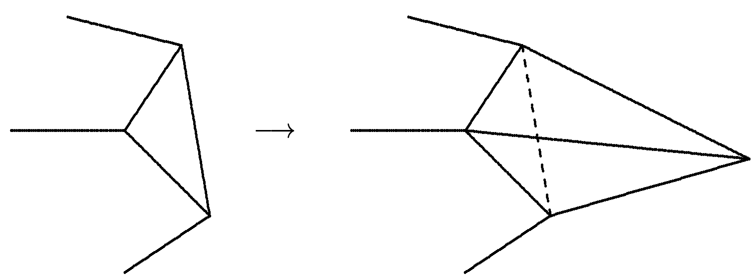

FIGURE 25.11. Adjoining pyramid to faces

Add pyramids to the faces of the flat octahedron of Figure 25.10 (we need, actually, only 6 pyramids, since the small triangles $AMB$ and $CND$ will not touch any other faces). We get a flexible polyhedron with 20 faces and with a very mild self-intersection: there will be two pairs of crossing edges. (The two halves of this polyhedron are shown in Figure 25.12, and the crossing point of the edges are marked as $E$ and $F$ in this figure.)

The dihedral angles at the crossing points have no other common point, they only touch each other as shown in Figure 25.13, left. But in the process of deformation these pairs of touching dihedral angles may behave as shown in Figure 25.13, right: they either go apart, or penetrate each other.

Actually, of the two pairs of touching dihedral angles, one behaves in one of the ways, and the other one behaves in the other way (this is not important for us, but can be easily confirmed by a calculation, or even by an experiment). Anyhow, this polyhedron still cannot be deformed without self-intersections. What to do? What

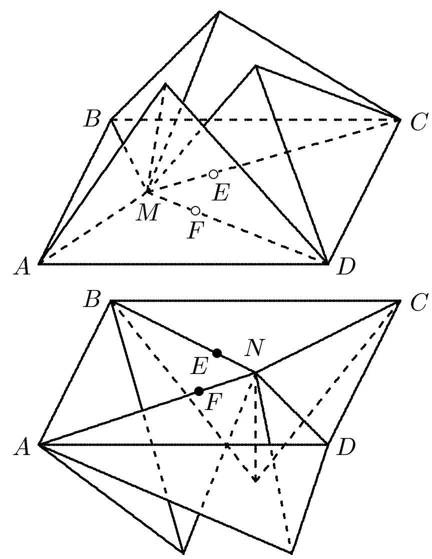


FIGURE 25.12. Two halves of an almost ready Connelly's polyhedron

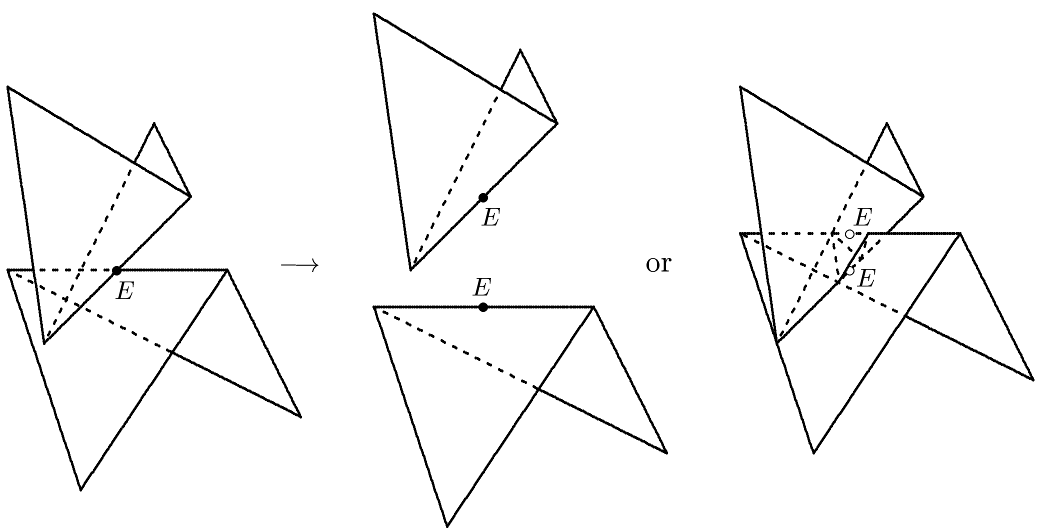


FIGURE 25.13. Deformation of touching dihedral angles

we want is to remove a small neighborhood of the touching point in (at least) one of the two touching dihedral angles (Figure 25.14, left). And this must be done in a "polyhedral" way. But we know how to do it: Figure 25.9, right, shows it! The arrow points at a small cavity, and all we need is to locate this cavity at and around the point $E$ (see also Figure 25.14, right). This completes Connelly's construction and the proof of Theorem 25.2.

It should be noted that the construction shown above is very good for proving Theorem 25.2 but not convenient for modeling and demonstration. The constructed

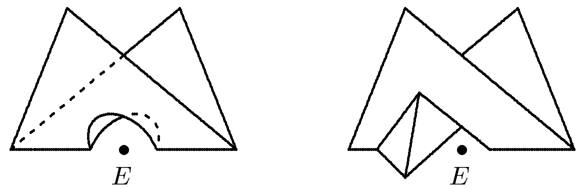


FIGURE 25.14. A final modification of a dihedral angle

polyhedron consists of 26 faces, of which 24 are triangles and 2 are non-convex hexagons. Even if you manage to make a model of this polyhedron, it will admit a very small deformation (compared with the size of the polyhedron), and you will never know, whether this deformability is ensured by the mathematical properties of the polyhedron or rather by flaws of the material used (the cardboard and the tape). However, there are modifications of Connelly's construction which yield quite a satisfactory model. We shall discuss these modifications in the next section.

**25.5 Better constructions.** After the breathtaking discovery of Connelly, many geometers tried to improve his construction. One possibility for an improvement is obvious: the insert in Figure 25.14 may be made bigger, so that it would eat up completely the two faces forming the dihedral angle. This will reduce the number of faces to 24, and all of them will be triangular. Then one can observe that not all the pyramids are really needed, and this gives rise, eventually, to a model with only 18 faces, all of which are triangular.

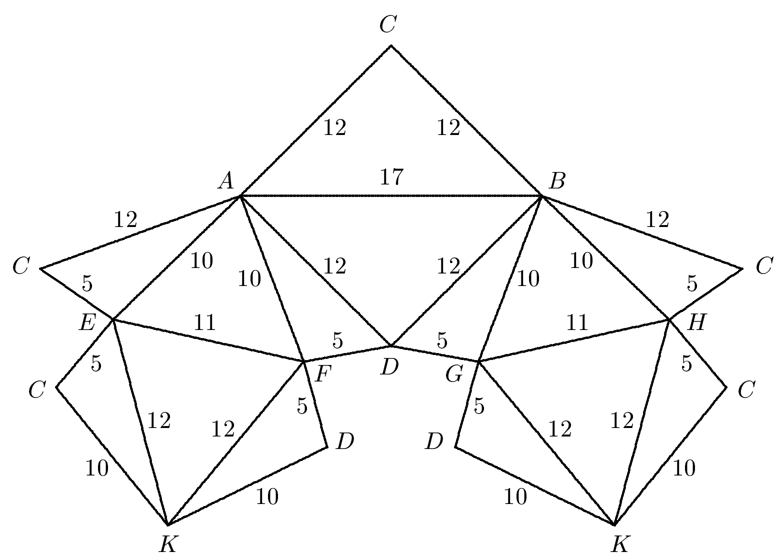


FIGURE 25.15. Cut this out of cardboard and make a model of Steffen's polyhedron

It was a young German mathematician Klaus Steffen who found, probably, the best possible construction. His polyhedron consists of 14 triangular faces and has only 9 vertices. You can make a model using the development on Figure 25.15.

A drawing of this polyhedron can be seen in Figure 25.16 (to make the drawing better understandable, we notice that the vertex $G$ is located in a cavity surrounded by the ridge $BDKH$).[2]

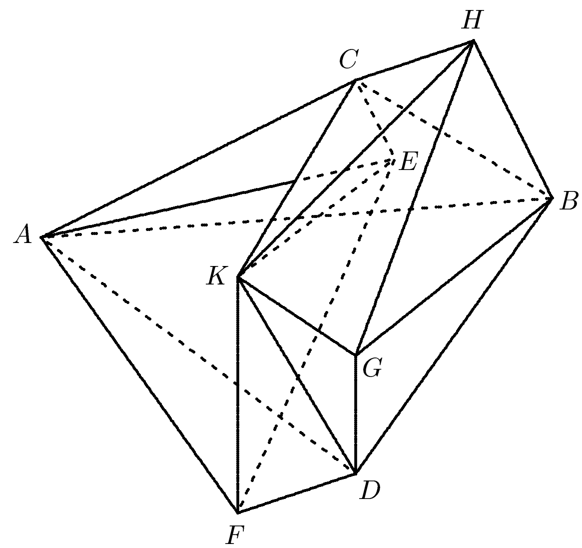


FIGURE 25.16. The Steffen polyhedron

We notice in conclusion that, as is seen from Figure 25.15, Steffen's polyhedron contains two identical 6-face pieces of Bricard's octahedron similar to those shown in Figure 25.8 (the two wings of Figure 25.15), and two more triangular faces (the middle part of Figure 25.15) which are attached to both octahedral pieces. These three parts of the Steffen polyhedron are shown separately in Figure 25.17.

These remarks make the flexibility of Steffen's polyhedron less surprising. We already know that the two octahedral pieces are deformable, and, certainly, we can deform them when they are attached to each other; thus the Steffen polyhedron less two faces ($ABC$ and $ABD$), is deformable. It is not hard to see that this deformation does not affect the distance $CD$ which makes deformable the whole polyhedron (and the dihedral angle formed by these two faces stays rigid in the process of deformation).

**25.6 The bellows conjecture.** There is one more natural problem: does the volume inside a flexible polyhedron vary in the process of deformation? There are indications that it does not. It is not hard to prove that the modification of a dihedral angle shown in Figure 25.14, right, does not affect the volume of the polyhedron.[3] From this, it is easy to deduce that the volume inside the Connelly polyhedron is equal to the sum of the volumes of 6 pyramids attached at the first step of the construction and does not vary in the process of the deformation. Similarly, the volume of the Steffen polyhedron (Figure 25.16) is equal to that of the

[2]An animated picture of Steffen's polyhedron showing its deformation is available on the web, e.g., at www.mathematik.com/Steffen/.

[3]With a right definition of the volume "inside" a self-intersecting polyhedron (we leave the details to the reader), one can prove that the volume inside any Bricard octahedron is zero.

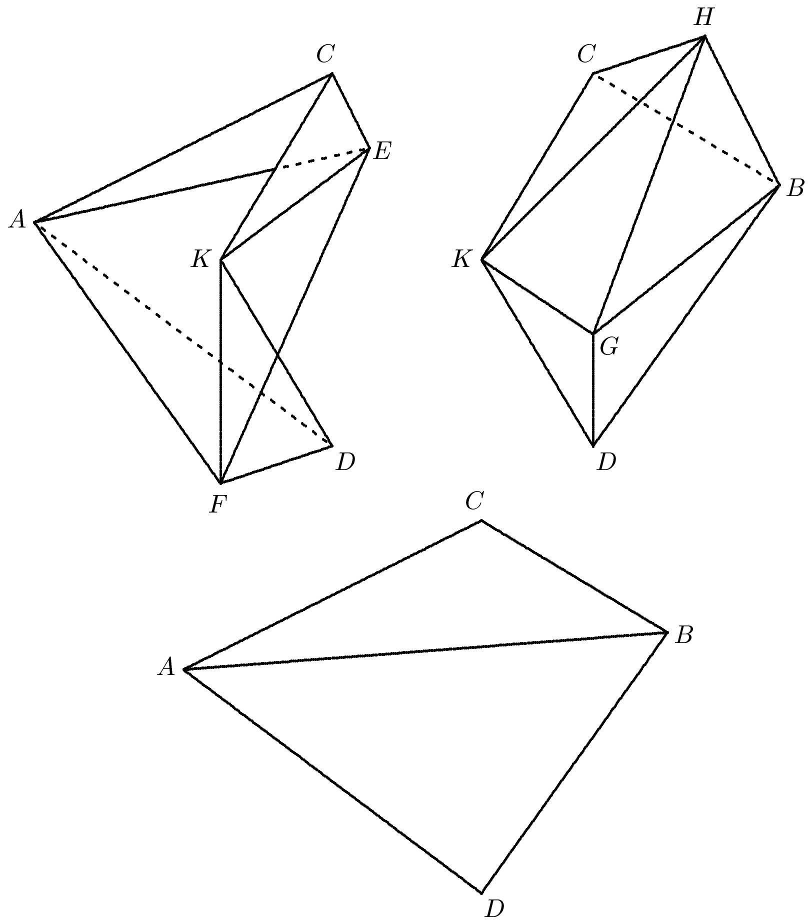


FIGURE 25.17. The Steffen polyhedron disassembled

tetrahedron $ABCD$ and is also constant. Still there remained a possibility of a construction of a flexible polyhedron with a variable volume. However, in 1995, I. Sabitov proved that such a construction is not possible; thus, Sabitov proved a statement which was called "the bellows conjecture". Actually, Sabitov's theorem states that, given a set of (rigid) faces of a polyhedron, the volume of the polyhedron can assume only countably many values, [**66**]. This, certainly, excludes any variation of the volume.

Let us mention, in conclusion, a somewhat paradoxical construction. Start with a tetrahedron and deform it, as shown in Figure 25.18. Namely, one subdivides each edge of the tetrahedron into two segments and each face into 10 triangles, and then pushes the new vertices on the edges inwards. This is an isometric deformation of the original tetrahedron.

The middle parts of the edges are pushed inwards, so one may expect the volume to decrease. However, the middle parts of the faces move outwards, and the total volume actually increases, by more than a third! Similar volume increasing

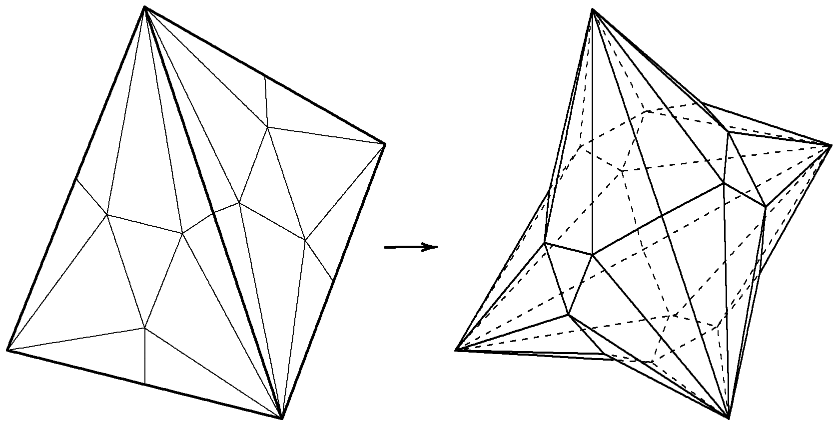

Figure 25.18. Isometric volume increasing deformation of a tetrahedron

isometric deformations can be made for all the Platonic solids [**7, 12**] and even all polyhedral surfaces [**58**].

It may appear that this construction contradicts the bellows conjecture. This is not the case: the deformation of a tetrahedron depicted in Figure 25.18 is not a continuous isometric deformation (the sizes of the small triangles, subdividing the faces of the original tetrahedron, change in the process).

| | | |
|---|---|---|
| John Smith<br>January 23, 2010 | Martyn Green<br>August 2, 1936 | Henry Williams<br>June 6, 1944 |

**25.7 Exercises.**

25.1. Let $ABCD$ be a non-self-intersecting quadrilateral in the plane. We are allowed to deform it in such a way that the lengths of the sides stay constant but the angles may vary.

(a) Prove that we can always deform the quadrilateral $ABCD$ into a triangle.

(b) Prove that we can always deform the quadrilateral $ABCD$ into a trapezoid.

(c) Is it always possible to deform the quadrilateral $ABCD$ into a trapezoid with $AB$ being one of two parallel sides?

25.2. Let $ABCD$ be a trapezoid. We want to deform it as in Problem 25.1 in such a way that in the process of deformation it remains a trapezoid. Prove that it is possible if and only if it is a parallelogram.

25.3. Let $A_1A_2 \dots A_n$ be an $n$-gon in the plane. An *admissible deformation* of this $n$-gon consists in a continuous motion of points $A_1, A_2, \dots, A_n$ not affecting the distances $|A_1A_2|, \dots, |A_{n-1}A_n|$, $|A_nA_1|$.

(a) Let $n = 4$. In terms of the four numbers, $|A_1A_2|, |A_2A_3|, |A_3A_4|, |A_4A_1|$, find a necessary and sufficient conditions for the existence of an admissible deformation joining the quadrilateral $A_1A_2A_3A_4$ with its mirror image $A'_1A'_2A'_3A'_4$ (the latter means that there exists a line $\ell$ such that $A_i$ is symmetric to $A'_i$ for all $i$).

*Hint.* See the comment below.

(b) Do the same for $n = 5$ and the numbers $|A_1A_2|, \dots, |A_4A_5|, |A_5A_1|$.

*Hint.* See the comment below.

*Comment.* There is a general result due to Kapovich and Milson [**43**] stating that for any $n$-gon $A_1A_2 \dots A_n$ the following two sattements are equivalent.

(1) For any $n$-gon $A'_1A'_2 \dots A'_n$ with $|A'_1A'_2| = |A_1A_2|, \dots, |A'_{n-1}A'_n| = |A_{n-1}A_n|, |A'_nA'_1| = |A_nA_1|$, there exists an admissible deformation of the $n$-gon $A_1A_2 \dots A_n$ into $A'_1A'_2 \dots A'_n$.

(2) Let $a_1, a_2, \dots, a_n$ be the numbers $|A_1A_2|, \dots, |A_{n-1}A_n|, |A_nA_1|$ arranged in the non-increasing order: $a_1 \geq a_2 \geq \cdots \geq a_n$. Then

$$a_2 + a_3 \leq a_1 + a_4 + \cdots + a_n$$

25.4. Let $ABCD$ be a non-self-intersecting quadrilateral in the plane, $M$ be a point not in this plane. The pyramid $MABCD$ becomes flexible if one removes the base $ABCD$ (see Section 25.2). Prove that in the process of deformation the points $A, B, C, D$ cannot remain coplanar.

25.5. A (possibly self-intersecting) polyhedron is called *two-sided* if one can paint the two sides of each face black and white in such a way that the colors match at each edge. Otherwise, a polyhedron is called *one-sided*.

(a) Prove that a non-self-intersecting polyhedron is two-sided.

(b) Take a regular (Plato's) octahedron as shown in Figure 25.19, remove the triangular faces $AMB, BNC, CMD, DNA$ and add the square faces $ABCD, AMCN, BMDN$. Prove that this construction creates a complete (every edge belongs to precisely 2 faces) one-sided polyhedron.

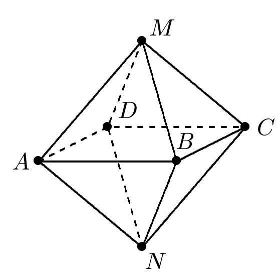


FIGURE 25.19. One-sided polyhedron made of an octahedron

(c) Prove that the Bricard octaherdron is two-sided. Prove also that the reflection in the axis of symmetry takes white into black and black into white.

25.6. Let $P$ be a complete two-sided polyhedron. Choose a black and white coloring of faces as in exercise 25.5 and choose a plane $\Pi$ not perpendicular to any face of $P$ and not crossing $P$. For a face $F$ define its underlying volume as the volume of the prism between $F$ and its orthogonal projection onto $\Pi$ (see Figure 25.20) multiplied by $-1$ if the upper face of the prism is white. Define the *signed volume* of $P$ as the sum of underlying volumes of all faces.

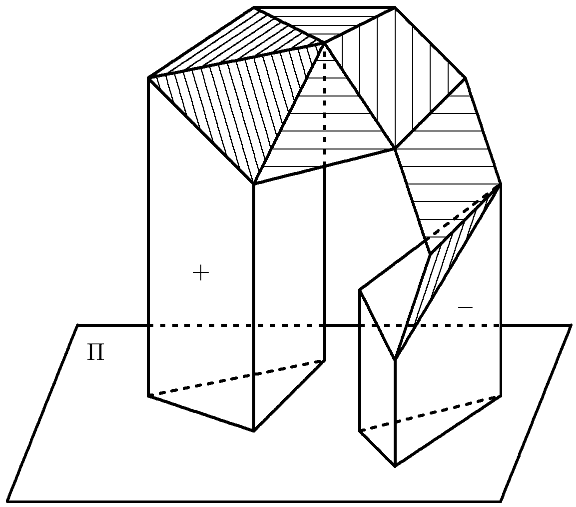


FIGURE 25.20. Signed volume

(a) Prove that the signed volume does not depend of $\Pi$.

(b) Prove that if $P$ is non-self-intersecting, and the exterior of is painted white, then the signed volume is the usual volume.

(c) Prove that the (signed) volume of the Bricard octahedron is zero.

*Hint*. Use the symmetry property from Exercise 25.5 (c).

In particular, this shows that the bellows conjecture holds for the Bricard octahedra.

(d) Prove that the signed volume of the Steffen polyhedron (Section 25.5) is equal to that of the tetrahedron $ABCD$. Deduce the bellows conjecture for this polyhedron.

25.7. (a)* Consider a smooth family of convex polyhedra $P_t$, where $t$ is a parameter, and denote by $l_j(t)$ its edge lengths and by $\varphi_j(t)$ the respective dihedral angles. Prove that

$$\sum_j l_j(t) \frac{d\varphi_j(t)}{dt} = 0.$$

(b) The *total mean curvature* of a polyhedron is defined as $\sum_j l_j \varphi_j$. Prove that the total mean curvature of a flexible polyhedron remains the same in the process of deformation.

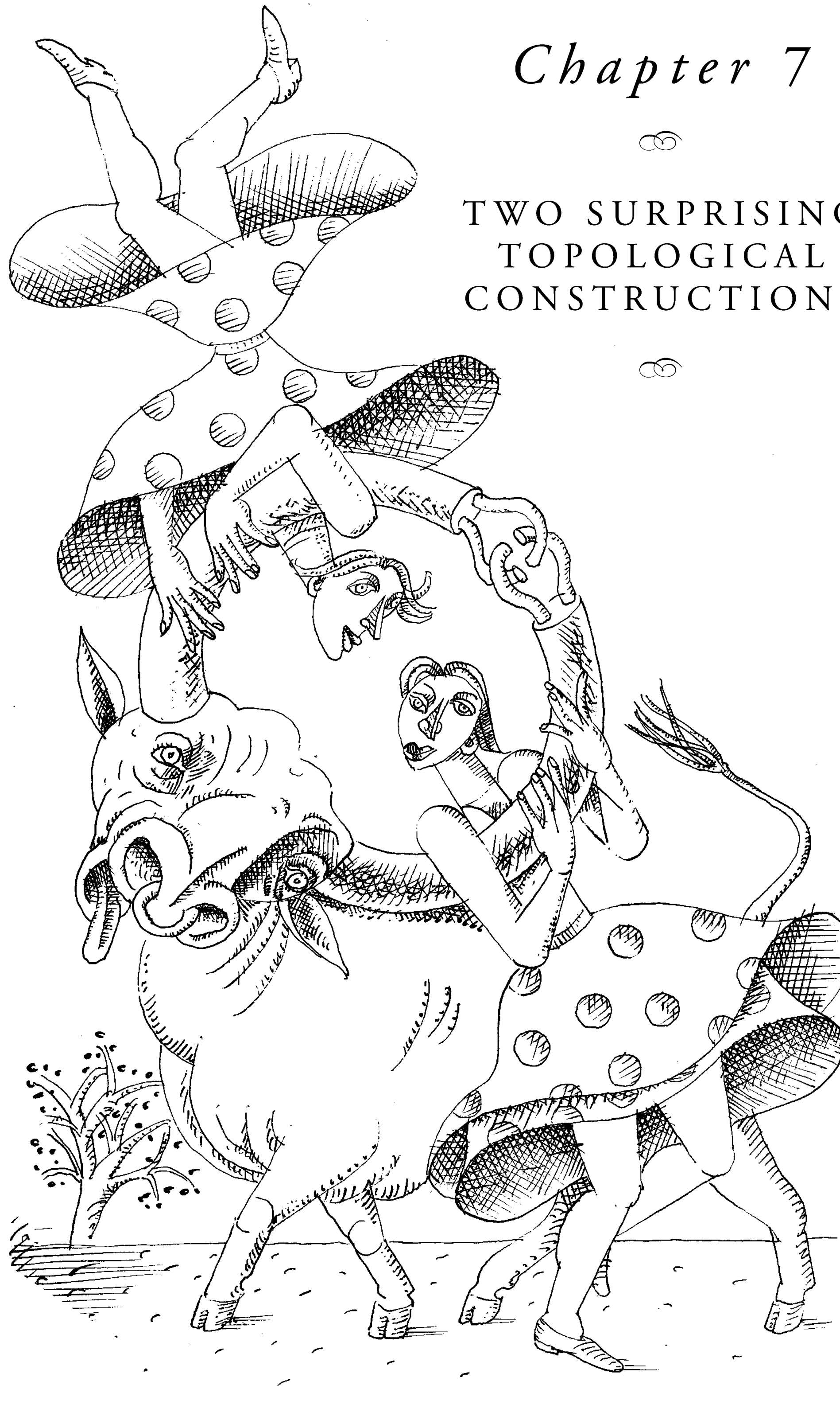

# *Chapter 7*

# TWO SURPRISING TOPOLOGICAL CONSTRUCTIONS

Two Topological Constructions] Two Surprising Topological Constructions

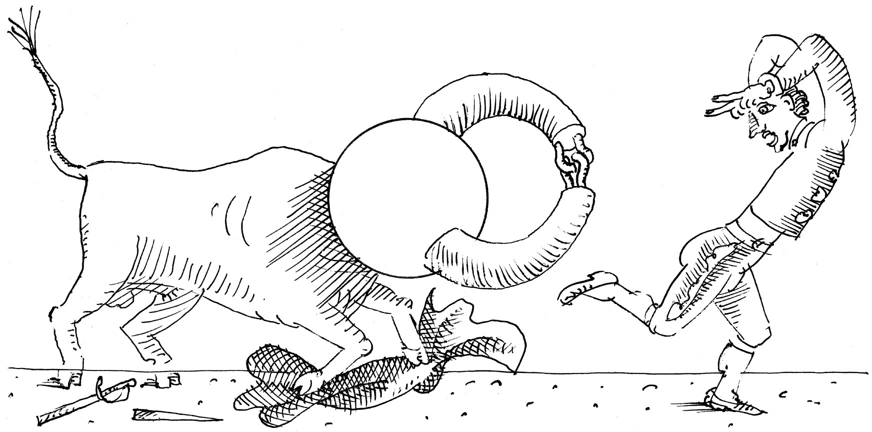

LECTURE 26

# Alexander's Horned Sphere

Two properties of the "horned sphere" make it worthy of describing in this book. First, it delivers a solution of an important and difficult problem. Second, it is really beautiful.

**26.1 Theorems of C. Jordan and A. Schoenflies.** A *curve* in the plane is a trace of a moving point. If the starting point of the movement coincides with the terminal point, the curve is called *closed*, if the positions of the moving point do not coincide at any two distinct moments of time, the curve is called *simple*, or *non-self-intersecting*. Jordan's theorem states that a simple closed curve $C$ divides the plane into two domains, "interior" and "exterior," in the sense that any two points from the same domain may be joined by a polygonal line disjoint from the curve $C$, while any polygonal line joining points from different domains crosses the curve (Figure 26.1).

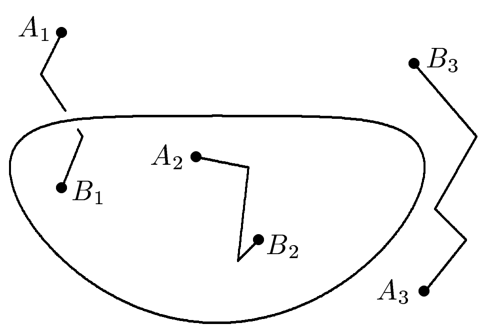


FIGURE 26.1. A closed curve divides the plane into two parts

This theorem is important in analysis, say, in integration theory where we need to consider domains bounded by a given simple closed curve; but it leaves unanswered a question belonging rather to *topology* than to analysis: what the parts into which the plane is divided by a simple closed curve, look like.

In mathematics this frivolous expression "look like" is usually replaced by a more rigorous word "homeomorphic": two domains are homeomorphic, if there exists a bijective map of one onto the other such that both this map and its inverse are continuous. For example, the interiors of a circle and a square are homeomorphic (although one can cay that they look different), while an annulus (the domain between two concentric circles) is not homeomorphic to either of them.

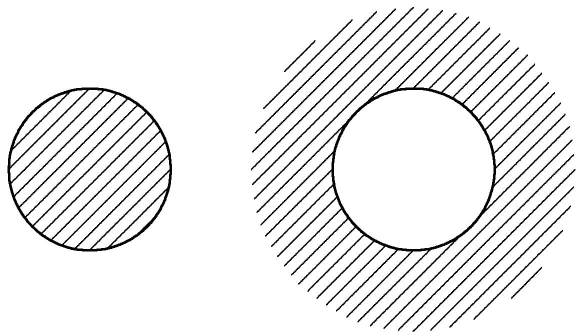

FIGURE 26.2. Interior and exterior

In 1908, A. Schoenflies proved that, whichever simple closed curve in the plane one takes, its interior and exterior will be homeomorphic to those of a usual circle: to an open disc and a plane with a round hole (Figure 26.2). Similarly, one can prove that a domain between two disjoint simple closed curves, of which one is contained in the interior of the other one, is homeomorphic to an annulus.

**26.2 Spatial generalizations.** One could expect that there should be theorems in space geometry similar to those of Jordan and Schoenflies – all you need is to find right statements. Closed curves, certainly, must be replaced by closed surfaces. Here, however, we encounter our first difficulty: while closed curves all look the same (homeomorphic), closed surfaces may be essentially different: there are spheres, tori, spheres with handles, etc (Figure 26.3). We shall resolve this difficulty by brute force: we shall simply ignore all this diversity, restricting our attention to surfaces obtained by a continuous deformation, without self-crossings, of the usual round sphere. For such surfaces we can hope to establish results similar to theorems of Jordan and Schoenflies.

As to Jordan's theorem, its spatial analog turns out to be true: the surface divides space into two parts, interior and exterior, and the statement of the planar Jordan theorem is true for them without any changes. The same is true for spheres with handles, and there are natural generalizations to arbitrary dimensions.

But what about the Schoenflies theorem? Its spatial counterpart should state that the interior and the exterior domains are homeomorphic to the those of the usual sphere, that is, to an open ball and the complement to a closed ball. It was an American topologist John Alexander, then very young, who proved in 1924 that this conjecture, however plausible it looked, was actually wrong. Alexander's work was very convincing: he presented an explicit construction of a deformed sphere in

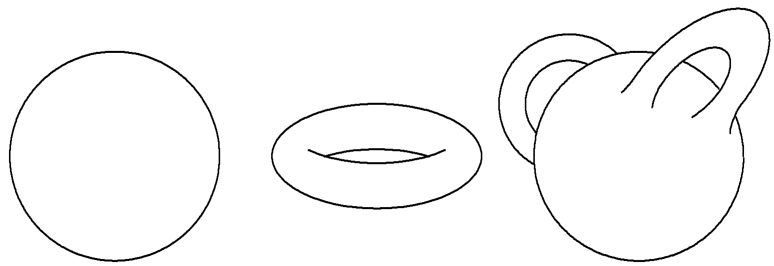

FIGURE 26.3. Different kinds of surfaces

space which divides space into non-standard parts. The details of his construction are described below.

**26.3 It is very beautiful.** And very simple. The main ingredient of the construction is shown in Figure 26.4: we take two disjoint small disks inside a bigger planar disc, pull out of them two "fingers" in such a way that their ends come close to each other but do not touch each other.

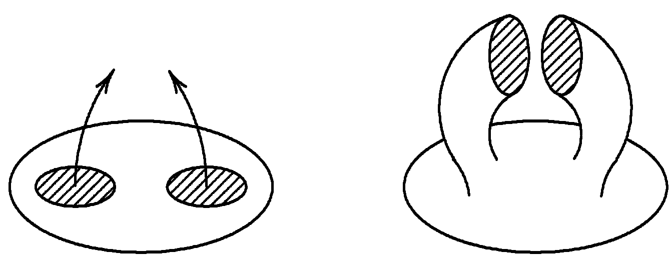

FIGURE 26.4. Pulling out fingers

The ends themselves remain planar discs. We shall usually perform this pulling fingers simultaneously from two parallel discs, and the four fingers will form a "lock" as shown in Figure 26.5.

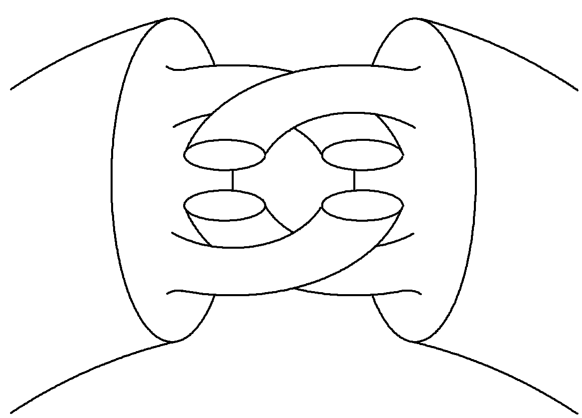

FIGURE 26.5. The lock

Now we can describe the whole construction. Take a round sphere. Then we pull out from two discs on this sphere two fingers, almost touching each other, as in Figure 26.4 – see Figure 26.6.

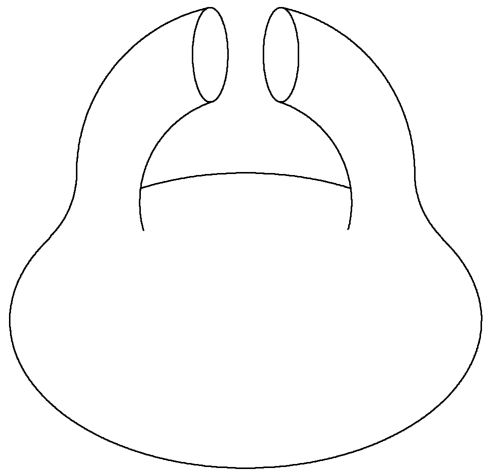

FIGURE 26.6. The first step: two fingers are pulled out of a sphere

The ends of the fingers are two parallel and close to each other planar discs; from these two discs we pull out four fingers, two from each disc, and lock them as in Figure 26.5 – see Figure 26.7.

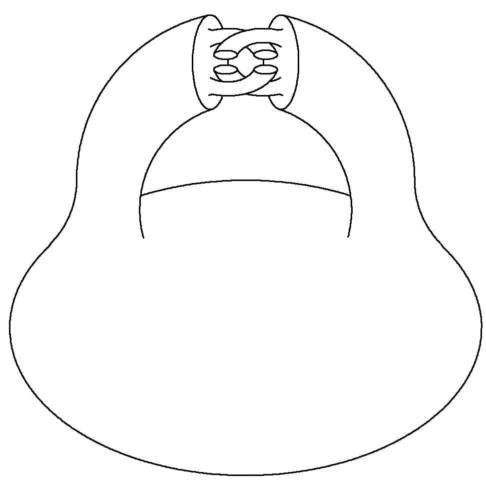

FIGURE 26.7. The second step: a lock is inserted between the fingers

Now we have two pairs of still smaller and still closer discs, and insert small copies of Figure 26.5 between the discs of each pair. And so on, infinitely many times. What we obtain after this "so on," is what is called "Alexander's horned sphere". It is hardly possible to make a satisfactory drawing of this sphere (because the fingers involved become smaller and smaller); still Figure 26.7 provides a reasonable visual approximation.

**26.4 It is an honest sphere.** On the first glance, this does cause some doubts.

Alexander's sphere looks like a weightlifter's weight with a slot sawed out of the handle and a complicated combinations of pieces of wire of different sizes inserted in the slot. Is it really true that the ends of the pieces of the handles do not meet? Seemingly, they could infinitely approach, and in the limit merge together, since on each step of the construction we pull together some parts of the surface.

No, this danger is purely imaginary. We can perform the previous construction in such a way that for every two different points of the sphere, the distance between their final positions is not less, than, say, 1% of their initial distance. (We say "say," since all the sizes – the lengths of the fingers, the width of the slots, etc. – are not specified on Figures 26.4 and 26.5, and we can choose them to our wishes.)

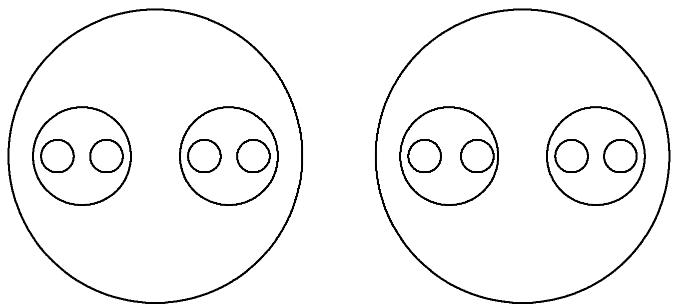

FIGURE 26.8. Discs involved in the construction

Examine our constructions, step by step. The first pulling of fingers involves two discs on a round sphere. The rest of the sphere remains untouched during the whole construction. The second step involves four smaller discs, two inside each of the previous discs (see Figure 26.8). The part of the sphere outside these four discs remains untouched by all steps of the construction after the first step. Similarly, there are 8 discs involved in the third step (see again Figure 26.8), 16 discs involved in the 4-th step (not shown on Figure 26.8), and so on. We shall refer to these discs as the discs of sizes $1, 2, 3, 4, \ldots$; thus, there are $2^n$ discs of size $n$, and each disc of size $n$ contains precisely two discs of size $n+1$. Points of the sphere not contained in any disc of size $n$ remain untouched by all steps of our construction starting with the $n$-th step.

Let us now examine the behavior of the distances between the points. Take two different points, $A$ and $B$, on the sphere. If neither $A$ nor $B$ belongs to either of the two discs of size 1, then these two points remain unchanged and so does the distance between them. If one of them is contained in one of the discs of size 1, and the other one is not, then the distance between them is not changed significantly, we can assume that even if it decreases, then it decreases not more than thrice. If $A$ and $B$ belong to *different* discs of size 1, then after the first step they become significantly closer, but we can assume that the distance between them decreases not more than 10 times. If, in addition to that, the two points belong to discs of size 2, then the next step makes them much closer, say not more than 10 times closer, to each other (see Figure 26.9). However, even if these points belong to discs of size 2 or more, they will not become significantly closer after all subsequent

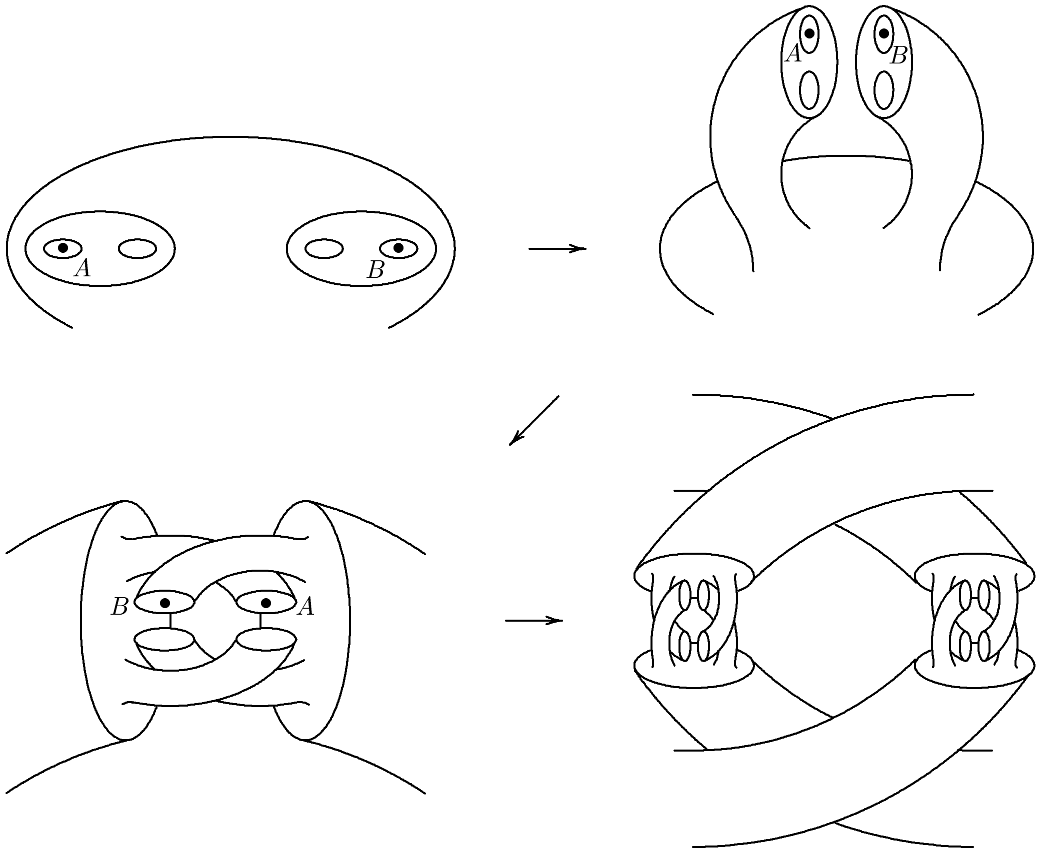


FIGURE 26.9. Points $A$ and $B$ do not approach each other

steps of our construction (see again Figure 26.9). This is because of the following fundamental property of the construction: on the $n$-th step of the construction, we pull together only points from the same disc of size $n-1$.

Now we can formulate the general Principle of Distances. *Let $n$ be the greatest number such that $A$ and $B$ belong to the same disc of size $n$. Then the distance between them remains unchanged under steps 1 through $n$. If neither of them belongs to a disc of size $n+1$, then the distance between them remains unchanged also under all the subsequent steps of the construction. If only one of the points $A, B$ belongs to a disc of size $n+1$, then after all the subsequent steps the distance between them decreases no more then thrice. If they both belong to discs of size $n+1$, then under the $n+1$-st step the distance between them decreases no more than 10 times. If neither of the points belong to discs of size $n+2$, then the distance between them remains unchanged after the $n+1$-st step. If precisely one of these points belongs to a disc of size $n+2$, then the distance between them may decrease thrice on the $n+2$-nd step and is not changed significantly after this. Finally, if both $A$ and $B$ belong to discs of size $n+2$, then the distance between them decreases at most 10 times on the $n+2$-nd step and is not changed significantly* *after this. In all cases, the distance between A and B decreases not more than 100 times.*

Thus, Alexander's horned sphere is indeed a sphere, that is, it is "homeomorphic" to the sphere as we stated above.

**26.5 The exterior of the horned sphere.** The interior of the horned sphere is homeomorphic to the usual ball (without the boundary); it is not hard to prove this, but we shall not need it. What is more important is that the *exterior* of the horned sphere is not the same as (not homeomorphic to) that of the usual sphere. The proof of this is simple but interesting, since it provides a sample of a topological proof. The exterior of the usual sphere (and the interior as well) possesses a property which topologists call *simply connectedness*: every closed curve can be continuously deformed to one point. It looks obvious (see Figure 26.10), although a rigorous proof of it involves some technicalities.

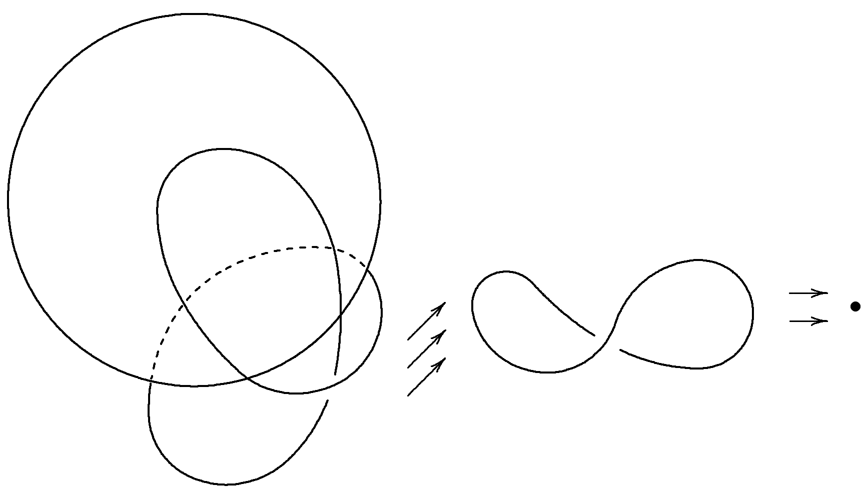

FIGURE 26.10. The exterior of the usual sphere is simply connected

Homeomorphic domains are simply connected simultaneously: if one is simply connected, then the other one should be also simply connected. However, the exterior of the horned sphere *is not* simply connected: a curve enclosing the handle of the weight (Figure 26.11) cannot be continuously pulled out of the handle. (To pull it out, we shall have to carry it between a pair of close parallel discs of any size; hence, in the process of deformation, the curve becomes arbitrarily close to the horned sphere, which means that it will touch the sphere at some moment, which is prohibited: our deformation should be performed in the exterior of the sphere.)

Thus, the exterior of the horned sphere is not simply connected and, hence, not homeomorphic to the exterior of the usual sphere. This shows that the conjectured spatial version of the Schoenflies theorem is false.

**26.6 What else?** Now, it is easy to be smart. We could pull the horns not outside but inside the sphere; then we get a sphere for which the interior, not the exterior, is not homeomorphic to the interior of the standard round sphere. Or we could pull two pairs of horns, one inside and one outside the sphere; then both the

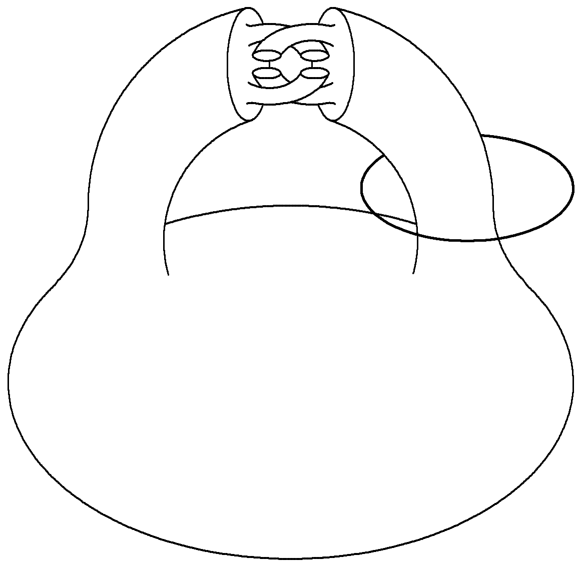

FIGURE 26.11. The exterior of Alexander's sphere is not simply connected

exterior and the interior of the sphere will be different from those for the usual sphere (not simply connected). Or we can pull not two, but, say, twenty two (or two hundred twenty two) pairs of horns, some inside and some outside the sphere and tangle them with each other in any way. This variety of possibilities does not surprise us any longer.

**26.7 Conclusion: further developments.** Years and decades passed after Alexander's discovery. Still topologists hoped that a spatial version of the Schoenflies theorem may exists: one only needs to exclude too complicated shapes. What if we take *polyhedral* spheres, that is spheres made out of finitely many polygonal pieces of a plane? Even in this case the problem turned out to be very hard. Still, in 1960, Morton Brown proved the polyhedral version of the Schoenflies theorem (actually, Brown's result holds for a wider class of surfaces, see Exercise 26.1).

Brown's theorem holds also in higher dimensions. However, in higher dimensions even polyhedral spheres sometimes provide unexpected surprises. For example R. Kirby and L. Siebenmann showed in the 1970's that two polyhedral spheres in four-dimensional space, one of which is contained in the interior of the other, may cobound a domain different from the standard domain cobounded by two concentric round spheres.

All this, however, goes beyond our technical possibilities.

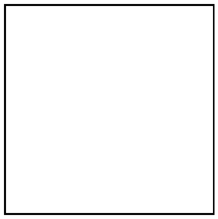

John Smith
January 23, 2010

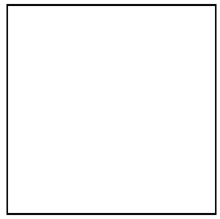

Martyn Green
August 2, 1936

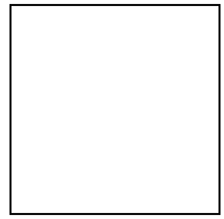

Henry Williams
June 6, 1944

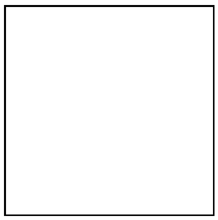

John Smith
January 23, 2010

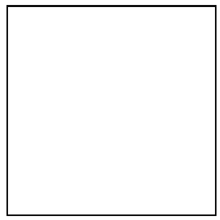

Martyn Green
August 2, 1936

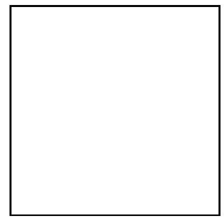

Henry Williams
June 6, 1944

**26.8 Exercises.** A surface $S$ is called *locally flat* at a point $P \in S$, if there exists a homeomorphism of a small ball $B$ centered at $P$ onto another ball, $B'$, which maps the intersection $B \cap S$ onto the intersection of $B'$ with a plane. Brown's theorem (see Section 26.7) states that if a surface in space is homeomorphic to a sphere and is locally flat at all its points, then it cuts space into two standard parts.

26.1. At which points is Alexander's sphere not locally flat (describe this set on the sphere both before and after the deformation)? Is this set countable or uncountable?

Further exercises are not related directly to Alexander's sphere, but they concern constructions which have a similar flavor. We begin with the classical Cantor set. Take the interval $[0, 1]$. Remove the middle third, $\left(\frac{1}{3}, \frac{2}{3}\right)$. Then remove the middle third from each of the two remaining intervals, that is, remove $\left(\frac{1}{9}, \frac{2}{9}\right)$ and $\left(\frac{7}{9}, \frac{8}{9}\right)$. Then remove the middle third of each of the 4 remaining intervals, and so on. The set obtained as a result of this infinite process is called the Cantor set. We denote it by $C$, and denote its complement by $D$.

26.2. (a) Prove that $\frac{1}{4}, \frac{10}{13}, \frac{19}{27} \in C$.

(b) More generally, let $x = [0.d_1 d_2 d_3 \dots]_3$ be a presentation of $x$ in the numerical system with the base 3; express the condition that $x$ belongs to $C$ in terms of the digits $d_i$.

Next, we shall define the Cantor function $\gamma\colon [0, 1] \to [0, 1]$. For $x \in \left(\frac{1}{3}, \frac{2}{3}\right)$, put $\gamma(x) = \frac{1}{2}$. On the two intervals deleted at the second step, $\left(\frac{1}{9}, \frac{2}{9}\right)$ and $\left(\frac{7}{9}, \frac{8}{9}\right)$, we set our function to be equal, respectively, to $\frac{1}{4}$ and $\frac{3}{4}$. On the four intervals deleted at the third step, we set the function to be equal, respectively, to $\frac{1}{8}, \frac{3}{8}, \frac{5}{8}$ and $\frac{7}{8}$. And so on. This process determines our function on $D$.

26.3. (a) Prove that for every $x \in C$ there exists a unique $y \in [0,1]$ such that $\gamma(z) \le y$ for every $z \in [0,x) \cap D$ and $\gamma(z) \ge y$ for every $z \in (x,1] \cap D$.

We put $\gamma(x) = y$. It is easy to see that $\gamma$ is a continuous monotonic function.

(b) Compute $\gamma\left(\frac{1}{4}\right), \gamma\left(\frac{5}{13}\right)$.

(c) More generally, let $x = [0.d_1d_2d_2\ldots]_3$. Find a presentation of $\gamma(x)$ in the numerical system with the base 2.

(d) Prove that if $x$ is rational, then $\gamma(x)$ is rational.

Now we will define the Peano curve in the square $[0,1]^2 = \{(x,y) \mid 0 \le x \le 1, 0 \le y \le 1\}$. Let $F\colon [0,1] \to [0,1]^2$ be a continuous curve with $F(0) = (0,0)$, $F(1) = (0,1)$. The coordinates of $F(t)$ are denoted by $(f(t), g(t))$. We define a curve $\widetilde{F}\colon [0,1] \to [0,1]^2$ by the formula

$$\widetilde{F}(t) = \begin{cases} \left(\frac{1}{2}g(4t), \frac{1}{2}f(4t)\right), & \text{if } 0 \le t \le \frac{1}{4} \\ \left(\frac{1}{2}(f(4t-1)+1), \frac{1}{2}g(4t-1)\right), & \text{if } \frac{1}{4} \le t \le \frac{1}{2} \\ \left(\frac{1}{2}(f(3-4t)+1), 1-\frac{1}{2}g(3-4t)\right), & \text{if } \frac{1}{2} \le t \le \frac{3}{4} \\ \left(\frac{1}{2}g(4-4t), 1-\frac{1}{2}f(4-4t)\right), & \text{if } \frac{3}{4} \le t \le 1. \end{cases}$$

In words: we compress the curve $F$ at the scale $1\colon 2$ and then compose the new curve of 4 copies of the rescaled old curve with the appropriate translations, rotations and reflections. See Figure 26.12. Starting from the arbitrary curve $F$ as above, we apply the transformation described infinitely many times, and denote the limit curve as $P\colon [0,1] \to [0,1]^2$; this is the *Peano curve*.

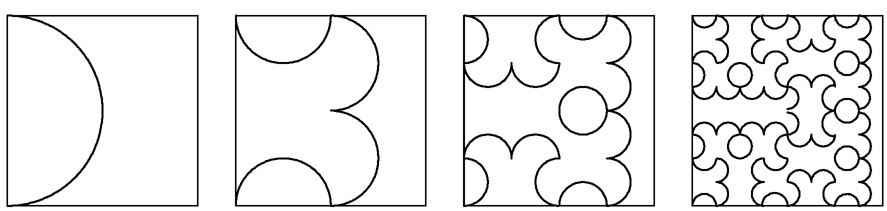

FIGURE 26.12. The Peano curve

26.4. (a) Prove that the limit exists and is continuous.

(b) Prove that $P$ does not depend on the initial curve $F$ (provided that it is continuous and joins $(0,0)$ with $(0,1)$).

(c) Prove that for every $(x,y) \in [0,1]^2$ there exists a $t \in [0,1]$ (maybe, not unique) such that $P(t) = (x,y)$ (in other words, the Peano curve fills the whole square).

(d) Find $P\left(\frac{1}{3}\right), P\left(\frac{1}{5}\right)$.

(e) For $t = [0.d_1 d_2 d_3 \dots]_2$ find (in the numerical system with the base 2) the coordinates of $F(t)$.

(f) Prove that if $t$ is rational, then the coordinates of $F(t)$ are rational.

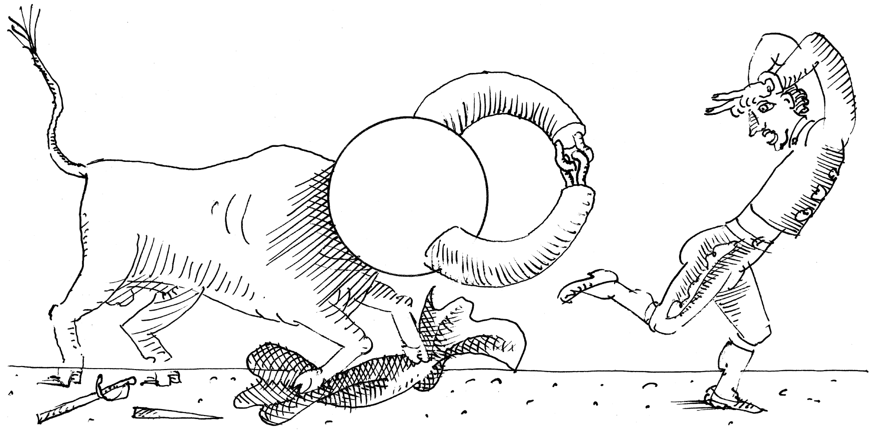

LECTURE 27

# Cone Eversion

**27.1 The problem.** In the plane with the origin deleted, consider two functions: $f_0(x,y) = \sqrt{x^2+y^2}$ and $f_1(x,y) = -\sqrt{x^2+y^2}$. Their gradients are the constant radial vector fields, from and to the origin, see Figure 27.1. One can easily deform the first field to the second so that no vector of any intermediate field vanishes: just rotate each vector 180°.

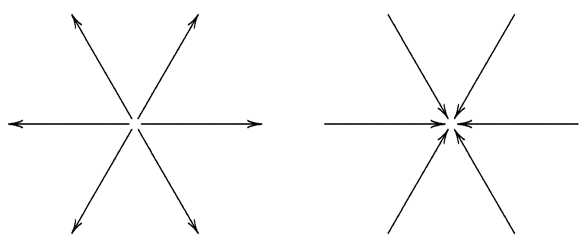

FIGURE 27.1. Two radial fields, from and to the origin

But can one perform such a deformation in the class of nondegenerate *gradient* vector fields? In other words, *can one include the functions $f_0(x,y)$ and $f_1(x,y)$ into a one-parameter family of smooth functions $f_t(x,y)$ without critical points in the punctured plane, continuously depending upon the parameter $t$?* This is the problem that we shall discuss in this lecture.

The problem is less innocent that it might appear at first glance. Simply looking at the flow-lines of a vector field, it is hard to tell whether this is a gradient field of some function. For example, the field in Figure 27.2 is not a gradient: it does non-zero work along circles centered at the origin. (Recall, from physics, that the work done by a force $F$ along a curve $\gamma$ is the line integral $\int_\gamma F \cdot ds$. The work done by a conservative force, that is, the gradient of a potential function, along a closed curve is always zero.)

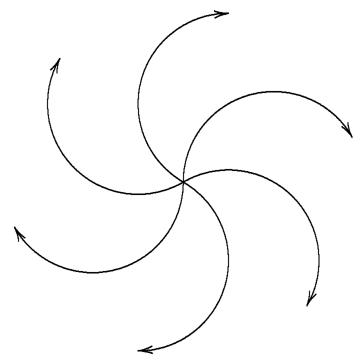

FIGURE 27.2. This is not a gradient field

We can formulate the problem more geometrically. Let $S_t$ be the graph of the function $f_t(x, y)$. The surfaces $S_0$ and $S_1$ are cones, see Figure 27.3. One wants to deform one cone to the other (in the class of surfaces whose projection on the punctured plane is one-one, that is, the graphs of functions defined in the punctured plane) in such a way that no intermediate surface $S_t$ has a horizontal tangent plane at any point. Indeed, the tangent plane is horizontal precisely when the function has a critical point, and its gradient vanishes.

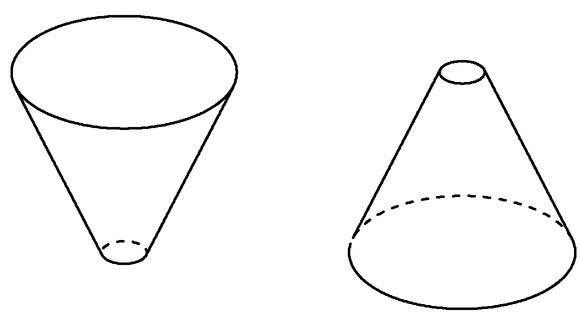

FIGURE 27.3. Can the left cone be everted to the right one without being horizontal anywhere at any time?

In the next section we shall construct such a cone eversion.

**27.2 A solution.** First, it is more convenient to deal with an annulus, say, $1 < \sqrt{x^2 + y^2} < 3$, than the punctured plane. The smooth mapping, given in polar coordinates by the formula

$$(\alpha, r) \mapsto \left(\alpha, \frac{r-1}{3-r}\right),$$

identifies the annulus and the punctured plane, and a solution of our problem in one domain yield a solution in the other.

Here is an explicit deformation. The surface $S_t$ is given by the equation

$$z_t(\alpha, r) = g_t(\alpha) + 0.25(r-2)\ h_t(\alpha)$$

in cylindrical coordinates $(\alpha, r, z)$; here $0 \le \alpha \le 2\pi,\ 1 < r < 3$ and $t$ varies from 0 to 1. The functions $g_t$ and $h_t$ are as follows:

$$g_t = 4t\sin\alpha, \quad h_t = (1-2t) + 4t\cos\alpha, \quad \text{for} \quad t \in [0, 0.25];$$

$$g_t = 2(1-2t)\sin\alpha + (4t-1)\sin 2\alpha, \quad h_t = \cos\alpha + (1-2t), \quad \text{for} \quad t \in [0.25, 0.5];$$

$$g_t = -2(2t-1)\sin\alpha + (3-4t)\sin 2\alpha, \quad h_t = \cos\alpha - (2t-1), \quad \text{for} \quad t \in [0.5, 0.75];$$

$$g_t = -4(1-t)\sin\alpha, \quad h_t = -(2t-1) + 4(1-t)\cos\alpha, \quad \text{for} \quad t \in [0.75, 1].$$

One could stop here: formulas are written, and an industrious reader is welcome to check that the surfaces $S_t$ have no horizontal tangent planes anywhere (that is, the functions $z_t$ have no critical points). But of course we owe the reader explanations.

Let us explain the genesis of these formulas. Since the original and the terminal functions are linear in $r$, it is natural to look for the function $z_t$ in the form:

$$z_t(\alpha, r) = g_t(\alpha) + \varepsilon(r-2)\ h_t(\alpha),$$

where $g$ and $h$ are periodic functions and $\varepsilon$ is a sufficiently small parameter (its actual value in our formulas is 0.25). The original cone corresponds to $g_0(\alpha) = 0$ and $h_0(\alpha) = const > 0$; the terminal cone – to $g_1(\alpha) = 0$ and $h_1(\alpha) = const < 0$.

It might be instructive to think of the surface $S_t$ as a closed rope ladder in space whose axis is the closed curve

$$z = g_t(\alpha), \quad 0 \le \alpha \le 2\pi, \quad r = 2,$$

and whose rungs are the radial segments

$$z = g_t(\alpha) + \varepsilon(r-2)\ h_t(\alpha), \quad \alpha = const, \quad 1 < r < 3$$

with the slope $\varepsilon h_t(\alpha)$. So, at the beginning, the axis is a horizontal circle and the slopes of all the rungs are positive. At the end, the axis is again a horizontal circle, but the slopes of the rungs are all negative.

What one wants to avoid in the deformation are the instances when the axis and the rungs are simultaneously horizontal. Thus the functions

$$\frac{dg_t(\alpha)}{d\alpha} + \varepsilon(r-2)\frac{dh_t(\alpha)}{d\alpha} \quad \text{and} \quad h_t(\alpha)$$

should have no common zeroes. If, for some $t$, the zeroes of

$$\frac{dg_t(\alpha)}{d\alpha} \quad \text{and} \quad h_t(\alpha)$$

are disjoint, then so are the zeroes of

$$\frac{dg_t(\alpha)}{d\alpha} + \varepsilon(r-2)\frac{dh_t(\alpha)}{d\alpha} \quad \text{and} \quad h_t(\alpha)$$

for a sufficiently small $\varepsilon$.

The strategy is clear now. First, change the shape of the axis of the rope ladder (i.e., the graph of $g(\alpha)$) into a non-horizontal curve, after which one can safely change the slope of the rungs (the sign of $h(\alpha)$) from positive to negative on its non-horizontal segments.

The graphs of $g_t(\alpha)$ are sketched in Figure 27.4 on the left. The graphs are drawn in solid or broken lines; the former means that $h_t(\alpha)$ is positive, and the latter, that it is negative at the corresponding points $\alpha$. The half-way picture, $t = 1/2$, is symmetric with respect to the time eversion: $t \mapsto 1-t$; from that point on, one just repeats the process backward. Figure 27.4, right, shows the

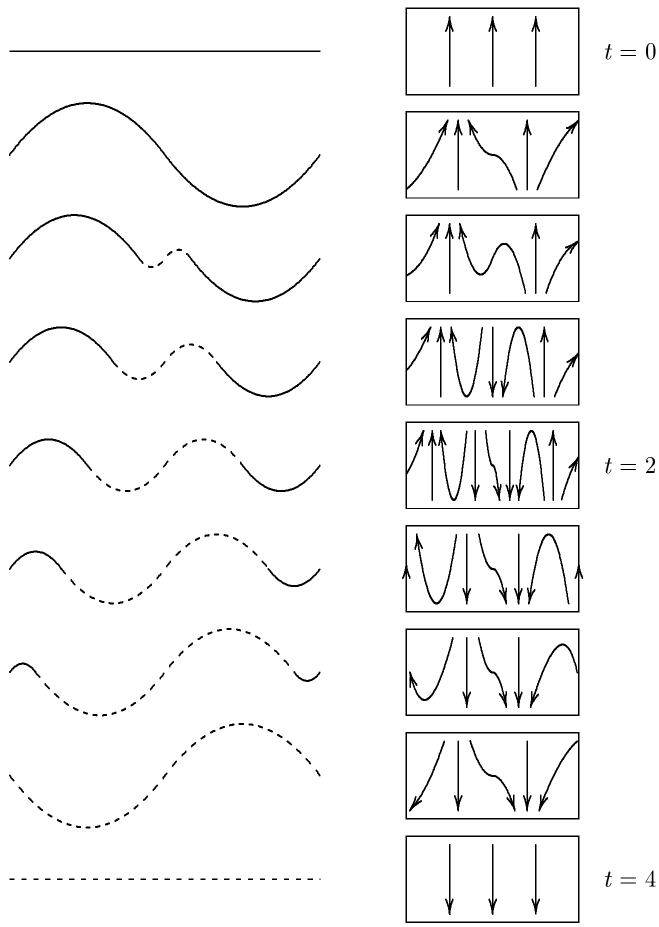


FIGURE 27.4. The deformation: geometry behind the formulas

corresponding deformation of the gradient vector fields, thus answering the original question.

Figure 27.5 shows level curves of the functions $z_t$ for $t = 1/8, 1/4, 3/8$ and $1/2$, and Figure 27.6 the whole deformation, from beginning to end.

**27.3 Comments.** The existence of a deformation, explicitly constructed in Section 27.2, follows from the $h$-principle theory, an actively developing chapter of differential topology. In fact, the existence of such a deformation is the first application of Gromov's $h$-principle, discussed in the book [**27**] (section 4.1); constructing an explicit deformation is an exercise in this book. Our construction is based on the article [**80**]. As far as we know, the problem, discussed in this lecture, was posed by M. Krasnosel'skii in his lecture titled "Mathematical divertissement" in the 1970s.

One of the early precursors of the $h$-principle theory was the Whitney theorem, discussed in Lecture 12; a sphere eversion, mentioned in the same lecture, is another manifestation of this theory (more precisely, the Smale-Hirsch immersion theory).

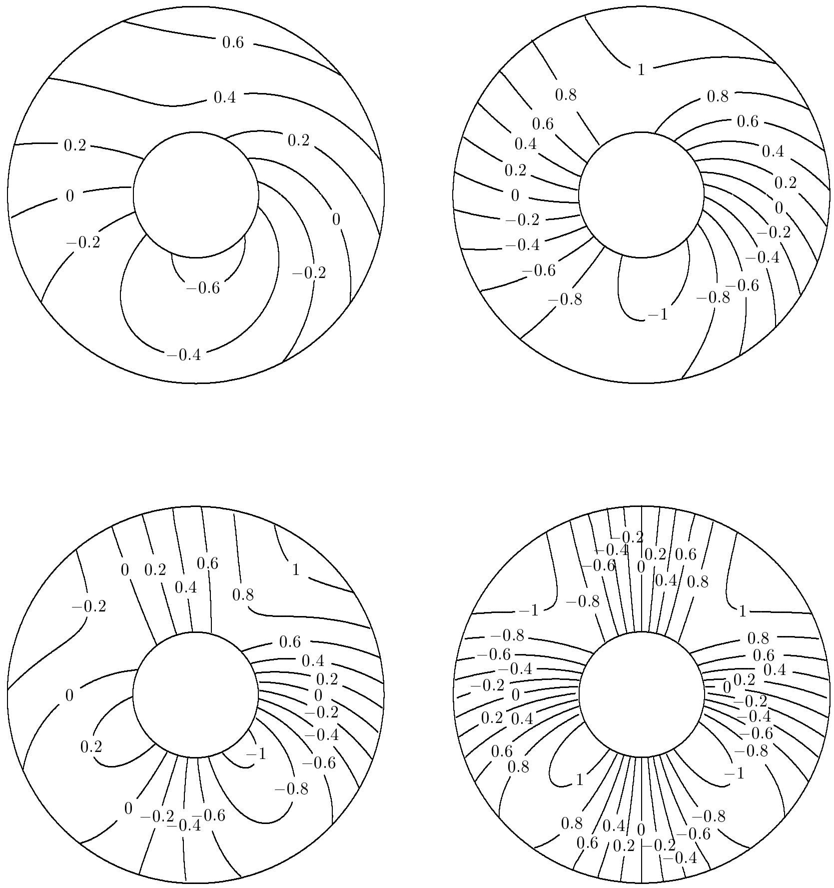


FIGURE 27.5. Level curves of the functions $z_t$ for $t = 1/8, 1/4, 3/8$ and $1/2$

Let us mention another famous result, the Nash-Kuiper theorem concerning differentiable, but not twice differentiable, maps. We shall not formulate the general theorem but instead mention one of its striking consequences: one can differentially and isometrically embed a unit sphere into an arbitrarily small ball (this would be impossible if the isometric embedding was twice differentiable)!

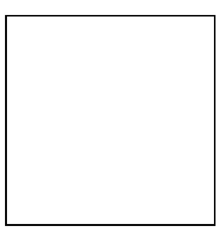

John Smith
January 23, 2010

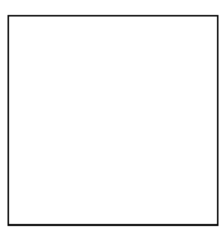

Martyn Green
August 2, 1936

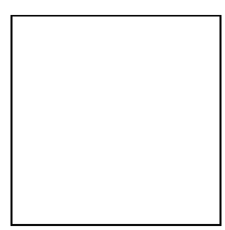

Henry Williams
June 6, 1944

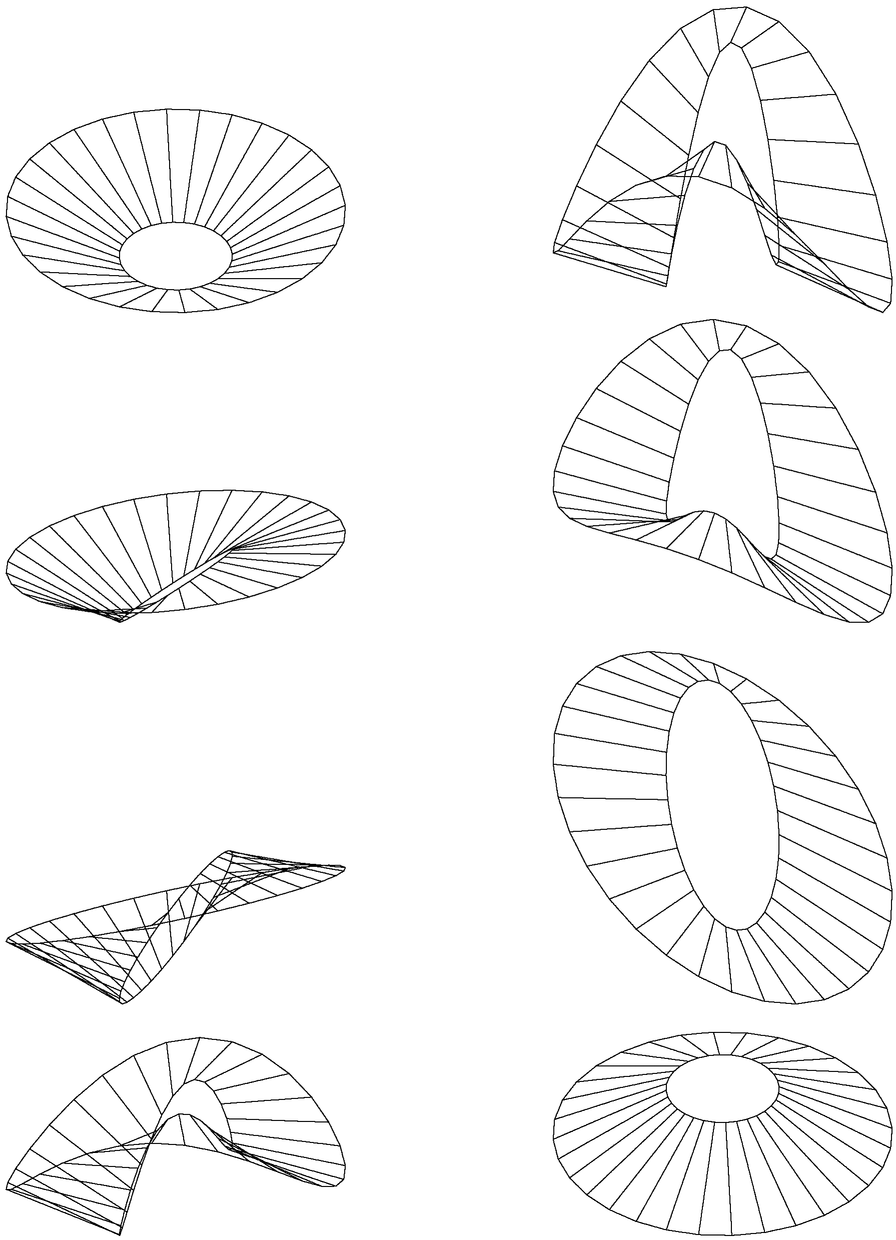

FIGURE 27.6. Cone eversion, from beginning to end

John Smith
January 23, 2010

Martyn Green
August 2, 1936

Henry Williams
June 6, 1944

John Smith
January 23, 2010

Martyn Green
August 2, 1936

Henry Williams
June 6, 1944

## 27.4 Exercises.

27.1. (a) Construct a function of two variables that has two local maxima and no local minima or saddle points. Draw level curves and gradient lines of this function.

(b)* Can one take a polynomial for such a function?

27.2. (a) Construct a function of two variables that has only one local minimum and no other critical points and such that this local minimum is not an absolute minimum. Draw level curves and gradient lines of this function.

(b)* Can one take a polynomial for such a function?

27.3. ** Let $f(x,y) = \cos x \cos y$. The critical point of the function $f$ form the lattice $(\pi k/2, \pi l/2)$ with $k+l$ even. Consider two nondegenerate vector fields in the complement to the lattice: the gradient of $f(x,y)$ and the gradient of $-f(x,y)$. Construct a continuous deformation of one field to the other in the class of nondegenerate gradient vector fields.

*Comment.* A similar fact holds for any smooth function with isolated local maxima, minima and saddle points.

27.4. Construct a polynomial of two variables whose range is the interval $(0,\infty)$?

*Comment*: essentially, this problem was given on the Putnam Competition in 1969. Only 1% of the contestants got a score of 8,9 or 10 for this problem. When the examination was printed it was believed that such a polynomial did not exist.

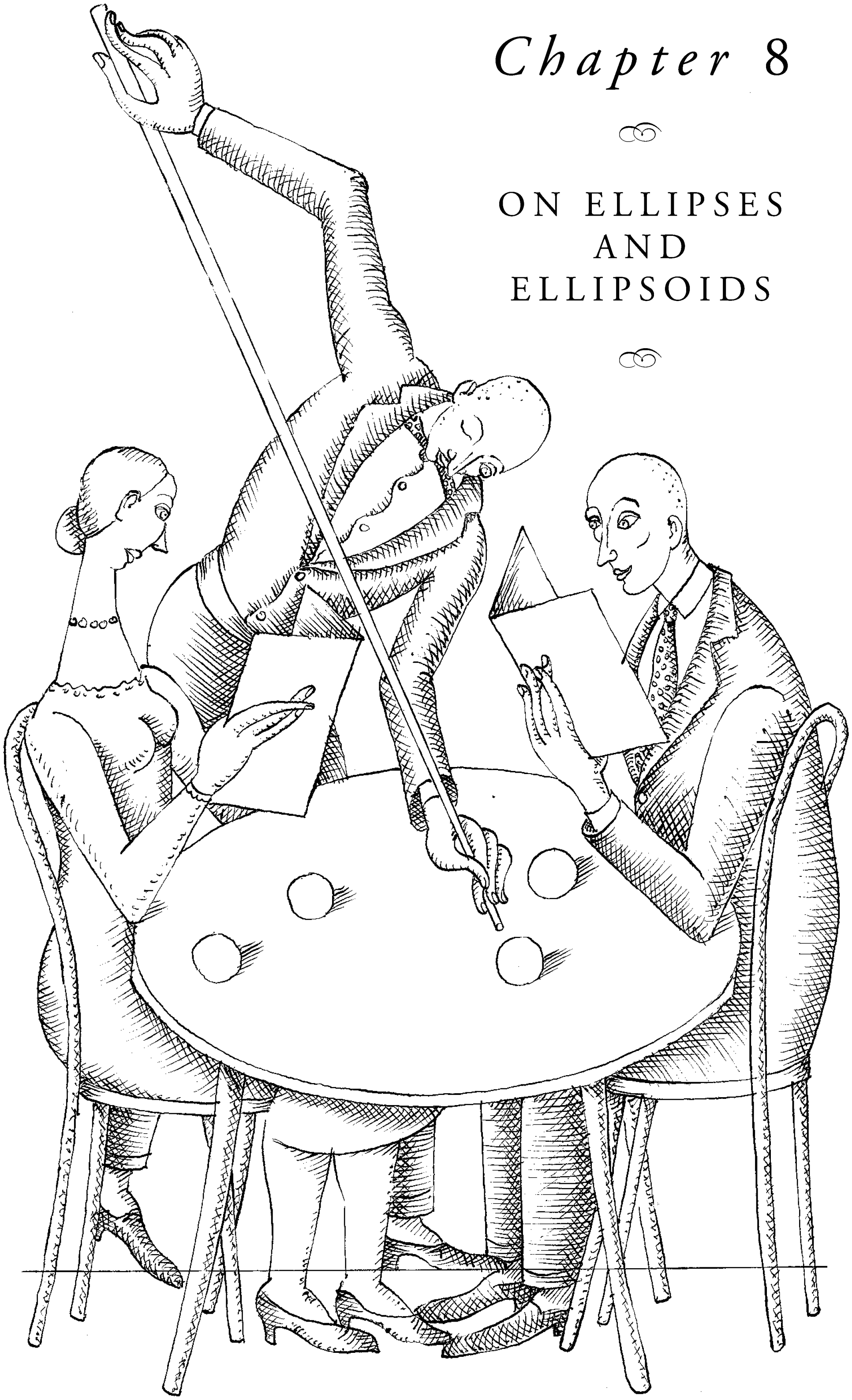

# *Chapter* 8

## ON ELLIPSES AND ELLIPSOIDS

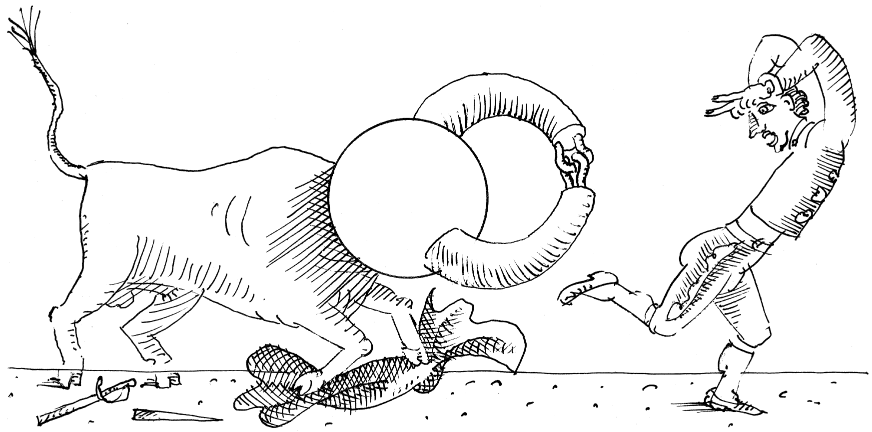

LECTURE 28

# Billiards in Ellipses and Geodesics on Ellipsoids

**28.1 Plane billiards.** The billiard system describes the motion of a free point inside a plane domain: the point moves with a constant speed along a straight line until it hits the boundary, where it reflects according to the familiar law of geometrical optics "the angle of incidence equals the angle of reflection". Equally well, one may imagine rays of light reflecting in the boundary which is a perfect mirror. We shall consider billiard tables bounded by smooth convex closed curves $\gamma$.

The billiard reflection is a mapping that sends the incoming billiard trajectory to the outgoing one. We shall denote this "billiard ball map" by $T$. The map $T$ acts on oriented lines that intersect the billiard table; if a line is tangent to the boundary, then $T$ leaves it intact.

One can characterize an oriented line by its two points of intersection with the boundary curve $\gamma$. The map $T$ sends $xy$ to $yz$, see Figure 28.1.

The reflection law can be interpreted as a solution to an extremal problem.[1] Fix points $x$ and $z$ and let $y$ vary.

LEMMA 28.1. *The angles made by lines $xy$ and $yz$ with $\gamma$ are equal if and only if $y$ is an extremal point of the function $|xy| + |yz|$:*

$$\frac{\partial(|xy| + |yz|)}{\partial y} = 0. \tag{28.1}$$

Proof. Assume first that $y$ is a free point, not confined to $\gamma$. The gradient of the function $|xy|$ is the unit vector from $x$ to $y$, and the gradient of $|yz|$ is the unit vector from $z$ to $y$. Indeed, if, say, $xy$ is an elastic string, fixed at one endpoint $x$, then the other endpoint $y$ will move directly toward $x$ with unit speed.

Point $y$, confined to $\gamma$, is a critical point of the function $|xy| + |yz|$ if and only if the sum of the two gradients is orthogonal to $\gamma$ (this is the Lagrange multipliers

[1]As many other laws of physics. The one describing propagation of light is called the Fermat principle: light "chooses" the trajectory that takes least time to get from one point to another.

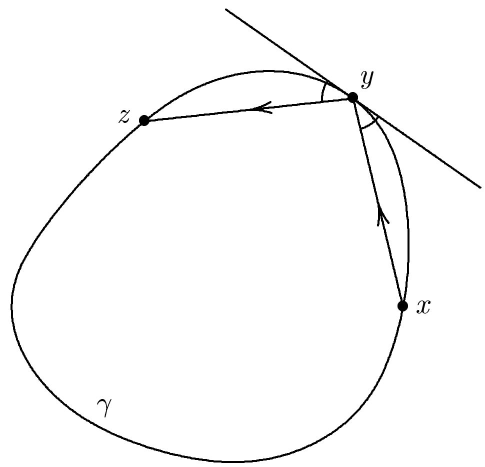


FIGURE 28.1. Billiard ball map

principle, familiar from calculus). This is equivalent to the fact that $xy$ and $yz$ make equal angles with $\gamma$. $\square$

In the language of mechanics, the point (or, better, a bead) $y$ on the "wire" $\gamma$ is acted upon by two unit forces exerted by the elastic string: from $y$ to $x$ and from $y$ to $z$. The point $y$ is in equilibrium if the total force is perpendicular to $\gamma$.

It is mentioned in Lecture 19 that the billiard ball map admits an invariant area element; this is the area on the space of oriented lines in the plane, which is the main character of Lecture 19. Now we shall deduce this fact from the variational principle of Lemma 28.1.

Consider an arc length parameterization of $\gamma$ and let $x$ and $y$ be two values of the parameter, that is, two points on the curve. Then $(x, y)$ are coordinates on the space of oriented lines intersecting the billiard table.

THEOREM 28.1. *The area element*

$$\omega(x, y) = \frac{\partial^2 |xy|}{\partial x \partial y}\, dxdy \tag{28.2}$$

*is invariant under the billiard ball map $T$.*

A necessary clarification before the proof: $dxdy$ is the *oriented* area of an infinitesimal box whose sides are parallel to the coordinate axes and have lengths $dx$ and $dy$. In this sense, $dydy = 0$, and $dxdy = -dydx$.[2]

Proof. Differentiate equation (28.1):

$$\frac{\partial^2 |xy|}{\partial x \partial y}\, dx + \frac{\partial^2 |xy|}{\partial y^2}\, dy + \frac{\partial^2 |yz|}{\partial y^2}\, dy + \frac{\partial^2 |yz|}{\partial y \partial z}\, dz = 0,$$

and multiply by $dy$. Taking into account that $dydy = 0$ and $dzdy = -dydz$, we obtain:

$$\frac{\partial^2 |xy|}{\partial x \partial y}\, dxdy = \frac{\partial^2 |yz|}{\partial y \partial z}\, dydz.$$

[2]The technically correct notation is $dx \wedge dy$; the wedge product is skew-symmetric.

The last equation means that $\omega(x,y) = \omega(y,z)$, as claimed. □

**28.2 Optical properties of conics.** Geometrically, an ellipse is defined as the locus of points whose sum of distances to two given points, $F_1$ and $F_2$, is fixed; these two points are called the foci. An ellipse can be constructed using a string whose ends are fixed at the foci, see Figure 28.2. This is sometimes called the "gardener" or "string construction" of an ellipse. A hyperbola is defined similarly, with the sum of distances replaced by the absolute value of their difference; and a parabola is the locus of points at equal distances from a point (focus) and a line.

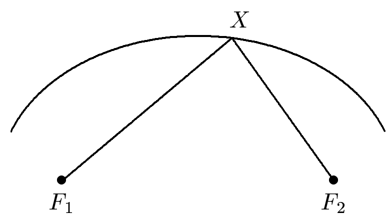


FIGURE 28.2. String construction of an ellipse: $|F_1X| + |F_2X| = \text{const}$

The following optical property of conics was known to the ancient Greeks.

LEMMA 28.2. *A ray from one focus of an ellipse reflects to a ray through the other focus.*

Proof. We want to prove that the angles made by $F_1X$ and $F_2X$ with the ellipse in Figure 28.2 are equal.

Assume that $X$ is free to vary in the plane. The ellipse is a level curve of the function $f(X) = |F_1X| + |F_2X|$, and the gradient of this function at point $X$ is orthogonal to the curve. Similarly to the proof of Lemma 28.1, the gradient of $f(X)$ is the sum of the two unit vectors, having directions $F_1X$ and $F_2X$. This sum is orthogonal to the curve if and only if the vectors make equal angles with it, as claimed. □

Likewise, a ray from the focus of a parabola reflects to a ray parallel to its axis, see Figure 28.3 – see Exercise 28.3. This optical property of parabolas has numerous applications in designs of projectors, flashlights, and other optical devices, and we already used it in Lecture 15.

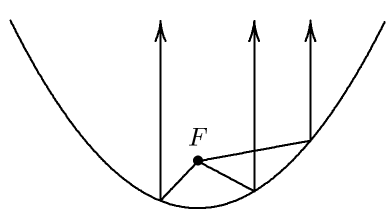


FIGURE 28.3. Optical property of parabola

Consider an ellipse and a hyperbola with the same foci passing through point $X$.

LEMMA 28.3. *The ellipse and the hyperbola are orthogonal to each other.*

Proof. The hyperbola is a level curve of the function $g(X) = |F_1X| - |F_2X|$, whose gradient at point $X$ is the difference of the two unit vectors, having directions $F_1X$ and $F_2X$. The difference of two unit vectors is orthogonal to their sum, hence the curves are perpendicular to each other. □

The construction of an ellipse with given foci has a parameter, the length of the string. The family of conics with fixed foci is called confocal. The equation of a confocal family, including ellipses and hyperbolas, is

$$\frac{x^2}{a^2+\lambda} + \frac{y^2}{b^2+\lambda} = 1 \tag{28.3}$$

where $\lambda$ is a parameter.

The next result generalizes Lemma 28.2 to billiard trajectories not through the foci.

Theorem 28.2. *A billiard trajectory inside an ellipse forever remains tangent to a fixed confocal conic. More precisely, if a segment of a billiard trajectory does not intersect the segment $F_1F_2$, then all the segments of this trajectory do not intersect $F_1F_2$ and are all tangent to the same ellipse with foci $F_1$ and $F_2$; and if a segment of a trajectory intersects $F_1F_2$, then all the segments of this trajectory intersect $F_1F_2$ and are all tangent to the same hyperbola with foci $F_1$ and $F_2$.*

Proof. Let $A_0A_1$ and $A_1A_2$ be consecutive segments of a billiard trajectory, see Figure 28.4. Assume that $A_0A_1$ does not intersect the segment $F_1F_2$ (the other case is dealt with similarly). It follows from the optical property of an ellipse, that the angles made by segments $F_1A_1$ and $F_2A_1$ with the ellipse are equal. Likewise, the segments $A_0A_1$ and $A_2A_1$ make equal angles with the ellipse. Hence the angles $A_0A_1F_1$ and $A_2A_1F_2$ are equal.

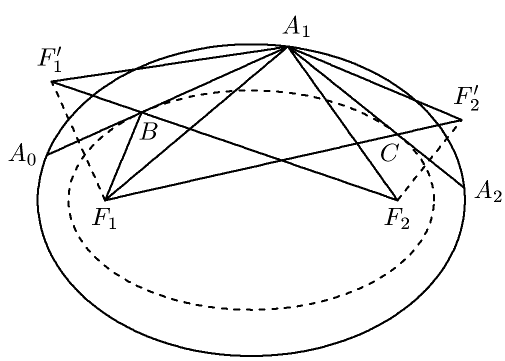


Figure 28.4. Proof of Theorem 28.2

Reflect $F_1$ in $A_0A_1$ to point $F_1'$, and $F_2$ in $A_1A_2$ to $F_2'$. Let $B$ be the intersection point of the lines $F_1'F_2$ and $A_0A_1$, and $C$ of the lines $F_2'F_1$ and $A_1A_2$.

Consider the ellipse $\Gamma_1$ with foci $F_1$ and $F_2$ that is tangent to the line $A_0A_1$. Since the angles $F_2BA_1$ and $F_1'BA_0$ are equal, and so are the angles $F_1'BA_0$ and $F_1BA_0$, the angles $F_2BA_1$ and $F_1BA_0$ are equal. By the optical property of ellipses, the ellipse $\Gamma_1$ touches $A_0A_1$ at the point $B$. Likewise the ellipse $\Gamma_2$ with foci $F_1$ and $F_2$ touches $A_1A_2$ at the point $C$. One wants to show that these two ellipses coincide or, equivalently, that $F_1B + BF_2 = F_1C + CF_2$, which boils down to $F_1'F_2 = F_1F_2'$.

We claim that the triangles $F_1'A_1F_2$ and $F_1A_1F_2'$ are congruent. Indeed, $F_1'A_1 = F_1A_1$ and $F_2A_1 = F_2'A_1$ by symmetry. In addition, the angles $F_1'A_1F_2$ and $F_1A_1F_2'$ are equal: the angles $A_0A_1F_1$ and $A_2A_1F_2$ are equal, hence so are the angles $F_1'A_1F_1$ and $F_2'A_1F_2$, and adding the common angle $F_1A_1F_2$ implies that $\angle F_1'A_1F_2 = \angle F_1A_1F_2'$.

Equality of the triangles $F_1'A_1F_2$ and $F_1A_1F_2'$ implies that $F_1'F_2 = F_1F_2'$, and we are done. □

As an application, here is a construction of a room with reflecting walls that cannot be illuminated from any of its points; this construction is due to L. and R. Penrose [**60**] – see Figure 28.5.[3] The upper and the lower curves are half-ellipses with foci $F_1, F_2$ and $G_1, G_2$. Since a ray passing between the foci reflects back again between the foci, no ray can enter the four "ear lobes" from the area between the lines $F_1F_2$ and $G_1G_2$, and vice versa. Thus if the source of light is above the line $G_1G_2$, the lower lobes are not illuminated; and if the source is below $F_1F_2$, the same applies to the upper lobes.

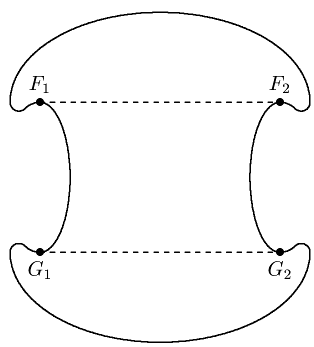


FIGURE 28.5. This room cannot be illuminated from a single point

**28.3 Caustics, string construction and the Graves theorem.** A *caustic*[4] is a curve inside a billiard table such that if a segment of a billiard trajectory is tangent to this curve, then so is each reflected segment. We assume that caustics are smooth and convex.

There is a *string construction*, similar to the string construction of ellipses, Figure 28.2, that recovers a billiard table from its caustic: wrap a closed non-stretchable string around the caustic, pull it tight at a point and move this point around to obtain the boundary of a billiard table, see Figure 28.6.

THEOREM 28.3. *The billiard inside $\gamma$ has $\Gamma$ as its caustic.*

[3]Roger Penrose is leading contemporary mathematical physicist. Lionel Penrose, his father, was a prominent psychiatrist and geneticists.

[4]Caustic also has a different meaning: the envelop of the normal lines to a curve; we used it in Lecture 10.

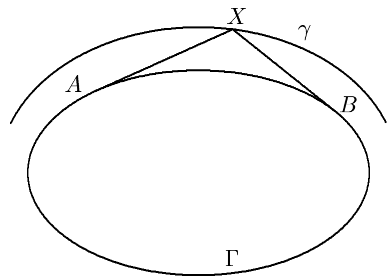


FIGURE 28.6. String construction: recovering a billiard table from a caustic

Proof. Choose a reference point $Y$ on $\Gamma$. For a point $X$, let $f(X)$ and $g(X)$ be the distances from $X$ to $Y$ by going around $\Gamma$ on the right and on the left, respectively. Then $\gamma$ is a level curve of the function $f(X) + g(X)$. We want to prove that the angles made by the segments $AX$ and $BX$ with $\gamma$ are equal.

We claim that the gradient of $f$ at $X$ is the unit vector in the direction $AX$. Indeed, the free end $X$ of the contracting string $YAX$ will move directly toward point $A$ with unit speed (compare with the proofs of Lemmas 28.1 and 28.2). It follows that the gradient of $f + g$ bisects the angle $AXB$. Since the gradient of a function is orthogonal to its level curve, $AX$ and $BX$ make equal angles with $\gamma$. □

Note that the string construction provides a one-parameter family of billiard tables: the parameter is the length of the string.

As a consequence of Theorem 28.2, one obtains the following Graves theorem: *wrapping a closed non-stretchable string around an ellipse produces a confocal ellipse*, see [**63**] for other proofs.

**28.4 Geometrical consequences.** The space of oriented lines, that intersect an ellipse, is, topologically, a cylinder. This cylinder is foliated by invariant curves of the billiard ball map, see Figure 28.7. Each curve represents the family of rays tangent to a fixed confocal conic. The $\infty$-shaped curve corresponds to the family of rays through the two foci. The two singular points of this curve represent the major axis with the two opposite orientations, a 2-periodic, back-and-forth billiard trajectory. Another 2-periodic trajectory is the minor axis represented by two centers of the regions inside the $\infty$-shaped curve.

Consider the invariant curves that go around the cylinder; they represent the rays tangent to confocal ellipses (other invariant curves, the ones inside the $\infty$-shaped curve, represent the rays, tangent to confocal hyperbolas).

THEOREM 28.4. *One can choose a cyclic coordinate on each invariant curve, $x$ mod 1, in such a way that the billiard ball map is given by the formula $T(x) = x + c$ (the value of the constant $c$ depends on the invariant curve).*

Proof. The construction of the desired coordinate $x$ depends on the two structures available to us: the family of invariant curves and the area element $\omega$ (28.2) on the cylinder.

Choose a function $f$ on the cylinder whose level curves are the invariant curves of the billiard ball map. Let $\gamma$ be a level curve $f = a$. Consider the nearby level curve $\gamma_\varepsilon$ given by $f = a+\varepsilon$. For an interval $I \subset \gamma$, consider the area $\omega(I, \varepsilon)$ between

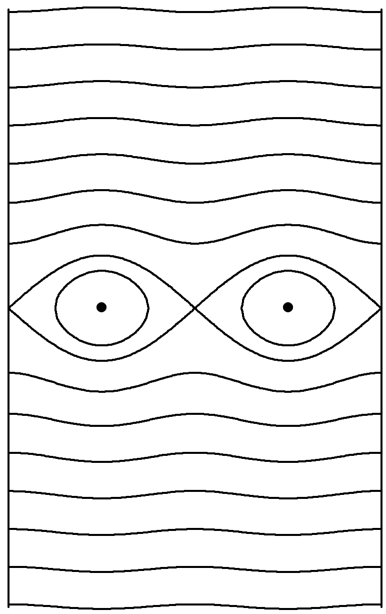

FIGURE 28.7. Phase portrait of the billiard ball map in an ellipse

$\gamma$ and $\gamma_\varepsilon$ over $I$; clearly, this area tends to zero as $\varepsilon \to 0$. Define the "length" of $I$ as

$$\lim_{\varepsilon\to 0} \frac{\omega(I,\varepsilon)}{\varepsilon}.$$

Choosing a different function $f$, one replaces the infinitesimal $\varepsilon$ by another one, say, $\delta$; then the length of every segment is multiplied by the same factor $\delta/\varepsilon$. Choose a coordinate $x$ so that the length element is $dx$ and normalize $x$ so that the total length is 1. This determines $x$ up to a shift $x \mapsto x + const.$

The billiard ball map $T$ preserves the area element $\omega$ and the invariant curves. Therefore it preserves the length element on the invariant curves, and hence it is given by the formula $x \mapsto x + c$ on each invariant curve (of course, the value of the constant $c$ depends on the invariant curve). □

The first consequence is a closure theorem for billiard trajectories in an ellipse, cf. Lecture 29.

COROLLARY 28.5. *Assume that a billiard trajectory in an ellipse $\gamma$, tangent to a confocal ellipse $\Gamma$, is $n$-periodic. Then every billiard trajectory in $\gamma$, tangent to $\Gamma$, is $n$-periodic.*

Proof. Consider the invariant curve that consists of the rays tangent to $\Gamma$. In the coordinate $x$ from Theorem 28.4, the billiard ball map is $x \mapsto x + c$. A point is $n$-periodic if and only if $nc$ is an integer. This condition does not depend on $x$, and the result follows. □

Let $\gamma_1, \gamma_2$ and $\Gamma$ be confocal ellipses, see Figure 28.8. One has two billiard ball maps, $T_1$ and $T_2$, corresponding to reflections in $\gamma_1$ and $\gamma_2$. Both maps act on the same space of oriented lines that intersect both ellipses, and they share a caustic,

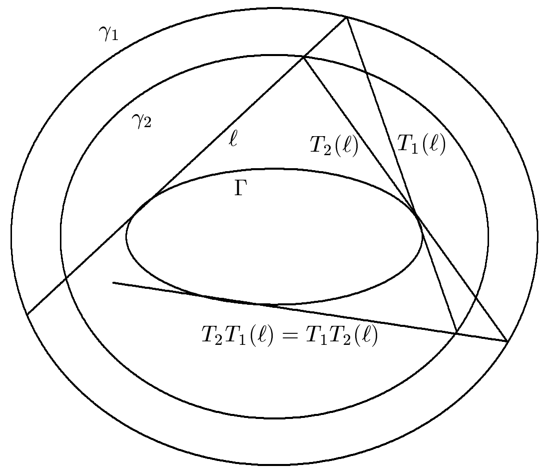


FIGURE 28.8. Commuting billiard ball maps in confocal ellipses

$\Gamma$. The choice of the parameter $x$ on the invariant curve, corresponding to this caustic, depended only on the area element in the space of oriented lines and the family of confocal ellipses, which are the same for both maps. We arrive at the next corollary.

COROLLARY 28.6. *The maps $T_1$ and $T_2$ commute: $T_1 \circ T_2 = T_2 \circ T_1$ (see Figure 28.9 for a resulting configuration theorem).*

Proof. Parallel translations $x \mapsto x + c_1$ and $x \mapsto x + c_2$ commute. □

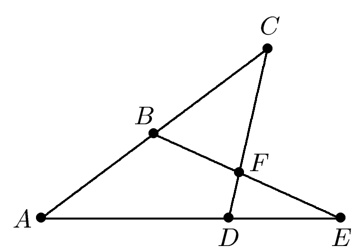


FIGURE 28.9. The most elementary theorem of Euclidean geometry

In the degenerate case, when $\Gamma$ is the segment connecting the foci, one obtains the following "most elementary theorem of Euclidean geometry":[5]

$$AB + BF = AD + DF \quad \text{if and only if} \quad AC + CF = AE + EF,$$

see Figure 28.9. Indeed, points $B$ and $D$ lies on an ellipse with foci $A$ and $F$ if and only if so do points $C$ and $E$.

[5]Discovered by M. Urquhart, 1902–1966, an Australian mathematical physicist; it was later found out that this theorem was published much earlier by De Morgan, in 1841. This is another manifestation of M. Berry's Law, mentioned in Lecture 15.

**28.5 Elliptic coordinates.** Let us return to the confocal family of conics (28.3). Through a generic point $P(x, y)$ there passes an ellipse and a hyperbola from this family (the point $P$ should not lie on the segment connecting the foci; this is the general position assumption in this case). Let $\lambda_1$ and $\lambda_2$ be the respective values of the parameter $\lambda$. Then $(\lambda_1, \lambda_2)$ are called the *elliptic coordinates* of the point $P$. The ellipses and hyperbolas from the confocal family (28.3) play the role of coordinate curves of this coordinate system; they are mutually orthogonal, see Figure 28.10.

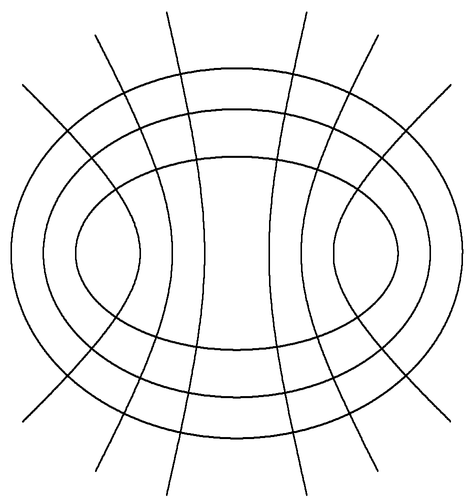

FIGURE 28.10. Confocal ellipses and hyperbolas

Consider now an ellipsoid $M$ in space

$$\frac{x^2}{a^2} + \frac{y^2}{b^2} + \frac{z^2}{c^2} = 1,$$

and assume that all semiaxes $a, b, c$ are distinct: $0 < a < b < c$. The confocal family of quadratic surfaces $M_\lambda$ is defined by the equation

$$\frac{x^2}{a^2 + \lambda} + \frac{y^2}{b^2 + \lambda} + \frac{z^2}{c^2 + \lambda} = 1 \tag{28.4}$$

where $\lambda$ is a real parameter. The type of the surface $M_\lambda$ changes as $\lambda$ passes the values $-b^2$ and $-a^2$: for $-c^2 < \lambda < -b^2$, it is a hyperboloid of two sheets, for $-b^2 < \lambda < -a^2$, a hyperboloid of one sheet, and for $-a^2 < \lambda$, an ellipsoid; see Figure 28.11.

Similarly to the plane case, we introduce elliptic coordinates of a point $(x, y, z)$ as the three values of $\lambda$ for which equation (28.4) holds. A justification is provided by the following theorem.

THEOREM 28.7. *A generic point $P = (x, y, z)$ is contained in exactly three quadratic surfaces, confocal with the given ellipsoid. These confocal quadrics are pairwise perpendicular at point $P$, see Figure 28.12.*

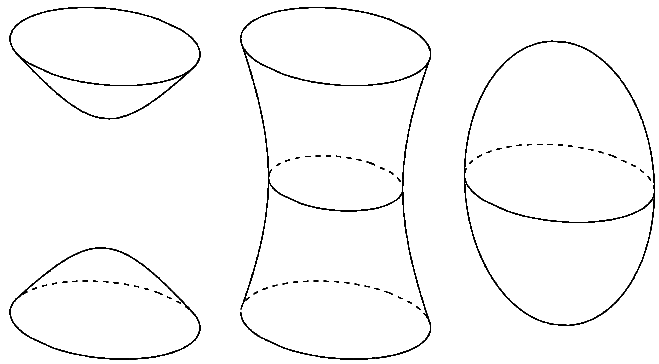

FIGURE 28.11. Confocal quadratic surfaces

Proof. Given a point $P$, equation (28.4) can be rewritten as a cubic equation in $\lambda$. We want to show that it has three real roots. Indeed, the graph of the left-hand side, as a function of $\lambda$, looks as depicted in Figure 28.13. Therefore this function assumes value 1 three times (assuming that $xyz \neq 0$: this suffices for the present argument; in general, we need to assume that the discriminant of the cubic equation in $\lambda$ does not vanish). Let $(\lambda_1, \lambda_2, \lambda_3)$ be the roots.

Next, we want to show that the quadrics are pairwise orthogonal at point $P$. Consider, for instance, $M_{\lambda_1}$ and $M_{\lambda_2}$. A normal vector to $M_{\lambda_1}$ at point $P$ is the gradient of the function on the right hand side of (28.4) (we divide it by 2 for convenience):

$$N_1 = \left( \frac{x}{a^2 + \lambda_1}, \frac{y}{b^2 + \lambda_1}, \frac{z}{c^2 + \lambda_1} \right),$$

and likewise for $N_2$. Hence

$$N_1 \cdot N_2 = \frac{x^2}{(a^2 + \lambda_1)(a^2 + \lambda_2)} + \frac{y^2}{(b^2 + \lambda_1)(b^2 + \lambda_2)} + \frac{z^2}{(c^2 + \lambda_1)(c^2 + \lambda_2)}. \tag{28.5}$$

Consider equations (28.4) for $\lambda_1$ and $\lambda_2$. The difference of their left-hand sides is equal to the right-hand side of (28.5) times $(\lambda_1 - \lambda_2)$. Hence this right-hand side is zero, and $N_1 \cdot N_2 = 0$, as claimed. □

**28.6 Apparent contours and Chasles' theorem.** Our goal in this section is to prove the following theorem, due to Chasles.

THEOREM 28.8. *A generic line in space is tangent to 2 distinct quadratic surfaces from a given confocal family. The tangent planes to these quadrics at the points of tangency with the line are orthogonal to each other.*

Let $\ell$ be the line. The strategy of the proof is to project space along $\ell$ to the orthogonal plane. A generic orthogonal projection of a surface on the plane (screen) is a domain bounded by a curve, the *apparent contour* (or, simply, the shadow) of the surface. The apparent contour is the locus of intersection points of the screen with the lines, parallel to $\ell$ and tangent to the surface. For example, the apparent contour of a convex surface is an oval.

The projection of the family of confocal quadrics yields a 1-parameter family of apparent contours.

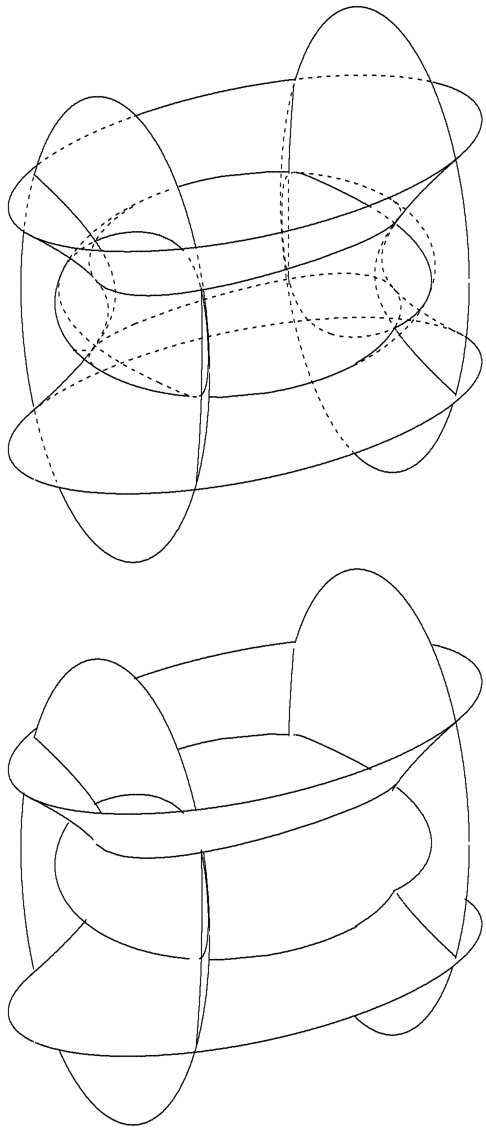

FIGURE 28.12. Three pairwise perpendicular confocal quadratic surfaces, transparent and opaque

PROPOSITION 28.4. *The apparent contours of confocal quadrics is a family of confocal conics.*

This proposition implies the Chasles Theorem.

Proof of Theorem 28.8. The projection of the line $\ell$ is a point. Through this point, there passes an ellipse and a hyperbola from a confocal family, and they are orthogonal to each other. Each of the two curves is the apparent contour of a quadratic surface from the given confocal family. Therefore these two surfaces are tangent to $\ell$ and are orthogonal at the tangency points. □

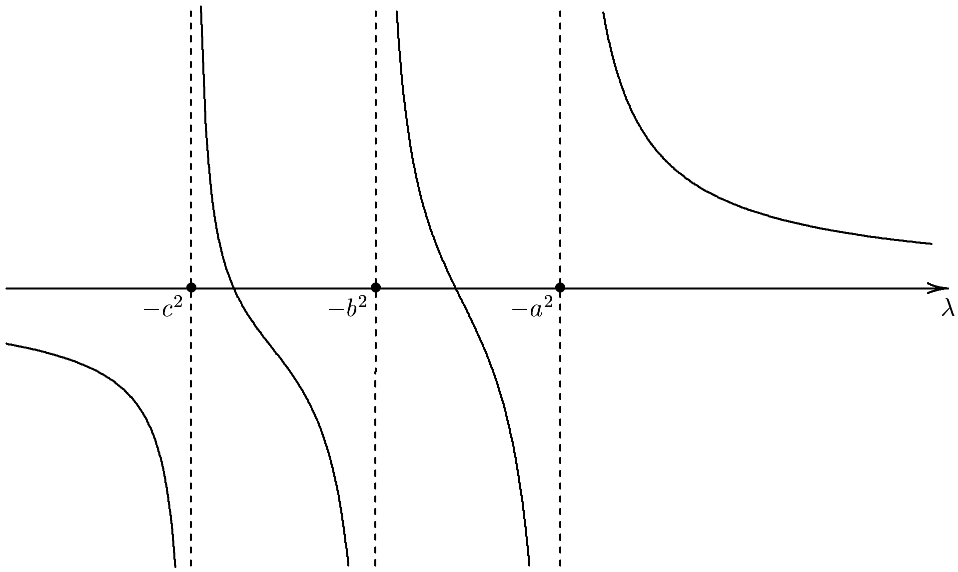


FIGURE 28.13. The graph of the equation of a confocal family

Proof of Proposition 28.4. First of all, it is easy to show that the apparent contour of an individual quadratic surface is a conic.

Assume that the screen is the horizontal $(x, y)$-plane and the line $\ell$ is vertical. Our quadratic surface $M$ is given by a quadratic equation in $x, y, z$; its specific form is not important to us (this equation is a combination of 10 terms: $x^2, y^2, z^2, xy, yz, zx, x, y, z$ and constants). For a given point of the screen $(x, y)$, the vertical line through this point has the parametric equation $(x, y, t)$. If we substitute this into the equation of $M$, we obtain a quadratic equation in $t$:

$$p_2(x, y)t^2 + p_1(x, y)t + p_0(x, y) = 0 \tag{28.6}$$

where $p_2$ is a constant, $p_1$ is a linear and $p_2(x, y)$ a quadratic function of $x, y$.

The apparent contour of $M$ consists of those points $(x, y)$ for which the vertical line through this point is tangent to $M$, that is, when equation (28.6) has a multiple root. This happens when the discriminant equals zero:

$$p_1(x, y)^2 - 4p_2(x, y)p_0(x, y) = 0.$$

This is a quadratic equation in $x$ and $y$, and it describes a conic on the screen.

It takes an extra work to prove that the apparent contours of a confocal family of quadrics is a confocal family of conics.

As we know, the normal vector to the quadric $M_\lambda$ at point $P(x, y, z)$ is

$$N(P) = (\bar{x}, \bar{y}, \bar{z}) = \left(\frac{x}{a^2 + \lambda}, \frac{y}{b^2 + \lambda}, \frac{z}{c^2 + \lambda}\right).$$

We have chosen the magnitude of the normal vector in such a way that $N(P) \cdot P = 1$; this equation holds due to (28.4).

As $P$ varies over $M_\lambda$, the point $N(P)$ describes the quadric $\overline{M}_\lambda$ given by the equation

$$(a^2 + \lambda)\bar{x}^2 + (b^2 + \lambda)\bar{y}^2 + (c^2 + \lambda)\bar{z}^2 = 1, \tag{28.7}$$

the latter equation being just another form of (28.4). Such a family of quadratic surfaces is called linear: the left hand side can be written as $Q_1 + \lambda Q_2$ where $Q_1$ and $Q_2$ are quadratic forms

$$a^2\bar{x}^2 + b^2\bar{y}^2 + c^2\bar{z}^2 \quad \text{and} \quad \bar{x}^2 + \bar{y}^2 + \bar{z}^2.$$

Denote the screen by $W$. A line, parallel to $\ell$, is tangent to $M_\lambda$ at point $P$ if and only if the normal $N(P)$ is orthogonal to $\ell$, that is, if $N(P)$ is parallel to $W$. Note that these vectors $N(P)$ are the normals to the apparent contour of the surface $M_\lambda$, see Figure 28.14.

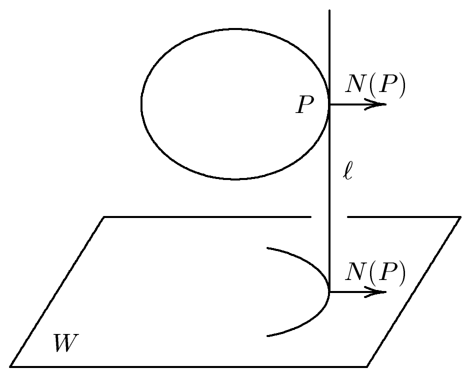


FIGURE 28.14. A surface and its apparent contour

The set of such vectors $N$ is the intersection curve of the quadratic surface $\overline{M}_\lambda$ with the plane $W$. This curve is a conic given, in appropriate Cartesian coordinates $(\xi, \eta)$ on $W$, by a formula, similar to (28.7):

$$(\alpha^2 + \lambda)\xi^2 + (\beta^2 + \lambda)\eta^2 = 1. \tag{28.8}$$

Thus the normals to the apparent contours of the surfaces $M_\lambda$ form a linear family of conics in the plane $W$.

In the plane, by the same token, it is also true that the normals to a confocal family of conics constitute a linear family of conics. It follows that these apparent contours form a confocal family on the screen. □

**28.7 Geodesics on ellipsoids.** Let $M$ be a surface. A geodesic curve on $M$ is a trajectory of a free particle confined to stay on $M$. If $\gamma(t)$ is an arc length parameterization of a geodesic, then the acceleration vector $\gamma''(t)$ is orthogonal to $M$ (physically, this means that the only force acting on the point is the normal force that confines the point to $M$). Geodesics locally minimize the distance between their points. For example, a geodesic on a developable surface becomes a straight line after the surface is unfolded to a plane. The geodesics on a sphere are its great circles. See Lecture 20 for a more detailed discussion.

Let $M$ be an ellipsoid. The behavior of geodesics is very regular; it is described by the following theorem, due to Chasles and Jacobi. This result is one of the great achievements of 19th century mathematics. We assume that the ellipsoid has distinct axes, so that the confocal family of quadratic surfaces is defined.[6]

THEOREM 28.9. *The tangent lines to a geodesic on $M$ are tangent to another fixed quadratic surface, confocal with $M$.*

Proof. Consider an arc length parameterized geodesic curve $\gamma(t)$ on $M$, and let $\ell(t)$ be the straight line, tangent to this geodesic at point $\gamma(t)$. By Theorem 28.8, $\ell(t)$ is tangent to another quadratic surface, $M_{\lambda(t)}$, confocal with $M$ and corresponding to parameter $\lambda(t)$ in equation (28.4). We want to prove that $\lambda(t)$ is independent of $t$, that is,

$$\frac{d\lambda(t)}{dt} = 0. \tag{28.9}$$

Fix a value of $t$, say, $t = 0$. Let $N$ be a normal vector to $M$ at point $\gamma(0)$ and let $\pi$ be the plane spanned by $N$ and the line $\ell(0)$. Consider a close point $\gamma(\varepsilon)$. Since the acceleration vector of the geodesic $\gamma$ is orthogonal to $M$, the line $\ell(\varepsilon)$ lies in the plane $\pi$, up to an error of order $\varepsilon^2$.

Indeed, using the "Big O" notation, one has:

$$\gamma(\varepsilon) = \gamma(0) + \varepsilon\gamma'(0) + O(\varepsilon^2), \quad \gamma'(\varepsilon) = \gamma'(0) + \varepsilon\gamma''(0) + O(\varepsilon^2).$$

The point $\gamma(0)$ and the vectors $\gamma'(0), \gamma''(0)$ lie in the plane $\pi$. Hence, up to an error of order $\varepsilon^2$, a point $\gamma(\varepsilon)$ of the line $\ell(\varepsilon)$ and its directional vector $\gamma'(\varepsilon)$ lie in $\pi$.

Let $y$ be the tangency point of the line $\ell(0)$ with $M_{\lambda(0)}$. By Theorem 28.8, the normal vector $N$ lies in the tangent plane to $M_{\lambda(0)}$ at $y$, that is, this tangent plane is the plane $\pi$, see Figure 28.15. Denote by $m(\varepsilon)$ the orthogonal projection of $\ell(\varepsilon)$ on the plane $\pi$. Note that $m(\varepsilon)$ and $\ell(\varepsilon)$ are close to order $\varepsilon^2$. Therefore, as far as equality (28.9) is concerned, we may replace $\ell(\varepsilon)$ by $m(\varepsilon)$, that is, to assume that the line $\ell(\varepsilon)$ lies in the plane $\pi$.

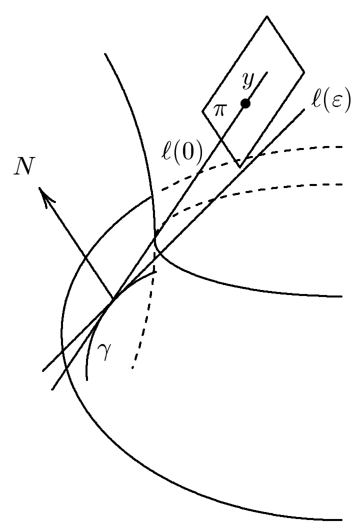


FIGURE 28.15. Proving Theorem 28.9

[6]Of course, the regular behavior of geodesics,, described in Theorem 28.9, extends, by continuity, to ellipsoids with coinciding axes, that is, ellipsoids of revolution.

We want to prove that $\lambda(\varepsilon) - \lambda(0) = O(\varepsilon^2)$. Intuitively, this is clear: the line $\ell(\varepsilon)$ lies on the tangent plane to the surface $M_{\lambda(0)}$ and is $\varepsilon^2$-close to this surface. To make an exact sense of this argument, we need a technical lemma.

Let $f(x, \varepsilon)$ be a smooth function of two variables; we think of this as a family of functions in variable $x$, with $\varepsilon$ being a parameter, and use the suggestive notation $f_\varepsilon(x)$. Assume that the function $f_0(x)$ has a critical point at $x = 0$, and this critical point is non-degenerate: $f_0''(0) \neq 0$. Assume also that the respective critical value is zero: $f_0(0) = 0$. Then, for every sufficiently small $\varepsilon$, the function $f_\varepsilon(x)$ has a critical point near $x = 0$; let $c(\varepsilon)$ be the respective critical value, see Figure 28.16.

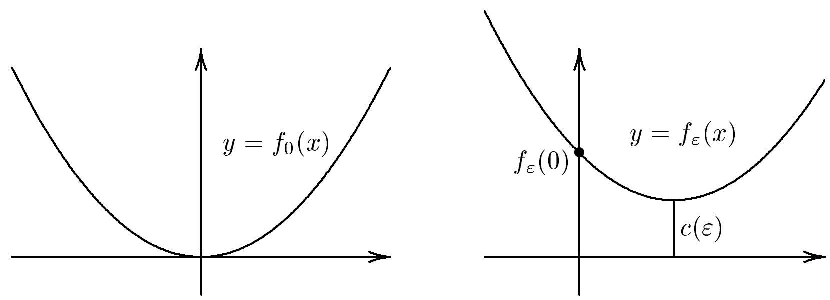


FIGURE 28.16. Lemma 28.5

LEMMA 28.5.

$$\lim_{\varepsilon \to 0} \frac{c(\varepsilon) - f_\varepsilon(0)}{\varepsilon} = 0. \tag{28.10}$$

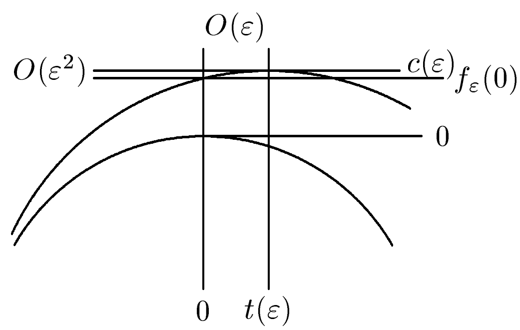


FIGURE 28.17. Proof of Lemma 28.5

Proof of Lemma. Expand $f_\varepsilon(x)$ in a series in $\varepsilon$:

$$f_\varepsilon(x) = f_0(x) + \varepsilon g(x) + O(\varepsilon^2). \tag{28.11}$$

Let $t(\varepsilon)$ be the critical point of the function $f_\varepsilon(x)$ near zero; since $t(0) = 0$, one has: $t(\varepsilon) = O(\varepsilon)$. It follows from (28.11) that

$$c(\varepsilon) = f_\varepsilon(t(\varepsilon)) = f_0(t(\varepsilon)) + \varepsilon g(t(\varepsilon)) + O(\varepsilon^2).$$

Since $f_0$ has a critical point at $x = 0$ with zero critical value, $f_0(x) = O(x^2)$, and hence $f_0(t(\varepsilon)) = O(\varepsilon^2)$. Also $g(t(\varepsilon)) = g(0) + O(\varepsilon)$. It follows that $c(\varepsilon) = \varepsilon g(0) +$

$O(\varepsilon^2)$. But (28.11) implies that $f_\varepsilon(0) = \varepsilon g(0) + O(\varepsilon^2)$. Hence $c(\varepsilon) - f_\varepsilon(0) = O(\varepsilon^2)$, and (28.10) follows. See Figure 28.17. □

Now we can finish the proof of Theorem 28.9. Assume that the tangency of line $\ell(0)$ with the surface $M_{\lambda(0)}$ is non-degenerate: for a quadratic surface, this means that the line does not lie on the surface (cf. Lecture 16). We shall prove the statement of the theorem for such a generic line, and then (28.9) extends to all lines by continuity.

Recall that the surface $M_{\lambda(0)}$ from the confocal family (28.4) passes through point $y$. Then, through every point in a vicinity of $y$, there passes a quadratic surface from this confocal family, and we consider the corresponding elliptic coordinate $\lambda$ as a function, defined in a neighborhood of $y$. In particular, the value of $\lambda$ at $y$ is $\lambda(0)$.

We can restrict the function $\lambda$ on a straight line. A line is tangent to a quadratic surface $M_c$ when the restriction of the function $\lambda$ on this line has a critical point with the critical value $c$. Identify all the lines, sufficiently close to $\ell(0)$, with the real line, assuming that the origin on $\ell(0)$ is at point $y$. Let $x$ be the variable on $\mathbf{R}$. Subtract $\lambda(0)$ from the function $\lambda$ and denote its restriction on the line $\ell(\varepsilon)$ by $f_\varepsilon(x)$.

Now we apply Lemma 28.5. Since the line $\ell(0)$ is tangent to $M_{\lambda(0)}$, the function $f_0(x)$ has a non-degenerate critical point at $x = 0$ with zero critical value. The distance between the origins on the lines $\ell(0)$ and $\ell(\varepsilon)$ is of order $\varepsilon$ (or higher). Since the line $\ell(\varepsilon)$ lies in the tangent plane $\pi$ to the level surface $\{\lambda = \lambda(0)\}$, the distance from the origin on this line to this surface is of order $\varepsilon^2$ or higher. That is, $f_\varepsilon(0) = O(\varepsilon^2)$. By Lemma 28.5, $\lim_{\varepsilon\to 0} c(\varepsilon)/\varepsilon = 0$ where $c(\varepsilon) = \lambda(\varepsilon) - \lambda(0)$, and (28.9) follows. □

Theorem 28.9 imposes very strong restrictions on the behavior of geodesics on ellipsoids. The lines, tangent to a fixed geodesic $\gamma$ on $M$, are tangent to another quadric $Q$, confocal with $M$. Let $x$ be a point of $\gamma$. The tangent plane to $M$ at $x$ intersects $Q$ along a conic (depending on $x$). The number of tangent lines to this conic from $x$ can be equal to 2, 1 or 0 (the intermediate case of a single tangent line, having multiplicity 2, occurs when $x$ belongs to the conic). Thus the surface $M$ gets partitioned into two parts depending on the number, 2 or 0, of common tangent lines of $M$ and $Q$, passing through a fixed point on $M$. The geodesic $\gamma$ is confined to the former part and can have only one of the two possible directions in every point, namely, the directions of the common tangent lines of $M$ and $Q$; see Figure 28.18.

In conclusion, two remarks. First, most of the results concerning billiards inside the ellipsoid and geodesics on the ellipsoid have multi-dimensional analogs; for example, *the tangent lines to a geodesic on an ellipsoid in $n$-dimensional space are tangent to $(n-2)$ other fixed quadratic confocal hypersurfaces.*

Secondly, if the smallest semi-axis of an ellipsoid tends to zero, the ellipsoid degenerates to a doubly covered ellipse. The geodesic lines on the ellipsoid become the billiard trajectories inside this ellipse, and Theorem 28.9 implies Theorem 28.2 as its limit case.

For more information about billiards in general, and in particular, billiards inside the ellipsoids and the geodesics on the ellipsoids, see, e.g., [**78, 83**].

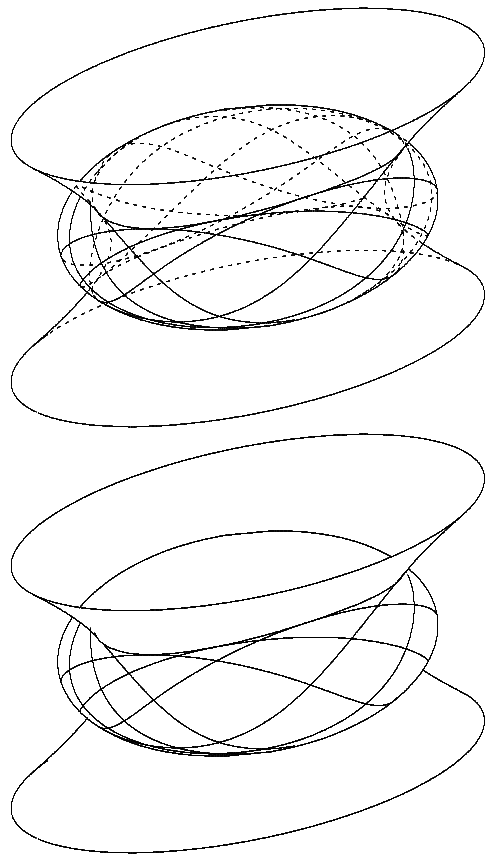

FIGURE 28.18. A geodesic on an ellipsoid: the lines tangent to the geodesic are tangent to a confocal hyperboloid (transparent and opaque)

| | | |
|---|---|---|
| John Smith<br>January 23, 2010 | Martyn Green<br>August 2, 1936 | Henry Williams<br>June 6, 1944 |

| | | |
|---|---|---|
| John Smith<br>January 23, 2010 | Martyn Green<br>August 2, 1936 | Henry Williams<br>June 6, 1944 |

### 28.8 Exercises.

28.1. Prove that, in terms of the angles in Figure 28.19, the area element (28.2) can be expressed as $\omega = \sin\alpha \; d\alpha dx$.

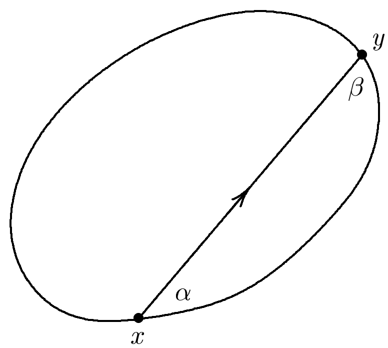


FIGURE 28.19. The angles associated with a chord

28.2. (a) Prove that the ellipse, hyperbola and parabola, given by the "gardener construction" of Section 28.2, indeed have familiar equations of second degree.

(b) Deduce the formula for a confocal family of conics (28.3).

28.3. Prove the optical property of the parabola.

28.4. Prove that a billiard trajectory in an ellipse that starts at a focus tends to the major axis of the ellipse.

28.5. (a) Consider a disc with center $O$ and let $A$ be a point inside the disc. For every point $X$ of the circle fold the disc so that the point $X$ coincides with point $A$. Prove that the envelope of the fold lines is the ellipse with the foci $A$ and $O$. What happens if $A$ lies outside of the disc?

(b)* Given a smooth curve $\gamma$ and a point $A$, reflect the lines emanating from $A$ in $\gamma$. Let $W$ be the locus of points obtained from $A$ by reflection in the tangent lines to $\gamma$. Prove that $W$ is a curve orthogonal to the reflected lines.

*Hint.* Approximate $\gamma$ by an ellipse and use (a).

28.6. According to the optical property of the ellipse, rays emanating from a point source of light $L$ located at a focus of the elliptic mirror will pass, after reflection, through the other focus. However, if $L$ is not located at a focus, then the reflected rays will not pass through one point; on the contrary, they will have an envelope, once again called the *caustic*. Draw a picture which allows to visualize these caustics; consider three cases: $L$ is close to the focus, $L$ is not close to the focus but still insuide the ellipse, $L$ is outside of the ellipse. In the last case we need to assume that the ellipse is both transparent and reflecting.

28.7. Geodesics emanating from a point of the sphere all arrive at the opposite point. This will not be true, however, if one replaces the sphere by an ellipsoid. Draw the family of geodesics emanating from a point of an ellipsoid (better take the ellipsoid close to a sphere) in the neighborhood of the opposite point. What does the envelope of this family look like? (*Warning*: your picture should not contradict to the fact that any two points of the ellipsoid can be joined by a geodesic.)

28.8. * Construct a trap for a parallel beam of light (by a trap we mean a non-closed curve such that if a family of rays having, say, the vertical direction enters the curve and starts to reflect in the curve according to the law of geometrical optics, then no ray will ever escape to infinity).

*Hint*. Use the optical properties of the ellipse and the parabola.

28.9. Find an elementary geometry proof of the "most elementary theorem of Euclidean geometry".

28.10. Show that the Cartesian coordinates are expressed in terms of the elliptic ones as follows:

$$x^2 = -\frac{(a^2+\lambda_1)(a^2+\lambda_2)}{b^2-a^2},\ y^2 = \frac{(b^2+\lambda_1)(b^2+\lambda_2)}{b^2-a^2}.$$

28.11. The apparent contour of an algebraic surface given by an equation of degree $n$ is an algebraic plane curve given by an equation $N$. Prove this and find the relation between $n$ and $N$.

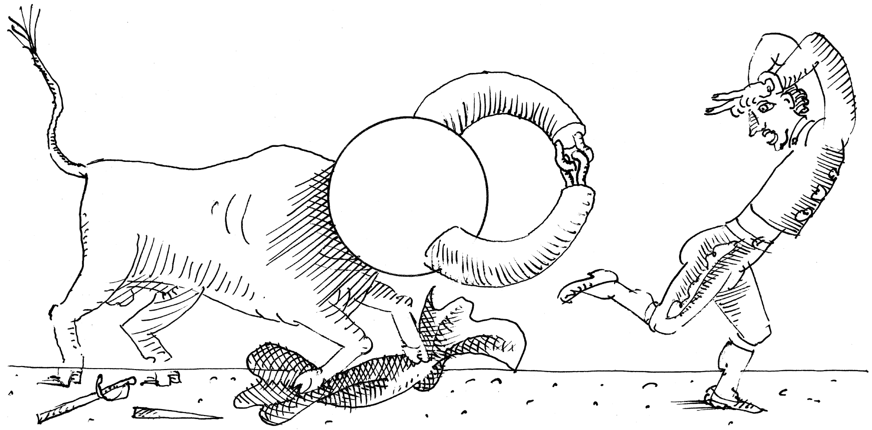

LECTURE 29

# The Poncelet Porism and Other Closure Theorems

**29.1 The closure theorem.** Consider two nested ellipses, $\gamma$ and $\Gamma$, choose a point $X$ on the outer one, draw a tangent line to the inner until it intersects the outer at point $Y$, repeat the construction, starting with $Y$, and so on. We obtain a polygonal line, inscribed into $\Gamma$ and circumscribed about $\gamma$. Suppose that this process is periodic: the $n$-th point coincides with the initial one. Now start at a different point, say, $X_1$. The Poncelet closure theorem states that again the polygonal line closes up after $n$ steps, see Figure 29.1.

Poncelet's porism[1] is a classical result of projective geometry. It was discovered by Jean-Victor Poncelet when he was a prisoner during the Napoleonic war in the Russian city of Saratov in 1813-1814, and published in 1822 in his "Traité sur les propriétés projectives des figures".

One can devise one's own closure theorem as follows. Start with a parametrized oval $\Gamma(t)$ with $t$ varying from 0 to 1. Choose a constant $c$ and consider the 1-parameter family of chords $\Gamma(t)\Gamma(t+c)$. These chords have an envelope $\gamma$. This envelope may have cusps (but not inflection points, see Lecture 8); suppose it is smooth, which will always be the case if $c$ is small enough. Then we obtain a pair of nested ovals, $\Gamma$ and $\gamma$, for which the statement of the closure theorem holds.

Indeed, the correspondence $X \mapsto Y$ is given, in the parameter $t$, by the formula $t \mapsto t+c$. A point returns back after $n$ iterations if and only if $nc$ is an integer. This condition depends only on $c$, that is, on the pair of ovals, but not on the choice of the starting point $X$, whence the closure theorem.

The question then is: given a pair of nested ellipses, how to choose a parameter $t$ on the outer one so that the correspondence $T : X \mapsto Y$ is given by the formula $t \mapsto t+c$?

**29.2 Proof.** First of all, stretch the plane so that $\Gamma$ becomes a circle (a technical name for stretching is an affine transformation). Since the Poncelet theorem

[1]For all practical purposes, the Greek word "porism" means "theorem". One of the lost books by Euclid was "Porisms".

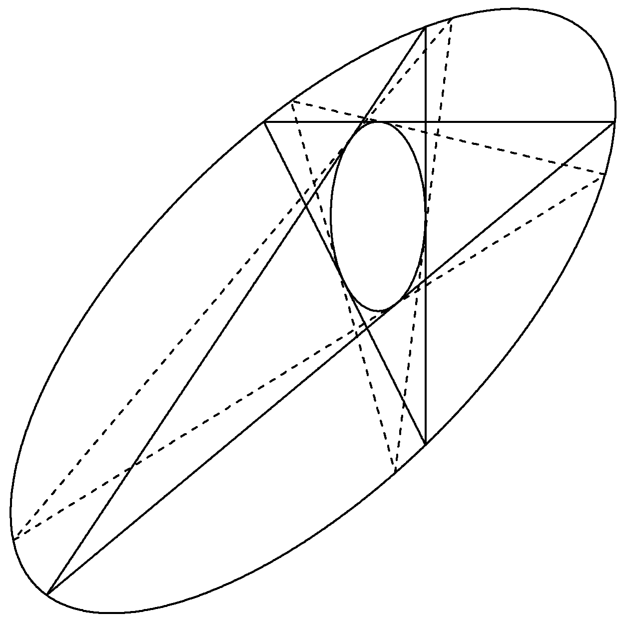

FIGURE 29.1. The Poncelet closure theorem

involves only lines (but not distances or angles), transformations of the plane that take lines to lines do not violate the theorem (such transformations are called projective). We consider the circle $\Gamma$ in its arc length parameter $x$.

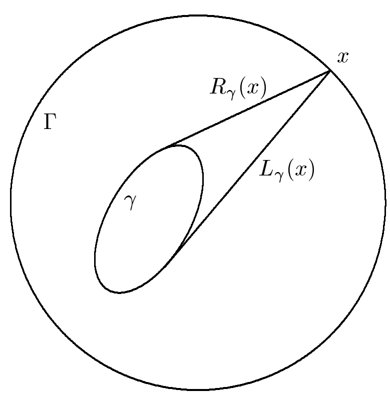


FIGURE 29.2. Left and right tangent segments

Denote by $R_\gamma(x)$ and $L_\gamma(x)$ the lengths of the right and left tangent segments from point $x$ to the curve $\gamma$, see Figure 29.2. Consider a point $x_1$, infinitesimally close to $x$. Let $O$ be the intersection point of the lines $xy$ and $x_1y_1$ and $\varepsilon$ the angle between these lines. The line $x_1y_1$, as every line, makes equal angles with the circle $\Gamma$; denote this angle by $\alpha$, see Figure 29.3.

What follows is, essentially, the argument from Theorem XXX, Figure 102, in I. Newton's "Principia" [**55**]; see also Lecture 30.

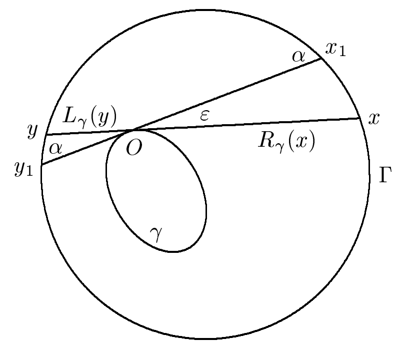


FIGURE 29.3. Distortion of the arc length

By the Sine theorem,

$$\frac{|yy_1|}{L_\gamma(y)} = \frac{\sin\varepsilon}{\sin\alpha} = \frac{|xx_1|}{R_\gamma(x)}$$

or

$$\frac{dy}{L_\gamma(y)} = \frac{dx}{R_\gamma(x)}. \tag{29.1}$$

Assume, for the moment, that $\gamma$ is a circle too. Then the right and left tangent segments are equal: $R_\gamma(x) = L_\gamma(x)$. Denote this common value by $D_\gamma(x)$. It follows from (29.1) that the length element $dx/D_\gamma(x)$ is invariant under the transformation $T$. It remains to choose a parameter $t$ so that this length element is $dt$; this is done by integrating:

$$t = \int \frac{dx}{D_\gamma(x)},$$

and the transformation $T$ becomes a translation $t \mapsto t + c$.

Finally, if $\gamma$ is not a circle, let $A$ be a stretching of the plane that takes $\gamma$ to a circle. An affine transformation does not change the ratio of parallel segments. Taking (29.1) into account, we have:

$$\frac{dx}{dy} = \frac{R_\gamma(x)}{L_\gamma(y)} = \frac{R_{A\gamma}(Ax)}{L_{A\gamma}(Ay)} = \frac{D_{A\gamma}(Ax)}{D_{A\gamma}(Ay)}.$$

One again obtains a length element $dx/D_{A\gamma}(Ax)$, invariant under the transformation $T$. As before, we choose a parameter $t$ so that $T(t) = t + c$, and Poncelet's theorem follows. □

REMARK 29.1. One can deduce the Poncelet porism from the complete integrability of the billiard inside an ellipse, see Corollary 28.5 which establishes the closure theorem for a pair of confocal ellipses – see Exercise 29.1.

**29.3 Ramifications.** A conic is determined by 5 of its points. A pencil of conics is a 1-parameter family of conics that share 4 fixed points. These points may be complex, and then they are "invisible" in the real plane. Algebraically, let $P(x, y) = 0$ and $Q(x, y) = 0$ be quadratic equations of two conics. These conics determine the pencil given by the equation $P(x, y) + tQ(x, y) = 0$ where $t$ is a parameter.[2]

The algebraic definition of a pencil does not exclude the cases when some of the 4 points coincide or lie at infinity. For example, the family of concentric circles is a pencil. Indeed, a conic is a circle if and only if it passes through two very special "circular" points at infinity, $(1 : i : 0)$ and $(-1 : i : 0)$. The concentric circles are all tangent to each other at these point, so in this case, the four points merge into two "double points".

Consider a number of nested conics from the same pencil $\gamma_1, \gamma_2, \cdots, \gamma_k, \Gamma$ where $\Gamma$ is the outmost one. Let us modify the game: choose a point $X$ on $\Gamma$, draw a tangent line to $\gamma_1$ to meet $\Gamma$ again at $Y$; draw a tangent line from $Y$ to $\gamma_2$, ..., draw a tangent line to $\gamma_k$ to meet $\Gamma$ at $Z$, see Figure 29.4. The correspondence $X \mapsto Z$ enjoys the same property: if its $n$-iteration takes a point $X$ to itself then every other point returns back after $n$ steps. This is a generalization of the Poncelet porism. (A different, projectively dual, generalization is given in Corollary 28.6.)

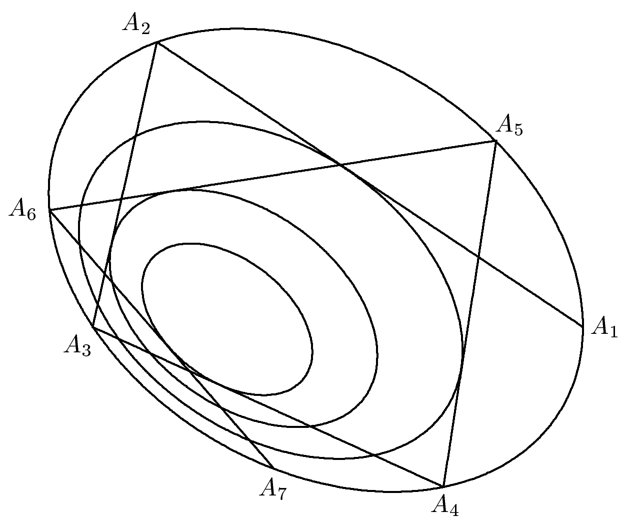


FIGURE 29.4. Generalized, or "Big", Poncelet theorem

Given two nested ellipses $\gamma$ and $\Gamma$, one wants to determine whether the inscribed-circumscribed Poncelet polygon closes up after $n$ steps. If both conics are circles (not necessarily concentric!) and $n = 3, 4$, explicit answers were known before Poncelet discovered his theorem. See Exercise 29.2.

A general answer was found by Cayley, see [**38**]. We shall describe this answer (without proof) in a particular case, when the outer conic is the unit circle $x^2 + y^2 = 1$ and the inner one is a concentric ellipse $a^2x^2 + b^2y^2 = 1$. Consider the Taylor series

$$\sqrt{(a^2 + t)(b^2 + t)(1 + t)} = c_0 + c_1 t + c_2 t^2 + \cdots$$

[2]In Lecture 28, we called a pencil a "linear system of conics".

where each $c_i$ is a function of $a$ and $b$ (for example, $c_0 = ab$). The Poncelet polygon closes up after $n$ steps if and only if

$$\det \begin{vmatrix} c_2 & \cdots & c_{m+1} \\ \cdot & \cdots & \cdot \\ c_{m+1} & \cdots & c_{2m} \end{vmatrix} = 0$$

for $n = 2m + 1$, and

$$\det \begin{vmatrix} c_3 & \cdots & c_{m+1} \\ \cdot & \cdots & \cdot \\ c_{m+1} & \cdots & c_{2m} \end{vmatrix} = 0$$

for $n = 2m$.

**29.4 The Poncelet grid.** Let $\gamma$ and $\Gamma$ be two nested ellipses. R. Schwartz recently discovered an interesting property of Poncelet polygons, that is, polygons inscribed into $\Gamma$ and circumscribed about $\gamma$ [**70**].

Let $L_1, \ldots, L_n$ be the lines containing the sides of the polygon and listed in the cyclic order of their tangency points with $\gamma$. Consider the intersection set of these lines: $A_{ij} = L_i \cap L_j$. Let us assume that $A_{ii}$ is the tangency point of $L_i$ with $\gamma$. Assume also that $n$ is odd (the formulation for even $n$ is a little different).

The points $A_{ij}$ constitute a finite set that we call the *Poncelet grid*. Let us decompose this grid into subsets in two ways. For each $j = 0, 1, \ldots, n-1$, the "circular" set $P_j$ consists of the points $A_{i,i+j}$ (of course, we understand the indices cyclically, so that $n + 1 = 1$, etc.), and the "radial" set $Q_j$ of the points $A_{j-i,j+i}$. Note that $P_j = P_{n-j}$, so there are $(n + 1)/2$ circular sets $P_j$, each containing $n$ points. There are $n$ radial sets $Q_j$, each containing $(n + 1)/2$ points. All this is illustrated in Figure 29.5 where $n = 7$.

According to the Schwartz theorem, each circular set $P_j$ lies on an ellipse,[3] say, $\gamma_j$, and $P_j$ consists of the vertices of a Poncelet polygon, inscribed into $\gamma_i$ and circumscribed about $\gamma$. Likewise, each radial set $Q_j$ lies on a hyperbola. Furthermore, all the circular sets $P_j$ are projectively equivalent: for all $j, j'$ there exists a projective transformation that takes $P_j$ to $P_{j'}$. The same projective equivalence holds for the radial sets $Q_j$.

Analogous results hold for even $n$. R. Schwartz proved his theorem using complex algebraic geometry. One can also deduce the Schwartz theorem from properties of billiards in ellipses, see [**52**].

**29.5 Money-Coutts theorem.** There is a number of other closure theorems that resemble the Poncelet porism. One is Steiner's theorem on a chain of circles, tangent to two given ones, $\gamma$ and $\Gamma$, see Figure 29.6. The statement is that if such a chain closes up after $n$ steps, starting from some point, then this will happen for any other starting point as well. Steiner's theorem becomes obvious if one applies an appropriate geometric transformation: there is an inversion that takes $\gamma$ and $\Gamma$ into concentric circles. (Note however that there is no such proof of the Poncelet porism which is therefore a much harder result.)

Another curious theorem concerns mutually tangent circles inscribed into polygons. Here is the simplest one. Consider a triangle $A_1A_2A_3$. Inscribe a circle $C_1$ into the angle $A_3A_1A_2$, then the circle $C_2$ into the angle $A_1A_2A_3$, tangent to $C_1$,

[3]This statement was known to Darboux [**19**].

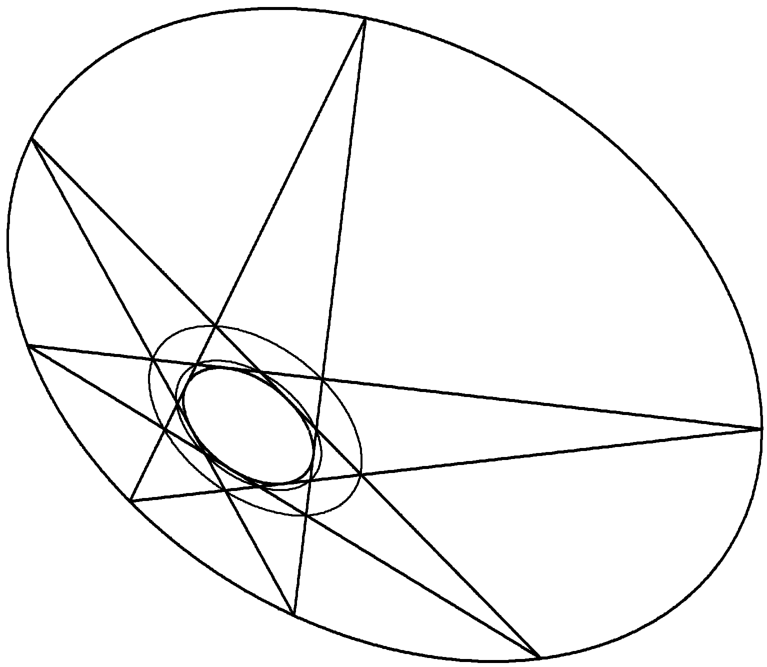

FIGURE 29.5. Poncelet grid

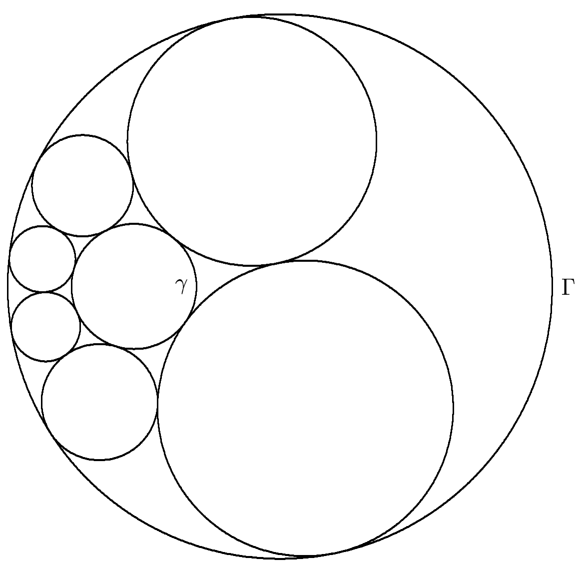


FIGURE 29.6. Steiner's theorem

then the circle $C_3$ into the angle $A_2A_3A_1$, tangent to $C_3$, and so on cyclically, see Figure 29.7.

THEOREM 29.1. *This sequence of circles is 6-periodic: $C_7 = C_1$, see Figure 29.8.*

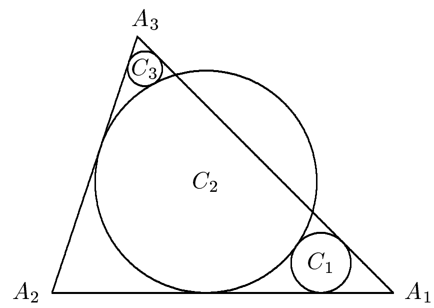


FIGURE 29.7. Inscribing consecutive circles in a triangle

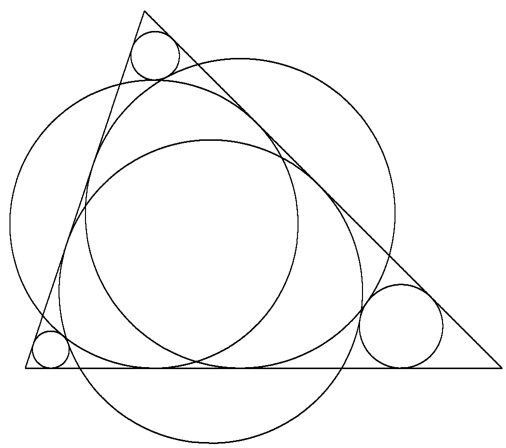

FIGURE 29.8. Six-periodicity of the process

Proof. The proof consists of a clever change of variables that appears somewhat of a miracle.

Let the angles of the triangle be $2\alpha_1, 2\alpha_2$ and $2\alpha_3$. Consider the first two circles; let $r_1$ and $r_2$ be their radii. We claim that

$$r_1 \cot \alpha_1 + 2\sqrt{r_1 r_2} + r_2 \cot \alpha_2 = |A_1 A_2|. \tag{29.2}$$

Indeed, in Figure 29.9,

$$|A_1 P_1| = r_1 \cot \alpha_1, |A_2 P_2| = r_2 \cot \alpha_2 \quad \text{and} \quad |P_1 P_2| = 2\sqrt{r_1 r_2}.$$

Set: $r_1 \cot \alpha_1 = u_1^2$, $r_2 \cot \alpha_2 = u_2^2$ and $\sqrt{\tan \alpha_1 \tan \alpha_2} = e$. Then equation (29.2) can be rewritten as

$$u_1^2 + 2e u_1 u_2 + u_2^2 = |A_1 A_2|. \tag{29.3}$$

Equation (29.3) implies:

$$u_1 + e u_2 = \sqrt{|A_1 A_2| - (1 - e^2) u_2^2},\ u_2 + e u_1 = \sqrt{|A_1 A_2| - (1 - e^2) u_1^2}. \tag{29.4}$$

Rewrite (29.3) as

$$u_1(u_1 + e u_2) + u_2(u_2 + e u_1) = |A_1 A_2|$$

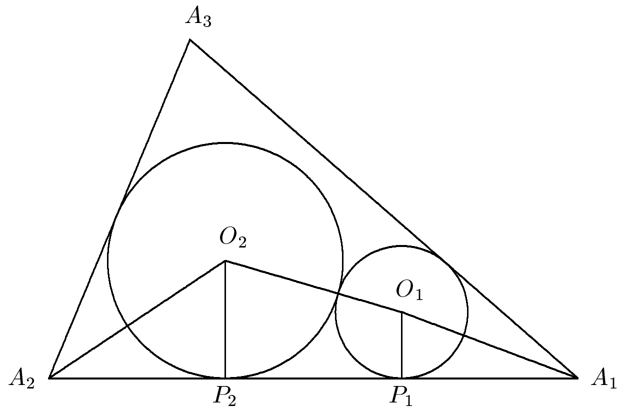


FIGURE 29.9. Relation between two inscribed circles

or, in view of (29.4), as

$$u_1\sqrt{|A_1A_2| - (1-e^2)u_2^2} + u_2\sqrt{|A_1A_2| - (1-e^2)u_1^2} = |A_1A_2|. \tag{29.5}$$

Inscribe a circle into our triangle; let $r$ be its radius and $a_1, a_2, a_3$ the tangent segments from the vertices to the circle, see Figure 29.10. Let $p = a_1 + a_2 + a_3$ be the semi-perimeter and $S$ the area. On the one hand, $S = rp$, and on the other, $S = \sqrt{pa_1a_2a_3}$ by the Heron formula. Therefore $r^2 = a_1a_2a_3/p$.

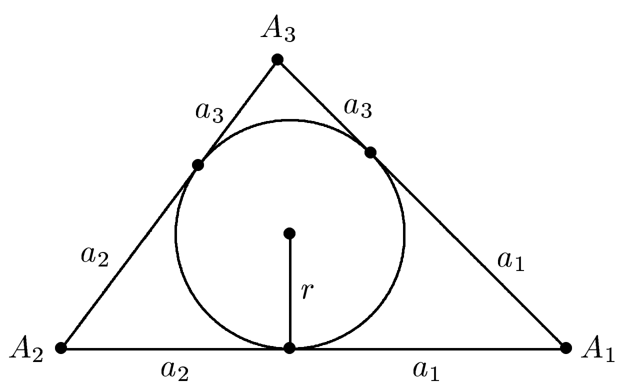


FIGURE 29.10. Proving 6-periodicity

Let us find $e$. One has: $\tan\alpha_1 = r/a_1,\ \tan\alpha_2 = r/a_2$, hence

$$e^2 = \frac{r^2}{a_1a_2} = \frac{a_3}{p}.$$

In particular, $e < 1$. It follows also that

$$1 - e^2 = \frac{p - a_3}{p} = \frac{|A_1A_2|}{p}.$$

We now rewrite equation (29.5) as

$$\frac{u_1}{\sqrt{p}}\sqrt{1-\frac{u_2^2}{p}}+\frac{u_2}{\sqrt{p}}\sqrt{1-\frac{u_1^2}{p}}=\sqrt{\frac{|A_1A_2|}{p}}. \tag{29.6}$$

A brief glance on this equation reveals the final substitution:

$$\frac{u_1}{\sqrt{p}}=\sin\phi_1,\ \frac{u_2}{\sqrt{p}}=\sin\phi_2,$$

and (29.6) is finally rewritten as

$$\sin(\phi_1+\phi_2)=\sqrt{\frac{|A_1A_2|}{p}}$$

or

$$\phi_1+\phi_2=\sin^{-1}\left(\sqrt{\frac{|A_1A_2|}{p}}\right):=\beta_3 \tag{29.7}$$

(the last equality is just a convenient notation).

Now, let us pause and reflect on what we have achieved. Initially, we characterized the circles inscribed into the two angles of the triangle by their radii, $r_1$ and $r_2$, and the tangency condition was a complicated equation (29.2). Then we changes the variables to $\phi_1$ and $\phi_2$, and the tangency condition simplified to (29.7).

Introduce the third class of circles, the ones inscribed into the angle $A_2A_3A_1$; they are characterized by their radius $r_3$ and by the variable $\phi_3$, related to $r_3$ the same way as $\phi_1$ and $\phi_2$ to $r_1$ and $r_2$.

Now, the final touch. For the first seven circles, we have:

$$\phi_1+\phi_2=\beta_3, \phi_2+\phi_3=\beta_1, \phi_3+\phi_4=\beta_2, \phi_4+\phi_5=\beta_1, \phi_5+\phi_6=\beta_2, \phi_6+\phi_7=\beta_1.$$

Take the first equation, subtract the second, add the third, subtract the forth,etc. The result is: $\phi_1-\phi_7=0$, that is, the 7-th circle coincides with the first one. □

Theorem 29.1 is closely related to the Malfatti problem of elementary geometry that asks to construct three pairwise tangent circles, inscribed into the three angles of a triangle. The problem was solved by G. Malfatti in 1803 but it continued to attract interest of prominent geometers of 19th century such as Steiner, Plücker and Cayley. A solution to the Malfatti problem readily follows from our formulas: for Malfatti circles, $\phi_4=\phi_1, \phi_5=\phi_2, \phi_6=\phi_3$, and

$$\phi_1=\frac{\beta_3+\beta_2-\beta_1}{2},\ \phi_2=\frac{\beta_1+\beta_3-\beta_2}{2},\ \phi_3=\frac{\beta_2+\beta_1-\beta_3}{2},$$

which uniquely describes the circles.

An amazing fact is that the statement of Theorem 29.1 still holds if one replaces a triangle with straight sides by one made of circular arcs! This was discovered by amateur mathematicians G. B. Money-Coutts and C. J. Evelyn by careful drawing,[4] and proved by Tyrrell and Powell in 1971, see [**86**]. The proof resembled our proof of Theorem 29.1 but the role of trigonometric functions was played by (more complicated) elliptic functions. (Incidentally, the invariant function for the billiard ball map in an ellipse can be expressed in elliptic functions as well.)

[4]The personal-computer era had still to arrive.

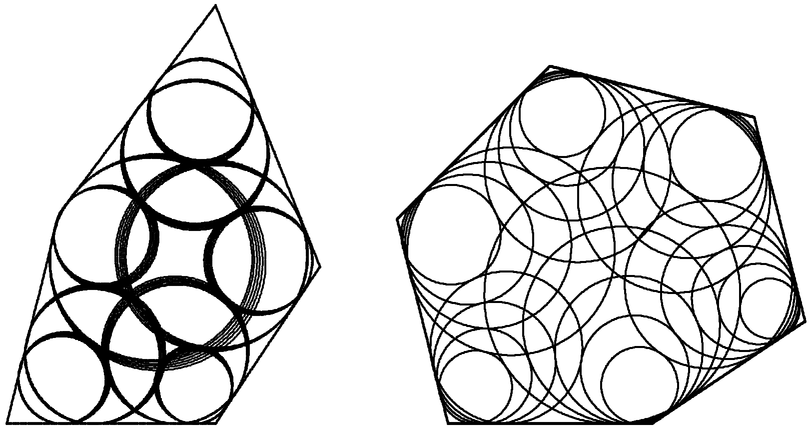

FIGURE 29.11. No periodicity for a generic polygon

What about other polygons? The game is to inscribe circles into consecutive angles, each circle tangent to the previous one. Figure 29.11 shows a generic pentagon and hexagon: we see that the inscribed circles do not exhibit any periodicity. For a generic quadrilateral, the behavior of the circles is quite chaotic [**84**].

However, periodicity is redeemed if the $n$-gon satisfies a special condition, depicted in Figure 29.12. Assume that $n \geq 5$. Let the vertices of a polygon be $A_1, A_2, \cdots$, and the the interior angles be $2\alpha_1, 2\alpha_2, \cdots$. Assume that $\alpha_i + \alpha_{i+1} > \pi/2$ for all $i$. Denote by $D_i$ the intersection point of the lines $A_{i-1}A_i$ and $A_{i+1}A_{i+2}$. Consider the excircles of the triangles $A_{i-1}A_iD_{i-1}$ and $A_iA_{i+1}D_i$, tangent to the sides $A_iD_{i-1}$ and $A_iD_i$, respectively. The condition is that these two excircles coincide for all $i$.

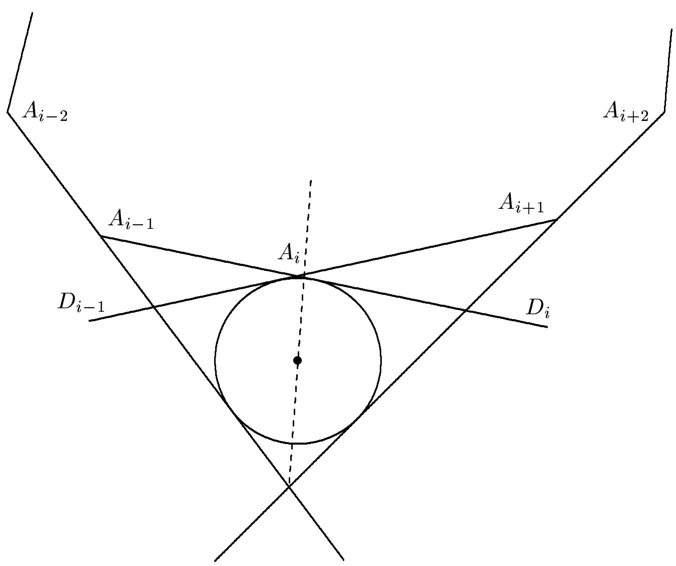


FIGURE 29.12. Condition that redeems periodicity

Then, for odd $n$, the sequence of inscribed circles is $2n$-periodic. For even $n$, one needs one additional condition:

$$\frac{\Pi_{i=1,\ i\,\mathrm{odd}}^{n}\left(\sqrt{1-\cot\alpha_i\cot\alpha_{i+1}}+1\right)}{\Pi_{i=1,\ i\,\mathrm{even}}^{n}\left(\sqrt{1-\cot\alpha_i\cot\alpha_{i+1}}+1\right)}=1,$$

and if this condition holds then the sequence of inscribe circles is $n$-periodic.

This result is proved similarly to Theorem 29.1, and like the latter, also has a version for polygons made of arcs of circles, see [**81**]. For more about the Poncelet porism, its history and generalizations, see [**5, 10**].

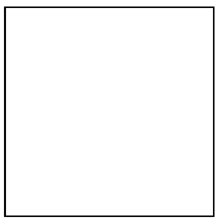
John Smith
January 23, 2010

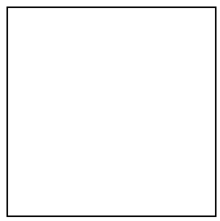
Martyn Green
August 2, 1936

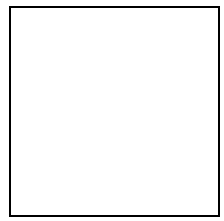
Henry Williams
June 6, 1944

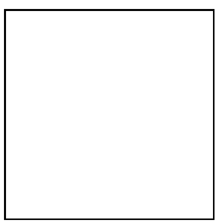
John Smith
January 23, 2010

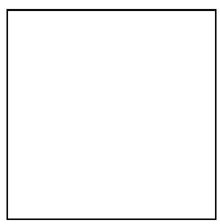
Martyn Green
August 2, 1936

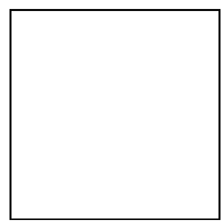
Henry Williams
June 6, 1944

### 29.6 Exercises.

29.1. Show that an arbitrary pair of nested ellipses can be taken to confocal ones by a projective transformation. Deduce the Poncelet porism from Corollary 28.5.

29.2. Let $\Gamma$ and $\gamma$ be circles of radii $R$ and $r$, and let $a$ be the distance between their centers. Assume that $\gamma$ lies inside $\Gamma$.

(a) Prove that there exists a triangle, inscribed into $\Gamma$ and circumscribed about $\gamma$, if and only if $a^2 = R^2 - 2rR$ (Chapple's formula).

(b) Prove that there exists a quadrilateral, inscribed into $\Gamma$ and circumscribed about $\gamma$, if and only if $(R^2 - a^2)^2 = 2r^2(R^2 + a^2)$ (Fuss's formula).

29.3. (a) Prove Steiner's theorem illustrated in Figure 29.6.

(b) Show that the centers of the circles, tangent to $\Gamma$ and $\gamma$, lie on an ellipse whose foci are the centers of $\Gamma$ and $\gamma$.

29.4. * Given a generic triple of lines $\ell_1, \ell_2, \ell_3$, how many triples of circles $C_1, C_2, C_3$ are there such that every two circles are externally tangent to each other, and $C_1$ is tangent to $\ell_2$ and $\ell_3$, $C_2$ to $\ell_3$ and $\ell_1$, and $C_3$ to $\ell_1$ and $\ell_2$?

29.5. The original Malfatti problem asked to inscribe three non-overlapping circles into a given triangle such that the sum of their areas is greatest possible. Malfatti assumed that this maximum is attained when each circle touches the other two. Prove that this assumption is wrong.

*Hint.* Consider an equilateral triangle.

*Comment.* A complete solution to this extremum problem was published as late as 1992 [**92**].

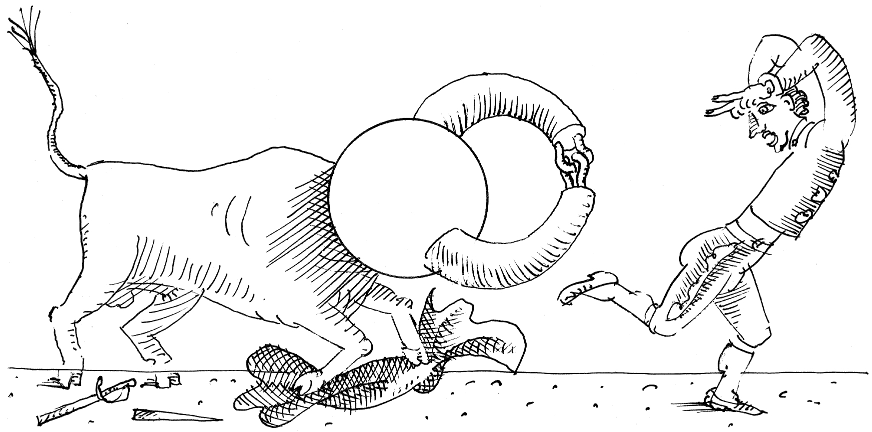

LECTURE 30

# Gravitational Attraction of Ellipsoids

In this last lecture we use freely physical terminology, assuming from the reader some basic knowledge of physics along with common sense. For example, a function is called a *potential* for a field of forces if the force vector is the gradient of this function; an *equipotential surface* is a level surface of a potential function, etc. Needless to say, the gravitational attraction is proportional to the masses and inverse proportional to the squared distance between the bodies, and likewise for the Coulomb attraction/repulsion of electrical charges.

**30.1 No gravity in a cavity.** I. Newton, one of the creators of mathematical analysis, was a great master of geometrical arguments. His main book, *Philosophiae Naturalis Principia Mathematica (Mathematical Principles of Natural Philosophy)* [**55**], is full of geometrical figures and is almost entirely devoid of formulas. Theorem 30 (Proposition 70) of Section 12 "The attractive forces of spherical bodies" from *Principia* states:

"If toward each of the separate points of a spherical surface there tend equal centripetal forces decreasing as the squares of the distances from the point, I say that a corpuscle placed inside the surface will not be attracted by these forces in any direction."

In other words, there is no gravity inside a uniform sphere (or rather, infinitesimally thin spherical shell).

Here is (slightly modified) Newton's proof (cf. Lecture 29). Let $P$ be a point inside the sphere. Consider an infinitesimal cone with vertex $P$. The intersection of the sphere and the cone consists of two infinitesimal domains $A$ and $B$, see Figure 30.1. Let us show that the forces of gravitational attraction exerted at $P$ by these two domains cancel each other.

The attraction forces from $P$ to the domains $A$ and $B$ are proportional to their masses, that is, their areas, and inverse proportional to the squares of their distances to $P$. The axis of the cone makes equal angles with the sphere. Therefore the two infinitesimal cones with the common vertex at $P$ are similar, and the ratios

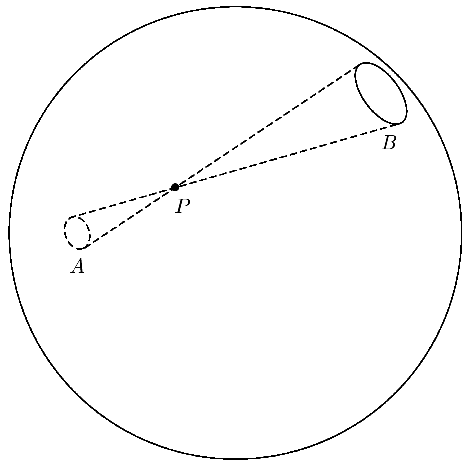


FIGURE 30.1. The attraction forces at point $P$ cancel each other

of the areas of their bases to the squares of the distances to $P$ are equal. Hence the attraction forces at $P$ are equal and have opposite directions. To quote Newton once again:

"Accordingly, body $P$ is not impelled by these attractions in any direction. Q.E.D."

Two remarks are in order. First, the same argument proves that there is no gravitational force inside a spherical shell of any width: it is made of infinitely thin shells, and for each of them the gravitational force vanishes. Secondly, the electric force inside a uniformly charged sphere vanishes as well: the Coulomb force is also subject to the inverse square law.

**30.2 Attraction outside a sphere.** Next, Newton considers the attraction force outside a homogeneous sphere. Theorem 31 (Proposition 71) states:

"With the same conditions being supposed as in prop. 70, I say that a corpuscle placed outside the spherical surface is attracted to the center of the sphere by a force inversely proportional to the square of its distance from the same center ".

That is, a uniform sphere attracts as a mass-point of equal total mass placed in the center.

Newton's proof is again geometrical, but rather involved; we shall give a different, more transparent and more conceptual, argument.

Consider the motion of non-compressible fluid toward a sink located at the origin $O$. The flow lines are radial, and the flux through any sphere, centered at $O$, is the same. The surface area of a sphere of radius $r$ is $4\pi r^2$. Hence the speed of fluid, as a function of the distance from the origin, is proportional to $r^{-2}$. Conclusion: the velocity field of spherically symmetric non-compressible fluid toward a sink is the same as the gravitational force field of a mass point.

The gravitational force field of any mass distribution is the sum of the forces exerted by the individual masses. It follows that the gravitational force field of any mass distribution has the same non-compressible property: the flux through the boundary of any domain that does not contain masses is zero.[1]

Back to the gravitational attraction of a uniform sphere centered at point $O$. Due to the spherical symmetry, the force at a test point $P$ depends only on the distance $PO$ and has the radial direction. Moreover, the force field is non-compressible. The only non-compressible spherically symmetric radial field is the field of gravitational attraction of a mass point located at $O$. To see that the mass of this point equals the total mass of the sphere, it suffices to compare the fluxes of the two fields through a sufficiently large sphere centered at $O$.

Both results, Newton's Theorems 30 and 31, hold in space of any dimension $n$, provided the attraction force of points at distance $r$ is proportional to $r^{1-n}$.

**30.3 Free distribution of charge.** Drop charged liquid on a closed conducting surface, and the charge will freely distribute on the surface. For example, for a sphere, this free distribution of charge is uniform.

Free distribution of charge has two properties. First, the potential on the surface itself is constant. This is obvious: a difference of potential at two points would cause the charged liquid to move from one point to another.

Secondly, the electric force inside the surface vanishes or, equivalently, the potential is constant. Indeed, assume that the potential is not constant. Being constant on the boundary surface, it attains either minimum or maximum at an interior point, say, $P$. Consider a small equipotential surface surrounding $P$. Then the electric force field enters (or exists) this surface, in contradiction to the fact that the force field is non-compressible.

This argument provides an alternative proof of Newton's theorem that the gravitational force inside a uniform sphere vanishes. Of course, we rely on a physical common sense here (for example, the existence of a unique free distribution of charge is a mathematically complicated matter!)

**30.4 Homeoids.** A *homeoid* is a domain between two homothetic ellipsoids with a common center.

THEOREM 30.1. *The gravitational force inside an infinitely thin homeoid is zero.*

Proof. First, consider an infinitesimally thin spherical shell. We know from Section 30.1 that the attraction force at a test point $P$ is zero, see Figure 30.2. Denote by $v$ and $V$ the volumes obtained by intersecting an infinitesimal cone with vertex $P$ and the shell, and by $r$ and $R$ the distances from $P$ to the sphere along the axis of the cone. Since the attraction force vanishes, $v/r^2 = V/R^2$.

A homeoid is obtained from a spherical shell by an affine transformation, a stretching in three pairwise orthogonal directions with different coefficients, see Figure 30.2. Denote the respective volumes and distances by $v', V', r', R'$. An affine transformation preserves the ratio of volumes and the ratio of collinear segments: $V'/v' = V/v, R'/r' = R/r$. It follows that $v'/(r')^2 = V'/(R')^2$, that is, the attraction forces at point $P'$ cancel each other. □

Thus the potential inside an infinitely thin (and hence, a finitely thin) homeoid is constant. Consider the distribution of charge on an ellipsoid whose density is

[1] In other words, the field is divergence free.

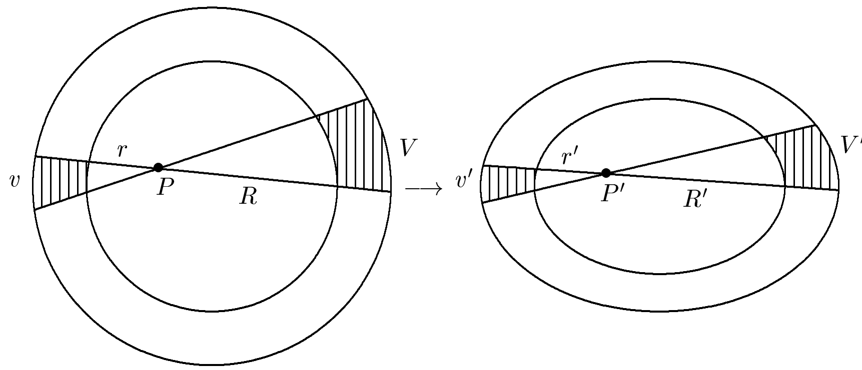


FIGURE 30.2. The attraction force inside a homeoid is zero

proportional to the width of the infinitely thin homeoid. For this distribution, the potential inside and on the ellipsoid is constant. Hence this is the free distribution of charge.

**30.5 Arnold's theorem.** Consider a smooth closed surface $M$ given by a polynomial $f(x, y, z) = 0$ of degree $n$. For example,

$$ax^4 + by^4 + cz^4 = 1$$

is the equation of a surface of degree 4. A point $P$ is called *interior* with respect to the surface $M$ if every line through $P$ intersects $M$ exactly $n$ times (of course, the number of intersections cannot exceed $n$). Figure 30.3 depicts two curves of degree 4; the interior points of the first one lie inside the inner-most oval, and the second curve has no interior points at all.

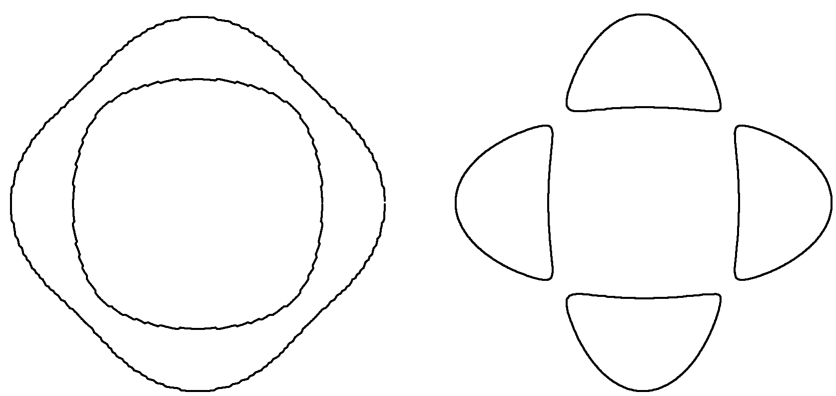

FIGURE 30.3. Two curves of degree four: one has interior points and the other does not

Consider the distribution of charge on surface $M$, whose density is proportional to the width of the infinitesimal shell between $M$ and the surface $M_\varepsilon = \{f(x, y, z) = \varepsilon\}$. This is a generalization of the homeoid density discussed in Section 30.4. Let $P$ be an interior point. The sign of the charge alternate: it is positive on the component of $M$, closest to $P$, negative on the next component, positive on the next, etc.

THEOREM 30.2. *The attraction force exerted by $M$ at point $P$ is equal to zero.*

Proof. As before, consider an infinitesimal cone with vertex at $P$ and axis $\ell$. The intersection of the cone with the shell between $M$ and $M_\varepsilon$ consists of $n$ domains, and we shall prove that their attractions at point $P$ cancel out.

Consider one of these domains, and let $Q$ be its point. Let $h$ be the length of the (infinitesimal) segment of $\ell$ inside the domain, and set $r = PQ$, see Figure 30.4. The volume of the domain equals $h$ times the area of the orthogonal section of the cone at point $Q$. The latter area is proportional to $r^2$. Therefore the domain exerts an attraction force at $P$ proportional to $r^2h/r^2 = h$. Thus we need to prove that the sum of signed lengths of the (infinitesimal) segments of the line $\ell$ between $M$ and $M_\varepsilon$ equals zero.

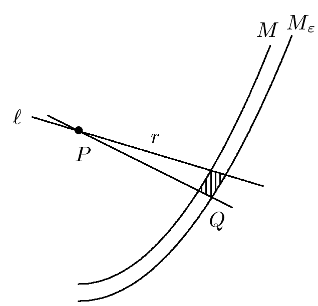


FIGURE 30.4. Computing the force exerted by domain $Q$ at point $P$

The latter is a one-dimensional statement: we can forget about the ambient space and restrict the polynomial $f$ on the line $\ell$. What we get is a polynomial of one variable, $f(x)$.

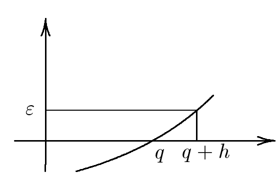


FIGURE 30.5. Computing the width of the infinitesimal shell

Let us express $h$ in terms of $f$. Consider Figure 30.5: $f(q) = 0, f(q+h) = \varepsilon$. One has: $f(q+h) = f(q) + hf'(q)$ (we ignore terms of order $h^2$ and higher), and hence $h = \varepsilon/|f'(q)|$. We need however to sum up with correct signs. We claim that, the signs taken into account, what we need to prove is the identity:

$$\frac{1}{f'(q_1)} + \frac{1}{f'(q_2)} + \cdots + \frac{1}{f'(q_n)} = 0 \tag{30.1}$$

where the sum is taken over all roots of a polynomial $f(x)$ of degree $n$.

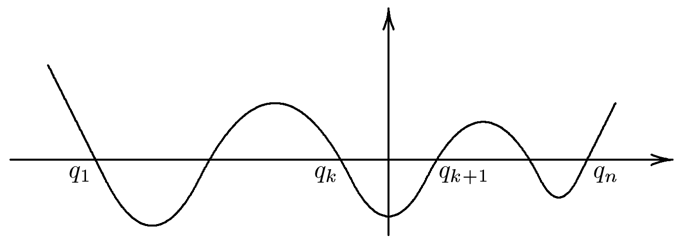


FIGURE 30.6. Sign bookkeeping

Indeed, the signs of derivatives at consecutive roots alternate, see Figure 30.6, and so do the signs of the charges. Let $q_1 < \cdots < q_k$ be the roots to the left of point $P$, and $q_{k+1} < \cdots < q_n$ to the right of it. To fix ideas, assume that $f'(q_{k+1}) > 0$. Then the total (positive) attraction force exerted by points $q_{k+1}, \cdots, q_n$ is $1/f'(q_{k+1}) + \cdots + 1/f'(q_n)$. Likewise, $f'(q_k) < 0$. The total (negative) attraction force exerted by points $q_1, \cdots, q_k$ is $1/f'(q_1)+\cdots+f'(q_k)$. Summing up the two yields (30.1).

Let us prove identity (30.1). Recall that all roots of $f$ are real: $f(x) = (x - q_1)\cdots(x - q_n)$. It follows that

$$f'(x) = (x - q_2)\cdots(x - q_n) + (x - q_1)(x - q_3)\cdots(x - q_n) + \cdots$$
$$+(x - q_1)(x - q_2)\cdots(x - q_{n-1}),$$

and hence $f'(q_i) = (q_i - q_1)(q_i - q_2)\cdots(q_i - q_n)$ (of course, the term $q_i - q_i$ is omitted). Then (30.1) is equivalent to the identity

$$\frac{1}{(q_1 - q_2)(q_1 - q_3)\cdots(q_1 - q_n)} + \frac{1}{(q_2 - q_1)(q_2 - q_3)\cdots + (q_2 - q_n)} + \cdots$$

$$+\frac{1}{(q_n - q_1)\cdots(q_n - q_{n-1})} = 0. \tag{30.2}$$

It remains to prove (30.2). Consider the polynomial of degree $n - 1$:

$$g(x) = \frac{(x - q_2)(x - q_3)\cdots(x - q_n)}{(q_1 - q_2)(q_1 - q_3)\cdots(q_1 - q_n)} + \frac{(x - q_1)(x - q_3)\cdots(x - q_n)}{(q_2 - q_1)(q_2 - q_3)\cdots + (q_2 - q_n)} + \cdots$$
$$+\frac{(x - q_1)(x - q_2)\cdots(x - q_{n-1})}{(q_n - q_1)\cdots(q_n - q_{n-1})}.$$

One has: $g(q_1) = g(q_2) = \cdots = g(q_n) = 1$. If a polynomial of degree $n - 1$ has $n$ roots then this polynomial is identically zero. Therefore $g(x) \equiv 1$. In particular, the leading term of $g(x)$ is equal to zero, and this is precisely identity (30.2). □

**30.6 Attraction outside a homeoid: Ivory's theorem.** We proved that the attraction force inside a homogeneous homeoid equals zero. What about its exterior? The answer was found by James Ivory early in the 19-th century.

An ellipsoid $M_0$

$$\frac{x^2}{a^2} + \frac{y^2}{b^2} + \frac{z^2}{c^2} = 1$$

includes into a 1-parameter family of quadratic surfaces $M_\lambda$

$$\frac{x^2}{a^2+\lambda}+\frac{y^2}{b^2+\lambda}+\frac{z^2}{c^2+\lambda}=1,$$

called confocal quadrics, see Lecture 28. Depending on the value of the parameter $\lambda$, this can be an ellipsoid, a hyperboloid of one sheet or a hyperboloid of two sheets.

THEOREM 30.3. *The equivipotential surfaces of the free distribution of charge on an ellipsoid are the confocal ellipsoids.*

Proof. The proof is based on a lemma due to Ivory. Consider two confocal ellipsoids, $M_0$ and $M_\lambda$. The latter is obtained from the former by an affine transformation stretching along the three coordinate axis:

$$A:(x,y,z)\mapsto(X,Y,Z)=\left(\frac{a'}{a}x,\frac{b'}{b}y,\frac{c'}{c}z\right) \tag{30.3}$$

where

$$a'=\sqrt{a^2+\lambda},\ b'=\sqrt{b^2+\lambda},\ c'=\sqrt{c^2+\lambda}.$$

We shall refer to $(x,y,z)$ and $(X,Y,Z)$ as the corresponding points.

LEMMA 30.1. *Let $P,Q$ be two points on an ellipsoid $M_0$ and $P',Q'$ the corresponding points on $M_\lambda$. Then $|PQ'|=|P'Q|$ (see Figure 30.7).*

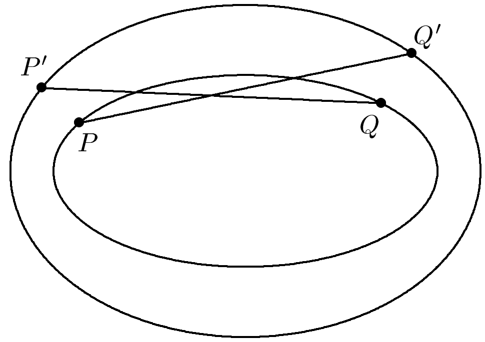


FIGURE 30.7. Ivory's lemma

Proof of Lemma. The proof is computational. Let $P=(x,y,z),Q=(u,v,w)$ and $P'=(X,Y,Z),Q'=(U,V,W)$. Then

$$|PQ'|^2=|P|^2+|Q'|^2-2P\cdot Q',\quad |P'Q|^2=|P'|^2+|Q|^2-2P'\cdot Q.$$

Note that $P\cdot Q'=P'\cdot Q$, as readily follows from (30.3). What remains to prove is

$$|P'|^2-|P|^2=|Q'|^2-|Q|^2.$$

Indeed, the left-hand side equals

$$\left[\left(\frac{a'}{a}\right)^2-1\right]x^2+\left[\left(\frac{b'}{b}\right)^2-1\right]y^2+\left[\left(\frac{c'}{c}\right)^2-1\right]z^2=\lambda\left(\frac{x^2}{a^2}+\frac{y^2}{b^2}+\frac{z^2}{c^2}\right)=\lambda,$$

and likewise for the right-hand side. □

Now we can complete the proof of Ivory's Theorem. Consider two infinitesimally thin confocal homeoids of equal volumes, $M_0$ and $M_\lambda$. Let $P$ and $P'$ be a pair of corresponding points on them. Then *the potential exerted by* $M_0$ *at point* $P'$ *equals the potential exerted by* $M_\lambda$ *at point* $P$.

Indeed, let $Q$ and $Q'$ be a pair of corresponding points. Consider an infinitesimal volume at $Q$ and an equal volume at $Q'$. By Lemma 30.1, the contribution of the former volume to the potential at point $P'$ equal the contribution of the latter volume to the potential at point $P$. Since this holds for all pairs of corresponding points $Q, Q'$, the statement follows.

Thus the potential exerted by $M_0$ at any point $P'$ of $M_\lambda$ equals the potential exerted by $M_\lambda$ at the corresponding point $P$ of $M_0$. But the potential inside a uniform homeoid $M_\lambda$ is constant. Therefore the potential exerted by $M_0$ at every point of $M_\lambda$ is the same. □

Let us mention, in conclusion, that Newton's and Ivory's theorems on gravitational attractions of quadratic surfaces have elegant magnetic analogs, discovered by V. Arnold, see [**4**]. Consider a conducting hyperboloid of one sheet and assume that there is a voltage drop between its ends at infinity. This voltage drop induces an electric current along the meridians of the hyperboloid. The claim is that *the magnetic field of this current inside the hyperboloid is zero, and outside the hyperboloid the magnetic field is directed along its parallels.*

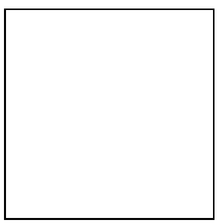

John Smith
January 23, 2010

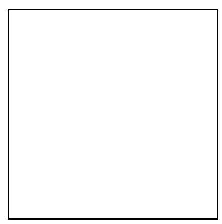

Martyn Green
August 2, 1936

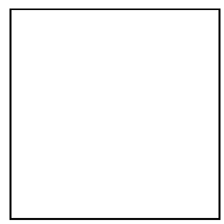

Henry Williams
June 6, 1944

### 30.7 Exercises.

30.1. Let $x_1, \dots, x_{n+1}$ and $a_1, \dots, a_{n+1}$ be two sets of distinct real numbers. Construct a polynomial of degree not greater than $n$ that takes value $a_i$ at point $x_i$. How many such polynomials are there?

30.2. Let $f(x)$ be a polynomial of degree $n$ with $n$ distinct real roots $q_1, \dots, q_n$. Prove that

$$\frac{q_1^k}{f'(q_1)} + \dots + \frac{q_n^k}{f'(q_n)} = 0$$

for $k = 0, 1, \dots, n-2$, and

$$\frac{q_1^{n-1}}{f'(q_1)} + \dots + \frac{q_n^{n-1}}{f'(q_n)} = 1.$$

30.3. Prove that the conclusion of Theorem 30.2 still holds if the density of the charge is multiplied by an arbitrary polynomial $\phi(x, y, z)$ of degree $n-2$ or less.

*Comment*: a generalization, due to A. Givental [**36**], states that if the density of the charge is multiplied by a polynomial of degree $m$ then the potential at the interior points is given by a polynomial of degree not greater than $m+2-n$.

30.4. A harmonic function $f(x, y)$ is a function satisfying the equality

$$\frac{\partial^2 f}{\partial x^2} + \frac{\partial^2 f}{\partial y^2} = 0$$

(for example, $x^2 - y^2$ or $\ln(x^2 + y^2)$).

(a) Prove that a harmonic function has neither local minima nor maxima.

(b) Prove that a level curve of a smooth harmonic function cannot be a simple closed curve.

(c) Prove that the following polynomials of degree $n$ are harmonic:

$$P_n(x) = \sum_{k \equiv n (mod 2)} (-1)^{\frac{n-k}{2}} \binom{n}{k} x^k y^{n-k}$$

and

$$Q_n(x) = \sum_{k+1 \equiv n (mod 2)} (-1)^{\frac{n-k-1}{2}} \binom{n}{k} x^k y^{n-k}.$$

These polynomials are the real and the imaginary parts of $(x + iy)^n$.

(d) Prove that every homogeneous harmonic polynomial of degree $n$ has the form $aP_n(x) + bQ_n(x)$ where $a$ and $b$ are real numbers.

30.5. Prove that any finite configuration of positive and negative charges cannot be stable.

*Hint*. The Coulomb potential is a harmonic function.

30.6. A polynomial equation $p(x, y) = 0$ determines an algebraic curve; an oval of the algebraic curve is a simple closed smooth curve satisfying this equation (see Lecture 10 for ovals of cubic curves).

(a) We saw in Lecture 17 that a curve of degree 4 may have four ovals. Prove that it cannot have five ovals.

*Hint*. A curve of degree 4 has at most 8 intersections with a generic conic.

(b) Show that at most two ovals of a curve of degree 4 or 5 are nested, and that if there are two nested ovals then there are no other ovals.

*Hint*. Consider the intersection with a line.

(c) What is the greatest number of pairwise nested ovals that a curve of degree $n$ may have?

*Comment*. The greatest number of components of an algebraic curve of degree $n$ in the projective plane is $(n^2 - 3n + 4)/2$ (Harnack's theorem). Hilbert's Sixteen problem asks to classify possible mutual positions of the ovals of algebraic curves.

30.7. Given two confocal ellipses, let $A$ be an affine transformation as in (30.3) that takes the first to the second. Prove that any point $P$ and its image $A(P)$ lie on a hyperbola, confocal with the ellipses.

30.8. Given a convex polyhedron, consider the vectors orthogonal to its faces whose magnitudes are equal to the areas of the faces. Prove that the sum of these vectors is zero.

*Hint*. Under orthogonal projection from one plane to another, the area is multiplied by the cosine of the angle between the planes.

*Comment*. The claim is physically obvious: the vectors in question are the pressures exerted by the air inside the polyhedron on its faces.

# Solutions to Selected Exercises

*LECTURE 1*

1.4. If $r = 0$, then

$$\alpha = [a_0; a_1, \dots, a_{d-1}, \alpha]$$

which can be rewritten as

$$\alpha = \frac{A\alpha + B}{C\alpha + D}, \qquad C\alpha^2 + (D - A)\alpha - B = 0.$$

To consider the general case, remark that if $\gamma$ is a root of quadratic equation $Kx^2 + Lx + M = 0$, then $a + \frac{1}{\gamma}$ is a root of a quadratic equation $Mx^2 + (L - 2aM)x + (Ma^2 - La + K) = 0$. If $\alpha$ is a periodic continued fraction with $r \neq 0$, then

$$\alpha = [a_0; a_1, \dots, a_{r-1}, \beta]$$

where $\beta$ is a periodic continued fraction with $r = 0$. Hence, $\beta$ is a root of a quadratic equation with integer coefficients, and $\beta_{r-1} = a_{r-1} + \frac{1}{\beta}$, $\beta_{r-2} = a_{r-2} + \frac{1}{\beta_{r-1}}, \dots, \beta_1 = a_1 + \frac{1}{\beta_2}, \alpha = a_0 + \frac{1}{\beta_1}$ are all roots of quadratic equations with integer coefficients.

1.5. See [**56**], Chapter 4.

1.6.

$$\begin{aligned} \sqrt{3} &= [1; 1, 2, 1, 2, 1, 2, \dots] \\ \sqrt{5} &= [2; 4, 4, 4, 4, \dots] \\ \sqrt{n^2+1} &= [n; 2n, 2n, 2n, 2n, \dots] \\ \sqrt{n^2-1} &= [n-1; 1, 2(n-1), 1, 2(n-1), 1, 2(n-1), 1, \dots] \end{aligned}$$

1.9. First notice that for any real $\gamma \neq 0$ and any integer $a$, the numbers $\gamma$ and $a + \frac{1}{\gamma}$ are related:

$$a + \frac{1}{\gamma} = \frac{a\gamma + 1}{\gamma + 0}, \quad a \cdot 0 - 1 \cdot 1 = -1.$$

If the continued fractions $\alpha$ and $\beta$ are almost identical, then

$$\alpha = [a_0; a_1, \dots, a_{m-1}, \gamma], \quad \beta = [b_0; b_1, \dots, b_{n-1}, \gamma].$$

Hence $\gamma$ is related to $\alpha_{m-1} = a_{m-1} + \frac{1}{\gamma}$, $\alpha_{m-2} = a_{m-2} + \frac{1}{\alpha_{m-1}}$, $\alpha_1 = a_1 + \frac{1}{\alpha_2}$, $\alpha = \frac{1}{\alpha_1}$ and also to $\beta_{n-1} = b_{n-1} + \frac{1}{\gamma}$, $\beta_{n-2} = b_{n-2} + \frac{1}{\beta_{n-1}}, \dots, \beta_1 = b_1 + \frac{1}{\beta_2}$, $\beta = b_0 + \frac{1}{\beta_1}$. Hence, $\alpha$ and $\beta$ are related. (We constantly use implicitly Exercise 1.8.)

1.10. **Lemma.** *If $\alpha$ and $\beta$ are related, then $\beta$ can be obtained from $\alpha$ by a sequence of operations $\gamma \mapsto -\gamma,\ \gamma \mapsto \gamma+1,\ \gamma \mapsto \dfrac{1}{\gamma}$.*

Proof of Lemma. Let $\alpha = \dfrac{a\beta+b}{c\alpha+d}$, $ad-bc=\pm 1$. Changing, if necessary, the sign of $\alpha$, we can assume that $a \geq 0,\ c \geq 0$. Then we follow the Euclidean algorithm for $(a,c)$: if $a = pc+q,\ 0 \leq q < c$, we change $\alpha$ into $\alpha - p$ (that is, $\alpha \mapsto -\alpha \mapsto -\alpha+1 \mapsto \ldots \mapsto -\alpha+p \mapsto \alpha - p$, and get $\dfrac{q\beta+r}{c\beta+d}$ where $r = b-pd$; obviously, $qd - rc = ad-bc = \pm 1$. We turn this into $\dfrac{c\beta+d}{q\beta+r}$, and so on. We arrive at $\dfrac{k\beta+\ell}{0\cdot\beta+m}$ with $km - 0\cdot\ell = \pm 1$ which implies $k=\pm 1, m = \pm 1$. Thus, $\alpha$ is reduced by our operations to $\pm\beta\pm\ell$, which, obviously, can be reduced by our operations to $\beta$. $\square$

To finish the proof of the statement of Exercise 1.10, we need only to observe that the continued fraction for each of $-\alpha, \alpha+1, \dfrac{1}{\alpha}$ is almost equal to that of $\alpha$ (see Exercise 1.2 for $-\alpha$).

1.11. Let $\alpha = [a_0; a_1, a_2, \ldots]$ be not related to the golden ratio. This means that there are infinitely many $a_n \geq 2$.

*Case* 1: infinitely many $a_n \geq 3$. Then the indicators of quality of corresponding convergent are $a_n + \cdots > 3 > \sqrt{8}$.

Let $a_n \leq 2$ for $n$ large.

*Case* 2: infinitely many $a_n = 1$. Then there are infinitely many $n$ with $a_n = 2, a_{n+1} = 1$. The indicators of quality of the corresponding convergents are $2 + \dfrac{1}{1+\ddots} + \dfrac{1}{a_{n-1}+\ddots} > 2 + \dfrac{1}{2} + \dfrac{1}{3} = \dfrac{17}{6} > \sqrt{8}$.

There remains

*Case* 3: $a_n = 2$ for $n$ large. Then the limit of the indicators of quality of the convergents is $[2;2,2,2,\ldots]+[0;2,2,2,\ldots] = 1+\sqrt{2}+\dfrac{1}{1+\sqrt{2}} = \sqrt{2}+1+(\sqrt{2}-1) = 2\sqrt{2} = \sqrt{8}$.

1.12. We use the notation of the previous solution.

*Case* 1: infinitely many $a_n \geq 3$. The indicators of quality of the corresponding convergents are $> 3 > \sqrt{\dfrac{221}{25}}$.

Since $\alpha$ is not related to the golden ratio and to $\sqrt{2}$, we can assume that, for $n$ large, $a_n \leq 2$ and there are infinitely many fragments $\{1,2\}$ in the sequence $\{a_n\}$.

*Case* 2: there are infinitely many fragments $\{1,2,1\}$ in the sequence $\{a_n\}$. The indicators of quality of the corresponding convergents will be greater than

$$2 + \frac{1}{1+\ddots} + \frac{1}{1+\ddots} > 3 > \sqrt{\frac{221}{25}}.$$

Let there be finitely many fragments $\{1,2,1\}$.

*Case* 3: there are infinitely many fragments $\{2,1,2\}$. Then there are infinitely many fragments $\{2,2,1,2,2\}$. Hence, infinitely many convergents have indicators of quality

$$2+\cfrac{1}{2+\ddots}+\cfrac{1}{1+\cfrac{1}{2+\cfrac{1}{2+\ddots}}}>2+\frac{1}{3}+\cfrac{1}{1+\cfrac{1}{2+\frac{1}{3}}}=2+\frac{1}{3}+\frac{7}{10}>3>\sqrt{\frac{221}{25}}$$

Let there be also finitely many fragments $\{2,1,2\}$.

*Case* 4: there are infinitely many fragments $\{2,2,2\}$. Then there are infinitely many fragments $\{a,1,1,2,2,2,2,b\}$ with $a\le 2,\ b\le 2$. Hence, there are infinitely many convergents with the indicators of quality of the form

$$\begin{aligned}2+\cfrac{1}{1+\cfrac{1}{1+\cfrac{1}{a+\ddots}}}+\cfrac{1}{2+\cfrac{1}{2+\cfrac{1}{b+\ddots}}}&>2+\cfrac{1}{1+\cfrac{1}{1+\frac{1}{3}}}+\cfrac{1}{2+\cfrac{1}{2+\frac{1}{3}}}\\&=2+\frac{4}{7}+\frac{7}{17}>\sqrt{\frac{221}{25}}\end{aligned}$$

Let there be also finitely many fragments $\{2,2,2\}$.

*Case* 5: there are infinitely many fragments $\{1,1,1\}$. Then there are infinitely many fragments $\{1,1,1,2,2,1,1\}$ and hence infinitely many convergents with the indicators of quality greater than

$$2+\cfrac{1}{1+\cfrac{1}{1+\frac{1}{2}}}+\cfrac{1}{2+\cfrac{1}{1+\frac{1}{2}}}=2+\frac{3}{8}+\frac{3}{5}>\sqrt{\frac{221}{25}}$$

In this case, $\alpha$ is related to $[2;2,1,1,2,2,1,1,\dots]=\dfrac{9+\sqrt{221}}{10}$.

There remains

*Case* 6: the continued fraction is periodic with the period $\{1,1,2,2\}$. In this case, the indicators of quality of the convergents corresponding to the incomplete fractions 1 are too low to consider, the indicators of quality of the convergents corresponding to the incomplete fractions 2 have the limit equal to

$$\begin{aligned}[2;2,1,1,2,2,1,1,\dots]\quad&+[0;1,1,2,2,1,1,2,2,\dots]\\&=\frac{9+\sqrt{221}}{10}+\frac{-9+\sqrt{221}}{10}=\sqrt{\frac{221}{25}}\end{aligned}$$

1.13. For the numbers provided in the hint, the limits of indicators of quality of the convergents corresponding to the incomplete fractions 2 is $2+[0;1,1,1,1,\dots]+[0;2,1,1,1,\dots]=2+\dfrac{\sqrt5-1}{2}+\dfrac{3-\sqrt5}{2}=3$.

1.15. The largest number with all incomplete fractions $\le n$ is, obviously,

$$[n;1,n,1,n,1,n,\dots]=\frac{n+\sqrt{n^2+4n}}{2}.$$

Hence, the maximal possible limit of indicators of quality of an infinite sequence of convergents is $[n;1,n,1,n,\dots]+[0;1,n,1,n,1,n,\dots]=\sqrt{n^2+4n}$. Thus, $\lambda_n=\sqrt{n^2+4n}$.

*LECTURE 2.*

2.3. let $m_{99}, m_{98}, \dots, m_1, m_0$ and $n_{99}, n_{98}, \dots, n_1, n_0$ be the digits of $m$ and $n$ in the numerical system with the base 2. According to the Kummer Theorem, $\binom{m+n}{n}$ is even if and only if there is at least one carry-over in the addition $m+n$, that is, if at least one of the pairs $(m_i, n_i)$ is $(1,1)$. Thus, there are 3 possibilities for each pair $(m_i, n_i)$, which shows that the total amount of pairs $(m, n)$ with $0 \le m < 2^{100}$, $0 \le n < 2^{100}$, with $\binom{m+n}{n}$ odd is $3^{100}$, which is

$$\frac{3^{100}}{4^{100}} \approx 3.21 \cdot 10^{-13}$$

of all numbers $\binom{m+n}{n}$.

2.4. We use the notations $m_i, n_i$ from the previous solution. According to the Kummer Theorem, $\binom{m+n}{n}$ is not divisible by 4 if and only if there is at most one carry-over in the addition $m+n$. In other words, there should be either no pairs $(1,1)$ at all, and we already know that there are $3^{100}$ such pairs $(m, n)$, or, the only such pair is $(m_{99}, n_{99})$, or, for some $k \le 98$, one must have $(m_{k+1}, n_{k+1}) = (0,0)$, $(m_k, n_k) = (1,1)$ with all other $(m_i, n_i)$ different from $(1,1)$. Thus the total amount of numbers $\binom{m+n}{n}$ not divisible by 4 is $3^{100} + 3^{99} + 99 \cdot 3^{98} = 111 \cdot 3^{98} = 37 \cdot 3^{99}$, which is

$$\frac{37 \cdot 3^{99}}{4^{100}} \approx 3.96 \cdot 10^{-12}$$

of all numbers $\binom{m+n}{n}$.

2.6. (a) $\binom{2n}{2} - \binom{n}{1} = \frac{2n(2n-1)}{2} - n = 2n(n-1)$ which is divisible by 8 if and only if $\frac{n(n-1)}{2} = \binom{n}{2}$ is even.

(b) $\binom{2n}{4} - \binom{n}{2} =$

$$\frac{2n(2n-1)(2n-2)(2n-3)}{24} - \frac{n(n-1)}{2} = \frac{2n^2(n-1)(n-2)}{3}.$$

This is not divisible by 8 if and only if $n$ is odd and $n-1$ is not divisible by 4, that is, $n \equiv 3 \bmod 4$.

2.7. (a) $\binom{3n}{3} - \binom{n}{1} =$

$$\frac{3n(3n-1)(3n-2)}{6} - n = \frac{n}{2}[(3n-1)(3n-2) - 2] = \frac{9n^2(n-1)}{2}.$$

This is not divisible by 27 if and only if neither $n$, nor $n-1$ is divisible by 3, that is, $n \equiv 2 \bmod 3$.

(b) $\binom{3n}{6} - \binom{n}{2}$

$$\begin{aligned} &= \frac{3n(3n-1)(3n-2)(3n-3)(3n-4)(3n-5)}{720} - \frac{n(n-1)}{2} \\ &= \frac{n(n-1)}{80}[(3n-1)(3n-2)(3n-4)(3n-5) - 40] \\ &= \frac{9n^2(n-1)(n-2)(9n^2-18n+13)}{80} \end{aligned}$$

which is always divisible by 27.

2.8. (a) This follows from the Newton formula

$$(1+y)^r = 1 + ry + \frac{r(r-1)}{2!}y^2 + \frac{r(r-1)(r-2)}{3!}y^3 + \dots$$

(which holds for any real $r$ and any $y$ with $|y| < 1$). Put $y = -4x, r = -\frac{1}{2}$. We get $\frac{1}{\sqrt{1-4x}} =$

$$1 - \frac{1}{2}(-4x) + \frac{\left(-\frac{1}{2}\right)\left(-\frac{3}{2}\right)}{2!}(-4x)^2 + \frac{\left(-\frac{1}{2}\right)\left(-\frac{3}{2}\right)\left(-\frac{5}{2}\right)}{3!}(-4x)^3 + \dots$$

The term with $(-4x)^n$ is

$$\begin{aligned} &\frac{\left(-\frac{1}{2}\right)\left(-\frac{3}{2}\right)\dots\left(-\frac{2n-1}{2}\right)}{n!}(-4x)^n \quad = (-1)^n\frac{1\cdot 3\cdot 5\dots(2n-1)}{2^n n!}(-4x)^n \\ &= \frac{1\cdot 2\cdot 3\cdot\dots\cdot 2n}{2\cdot 4\cdot\dots\cdot 2n\cdot 2^n n!}4^n x^n = \frac{(2n)!}{2^n n!\cdot 2^n n!}4^n x^n = \binom{2n}{n}x^n. \end{aligned}$$

Thus,

$$\frac{1}{\sqrt{1-4x}} = \sum_{n=0}^{\infty}\binom{2n}{n}x^n.$$

(b) It follows from Part (a) that

$$\left(\sum_{n=0}^{\infty}\binom{2n}{n}x^n\right)\left(\sum_{n=0}^{\infty}\binom{2n}{n}x^n\right) = \frac{1}{4x-1} = 1 + 4x + (4x)^2 + (4x)^3 + \dots$$

Equate the terms with $x^n$:

$$\sum_{p+q=n}\binom{2p}{p}x^p\cdot\binom{2q}{q}x^q = (4x)^n,$$

that is, $\sum_{p+q=n}\binom{2p}{p}\binom{2q}{q} = 4^n$.

2.9. (a) One of many possible proofs:

$$\begin{aligned} C_n &= \frac{(2n)!}{n!(n+1)!} = \frac{1}{n(n+1)}\cdot\frac{(2n)!}{(n-1)!n!} = \left(\frac{1}{n} - \frac{1}{n+1}\right) \\ &= \frac{(2n)!}{n!n!} - \frac{(2n)!}{(n-1)!(n+1)!} = \binom{2n}{n} - \binom{2n}{n+1} \end{aligned}$$

(c) By (b), $(xC(x))' = \sum_{n=0}^{\infty} \binom{2n}{n} x^n = (1-4x)^{-\frac{1}{2}}$. Hence,

$$xC(x) = \int (1-4x)^{-\frac{1}{2}} dx = -\frac{1}{4} \cdot \frac{(1-4x)^{-\frac{1}{4}}}{\frac{1}{2}} + C = -\frac{\sqrt{1-4x}}{2} + C,$$

and since $0 \cdot C(0) = 0$, $C = \dfrac{1}{2}$. Thus

$$xC(x) = \frac{1}{2} - \frac{\sqrt{1-4x}}{2}, \text{ and } C(x) = \frac{1-\sqrt{1-4x}}{2x}.$$

(d) From the formula proved in Part (c), $C(x) = \dfrac{1-\sqrt{1-4x}}{2x}$, we deduce that $xC(x)^2 - C(x) + 1 = 0$. Since $C(x)^2 = \sum_{n=0}^{\infty} \left( \sum_{p+q=n} C_p C_q \right) x^n$, this implies

$$\sum_{n=0}^{\infty} \left( \sum_{p+q=n} C_p C_q \right) x^{n+1} - \sum_{n=0}^{\infty} C_n x^n + 1 = 0,$$

that is,

$$\begin{aligned} 0 &= \sum_{n=1}^{\infty} \left( \sum_{p+q=n-1} C_p C_q \right) x^n - 1 - \sum_{n=1}^{\infty} C_n x^n + 1 \\ &= \sum_{n=1}^{\infty} \left( \left( \sum_{p+q=n-1} C_p C_q \right) - C_n \right) x^n. \end{aligned}$$

Thus,

$$C_n = \sum_{p+q=n-1} C_p C_q \text{ for } n \geq 1.$$

(e) Apply induction on $n$. If $n = 0$ then our expression is just $a_1$ which does not involve any multiplications and has only $1 = C_0$ meaning. Assume that our statement is true for all products $a_1 * \cdots * a_{k+1}$ with $k < n$. Let $A$ be one of the meanings of the product $a_1 * \cdots * a_{n+1}$. Break $A$ at the multiplication performed last: $A = B * C$ where $B$ and $C$ are obtained from $a_1 * \cdots * a_k$ and $a_{k+1} * \cdots * a_{n+1}$ ($1 \leq k \leq n$ by specifying the order of multiplications. We see that the number of meanings for $a_1 * \cdots * a_{n+1}$ is

$$\sum_{k=1}^{n} C_{k-1} C_{n-k} = \sum_{p+q=n-1} C_p C_q = C_n.$$

(f) Apply induction on $n$. If $n = 3$ then the number of triangulations is $1 = C_1$. Assume that our statement is true for all convex $k$-gons with $k < n$. Let $P = A_1 A_2 \dots A_n$ and consider a triangulation of $P$. Let $A_1 A_2 A_k$ ($3 \leq k \leq n$) be the triangle of the triangulation that contains $A_1 A_2$. Then our triangulation is determined by triangulations of the $(k-1)$-gon $A_2 A_3 \dots A_k$ (which is nothing, if $k = 3$ and the $(n-k+2)$-gon $A_1 A_k A_{k+1} \dots A_n$. Thus, the number of triangulations of $P$ is

$$C_{n-3} + \sum_{k=4}^{n-1} C_{k-3} C_{n-k} + C_{n-3} = \sum_{p+q=n-3} C_p C_q = C_{n-2}.$$

*LECTURE 3*

3.1. Let $n = n_1 + \cdots + n_k$ be a partition from the left box, and let $n_i = m_i \cdot 2^{d_i}$ where $m_i$ is odd. Replace $n_i$ by $\underbrace{m_i + \cdots + m_i}_{2^{d_i}}$ and then reorder the summands in a non-decreasing order. We get a partition of $n$ from the right box.

Let $n = n_1 + \cdots + n_k$ be a partition from the right box. For an odd number $m$, let $r_m$ be the number of $m$'s in the partition. Let $r_m = 2^{d_{m,1}} + \cdots + 2^{d_{m,s}}$, $d_{m,1} > \cdots > d_{m,s} \geq 0$ (this is equivalent to the presentation of $r_m$ in the numerical system with the base 2). For every $m$, replace the group $\underbrace{m + \cdots + m}_{r_m}$ by $m \cdot 2^{d_{m,1}} + \cdots + m \cdot 2^{d_{m,s}}$ and then reorder the summands in the increasing order. We get a partition of $n$ from the left box.

These two transformations between partitions in the left box and partitions in the right box are inverse to each other.

3.2.

$$\frac{p^s}{p^s - 1} = \left(1 - \frac{1}{p^s}\right)^{-1} = 1 + \frac{1}{p^s} + \frac{1}{p^{2s}} + \frac{1}{p^{3s}} + \ldots$$

Hence,

$$\begin{aligned} \prod \left(\frac{p^s}{p^s - 1}\right) &= \prod \left(1 + \frac{1}{p^s} + \frac{1}{p^{2s}} + \ldots\right) \\ &= \sum_{k_2, k_3, k_5, \ldots} \frac{1}{(2^{k_2} 3^{k_3} 5^{k_5} \ldots)^s} = \sum_{n=1}^{\infty} \frac{1}{n^s}. \end{aligned}$$

3.3.

$$\begin{aligned} \mathbf{d}(2^{k_2} 3^{k_3} 5^{k_5} \ldots) &= \textstyle\sum_{0 \leq \ell_p \leq k_p} (2^{\ell_2} 3^{\ell_3} 5^{\ell_5} \ldots) \\ &= \prod_{p \in \{\text{primes}\}} (1 + p + p^2 + \cdots + p^{k_p}) = \prod_{p \in \{\text{primes}\}} \frac{p^{k_p + 1} - 1}{p - 1}. \end{aligned}$$

3.5. First,

$$-(kl + km + lm) = \frac{k^2 + l^2 + m^2 - (k + l + m)^2}{2} = \frac{k^2 + l^2 + m^2 - 1}{2} \geq 0.$$

Second, the residues of the squares modulo 8 are 0, 1, or 4, and $k^2 + l^2 + m^2 - 1$ cannot be 6 modulo 8.

3.8. We restrict ourselves to Parts (a) – (d); we hope that the reader will be able to reconstruct the solutions of the remaining parts.

LEMMA 30.2. *For every $k$,*

$$F_1 + F_2 + \cdots + F_k = F_{k+2} - 2.$$

Proof. Induction. For $k = 1$, it is true $(1 = 3 - 2)$. If $F_1 + F_2 + \cdots + F_k = F_{k+2} - 2$, then $F_1 + F_2 + \cdots + F_{k+1} = (F_1 + F_2 + \cdots + F_k) + F_{k+1} = F_{k+2} - 2 + F_{k+1} = F_{k+3} - 2$.

LEMMA 30.3. *For every $k$,*

$$\begin{aligned} F_1 + F_3 + \cdots + F_{2k-1} &= F_{2k} - 1, \\ F_2 + F_4 + \cdots + F_{2k} &= F_{2k+1} - 1. \end{aligned}$$

Proof. Induction. For $k = 1$ it is true $(1 = 2 - 1,\ 2 = 3 - 1)$. If $F_1 + F_3 + \cdots + F_{2k-1} = F_{2k} - 1$,, then $F_1 + F_3 + \cdots + F_{2k+1} = (F_1 + F_3 + \cdots + F_{2k-1}) + F_{2k+1} = F_{2k} - 1 + F_{2k+1} = F_{2k+2} - 1$. If $F_2 + F_4 + \cdots + F_{2k} = F_{2k+1} - 1$, then $F_2+F_4+\cdots+F_{2k+2} = (F_2+F_4+\cdots+F_{2k})+F_{2k+2} = F_{2k+1}-1+F_{2k+2} = F_{2k+3}-1$.

(a) Induction. For $n = 1$ it is true $(1 = F_1)$. Let it be true for all numbers less than $n$, and let $F_k$ be the largest Fibonacci number $\leq n$. If $F_k = n$, then $n = F_k$ is our partition; let $F_k < n$. According to the induction hypothesis, $n - F_k = F_{k_1} + \cdots + F_{k_s},\ k_1 < \cdots < k_s$. But $n < F_{k+1}$ implies $n - F_k < F_{k+1} - F_k = F_{k-1}$; hence $k_s < k - 1$, and $n = F_{k_1} + \cdots + F_{k_s} + F_k$ satisfies our requirements.

(b) The existence of a partition $n = F_{k_1} + \cdots + F_{k_s}$ with $k_i - k_{i-1} \geq 2$ is actually proved in Part (a): it is sufficient to include the condition $k_i - k_{i-1} \geq 2$ in the induction hypothesis. Let us prove the uniqueness. Let

$$F_{k_1} + \cdots + F_{k_s} = F_{\ell_1} + \cdots + F_{\ell_t}$$

be two different partitions of the same number with $k_i - k_{i-1} \geq 2$ for $1 < i \leq s$ and $\ell_j - \ell_{j-1} \geq 2$ for $1 < j \leq t$. If $F_{k_s} = F_{\ell_t}$, we cancel them, and we keep on canceling until the largest parts of the partition become different. So, we can assume that $k_s < \ell_t$. Then

$$\begin{aligned} F_{k_1} + \cdots + F_{k_s} \quad &\leq F_{k_s} + F_{k_s-2} + \cdots + (F_2 \text{ or } F_1) \\ &= F_{k_s+1} - 1 < F_{k_s+1} \leq F_{\ell_t} \\ &\leq F_{\ell_1} + \cdots + F_{\ell_t} \end{aligned}$$

(we use Lemma 30.3); a contradiction.

(c) Let $n = F_{k_1} + \cdots + F_{k_s}$ be some partition as in (a). If for some $i$, $i > 1$ and $k_i > k_{i-1} + 2$, or $i = 1$ and $k_1 > 2$, then we replace $F_{k_i}$ by $F_{k_i-2} + F_{k_i-1}$. We get another partition as in (a), with a bigger number of parts. If the condition in (c) is still not satisfied, we apply the same trick again, and the process must stop at some moment, since the number of summands cannot grow infinitely. This prove the existence of a partition with the required property; let us prove that it is unique.

Let

$$F_{k_1} + \cdots + F_{k_s} = F_{\ell_1} + \cdots + F_{\ell_t}$$

be two different partitions of the same number with $k_1 \leq 2$, $\ell_1 \leq 2$, $k_i - k_{i-1} \leq 2$ for $1 < i \leq s$, and $\ell_j - \ell_{j-1} \leq 2$ for $1 < j \leq t$. As in Solution of (b), we may assume that $k_s < \ell_t$. Then

$$\begin{aligned} F_{k_1} + \cdots + F_{k_s} \quad &\leq F_1 + F_2 + \cdots + F_{k_s} = F_{k_s+2} - 2 \\ &< F_{k_s+2} - 1 = F_{k_s+1} + F_{k_s-1} + \cdots + (F_2 \text{ or } F_1) \\ &\leq F_{\ell_t} + F_{\ell_t-2} + \cdots + (F_2 \text{ or } F_1) \\ &\leq F_{\ell_1} + \cdots + F_{\ell_t} \end{aligned}$$

(we used Lemmas 30.2 and 30.3); a contradiction.

(d) It is shown in Solution of (c) that any partition $n = F_{k_1}+\cdots+F_{k_s}$, $1 \leq k_1 < \cdots < k_s$, can be reduced to the partition described in (c) by a finite sequence of replacements $F_k \to F_{k-1} + F_{k-2}$ applied to $k = k_i$ such that $k_i > k_{i-1} + 2$ or $i = 1$ and $k_1 > 2$. Conversely, any partition as in (a) can be obtained from a partition as in (c) by finitely many replacements $F_k + F_{k+1} \to F_{k+2}$ applied when $k_i = k$, $k_{i+1} = k+1$, and $k_{i+2} > k+2$

(or $i+2>s$). For positive integers $j_1, j_2, \ldots, j_q$ put

$$\begin{aligned} S(j_1, j_2, \ldots, j_q) &= \underbrace{(F_1 + \cdots + F_{j_1})}_{j_1} + \underbrace{(F_{j_1+2} + \cdots + F_{j_1+j_2+1})}_{j_2} + \ldots \\ &+ \underbrace{(F_{j_1+\cdots+j_{q-1}+q} + \cdots + F_{j_1+\cdots+j_q+q-1})}_{j_q} \\ T(j_1, j_2, \ldots, j_q) &= \underbrace{(F_2 + \cdots + F_{j_1+1})}_{j_1} + \underbrace{(F_{j_1+3} + \cdots + F_{j_1+j_2+2})}_{j_2} + \ldots \\ &+ \underbrace{(F_{j_1+\cdots+j_{q-1}+q+1} + \cdots + F_{j_1+\cdots+j_q+q})}_{j_q} \end{aligned}$$

According to Part (c), every $n$ is either $S(j_1, \ldots, j_q)$ or $T(j_1, \ldots, j_q)$. We will consider the case when $n = S(j_1, \ldots, j_q)$ (the proof for $n = T(j_1, \ldots, j_q)$ is the same, up to the obvious change of notations and a shift of indices). For $n = S(j_1, \ldots, j_q)$, we put $K_n = K(j_1, \ldots, j_q)$, $H_n = H(j_1, \ldots, j_q)$, and $K_n - H_n = M(j_1, \ldots, j_q)$. We begin with the case $q = 1$, that is, $n = S(j)$ (which is equal to $F_{j+2} - 2$, but is not important for us). In this case, all the partitions of $n$ into distinct Fibonacci numbers are

$$\begin{aligned} n &= F_1 + \cdots + F_j = F_1 + \cdots + F_{j-2} + F_{j+1} \\ &= F_1 + \cdots + F_{j-4} + F_{j-1} + F_{j+1} \\ &= \cdots = \begin{cases} F_3 + F_5 + F_7 + \cdots + F_{j+1}, & \text{if } j \text{ is even} \\ F_1 + F_4 + F_6 + \cdots + F_{j+1}, & \text{if } j \text{ is odd} \end{cases} \end{aligned}$$

We see that $K_n$ and $H_n$ are, respectively, the numbers of even and odd numbers among $j, j-1, \ldots, \left[\dfrac{j+1}{2}\right]$. From this,

$$\begin{aligned} K_n &= \begin{cases} m, & \text{if } n = 4m+1, \\ m+1, & \text{if } n = 4m, 4m+2, \text{or } 4m+3, \end{cases} \\ H_n &= \begin{cases} m, & \text{if } n = 4m, \\ m+1, & \text{if } n = 4m+1, 4m+2, \text{or } 4m+3. \end{cases} \end{aligned}$$

and hence

$$M(j) = K_n - H_n = \begin{cases} 1, & \text{if } n \equiv 0 \bmod 4, \\ -1, & \text{if } n \equiv 1 \bmod 4, \\ 0, & \text{if } n \equiv 2 \text{ or } 3 \bmod 4. \end{cases}$$

Let now $n = S(j_1, \ldots, j_q)$, $q \geq 2$; we may assume that $|M(h_1, \ldots, h_r)| \leq 1$ whenever $r < q$. Any partition of $n$ into distinct Fibonacci numbers can be obtained from the partition of $S(j_1, \ldots, j_q)$ shown above by a sequence of steps $F_k + F_{k+1} \to F_{k+2}$. This sequence either contains the step $F_{j_1-1} + F_{j_1} \to F_{j_1+1}$ or does not contain this step. Accordingly, we break each of $K_n$ and $H_n$ into two parts: $K'_n + K''_n$ and $H'_n + H''_n$. If this step is not applied, then the resulting partitions 1–1 correspond to that of $S(j_2, \ldots, j_q)$ and the parity of the number of summands differs from that for $n$ by the parity of $j_1$. In other words,

$$K''_n - H''_n = (-1)^{j_1} M(j_2, \ldots, j_q).$$

If $F_{j_1-1} + F_{j_1} \to F_{j_1+1}$ is one of our steps, then we can begin with this step. Further steps for $F_1 + \cdots + F_{j_1-2}$ and $(F_{j_1} + \cdots + F_{j_1+j_2}) + \ldots$ are performed independently. Hence,

$$\begin{aligned} K'_n &= K(j_1-2)K(j_2+1, j_3, \ldots, j_q) + H(j_1-2)H(j_2+1, j_3, \ldots, j_q) \\ H'_n &= K(j_1-2)H(j_2+1, j_3, \ldots, j_q) + H(j_1-2)K(j_2+1, j_3, \ldots, j_q) \end{aligned}$$

and

$$K'_n - H'_n = M(j_1-2)M(j_2+1, j_3, \ldots, j_q).$$

Thus,

$$M(j_1, \ldots, j_q) = (-1)^{j_1} M(j_2, \ldots, j_q) + M(j_1-2)M(j_2+1, \ldots, j_q).$$

If $j_1 \equiv 0$ or 1 mod 4, then $M(j_1-2)=0$ and

$$M(j_1,\dots,j_q)=(-1)^{j_1}M(j_2,\dots,j_q)=0 \text{ or } \pm 1.$$

If $j_1 \equiv 2$ or 3 mod 4, then $M_(j_1-2)=(-1)^{j_1}$, and

$$\begin{aligned} M(j_1,\dots,j_q) &= (-1)^{j_1}\left(M(j_2,\dots,j_q)+M(j_2+1,j_3,\dots,j_q)\right) \\ &= (-1)^{j_1}\left((-1)^{j_2}+(-1)^{j_2+1}\right)M(j_3,\dots,j_q) \\ &+(-1)^{j_1}\left(M(j_2-2)+M(j_2-1)\right)M(j_3+1,j_4,\dots,j_q). \end{aligned}$$

Since $(-1)^{j_2}+(-1)^{j_2+1}=0$ and $M(j_2-2)+M(j_2-1)=0$ or $\pm 1$ (for any $j_2$), we have

$$M(j_1,\dots,j_q)=0 \text{ or } \pm 1$$

which completes the proof.

*LECTURE 4.*

4.1. One can take $x^3+3rx+(r^3-1)=0$ with $r$ odd (if $r$ is even, the formula works perfectly well, but the roots will be rather half-integers than integers). There are other solutions.

4.4. The formula is

$$x=\sqrt{\frac{4p}{3}}\sinh\left(\frac{1}{3}\sinh^{-1}\left(-\frac{3q\sqrt{3}}{20\sqrt{p}}\right)\right).$$

It works for $p>0$ and gives one solution. By the way, $\sinh^{-1}=\ln(x+\sqrt{1+x^2})$.

4.5. (a) The auxiliary cubic equation is $y^3-12y+16=0$; its roots are $-4,2,2$ (can be found either by the formula or by guessing). The plus-minus roots of the given equation are $\dfrac{\pm 2\pm i\sqrt{2}\pm i\sqrt{2}}{2}=\pm 1,\pm 1\pm i\sqrt{2}$. The roots of our equation are

$$-1,-1,1+i\sqrt{2},1-i\sqrt{2}.$$

(b) The auxiliary cubic equation is $y^3-4y^2-4y+16=0$, the roots are $-2,2,4$ (found by guessing). The plus-minus roots of the given equation are

$$\frac{\pm\sqrt{2}\pm i\sqrt{2}\pm 2i}{2}=\pm\frac{\sqrt{2}}{2}\pm\left(1\pm\frac{\sqrt{2}}{2}\right)i.$$

It can be checked directly that

$$\frac{\sqrt{2}}{2}+\left(1+\frac{\sqrt{2}}{2}\right)i$$

is a root. Hence, the complex conjugate

$$\frac{\sqrt{2}}{2}-\left(1+\frac{\sqrt{2}}{2}\right)i$$

is also a root. The remaining roots are not minus the roots found, and the sum of all roots is 0. This implies that

$$-\frac{\sqrt{2}}{2}+\left(1-\frac{\sqrt{2}}{2}\right)i,-\frac{\sqrt{2}}{2}-\left(1-\frac{\sqrt{2}}{2}\right)i$$

are the roots.

(c) The auxiliary cubic equation is $y^3-7696y+230400=0$, its roots are $36,64,-100$. The plus-minus roots of the given equation are

$$\frac{\pm 10\pm 6i\pm 8i}{2}=\pm 5\pm 3i\pm 4i=\begin{cases}\pm 5\pm i\\ \pm 5\pm 7i\end{cases}$$

An easy checking shows that $-5+i$ is a root of our equation, and the same arguments as in $(b)$ show that all the four roots of the given equation are

$$-5\pm i,5\pm 7i.$$

4.6. The auxiliary cubic equation will be

$$y^3 - py^2 - 4ry + (q^2 - 4pr) = 0.$$

If $y_1, y_2, y_3$ are the roots of this equation, then the eight numbers $\pm x_i$ (where $x_1, x_2, x_3, x_4$ are the roots of the given equation) are

$$\frac{\pm\sqrt{-y_1 - y_2} \pm \sqrt{y_1 - y_3} \pm \sqrt{-y_2 - y_3}}{2}.$$

*LECTURE 5*

5.1. The radical solution of the equation $x^4 + qx + r = 0$ is presented in 7 equalities below (as usual, $\varepsilon$ is $\frac{-1+i\sqrt{3}}{2}$).

$$x_1^2 = -\frac{64r^3}{27} + \frac{q^2}{4} \qquad x_4^2 = -x_2 - x_3$$

$$x_2^3 = -\frac{q^2}{2} + x_1 \qquad x_5^2 = -\varepsilon x_2 - \overline{\varepsilon} x_3$$

$$x_3^3 = -\frac{q^2}{2} - x_1 \qquad x_6^2 = -\overline{\varepsilon} x_2 - \varepsilon x_3$$

$$x_7 = \frac{x_4 + x_5 + x_6}{2}$$

The number of solutions is 24. (Why not $2\cdot 3\cdot 3\cdot 2\cdot 2\cdot 2 = 144$? An alternative choice of $x_1$ will lead only to switching $x_2$ and $x_3$; similarly, replacing $x_2, x_3$ by $\varepsilon x_2, \overline{\varepsilon} x_3$ or by $\overline{\varepsilon} x_2, \varepsilon x_3$ will result in a permutation of $x_4, x_5, x_6$ .) The 24 solutions are solutions of 6 equations, $x^4 \pm qx + r = 0, x^4 \pm qx + \varepsilon r = 0, x^4 \pm qx + \overline{\varepsilon} r = 0$.

5.2. Let $S$ be the set of partitions of a 4-element set into 2 pairs: $\{12/34\}$, $\{13/24\}$, $\{14/23\}$. It is easy to check that every even permutation of the set $\{1, 2, 3, 4\}$ gives rise to an even (cyclic) permutation in $S$. Since cyclic permutations commute, a commutator of even permutations must be an identity on $S$. There are four such permutations: the identity and $(2, 1, 4, 3), (3, 4, 1, 2)$, $(4, 3, 2, 1)$. All of them are commutators of even permutations:

$$\begin{aligned} (2,1,4,3) &= [3,1,2,4),(4,1,3,2)], \\ (3,4,1,2) &= [(3,1,2,4),(1,3,4,2)], \\ (4,3,2,1) &= [(3,1,2,4),(1,4,2,3)]. \end{aligned}$$

*LECTURE 6*

6.5. Let

$$f_n(x) = 1 + \frac{x}{1!} + \frac{x^2}{2!} + \cdots + \frac{x^n}{n!}.$$

Then $f_n' = f_{n-1} = f_n - x^n/n!$ Therefore

$$(f_n e^{-x})' = (f_n' - f_n)e^{-x} = -e^{-x}\frac{x^n}{n!}$$

If $n$ is even then the last function is everywhere negative (except $x = 0$ where it equals zero). It follows that $f_n e^{-x}$ is a decreasing function. Since $\lim_{x\to+\infty}(f_n e^{-x}) = 0$, one has: $f_n e^{-x} > 0$ for all $x$, and hence $f_n$ has no roots. If $n$ is odd then $f_n(x)$ is negative for very small $x$ and positive for very large $x$, hence $f_n$ has a root. If it has more than one root then, by Rolle's theorem, $f_n'$ has a root. But $f_n' = f_{n-1}$, and we already proved that $f_{n-1}$ has no roots.

Alternatively, it suffices to prove that $f_n$ cannot have two consecutive negative roots. Assume that $a$ and $b$ are negative roots. Then

$$f_n(a) = f_n'(a) + \frac{a^n}{n!} = 0,\ f_n(b) = f_n'(b) + \frac{b^n}{n!} = 0,$$

and hence $f_n'(a)$ and $f_n'(b)$ are either both positive (if $n$ is odd) or negative (if $n$ is even). But the signs of the derivative at the consecutive roots are opposite.

6.7. Denote the number of sign changes in the sequence $a_1, \dots, a_n$ by $S$ and the number of roots of $f(x)$ by $Z$. Argue by induction on $S$. If $S = 0$ then obviously $Z = 0$. Let $k$ be such that $a_k a_{k+1} < 0$ and choose $\lambda \in (\lambda_k, \lambda_{k+1})$. Set

$$g(x) = e^{\lambda x}\left(e^{-\lambda x} f(x)\right)' = \sum a_i(\lambda_i - \lambda)e^{\lambda_i x}.$$

Let $s$ and $z$ have the same meanings for $g$ as $S$ and $Z$ for $f$. By Rolle's theorem, $z \geq Z-1$. The coefficients of $g$ are

$$-a_1(\lambda - \lambda_1), \dots, -a_k(\lambda - \lambda_k), a_{k+1}(\lambda_{k+1} - \lambda), \dots, a_n(\lambda_n - \lambda),$$

and hence $s = S - 1$. By the induction assumption, $s \geq z$, therefore $S \geq Z$.

6.9. We assume that $f(x)$ is in general position: no two derivatives $f^{(i)}(x)$ and $f^{(j)}(x)$ have common roots; in particular, no derivative has a multiple root (the argument in the general case is similar, see [**64**]). Let $x$ vary from $a$ to $b$. If $x$ passes a root of $f$, say, $c$, then, near point $c$, the signs of the sequence $f(x), f'(x), f''(x), \dots, f^{(n)}(x)$ are those of $(x-c)g(c), g(c), g'(c), g''(c)\dots$ where $f(x) = (x-c)g(x)$. As $x$ passes $c$ the number of sign changes in the latter sequence decreases by 1.

Assume now that $x$ passes a root of $f^{(i)}$ with $i \geq 1$, again denoted by $c$. We need to show that the number of sign changes in the sequence $f^{(i-1)}(x), f^{(i)}(x), f^{(i+1)}(x)$ changes by an even non-negative number. As before, there is a sign change in $(f^{(i)}(x), f^{(i+1)}(x))$ left of $c$, and none right of $c$. As to $(f^{(i-1)}(x), f^{(i)}(x))$, the sign changes here are the same as in $(f^{(i-1)}(c), (x-c)g(c))$ where $f^{(i)}(x) = (x-c)g(x)$. If the signs of $f^{(i-1)}(c)$ and $g(c)$ coincide then, as $x$ passes $c$, the number of sign changes decreases by 1, and if these signs are opposite then the number of sign changes increases by 1. This implies the claim.

*LECTURE 7*

7.3. Arguing as in the proof of Theorem 7.1, it suffices to find a function $ax+b$ such that $f(x) = e^x - ax - b$ has equal maximum values at the end points 0 and 1, and the minimal value opposite to this maximum. Thus $1 - b = f(0) = f(1) = e - a - b$, and therefore $a = e - 1$. To find the minimum, set $f'(x) = 0$, hence $e^x = a$. Thus the minimal value is $a - a\ln a - b$. Therefore $a - a\ln a - b = b - 1$, and the least deviation of $f(x)$ from zero equals

$$\frac{2 - e + (e-1)\ln(e-1)}{2} \approx 0.1$$

7.8. (A sketch.) A linear substitution $\phi(x) = ax + b$ changes a polynomial $f(x)$ to $\bar f(x) = \phi^{-1} \circ f \circ \phi = (f(ax+b) - b)/a$. If $f \circ g = g \circ f$ then $\bar f \circ \bar g = \bar g \circ \bar f$. Let $f_n$ be a sequence of commuting polynomials, $\deg f_n = n$. Applying a linear substitution, one can change $f_2(x)$ to $x^2 + \gamma$. Let $f_3(x) = ax^3 + bx^2 + cx + d$. The equality $f_2 \circ f_3 = f_3 \circ f_2$ is equivalent to the system of equations

$$\begin{cases} a^2 = a, ab = 0, b^2 + 2ac = 3a\gamma + b, ad + bc = 0 \\ c^2 + 2bd = 3a\gamma^2 + 2b\gamma + c, cd = 0, d^2 + \gamma = a\gamma^3 + b\gamma^2 + c\gamma + d \end{cases}$$

This system has only two solutions: $\gamma = 0$ or $\gamma = -2$.

In the first case, $f_2(x) = x^2$, hence $f_n(x^2) = f_n^2(x)$ and more generally, $f_n(x^{2^k}) = f_n^{2^k}(x)$ for all $n, k$. Therefore every root of $f_n(x^{2^k})$ is a root of $f_n(x)$. If $f_n(x)$ has a root other than 0 then the set of distinct (complex) roots of the polynomials $f_n(x^{2^k})$, $k = 1, 2, \dots$ is infinite. But $f_n(x)$ has finitely many roots, and thus $f_n(x) = ax^n$. Since $f_n(x^2) = f_n^2(x)$ one has $a = 1$.

If $f_2(x) = x^2 - 2$ then $f_n(x^2 - 2) = f_n^2(x) - 2$ for all $n$. Differentiate to obtain $xf_n'(x^2 - 2) = f_n(x)f_n'(x)$. Set $g_n(x) = (4 - x^2)f_n'(x) + n^2(f_n^2(x) - 4)$. On the one hand, the leading coefficient of $g_n(x)$ is zero so $g_n$ has degree less than $2n$. On the other hand, one can check that $g_n(x^2 - 2) = g_n(x)f_n^2(x)$, and hence $\deg g_n$ is $2n$. It follows that $g_n(x) \equiv 0$. Therefore $f_n$ satisfies the differential equation $(4 - x^2)f_n'(x) + n^2(f_n^2(x) - 4) = 0$

which can be explicitly solved: $f_n(x) = 2\cos(n \arccos(x/2) + c)$. To find the constant, use the equality $f_n(x^2 - 2) = f_n^2(x) - 2$ which implies that $f_n(2) = 2$, and hence $c = 0$.

*LECTURE 10*

10.1. (a) See Figure 30.8.

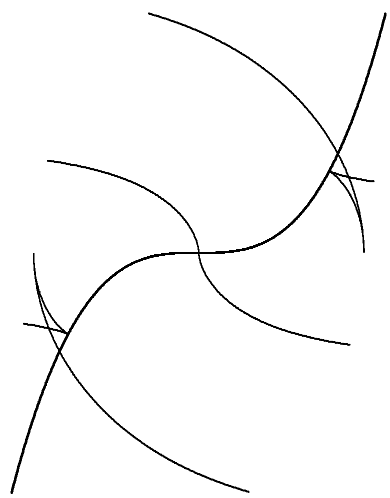

FIGURE 30.8. Solution to Exercise 10.6 (a)

10.1. (b) See Figure 30.9.

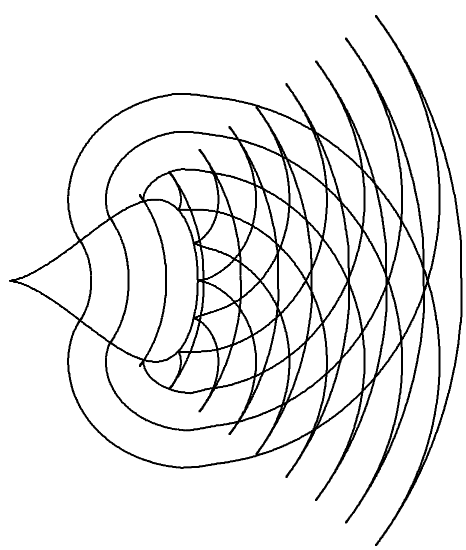

FIGURE 30.9. Solution to Exercise 10.6 (b)

10.4. (a) *Answer*:

$$L = \int_0^{2\pi} p(\phi)\ d\phi, \quad A = \frac{1}{2}\int_0^{2\pi} p(\phi)(p(\phi) + p''(\phi))\ d\phi.$$

10.5. Assume that $f^{(n+1)}(t) > 0$ on $I$. Let $a < b$ and suppose that $g_a(x) = g_b(x)$ for some $x$. One has

$$\frac{\partial g_t}{\partial t}(x) = \sum_{i=0}^{n} \frac{f^{(i+1)}(t)}{i!}(x-t)^i - \sum_{i=0}^{n} \frac{f^{(i)}(t)}{(i-1)!}(x-t)^{i-1} = \frac{f^{(n+1)}(t)}{n!}(x-t)^n,$$

and hence $(\partial g_t/\partial t)(x) > 0$ (except for $t = x$). It follows that $g_t(x)$ increases, as a function of $t$, therefore $g_a(x) < g_b(x)$. This is a contradiction.

10.6. Consider the sequence of functions $f_q = (-1)^q (kI)^{2q}(f)$, namely,

$$f_q(x) = a_k \cos kx + b_k \sin kx + \left(\frac{k}{k+1}\right)^{2q} (a_{k+1} \cos(k+1)x + b_{k+1} \sin(k+1)x)$$
$$+ \cdots + \left(\frac{k}{n}\right)^{2q} (a_n \cos nx + b_n \sin nx).$$

By the Rolle theorem, for every $q$, one has: $Z(f) \geq Z(f_q)$. For large $q$, the function $f_q(x)$ is arbitrarily close to $a_k \cos kx + b_k \sin kx$, therefore $f_q$ has $2k$ sign changes. Thus $Z(f) \geq 2k$.

*LECTURE 11*

11.6. In both cases, this equals the number of tangent lines from a given point to the envelope of the family of lines that bisect the area of the polygon. This envelope is a concave triangle made of arcs of hyperbolas, and the answer is either one or three, if the point is not on the envelope, and two if it lies on the envelope.

11.7. Order the vertices cyclically $V_1, V_2, \ldots, V_n$ and assume that the correspondence side $\mapsto$ opposite vertex is one-to-one. Let side $V_{i-1}V_i$ be opposite to vertex $V_j$. Then side $V_iV_{i+1}$ is opposite to the next vertex $V_{j+1}$, otherwise the correspondence between the sides and the opposite vertices cannot be one-to-one. It follows that there exists $k$ such that, for every $i$, side $V_iV_{i+1}$ is opposite to the vertex $V_{i+k}$ (of course, we understand the indices cyclically mod $n$). It is clear that side $V_{i+k-1}V_{i+k}$ is opposite to the vertex $V_i$, and hence $(i+k-1)+k = i \bmod n$. It follows that $n$ is odd.

*LECTURE 12*

12.3. Orient one curve and consider the number of intersections of its positive tangent half-line with the other curve. As the tangency point traverses the first curve, this number changes as described in Section 12.2. Computed for both orientations of the first curve, the total contribution of each outer double tangent is 2, of inner double tangent is -2, and of each intersection point -2. Thus $t_+ = t_- + d$.

12.5. The solution is based on [**40**]. Let $I$ be a positive even number and $T_+ - T_- - I/2 = D$. We need three preparatory constructions. First, let $I = 2, D = 2$ and $T_-$ arbitrary. A curve is shown in Figure 30.10, left or right, depending on the parity of $T_-$.

Next, let $T_- = 0, D = 0$ and $I$ an arbitrary even number. A curve is shown in Figure 30.11.

Third, one can adjust two nearly parallel arcs to obtain additional self-intersections and without affecting $I$ or $T_-$ as shown in Figure 30.12.

Now, starting with the first construction with the desired $T_-$, adjust it by the second and third constructions as shown in Figure 30.13. This solves (a).

To prove (b), let $\gamma(\alpha)$ be a parameterization of the given curve by the angle made by its tangent direction with a fixed direction in the plane. Denote by $w$ the winding number; the parameter $\alpha$ varies between 0 and $2\pi w$. One has a double tangent line at points $\gamma(\alpha)$ and $\gamma(\beta)$ if and only if the vectors $\gamma'(\alpha)$ and $\gamma(\beta) - \gamma(\alpha)$ are parallel. This implies that $\beta = \alpha + \pi k$, and the double tangent is inner if and only if $k$ is odd. For a fixed $k$, let

$$A_k^{\pm} = \{\alpha \mid \gamma'(\alpha) = t(\gamma(\alpha + \pi k) - \gamma(\alpha))\} \tag{30.4}$$

with $t$ positive or negative, respectively. We make three claims whose proofs are left to the reader:

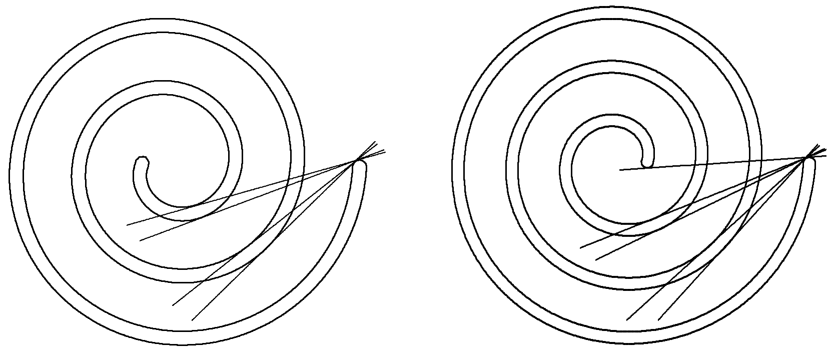

FIGURE 30.10. The case of $I = 2, D = 2$

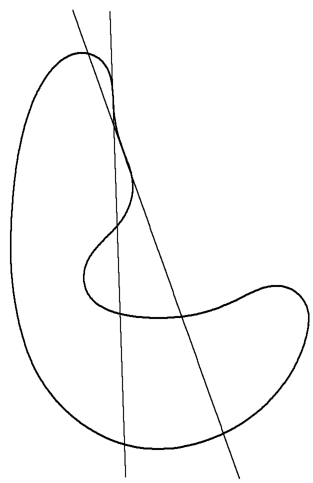

FIGURE 30.11. The case of $T_{-} = 0, D = 0$

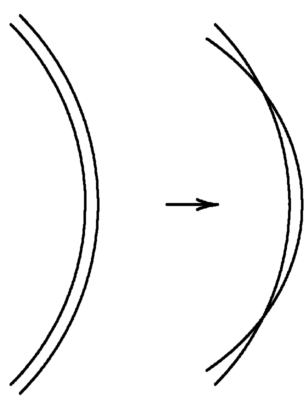

FIGURE 30.12. Making additional self-intersections

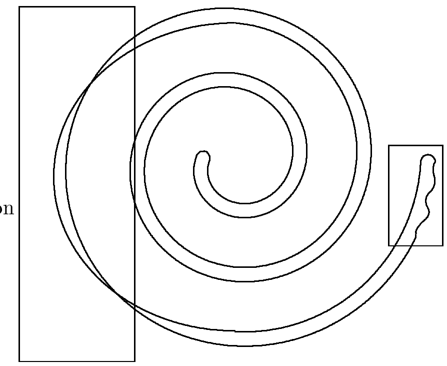


FIGURE 30.13. Combining the preceding constructions in one curve

(1) the points of $A_k^+$ and $A_k^-$ alternate;
(2) if distinct $\alpha, \beta \in A_k^+$ then $|\beta - \alpha| > \pi$;
(3) $A_1^+$ and $A_{2w-1}^+$ are empty.

One has:

$$2T_- = \sum_{1 \le k \le 2w-1;\ k \text{ odd}} |A_k^+| + |A_k^-|.$$

By claim (1), $|A_k^+| = |A_k^-|$; by claim (2), $|A_k^+| \le 2w - 1$ for each $k$; and then , by claim (3), $T_- \le (w-2)(2w-1)$. By Exercise 12.11, $w \le D+1$, and it follows that $T_- \le (2D+1)(D-1)$. Finally, the number $T_-$ splits into two summands, according as $t > 0$ or $t < 0$ in (30.4). These summands equal

$$\frac{1}{2} \sum_{1 \le k \le 2w-1;\ k \text{ odd}} |A_k^\pm|,$$

respectively. By claim (1), the two sums are equal and hence $T_-$ is even.

Considering (c), let $T_-$ be even and $T_- \le D(D-1)$. Then there exists $n \le D$ such that $\binom{n-1}{2} \le T_-/2 \le \binom{n}{2}$. Set $k = \binom{n}{2} - T_-/2$. Then $k \le n-1$. Set $q = D - n$. A desired curve is constructed in three steps. First, consider a closed curve without inflections which makes $q+1$ loops, then insert $n-k$ *small loops* into the inner large loop of the curve, and then insert $k$ *very small loops* into one of the small loops. See Figure 30.14 where $q = 2, n = 8, k = 3$. This curve has $q + n = D$ double points. Every pair of small or very small loops contribute two inner tangents, except for the pairs (small loop, one of the very small loops inside it). Thus the number of inner double tangents is $2\left(\binom{n}{2} - k\right) = T_-$.

12.7. See [**89**].

12.8. See [**29**].

*LECTURE 13*

13.1. The equation of the plane $\Pi$ has the form

$$A(x - x(t_0)) + B(y - y(t_0)) + C(z - z(t_0)) = 0.$$

The plane $\Pi$ contains the tangent line

$$x = x(t_0) + ux'(t_0),\ y = y(t_0) + uy'(t_0),\ z = z(t_0) + uz'(t_0)$$

($u$ is a parameter on the line) if and only if

$$Ax'(t_0) + By'(t_0) + Cz'(t_0) = 0.$$

Consider the function

$$h(t) = A(x(t) - x(t_0)) + B(y(t) - y(t_0)) + C(z(t) - z(t_0))$$

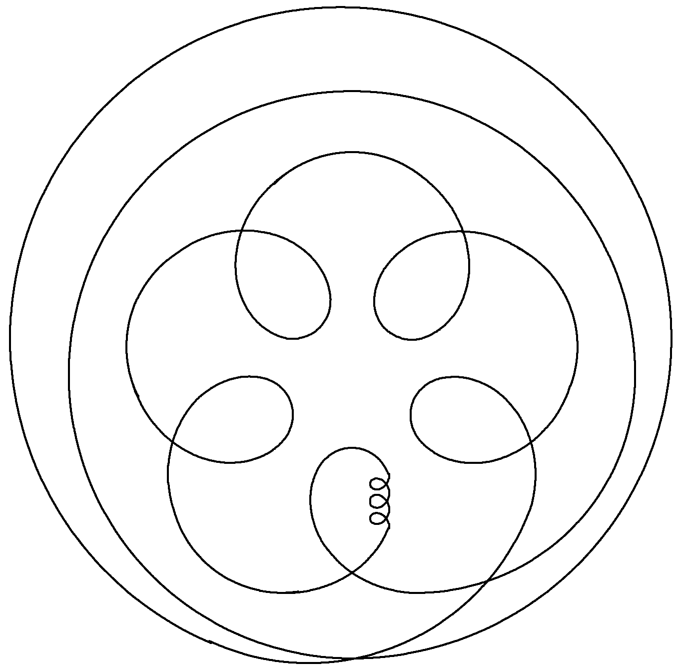

FIGURE 30.14. Solution to Exercise 12.5 (c)

(on the curve). Obviously, $h(t_0) = h'(t_0) = 0$, and, since the curve passes at $P$ from one side of the plane to the other one, it changes sign at $t = t_0$. Hence, the second derivative of $h$ also equals 0 at $t_0$. Thus,

$$Ax''(t_0) + By''(t_0) + Cz''(t_0) = 0,$$

that is, the plane contains not only the velocity vector, but also the acceleration vector. It is the osculating plane.

13.2. If $x = x(t),\ y = y(t),\ z = z(t)$ are parametric equations of the cuspidal edge, then the parametric equations of the developable surface (made of the tangent lines to the curve) are

$$x = x(t) + ux'(t),\ y = y(t) + uy'(t),\ z = z(t) + uz'(t).$$

The tangent plane to the surface at the point $(t, u)$ is spanned by the vectors

$$\begin{aligned}(x'_t, y'_t, z'_t) &= (x'(t) + ux''(t), y'(t) + uy''(t), z'(t) + uz''(t))\\ (x'_u, y'_u, z'_u) &= (x'(t), y'(t), z'(t)).\end{aligned}$$

It is the same as the osculating plane to the cuspidal edge.

13.3. (A sketch.) Let $\Pi(t)$ be our family. The intersection line of the planes $\Pi(t), \Pi(t+\varepsilon)$ $(\varepsilon \neq 0)$ has a limit $\ell(t) \subset \Pi(t)$ as $\varepsilon \to 0$. The point of intersection of the three planes $\Pi(t), \Pi(t+\varepsilon_1), \Pi(t+\varepsilon_2)(\varepsilon_1 \neq \varepsilon_2,\ \varepsilon_1 \neq 0,\ \varepsilon_2 \neq 0)$ has a limit $\gamma(t) \in \ell(t)$ as $\varepsilon_1 \to 0,\ \varepsilon_2 \to 0$. The union of lines $\ell(t)$ is a developable surface whose tangent planes are $\Pi(t)$; the union of points $\gamma(t)$ is a curve whose osculating planes are $\Pi(t)$.

13.5. The parametric equations of the surface made of the tangent lines to the given curve is

$$x = t + u,\ y = t^3 + 3t^2u,\ z = t^4 + 4t^3u.$$

The intersection of this surface with the plane $x = c$ (in the coordinate system $y, z$) is

$$\begin{array}{rclcl} y & = & t^3 + 3t^2 & = & t^2(3c - 2t), \\ z & = & t^4 + 4t^3(c - t) & = & t^3(4c - 3t). \end{array}$$

The derivatives $y' = 6t(c - t), z' = 12t^2(c - t)$ have two common zeroes: $t = 0$ and $t = c$; thus the curve has two cusps, $(0, 0)$ and $(c^3, c^4)$. Accordingly, the surface has two cuspidal edges: the given curve $x = t,\ y = t^3,\ z = t^4$ and, more surprisingly, the $x$ axis $x = t, y = z = 0$.

Besides two cusps, our curve has also a self-intersection. Indeed, the system

$$\left\{ \begin{array}{rcl} t_1^2(3c - 2t_1) & = & t_2^2(3c - 2t_2) \\ t_1^3(4c - 3t_{)} & = & t_2^3(4c - 3t_2) \end{array} \right. \Longleftrightarrow 3(t_1^4 - t_2^4) = 4c(t_1^3 - t_2^3) = 6c^2(t_1^2 - t_2^2),$$

besides the obvious solution $t_1 = t_2$, has solutions

$$t_1 = \frac{1 + \sqrt{3}}{2}c, t_2 = \frac{1 - \sqrt{3}}{2}c, \text{ and } t_1 = \frac{1 - \sqrt{3}}{2}c, t_1 = \frac{1 + \sqrt{3}}{2}c,$$

which means that at the parameter values $\frac{1 \pm \sqrt{3}}{2}c$ the values of the coordinates $y, z$ are the same. An easy computation shows that these values are $y = \frac{c^3}{2}, z = -\frac{c^4}{4}$. Thus, besides two cuspidal edges, the surface has a self-intersection along the curve

$$x = t,\ y = \frac{t^3}{2},\ z = -\frac{t^4}{4}.$$

We leave to the reader the pleasant work of visualizing these results.

13.6. The solution is described in [**82**]. For (a), unfold the disc to the plane to obtain a plane disc foliated by straight segments, the ruling of the developable surface, and a curve $\gamma$ on it. We need to prove that there are two intersection points of $\gamma$ with a ruling at which the tangent lines to $\gamma$ are parallel. Since the tangent planes along a ruling of a developable surface are the same, the respective tangent lines to $\gamma$ in space will be parallel as well.

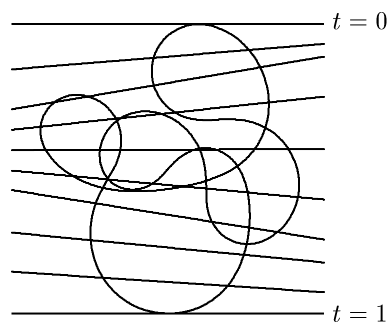


Figure 30.15. Curve and rulings

Let $l_t,\ t \in [0, 1]$, be the family of lines foliating the domain; think of these lines as oriented from left to right. Assume that $\gamma$ lies between $l_0$ and $l_1$, and that these lines touch the curve, see Figure 30.15. Let $C_+(t)$ and $C_-(t)$ be the rightmost and the leftmost points of $\gamma \cap l_t$. The curves $C_\pm(t)$ are piecewise smooth. Let $\alpha_\pm(t) \in [0, \pi]$ be the angle between $C_\pm(t)$ and $l_t$. The functions $\alpha_\pm(t)$ are not continuous but their discontinuities are easily described. The three types of discontinuities of $\alpha_-(t)$ are shown in Figure 30.16: in each case the graph of $\alpha_-(t)$ has a descending vertical segment. Likewise, there are three types of discontinuities of $\alpha_+(t)$, and in each case the graph has an ascending vertical segment.

Note that, for $t$ close to 0, $\alpha_-(t)$ is close to 0, while $\alpha_+(t)$ is close to $\pi$. Similarly, for $t$ close to 1, $\alpha_-(t)$ is close to $\pi$ and $\alpha_+(t)$ is close to 0.

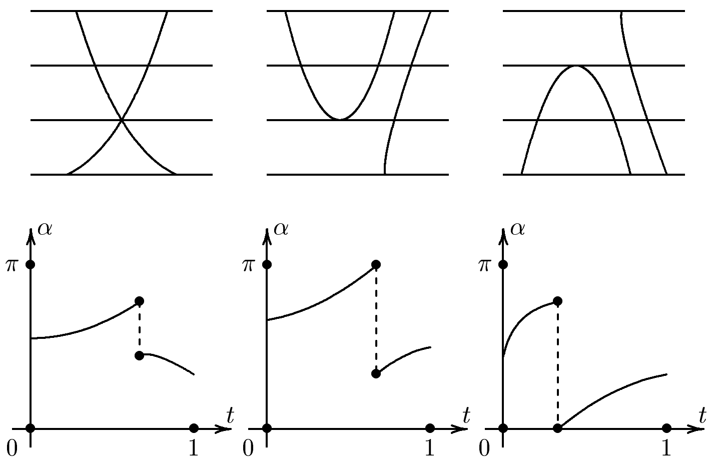


FIGURE 30.16. Discontinuities of the functions $\alpha_\pm(t)$

We claim that that the graphs of $\alpha_-(t)$ and $\alpha_+(t)$ have a common point not on a vertical segment of either graph. Approximate both functions by smooth ones so that the vertical segments of the graphs become very steep: $\alpha'_-(t) \ll 0$ and $\alpha'_+(t) \gg 0$ on the corresponding small intervals. Consider the function $\beta(t) = \alpha_+(t) - \alpha_-(t)$. For $t$ near 0, $\beta(t) > 0$, and for $t$ near 1, $\beta(t) < 0$. Let $t_0$ be the smallest zero of $\beta(t)$. Since $\beta$ changes sign from positive to negative, $\beta'(t_0) \le 0$. Therefore $t_0$ is not on the segments where $\alpha'_-(t) \ll 0$ or $\alpha'_+(t) \gg 0$. Thus $t_0$ is a desired common value of the two angles.

For (b), take an equilateral triangle in the plane and draw three lines near each corner, cutting across and not parallel to opposite sides. Fold smoothly along these lines (that is, approximate a fold line by a cylinder of a small radius) so that the obtained surface consists of a flat hexagon with three triangular flaps going more-or-less vertically. The curve $\gamma$ is a simple smooth convex curve approximating the perimeter of the original triangle. After the flaps are folded, the curve doesn't have parallel tangents in space, see Figure 30.17.

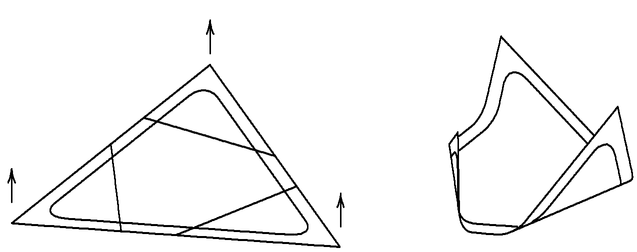

FIGURE 30.17. A curve without parallel tangents

*LECTURE 15*

15.3. Denote the unit tangent, the unit normal and the binormal vectors of the arc length parameterized curve $\gamma(t)$ by $T(t), N(t)$ and $B(t)$. One has the Frenet formulas:

$$T'(t) = \kappa(t)N(t),\ N'(t) = -\kappa(t) - \tau(t)B(t),\ B'(t) = \tau(t)N(t).$$

Let $v(t)$ be a vector along the ruling at point $\gamma(t)$. The surface generated by the rulings has a parameterization $r(t,s) = \gamma(t) + sv(t)$. Then $r_t = \gamma' + sv',\ r_s = v$ are tangent vectors to the surface. Since the surface is developable, the normal $\nu(t)$ along a ruling remains the same. Then $\nu(t)$ is orthogonal to $v$ and to $\gamma' + sv'$ for all $s$, and hence to $\gamma'$ and to $v'$. Therefore the vectors $v, v', \gamma'$ are coplanar. It is easy to express $v$ in terms of $T(t), N(t)$ and $B(t)$:

$$v = T\cot\beta + N\cos\alpha + B\sin\alpha.$$

Differentiate using the Frenet formulas:

$$v' = -T(\kappa\cos\alpha + \beta'\operatorname{cosec}^2\beta) + N(\kappa\cot\beta + (\tau - \alpha')\sin\alpha) + B(\alpha' - \tau)\cos\alpha.$$

It is now straightforward to compute the determinant of the vectors $v', v, T$ which equals $\kappa\sin\alpha\cot\beta + \tau - \alpha'$. Equating to zero yields formula (15.2).

15.6. If there is a hole inside the fold then the straight rulings that go inside it have their other end points on the boundary of the hole. If there is no hole then the other end points of the rulings must lie on the fold as well. Since the family of rulings is continuous, there will be rulings that are tangent to the fold, and this contradicts to the fact that the rulings make non-zero angles with the fold.

*LECTURE 16*

16.1. *Answer*: a hyperbolic paraboloid.

16.2. Let $ABCD$ be the quadrilateral given. Take the union, for all planes $\Pi$ parallel to the lines $AB$ and $CD$, of lines $KM$ where $K$ and $M$ are points of intersection of $\Pi$ with the lines $BC$ and $DA$.

16.6. (a) The ruling chosen is projected onto a point, denote it by $P$. The family containing this ruling is projected onto a family of parallel lines not passing through $P$. The other family is projected onto the family of lines passing through $P$ except the line parallel to the images of the rulings of the first family.

(b) The projections will form two families of parallel lines.

*LECTURE 17*

17.1. The 12 lines passing through the points $(0,0,0), (1,0,0), (0,1,0),\ (0,0,1)$ are

$$\begin{array}{llll} x=0, y=-z; & x=1, y=0; & y=1, x=0; & z=1, x=0; \\ y=0, x=-z; & x=1, z=0; & y=1, z=0; & z=1, y=0; \\ z=0, x=-y; & x=1, y=-z; & y=1, x=-z; & z=1, x=-y. \end{array}$$

To find the remaining line we use the fact that each of the 27 lines intersects 10 other lines. This shows that every known line intersects some unknown lines. Say, take the line $x = 0, y = z$. Its general point is $(0, t, -t)$. Thus, for some values of $t$, and some $p, q, r$, the point $x = pu, y = t + qu, z = -t + ru$ must belong to the surface for all $u$. Plug the point into the equation of the surface. We will get a polynomial in $u$ of degree 3 without the constant term (for $u = 0$, the point lies on the surface for every $u$). Equate to 0 the coefficients at $u, u^2, u^3$, and determine, for which $t$ the system has a non-zero solution in $p, q, r$.

In this way, we find one more line on the surface; it is given by parametric equations

$$x = \frac{\sqrt{5}+1}{2} + \frac{\sqrt{5}-1}{2}t,\ y = \frac{1-\sqrt{5}}{2}t,\ z = 1 + t.$$

The remaining 11 lines can be obtained from the last one by permutations $x$, $y$ and $z$ and replacing $\sqrt{5}$ by $-\sqrt{5}$.

17.2. It is easy to find 12 lines on our surface. One of them is given by the equations $y = ax, z = b$ where $b^2 = \dfrac{\gamma}{\beta}, \beta a^2 + ba + \beta = 0$; 11 more can be obtained by varying the values of $a$ and $b$ and by permutations of $x, y$, and $z$. One more line can be found by the method described in the previous solution; it is $z = x + \dfrac{2\beta}{a} + b,\ y = -2\beta$; 11 more by varying the values of $a$ and $b$ and by permutations of the coordinates. Three lines are infinite (this follows from the fact that our surface, for big $x, y, z$, is asymptotically close to $xyz = 0$ which is the union of three planes. The intersection with the infinite plane consists of three lines.

*LECTURE 18*

18.6. Let the zero element $E$ be one of the inflection points of the cubic curve. Given a point $A$ of the cubic curve, let $B$ be the third intersection point of the line $AE$ with the curve. We claim that $A + B = E$. Indeed, since $E$ is an inflection, the third intersection point of the tangent line at $E$ with the cubic curve is $E$. (This implies that points $A, B$ and $C$ are collinear if and only if $A + B + C = E$.)

Let $A$ be an inflection point. Then the construction for the addition of points implies that $A + A = -A$, that is, $3A = E$. Conversely, if $2A = -A$ then the third intersection point of the tangent line at point $A$ with the cubic curve is again $A$, hence this tangent line has third order tangency with the curve and $A$ is an inflection point. Thus the inflection points are precisely the points of order three, satisfying $3A = E$. Finally, if $A$ is an inflection point then $3A = E$ and hence $3(-A) = E$. Therefore $-A$ is an inflection point as well, and the three inflection points, $A, E, -A$, are collinear.

*LECTURE 19*

19.7. (c) Choose a direction, say, $\alpha$, and consider the support lines to the given curve of constant width $\gamma$ having the directions $\alpha, \alpha+\pi/3, \alpha+2\pi/3, \alpha+\pi, \alpha+4\pi/3$ and $\alpha+5\pi/3$. These lines form a hexagon with all the angles equal to $2\pi/3$. Let $d$ be the distance between the opposite, parallel sides of the hexagon (equal to the diameter of $\gamma$) and $a, b$ two adjacent sides. Then $d = (a + b)\cos\pi/6$. Therefore the sum of any two adjacent sides is the same. Hence the odd-numbered sides are of equal length, and so are the even numbered sides. Let $c(\alpha)$ be the difference of the former and the latter.

Let $\alpha$ continuously increase by $\pi/3$. Then the sign of $c(\alpha)$ changes to the opposite. Therefore, for some intermediate value of the angle, $c(\alpha) = 0$ and the hexagon is regular.

(d) Let $\gamma$ be a curve of constant width $d$ and $ABCDEF$ be a regular circumscribed hexagon. Let $\gamma_1$ be a Reuleaux triangle inscribed into $ABCDEF$ and touching it at points $B, D, F$. Choose the origin at the center of the hexagon and the horizontal axis parallel to $AB$. Denote the support function, the curvature radius and the area of $\gamma$ by $p(\phi), \rho(\phi)$ and $A$ respectively, and let $p_1(\phi), \rho_1(\phi), A_1$ be those for $\gamma_1$. Then, by Exercise 10.4, $\rho(\phi) = p''(\phi) + p(\phi)$ and $A = (1/2)\int p(\phi)\rho(\phi)\ d\phi$.

Considering the arc $BD$ of the Reuleaux triangle $\gamma_1$, it is clear that $p(\phi) \geq p_1(\phi)$ for $\pi/3 \leq \phi \leq 2\pi/3$, and similarly for $\pi \leq \phi \leq 4\pi/3$ and $5\pi/3 \leq \phi \leq 2\pi$. Considering the centrally symmetric Reuleaux triangle, we conclude that $p(\phi+\pi) \geq p_1(\phi+\pi)$ for $\pi/3 \leq \phi \leq 2\pi/3, \pi \leq \phi \leq 4\pi/3$ and $5\pi/3 \leq \phi \leq 2\pi$. Therefore $2A =$

$$\int_0^{2\pi} p(\phi)\rho(\phi)\ d\phi = \left(\int_{\pi/3}^{2\pi/3} + \int_{\pi}^{4\pi/3} + \int_{5\pi/3}^{2\pi}\right)(p(\phi)\rho(\phi) + p(\phi+\pi)\rho(\phi+\pi))\ d\phi \geq$$

$$\left(\int_{\pi/3}^{2\pi/3} + \int_{\pi}^{4\pi/3} + \int_{5\pi/3}^{2\pi}\right)(\rho(\phi) + \rho(\phi+\pi))p_1(\phi)\ d\phi.$$

Since $p(\phi) + p(\phi + \pi) = d$ we have $\rho(\phi) + \rho(\phi + \pi) = d$, and therefore the last integral equals

$$d\left(\int_{\pi/3}^{2\pi/3} + \int_{\pi}^{4\pi/3} + \int_{5\pi/3}^{2\pi}\right) p_1(\phi)\ d\phi = \int_0^{2\pi} \rho_1(\phi) p_1(\phi)\ d\phi = 2A_1,$$

as needed.

19.9. Let $\gamma(t)$ be the arc length parameterization of the curve. Then $|\gamma(t)| \leq 1, |\gamma'(t)| = 1$ and $|\gamma''(t)| = |k(t)|$ for all $t$. One has:

$$L = \int_0^L \gamma' \cdot \gamma' dt = \gamma \cdot \gamma' \big|_0^L - \int_0^L \gamma \cdot \gamma'' dt \leq 2 + \int_0^L |\gamma||\gamma''| dt \leq 2 + \int_0^L |k| dt = 2 + C,$$

as claimed.

19.10. The formulation is the same as in the plane (for a closed curve inside a unit ball, $L \leq C$), and the proof given in the solution of Exercise 19.9 applies.

19.11. By approximation of a smooth curve by a polygonal one, it suffices to prove the statement for a single wedge. Let $\alpha$ be the exterior angle of a wedge. Since the measure $dv$ is invariant under isometries of space, $I(\alpha) = \int C_v dv$ does not depend on the position of the wedge but only on the value of $\alpha$. It is clear that $I(\alpha)$ is a continuous function of $\alpha$ and that $I(\alpha + \beta) = I(\alpha) + I(\beta)$ (since this additivity holds for each projection). A continuous additive function is linear: $I(\alpha) = C\alpha$. To find the constant $C$ consider the case $\alpha = \pi$. Almost every projection of such a wedge also has curvature $\pi$, and hence $C$ equals the area of the unit sphere, $4\pi$. This implies the result.

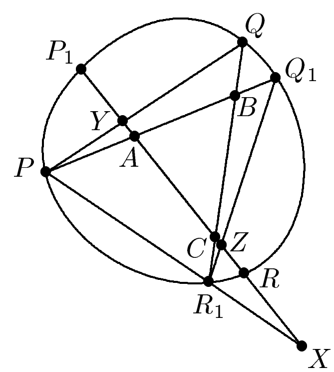


FIGURE 30.18. Proving the triangle inequality in Hilbert's metric

19.12. Let $ABC$ be a given triangle. Extend its sides to their intersections with the boundary of the convex domain and call the intersection points $P, P_1, Q, Q_1, R, R_1$, see Figure 30.18. We want to show that

$$[P, A, B, Q_1][Q, B, C, R_1] \geq [P_1, A, C, R].$$

Let $X, Y, Z$ be the intersection points of the line $P_1R$ with the lines $PR_1, PQ$ and $Q_1R_1$, respectively. The cross-ratio is invariant under a central projection. Projecting the line $PQ_1$ to the line $P_1R$ from point $R_1$ yields $[P, A, B, Q_1] = [X, A, C, Z]$. Likewise, projecting $QR_1$ to $P_1R$ from $P$ yields $[Q, B, C, R_1] = [Y, A, C, X]$. Since $[X, A, C, Z][Y, A, C, X] = [Y, A, C, Z]$, what we need to show is $[Y, A, C, Z] \geq [P_1, A, C, R]$. But this inequality holds since $Y$ and $Z$ are closer to $A$ and $C$ than $P_1$ and $R$.

*LECTURE 20*

20.4. When the loop is pulled down it minimizes its length and becomes a geodesic line on the cone. Cut the cone along the ruling through the point of the loop that is being pulled down and flatten the cone in the plane. One obtains a plane wedge, and the geodesic unfolds to a straight segment. If this wedge has the angle measure less than $\pi$ then the segment lies within the wedge and the loop stays on the cone, but if this angle measure is greater than $\pi$ then the loops slides off from the cone.

Consider the plane section of the cone through its axis and let $2\alpha$ be its angle. Cutting the cone along its ruling and flattening it yields a sector with perimeter length $2\pi l \sin\alpha$ where $l$ is the length of a ruling. The borderline case is when this sector is half a circle; then $2\pi l \sin\alpha = \pi l$, and hence $\alpha = \pi/6$.

20.6. (a) The result will follow once we prove that $\gamma_\varepsilon$ is orthogonal to the normals to $\gamma$ (the notation is introduced in Exercise 20.6 (c)).

This claim is obvious if $\gamma$ is a circle – then each $\gamma_\varepsilon$ is a concentric circle. In the general case, one approximates $\gamma$ at each point by its osculating circle, and then the concentric circles are tangent to $\gamma_\varepsilon$ at the respective points.

(b) Let $C(\gamma)$ be the total geodesic curvature of $\gamma$. If one proves that $\ell(\gamma^*) = C(\gamma)$ then the result will follow from the Gauss-Bonnet theorem for spherical curves.

To prove that $\ell(\gamma^*) = C(\gamma)$, approximate the curve by a spherical polygon. So assume that $\gamma$ is a convex polygon. Let $C$ be the polyhedral cone whose intersection with the unit sphere is $\gamma$ and $C^*$ the dual cone whose intersection with the unit sphere is $\gamma^*$. Then $\ell(\gamma^*)$ is the sum of the angles between the edges of $C^*$ and $C(\gamma)$ is the sum of the complements to $\pi$ of the dihedral angles of $C$. It remains to use Lemma 20.2.

(c) Assume that $\gamma$ is a convex spherical $n$-gon (if $\gamma$ is smooth then the result is obtained by approximation). Let $l_1, \ldots, l_n$ be the side lengths, $\alpha_1, \ldots, \alpha_n$ be the angles and $\beta_1, \ldots, \beta_n$ the exterior angles of $\gamma$. The domain enclosed by $\gamma_\varepsilon$ consists of $n$ domains bounded by the sides of $\gamma$ and the arcs of great circles obtained from these sides by moving distance $\pi/2$ in the orthogonal direction, and of $n$ spherical isosceles triangles with equal sides $\varepsilon$ and the vertex angles $\pi - \alpha_i = \beta_i$. The perimeter lengths of the outer boundaries of the former domains are equal to $l_i \cos\varepsilon$ and of the latter ones to $\beta_i \sin\varepsilon$. Therefore

$$\ell(\gamma_\varepsilon) = (\sum l_i)\cos\varepsilon + (\sum \beta_i)\sin\varepsilon = \ell(\gamma)\cos\varepsilon + (2\pi - A(\gamma))\sin\varepsilon$$

(the last equality follows from the Gauss-Bonnet theorem). Since $\gamma_{\varepsilon+\pi/2} = \gamma_\varepsilon^*$, it follows from the Gauss-Bonnet theorem that

$$A(\gamma_\varepsilon) = 2\pi - \ell(\gamma_{\varepsilon+\pi/2}) = 2\pi + \ell(\gamma)\sin\varepsilon - (2\pi - A(\gamma))\cos\varepsilon.$$

Alternatively, one argues that

$$\frac{dA(\gamma_\varepsilon)}{d\varepsilon} = \ell(\gamma_\varepsilon),\ \frac{d\ell(\gamma_\varepsilon)}{d\varepsilon} = 2\pi - A(\gamma_\varepsilon)$$

(the second equality follows from the Gauss-Bonnet theorem), and therefore

$$\frac{d^2A(\gamma_\varepsilon)}{d\varepsilon^2} = 2\pi - A(\gamma_\varepsilon),\ \frac{d^2\ell(\gamma_\varepsilon)}{d\varepsilon^2} = -\ell(\gamma_\varepsilon).$$

These second order differential equations are easily solved and the initial conditions uniquely chosen, which implies the result.

(e) Again we assume that $\gamma$ is a convex spherical $n$-gon. Let $\alpha_1, \ldots, \alpha_n$ be its exterior angles. Then the total curvature, $C(\gamma) = \sum \alpha_i$. The domain inside $\gamma'$ is the union of the interior of $\gamma$ and $n$ spherical isosceles triangles with equal sides $\pi/2$ and the vertex angle $\alpha_i$. The area of the former is $\alpha_i$, therefore the area inside $\gamma'$ equals $\sum \alpha_i + A(\gamma) = C(\gamma) + A(\gamma) = 2\pi$ by the Gauss-Bonnet theorem.

20.9, 20.10. See [**31**].

*LECTURE 21*

21.2. Let $(x, y, z)$ be a point of the unit sphere $x^2 + y^2 + z^2 = 1$ and $(X, Y)$ be its stereographic projection on the plane. The explicit formula is easy to derive from similar triangles:

$$x = \frac{2X}{R^2+1},\ y = \frac{2Y}{R^2+1},\ z = \frac{R^2-1}{R^2+1}$$

where $R^2 = X^2 + Y^2$. Consider a plane circle $(X + a)^2 + (Y + b)^2 = c^2$. This equation can be rewritten as $R^2 + 2aX + 2bY = d$ with $d = c^2 - a^2 - b^2$. Further rewrite it as

$$\frac{2aX}{R^2+1} + \frac{2bY}{R^2+1} + \frac{(d+1)(R^2-1)}{2(R^2+1)} = \frac{d-1}{2},$$

that is, as $2ax + 2by + (d + 1)z = (d - 1)$. This is an equation of a plane (not through the North Pole $(0, 0, 1)$); and the intersection of this plane with the sphere is a circle. Hence the preimage of a plane circle under the stereographic projection is a spherical circle. By continuity, one can conclude that the preimage of a straight line is a circle on the sphere that passes through the North Pole.

To prove that the stereographic projection preserves the angles between circles, it suffices to assume that one of the circles, say, $C_1$, is a meridian. Let $C_2$ be another circle on the sphere, and let $X$ be an intersection point of $C_1$ with $C_2$. Replace $C_2$ by the circle $C_3$ that passes through $X$, is tangent to $C_2$ at this point and passes through the North Pole. Let $C_0$ be the meridian tangent to $C_3$ at the North Pole. Let $L_0, L_1$ and $L_3$ be the images of $C_0, C_1$ and $C_3$ under the stereographic projection; these are lines in the plane, $L_0$ is parallel to $L_3$. It suffices to prove that the angle between $C_1$ and $C_3$ equals the angle between $L_1$ and $L_3$. Indeed, the angle between $L_1$ and $L_3$ equals that between $L_1$ and $L_0$ (property of parallel lines); the latter equals the the angle between $C_1$ and $C_0$ (obvious); and this angle equals the angle between $C_1$ and $C_3$ (two angles made by two circles are equal).

21.3. The idea is similar (and, in a sense, dual) to the proof of Theorem 21.1.

Assume that $P$ is circumscribed. Consider a face $A_1, A_2, \cdots, A_n$ and let $O$ be its tangency point with the sphere. Clearly, the sum of angles $A_iOA_{i+1}$ is $2\pi$. As before, we shall sum up all these angles over all faces, taking the ones in the white faces with the positive signs, and the ones in the black faces with the negative signs. Since there are more black faces, this sum, $\Sigma$, is negative.

On the other hand, consider two adjacent faces with a common edge $AB$, see Figure 30.19. The angles $AOB$ and $AO'B$ are equal. Indeed, revolve the plane $AOB$ about the line $AB$ (as if it were a hinge) until it coincides with the plane $AO'B$. This rotation takes point $O$ to $O'$, see Figure 30.19, and hence the triangles $AOB$ and $AO'B$ are congruent.

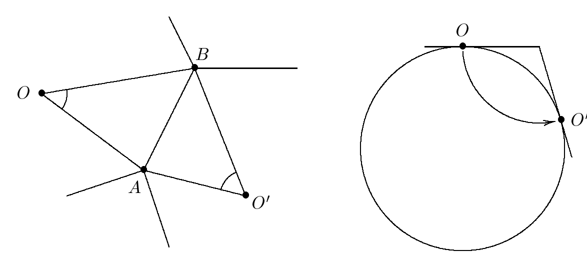


FIGURE 30.19. Solution to Exercise 21.3

There are two kinds of adjacent faces: black–white and white–white; the former's contribution to $\Sigma$ cancels, and the latter contribute a positive number. Thus $\Sigma \geq 0$, a contradiction.

21.4. Let $k$ be the number of faces adjacent to every vertex, $e$ the number of edges and $b$ and $w$ the number of black and white vertices. Let us count, in two ways, the number of edges. On the one hand, there are $k$ edges adjacent to every black vertex, so $e = bk$. For the same reason, $e = wk$, and hence $b = w$.

*LECTURE 22*

22.5. Let $P$ be our polyhedron. Let $\mathrm{Dehn}(P) \neq 0$; more specificaly, let the coefficient of $a_i \otimes \alpha_j$ in $\mathrm{Dehn}(P)$ be $c \neq 0$ (see the definition of $\mathrm{Dehn}(P)$ in Section 22.4). Let $V$ be the volume of the polyhedron $P$ and $d$ be the diameter of $P$. Let, further, $C$ be the sum of the absolute values of the coefficient of $a_i \otimes \alpha_j$ contributed by all the edges of $P$in $\mathrm{Dehn}(P)$. Consider a tiling of space by polyhedra congruent to $P$. Fix in space some ball $B$ of radius $R$, and let $Q$ be the union of tiles whose intersection with $B$ is not empty. Let $N$ be the number of the tiles in $Q$. Since $Q \supset B$,

$$N \geq \frac{\mathrm{Volume}(B)}{\mathrm{Volume}(P)} = \frac{4\pi R^3}{3V}.$$

The absolute value of the coefficient of $a_i \otimes \alpha_j$ in $\mathrm{Dehn}(Q)$ is $N|c|$. On the other hand, the edges of $Q$ all belongs to the copies of $P$ which are contained in the domain between two concentric spheres of radii $R + d$ and $R - d$. (See Figure 30.20.)

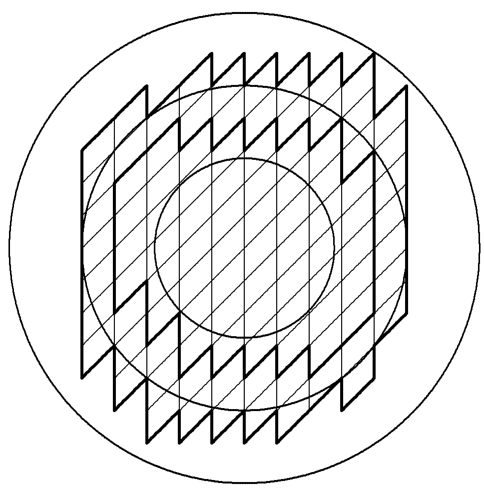

FIGURE 30.20. Exercise 22.5: the outer solid contour symbolizes the polyhedron $Q$, the tiles between the two solid contours contribute into the Dehn invariant of $Q$

The volume of this domain is

$$\frac{4}{3}\pi((R+d)^3 - (R-d)^3) = \frac{4}{3}\pi(6R^2 d + 2d^3) = \frac{8}{3}\pi d(3R^2 + d^2).$$

Hence, the number of tiles within this domain does not exceed $\dfrac{8\pi d(3R^2 + d^2)}{3V}$ and the absolute value of contribution of edges of these copies of $P$ cannot exceed $\dfrac{8\pi d(3R^2 + d^2)}{3V} \cdot C$. Thus,

$$\frac{4\pi R^3}{3V} \cdot |c| \leq \frac{8\pi d(3R^2 + d^2)}{3V} \cdot C, \ |c| \leq \frac{2d(3R^2 + d^2)}{R^3} \cdot C,$$

and since $R$ may be chosen arbitrarily large, this means that $|c|$ is less than any positive number. This contradicts to the positivity of $|c|$. See [**48**] and the references therein.

*LECTURE 23*

23.1. There are as many black as white squares here. However, the left half of the figure contains more black squares and the right half more white ones (16 against 9, in each half). Suppose that there exists a tiling. Then at most one tile intersects the wavy line in the middle in Figure 23.24, and the left part of the polygon (except, possibly, one right-most square, adjacent to the wavy line) is tiled by dominos. But this is impossible, due to the lack of balance between the black and white squares.

23.4. Argue as in the proof of the Theorem 23.1. That a tiling exists for $n \equiv 0, 2, 9, \text{or } 11 \bmod 12$ is shown by explicit constructions for $n \leq 12$ and then extending from a tiling for $n = 12k$ to $n = 12k + l$ where $l = 2, 9, 11, \text{or } 12$.

To prove that no tiling exists for other values of $n$, note first that a necessary condition for a tiling to exist is that the number of dots is divisible by 3: $n(n+1)/2 \equiv 0 \bmod 3$, and hence $n \equiv 0$ or $2 \bmod 3$. Thus we need to consider $n \equiv 3, 5, 6, \text{or } 8 \bmod 12$. The boundary words of the tiles are $x^2yx^{-1}yx^{-1}y^{-2}$ and $xy^2x^{-2}y^{-1}xy^{-1}$. Their shadows on the hexagonal grid are closed. Assign to an oriented closed path on the hexagonal grid the sum of its rotation numbers about the hexagonal regions. These numbers are equal to $\pm 1$ for the boundary paths of the tiles and to $[(n+1)/3]$ for the boundary path of the region. It follows that if the region is tiled by $m$ tiles then $[(n+1)/3] \equiv m \bmod 2$. On the other hand, $n(n+1)/2 = 3m$, hence $n(n+1)/2 \equiv m \bmod 2$. Therefore $[(n+1)/3] \equiv n(n+1)/2 \bmod 2$, and it is easy to see that this congruence does not hold for $n \equiv 3, 5, 6, \text{or } 8 \bmod 12$.

23.5. Argue as in the proof of Theorem 23.3. Define an additive function $f(x)$ such that $f(1) = 1, f(\sqrt{2}) = -0.5$ and $f(x) = 0$ if $x$ is not a rational combination of 1 and $\sqrt{2}$. Define the "area" of a $u \times v$ rectangle as $f(u)f(v)$. Then the "area" of the polygon in Figure 23.25 equals $-0.75$. If a polygon is tiled by squares then its "area" is non-negative, whence the result.

*LECTURE 24*

24.3. The following argument resembles the proof of Theorem 10.3. Let $\gamma(\phi)$ and $\gamma_1(\phi)$ be the two ovals, parameterized by the directions of their tangent lines. Then $\gamma_1'(\phi) = h(\phi)\gamma'(\phi)$ where the function $h$ is the ratio $ds_1/ds$. We want to show that $h$ has at least four extrema.

Let $f_1(\phi)$ and $f_2(\phi)$ be the components of the vector-valued function $\gamma(\phi)$. Since $\gamma_1$ is a closed curve,

$$0 = \int_0^{2\pi} \gamma_1'(\phi)\ d\phi = \int_0^{2\pi} h(\phi)(f_1'(\phi), f_2'(\phi))\ d\phi,$$

hence $\int hf_1' d\phi = \int hf_2' d\phi = 0$. It follows, by integration by parts, that $\int h' f_1\ d\phi = \int h' f_2\ d\phi = 0$. Clearly, $\int h'\ d\phi = 0$ as well.

Assume that $h'$ has only 2 sign changes. We can find a combination of the functions $f_1, f_2$ and 1, say, $af_1 + bf_2 + c$, that changes sign at the same points as $h'$. The function $af_1 + bf_2 + c$ has no other zeros – otherwise the line $ax + by + c = 0$ would intersect the oval $\gamma_1$ at more than 2 points. Therefore $af_1 + bf_2 + c$ has the same intervals of constant sign as $h'$ and $\int h'(af_1 + bf_2 + c)\ d\phi \neq 0$. This contradicts the previous paragraph.

24.4. This is a discrete analog of the previous problem. Denote the position vectors of the vertices of $P$ by $V_1, \ldots, V_n$ and let $\ell_i = |V_{i+1} - V_i|$. Set $h_i = \ell_i'/\ell_i$. Since $P'$ is a closed polygon, $\sum h_i(V_{i+1} - V_i) = 0$. It follows that $\sum(h_{i+1} - h_i)V_i = 0$ (discrete integration by parts). Set $g_i = h_{i+1} - h_i$. We claim that the cyclic sequence $g_i$ is either identically zero or it changes sign at least four times. Since $\sum g_i = 0$, there are at least two sign changes or $g_i = 0$ for all $i$. Assume that there are exactly two sign changes. Then there exist a line $m$ such that for the vertices of $P$ on one side of $m$ one has $g_i \geq 0$ and on the other side $g_i \leq 0$ and there is at least one positive and one negative value. Choose the origin on the line $m$. Then the point $\sum g_i V_i$ lies on the side of $m$ where $g_i > 0$, and hence the vector $\sum g_i V_i$ is not zero. This is a contradiction.

Finally, if $g_{i-1} < 0 < g_i$ then $h_{i+1} > h_i < h_{i-1}$, and hence $\ell'_{i+1}/\ell_{i+1} > \ell'_i/\ell_i < \ell'_{i-1}/\ell_{i-1}$. Therefore $a_i > 0$, and likewise for $g_{i-1} > 0 > g_i$.

24.5. See [**39**], Theorem 2.19.

*LECTURE 25*

25.7. (a) Consider an edge $E$ of $P_t$ of length $l(t)$ with the dihedral angle $\varphi(t)$. Let $n(t)$ and $n_1(t)$ be the unit outer normal vectors to the faces $F$ and $F_1$ that share $E$, and let $w(t)$ and $w_1(t)$ be the inner normal vectors to $E$ in $F$ and $F_1$ having magnitude $l(t)$. We claim that

$$-l(t)\varphi'(t) = n'(t) \cdot w(t) + n_1'(t) \cdot w_1(t) \tag{30.5}$$

where prime is $d/dt$. Indeed, choose a Cartesian coordinate system in the plane orthogonal to $E$, and let $\theta$ and $\theta_1$ be the angles made by $n(t)$ and $n_1(t)$ with the $x$-axis. Then the vectors involved are

$$n = (\cos\theta, \sin\theta), n_1 = (\cos\theta_1, \sin\theta_1), w = l(\sin\theta, -\cos\theta), w_1 = l(-\sin\theta, \cos\theta).$$

Therefore

$$n' = \theta'(-\sin\theta, \cos\theta) = -\frac{1}{l}\theta' w,\ n_1' = \theta_1'(-\sin\theta_1, \cos\theta_1) = \frac{1}{l}\theta_1' w_1,$$

and hence $n' \cdot w + n_1' \cdot w_1 = l(\theta_1' - \theta')$. It remains to notice that $\theta_1(t) - \theta(t) = \pi - \varphi(t)$.

For every face $F$ of $P$, the sum of the inner normal vectors to the edges inside this face, whose magnitudes are equal to the lengths of these edges, is zero (compare with Exercise 30.8). Dot multiply this sum by the derivative of outer unit normal vector to $F$ and sum over all faces. The resulting sum is zero and it equals the sum, over all edges, of the right hand sides of (30.5). The result follows.

*LECTURE 26*

26.2. (b) The interval $\left(\frac{1}{3}, \frac{2}{3}\right)$ consists of numbers $[0.1\ldots]_3$ besides $[0.1]_3$. The intervals $\left(\frac{1}{9}, \frac{2}{9}\right)$ and $\left(\frac{7}{9}, \frac{8}{9}\right)$ consist of numbers $[0.01\ldots]_3$ and $[0.21\ldots]_3$ besides $[0.01]_3$ and $[0.21]_3$ and so on. Thus, $C$ consists of all $[0.d_1d_2d_3\ldots]_3$ with $d_i \neq 1$ for all $i$, and the numbers $[0.d_1d_2\ldots d_{n-1}1]_3$ with $d_i \neq 1$ for $1 \leq i < n$.

(a)

$$\begin{aligned}
\frac{1}{4} &= 2 \cdot \frac{1}{8} = 2 \cdot \left(\frac{1}{9} + \frac{1}{9^2} + \frac{1}{9^3} + \ldots\right) = [0.020202\ldots]_3,\\
\frac{10}{13} &= 20 \cdot \frac{1}{26} = [202]_3 \left(\frac{1}{27} + \frac{1}{27^2} + \ldots\right) = [0.202202202\ldots]_3,\\
\frac{19}{27} &= \frac{2}{3} + \frac{1}{27} = [0.201]_3
\end{aligned}$$

These number belong to $C$ by the result in Part (b).

26.3. (a) The definition of $\gamma$ shows that

$$\begin{aligned}
\gamma[0.1\ldots]_3 &= [0.1]_2, & \gamma[0.001\ldots]_3 &= [0.001]_2,\\
\gamma[0.01\ldots]_3 &= [0.01]_2, & \gamma[0.021\ldots]_3 &= [0.011]_2,\\
\gamma[0.21\ldots]_3 &= [0.11]_2, & \gamma[0.201\ldots]_3 &= [0.101]_2,\\
& & \gamma[0.221\ldots]_3 &= [0.111]_2.
\end{aligned}$$

The apparent rule of forming $\gamma(x)$ is the following: if $x = [0.d_1d_2d_3\ldots]_3$ and there are 1's among $d_i's$, then one should take the first $n$ with $d_n = 1$ and put

$$\gamma[0.d_1d_2d_3\ldots]_3 = [0.e_1\ldots e_{n-1}1]_2,\ e_i = \frac{d_i}{2}.$$

It is clear that to extend $\gamma$ to a continuous function on the whole interval $[0,1]$, one should put

$$\gamma[0.d_1d_2d_3\dots]_3 = [0.e_1e_2e_3\dots]_2,\ e_i = \frac{d_i}{2},\ \text{if } d_i \neq 1 \text{ for all } i.$$

(b) Since $\frac{1}{4} = [0.020202\dots]_3, \gamma\left(\frac{1}{4}\right) = [0.010101\dots]_2 = \frac{1}{4} + \frac{1}{4^2} + \dots = \frac{1}{3}$. Since $\frac{5}{13} = 10 \cdot \frac{1}{26} = [0.101101101\dots]_3 = [0.1]_2 = \frac{1}{2}$.

(c) Solved in (a).

(d) Obviously follows from (a).

26.4. (a) Denote the initial curve $F$ by $F_0$, then put $F_1 = \widetilde{F}_0, F_2 = \widetilde{F}_1$ and so on. It is clear from the construction that $F_n$ maps every interval $\left[\frac{k}{4^n}, \frac{k+1}{4^n}\right]$ into a square of the form $\left[\frac{\ell_1}{2^n}, \frac{\ell_1+1}{2^n}\right] \times \left[\frac{\ell_2}{2^n}, \frac{\ell_2+1}{2^n}\right]$; moreover it maps $4^n$ different intervals of the indicated form into $4^n$ different squares of the indicated form, and maps adjacent interval into adjacent squares. In addition to that, if

$$F_n\left[\frac{k}{4^n}, \frac{k+1}{4^n}\right] \subset \left[\frac{\ell_1}{2^n}, \frac{\ell_1+1}{2^n}\right] \times \left[\frac{\ell_2}{2^n}, \frac{\ell_2+1}{2^n}\right],$$

then

$$F_p\left[\frac{k}{4^n}, \frac{k+1}{4^n}\right] \subset \left[\frac{\ell_1}{2^n}, \frac{\ell_1+1}{2^n}\right] \times \left[\frac{\ell_2}{2^n}, \frac{\ell_2+1}{2^n}\right],$$

for every $p > n$. This shows that for every $t \in [0,1]$ and every $p, q \geq n$, the distance between $F_p(t)$ and $F_q(t)$ cannot exceed $\frac{\sqrt{2}}{2^n}$. It remains to use standard theorems from Analysis; "Cauchy criterion" asserts that the sequence $F_n$ converges uniformly to a certain map $[0,1] \to [0,1]^2$, call it $P$, and there is another theorem which states that a uniform limit of a sequence of continuous function is continuous, so $P$ is continuous.

(b) Obviously, $F_n\left(\frac{k}{4^n}\right)$ does not depend on the initial map $F$ and

$$F_n\left(\frac{k}{4^n}\right) = F_{n+1}\left(\frac{k}{4^n}\right) = \dots = P\left(\frac{k}{4^n}\right).$$

Thus, the values of $P$ at the fractions with denominators of the form $4^n$ do not depend on $F$, and, since these fractions form a dense subset of $[0,1]$, $P$ does not depend on $F$ at all.

(c) It was shown in the solution of Part (a) that the image of $P$ contains points in every square $\left[\frac{\ell_1}{2^n}, \frac{\ell_1+1}{2^n}\right] \times \left[\frac{\ell_2}{2^n}, \frac{\ell_2+1}{2^n}\right]$, for every $n$. This shows that the image of $P$ is dense in $[0,1]^2$. But the image of $[0,1]$ with respect to any continuous map is closed; hence it must be the whole square $[0,1]^2$.

(e) Any $t \in [0,1]$ may be presented as $[0.A]_2$ where $A$ is an *infinite* sequence of zeroes and ones (it may consist, after some moment, only of zeroes or only of ones). For a sequence $A$, we denote by $\overline{A}$ the "opposite" sequence: zeroes are replaced by ones and ones are replaced by zeroes. Suppose that $F[0.A]_2 = ([0.B]_2, [0.C]_2)$. According to Part (b) we may assume that $F$ is "symmetric," that is, $F[0.\overline{A}]_2 = ([0.B]_2, [0.\overline{C}]_2$. The definition of $\widetilde{F}$ given before Exercise 26.4 may be restated in the following way:

$$\begin{aligned}\widetilde{F}[0.00A]_2 &= ([0.0C]_2, [0.0B]_2), \quad F[0.01A]_2 = ([0.1B]_2, [0.0C]_2),\\ \widetilde{F}[0.10A]_2 &= ([0.1B]_2, [0.1\overline{C}]_2), \quad F[0.11A]_2 = ([0.0C]_2, [0.1\overline{B}]_2).\end{aligned}$$

It is permissible to replace in all these formulas $F$ and $\widetilde{F}$ by $P$.

(f) The formulas above show that for any $2n$-term sequence $a$ of digits 0 and 1, $F_n[0.aA]_2 = ([0.bB']_2, [0.cC']_2)$ or $([0.cC']_2, [0.bB']_2)$ where $b$ and $c$ are $n$-term sequences depending only on $a$, $B' = B$ or $\overline{B}$, $C' = C$ or $\overline{C}$. Repeating this procedure 4 times, we obtain the following result: if $P[0.A]_2 = ([0.B]_2, [0.C]_2)$ then for any word $a$ of even length, $P[0.aaaaA]_2 = ([0.bB]_2, [0.cC]_2$ where $b$ and $c$ depend only on $a$. This implies that if $A$ is periodic, then $B$ and $C$ are periodic. (If $A$ is periodic starting from some place, then $A = aA_1$ where $A_1$ is (pure) periodic and $a$ has even length. The formulas above show that in this case $B$ and $C$ also will be periodic starting from some place.)

(d) $\frac{1}{3} = [0.010101\dots]_2$. Let $A = 010101\dots$ and let $P[0.A]_2 = ([0.B]_2, [0.C]_2)$. Then

$$P\left(\frac{1}{3}\right) = P[0.01A]_2 = ([0.1B]_2, [0.0C]_2) = ([0.B]_2, [0.C]_2).$$

Thus, $B = 1B,\ C = 0C$, hence $B = 11111\dots,\ C = 00000\dots$, hence

$$P\left(\frac{1}{3}\right) = (1, 0).$$

$\frac{1}{5} = [0.001100110011\dots]_2$. Let $A = 001100110011\dots$ and let $P[0.A] = ([0.b]_2, [0.C]_2)$. Then

$$P[0.11A]_2 = ([0.0C]_2, [0.1\overline{B}]_2),\ P[0.0011A] = ([0.01\overline{B}]_2, [0.00C]_2),$$

and hence

$$P[0.00110011A]_2 = ([0.0110B]_2, [0.0000C]_2).$$

Thus, $B = 0110B,\ C = 0000C$, hence $B = 011001100110\dots, C = 000000\dots$ and

$$P\left(\frac{1}{5}\right) = ([0.B]_2, [0.C]_2) = \left(\frac{2}{5}, 0\right).$$

(The reader who wants to perform a more challenging computation may try to compute $P\left(\frac{1}{7}\right)$. According to our computations, it is $\left(\frac{29}{65}, \frac{28}{65}\right)$.)

*LECTURE 27*

27.1. (b) *Answer*: $-(x^2y - x - 1)^2 - (x^2 - 1)^2$.

27.2. (b) *Answer*: $x^2(1 + y)^3 + y^2$.

27.3. See [**27**].

*LECTURE 28*

28.8. See Figure 30.21: the focus of the parabola is also a focus of the ellipse; the two conics are smoothly connected by arbitrary curves. The construction makes use of Exercise 28.4.

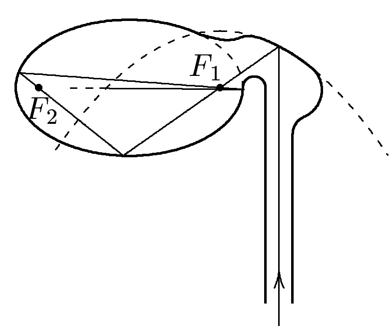


FIGURE 30.21. Trap for a parallel beam

28.9. See [**59, 88**].

*LECTURE 29*

29.5. Let us compare the areas of two triples of circles inside an equilateral triangle with unit sides. The first configuration consists of three equal circles, each inscribed in its own angle of the triangle and tangent to two other circles. Let $r$ be the radius of such a circle. Then $2r + 2\sqrt{3}r = 1$ and hence $r = 1/(2(1+\sqrt{3}))$. The area of the three circles, $A_1 = 3\pi/(4(1+\sqrt{3})^2)$ and $A_1/\pi \approx 0.1005$.

The second configuration consists of the circle inscribed into the triangle and two equal smaller circles, inscribed into two angles of the triangle and each tangent to the larger circle (but not to each other). Let $R$ be the radius of the larger circle and $r$ those of the smaller ones. Then $R = \sqrt{3}/6$. The other radius is found from the equation $(0.5 - \sqrt{3}r)^2 + (R-r)^2 = (R+r)^2$. This quadratic equation has two roots $\sqrt{3}/2$ and $\sqrt{3}/18$, and $r$ is the latter. The total area of the three circles, $A_2 = \pi/12 + \pi/54$ and $A_2/\pi \approx 0.1018$. Thus the second configuration has a greater area.

Another competing configuration consists of three circles that make a chain and are inscribed into one angle of the triangle. If the triangle is isosceles and very long and thin then the total area of such a chain of circles is almost twice as large as the total area of the Malfatti configuration of three circles, each tangent to two others .

*LECTURE 30*

30.1. *Answer*:

$$\sum_{k=1}^{n+1} a_k \frac{(x-x_1)(x-x_2)\dots(x-x_{k-1})(x-x_{k+1})\dots(x-x_{n+1})}{(x_k-x_1)(x_k-x_2)\dots(x_k-x_{k-1})(x_k-x_{k+1})\dots(x_k-x_{n+1})}.$$

The polynomial is unique.

30.2. Consider the polynomial $g(x)$ from the proof of Theorem 30.2. Since $g(x) \equiv 1$, its coefficients of degree $0, 1, \dots, n-2$ vanish. This gives all but one desired identities. The last one is obtained by equating the leading coefficient to 1.

30.3. The claim will follows once we prove that

$$\frac{h(q_1)}{f'(q_1)} + \frac{h(q_2)}{f'(q_2)} + \dots + \frac{h(q_n)}{f'(q_n)} = 0$$

where the sum is taken over all roots of a hyperbolic polynomial $f(x)$ of degree $n$ and $h(x)$ is a polynomial of degree $n-2$ or less. Since a polynomial $h(x)$ is a linear combination of the monomials $1, x, \dots, x^{n-2}$, the result follows from Exercise 30.2.

30.7. Recall the notion of elliptic coordinates introduced in Lecture 28. Given a confocal family of conics

$$\frac{x^2}{a^2+\lambda} + \frac{y^2}{b^2+\lambda} = 1,$$

the elliptic coordinates of a point $(x, y)$ are the two values of $\lambda$ for which this equation holds. Fixing one of the elliptic coordinates describes an ellipse, fixing the other – a confocal hyperbola. It is easy to calculate that if $(\lambda, \mu)$ are the elliptic coordinates of a point $(x, y)$ then

$$x^2 = \frac{(a^2+\lambda)(a^2+\mu)}{a^2-b^2},\ y^2 = \frac{(b^2+\lambda)(b^2+\mu)}{b^2-a^2}.$$

Let $P = (x, y)$ be a point of the ellipse

$$\frac{x^2}{a^2} + \frac{y^2}{b^2} = 1,$$

and $Q = (X, Y) = A(x, y)$ be the respective point of the ellipse

$$\frac{x^2}{a^2+\lambda} + \frac{y^2}{b^2+\lambda} = 1,$$

where $X = x\sqrt{a^2+\lambda}/a, Y = y\sqrt{b^2+\lambda}/b$. Let the elliptic coordinates of $P$ be $(0, \mu)$; let those of $Q$ be $(\lambda, \eta)$. We want to prove that $\mu = \eta$. Indeed, expressing the Cartesian coordinates in terms of the elliptic ones,

$$x^2 = \frac{a^2(a^2+\mu)}{a^2-b^2},\ X^2 = \frac{(a^2+\lambda)}{a^2}\frac{a^2(a^2+\mu)}{a^2-b^2} = \frac{(a^2+\lambda)(a^2+\eta)}{a^2-b^2}.$$

Hence $\mu = \eta$, as needed.

# Bibliography


[1] C. Adams. *The knot book. An elementary introduction to the mathematical theory of knots*, Amer. Math. Soc., Providence, RI, 2004.

[2] M. Aigner, G. Ziegler, K. H. Hofmann. *Proofs from THE BOOK*, Springer-Verlag, Berlin–Heidelberg–New York, 2004.

[3] J.-C. Alvarez. *Hilbert's fourth problem in two dimensions*, MASS Selecta, Amer. Math. Soc., Providence, RI, 2003, pp. 165–184.

[4] V. Arnold. *Mathematical methods of classical mechanics*, 2-nd edition, Springer-Verlag, New York, 1989.

[5] W. Barth, Th. Bauer. *Poncelet theorems*, Expos. Math. **14** (1996), 125–144.

[6] L. Bianchi. *Vorlesungen über Differentialgeometrie*, Teubner, Leipzig, 1910.

[7] D. Bleecker. *Volume increasing isometric deformations of convex polyhedra*, J. Diff. Geom. **43** (1996), 505–526.

[8] W. Blaschke. *Einführung in die Geometrie der Waben*, Birkhauser, Basel, Stuttgart, 1955.

[9] V. Boltianskii. *Hilbert's Third problem*, John Wiley & Sons, Wash., New York, 1978.

[10] H. Bos, C. Kers, F. Oort, D. Raven. *Poncelet's closure theorem*, Expos. Math. **5** (1987), 289–364.

[11] V. Brun, J. O. Stubban, J. E. Fjeldstad, L. Tambs, K. E. Aubert, W. Ljunggren, E. Jacobsthal. *On the divisibility of the difference between two binomial coefficients*, Den 11te Skandinaviske Matematikerkongress, Trondheim, 1949, 42–54.

[12] Yu. Burago, V. Zalgaller. *Isometric piecewise-linear embeddings of two-dimensional manifolds with a polyhedral metric into* $\mathbf{R^3}$, St. Petersburg Math. J. **7** (1996), 369–385.

[13] P. Cartier. *Decomposition des polyèdres: le point sur le troisième problème de Hilbert*, Astérisque **133–134** (1986), 261–288.

[14] S.-S. Chern. *Web geometry*, Bull. Amer. Math. Soc. **6** (1982), 1–8.

[15] Yu. Chekanov, P. Pushkar'. *Combinatorics of fronts of Legendrian links, and Arnold's 4-conjectures*, Russian Math. Surveys **60** (2005), 95–149.

[16] A. Colton, D. Freeman, A. Gnepp, T. Ng, J. Spivack, C. Yolder. *The isoperimetric problem in some singular surfaces*, J. Austral. Math. Soc. **78** (2005), 167–197.

[17] J. Conway, J. Lagarias. *Tiling with polyominoes and combinatorial group theory*, J. Combin. Theory Ser. **A 53** (1990), 183–208.

[18] D. Cox, S. Katz. *Mirror symmetry and algebraic geometry*, Amer. Math. Soc., Providence, RI, 1999.

[19] G. Darboux. *Principes de géométrie analytique*, Gautier-Villars, Paris, 1917.

[20] M. Dehn. *Über raumgleiche Polyeder*, Nachr. Acad. Wiss. Göttingen Math.-Phys. Kl. (1900), 345–354.

[21] M. Dehn. *Über die Zerlegung von Rechtecken in Rechtecke*, Math. Ann. **57** (1903), 314–332.

[22] M. Dehn. *The mentality of the mathematician. A characterization*, Math. Intelligencer **5** No. 2 (1983), 18–26.

[23] F. Dogru, S. Tabachnikov. *Dual billiards*, Math. Intelligencer **27** No. 4 (2005), 18–25.

[24] J. P. Duncan, J. L. Duncan. *Folded developables*, Proc. Roy. Soc. London Ser. A **383** (1982), 191–205.

[25] J. Dupont. *Scissors congruences, group homology and characteristic classes*, World Scientific, River Edge, NJ, 2001.

[26] F. Dyson. *Missed opportunities*, Bull. Amer. Math. Soc. **78** (1972), 635–652.

[27] Ya. Eliashberg, N. Mishachev. *Introduction to the h-principle*, American Math. Soc., Providence, RI, 2002.

[28] F. Fabricius-Bjerre. *On the double tangents of plane curves*, Math. Scand. **11** (1962), 113–116.

[29] E. Ferrand. *On the Bennequin invariant and the geometry of wave fronts*, Geom. Dedicata **65** (1997), 219–245.

[30] C. Freiling, D. Rinne. *Tiling a square with similar rectangles*, Math. Res. Lett. **1** (1994), 547–558.

[31] D. Fuchs, E. Fuchs. *Closed geodesics on regular polyhedra*, Moscow Math. J., to appear.

[32] D. Fuchs, S. Tabachnikov. *More on paperfolding*, Amer. Math. Monthly, **106** (1999), 27–35.

[33] I. Gelfand, M. Kapranov, A. Zelevinsky. *Discriminants, resultants, and multidimensional determinants*, Birkhauser, Boston, MA, 1994.

[34] P. Giblin, P. Holtom. *The centre symmetry set*, CAUSTICS '98 (Warsaw), 91–105, Banach Center Publ., **50**, Warsaw, 1999.

[35] S. Gindikin. *Tales of physicists and mathematicians*, Birkhauser, Boston, MA, 1988.

[36] A. Givental. *Polynomiality of electrostatic potential*, Uspekhi Mat. Nauk **39** No. 5 (1984), 253–254.

[37] A. Granville. *Arithmetic properties of binomial coefficients*, http://www.dms.umontreal.ca/ andrew/Binomial/

[38] P. Griffith, J. Harris. *On Cayley's explicitsolution of Poncelet's porism*, l'Enseign. Math. **24** (1978), 31–40.

[39] H. Guggenheimer. *Diffferential geometry*, Dover, New York, 1977.

[40] B. Halpern. *An inequality for double tangents*, Proc. Amer. Math. Soc. **76** (1979), 133–139.

[41] B. Halpern, K. Weaver. *Inverting a cylinder through isometric immersions and isometric embeddings*, Trans. Amer. Math. Soc. **230** (1977), 41–70.

[42] D. Hilbert, S. Cohn-Vossen. *Geometry and the imagination*, Providence, RI, AMS Chelsea Publ., 1999.

[43] M. Kapovich, J. Millson. *On the moduli space of polygons in the Euclidean plane*, J. Differential Geom. **42** (1995), 430–464.

[44] S. Katz. *Enumerative geometry and string theory*, Amer. Math. Soc., Providence, RI, 2006.

[45] R. Kenyon. *Tilings of convex polygons*, Ann. Inst. Fourier **47** (1997), 929–944.

[46] J. King. *Three problems in search of a measure*, Amer. Math. Monthly **101** (1994), 609–628.

[47] D. Konhauser, D. Velleman, S. Wagon. *Which way did the bicycle go? And other intriguing mathematical mysteries*, MAA, Washington, 1996.

[48] J. Lagarias, D. Moews, D. *Polytopes that fill $R^n$ and scissors congruence*, Discrete Comput. Geom. **13** (1995), 573–583.

[49] J. Lagarias, T. Richardson. *Convexity and the average curvature of plane curves.* Geom. Dedicata **67** (1997), 1–30.

[50] Z. Leibenzon. *A simple combinatorial method for proving the Jacobi identity and its generalizations*, Funct. Anal. Appl. **20** (1986), no. 1, 66–68.

[51] M. Levi. *A "bicycle wheel" proof of the Gauss-Bonnet theorem*, Exposition. Math. **12** (1994), 145–164.

[52] M. Levi, S. Tabachnikov. *The Poncelet grid and the billiard in an ellipse*, Amer. Math. Monthly, to appear.

[53] Yu. Manin. *Cubic forms. Algebra, geometry, arithmetic*, North-Holland Publ. Co., Amsterdam, 1986.

[54] A. Nazarov, F. Petrov. *On S. L. Tabachnikov's conjecture*, preprint math.MG/0507379.

[55] I. Newton. *The Principia. Mathematical principles of natural philosophy*, Univ. California Press, Berkeley, CA, 1999.

[56] C. D. Olds. *Continued fractions*, Random House, New York, 1963.

[57] V. Ovsienko, S. Tabachnikov. *Projective differential geometry, old and new: from Schwarzian derivative to cohomology of diffeomorphism groups*, Cambridge Univ. Press, 2005.

[58] I. Pak. *Inflating polyhedral surfaces*, preprint.

[59] D. Pedoe. *The most "elementary" theorem of Euclidean geometry*, Math. Mag. **49** (1976), 40–42.

[60] L. Penrose, R. Penrose. *Puzzles for Christmas*, New Scientist. 25 December (1958), 1580-1581, 1597.

[61] A. Pogorelov. *Hilbert's fourth problem*, J. Wiley & Sons, 1979.

[62] G. Polya. *Induction and analogy in mathematics. Mathematics and plausible reasoning*, vol. I. Princeton University Press, Princeton, N. J., 1954.

[63] K. Poorrezaei. *Two proofs of Graves's theorem*, Amer. Math. Monthly **110** (2003), 826–830.

[64] V. Prasolov. *Polynomials*, Springer-Verlag, Berlin, 2004.

[65] J. Propp. *A pedestrian approach to a method of Conway, or, A tale of two cities*, Math. Mag. **70** (1997), 327–340.

[66] I. Sabitov. *The volume as a metric invariant of polyhedra*, Discrete Comput. Geom. **20** (1998), 405–425.

[67] C. Sah. *Hilbert's third problem: scissors congruence*, Research Notes in Mathematics, 33. Pitman, Boston–London, 1979.

[68] I. Schoenberg, S. Zaremba. *On Cauchy's lemma concerning convex polygons*, Canad. J. Math. **19** 1967, 1062–1071.

[69] O. Schramm. *How to cage an egg*, Invent. Math. **107** (1992), 543–560.

[70] R. Schwartz. *The Poncelet grid*, Advances in Geometry (2006), to appear.

[71] B. Segre. *The non-singular cubic surfaces*, Oxford University Press, Oxford, 1942.

[72] A. Sossinsky. *Mathematics with a twist*, Harvard Univ. Press, Cambridge, MA, 2002.

[73] R. Stanley. *Enumerative Combinatorics* v. 2, Cambridge Univ. Press, Cambridge, 1999.

[74] R. Stanley. Catalan Addendum.
http://www-math.mit.edu/ rstan/ec/catadd.pdf

[75] S. Stein, S. Szabo. *Algebra and tiling*, Washington, DC, MAA 1994.

[76] J.-P. Sydler, *Conditions nécessaires et suffisantes pour l'equivalence des polyèdres de l'espace euclidien à trois dimension*, Comment. Math. Helv. **40** (1965), 43–80.

[77] G. Szegö. *Über eine Eigenschaft der Exponentialreihe, Sitzungsber. Berl. Math. Ges.,* **23** *(1924), 500-64.*

*[78] S. Tabachnikov.* Billiards, *Soc. Math. France, "Panoramas et Syntheses", No 1, 1995.*

*[79] S. Tabachnikov. The four vertex theorem revisited – two variations on the old theme, Amer. Math. Monthly* **102** *(1995), 912–916.*

*[80] S. Tabachnikov. A cone eversion, Amer. Math. Monthly* **102** *(1995), 52–56.*

*[81] S. Tabachnikov. Going in circles: variations on the Money-Coutts theorem, Geom. Dedicata* **80** *(2000), 201–209.*

*[82] S. Tabachnikov. On skew loops, skew branes and quadratic hypersurfaces, Moscow Math. J.* **3** *(2003), 681–690.*

*[83] S. Tabachnikov.* Geometry and billiards, *Amer. Math. Soc., Providence, RI, 2005.*

*[84] S. Troubetzkoy. Circles and polygons, Geom. Dedicata* **80** *(2000), 289–296.*

*[85] W. Thurston. Conway's tiling groups, Amer. Math. Monthly* **97** *(1990), 757–773.*

*[86] J. Tyrrell, M. Powell. A theorem in circle geometry, Bull. Lond. Math. Soc.* **3** *(1971), 70–74.*

*[87] S. Wagon. Fourteen proofs of a result about tiling a rectangle, Amer. Math. Monthly* **94** *(1987), 601–617.*

*[88] G. Wanner. The Cramer-Castillon problem and Urquhart's 'most elementary' theorem, Elem. Math.* **61** *(2006), 58–64.*

*[89] J. Weiner. Global properties of spherical curves, J. Diff. Geom.* **12** *(1977), 425–438.*

*[90] J. Wilford. The mapmakers, Vintage, 2001.*

*[91] B. Yandell. The honors class: Hilbert's problems and their solvers, A. K. Peters, 2001.*

*[92] V. Zalgaller, G. Los'. Solution of the Malfatti problem, J. Math. Sci.* **72** *(1994), 3163–3177.*

*[93]* Mathematical developments arising from Hilbert's problems, *F. Browder, ed., Proc. Symp., Pure Math.,* **XXVIII** *(1976).*

*[94]* Outside In: A video about turning the sphere inside out, *The Geometry Center, University of MN, A.K. Peters, 1994.*

# Index